INDC-217

FUNDAMENTAL NUCLEAR ENERGY RESEARCH

1967

A Supplemental Report to the
Annual Report to Congress for 1967
of the

UNITED STATES ATOMIC ENERGY COMMISSION

JANUARY 1968

FUNDAMENTAL NUCLEAR ENERGY RESEARCH

1967

A Supplemental Report to the
Annual Report to Congress for 1967
of the
UNITED STATES ATOMIC ENERGY COMMISSION
JANUARY 1968

Edited by the Division of Plans and Reports in cooperation with the Office of the Assistant General Manager for Reactors, the Division of Biology and Medicine, and the Division of Research.

PREVIOUS PUBLICATIONS

Previous reports in this series were: "Atomic Energy Research in the Life and Physical Sciences—1960" ($1.25); "Atomic Energy Research—Life and Physical Sciences, Reactor Development, Waste Management—1961" ($2.25); "Fundamental Nuclear Energy Research—1962" ($2.50); "Fundamental Nuclear Energy Research—1963" ($2.50); "Fundamental Nuclear Energy Research—1964" ($2.00); "Fundamental Nuclear Energy Research—1965" ($2.25); and "Fundamental Nuclear Energy Research—1966" ($2.50), which are available, at the indicated prices, from the Superintendent of Documents, U.S. Government Printing Office, Washington, D.C. 20402.

For sale by the Superintendent of Documents, U.S. Government Printing Office
Washington, D.C. 20402 - Price $2.50

FOREWORD

". . . Our work and our investigations are constant reminders of how much more we need to do and to learn. Therefore, in the nuclear field we continue to put great emphasis on research . . . our National Laboratories across the country are busy exploring many basic phenomena of nature and delving deeper and deeper into the heart of the atom. Indeed, one of the most fascinating aspects of this whole field of nuclear energy is the extreme range of the work—for while we develop nuclear propulsion to take us to the stars and at the same time analyze the cosmic rays that come from them, we also explore the very nature of matter, the very substance of the stars, of ourselves and all that exists. It is a most exciting field and a most exciting time to be working in it."

—Dr. Glenn T. Seaborg, Chairman
U.S. Atomic Energy Commission
In an address upon visiting
Bangkok, Thailand
January 10, 1967

PREFACE

The Atomic Energy Commission's responsibility for research and development in nurturing the Nation's nuclear energy program is twofold: (*a*) to foster the growth of basic scientific and technical knowledge, and (*b*) to promote the beneficial applications of the knowledge thus attained. Toward the end of providing a public accounting of its conduct of this dual responsibility, the Atomic Energy Commission annually publishes two reports: "Fundamental Nuclear Energy Research," and the "Annual Report to Congress." In this, its "Fundamental Nuclear Energy Research—1967," the AEC reports on some of the more significant advancements that have been made recently in the basic research and exploratory development work conducted in the areas of biomedical and environmental sciences, the physical sciences, and nuclear reactor technology. This report is a supplement to the "Annual Report to Congress for 1967" [1] in which the AEC reports upon the specific activities and programs it conducted during the year for the purpose of applying the beneficial aspects of nuclear energy for the good of civilization.

This report is not a complete review of the AEC's overall fundamental nuclear research effort. The several thousand research tasks assigned to its contractors and laboratories are too broad and too varied to be discussed in a single volume. Thus, this volume only briefly summarizes some of the more noteworthy advancements currently being made—many of a purely basic nature, some on an exploratory development phase, and a few at the beneficial application stage.

The pace of today's basic research effort is swift and efficient and more often than not, it is conducted as a team-effort involving members of several scientific and/or technical disciplines. Experiments are set up with engineering skill and the results of individual trials can, in some instances, be matched with related knowledge and theory already stored in computer banks. Modern communications and travel make possible the interplay of ideas and results between individuals and groups on a current basis. Thus the chain of knowledge necessary for a scientific "breakthrough," however big or small, is forged effectively and quickly. In the area of nuclear energy especially, very little new basic knowledge "sits on the shelf" for long; in fact, at times, exploratory development on the application of an experimental objective may begin before all the details of the new knowledge have been fully attained. As a result, some of the advancements in fundamental nuclear research that were reported in prior editions of this report may be recognized as current project-oriented applications in the "Annual Report to Congress."

AEC-fostered research in the fields of biology and medicine is aimed toward determining the various effects of radiation on the life processes so that effective precautionary and remedial measures can be developed. However, in many instances, the basic knowledge of a particular aspect of life—human, animal, or plant—has not yet been attained through conventional biomedical research. For this reason, much of the biomedical work sponsored by the AEC is on a two-step basis: first, to evolve a knowledge of a specific life process itself, and then, second, to determine the manner and effect of radiation interactions. Thus, some of the biological-medical-environmental advances reported here may, at first glance, appear to have little immediate bearing on the atomic energy program.

Several hundred individual studies are mentioned in this report. Those that are "highlighted" on the next 9 pages are considered as representative samples of the progress being made under AEC-sponsorship in the field of fundamental nuclear energy research.

[1] Publicly available mid-February 1968 under the title "Major Activities in the Atomic Energy Programs—January–December 1967" from the Superintendent of Documents, U.S. Government Printing Office, Washington, D.C. 20402.

Part One

BASIC PHYSICAL RESEARCH PROGRAMS

HIGH ENERGY PHYSICS

"Quark Model"

● Calculations have been made to test the new "quark model" based upon the existence of three particles which may have fractional electric charges and which may be the fundamental constituents of matter (p. 4).

Interference Theory

● An interference model has been developed to explain the experimentally observed features of high velocity collisions between two types of particles—pions and nucleons (p. 5).

Electromagnetic Radiation

● Interpretation of very high energy experiments conducted at electron accelerators have confirmed the theory that electromagnetic radiation manifests several forms upon interaction (p. 5).

K-Meson Cross Section Measurements

● A number of new enhancements, possibly "resonant" particles, have been discovered by measuring the total cross section for K^- and K^+ mesons on protons and deuterons (p. 8).

Discovery of New Strangness -1 Particles

● A new photoproduction method has resulted in the discovery of two new members of the Y* family of particles (p. 9).

External Proton Beam

● The successful extraction of the proton beam directly into a large experimental hall makes it possible to obtain mesons produced at 0° to the forward direction (p. 11).

Beam Magnet Improvements

● Superconducting beam magnets have been developed which produce magnetic fields two to three times greater than the 20 kilogauss limit for iron pole beam magnets (p. 12).

Photon Spectrometer

● A unique tool, which employs the conversion of photons into electron-positron pairs, has been developed to analyze the spectrum of a beam of high energy photons (p. 16).

MEDIUM ENERGY PHYSICS

K- and Pi-Mesonic X-rays

● K-mesonic atoms of lithium, beryllium, boron, and carbon have been identified (p. 21).

LOW ENERGY PHYSICS

Nuclear Lifetimes Using Doppler Shift

● A combination of the *Coulomb* excitation process and *Doppler* shift is being applied to the study of nuclear lifetimes in the 10 picosecond (10^{-11} of a sec.) range (p. 27).

New Radioisotope, Helium-7

● One particularly significant result of nuclear reactions induced by tritons from a three-stage tandem Van de Graaff accelerator is the discovery of the nucleus, helium-7 (p. 31).

Iodine Clock

● Radioactive iodine, alive in the early times of our solar system, but now completely died

out, has brought forth the discovery that an extinct radioactivity clock can be extremely useful in dating other events in the early solar system (p. 35).

CHEMISTRY RESEARCH

Improved Particle Identifier System

● New techniques of measurement have resulted in the discovery of nuclei of boron and lithium never before identified. These include boron-14, boron-15, and lithium-11. Many other details of important nuclear reactions are being unraveled by this method (p. 38).

Improved Cross Section Measurements

● Lithium-drifted germanium detectors have recently been applied to new measurements of neutron activation cross sections, which are used in activation analysis of a wide variety of materials. The new techniques permit more rapid analyses at lower cost because no chemical separations are necessary (p. 40).

Electronic Structure of the Actinides

● Major advances in spectral interpretations of the electronic structures of the actinide elements have been made at a number of AEC laboratories using computer programs to make theoretical calculations (p. 42).

Mössbauer Spectroscopy of Iron in Coal

● The iron-57 isotope has been used in Mössbauer spectroscopy to give new information about the chemical composition or state of combination of iron in native coal. This information is expected to be useful because it is related to problems of ash and clinker formation, waste disposal, and of possible pollution control (p. 54).

Penta-Covalent Silicon

● All ordinary compounds of silicon have a valence of four. That is, each silicon atom is chemically bonded to four other atoms. Recently, a compound of silicon showing a valence of five has been prepared and its structure determined for the first time. This opens up a new field of silicon chemistry of considerable theoretical and possible practical interest (p. 57).

Structure and Properties of Molten Salts

● New experimental and theoretical investigations, including the development of laser-excited *Raman* spectroscopy, are providing improved understanding of the compositions and structures of fused salts (p. 60).

METALLURGY AND MATERIALS

Channeling of Charged Particles

● In experiments on channeling, iodine ions of 50 Mev. energy were found to pass through gold crystals and emerge with discrete energy bands (p. 66).

Radiation Effects in Nickel

● Normal grain boundaries in nickel have been observed to absorb defects created during neutron irradiation more readily than twin boundaries (p. 69).

Thermal Expansions at Low Temperatures

● A device has been developed for measuring temperature-induced length changes of the order of 1 percent of the average spacing between atoms in the solid—10 times better than previously possible (p. 71)

Tunneling Between Superconductors

● A new superconducting phenomenon has been discovered involving electronic tunneling between superconductors (p. 73).

Electron Spin Resonance

● A new electron spin resonance technique has been developed and used to study the excited states of impurity atoms in crystals (p. 77).

Polarized Neutron Beam Research

● A new limit for the electric dipole moment of the neutron has been established by neutron scattering of a high flux beam of neutrons (p. 81).

Superplasticity in Metallic Materials

● Recent observations on superplasticity in metallic materials point to a plausible explanation for this phenomenon, namely the appearance and growth of new grains and the constant motion of grain boundaries during stretching (p. 83).

TRIP Steels

● A new high-strength-high-ductility material, TRIP (transformation-induced plasticity) steel, has been developed (p. 87).

CONTROLLED THERMONUCLEAR RESEARCH

Stellarator

● For the first time, a high temperature plasma has been contained in a low-beta toroidal device without the existence of anomalous diffusion (p. 95).

Astron

● The Astron device achieved magnetic field reversal of a few percent which represents a significant step toward proving the feasibility of the Astron concept (p. 98).

MATHEMATICS AND COMPUTERS

Processing of Pictorial Information

● Two devices to assist in the computer processing of line drawings employing novel high-speed digitally controlled analogue circuits have been developed under AEC sponsorship. The machines are relatively cheap and offer the possibility of considerably simplifying the operations of computer graphics (p. 104).

Fluid Dynamics

● A method has been developed for calculating the circulating motion which occurs when a layer of compressible heat-conducting viscous liquid is heated from below. This type of phenomenon occurs frequently in nature. As a result, the work is of interest to scientists in many fields (p. 107).

Erythron Behavior

● Important information concerning the generation and maturation period of red blood cells has been discovered as a result of a mathematical model which was developed to simulate the behavior of such blood cells and their precursors (erythrons) (p. 107).

Part Two

REACTOR TECHNOLOGY PROGRAMS

NUCLEAR SAFETY RESEARCH

Primary Vessel Integrity

● Brittle-fracture tests on the highly irradiated pressure vessel of the PM–2A demonstrated that the degree of design conservatism in establishing a margin of safety for the vessel was much more than adequate. The vessel did not test fail until subjected to conditions that were much more severe than those predicted by prior analysis (p. 114).

Containment Integrity

● Blowdown of water and steam from small pressurized vessels in the LOFT and CSE projects is providing confirmation of the analytical methods for determining the pressure transient resulting from stored heat energy in the water coolant. Likewise, experiments conducted at laboratories on small samples of metal-clad fuel are providing basic data on the amount of additional energy to be expected from metal-water reactions (p. 123).

Design for Seismic Loading

● A study of four separate reactor designs is being made to develop improved antiseismic designs. These designs describe reactors which can withstand a range of severe vibration and displacement loads due to earthquakes combined with loads which may be caused by reactor accidents (p. 124).

REACTOR FUELS AND MATERIALS

Coated-Particle Fuels

● A mathematical model relating irradiation performance of carbon-coated fuel particles for high-temperature gas-cooled reactors to their physical characteristics has successfully predicted particle stability in use. In addition, the substitution of propylene for methane as a coating gas in the carbon coating process has markedly reduced the required coating time and temperature (p. 134).

Radiation Effects on Stainless Steels

● In a series of in-reactor creep tests on type AISI 304 stainless steel, over the temperature range 400–760° C., it has been discovered that neutron flux has little effect on dynamic creep rate but does consistently shorten the time to failure. Careful examination with electron microscope discloses that this loss of ductility is due to the formation of metallic carbides promoted by neutron irradiation and possibly by radiation-induced gas atoms (p. 139).

Graphite Sublimation in Reactors

● Studies of the sublimation of structural graphite from a high-temperature gas-cooled reactor by the corrosive action of oxidant impurities in the helium coolant have determined factors controlling the rate of loss. If the coolant flow rate, geometry of the system, and pressure are maintained constant, the reaction rate of loss is a function of the temperature and oxidant concentration (p. 147).

Electromagnetic Testing

● A significant new development in eddy current testing of reactor tubing has been the demonstration of a technique for simultaneously displaying the location and size of a flaw on an oscilloscope. This display, similar to a radar display of a cross section of the tube, indicates the relative magnitude and positions of the flaws, whereas previous eddy current displays had been in the form of blips on an oscilloscope (p. 155).

REACTOR PHYSICS RESEARCH

ZPR–3 Assembly 48

● A plutonium-fueled critical experiment of special interest to fast reactor physicists, designated Assembly 48, was constructed in ZPR–3. The reactor core was designed to be similar to that of a very large power reactor in its neutron energy spectrum, yet simple enough in the arrangement of its constituents to permit detailed analysis (p. 158).

High Burnup Studies of Pu^{241} and U^{233}

● Irradiations of the fissile isotopes uranium-233 and 235, and plutonium-239 and 241, together with measurements of the resulting changes in reactivity caused by depletion of the

fissile isotope, have disclosed a depletion pattern which indicates that, on the average, the cross sections of daughter products do not differ from the cross sections of the original fission products after 500 hours of irradiation (p. 164).

Capture and Fission Cross Sections

● An experiment in which the neutron capture and fission cross sections of U^{233} were measured simultaneously over the neutron energy range of 0.5 to 100 ev. was performed successfully, yielding the first direct measurements of the capture cross section ever made (p. 167).

Pulsed Research Reactor Studies

● In studies of concepts for high-performance pulsed fast research reactors, a peak power of some 20,000 megawatts for about 60 microseconds appears to be feasible. The neutrons generated during these power bursts would provide an intense source for neutron physics research (p. 176).

REACTOR INSTRUMENTATION

Fluidic Temperature Sensor

● A fluidic temperature sensor, specifically designed for operation in a high radiation and high temperature environment, has been developed and successfully demonstrated. This instrument senses the temperature of the fluid and generates an output pressure signal proportional to the fluid temperature (p. 183).

Carbon Meter for Liquid Metals

● An instrument to provide a continuous measure of carbon activity in flowing sodium, for use in liquid metal-cooled fast breeder reactors, has been under development. This meter will be particularly important, since sodium can change the carbon content of the structural materials it contacts enough to seriously impair their mechanical properties (p. 184).

Digital Computer for UHTREX

● A digital computer, programmed to perform a variety of recording, checking, calculating, and operating functions, has been incorporated in the high-temperature gas-cooled graphite reactor, UHTREX. This computer checks over 600 temperatures and pressures every 15 seconds and checks the position of all valves in the system each second, recording the data and sounding an alarm if any changes take place which endanger the system. The computer also handles the fuel loading process, opening and closing valves in a prescribed sequence to load fuel when requested to do so by the operator (p. 185).

HEAT TRANSFER AND FLUID DYNAMICS

Heat Transfer Through Rod Bundles

● It has been concluded that for the flow rates normally encountered in liquid-metal heat exchangers, heat transfer coefficients obtained experimentally with only one test rod may be applied directly to commercial exchangers, where all rods in the bundle are transferring heat (p. 188).

Boiling-Inception Superheats

● Investigations of the conditions under which a liquid-metal reactor coolant might inadvertantly boil, should there be a flow stoppage or sudden insertion of reactivity, have shown that alkali metals must reach very high superheats before initiation of boiling, which then tends to occur "explosively" with rapid oscillation in fluid temperature and pressure. There is a slight, but noticeable increase in this boiling initiation superheat with repetition in a series of runs (p. 190).

Turbine Blade Erosion Studies

● By using a novel technique for high-speed impingement of liquid potassium droplets of

known size against a wedge of pre-chosen material, information has been obtained which pertains to the rate of erosion of high-speed turbine blades. Likewise, by running a supersonic turbine for a stated time period in wet potassium vapor, it has been determined that while damage does occur to the turbine blades, it is not sufficient to cause serious deterioration of the turbine performance (p. 192).

FUEL PROCESSING DEVELOPMENT

Centrifugal Extractor

● Centrifugal extractors of a new design are now separating plutonium and uranium from radioactive fission products. The new extractors have replaced conventional mixer settlers, in which the two phases are separated by gravity. Because the centrifugal separation is much faster, the holdup time of the process solutions is 50 times shorter than in the mixer-settler equipment (p. 198).

Ion Exchange Method

● Ion exchange membranes have been developed to continuously concentrate and purify aqueous solutions of metal ions. Several small concentrating units have been built and successfully tested to concentrate uranium solutions (p. 198).

Fast Breeder Process Development

● Investigations have indicated that existing reprocessing plants, using well established solvent extraction methods, can probably be modified for processing the spent fuels from fast breeder reactors. Also, it appears that the remotely operable sol-gel process for fuel refabrication can be readily adapted for use as an important step in the fuel cycle (p. 199).

Thermal Fuel Burnup Analysis

● A more accurate method for measuring the percentage of uranium and plutonium which has fissioned in a spent fuel element has been developed by measuring the amount of a specific non-volatile, low neutron cross section fission product produced within the fuel. Neodymium-148 has been found to meet these requirements for a burnup indicator (p. 205).

DIRECT ENERGY CONVERSION

Development of Adsorption Cesium Reservoir

● A new high-temperature adsorption cesium reservoir has been developed for operation within thermionic converters. Consisting of a multiplicity of small elements to which cesium adheres, the reservoir contains a relatively large amount of cesium in a small volume (p. 210).

Part Three

BIOLOGICAL, MEDICAL, AND ENVIRONMENTAL RESEARCH

SELECTED BENEFICIAL APPLICATIONS

Treatment of Diseases

● Techniques have been perfected to synthesize human insulin for the first time. The perfection of such techniques is an important event in efforts to understand body processes and opens new avenues for research on diabetes (Fig. III-3, p. 220).

Diagnostic Uses of Technetium-99^m

● Technetium-99^m a radioisotope, has been shown to be as useful as radioactive iodine-131 in the diagnosis of abnormal conditions of the thyroid gland (p. 222). Retention of technetium-99^m in the kidney has also proved to be a useful characteristic for making good scans without unduly high radiation dose to the kidneys (p. 224).

Plant Research

● Recent work in plant seedlings has shown that lower doses of radiation from neutrons are required to reduce growth comparable to the reductions induced by higher doses of gamma rays. Okra seeds were used in the experiment (p. 227).

INSTRUMENTATION

Scanning Electron Microscope

● A newly developed scanning electron microscope has achieved a series of highly magnified photographs of living flour beetles. This appears to be one of the first times that living organisms have been visualized by electron microscopy (p. 230).

RADIOLOGICAL PHYSICS

Dosimetry in Cell-Sized Volumes

● Measurements of energy deposition in sample targets which simulate living tissue (ten-millionths of a centimeter thick) indicate that a maximum of 100 to 110 thousand electron volts of energy can be deposited by energetic protons in a cell one ten-thousandth of a centimeter in diameter. This is about 20 percent more than previous estimates (p. 233).

CANCER RESEARCH

Cancer Therapy

● Implants of radioactive chromium wire introduced into cancer patients by means of a special injection "gun" have had results promising enough to deserve more attention (p. 235).

● Needles containing californium-252 show some promise of becoming a new method for treating cancer. Dose rate measurements are now underway before biological studies begin. Patients will not be treated until preliminary trials in animals show this to be a safe technique (Fig. III–16, p. 236).

SOMATIC EFFECTS OF RADIATION

Aging in Germ-Free Mice

● In tests with germ-free mice, investigators have found that the absence of detectable micro-organisms does not increase the maximum length of life, but does increase the number of mice reaching "old age." This suggests that aging cannot be prevented by exclusion of micro-organisms from the environment (p. 244).

Reproduction in a Life Study Herd

● A bovine herd is under a life-time study to observe the effects of radiation on: (*a*) fertility; (*b*) growth and viability of the calves; (*c*) pathological response in the cows; and (*d*) performance of the offspring by sire groups. Information acquired to date does not demonstrate that wholebody irradiation at levels of 200, 300, 400, and 600 roentgens has had an effect on the total reproductive performance of this herd (p. 252).

TOXICITY OF RADIOELEMENTS

Neoplasms in Miniature Swine

● The biological effects of daily ingestion of various levels of strontium-90 in miniature swine have been under investigation since 1958. To date, 53 cases of lymphopoietic (lymph-forming tissue) or hematopoietic (blood-forming tissue) neoplasms have been observed in animals ingesting 250 to 625 microcuries of strontium-90 a day. Four of these swine had multiple bone tumors in addition to indications of leukemia. Most cases occurred in animals ingesting 125 microcuries a day. This amount is more than 100 times greater than the limits set for workers in atomic energy industries (p. 254).

Plutonium-238 Lung Deposition

● Whole body counters are being studied for their usefulness in determining deposition of plutonium-238 in the human lung. At one lab-

oratory, it was concluded that the detection of a lung burden of plutonium-238 (0.016 nanocuries or 16 billionths of a curie) could be detected with existing equipment and that with some refinements in equipment, one-half this amount could be detected (p. 257).

COMBATING RADIATION'S DETRIMENTAL EFFECTS

Protective Agents

● In tests of three chemicals for reduction in dose factors, one, MEA (mercaptoethylamine), was superior to the others in protecting mice from lethal irradiation of the head region while the rest of the body was protected by a lead shield (p. 261).

RADIATION GENETICS

Studies With Synchronized Cells

● Better synchronization of stages in a cell's cycle during periods of pre- and post-deoxyribonucleic acid (DNA) synthesis has been attained in cell cultures. With these refinements, it has been noted that most responses to X-ray vary greatly depending on the stage of the cycle at which the cell is irradiated (p. 266).

Radiosensitivity and Chromosome Volume

● Work with plants has shown that a direct proportionality exists between the radiosensitivity of herbaceous plants and the volume of the chromosomes at the interphase stage of division in the cells of such plants. Continuing work extended to other forms of life, ranging from viruses and bacteria to the higher animals, has now shown that: (*a*) similar relationships between chromosome volume and radiosensitivity exist; and (*b*) that these relationships can be used to classify all the forms studied thus far in seven distinct groups (p. 268).

MOLECULAR AND CELLULAR LEVEL STUDIES

DNA Replication and Repair in Human Cells

● In studies of the synthesis of deoxyribonucleic acid (DNA) in cultured human cells, a new technique has shown that after irradiation, synthesis of DNA occurs in a manner completely different from that in normal unirradiated cells. This synthesis after irradiation may be a part of a repair process that eliminates some of the radiation-induced damage to the cells' genetic material. This is the first evidence to come to light for the repair of genetic damage by human cells (p. 272).

Protein Synthesis in Development

● A study has shown that the removal of the nucleus from a developing egg (frog embryo) has no effect on the rate of protein synthesis. A conclusion is that although the nucleus must provide the utimate control of growth and synthesis, the expression of the genetic characteristics coded in the nucleus does not necessarily occur as a simple, timed sequence of events (p. 276).

Purified Viruses for Vaccines

● Ultracentrifuge rotors are being used to obtain large amounts of purified viruses for use in new vaccines. Several common cold viruses, as well as influenze virus, *Rauscher* and *Moloney* leukemia viruses, and bacteriophages have been obtained in a highly purified state using the ultracentrifuge (p. 279).

ENVIRONMENTAL RADIATION STUDIES

Cycling of Radioactive DDT in a Marsh

● Translocation and accumulation of DDT labeled with a radioactive isotope have been studied in a freshwater marsh. Results have shown that DDT is rapidly translocated through the marsh ecosystems and is rapidly accumulated by many organisms of which

aquatic plants are the greatest accumulators—taking up 3,000 times the concentration applied initially 3 days before (p. 284).

Ecology of Tick Vectors of Disease

● Radioactive labeling of ticks has been achieved and the method is giving promise of being a useful technique for studying the transfer of a number of diseases that plague mankind (p. 285).

ATMOSPHERIC RADIOACTIVITY AND FALLOUT

High Altitude Sampling

● A new high altitude rocket sampling system designed and developed by the AEC and the Department of Defense marks a significant increase in altitude range over that attainable by balloon sampling for atmospheric radioactivity. An option in sampling altitudes allows selection of one of three essentially equal altitude increments between 150,000 and 250,000 feet or an integral sample taken over this entire range (p. 293).

Iron–55 in Man and the Biosphere

● Iron-55 has increased from a minor fraction of fallout to the most abundant of all fallout isotopes since the 1961–62 nuclear tests. The study of the transfer of iron-55 and its concentration in the biosphere is of interest because iron is an essential element to many organisms and it is easily measured in almost all living organisms. The weak radiation associated with the iron-55 decay produces an extremely small radiation exposure as compared even with the normal potassium-40 content of the body (p. 295).

ATMOSPHERIC SCIENCES

Plume Rise Variables

● Theoretical studies of smoke plume rise have led to conclusions that the rise depends mostly upon buoyancy and momentum, and only somewhat on the temperature of the surrounding air (p. 299).

Aircraft Sampling

● Measurements of atmospheric tracers using aircraft have shown an expected limitation on the upward plume growth when there is warmer air above. The effects of terrain variations on the plume growth have been observed. Mixing caused by mountains masks the mixing from ordinary surface roughness and that due to convective activity, and the usual seasonal and day-to-night differences in concentrations are considerably reduced. Deviations in plume paths over large distances as a result of large terrain obstructions have also been observed (p. 305).

SEMICONDUCTOR DETECTOR APPLICATIONS

In-Vivo Plutonium-239 Mapping

● A technique has been developed to determine the depth of plutonium contamination in a wound and an *in vivo* probe has also been developed for use in surgical removal of embedded plutonium (p. 325).

Blood Flow in Brain

● Miniature semiconductor detectors have been developed for the purpose of studying blood flow in the interior of the brain. They have been semi-permanently implanted in the brains of experimental animals, and after injection of radioactive rare gases, clearance patterns of the radioactive material give valuable information about blood circulation patterns in the vicinity of the detectors (p. 328).

Brain Tumor Localization

● A semiconductor detector probe has been developed with which the boundaries of brain tumor sites can more accurately be determined (p. 329).

CONTENTS

Part One

BASIC PHYSICAL RESEARCH PROGRAMS

275-845 O—68——2

Part Two

REACTOR TECHNOLOGY PROGRAMS

Part Three

BIOLOGICAL, MEDICAL, AND ENVIRONMENTAL RESEARCH PROGRAMS

Part One

BASIC PHYSICAL RESEARCH PROGRAMS

PERIODIC TABLE OF THE ELEMENTS

	GROUP IA	IIA											IIIA	IVA	VA	VIA	VIIA	NOBLE GASES
1	H 1																	He 2
2	Li 3	Be 4											B 5	C 6	N 7	O 8	F 9	Ne 10
3	Na 11	Mg 12	IIIB	IVB	VB	VIB	VIIB	VIII			IB	IIB	Al 13	Si 14	P 15	S 16	Cl 17	Ar 18
4	K 19	Ca 20	Sc 21	Ti 22	V 23	Cr 24	Mn 25	Fe 26	Co 27	Ni 28	Cu 29	Zn 30	Ga 31	Ge 32	As 33	Se 34	Br 35	Kr 36
5	Rb 37	Sr 38	Y 39	Zr 40	Nb 41	Mo 42	Tc 43	Ru 44	Rh 45	Pd 46	Ag 47	Cd 48	In 49	Sn 50	Sb 51	Te 52	I 53	Xe 54
6	Cs 55	Ba 56	La 57	Hf 72	Ta 73	W 74	Re 75	Os 76	Ir 77	Pt 78	Au 79	Hg 80	Tl 81	Pb 82	Bi 83	Po 84	At 85	Rn 86
7	Fr 87	Ra 88	Ac 89	(104)	(105)	(106)	(107)	(108)	(109)	(110)	(111)	(112)	(113)	(114)	(115)	(116)	(117)	(118)

LANTHANIDE SERIES	Ce 58	Pr 59	Nd 60	Pm 61	Sm 62	Eu 63	Gd 64	Tb 65	Dy 66	Ho 67	Er 68	Tm 69	Yb 70	Lu 71
ACTINIDE SERIES	Th 90	Pa 91	U 92	Np 93	Pu 94	Am 95	Cm 96	Bk 97	Cf 98	Es 99	Fm 100	Md 101	No 102	Lr 103

Fig. I–1. Periodic Chart of the Elements. The Periodic Chart of the Elements is an orderly classification based on the extent to which the elements exhibit similarities in their chemical and physical properties. The name of each element on the Periodic Table is abbreviated to a chemical symbol for easy usage (note that element 103, lawrencium, is now abbreviated Lr instead of the Lw that was previously used). The number in the lower left corner of each rectangle is the element's atomic number. All of the elements are listed in order of their atomic numbers. The atomic number of an element represents the positive charge (number of protons) of the nucleus; the atoms of the elements are electrically neutral bodies; thus, the atomic number designates also the number of electrons in a neutral atom. The dependence of both chemical and physical properties upon the atomic number is expressed by the *periodic law* which is: *the properties of the elements are periodic functions of their atomic numbers.* The rare earth (lanthanide) series of elements, are shown in a horizontal row below the main diagram, and the transuranium elements (in shaded squares) are known as the "heavy elements" and are part of the actinide series.

BASIC PHYSICAL RESEARCH

The ever increasing necessity for control over the physical universe is reflected in the AEC's basic physical research program which seeks new knowledge of the natural laws of science as well as a better understanding of the knowledge already in existence. The AEC maintains a broad program of basic physical research which includes high energy physics, medium energy physics, low energy physics, chemistry, metallurgy and materials, controlled thermonuclear research, and mathematics and computers. Knowledge derived from this program is responsible for the maintenance of U.S. leadership in nuclear science.

Basic to nuclear science and technology are fundamental studies of atomic nuclei, the particles that constitute them, and the forces involved in their structure. Investigations concerned with the interactions of radiation with matter, and of the properties of materials; the synthesis of new compounds having improved properties and the prediction of the effects of time, use, and radiation upon these properties also must be included as most necessary for a successful nuclear science program.

Another important area of research combines the skill of nuclear and solid state physics in structure studies of nearly perfect crystals. The classes of solids under investigation run the gamut from metals and alloys, semi- and superconductors, ionic and covalent crystals, ceramics, and organic polymers.

Many basic investigations are not necessarily of a nuclear nature but knowledge derived from such studies help to solve the many problems inherent in a vigorous nuclear energy program. Among the more basic aspects under this category can be included the chemistry of elements and compounds of special interest, isotope effects, the metallurgy of materials used in nuclear reactors, the neutron scattering and absorbing properties of substances used in nuclear reactors, and other nuclear devices.

One aspect of the basic physical research program with an obvious potential for practical application is the controlled thermonuclear research program. The goal of this program is the demonstration of the feasibility of a controlled fusion power reactor. Such an event will be one of the most dramatic achievements in the history of mankind. In essence, such a development would pave the way for unlimited power, as far into the future as one can possibly see.

In support of all major basic and applied research activities is the mathematics and computer program. Research is conducted in mathematical formulation and analysis of physical problems and in obtaining higher performance computers with increased capacity.

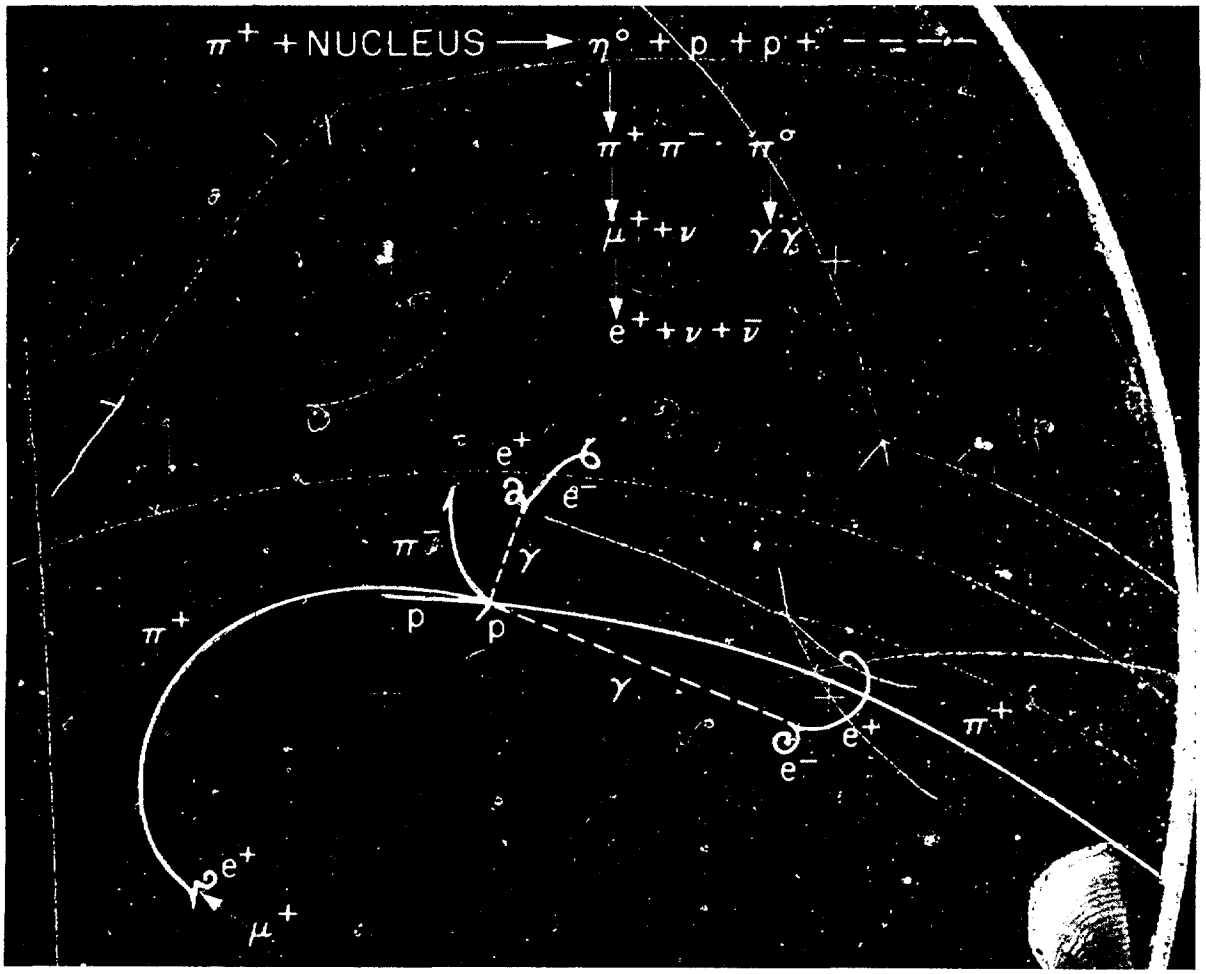

Fig. I–2. Heavy Liquid Bubble Chamber. Argonne National Laboratory photo shows how a positive pi-meson (π^+) beam interacts in the new 40-inch heavy liquid bubble chamber (filled with freon for this experiment) to produce a neutral eta-meson (η°) which is identified only by the total mass of its decay products, the $\pi^+\pi^-$ and π° mesons. Since the neutral eta carries no electrical charge and leaves no tracks, the occurrence of the η° meson is positively established by the presence of the two charged pi mesons, and electron positron pairs produced by the conversion of the photon decay products of the neutral pi meson. Details of the new bubble chamber and another photo appear on page 15.

HIGH ENERGY PHYSICS

The AEC's high energy physics research program is directed toward understanding the forces of nature which determine the properties of, and the interrelationship between, members of the ever expanding states of subnuclear matter. The research effort is both theoretical and experimental, with very close liaison between them. The experimental program relies on the use of high energy accelerators. Accelerator technology is an integral part of the overall program. Cosmic ray research relating to high energy particle interactions is also included in the research effort.

THEORETICAL RESEARCH

The description of the particle interaction processes is the principal goal of the theoretical research effort. Considerable emphasis is placed on the classification of elementary particles and resonances in terms of unitary symmetry and other models, phenomenological study of reactions at high energy, and the development of dynamical models.

"Quark Model"

Within the past decade, so many new particles have been discovered that it is no longer possible to believe that all of them are fundamental constituents of matter. The particles that have strong interactions with each other (proton, neutron, and pion) are called hadrons. The particles that experience weak interactions primarily (electron, neutrino, and muon) are called leptons. The recent successes of the SU_3 [1] unitary symmetry have led to a hypothesis that quarks—three particles that may have fractional electrical charges—may be the fundamental constituents of hadrons. This is called the "quark model" of elementary particles. Theoretical tests of the quark model have yet to be made since quarks with a fractional electric charge have not yet been observed.

In order to develop a theory which explains the properties of all hadrons as bound states of quarks it is necessary to have theoretical calculations with composite systems of quarks giving rise to the observed hadrons. A development in this area has been a method called the algebra of currents.[2] When this method is applied to electromagnetic currents constructed out of quarks, the dynamical predictions depend on whether the quarks possess fractional or integral electric charge. In this way, the algebra of currents permits the testing of different theoretical models for the fundamental constituents of the strongly interacting particles.

Theoretical calculations made by the University of Rochester, N.Y., and other universities, to test this quark model have employed the algebra of currents method. The lifetime of the neutral pion decaying into two photons, the axial vector weak coupling constant associated with the beta decay of the neutron into the proton, and the lifetime of two neutral unstable particles, rho (ρ°) and omega (ω°), decaying into electron-positron pairs, were computed and compared with the corresponding experimental data. The results further strengthened the preference for the quark model. There is a possibility that, if quarks possess large masses, they may be inaccessible to present day high energy accelerators and their observation must consequently await the advent of very large machines.

Low Energy Pion Emission

The problem of understanding processes involving emission of low energy pions (pi mesons) has been investigated at the University of Chicago. Using a mathematical technique, it was found possible to account for a number of decay processes of K mesons and hyperons (so-called "strange particles" in which pions were emitted. The calculations are based on the widely accepted hypotheses that: (*a*) the baryons and mesons (strongly interacting particles) are made up of more fundamental subunits (quarks) at least in a symbolical sense, and (*b*) their decays are induced by interacting currents of the constituents. Therefore, the results lend a further support to these fundamental hypotheses about the nature of elementary particles.

The mathematical technique employed in this project is known as the "partially conserved axial current" (PCAC) relation which originated at the University of Chicago in 1960. The

[1] SU_3—A mathematical representation of related states of matter.

[2] *Algebra of Currents*—Currents algebra treats the description of elementary particle interactions in terms of incoming or outgoing currents. The description of particles by waves or currents is a consequence of the quality of matter, whereby matter can exhibit both particulate and wave-like properties. The relationships between the currents arise from the symmetry exhibited between the properties of various particles. Such relationships make up current algebra and permit a comparison of theory with experimental measurement.

full significance of PCAC came to light only when it was combined with the above-mentioned quark hypothesis. The PCAC relation is now part of the more general framework of the algebra of currents, which makes use of the algebraic properties of fundamental observables to derive relations among measureable quantities. Applications of this technique have greatly advanced the understanding of the strong, electromagnetic, and weak interactions of elementary particles.

Interference Theory

A principal aim of fundamental particle theory is the description of the scattering which occurs in collisions of particles at high velocities. A theoretical interference model has been developed at the University of Wisconsin, Madison, to explain the experimentally observed features of high velocity collisions between two types of particles, namely, pions and nucleons. The significance of this development is twofold: (*a*) The interference theory describes the observed scattering and serves as a useful tool for the determination of properties of fundamental particles; and (*b*) The theory can be used to predict the behavior of some types of collisions that have not yet been studied experimentally.

As the terms "interference theory" implies, the likelihood of a collision between two particles tends to show a fluctuation pattern (similar to interference patterns with light) as the velocity of the colliding particles is changed. This pattern can be considered as an interplay between two basic ways that the particles can scatter. In the first way, the two incident particles "exchange" a third particle. Pictorially, this exchange scattering can be visualized as a capital H in which the lower legs of the H represent the two incoming particles before collision, the upper legs of the H represent two outgoing particles after collision, and the rung (or bar) of the H represents the particle which is exchanged. The amount of exchange scattering changes slowly with the velocity of the colliding particles. In the second way of scattering the two incident particles tend to remain together for a short period of time during the collision and then separate. When the incident particles remain together in such a fashion they appear as a single new particle (usually called a resonance). This second type of scattering displays rather sharp peaks at certain velocities where the resonances can occur. When both types of scattering are taken into account in the interference theory, the likelihood of collision is predicted to show the fluctuations observed experimentally.

The theory in its present form applies only to the case of two-particles-in and two-particles-out type of collisions. However, since the outgoing particles can be different from the incident particles, there are still a considerable variety of collisions that can be analyzed. Further investigation along these lines should contribute substantially to present understanding of the nature of elementary particle collisions at high velocity.

Electromagnetic Radiation

The study of electromagnetic interactions may be split into two main categories: (*a*) interactions involving hadrons, or strongly interacting particles, and (*b*) interactions involving only photons and leptons. In the former category the photon is used principally as a tool to probe the structure of the elementary particles and to understand their interactions, whereas in the latter category the main interest is in detailed testing of the theory of quantum electrodynamics, which at present is the only successful field theory. Much work has been done in these two areas at the high-energy accelerators at the Cambridge Electron Accelerator (CEA) in Massachusetts, and at the Deutsches Elektronen Synchrotron (DESY), in Hamburg, Germany.

Recently, it has been suggested that electromagnetic radiation might be used to investigate the process of diffraction dissociation. This process is probably the dominant inelastic process between strongly interacting particles at extremely high energies, and it is therefore im-

portant to understand it and to test the various theoretical models that have been devised. The process of diffraction dissociation may be described by considering the colliding particles to be a composite system which may have several components, *e.g.*, $d \rightarrow n + p$, $\pi \rightarrow 3\pi$, and $\gamma \rightarrow \rho$ (or ω, or ϕ). These dissociations cannot be realized in free space because of energy-momentum conservation, but at very high energy a small momentum transfer between the incident projectile and the target can materialize the components.

The cases of the deuteron and pion dissociations have received much attention but are experimentally difficult because of the presence of other "low" energy processes. However, the coupling of the photon to the vector mesons (ρ, ω, ϕ) is a particularly useful tool in understanding this diffraction process, as experiments at CEA and DESY indicate that it dominates the photon interaction even at fairly low energies (2–3 Bev.). Experiments are now underway at CEA, DESY, and the Stanford Linear Accelerator (SLAC), near Palo Alto, Calif., to test the various predictions for the process and to extend its study to higher energies.

Regge Model and High-Energy Scattering

Exploration of the *Regge*[3] model for high-energy scattering has been one of the liveliest fields of current activity in particle physics, and has led to significant progress in the fundamental understanding of particle processes in their relationship to each other. For some time, it has been clear to physicists that the interactions of strongly interacting particles involved the exchange of other particles within the interacting system; in certain cases the interactions can be completely explained by this exchange. For example, nucleon-nucleon scattering at energies of a few hundred million electron volts (Mev.) and for cases in which the nucleons do not come too close together, can be well explained by the assumption that a single pion is exchanged between the nucleons in the scattering process.

The *Regge* model is an extension of this concept to the much more complex high-energy processes. In this model, it is assumed that the interactions come about as the result of an exchange of "*Regge* poles;" these latter being analogous to pions, but with certain significant differences. The most important of these has to do with the spin (angular momentum) of the poles. According to established quantum mechanical principles, the spin of a physical particle must be (n/2) h, where n is an integer and h is a known constant. The previously mentioned principles do not apply for the *Regge* poles in which case n is taken to be a continuous function of the mass of the particle. Also, for physical particles the mass is fixed, but for the *Regge* poles it is variable. However, a connection with the physical particles can be achieved, since for *Regge* poles with allowed physical values of spin, the model predicts that physical particles will be found. This leads to the classification of particles in families which are manifestations of the same "*Regge* Trajectory."

Two particularly simple cases have been very successfully treated at the Lawrence Radiation Laboratory, Berkeley: first, negative pion+proton→neutral pion+neutron ($\pi^- + p \rightarrow \pi^\circ + n$) and second, negative pion+proton→neutral eta+neutron ($\pi^- + p \rightarrow \eta^\circ + n$). In the former case, "dips" in the differential cross section were observed, and these were explained by assuming that the spin of the pole went through zero. An analysis of negative pion-proton ($\pi^- p$) elastic scattering in the backward direction[4] provided a prediction and observation of similar dips in this case. Furthermore, an analysis of negative pion-proton elastic scattering for forward angles (which included 3 poles) led to a prediction for the polarization which was in agreement with later experiments both in sign and in order of magnitude. The difference between the polarizations in negative and positive pion-proton ($\pi^- p$ and $\pi^+ p$) scattering was also correctly predicted. From an analysis of nega-

[3] See p. 219, "Fundamental Nuclear Energy Research—1965," and p. 176, "Fundamental Nuclear Energy Research—1966."

[4] See p. 176, "Fundamental Nuclear Energy Research—1966."

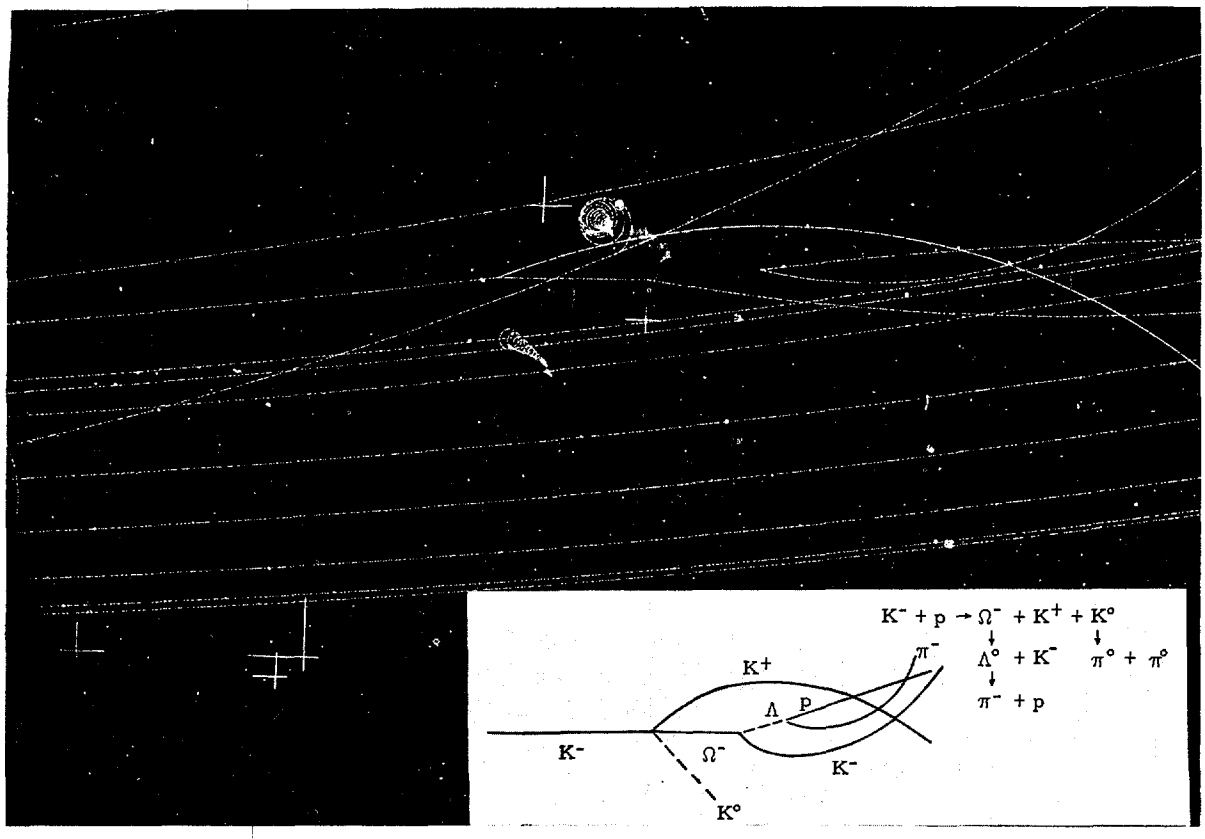

Fig. I–3. Accurate Measurement of the Ω⁻ Mass. The rare omega minus (Ω⁻) is one of the particles theoretically predicted by the symmetry schemes classifying elementary particles into definite multiplets. The original observation of this particle at Brookhaven National Laboratory in 1964 (see pp. 220–221, "Fundamental Nuclear Energy Research—1965") provided a dramatic confirmation of the prediction; however, more detailed tests of the theory depend on accurate measurements of its properties. To date, a total of 19 examples have been observed in laboratories in the U.S.A. and Europe. Four of these cases were observed in the 30-inch hydrogen bubble chamber exposed to the 5.5 Bev./c. K⁻ beam at the Argonne National Laboratory Zero Gradient Synchrotron (ZGS). This chamber has both a high magnetic field and a good optical system so that the mass of the Ω⁻ has been measured to much better accuracy than was previously possible. The sub-particle's mass of 1671.9 Mev. is now known to an accuracy of within 1 Mev. The above is one of the Ω⁻ events observed in a ZGS experiment which was carried out by a collaboration of scientists from Argonne, the University of Illinois, Northwestern University, and the University of Wisconsin. The diagram shows the interpretation of the nuclear event.

tive K meson-proton (K^-p) elastic scattering and an assumption about the reasonably well established SU_3 symmetry in the strong interactions, a satisfactory prediction of the neutral eta (η°) production was also obtained.

EXPERIMENTAL RESEARCH

The experimental effort in high energy physics has concentrated on strong interactions, electromagnetic interactions, and weak interaction research using existing high-energy machines.

Strong Interactions

Proton-Proton Elastic Cross Sections

A series of measurements have been made of proton proton elastic scattering at an angle of 90° (where the cross section is smallest and deep

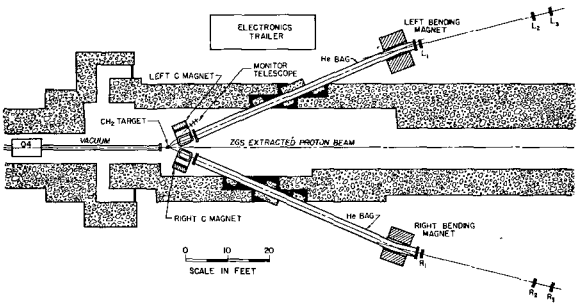

Figs. I–4 and 5. Proton-Proton Scattering Experiment. Drawing *above* shows the layout of the 90° proton-proton scattering experiment at Argonne National Laboratory. The protons in the ZGS extracted beam are focused by quadrupole Q4 and strike the protons in the polyethylene (CH_2) target. Both scattered protons pass through helium (He) bags and then through bending magnets which provide momentum analysis (helium scatters the protons less than air). The protons then trigger the scintillation counters L_1, L_2, L_3, and R_1, R_2, R_3 which send out signals processed and recorded in the electronics trailer. The two C magnets realign the scattered protons for each incident momentum selected, thus eliminating the need for 50 costly moves of heavy magnets and counters. Chart *below* plots the logarithm of the differential cross section for proton-proton elastic scattering at 90° in the center of mass as plotted against p^2_{cm} (the total momentum in the center of mass system of the two protons) and p_{Lab} (the momentum of the incident particle in the laboratory).

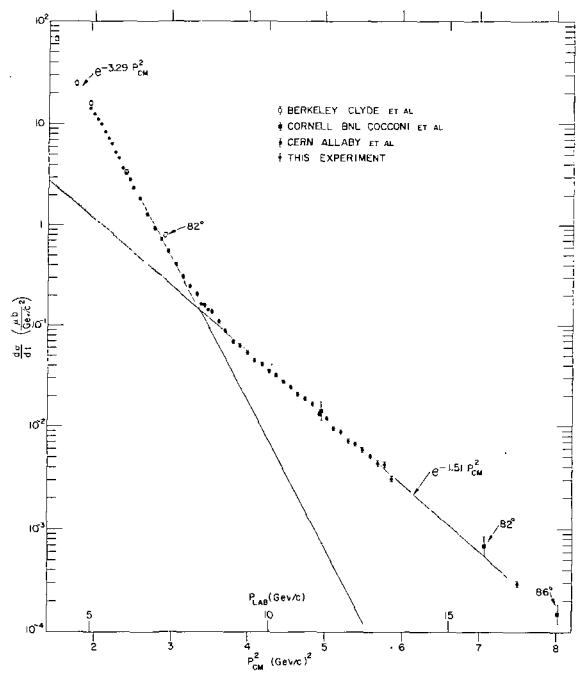

probes can be made into the center of the proton). The experiments were done at the Zero Gradient Synchrontron (ZGS) at Argonne National Laboratory (ANL) by a team of physicists from ANL, the University of Michigan, the University of Minnesota, and the University of Iowa. The differential cross section for this process was measured at 51 different energies in the momentum range 5.0 to 13.4 Bev./c.[5] The protons from the slow extracted proton beam were scattered from the protons held fixed in a polyethylene target (see Fig. I–4). Each scattered proton was detected by a spectrometer consisting of a magnet for momentum analysis and a telescope of scintillation counters for detection. The energy of the protons was varied by taking advantage of the ZGS ability to provide a variable energy external proton beam.

The large number of points measured (see Fig. I–5), together with the high accuracy obtained, allowed several interesting new conclusions to be drawn about the nature of the proton. The most interesting feature of the data is the sharp break in the differential cross section which occurs at about 8 Bev./c. Previous experiments had not shown this structure so clearly. The smooth behavior places a severe upper limit on the cross section for production of resonances with a baryon number of 2.

K-Meson Cross Section Measurements

A Brookhaven National Laboratory group, using the Alternating Gradient Synchrotron (AGS), and joined by guest scientists from Europe, have discovered a number of new "resonant" particles by measuring the total cross section for K^- and K^+ mesons on protons and deuterons. It is essential to the understanding of the strong interaction to uncover and identify such particle "states" because all theory which is valid must be able to predict the existence of such states. In this way, choices can be made between competing theories.

[5] *Bev./c.*—A convenient unit of momentum; *Bev.* (billion electron volts) being the unit of energy and *c.* standing for the speed of light.

The experiment was performed by varying the momentum of the kaons (K-mesons) which bombard the protons in a liquid hydrogen target (or the deuterons in a liquid deuterium target). "Resonant" particles reveal their existence since their formation causes an increase in the cross section at certain values of the momentum of the incoming kaon. The mass of the resonance may be determined from the value of the kaon momentum at which the cross section increase is observed. Their measurements were made in the momentum range 0.9–2.45 Bev./c. at intervals of 50 Mev./c. Preliminary analysis indicates two new K^--nucleon resonances in the isospin [6] 0 state and very likely three in the isospin 1 state above the Y^*_0 (1815) as follows:

Resonance	*Mass (Mev./c.²)*	*Full Width (Mev./c.²)*
Y^*_0	2092±20	160
Y^*_0	2343±20	105
Y^*_1	1915±20	65
Y^*_1	2030±20	150
Y^*_1	2260±20	180

It is possible that these Y^* resonances may fit the *Regge* model which predicts recurrences of resonances at higher mass values with higher spin assignments.

The analysis of the K^+ cross section data reveals the existence of previously unreported structure in each of the two possible isospin states I=0 and I=1. The effect observed in the isospin 0 channel is interpreted as a resonance, Z_0^*, with a mass of 1868±20 Mev./c.². This would be the first resonance observed with strangeness [7] +1. The only SU_3 representation into which the Z_0 would fit is an antidecuplet.[8]

Nucleon-Nucleon Scattering

The problem of determining the structure of nucleons—protons and neutrons—is still only partially solved. One of the best methods of exploring such problems is by scattering nucleons from nucleons. Recently, it has been possible at the Lawrence Radiation Laboratory, Berkeley, to make more precise measurements of both elastic and inelastic proton-proton scattering. Results can be interpreted in terms of a model for the nucleon in which the "size" of the nucleon increases with energy, while the nucleon at the same time becomes more transparent.

Recent proton-proton scattering experiments in the region of 3 to 7 Bev./c. have led to a better understanding of both the elastic and inelastic processes. Collisions are called elastic if a new particle is not created as a result of the collision; all other collisions are called inelastic. An interference between the *Coulomb* (electric) force and other nuclear forces was observed. The experiment also showed narrowing or shrinkage of the forward diffraction peak as the incident proton energy is increased as predicted by the above interpretation.

Studies of inelastic processes provided cross sections for production of resonances at 1,238, 1,512, and 1,688 million electron volts (Mev.) that decrease both with incident energy and with the momentum transferred. No other significant resonance effects were found below 2,400 Mev.

Discovery of New Strangeness −1 Particles

Most of the discoveries of new kinds of heavy particles (baryons) have been made with the aid of beams of very-high-energy protons. When such protons hit a nucleus of an atom, various baryons of strangeness 0, strangeness −1, strangeness −2, etc., are produced, as well as mesons. A group from Yale University, New Haven, Conn., working at the Cambridge Electron Accelerator, created strangeness −1 par-

[6] *Isospin*—A quantum number relating to the charge of a particle or state. For particles, an isospin of zero means a particle which has only one charge state. Isospin of one indicates a charge triplet; for example, the pi meson (pion) having members with charge +1, 0, −1.

[7] *Strangeness*—After the discovery of the various hyperons and K-mesons, it was found that the details of the production and decay of these particles could not be understood within the context of existing theories. For this reason, they were called "strange particles." The word was formalized by Dr. Murray Gell-Mann, California Institute of Technology, Pasadena, when he suggested assigning a "strangeness" quantum number +1, 0, −1, or −2 to all particles. This makes it possible to better understand the observations by assuming that the total strangeness is conserved in a strong interaction, such as the production of strange particles, but not conserved in weak interactions, such as their decay.

[8] A decuplet is a family of 10 particles, an antidecuplet is a family of 10 particles in antimatter states.

275-845 O—68——3

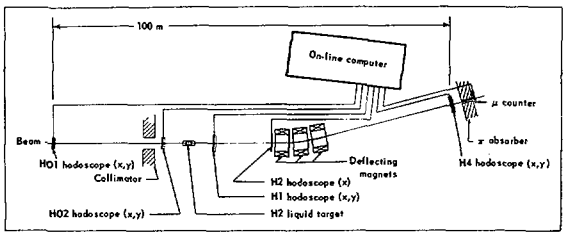

Fig. I–6. Microscopic Causality Experiment. Diagram of the small-angle scattering experimental arrangement used in the Brookhaven National Laboratory study of the principle of microscopic causality. In this experiment, the laboratory used an on-line computer technique with a massive system of counter hodoscopes which BNL had originally developed several years earlier. More than 1 trillion (10^{12}) counter combinations are possible in this system which extends over 500 feet and allows angles to be measured to a few-tenths of a milliradian and momentum measured to a few-tenths of a percent.

ticles (called Y* particles) using photons instead of protons. This was achieved by directing a high-energy beam of gamma radiation at a target of liquid hydrogen. Y* particles were produced fairly abundantly by this "photoproduction" method, and two entirely new members of the Y* family of particles also were observed. The heavier of the two has a mass almost three times that of the familiar proton, and thus ranks as one of the most massive of the particle states produced to date. This new approach of photoproduction opens the way to further study of the properties of these particles, and perhaps to the discovery of additional members of the family.

Principle of Microscopic Causality

Brookhaven National Laboratory used the very high energies of the Alternating Gradient Synchrotron to check the principle of microscopic causality (see Fig. I–6). This fundamental principle assumes that signals cannot travel faster than the velocity of light even over distances comparable with a nucleon radius. In this experiment, positive or negative pion-proton ($\pi\pm$p), elastic scattering was studied at very small angles. At small angles, the scattering due to *Coulomb* interaction is large enough to interfere with the scattering due to strong interactions. The study of these effects together affords the opportunity to analyze the scattering amplitude or cross section into two parts. The one part is directly due to the forces between pion (π) and proton (p). The other is a secondary effect; absorption of particles is always accompanied by elastic scattering. The predictions of miscroscopic causality were accurately verified up to energies of 29 Bev. for positive or negative pion-proton ($\pi\pm$p) interactions. It is concluded that a breakdown of this principle should not occur for distances greater than one-hundredth of a proton radius.

Electromagnetic Interactions

Wide-Angle Electron Pair Production

In a collaboration experiment between Columbia University, New York, N.Y., and Deutsches Elektronen Synchrotron (DESY) in Germany, the wide-angle photoproduction of electron-positron pairs was investigated in order to determine the range of applicability of quantum electrodynamics when the momentum transfer to the electron or positron is very large. Previous experiments of this type carried out at Cornell University, Ithaca, N.Y., and Cambridge Electron Accelerator[9] had shown deviations from first order quantum electrodynamics which increased with increasing momentum transfer to the fermion. However, because of the importance of such a deviation, it seemed necessary to repeat these measurements independently. A carbon target was used and only nearly symmetrical pairs were accepted so that the momentum transfer to the nucleus was kept small thus minimizing the form factor corrections. The pairs produced in the target were analyzed in momentum and angle by a symmetric magnetic double spectrometer. Based on the results from this experiment, it was concluded that within experimental accuracy, quantum electrodynamics theory correctly describes the process up to momentum transfers of 388 Mev./c. which corresponds to 548 Mev./c.^{2} invariant mass.

[9] See p. 184, "Fundamental Nuclear Energy Research Report—1966."

Weak Interactions

Invariance Studies

One of the most important and far reaching experiments in the high energy physics program was conducted at the Princeton-Pennsylvania Proton Accelerator Laboratory, Princeton, N.J., and resulted in the discovery that the (neutral kaon of the second kind) K°_2 meson decays into two neutral pions (π°). The rate of this reaction was measured relative to the rate of K°_2 decaying to positive (π^+) and negative (π^-) pions. These two reactions indicate a breakdown of CP, invariance under charge conjugation and space inversion, two of the fundamental symmetries of nature.

Symmetry involves the behavior of subatomic particles under changes in the system which are of a fundamental philosophical nature such as, reversal of direction of time flow (time reversal symmetry, T); change in sign of isospin projection for each particle (charge conjugation symmetry, C); or change of sign of spatial coordinates for each particle (parity symmetry, P). A further consequence of this CP breakdown comes about through a very fundamental theorem which states that the combined action of C, P, and T on a system of particles should lead to a final system which is indistinguishable from the original one. Therefore, if CP is found to be violated, then time reversal (T) is inferred to be invalid in order to make the product TCP valid. Several experiments have been performed to test the TCP theorem. These primarily compare the lifetimes of particles and their antiparticles. Should the lifetimes be diffierent, the result would be in contradiction to the above theorem. A University of Rochester group working at Brookhaven National Laboratory found the K^+ and K^- lifetimes to be identical within 0.2 percent.

ACCELERATOR TECHNOLOGY

The high energy physics program, a most basic area of physical research, is dependent upon a most advanced and sophisticated technology. Continuous advancements in accelerator technology are necessary to meet the needs of the experimental program. Thus, the technology includes not only accelerator components, but also such areas as shielding, superconducting magnet development, spark chambers, bubble chambers, and data analyses.

Beam Developments

PPA External Proton Beam

A major accomplishment at the Princeton-Pennsylvania Proton Accelerator, Princeton, N.J., is the successful slow extraction of the proton beam directly into the large experimental hall. Approximately 80 percent of the circulating current has been extracted and focused 80 feet away into a ⅛-inch diameter spot. The remaining 20 percent of the beam is directed into an internal target, thereby making protons available in two experimental areas rather than just one. This extraction system is unique for a weak focusing synchrotron because it depends upon a resonant buildup of radial betatron-type oscillations to cause the beam to spiral out into a final magnetic extraction channel. Earlier extraction methods using a jump target had a lower extraction efficiency and resulted in a poorly focused beam. This method, in addition to doubling the number of experiments which can be performed simultaneously, makes it possible to obtain mesons produced at zero degrees to the forward direction.

SLAC Positron Beam

The highest energy positron beams ever achieved (more than 10 Bev.) have been produced at the Stanford Linear Accelerator Center (SLAC), near Palo Alto, Calif. The positron beam is produced by bombarding a special conversion target with a high-intensity electron beam, and then reverse-phasing the SLAC machine so that it accelerates the positrons that emerge from the target. A beam of about three

billion (3×10^9) positrons per pulse (360 pulses per second) can be achieved in this way, compared with the SLAC electron current of about 300 billion (3×10^{11}) electrons per pulse.

As expected, the SLAC accelerator has also proved to be a copious source of secondary particles (muons, pions, kaons, etc.), the usable yields of the strongly interacting particles being roughly comparable to those obtained from the Brookhaven National Laboratory Alternating Gradient Synchrotron (AGS) and the CERN Proton Synchrotron at Geneva, Switzerland.

ZGS Fast Extraction System

Argonne National Laboratory (ANL) has developed a method for extracting a short pulse with a high efficiency from the weak focusing Zero Gradient Synchrotron (ZGS). The characteristics desired of the proton beam extracted from an accelerator depend strongly on the nature of the experiment to be performed. Most experiments using scintillation counters or spark chambers as particle detectors require a "long spill," that is, a beam that is spread out in time for 200 to 400 milliseconds. For bubble chamber runs, a pulse of short duration is necessary. Short pulse duration is also necessary when radiofrequency separators are used to obtain a high momentum separated secondary beam. Methods for extracting such a short pulse from strong focusing machines which characteristically have an internal circulating beam of small cross sectional area, have been known for some time. In the weak focusing ZGS the same methods do not apply since the beam has a large cross section. The method developed at ANL employs a fast bumper magnet to shift the orbit of the internal beam. A portion of the beam then passes through a beryllium target on the outside during each turn, and energy loss in the target causes the protons to enter the first extraction magnet downstream from the target. This system has been used to produce an external beam of 40 microseconds duration with an efficiency of greater than 50 percent (see Fig. I–7).

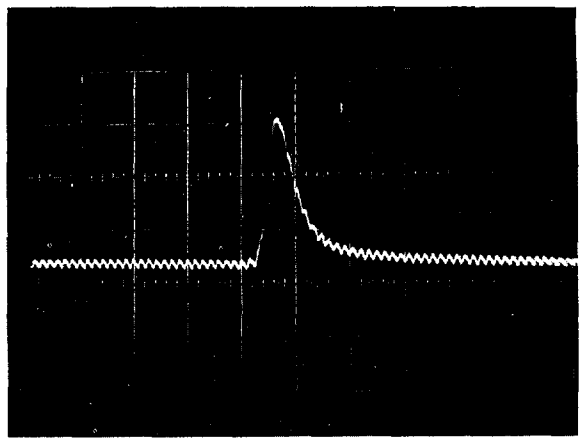

Fig. I–7. ZGS Fast Extraction System. Photo shows a result of the fast proton extraction system from the ZGS used at Argonne National Laboratory. The curve is an oscilloscope tracing of the intensity of the extracter beam (vertical coordinate) plotted against time. The time interval between each pair of vertical lines is one ten-thousandth of a second and most of the pulse takes place in about 50 millionths of a second.

Spark Chambers

Streamer Spark Chambers

The first practical large-volume streamer spark chamber designed for use at high energy accelerators in the United States has recently had a successful engineering run in a 17-Bev. *bremsstrahlung* beam at the Stanford Linear Accelerator Center. The $2.5\times1.5\times0.6$-meter ($8.2\times4.9\times1.9$-foot) chamber had a target consisting of a 1 centimeter (0.39-inch) mylar tube filled with hydrogen at atmospheric pressure. The chamber operated with a gradient of 20 kilovolts/cm. in a magnetic field.

Superconducting Magnet Development

Beam Magnet Improvements

Superconducting beam magnets have been developed at Brookhaven National Laboratory which produce magnetic fields two to three times greater than the 20 kilogauss limit for iron pole beam magnets. This higher field

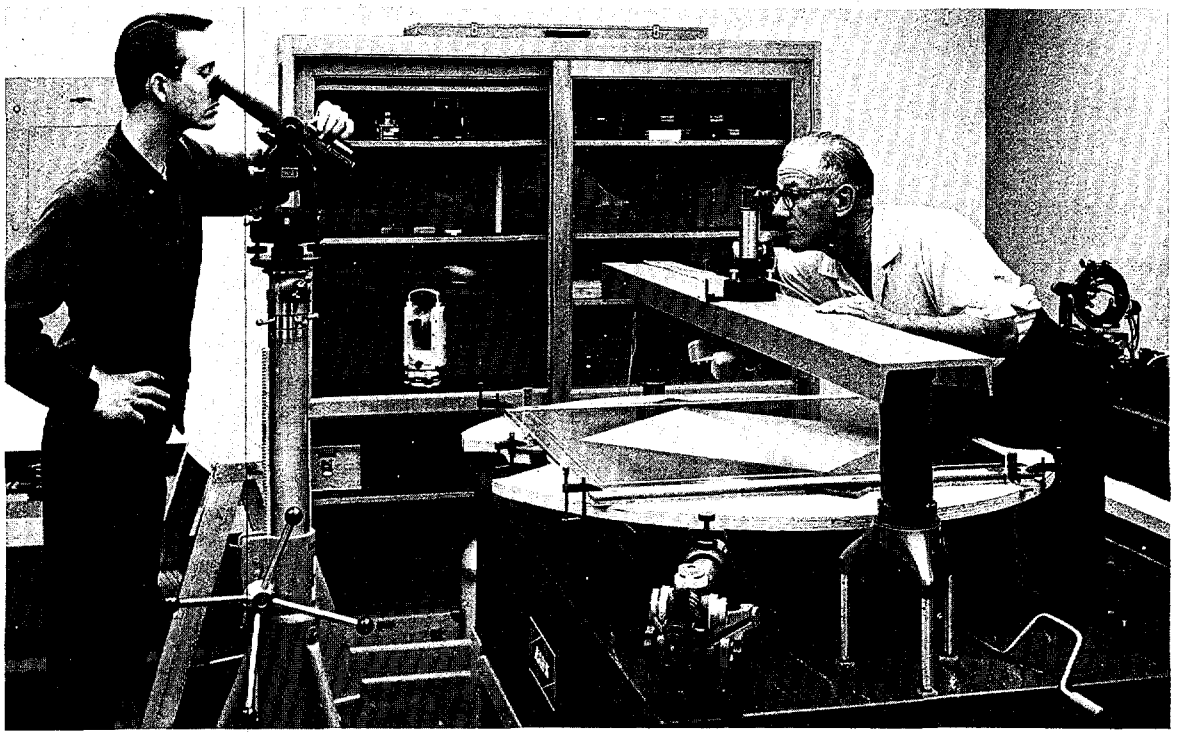

Fig. I–8. Magnetostrictive Readout Technique. An important innovation in high energy physics technology at the Lawrence Radiation Laboratory, Berkeley, has been the magnetostrictive method of recording spark chamber tracks electronically and producing signals that can be stored in coded form on magnetic tape for direct analysis by computers. The spark chamber is constructed of wire planes, with wires in adjacent planes oriented perpendicularly in order to provide a system of coordinates. Photo shows technicians checking plane for accuracy of wire positions. Position of the particle track in each gap is then determined by identifying the wires in the planes which carry the spark current. Alloys used in the sensor wires are magnetostrictive, *i.e.*, their linear dimensions change locally under the action of the magnetic field produced by the current carrying wires. This deformation travels down the sensor wire at the velocity of sound in that alloy. Its arrival is indicated by the induced electrical signal produced by the inverse magnetostrictive effect in a pick-up coil which can be conveniently located outside the chamber. Some saturation problems are experienced when chambers of this type are placed in strong magnetic fields. Techniques by which they can be used in magnetic fields up to 20 kilogauss have been tested, and alternative techniques which are satisfactory for higher fields, such as would be produced when superconducting magnets become available, have been developed. The simplicity of the magnetostrictive technique, compared to other known filmless techniques for track reading, has enabled the development of compact electronic readouts of high reliability. (See also pp. 193–194, "Fundamental Nuclear Energy Research—1966.")

strength combined with more compact construction can greatly reduce the bulk and cost of radiation shielding required around future particle experiments. At present, almost all magnets are made of copper and iron. They may weigh tens of tons and their bulk is often 20 times the volume of the useful magnetic field.

Another new development at Brookhaven is a magnetic pump for converting high voltage at low current to magnetic flux energy. This device will be useful for powering high current superconductive magnets through small electrical leads, so that the magnet may be thermally isolated from the electric power source. A new superconducting ribbon has also been developed that will boost by 30 to 50 percent the field attainable in the beam magnets now under construction.

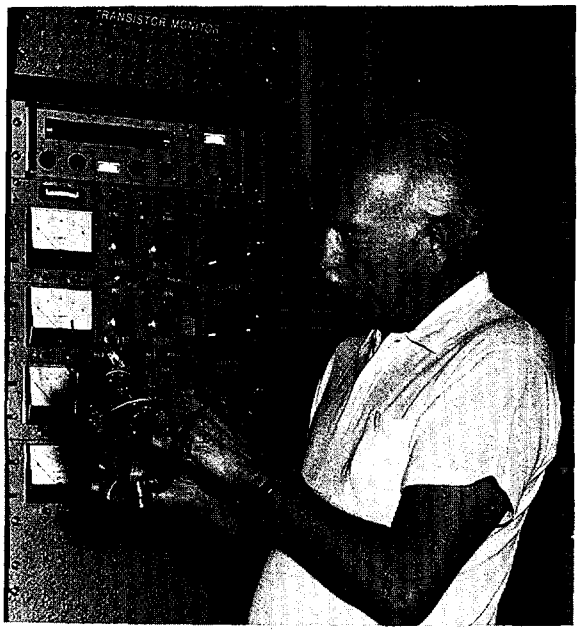

Fig. I–9. Beam Magnet Improvements. Photo is of a superconducting quadrupole lens, designed and fabricated at Brookhaven National Laboratory. The superconducting material is niobium-tin ribbon. Field gradients have been attained which are about five times higher than those available with standard copper-coil, iron magnets. The lens has a 1-inch bore and an effective length of 6 inches. In the back of the magnet is the panel for the special electrical supply system.

SLAC Superconducting Coils

The Stanford Linear Accelerator Center (SLAC) has built and is now testing a 12-inch inner-diameter, 24-inch-long superconducting *Helmholtz* coil capable of producing fields up to 60–70 kilogauss. The coil is wound in two sections, inner and outer. The inner coil is wound from niobium-titanium (NbTi) formed in a cable which is fully stabilized, *i.e.*, there is enough copper to carry the full current in case the superconductor goes normal. The outer coil is wound from niobium-zirconium (NiZr). The inner section has been run successfully at 43 kilogauss.

The SLAC 12-inch coil is intended as a test model for a larger coil which could be installed on the SLAC 40-inch bubble chamber to advance it from a 6–8 Bev. instrument to one useful at 10–12 Bev. The model itself could also be used, for example, as a magnet for a polarized proton target.

Bubble Chamber Magnet

Superconducting magnet development at Argonne National Laboratory has concentrated on factors allowing stable and reliable operation of exceedingly large superconducting magnets in bubble chambers. The completed design of a superconducting magnet for the 12-foot hydrogen bubble chamber [10] uses the results of these investigations on stability and reliability. Figure I–10 shows a cross section of the conductor which will be used in the superconducting magnet for the 12-foot chamber. To achieve the goal of conservative design in every aspect of the coil, it was necessary to develop a quantitative understanding of heat transfer from the conductor to the liquid helium bath, as well as of the current transfer which can take place between the superconductor and the large copper conductor in which the superconducting material is imbedded. This work will be helpful in the design of superconducting magnets for a wide variety of practical applications in high energy physics. In addition to bubble chamber magnets, future superconducting quadrupoles and bending magnets used to transport external beams to experiments will use very similar design principles.

Bubble Chamber Development

SLAC 40-Inch Bubble Chamber

The Stanford Linear Accelerator Center's (SLAC) 40-inch hydrogen bubble chamber has had a successful engineering run during which it was expanded about 100,000 times with liquid hydrogen in the chamber (see Fig. I–11). The magnetic field in the chamber has been measured to be 26 kilogauss. Photographs of

[10] See p. 191, "Fundamental Nuclear Energy Research—1966."

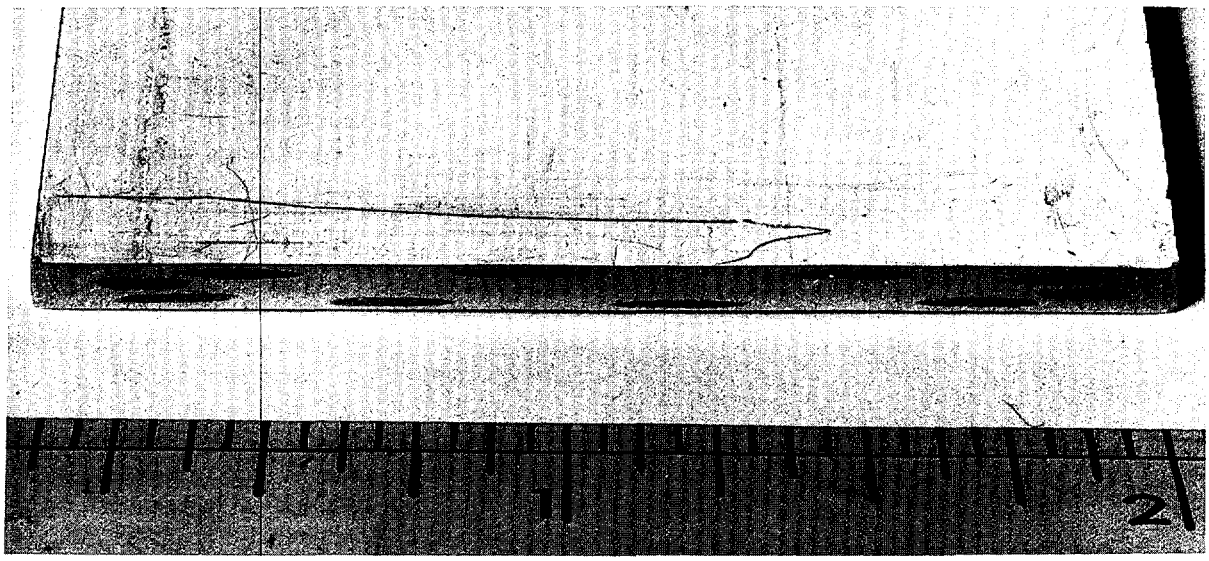

Fig. I–10. Bubble Chamber Magnet. Photo shows a cross section of the stabilized superconductor magnet to be used in Argonne National Laboratory's 12-foot hydrogen bubble chamber. The dimensions of the copper conductor are 2 inches × 0.1 inch. Ten niobium-titanium (NbTi) superconductors, embedded in the copper conductor, are shown (*dark spots* just above the ruler). This integral conductor, supplied by the Supercon Division (Natick, Mass.) of National Research Corp. was developed specifically for use in the ANL magnet.

events from photon and muon beams passing through the chamber were taken at f/22 and a demagnification of 17 to 1, and the preliminary pictures show clearly delineated multiprong events from the interactions of photons with protons. This chamber began physics operation in mid-1967 with a quasimonochromatic photon beam, obtained from annihilation-in-flight of positrons by electrons, a technique developed at the Stanford Linear Accelerator Center (SLAC). The chamber is being used initially to study multibody final states in photon-proton (γ-p) interactions.

Heavy Liquid Bubble Chambers

A 40-inch heavy liquid chamber has been put into operation at Argonne National Laboratory (see Fig. I–12). Bubble chambers, making use of heavy liquids (freon, propane, or freon-propane mixtures), are particularly suitable for identifying neutral particles such as neutral pi-mesons (π°) since the gamma rays into which they decay are quickly converted into electron-positron pairs which can easily be identified in the chamber (see Fig. I–2). The heavy liquid also offers advantages for distinguishing between electrons, mu-mesons, and pi-mesons. All three liquid combinations mentioned above will be used in the 40-inch chamber. By varying the composition of the liquid mixture, the conditions can be controlled for a particular experiment.

The bubble chamber was designed and built at the University of Michigan, Ann Arbor, for installation at Argonne. The magnet has a measured field of 46 kilogauss produced by 11 megawatts of electrical power at 22,000 amperes and 500 volts. To remove the generated heat, 800 gallons per minute of cooling water are passed through the magnet. The magnet weighs 411 tons and is designed with built-in mobility so that it can be moved by "walking" at the rate of 12 feet per hour.

Argonne's 12-foot hydrogen bubble chamber is under construction. Major components of the chamber are being fabricated with delivery scheduled for the first quarter of 1968. These

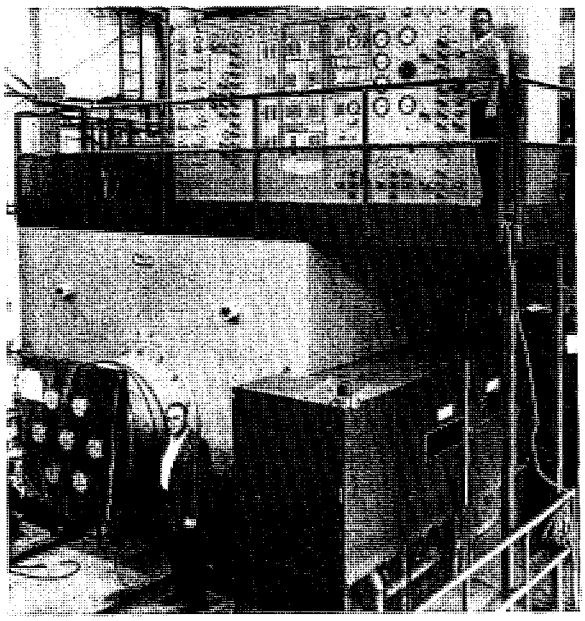

Fig. I–11. SLAC 40-Inch Bubble Chamber. The 40-inch hydrogen bubble chamber at the Stanford Linear Accelerator Center (SLAC) has a cylindrical hydrogen volume 40 inches in diameter and 20 inches deep. The bellows-connected piston is designed to expand the chamber at rates up to two cycles per second. The chamber magnet can produce a field of 26 kilogauss. Intended for general experimental use at SLAC, this chamber will be used initially to study the interactions produced in hydrogen by a high-energy beam of quasi-monochromatic photons obtained from positron annihilation. The chamber is also suited to eventual use with deuterium, rather than hydrogen.

large components include the chamber vessel and vacuum container, 1,600 tons of magnet iron, and the large *Dewar* vessel for the superconducting coils. Initial preoperational cooldown of the mammoth particle detector is scheduled for the summer of 1969.

Spectrometers

SLAC Spectrometers

Three large magnetic spectrometers capable of high-precision analyses in the momentum ranges up to 1.6, 8, and 20 Bev./c., respectively, are now in use at the Stanford Linear Accelerator Center (SLAC) (see Fig. I–13). Together, these instruments give SLAC the capability of carrying out a wide variety of scattering and photoproduction experiments, ranging from studies of those high-momentum, small-angle events which have relatively high cross sections to the lower-momentum, large-angle events which have smaller cross sections. The use of three separate spectrometers provides for a more economical coverage than would be possible with a single large instrument that would have to combine high momentum capability with large angular acceptance. Each of the spectrometers has momentum and angular resolution on the order of 0.1 percent; this extremely high precision makes it possible to distinguish, for example, between interaction processes that differ only in the production of a single pion. The precise angle and momentum of the particles passing through the spectrometers are defined by gridded arrays of counters (hodoscopes) in the focal planes of the spectrometers. Computerization and TV displays are used to log and partially analyze the data from the spectrometers.

CEA Photon Spectrometer

A unique tool for analyzing the spectrum of a beam of high energy photons was perfected and put into operation at the Cambridge Electron Accelerator, Cambridge, Mass. The device, a pair-spectrometer of special type, employs an indirect principle: the gamma rays strike a thin sheet of copper, and produce pairs of electrons and positrons which are, in turn, used in the measurement process. An individual photon in the gamma beam produces one such pair, and the entire energy of the photon is carried by the electron and positron. The spectrometer uses a 20-ton electromagnet to "bend" the paths of the electron and the positron; the greater the bend, the less the momentum of the particle in question. Large arrays of detectors evaluate the extent of bend, and thus permit evaluation of the momentum and energy of the individual particles. By this indirect process it is possible to

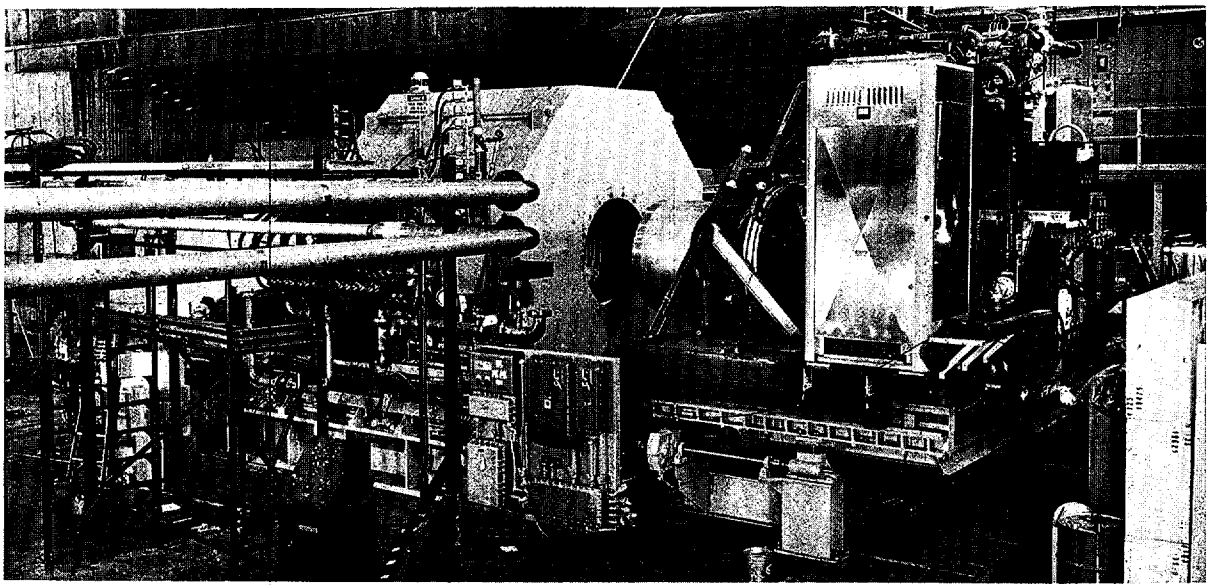

Fig. I–12. Heavy Liquid Bubble Chamber. The 40-inch Michigan-Argonne heavy liquid bubble chamber showing the 46 kilogauss magnet (octagonal structure) in the center. The chamber proper is the cylindrical structure shown withdrawn to the right of the magnet. The cabinets to the right of the chamber proper contain the firing equipment for the flash lamps. The two pipes entering from *left* provide 800 gallons per minute of cooling water required to remove the heat of the 11 megawatts of excitation power.

evaluate the entire spectral energy distribution in the original gamma beam in the course of 30 minutes, within an accuracy of about 0.5 percent in terms of energy. Using such a pair spectrometer, physicists studying the production of rare kinds of fundamental particles by means of a 0 to 6 Bev. gamma beam will have full knowledge of the detailed composition of the gamma ray beam.

Data Analyses

Spark Chamber Film Scanner

A spiral automatic scanning system (SASS) has been developed at the Lawrence Radiation Laboratory, Berkeley, for the scanning of spark chamber film. A spot of light generated by a computer-controlled cathode ray tube searches the film for sparks. Coordinates of the sparks on the film are automatically recorded by the computer and the scanning criteria are applied to this information. If the particular frame that is being measured satisfies all the scanning criteria, the coordinates of the sparks are written on magnetic tape for further analysis. The device then moves the film to the next frame and proceeds with the analysis. Film is scanned at an average rate of 5 seconds per frame, which includes moving the film and instructing the operator of the machine about special action that must be taken.

Precision Encoding and Pattern Recognition

A precision encoding and pattern recognition (PEPR) device at the Massachusetts Institute of Technology, Cambridge, has been operated successfully in its prototype form. The main objectives sought with the prototype were to: (*a*) develop a digitally controlled cathode ray tube measuring device whose accuracy would approach that of the mechanical equivalents in use with other systems; (*b*) develop a digitally controlled cathode ray tube line pattern and to investigate the efficiency of this pattern in analyzing bubble chamber film; and (*c*) develop techniques and computer programs leading to a system capable of analyzing bubble chamber

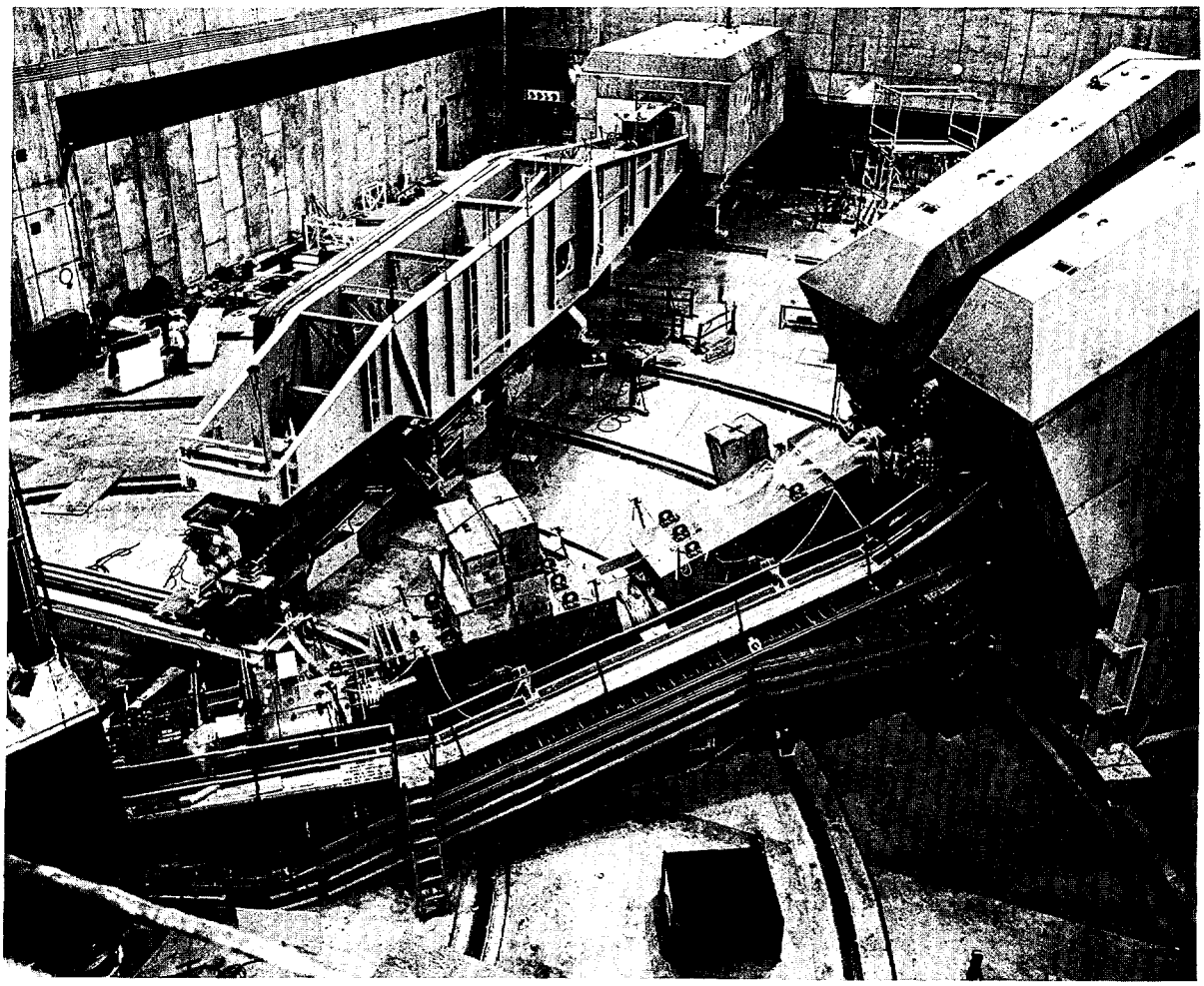

Fig. I–13. SLAC Spectrometers. Photo shows the 8 and 20 Bev./c. spectrometers at the Stanford Linear Accelerator Center (SLAC). The magnets on the 20 Bev./c. spectrometer, on the *top left*, are slung low in the frame and are thus not readily visible. The size of these high-precision instruments is illustrated by the two workmen on the ramp of the 8 Bev./c. spectrometer, at the *right*. The electronic counters that detect the particles traversing the spectrometers are housed in large concrete shielding pods so as to reduce accidental counts from cosmic-rays and stray radiation. The larger spectrometer is 160 feet long and weighs 1,700 tons. The multiple-wheel spectrometer carriages ride on the circular floor rails and enable the instruments to be swung through the wide range of angular positions necessary for the varied experimental program.

events under computer control. However, there is no immediate plan to operate this device without prescanning.

The prototype developed has demonstrated not only the feasibility of the cathode ray system, but also that its stability and accuracy exceeds that of most of the mechanical devices in use. Its absolute precision exceeds one part in 40,000. The measuring speed is hundreds of times greater than that achievable by mechanical stages. A cathode ray pattern has been created which has been demonstrated to be effective in distinguishing and identifying bubble chamber tracks from the usual background in bubble chamber film. In addition, a prototype bubble chamber analysis system (Point Guidance) has been applied successfully to the measurement of over 1,000 real events. The input to this

system is a minimal number of points for each event plus the film number of the event. From this point forward, the PEPR system finds and measures fiducial points and event tracks and the ionization density of each track.

Digital Automatic Pattern Recognition

Computer programs for entirely automatic scanning and measuring of bubble chamber film have been demonstrated at the Lawrence Radiation Laboratory, Berkeley.

Although hardware capable of digitizing (converting tracks on the film to numbers suitable for computational use) this film has been operated since 1963, the computer controlled measurement process has required a previous manual scanning operation to find and point out events of interest. The goal of DAPR (digital automatic pattern recognition) is to find, measure, and analyze bubble chamber events under computer control, without manual intervention. Achieving this will release substantial numbers of people from the tedious task of searching each picture for events, and will improve the processing time of events by avoiding the many extra steps required by separate scanning and measuring operations. Because the system is entirely automatic, continuous monitoring of film, hardware, and program performance is required to maintain high standards of reliability. Some of this can be done by searching for fixed elements common to all pictures, but the most adequate controls are achieved by intercomparison of the three views of the chamber made from separate camera positions for each event exposure. Substantial effort has been devoted to the development of a multiview spatial reconstruction program which enhances the quality of conventional output, but which primarily provides the artificial intelligence that substitutes for the human scanners who are not used in the DAPR system. By comparing all views, it can resolve ambiguities, improve analysis accuracy, and guarantee the reliability of the automatically obtained data.

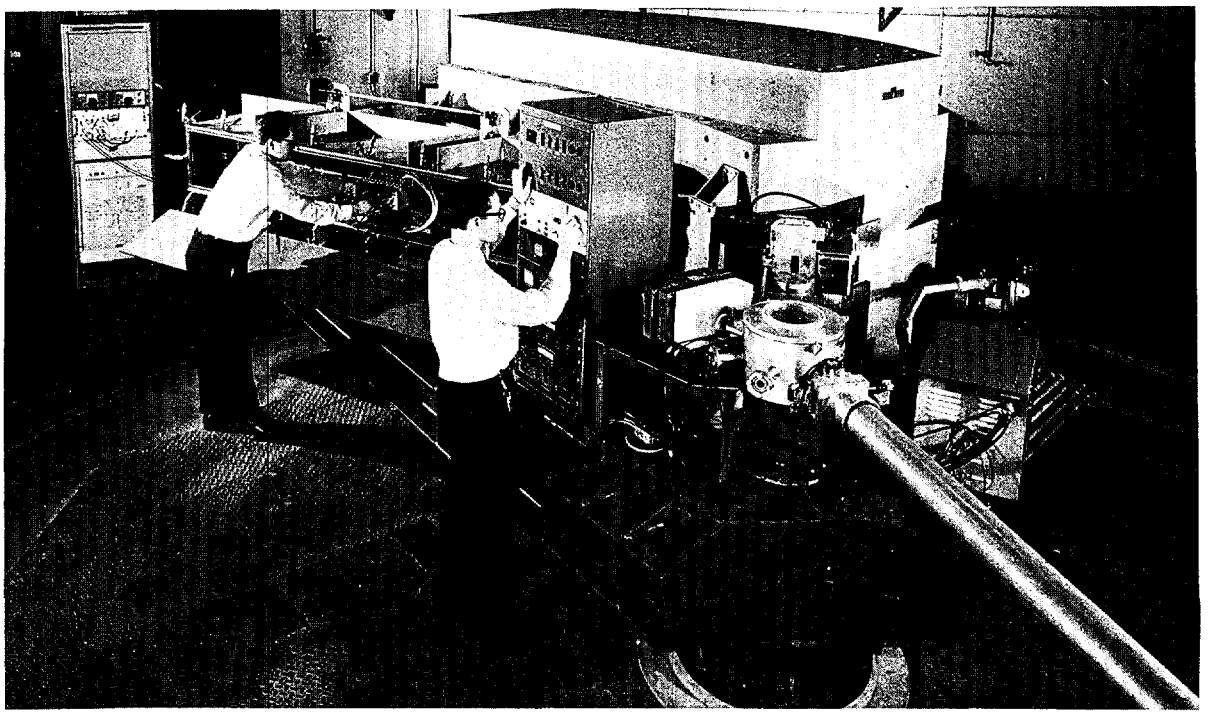

Fig. I–14. Broad-Range Spectrograph. A precision magnetic spectrograph installed at the Oak Ridge Isochronous Cyclotron (ORIC) at Oak Ridge National Laboratory is used to analyze nuclear reaction products of various masses over a broad range of energies. The 60-ton magnet, one-fourth the weight of the cyclotron magnet itself, can be rotated readily from 10° to the left of the cyclotron beam to 160° to the right. Particles emitted from the target are focused by the magnet onto a focal plane, where their arrival may be recorded on photographic emulsions or by a digital spark chamber shown here being inserted in the focal plane. This device can distinguish particles that differ in energy by as little as one part in two thousands. Such resolution is required for the separation of particle groups from closely spaced energy levels within a given nucleus. An analysis of the character of the individual groups then yields the nuclear properties of the associated level.

MEDIUM ENERGY PHYSICS

Research investigations in the medium energy region (50 to 1,000 Mev. primary proton or electron beam energy) are involved with obtaining detailed knowledge about how neutrons and protons are bound together to form the atomic nucleus and the various configurations the nucleus takes when it is excited. The proton and electron beams are delivered by intermediate energy accelerators such as sector-focussed cyclotrons, proton and electron linacs and synchrocyclotrons. The data obtained from such experiments are required to test theories, which include descriptions of the forces holding the nucleons together within the nucleus.

K- and Pi-Mesonic X-rays

At Lawrence Radiation Laboratory, Berkeley, K-mesonic atoms of lithium, beryllium, boron and carbon have been identified. Mesonic atoms differ from natural atoms in that a negative meson moves about the positively charged nucleus replacing a negatively charged electron. High-energy accelerators produce several kinds of elementary particles that can be substituted for one of the electrons in natural atoms. These new atoms are described by the kind of particle that has replaced an electron; for example, mu-mesonic and pi-mesonic atoms contain muons

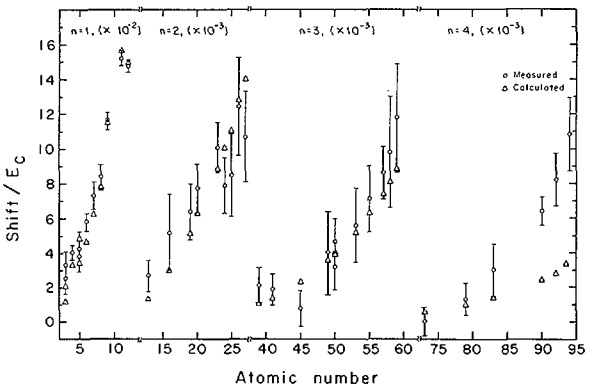

Fig. I–15. Pi Mesonic X-Rays. X-ray energies are measured by means of a solid-state detector, which has the property of collecting all the charge pairs created by the X-ray so that the size of the output pulse is directly proportional to the energy of the X-rays. The system can be calibrated by using X-rays of known energy from radioactive sources. The Lawrence Radiation Laboratory, Berkeley, chart shows the energy shift of X-rays for various elements due to pion-nucleus interaction; n is the principal quantum number of the orbit to which the pion makes a transition and the mean radius of an orbit is proportional to n^2.

and pions. The lifetimes of mesonic atoms are generally shorter than one millionth of a second because the substituted particle may be captured by the nucleus or may decay naturally. They are studied by observing the light they emit. For mesonic atoms this light is in the X-ray region of the electromagnetic spectrum.

Mu-mesonic and pi-mesonic atoms have been studied for about 20 years. Although K particles were discovered about 15 years ago, their scarcity has until recently prevented the study of K-mesonic atoms. The first K-mesonic X-rays were observed in helium by a group at Argonne National Laboratory in 1965.[11]

Characteristic X-rays of lithium and beryllium corresponding to transitions from orbital numbers n=3 to n=2 were observed at 15.3 thousand electron volts (Kev.) and 27.6 Kev., respectively. In carbon transitions from n= 4, 5, and 6 down to n=3 were observed at energies of 22.0, 32.2, and 37.8 Kev., respectively. Similar radiations were detected from boron. The number of X-rays of a given energy emitted per stopped K^- particle depends upon the atomic species and the transition involved and ranges up to about 0.3. Such studies of K^--mesonic atoms should give information on nuclear structure and the K^--nucleon interaction.

Negative pi-mesons when stopped in a given material, are captured into orbits around the positively charged nuclei of the material. Although they remain in the orbit an extremely short time before being captured in the nucleus itself, it is a sufficient time for them to emit X-rays as they transfer from one orbit to another of lower energy. These X-rays have a unique energy; a measurement of this energy and a comparison with its expected value calculated on the basis of the pi-meson's electric interaction with the nucleus, yields information on the way in which the pion interacts with the nucleus through the nuclear force. The results obtained for the pion-nucleus interaction agree very well with those calculated on the basis of the known interactions of pions with individual neutrons and protons (see Fig. I–15).

Nuclear Shapes and Sizes

The muon is a particle that is identical to an electron except that it is 207 times as heavy. Consequently, it can form an atom similar to a normal electronic atom. But because of its greater mass, the muon orbits are only $\frac{1}{207}$ as large as the corresponding electron orbits. Therefore, since the muon spends most of its time near, or even inside, the nucleus, it is a useful particle for probing the interior of the nucleus. A collaborative series of experiments were undertaken by Argonne National Laboratory, Carnegie-Mellon University, Pittsburgh, Pa., and the State University of New York, Binghamton, to measure the spectra of X-rays from muonic atoms produced by the muon beam from the Carnegie synchrocyclotron. The shapes of nuclei and the distributions of electric charge and magnetism in nuclei have been extracted from the data (see Fig. I–16). The results agree with earlier nuclear size measurements but are more precise and offer definite information on the size and shape of nonspherical

[11] See pp. 182–183, "Fundamental Nuclear Energy Research—1966."

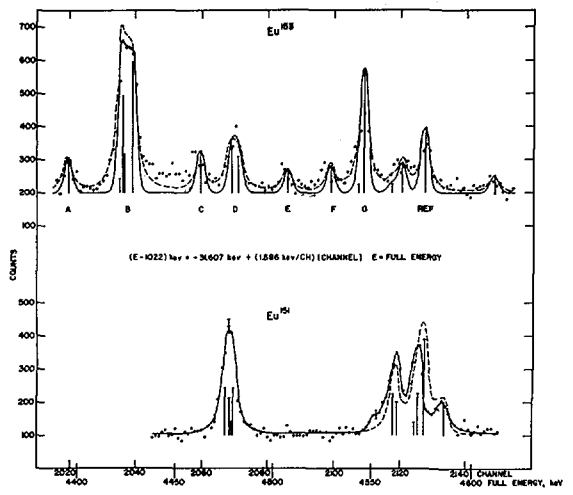

Fig. I–16. Nuclear Shapes and Sizes. A collaborative series of experiments were undertaken by Argonne National Laboratory, Carnegie-Melon University, Pittsburgh, Pa., and the State University of New York at Binghamton, to measure the spectra of X-rays from muonic atoms produced by the muon beam from the Carnegie synchrocyclotron. Many of these effects are dramatically illustrated in the spectra of the rare separated isotopes of europium-151 and -153. The isotope shift is visible as a large shift in the prominent line on the left of the two spectra while the nuclear magnetism causes broadening in the left peak of europium-151. The "Eu^{153}" spectrum is more complicated because the europium-153 nuclear shape is more distorted.

nuclei, and the difference in size between isotopes.

In these experiments, a beam of muons strike a target, and some of the muons are captured in the outer orbits of the target atoms. Through emission of X-rays or by other energy transfers, the muon drops into orbits lying successively closer to the nucleus. It very quickly reaches the most tightly bound orbit, which is very small. In fact, within a heavy nucleus, the muon in the innermost orbit may spend half of its life actually within the nucleus. Eventually (after about one ten-millionth of a second in a heavy atom) it is captured by the nucleus itself. The energies and intensities of the X-rays emitted in these muon transitions, especially those to the most tightly bound orbits, depend critically on the electric and magnetic fields in which the muon moves. These, of course, are directly related to the shape and size of the particular nucleus involved.

Nearly spherical nuclei were studied in one series of measurements. In gold, the hyperfine splitting due to the nonspherical charge distribution in the nucleus was observed in detail for the first time. The magnetism of the bismuth nucleus was shown to be distributed over a volume, not concentrated at a point. The isotope shift (an electrostatic effect associated with the muon penetrating farther into a larger nucleus than into a smaller one) was observed clearly in silver and cerium.

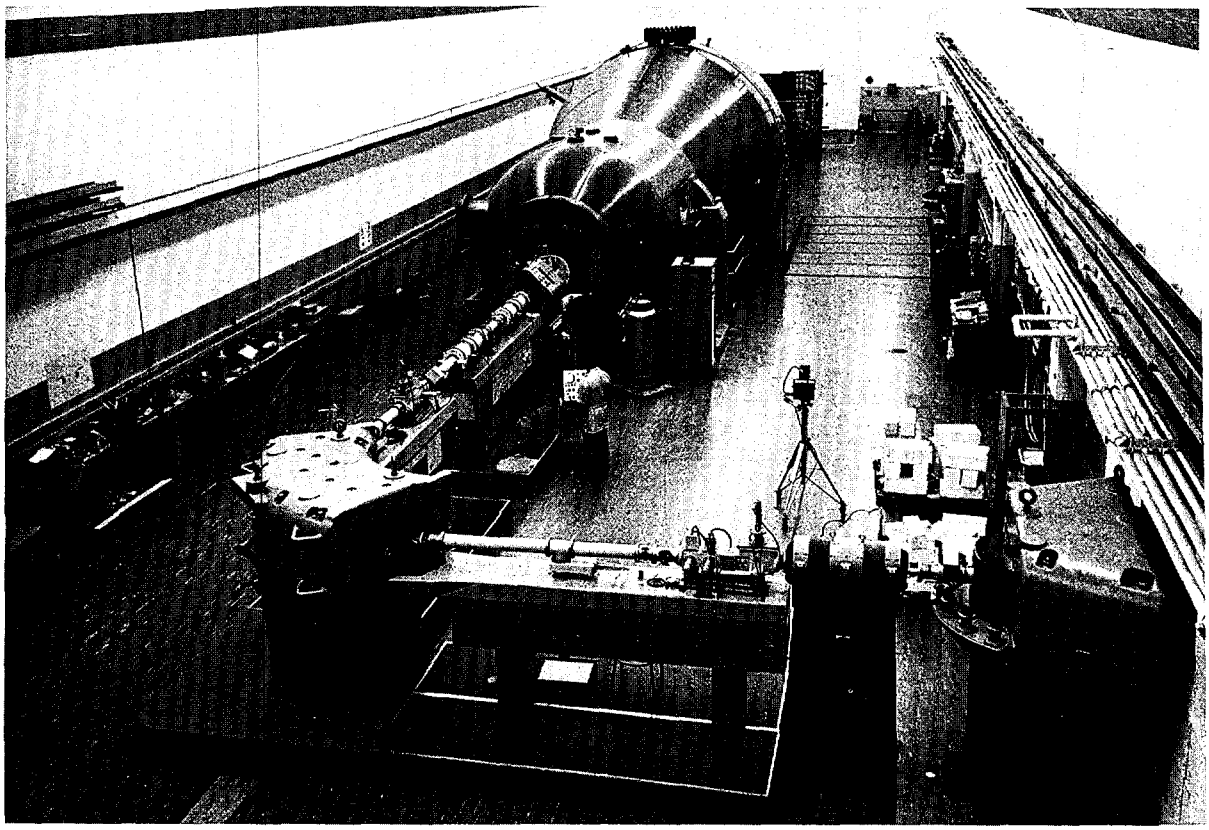

Fig. I–17. New Accelerator. The world's first Emperor Tandem Van de Graaff electrostatic accelerator has been installed and brought into full operation for AEC-sponsored research at Yale University, New Haven, Conn. Built by High Voltage Engineering Corp., Burlington, Mass., there are only five additional Emperor-type accelerators in existence or under construction in the western hemisphere. The negative ion injector appears in the shielding enclosure in the extreme *background* and the beam energy defining and first beam switching magnets appear in the *foreground*, leading to the experimental areas. The accelerator tank is 81 feet in length, 20 feet in diameter, and is constructed of 2-inch steel and weighs 400,000 pounds. The projectile beams travel up to 300 feet at speeds up to 500 million miles per hour before reaching the targets under study. The Emperor is capable of producing proton beams four times more energetic than those produced by conventional one-stage Van de Graaffs and 20 percent more energetic than those produced by other existing tandem accelerators. It is also designed to produce intense beams of a wide variety of heavy ions.

LOW ENERGY PHYSICS

Research in low energy physics seeks to further existing knowledge on the behavior and structure of nuclei, nuclear components, and nuclear forces. Areas of investigation include nuclear theory, charged particle physics, neutron physics, and atomic and classical physics.

NUCLEAR THEORY

Research in the area of nuclear theory is based in large part on nuclear models. Such models are useful in interpreting experiments and have advanced significantly from the early model of the atom.

Non-Spherical Light Nuclei

In general it is assumed that light nuclei, *i.e.*, nuclei with masses less than 100 times the mass of the hydrogen atom, are spherical. However, a large number of observed properties such as locations of energy states corresponding to var-

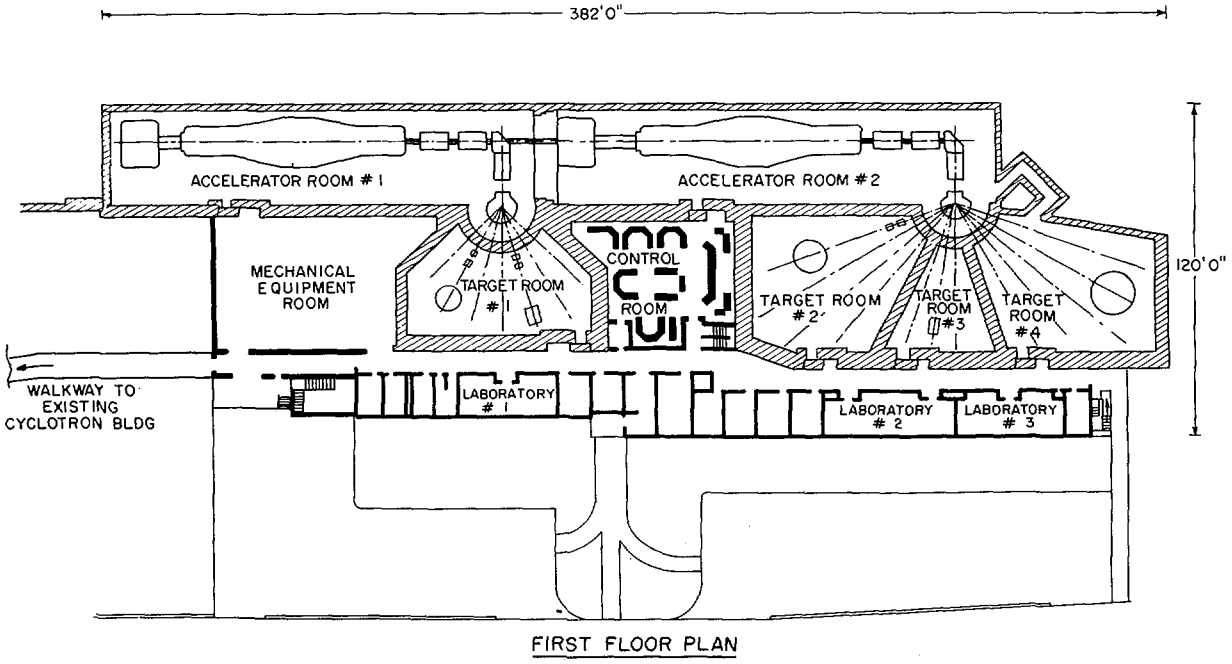

Fig. I–18. New Brookhaven Facility. Two Emperor Tandem Van de Graaffs will be installed in line in Accelerator Rooms No. 1 and 2 as shown in this drawing of Brookhaven National Laboratory's new Tandem Van de Graaff facility. Accelerator No. 1 can provide a beam into Target Room No. 1 operating as a conventional two-stage Emperor Tandem Van de Graaff. Accelerator No. 2 can also provide a beam into Target Rooms No. 2, 3, or 4 when operating as a standard two-stage Emperor Tandem Van de Graaff. In order to operate the facility as a three-stage unit, a special terminal ion source designed by BNL will be installed in the terminal of Accelerator No. 1. This machine will then be operated to accelerate negative ions from the terminal ion source to ground potential. These ions which have now attained an energy of 10 Mev. are then injected into Accelerator No. 2 and accelerated through the last two stages for an additional energy gain of 20 Mev. which results in a final energy of 30 Mev. The primary use of the facility will be as a three-stage accelerator; hence, the three-target rooms for the three-stage beam allow for easy access and experimental set up in two of the rooms while the third is being used with beam for experimental measurements.

ious modes of excitation, the decay probabilities of these excited nuclei to other excited or ground states, and the gradient of the charge distribution (*quadrupole moments*), cannot be adequately understood in terms of this basic assumption. This led to the proposition that the mass distribution of light nuclei could be ellipsoidal, and hence, particles inside these nuclei move within an ellipsoidal potential surface. The initial consequences of this proposition look very encouraging. It explains the above-mentioned difficulties for many light nuclei with an odd number of particles. The theoretical consequences of particles moving in an aspherical potential is more complex than in the spherical case. The ellipsoidal nature of these nuclei implies a rotational motion, and the motion of particles inside the nucleus gets coupled to this rotation. A theoretical calculation of this coupled motion was performed at Yale University, New Haven, Conn. This coupling influences profoundly the above-mentioned observed properties, and the calculation of them agrees with the observed results.

CHARGED PARTICLE PHYSICS

Protons, deuterons, heavy ions, and photons are used as nuclear probes. These particles are obtained from accelerators such as Van de Graaffs, linacs, and cyclotrons. Some of the

types of research conducted under this program are elastic, inelastic and reaction differential cross section measurements as well as heavy ion reaction studies, fission studies, and studies using polarized targets and polarized bombarding particles. Other programs include the study of nuclear reactions induced by gamma rays, double beta decay studies, particle channeling studies, and studies involving the unraveling of nuclear decay schemes.

Study of Excited States of Nuclei

A recently developed method of analyzing nuclear particle bombardment of nuclei by fluctuations in the yield has been used by the Los Alamos Scientific Laboratory to continue the study of the states of excitation of nuclei and to obtain significant new information in the continuum region of nuclear excitation energy where the states are so numerous that they are no longer distinct. Different bombardment conditions allowed determinations of the change of the widths of these states both with the excitation energy and with the amount of the nuclear spin. These widths can then be related to the state lifetimes by means of the uncertainty principle of quantum mechanics, which states that the width is inversely proportional to the lifetime. The results showed that the time in which nuclei de-excite decreases as the energy increases and increases as the spin increases.

The fluctuations in the cross section have been analyzed for the production of alpha particles, helium-4 nuclei, from proton bombardment of phosphorus-31 to determine the width change with energy for the sulfur-32 nucleus formed by this bombardment. Use was made of a change of proton energy from 5 to 22 Mev. obtained, respectively, from single-stage and three-stage use of the Los Alamos tandem Van de Graaff accelerator (see Fig. I–19). Analysis showed a change in average width from 10 Kev. to 95 Kev., which confirms the expected trend.

For the study of the change of width with the amount of rotation or spin, of the nucleus, the fluctuations in the cross section for producing alpha particles from oxygen-16 bombardment of oxygen-16 were measured over the energy range from 24.9 to 29.2 Mev. in 25 Kev. steps. This enabled a comparison of the average level width from the same sulfur-32 nucleus at the same excitation energy as for the higher-energy proton bombardment of phosphorus-31. Oxygen ions were obtained from two-stage use of the tandem Van de Graaff. Oxygen ions impart more rotation to the compound nucleus than protons, and this larger amount of spin was found to reduce the width to 73 Kev. from the 95 Kev. found for proton bombardment. The higher-spin states are expected to live longer because few particles emitted from an excited nucleus in its decay are capable of providing the required reduction in spin. The resulting longer lifetime of excited states for larger-spin nuclei results in the smaller width observed.

Nuclear Lifetimes Using Doppler Shift

Nuclei generally exist in unstable configurations for very short periods of time. This time, which is intimately related to the nuclear structure, becomes increasingly more difficult to measure for times shorter than ten picoseconds (10^{-11} second). A combination of the *Coulomb* excitation process and Doppler shift is now being applied at the Oak Ridge National Laboratory to a study of nuclear lifetimes in this range. In *Coulomb* excitation, a nucleus is forced into an unstable configuration by bombarding it with high-velocity charged particles. If the charged particles are heavy (oxygen ions are presently being used), the bombarded nucleus is also left with a significant velocity (typically a few percent of the velocity of light). The energy of the gamma ray emitted by the nucleus in returning to its normal condition depends, according to the Doppler principle, on the velocity of the nucleus. (A frequently observed example of the *Doppler* shift dealing

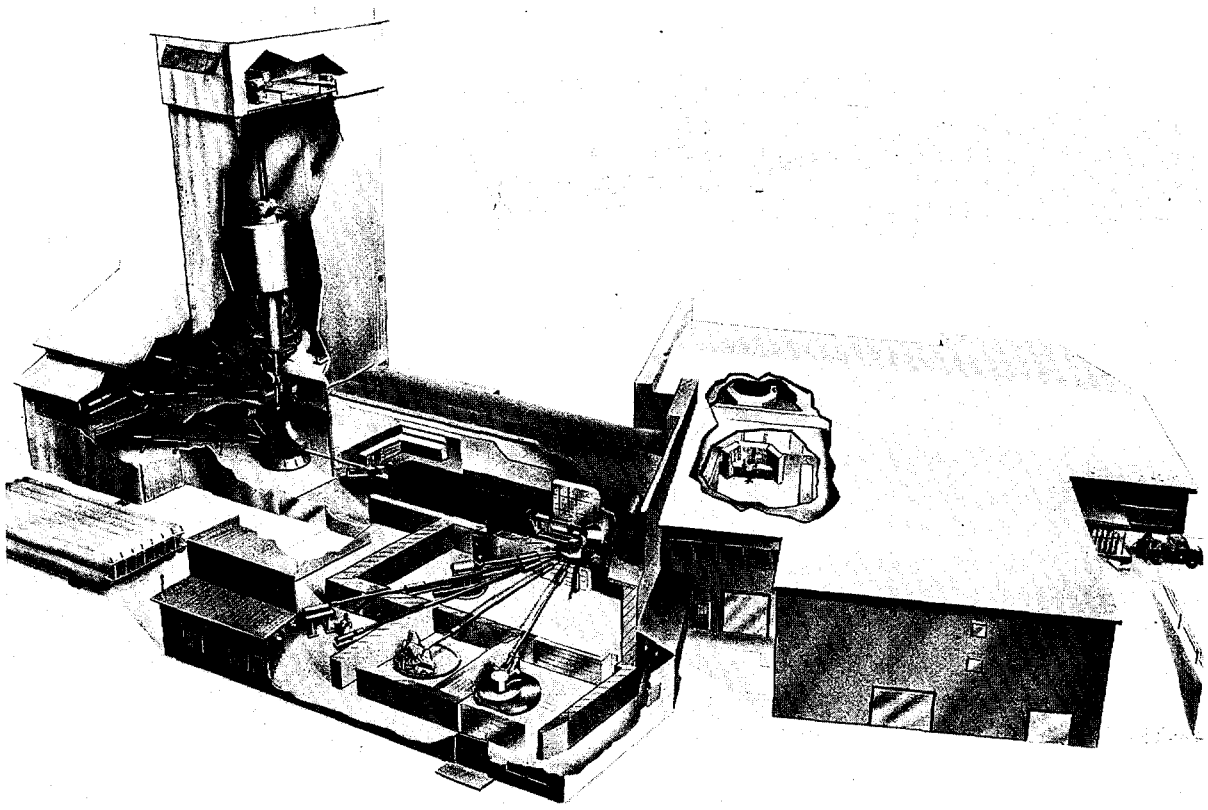

Fig. I–19. Los Alamos Three-Stage Van de Graaff Facility. Cutaway drawing shows the two electrostatic accelerators making up the Los Alamos Scientific Laboratory's three-stage Van de Graaff facility. On the *left* is the vertical accelerator that can accelerate protons to 8 million electron volts (Mev.) and can also produce beams of deuterons, tritons, and helium ions. It is used independently (mostly for neutron research), or is used as an injector for the two-stage horizontal machine (*center* of drawing), a 17-Mev. tandem Van de Graaff that produces beams of the same variety as the vertical machine and can be operated independently, primarily for charged particle experiments. When operated in series the two machines can produce a maximum proton energy of over 25 Mev. The facility produces the world's only tritons (tritium nuclei) with a greater than 20-Mev. energy, a factor instrumental in the recent discovery of the new helium-7 radioisotope (see p. 31).

with sound waves is the change in pitch of a railroad warning signal heard by a passenger on a fast moving train). Since the nucleus is slowed down by collisions with other nearby atoms, the velocity at the moment of gamma-ray emision depends on how quickly the nucleus returns to its stable configuration. Thus, the magnitude of the *Doppler* shift is directly related to the nuclear lifetime. A measure of this has, for example, established that two excited configurations of tin-117 have lifetimes of two trillionths (2×10^{-12}) of a second and nine-tenths of one-trillionth (9×10^{-13}) of a second. These measurements would not have been possible without the recently developed high-resolution germanium detectors.

Resolution vs. Energy in Detectors

One of the less desirable properties of silicon and germanium lithium drifted detectors is the change in resolution of the detector with energy (see also "Semiconductor Detectors" section, p. 319, in Part Three—Biological, Medical and Environmental Research). Ideally these detectors would collect 100 percent of the hole-

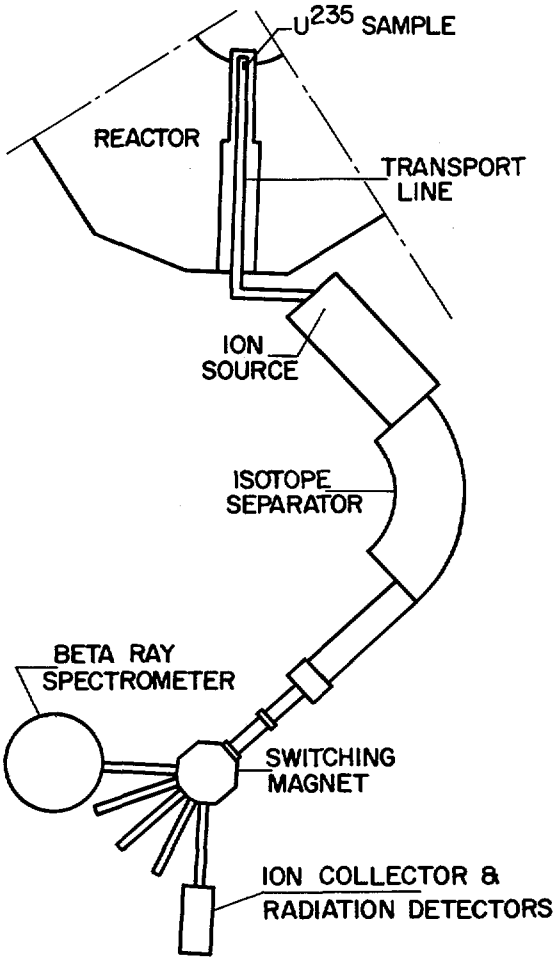

Fig. I–20. Isotope Separator System. The first successful operation of an isotope separator connected to a reactor for the purpose of continuously studying short-lived radioactivity produced by fission of uranium-235 (U^{235}) has been achieved at the Ames Laboratory research reactor. Gamma ray spectra of xenon and krypton isotopes (with half-lives down to less than 2 seconds) have been analyzed, and some observations have been made of other types of radiation, such as neutrons. In the operation, a sample of U^{235} is placed in the reactor neutron flux (near the reactor core) and, through fission, acts as a source of gaseous radioactive atoms. These atoms then travel from the uranium-235 sample to the ion source of the isotope separator through a transport line. The isotope separator serves to produce—for collection and simultaneous study of radioactive decay—pure radioisotopes so that competing activities from neighboring masses are eliminated. The collection of the activities can be made either in a beta ray spectrometer or in a variety of other arrangements with suitable detectors for specific studies of the different aspects of the radioactive decays.

electron [12] pairs produced by the incoming ionizing radiation and (together with the associated electronics) produce a pulse the amplitude of which is directly proportional to the number of hole-electron pairs. However, this pulse height would not always be the same for identical events but would show statistical fluctuations resulting from the statistics involved in the production of the hole-electron pairs. A spectrum for mono-energetic ionizing events in the detector should then be a gaussian line with a characteristic full width at half maximum *i.e.*, resolution, increasing with the square root of the number of hole-electron pairs produced. However, it is only at the lowest energies that the line shape is even approximately gaussian. As the energy increases the line broadens on the low energy side as though efficiency for the collection of hole-electron pairs is not uniform.

Studies have been made at Brookhaven National Laboratory on the line shape as a function of pulse rise time to try to eliminate pulses which degrade the resolution. This idea of such pulse shape discrimination in counters is not new but has been used (on a different time scale) in both gas and solid state counters.

Using a small (1 cm^2 × 1.5 mm) silicon lithium drifted detector the resolution before pulse shape discrimination was measured to be 0.850 Kev. at 14 Kev., 1.3 Kev. at 68 Kev., and 1.6 Kev. at 122 Kev. The line shape at the higher energies was very asymmetric on the low energy side of the line. With pulse shape discrimination the resolution could be 0.850 Kev. at all the above energies. The curious and unanticipated result of this investigation at Brookhaven is that it is the slowly rising pulses and not the fast ones which give the improved resolution. This appears to be inconsistent with the reasons commonly given for the degradation of resolution with increasing energy.

[12] A "hole" is the absence of an electron, or an effective positive charge.

Fission Cross Section of Am^{242m}

The fission cross section of metastable [13] americium-242 (Am^{242m}) at thermal energy is 7,200 barns,[14] much larger than that of any other known nucleus. However, only recently has Am^{242m} been available in sufficiently large quantities for detailed measurements to be attempted at other energies. A severe problem with measurements on this nucleus is its short alpha-decay half life which makes it very difficult to detect fission fragments in the high background of alpha particles which the sample emits continuously. This problem has been solved at the Lawrence Radiation Laboratory, Livermore, by using spark chamber detectors. Cross section measurements for neutrons ranging in energy from thermal (0.02 ev.) to 6 Mev. have been obtained. The measurements were carried out using the beam from an electron linear accelerator as a pulsed neutron source. The whole unnormalized cross section curve as a function of energy can be normalized to the easily-measured thermal fisson cross section. Thus, there is no need for carrying out measurements in different energy ranges on different kinds of apparatus and then trying to piece the results together to get a broad energy region, as has been done in the past on most other fissile nuclides. The fission cross section below 4 ev. is shown in Figure I-21. The fission cross section from below thermal to 0.2 ev. is relatively flat and has a value of about 6,000 barns. This is more than 10 times larger than that of any of the common fissile nuclides over most of that energy range. The cross section falls rapidly from 0.2 to 1 ev., but even at 1 ev. the cross section is as large as the uranium-235 cross section is at thermal energy. This extremely large cross section over the neutron energy range in which thermal reactors operate suggests the possibility of building much smaller and lighter reactors than are presently possible provided the americium-242 can be made in useful quantities. Such reactors could have important applications, for example, in space power systems.

This is the only odd-odd [15] nucleus for which the fission cross section has been studied. These measurements have demonstrated a capability for measuring fission cross sections of other rare heavy nuclides which now are becoming available in samples of adequate size for such studies. The measurements promise to be a source of information which could lead to applications of the fission properties of these rare heavy nuclides which might be uniquely different from those of the more common fissile materials.

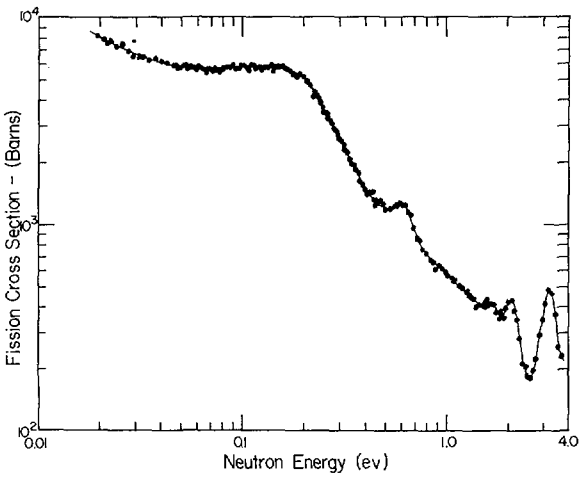

Fig. I-21. Fission Cross Section of Am^{242m}. The fission cross section of metastable americium-242 (Am^{242m}) at thermal energy is 7,200 barns, much larger than that of any other known nucleus. Since Am^{242m} has become available in quantities large enough for detailed measurements to be attempted at other energies, the Lawrence Radiation Laboratory, Livermore, has measured the fission cross section for neutron energies less than 4 electron volts (ev.). As indicated in the above figure, the fission cross section from below thermal (0.025 ev.) to thermal (0.2 ev.) is relatively flat and has a value of about 6,000 barns which is more than 10 times larger than any of the more common fissile nuclides over most of that energy range. The figure shows a rapid decline to about 300 barns in the range from 0.2 to 1 ev. but even above 1 ev. the cross section is as large as the uranium-235 cross section at thermal energy.

[13] *Metastable Americium-242*—The radioisotope decays without particle emission to a more stable form of the element.

[14] *Barn*—The unit of measure of the probability that a given nuclear reaction will occur; more specifically, the unit for expressing cross-section values for reactions between particular nuclides and particular incident particles of particular energies. In physical terms, the barn is a unit of area—10^{-24} square centimeters.

[15] Odd number of neutrons and protons.

New Isotope, Copper-69

Nuclear disintegrations in which protons are selectively removed from nuclei are conveniently performed by irradiation of elements with high energy X-rays. A recent result of a continuing research program at the Ames Laboratory to investigate possible new radioactivities formed in this way has been the discovery of a new isotope, copper-69. This isotope was produced by bombarding an enriched sample of the isotope zinc-70 with X-rays from the Iowa State University electron synchrotron. The half-life of the new activity in copper was determined to be 3.0±0.1 minutes, and quantum numbers of several of the energy levels were identified.

New Isotope, Helium-7

Very light nuclei have been studied at the Los Alamos Scientific Laboratory by means of nuclear reactions induced by tritons from a three-stage tandem Van de Graaff accelerator and one particularly significant result has been the discovery of the nucleus helium-7 (He^7).

The LASL tandem accelerator produces the world's only tritons (tritium nuclei) with an energy greater than 20 Mev. This triton beam permits unusual neutron-rich light nuclei to be formed by nuclear reactions. For example, when a triton beam strikes a tritium target, one reaction that may take place is: triton+triton →hydrogen-5+proton, ($t+t \rightarrow H^5+p$). The proton energy spectrum from the reaction can be measured in a detector system, and the spectral shape will indicate the possible existence of the residual hydrogen-5 (H^5) nucleus. A series of experiments using this technique have been performed to study nuclear systems having mass numbers 3 through 7. These experiments explore a new region of high excitation energy in these nuclei and permit a search for hitherto undiscovered nuclei. In addition, measurements of the spectra of reactions such as triton+triton→(3 neutrons)+helium-3 ($t+t \rightarrow (3n)+He^3$) are expected to shed further light on the three-body nuclear force.

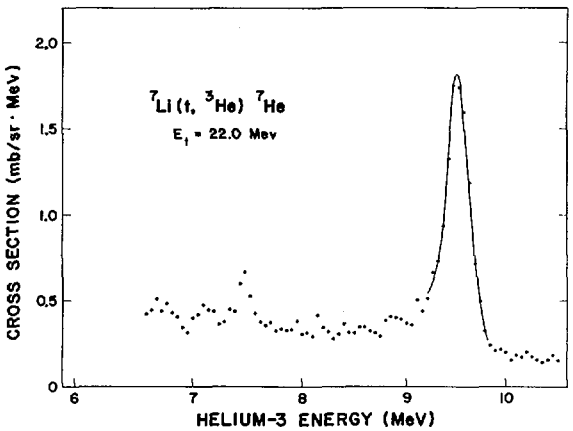

Fig. I–22. New Radioisotope, Helium-7, Found. Using the triton beam from the Los Alamos three-stage tandem Van de Graaff accelerator to bombard a lithium target, experiments have produced a new isotope of helium, helium-7 (He^7). The figure shows the energy spectrum of He^3 particles arising from the $H^3+Li^7 \rightarrow He^7+He^3$ reaction. The He^3 particles were observed in detectors placed at an angle of 10° to the incoming triton beam. The data points rise to a peak between 9 and 10 Mev. and this peak together with data taken at other angles shows the existence of the new isotope He^7. The energy width of the peak has been measured and is related to the detailed nuclear structure of He^7.

The He^7 nucleus was observed by use of the tritium+lithium-7→helium-7+helium-3 ($t+Li^7 \rightarrow He^7+He^3$) reaction. From a peak in the He^3 energy distribution the existence of He^7 was shown, and its nuclear mass was determined (see Fig. I–22). Helium-7 is unstable for it decays into He^6+n, but nevertheless clearly appears as a fairly narrow peak in the He^7 excitation spectrum. Based on the mass of He^7, the systematics of neutron binding in light nuclei can be extended. For instance, the neutron pairing energy of He^8 is determined now that the mass of He^7 is known. Also, from the masses of He^7 and its analogues in Li^7 and beryllium-7 (Be^7), the mass of the undiscovered nucleus of boron-7 (B^7) can be predicted.

Negative Helium Ion Source

The University of Wisconsin at Madison has developed a new type of ion source capable of producing much more intense beams of nega-

tive helium ions. Negative ions are required for the operation of tandem Van de Graaff accelerators. By injecting negative helium ions into a tandem Van de Graaff an emergent beam with an energy three times that of the terminal voltage becomes available. The new ion source uses the interaction of cesium vapor with low energy positive helium ions to convert approximately two percent of the positive ions to negative ions. Previous ion sources employed hydrogen as the converting gas and only about 0.01 percent conversion of the positive ions was achieved. The new source will now make practical accurate studies of many more alpha-particle and helium-3 ion induced nuclear reactions.

Analog States in Barium Isotopes

If a nucleus is excited to a high enough energy to have many different ways of giving up this energy, the notions of its particles are usually too complicated to be understood on the basis of the present theoretical models. One of the few types of high-energy nuclear states to escape this general complexity is the isobaric analog state. This is a state whose structure is nearly identical to that of a clearly identified state of an isobaric nucleus—a nucleus with the same total number of particles but with a neutron replaced by a proton. The remarkable similarity of a state and its isobaric analog is fundamentally due to the dynamical similarity of neutrons and protons, which enables nuclear theory to relate the properties of a nucleus to those of its isobar. This simplification has been used by Argonne National Laboratory in a detailed study of analog states in the barium isotopes, which are near the neutron closed shell with 82 neutrons. Observations of the decay of analog states have yielded detailed information about states that correspond to basically simple motions of neutrons in the barium isotopes of even mass numbers.

In this experiment, protons from the tandem Van de Graaff are scattered inelastically from isotopically separated barium targets. When the energy of the incident proton is exactly right to excite an analog state, groups of protons in the measured spectra stand out dramatically above the background (see Fig. I–23). At other energies (middle spectrum), such groups are missing. In the nuclear reaction producing these particular spectra, the proton enters the barium-138 nucleus to produce the compound nucleus lanthanum-139. The latter emits a proton with less energy than the incident one, so the nucleus that remains is barium-138 in an excited state. Specific states of barium-138 are excited strongly only by way of those states of lanthanum-139 that are isobaric analogs of low-

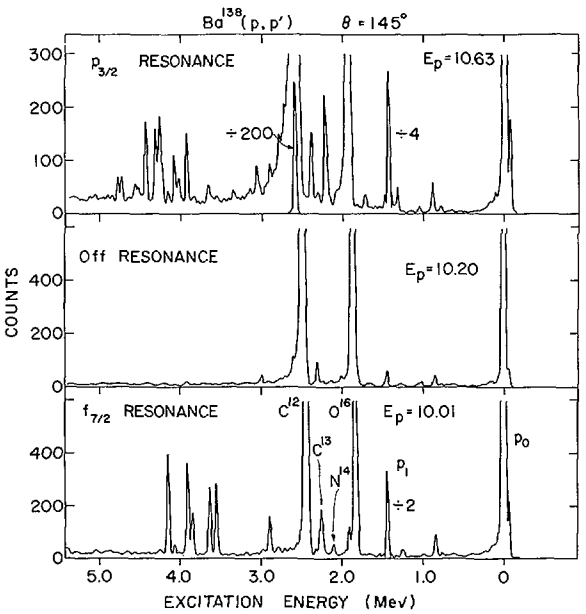

Fig. I–23. Analog States in Barium Isotopes. The graphs show the spectra of protons scattered elastically and inelastically from barium-138 in an Argonne National Laboratory study. The energy (Ep) of the incident protons (in Mev.) is indicated for each spectrum. Peaks due to impurities (carbon-12, carbon-13, nitrogen-14, and oxygen-16) are labeled. The top and bottom spectra were obtained at resonances (at which the protons had exactly the right energy to excite an analog state). The middle spectrum was obtained at an energy between resonances. The strong peak at zero excitation energy in barium-138 represents protons scattered elastically (without loss of energy). The group of strong peaks at about 4 Mev. appear selectively at the resonance energies. These states correspond to basically simple motions of the nuclear particles, but despite this they would be very hard to excite in any other reaction.

lying states in barium-139 and have the same simple structure.

If the states seen in these experiments have the simple structure they appear to have, the effective law of force between two neutrons in a nucleus can be extracted from this experiment. This is one of the first intermediate-mass nuclei for which there has been sufficient experimental data to make this extraction possible. The properties of the force law thereby determined can be used in two important ways: (*a*) they enable the making of fairly reliable theoretical predictions about the structure of other nuclei in this mass region, and (*b*) they can be used to examine whether or not the effective law of force between neutrons in a nucleus can be derived from the force between free nucleons.

NEUTRON PHYSICS

Neutron physics is of special importance to the AEC's reactor and weapons development program. Included in this category are basic studies of neutron scattering (elastic and inelastic), neutron-induced reactions, and neutron-induced fission research. Neutrons used in these studies are produced in nuclear reactors and by beams of charged particles from particle accelerators.

Spin Dependence of Nuclear Forces

Neutrons and protons possess nuclear spin, *i.e.*, they may be visualized as spinning rapidly about an axis and when they are all spinning in the same direction they are said to be polarized. The fundamental force acting between neutrons and protons, which is the force which binds all nuclei together, is greatly affected by the spin of these particles. Consequently, a variety of experiments sensitive to the presence of spin, at many energies, are required for the understanding of the nature of the force. Two recent experiments at the Los Alamos Scientific Laboratory (LASL) bear on this problem.

Neutron-proton scattering. In the first experiment of its kind, a polarized beam of 23 Mev. neutrons was scattered from a target of polarized protons to study the spin dependence of nuclear forces. The object of the experiment was to measure the difference in the rate at which protons were knocked out of the target, when the neutron and proton spin polarizations were parallel, as compared to the case where they were anti-parallel. This measurement is called a "C_{NN}" spin-correlation experiment in neutron-proton scattering. The LASL results have caused definite modifications in the empirical data analyses made by a Lawrence Radiation Laboratory, Livermore, theoretical group. In addition, the data are also being employed in similar analyses at Yale, at Harwell in Great Britain, and at Dubna in the U.S.S.R. The experiment, which is diagrammed in Fig. I–24, required cooperation between widely different disciplines for its success. Nuclear physics techniques produced the neutron flux and provided particle detection. Target polarization required microwave and radio methods in a low temperature cryostat operating near absolute zero temperature (−273° C.) in a 14,000 gauss magnetic field. The results, together with certain theoretical phase shift calculations are shown in Fig. I–25. It should be noted that the Yale curve is a prediction, since Yale did not have prior knowledge of these data, whereas the Livermore and Dubna curves were obtained after fitting the data at 140° and 174°. Both these latter curves represent substantial changes from their original predictions. Further work remains to be done in order to obtain better agreement at small angles.

Proton-proton scattering. In the second LASL experiment, done cooperatively with the University of Colorado, the relative orientation of the spins of the two scattered particles in proton-proton scattering was studied, and the spin correlation, "C_{NN}" was measured. The results were used along with the other various types of spin-dependent scattering measurements to seek a complete experimental description for the proton-proton interaction, which a successful theory of nuclear forces must explain. As shown in Fig. I–26, the 27-Mev. proton

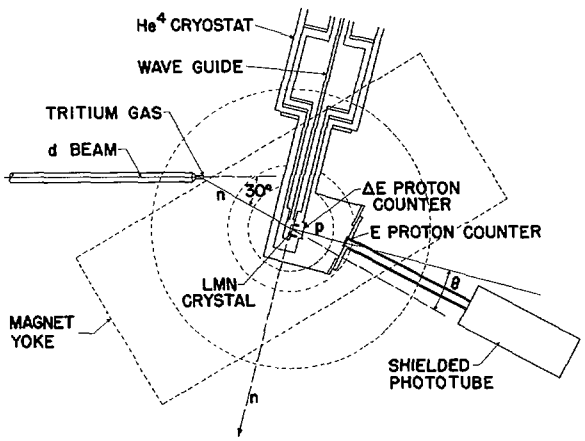

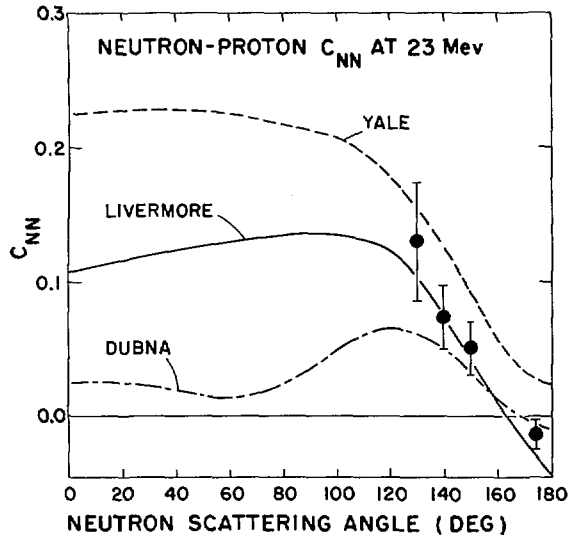

Figs. I–24 and 25. Polarized Neutron-Proton Experiment. The schematic diagram, *left*, shows the arrangement for a Los Alamos Scientific Laboratory experiment in which a polarized beam of 23-Mev. neutrons were scattered from a polarized proton target to study the dependence of nuclear forces on neutron and proton spin. The polarized neutrons are produced by bombarding tritium gas with a beam of deuterons. The polarized protons are contained in a "LMN" crystal [$La_2Mg_3(NO_3)_{12} \cdot 24H_2O$] immersed in liquid helium in a 14,000 gauss magnetic field. The protons knocked out of the target were detected by a scintillation crystal and photo tube. The results of the study of the dependence of the fundamental nuclear binding forces on the spin of neutrons and protons are shown in the curve *at right*. The circled points are the measured values of the differences in the rate at which protons are knocked out of a polarized proton target by polarized neutrons when the neutron and proton spin polarization are paralleled from the rate when the polarizations are anti-parallel. This measurement is called a "C_{NN}" spin-correlation experiment. The curves are various theoretical calculations of these values.

beam of the University of Colorado cyclotron struck a thin liquid hydrogen (proton) target. The emergent proton pairs from this collision were then analyzed for their simultaneous polarizations by scattering from thin liquid helium targets. The final data were obtained in a 200-hour run in which the desired events occurred at a rate of 20 per hour. An involved Monte Carlo computer analysis showed that for 90° scattering (center of mass), 84.4 percent of the scattering events take place with the proton spins anti-parallel. This information in conjunction with the neutron-proton information has been employed in theoretical analyses of the generalized nucleon-nucleon interaction.

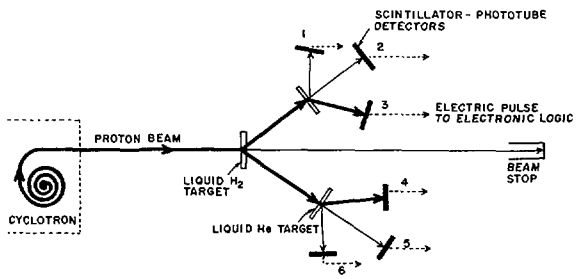

Fig. I–26. Proton-Proton Scattering. Drawing shows the arrangement of a Los Alamos Scientific Laboratory experiment, done in cooperation with the University of Colorado, to study the spin dependence of the binding forces between protons. A beam of 27-Mev. protons from the University of Colorado cyclotron was directed at a liquid hydrogen target. The polarizations of the proton pairs scattered from the target were determined by scattering these protons from two liquid helium targets. As shown in the drawing, simultaneous pulsing of detectors *3* and *4* indicates that the two protons are spinning in opposite directions, that is, their polarizations are anti-parallel.

ATOMIC AND CLASSICAL PHYSICS

Research in the area of atomic and classical physics includes spectroscopy studies of atoms

and molecules, crystals, atomic beam studies, low temperature physics, and atomic cross section measurements.

Quadrupole Moment Correction

The distribution of electric charge in the nucleus of an atom can be characterized by what is called the nuclear electric quadrupole moment. The magnitude and sign of the moment can be predicted theoretically for any particular nuclear state once a nuclear model has been assumed. Although such predictions have been strikingly successful in all similar cases, the prediction for the nuclear ground state of vanadium-51 has been in sharp disagreement with the only experimental value. For this reason, the validity of the theory has been in question. Argonne National Laboratory remeasured the quadrupole moment with a more precise technique than had been used previously. The final result is in agreement with theory and shows that the previous measurement was in error.

In this experiment, the atomic-beam magnetic-resonance technique was employed to examine in detail the hyperfine spectra of nine atomic levels in two distinct electronic configurations of vanadium-51. After the electric-quadrupole part of the hyperfine structure had been separated from the part due to other causes, it was possible to use the data from each of eight atomic levels separately to calculate the quadrupole moment of the nucleus in its ground state. Although the eight values obtained should have been the same, large differences were found. The differences between the values obtained for the four states of each configuration were much larger than the estimated experimental errors (see Fig. I–27). This large scatter among the measured values of the quadrupole moment was at first disturbing. However, further consideration of the theory showed that each level should be suitably corrected for the effects of admixture with nearby atomic energy levels. The final values of the quadrupole moment were found to be the same for states of both electronic configurations.

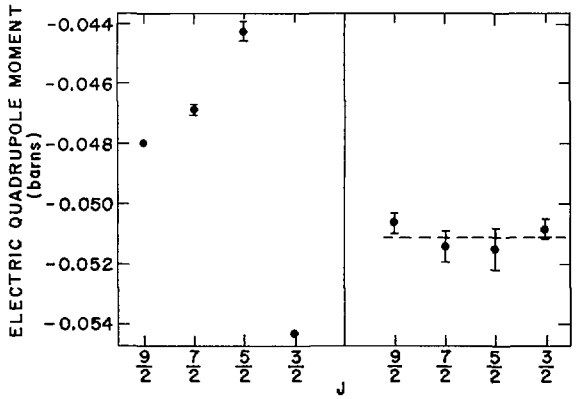

Fig. I–27. Quadrupole Moment Correction. The chart shows the values of the electric quadrupole moment of the vanadium-51 nucleus in its ground state, as computed at Argonne National Laboratory from the measured hyperfine structure of the atom in four electronic states in one configuration. These states correspond to four values of the angular momentum J in this electronic configuration. Before correcting for the effects of admixture with other states (left-hand portion), the values differed widely from one to another. After the correction, all measurements are consistent with a single value (dotted line in the right-hand portion).

Iodine Clock

Radioactivity which was still alive at early times in the solar system, but has now completely died out, has led to the interesting discovery that very stable minerals in 10 different stone meteorite samples were all formed within 1 or 2 million years of each other. This finding by the University of California, Berkeley, illustrates the unique advantage of an extinct radioactivity "clock", because the minerals in question were formed about 5 billion years ago. With ordinary radioactive clocks, such coincidences in time can be established only 100 million years or so back.

It is likely, but not yet proven, that the minerals giving this result are "remembering" a rapid cooling of chondrules in the early solar system. Chondrules are mysterious stony spheres which occur in most stone meteorites. The 10 samples studied contained chondrules, and one of the samples was an individual chondrule pried out of a meteorite. Aside from all having

chondrules, the stone meteorites in the study were quite diverse in character.

The meteorite samples were irradiated in a Brookhaven National Laboratory reactor which resulted in a little of the iodine in these objects changing into a xenon-128 (Xe^{128}) isotope. In early days of the solar system these samples also contained a trace of radioactive iodine-129, which decayed within 25 million years, on the average, to stable xenon-129. After the irradiation, the samples were heated in steps and the xenon driven off was examined in a sensitive mass spectrometer, which could measure for each temperature fraction the ratios Xe^{128}/Xe^{132} and Xe^{129}/Xe^{132}. If the early iodine-129 was present to a random extent in these objects or if the time of cooling of the primitive minerals in these objects was variable, there would be no relation between the two ratios. But for all 10 samples these ratios for fractions expelled above 1,100° C. when plotted against each other on an "x-y" plot, fell accurately on a single straight line. The straight line plot is a consequence of synchronous cooling of the chondrules.

Just why the early solar system contained radioactive iodine-129 in the first place is still open to question, but these results show that this fossil radioactivity was well mixed with ordinary iodine to very nearly one part in 10,000 at the time when stable minerals in stone meteorites took form. It is hoped that the iodine clock will become useful in dating other solar events, thus verifying theories of the creation and evolution of the early solar system.

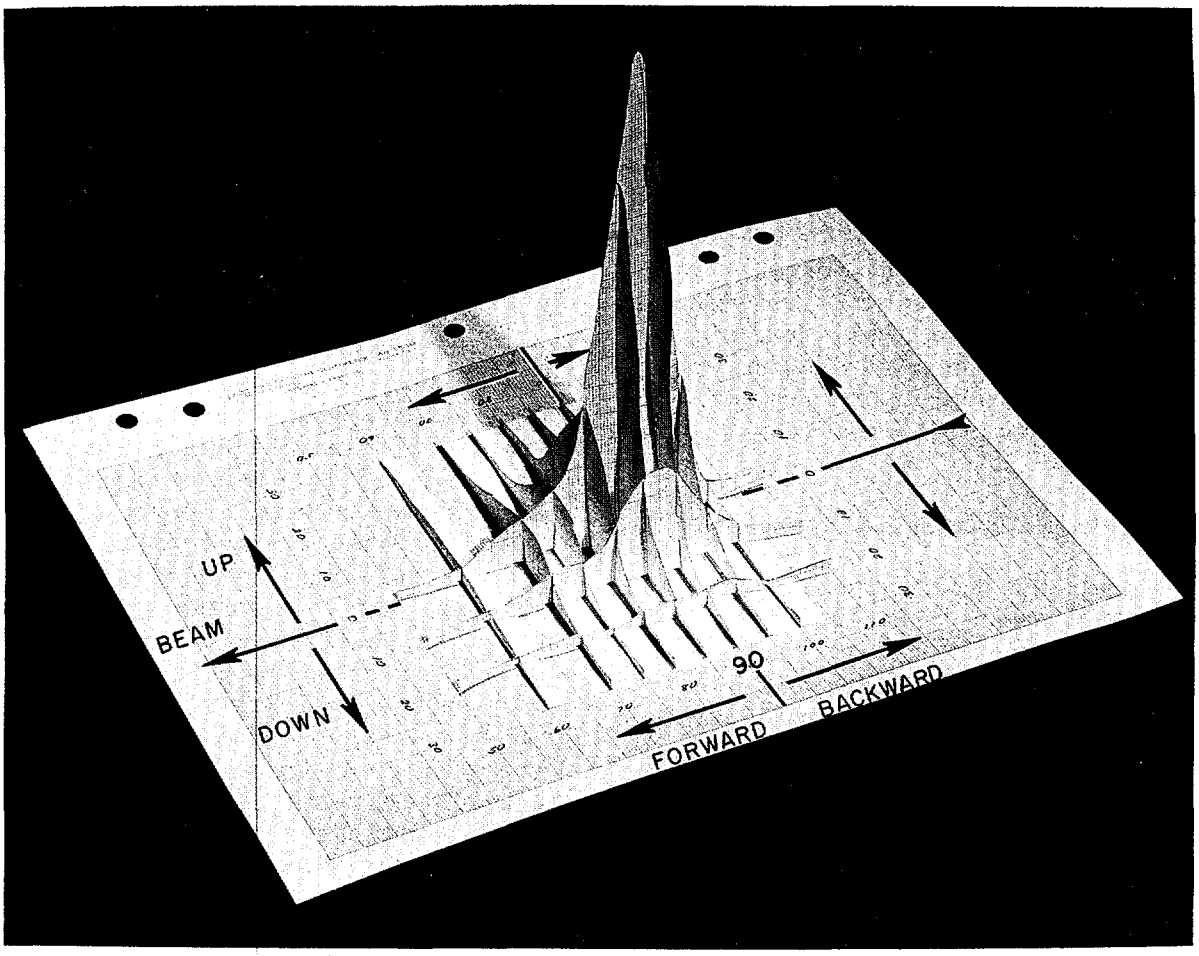

Fig. I–28. High Energy Fission Studies. Brookhaven National Laboratory has studied the angular correlation between fragments produced in uranium fission induced by 3-Bev. protons from an accelerator. The probability of fission events as a function of the angle between fragments is shown above on a three-dimensional basis. The proton beam direction is indicated, and the thin uranium target was located at the intersection of the beam line with the 90° line. One of the two fragment detectors was directly below that point. By moving the second detector on the opposite side, the relative probability of the occurrence of fission is shown by the height of the peak at the angle of interest (see page 40 for details).

CHEMISTRY RESEARCH

Basic research in chemistry deals with matter, its properties, and the transformations it undergoes. Investigations on materials range from forms as simple as atoms of hydrogen and as complex as the large molecules of enzymes and nucleic acids. The research is basic in nature and provides the discoveries on which advances in nuclear science and technology depend. The program includes research in nuclear chemistry, heavy element chemistry, radiation chemistry, theoretical and structural chemistry, analytical chemistry, physical chemistry, inorganic chemistry, separation chemistry and technology, high temperature chemistry, and isotopic geochemistry.

NUCLEAR CHEMISTRY

Research in nuclear chemistry deals with nuclear structure, nuclear reactions, and radioactive transformations. Emphasis is placed on complex phenomena such as the structure and synthesis of the heavier nuclei, high energy nuclear reactions, the preparation and separation of different nuclei formed in accelerator bombardments or reactor irradiation, and applications and measurements of stable and radioactive nuclei to study fundamental chemistry and physics.

Alpha Particle Reactions on Calcium

The half-life and characteristic radiation of calcium-47 make it by far the best radioactive tracer for studying the role of calcium in biological systems. Yields of calcium-47 formed by cyclotron bombardment of calcium-48 have been measured experimentally at Brookhaven National Laboratory, and shown to be substantially higher than that predicted by theory. It was shown that if a thick target of calcium-48 was bombarded with alpha particles of 40 million electron volts (Mev.) energy the yield of calcium-47 would be substantial. The isotope can be produced by reactions in which various nuclear projectiles bombard either calcium-46 or calcium-48. Because of the importance of the calcium-47 produced and the expense of these targets, it is worthwhile to make maximum use of the reaction yields. The experimentally measured curve of yield *versus* energy of bombarding particle showed interesting differences from the theoretically predicted curve. These differences suggest that the mechanism for the reaction between an alpha particle and a calcium-48 atom to produce a calcium-47 atom [16] differs from the mechanism of most other alpha in, alpha plus neutron out (α, αn) reactions that have been reported. The interpretation of these results is expected to lead to information concerning the nuclear structure of unusual nuclides such as calcium-48; therefore assisting in the understanding of nuclear structure in general.

Improved Particle Identifier System

The identification of energetic light nuclei in the complex mixture of products produced by nuclear reactions, nuclear fission, and high energy nuclear fragmentation has always posed problems. A mixture might contain isotopes of hydrogen (H), helium (He), lithium (Li), beryllium (Be), etc., with kinetic energies of many million electron volts. A common solution to the identification problem is to place a thin particle detector made of a silicon semiconductor crystal in front of a thick detector of the same material. When a particle traverses the detector assembly, the thin detector produces an electrical pulse proportional to the energy loss rate of the particle and the thick detector gives a signal proportional to the particle's total energy. The type of particle can be identified by suitable calculations performed with the detector signals because different kinds of particles of the same energy lose energy at different rates. Now a much improved particle identifier system has been developed at the Lawrence Radiation Laboratory, Berkeley.

The improved system makes use of an assembly of two thin detectors and one thick detector of silicon semiconductor material. Electrical signals are passed through fast-timing circuits and then introduced to an analog computer which generates an output pulse characteristic of the identity of the particle and the second pulse proportional to its kinetic energy. An important feature is that the identification is made twice by independent calculations based on the electrical pulses from the two thin detectors and only those events in which the two identifications agree are recorded. This feature markedly improves the capability of the system to identify closely similar particles. This improved particle identifier technique has been successfully applied to a variety of problems and has brought much acclaim from nuclear chemists.

In one study of light fragments ejected from heavy target elements such as gold or uranium

[16] Such a reaction is termed an alpha, alpha neutron (α, αn) reaction to indicate that an alpha particle has caused the removal of a neutron from a target atom.

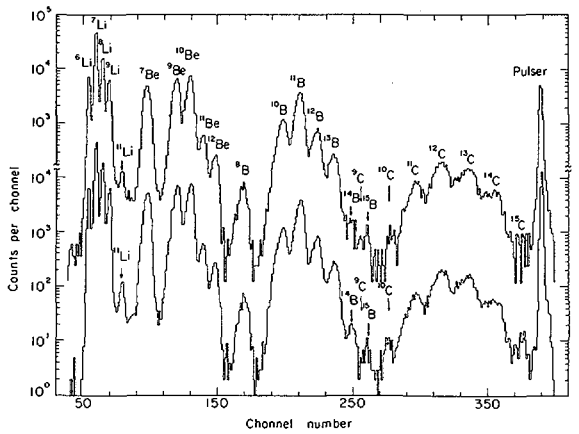

Fig. I–29. Improved Particle Identifier System. Shown above is a particle spectrum resulting from the improved particle identifier system that has been developed at Lawrence Radiation Laboratory, Berkeley. This new system allows the systematic identification of all energetic fragments of hydrogen, helium, lithium, beryllium, boron, and carbon. An additional bonus of this new system is that boron-14, boron-15, and lithium-11 nuclei have been identified for the first time.

bombarded with 5.4 billion electron volts (Bev.) protons in the external beam of the Bevatron, the new technique allowed systematic identification of all fragments of hydrogen, helium, lithium, beryllium, boron, and carbon (see Fig. I–29). Heretofore, photographic emulsions and radiochemical methods were used to gather information on only a selected few of the fragments.

The spontaneous fission of californium-252 was reinvestigated using this new system to gain information on very rare events in which the splitting of the californium nucleus into two massive fragments is accompanied by the ejection of a light fragment. Results showed the emission of 13 fragments: H^1, H^2, H^3, He^3, He^4, He^6, He^8, Li^6, Li^7, Li^8, Li^9, Be^9, and Be^{10}. The presence of these light fragments is of interest for the detailed description of the extremely distorted shapes occurring in nuclear matter at the exact moment of nuclear scission, *i.e.*, the precise moment of the division of an atom. In addition, the presence or absence of specific fragments provides information on the particle stability of previously unstudied species.

New Theory of Nuclear Structure

A partial theory of nuclear structure has been formulated at the Lawrence Radiation Laboratory, Berkeley, which is both fairly accurate and simple and goes beyond the simplest "liquid drop" model of nuclei which describes a nucleus as a fluid with properties built mainly on two kinds of force: surface tension, and electrostatic repulsion. It takes account of the principal effects of nuclear shell structure, but remains comparable in simplicity to the liquid drop model, which has been used for 30 years in describing trends in nuclear masses (or binding energies) throughout the periodic table.

The description of these trends, considered as functions of the numbers of neutrons and protons in a nucleus, has been a long standing problem in nuclear physics. The liquid drop formula of *Bethe* and *Weizsäcker* introduced in the 1930's, had for a long time served as a standard tool for representing, approximately, nuclear masses or binding energies. Over the years, a vast amount of experimental information has accumulated on the details of the deviations of nuclear masses from the liquid drop formula and on the related question of the deviations of nuclear shapes from the spherical form, which is the shape predicted by a liquid drop formula. The reasons for these deviations were understood in principle as caused by nuclear shell structure. These deviations, when plotted as functions of the number of neutrons and protons in a nucleus show irregular oscillations. Previous attempts at taking account of these effects had led to unwieldly expressions with dozens of adjustable parameters.

The new theory, with only three parameters beyond those of the liquid drop theory, approximately reproduces the oscillations in nuclear binding energies due to shell structure and in addition, gives a rough account of the nonspherical equilibrium shapes of nuclei. It is suited for the discussion of arbitrarily deformed nuclear configurations and gives a fair description of the critical shapes and barrier energies relevant for the theory of nuclear fission.

Even this new theory is by no means in perfect agreement with all experimental data, but its extreme simplicity has made it possible to isolate clearly the remaining defects. Some new insight into nuclear structure has already been achieved by recent attempts to interpret the newly seen discrepancies. The theory is expected to serve for some time as a useful replacement of the *Bethe-Weizsäcker* formula.

High Energy Fission Studies

Uranium is the only naturally occurring element which can fission at very low energies. At higher energies, lighter nuclei undergo reactions in which one or more heavy fragments are emitted but these results cannot be described by a simple extrapolation of the fission theory based on low energy data. It is now possible to study in detail the mass and energy of the fragments emitted in these high energy reactions using new techniques of particle detection and electronic instrumentation. Brookhaven National Laboratory has investigated the nature of the fragments produced by the interaction of 3-Bev. protons with uranium and bismuth targets. Results showed a broader distribution in the angle between pairs of fissions fragments produced at high energies compared to low energies where all fragment pairs are emitted very close to 180°. The greatest probability for fission occurred at angles which correspond to the motion of the fissioning parent in the beam direction. Interestingly, the experiments of fragment pairs show no evidence for the relatively slow, massive neutron-deficient fragments found in radiochemical experiments. Evidence about these fragments may appear in the results accumulated in the events in which only a single heavy fragment was observed (see Fig. I–28).

Improved Cross Section Measurements

An improved technique for determining activation cross sections of neutron reactions which lead to gamma-ray emitting radioactive nuclei has been found at the Georgia Institute of Technology, Atlanta. This method takes advantage of the high resolution of lithium-drifted germanium detectors and permits the identification of very low (long-lived) activities and accurate measurement of their neutron formation cross sections. Although the method is limited to nuclides emitting gamma-rays of well-established intensities, it has the additional advantage that natural elements often can be used as targets in place of expensive highly enriched isotopes, since all of the gamma activities can be identified and their half-lives followed simultaneously. Radiochemical separation often becomes unnecessary for identification and measurements, permitting shorter-lived nuclei to be measured.

If the cross section of one of the resulting activities in the natural sample under investigation is known to be accurate, it may be used as an internal monitor for the neutron flux. Otherwise, internal monitors can be added by mixing the powdered sample with aluminum and/or iron powders of the same grain size. From the ratio of manganese-56/sodium-24 (Mn^{56}/Na^{24}) activities formed from iron and magnesium in 14.4-Mev. neutron irradiations, it is possible to recognize any error arising from possible non-uniform mixing of sample and monitor powders. In cases where a stoichiometric [17] chemical compound is available, one of the constituents often can be used as an internal monitor. The procedure of mixing the monitor uniformly with the sample to be investigated eliminates geometrical errors present in the normal procedure of sandwiching the sample between foils that act as flux standards. This method can be applied only when the high resolution of lithium-drifted germanium detectors permits all of the gammas from sample and monitor activities to be identified simultaneously. This feat was not possible with former low-resolution detectors, such as sodium iodide scintillation spectrometers which have been in use for at least 10 years for neutron cross section measurements. The technique has been applied to cross section studies of selenium,

[17] *Stoichiometric*—Having the exact proportions of elements to make a pure chemical compound.

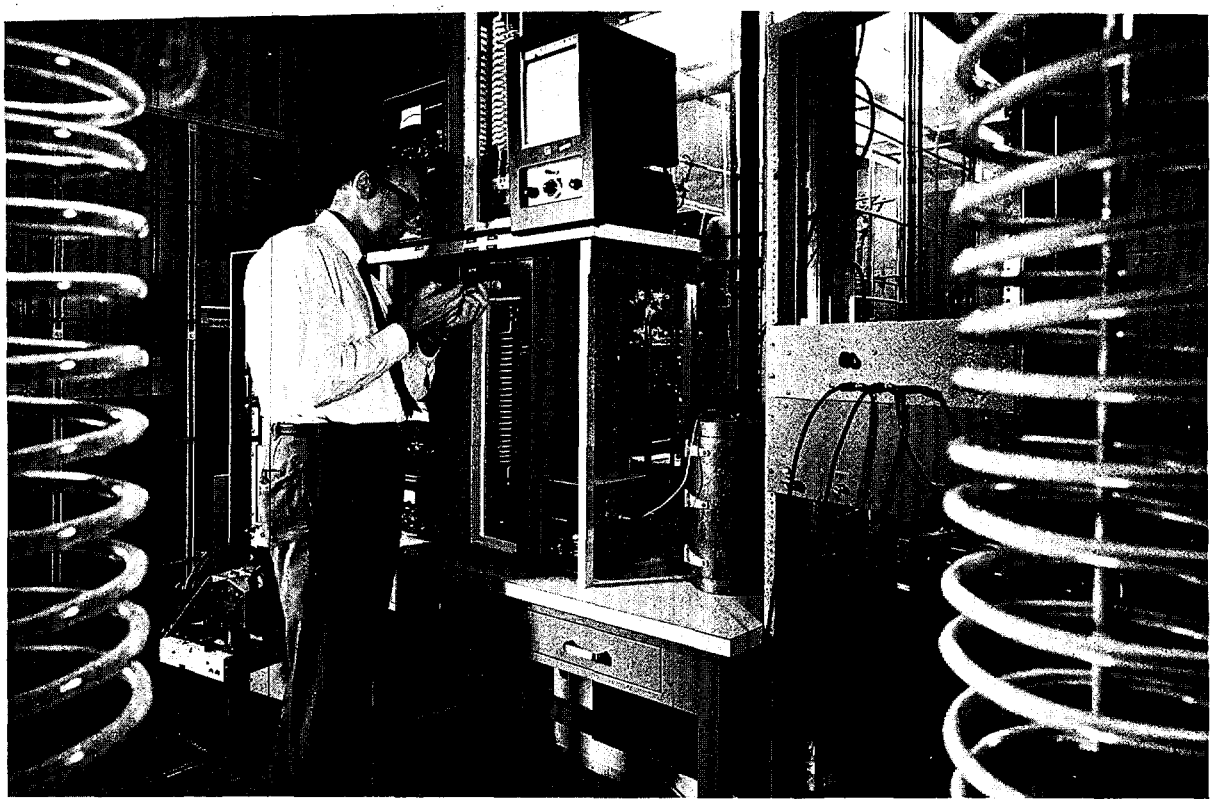

Fig. I–30. Chemical Effects of High-Energy Recoiling Atoms. Using the gas-liquid chromatographic apparatus, chemists at Brookhaven National Laboratory are investigating the products formed when atoms of very high kinetic energy interact with organic molecules. After irradiation, either in a reactor or accelerator, a very small amount of target material is injected into the apparatus with a hypodermic syringe, as shown in photo. As the material passes through the spiral column, the different organic species travel at different rates and are separated one from the other. The material passes through a radiation detector after leaving the column and thus the amount of radioactive content of each species is determined. Analyses are carried out automatically on samples containing such short-lived radioactive products as carbon-11, nitrogen-13, and oxygen-15 and the data recorded on magnetic tape. The results are then evaluated and corrected on a computer.

bromine, mercury, and germanium isotopes with 14.4-Mev. neutrons.

The neutron cross sections are important for basic cross section systematics leading to an understanding of the mechanism of neutron reactions at higher energies, and some of the cross sections are of interest in reactor physics and in nuclear astrophysical theories of the nucleosynthesis of the elements in stars.

HEAVY ELEMENT CHEMISTRY

The elements heavier than uranium (element 92) have all been synthesized and produced by man—and represent one of the greatest advances of modern science. These heavy elements have increased by ten percent the number of known elements as shown in the Periodic Table. The study of their chemical behavior and of their various isotopes is vital to the success of the atomic energy program, because they offer so many opportunities for use of nuclear radiations such as isotopic power in "small packages" and radiation sources for industry and medicine. Further knowledge of nuclear, atomic, and molecular structure is increasingly being shaped by discoveries and theories concerning this new group of elements.

275-845 O—68——5

Electronic Structure of the Actinides

The actinide elements[18] have long been recognized as forming a second rare earth series, similar to the lanthanides but with important differences. The lanthanide elements have similar chemical properties because they have the same number and arrangement of electrons on the outside of the atom. They differ from one another in that the successive members of this group have an increasing number of electrons put into an incomplete inner shell (the 4f shell[19]) where they are protected and do not participate when the rare earth atom reacts chemically with other atoms to form a compound. However, if energy is supplied to the lanthanide atom a 4f electron can be promoted to an outer electron in the 5d shell where it can react, increasing the valence. The actinide elements have an analogous incomplete inner shell (the 5f shell) with the same possibility of promotion to the appropriate d shell giving higher valences. For the actinides, however, the f-level to the d-level energy is less, resulting in the possibility of promoting more f electrons and consequently of having higher valences than the corresponding lanthanides. The energy is measured most precisely by atomic spectroscopy, and enough lanthanide and actinide spectra have now been analyzed to permit description of the variation of the binding energies of the different types of electrons as a function of atomic number and degree of ionization. These variations show a good correlation with chemical behavior.

Plutonium studies. Actinide spectra contain numerous lines of different wavelengths, which makes it difficult to determine those energy levels giving rise to the transitions and even more difficult to identify the levels in terms of quantum numbers and electron configurations.

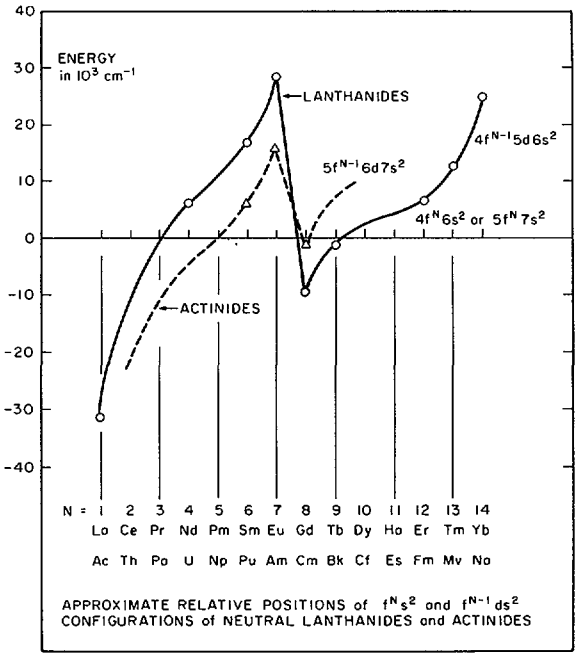

Fig. I–31. Electronic Structure of the Actinides. Some of the results of a cooperative study of electronic structure of the actinides at Argonne National Laboratory are presented graphically above. Relative energies of two configurations, one with N electrons in the f shell and the other with one d electron leaving only (N–1) f electrons. The figure, therefore, shows the tendency for an inner non-bonding electron to be promoted to an outer valence electron, and has a good correlation with the tendency of a lanthanide or actinide element to exist in more than one valence state. Working with Argonne on this study were Lawrence Radiation Laboratory, Berkeley and Livermore, Los Alamos Scientific Laboratory, and the French Centre National de la Recherche Scientifique.

A complete study has been made for plutonium, as a joint project of Argonne National Laboratory, Lawrence Radiation Laboratory at Livermore, and the Centre National de la Recherche Scientifique at Bellevue, France (see Fig. I–31). The interpretation was aided by comparison with theoretical calculations using computer programs developed mostly at Argonne, but also in part at Los Alamos and Berkeley. The plutonium analysis indicates that for the other actinide elements, with less data available, the relative positions of the most stable configurations for these elements can nevertheless be derived with some confidence.

[18] *Actinide elements* refer to a series of elements starting with actinium, atomic number 89 and going through to lawrencium, atomic number 103. The *lanthanide* or rare earth elements refer to a series of elements from lanthanum, atomic number 57 through lutetium, atomic number 71.

[19] *4f shell*—Electrons can be considered to be located in shells and subshells of different energies. The number 4 refers to the fourth shell and f refers to one of the subshells in the fourth shell.

Oxidation states. For the major part, electronic spectroscopy has been used to identify various oxidation states of actinides and lanthanides. A more difficult task is to explain the chemistry of a given oxidation state. The difficulty stems from the relatively small effect of external environment on the electrons. This is especially true for the lower oxidation states. Studies in this area are underway at Pacific Northwest Laboratory (PNL).

For an actinide chemist, it is encouraging to note that the external effect is larger for actinides than for lanthanides, although it is generally much less than for the d-transition elements(scandium through copper and yttrium through palladium). The fact that f electrons are shielded from the environment requires careful examination of the electronic spectra (f→f transition) in order to determine the nature of the environment. Whereas the identification of an oxidation state or of the environment of a d-transition element requires only relatively crude qualitative analysis, actinides require careful quantitative analysis, not only of energy levels, but of transition probabilities and perturbations of transitions probabilities as a function of temperature and energy.

Few such careful analyses have been made, the most outstanding being that of tetravalent uranium in an octahedrally coordinated environment. Protactinium has also been examined in octahedral fields. Some preliminary efforts have been made to calculate intensities of actinide spectra of aqueous solutions but the approximations necessary for these analyses were rather severe.

Crystal studies. Some work has been done at Pacific Northwest Laboratory and at the University of California at Los Angeles with actinides incorporated into the host crystals, thorium dioxide (ThO_2) and lanthum chloride ($LaCl_3$). The spectra of actinides in fused chlorides have been examined at PNL with partial success in identifying the configuration about some actinide ions. This has only been possible where comparisons could be made with compounds whose structure and spectra were known. The theory simply has not progressed to the point that configurations can be predicted on the basis of spectra alone. This inadequacy has necessitated a turn to the general theory in attempt to make it more useful.

New Isotopes of Heavy Elements

Four new heavy element isotopes have been discovered: berkelium-251 (Bk^{251}), californium-242 (Cf^{242}) and Cf^{243}, and mendelevium-258 (Md^{258}).

Californium-242 and -243 were found by both LRL–Berkeley, and ANL, using different approaches. At Berkeley, Cf^{242} and Cf^{243} were produced by bombardment of certain uranium isotopes with carbon-12 ions in the Heavy Ion Linear Accelerator (HILAC). At Argonne, the same isotopes were produced by helium-3 (He^3) reactions with curium-242 (Cm^{242}) and Cm^{243}.

Argonne also found berkelium-251 by determining that einsteinium-255 (Es^{255})—produced in thermonuclear weapons tests—in addition to emitting beta particles also emitted alpha particles to produce Bk^{251}. Based on this observation, it was possible to isolate Bk^{251} from reactor-produced einsteinium and demonstrate that it has a 57-minute half-life.

A lower limit to the spontaneous fission half-life of einsteinium-255 has been set at 24 million (2.4×10^7) years. This means that, contrary to previous beliefs, there is no odd-odd nucleus whose ground state decays perceptibly by spontaneous fission.

The heaviest known isotope of firmly established mass number, mendelevium-258 was produced by a Berkeley-Livermore team using the HILAC at Berkeley to bombard einsteinium with helium ions. This isotope of mendelevium is particularly significant because it has a half-life of about two months which is unusually long for any isotope appearing in this extremely high region of the Periodic Table of the Elements. This means that it can be made in sufficient quantities to carry on substantial tracer chemical studies.

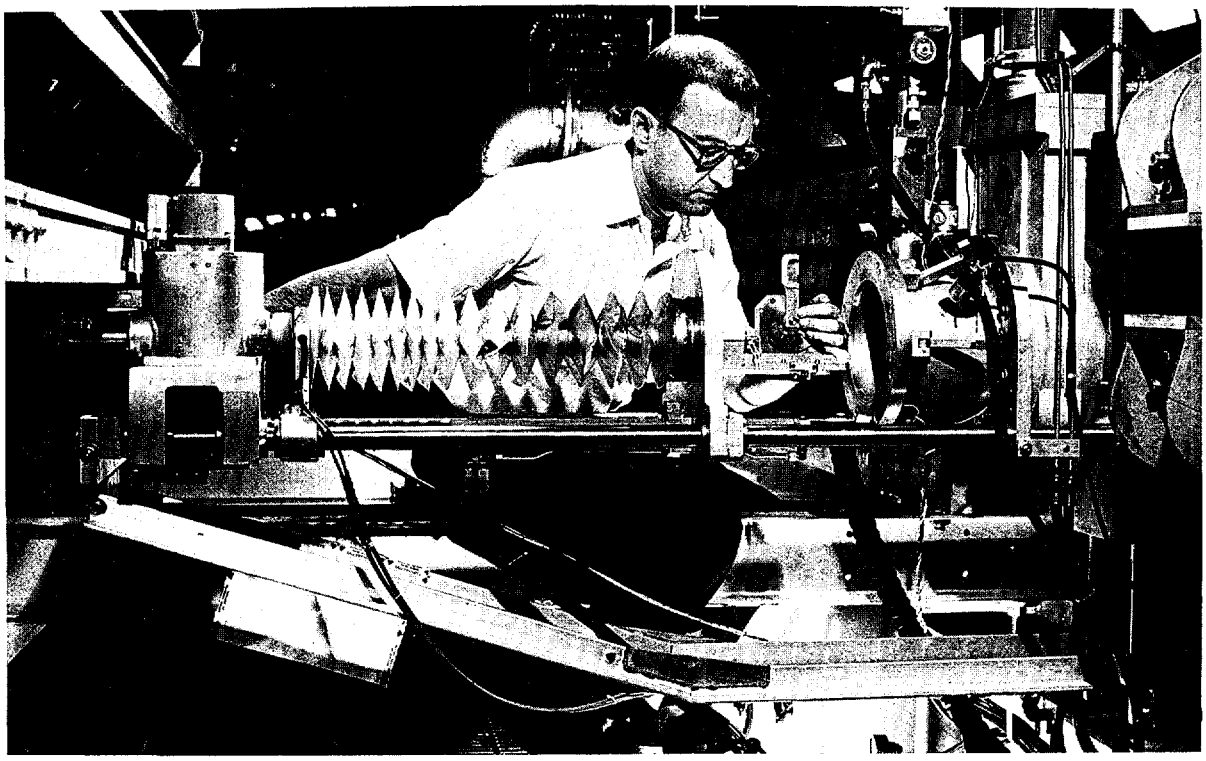

Fig. I–32. Proton Bombardment Study. A copper foil is placed on a target mechanism at the Alternating Gradient Synchrotron at Brookhaven National Laboratory. By measuring the radioactive products formed in such targets after irradiation with 30-Bev. protons, nuclear chemists are studying details of interaction between high energy particles and complex nuclei. Since the accelerator can operate only under very good vacuum, all targets must be pumped out in an air lock (round opening at *right*) before they can be inserted into the operating portion of the accelerator. To the *left* of the target an expandable plastic jacket prevents dust particles from settling on the shaft which drives the target mechanism.

RADIATION CHEMISTRY

The area of radiation chemistry investigation is concerned with the chemical effects of ionizing radiation and of related chemical effects of ultraviolet light and other radiant energy. The interaction of energetic radiation—gamma rays and X-rays, fast electrons, alpha and other charged particles—with matter is extremely complex. Very high-speed measurements of primary physical and chemical events caused by radiation have led to the investigations of previously little known transient chemical species. Theoretical studies are concerned with the mechanism of the dissipation of absorbed energy, delineation of the role of diffusion and of ions and radicals in chemical reactions.

Silica and Silica-Alumina Gels

Silica and silica-alumina gels are hard solids, chemically similar to sand or quartz; however, the gels are sponge-like in their high porosity and, hence, possess a very large internal surface area that is accessible to the molecules of chemical reagents. Silica-alumina gel is an important catalyst for various chemical reactions (notably those involved in petroleum cracking) at elevated temperatures. Gamma irradiation of silica and silica-alumina gels produces localized centers that exhibit chemical activity. At the AEC's Radiation Laboratory, University of Notre Dame, the behavior of such centers is being studied by a number of methods. They include measurement of chemical products, thermolu-

minescence, chemiluminescence, and electron spin resonance (ESR) signals. These measurements have been made under a variety of experimental conditions and include measurements at temperatures ranging from —196° C. to above room temperature. By using a combination of methods and experimental conditions, it is possible to associate radiation-induced chemical activity with specific radiation-produced color centers and thus to gain some insight into the "why" and "how" of radiation-induced chemical activity and perhaps of ordinary catalytic activity. For example, the behavior of isopropylbenzene in conversion to benzene on irradiated silica gel was found to parallel that of certain color centers identified as electrons trapped at oxygen vacancies in the silica matrix. In irradiated silica-alumina gel, certain color centers (which, in this case, impart a visible color to the solid) have been identified as positive holes trapped on aluminum atoms present in the matrix. Such color centers have a characteristic ESR signal, the intensity of which is a measure of the number of color centers. The chemical activity of an irradiated silica-alumina sample (in this case, in conversion of isopropylbenzene to benzene) has been shown to correlate with the visible color and the intensity of the ESR signal (see Fig. I–33). The addition of isopropylbenzene destroys both the color and the ESR signal of an irradiated silica-alumina sample with concomitant formation of benzene.

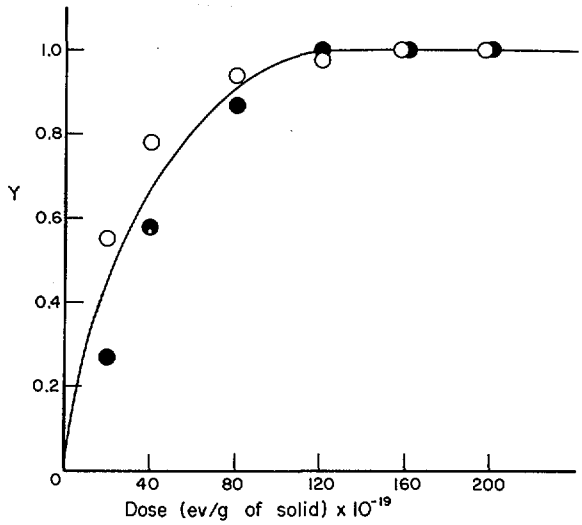

Fig. I–33. Silica and Alumina Gels. This diagram from the Radiation Laboratory at the University of Notre Dame, illustrates the yield "Y" of radiation-produced centers in silica-alumina (relative to the maximum value) as a function of dose: O, color centers as measured by electron spin resonance (ESR) signal- intensity; ● centers of chemical activity for conversion of isopropylbenzene to benzene. The ESR signal intensity and the chemical activity grow in the same manner with increase in radiation dose.

Pressure Effect on Hydrated Electron

Research at AEC laboratories and elsewhere has established that the hydrated electron (electron in a cavity of water molecules to which it is bound by electrostatic forces) is produced in the radiolysis of aqueous solutions. An important property of such hydrated electrons is their partial molal volume, $\overline{V}$, defined as the change in volume of a relatively large amount of water on addition of one mole of a solute (in this case, the electron). When the solute is a charged particle such as an ion or electron, the partial molal volume may be negative; in such a case, contraction of water molecules around the charged particle causes a decrease in volume that exceeds the intrinsic volume of the added particle. For the occurrence of a chemical reaction, the reactants generally must come together with sufficient energy to surmount an energy barrier to the reaction. In such a reactive state, the combined reactants constitute an "activated complex" which has the properties of a molecule, including a partial molal volume. The difference between the partial molal volume of the activated complex and the sum of those of the reactants determines how pressure affects the rate of a chemical reaction. Therefore, study of the effect of pressure on the rate of an appropriate hydrated-electron reaction provides a possibility of determination of the partial molal volume of an electron (partial molal volumes of various ions being known). A 10- fold increase in the rate of such a reaction at 1,000 atmospheres corresponds to a decrease in volume of approximately 57 milliliters per mole on forma-

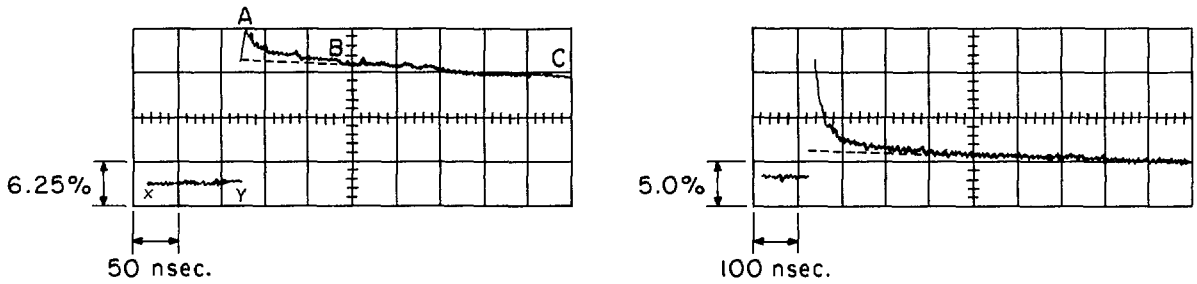

Fig. I–34. Nanosecond Pulse Radiolysis. On the left is a graphic presentation of pulse radiolysis of pure water data as obtained at Argonne National Laboratory through an oscilloscope picture of the reaction of hydrated electrons in a "spur." The abscissa represents time, with one small square being 50 nanoseconds, and the ordinate represents light absorption, with one small square being 6.25 percent absorption. The light absorption is proportional to the concentration of hydrated electrons. On the *right* is a pulse radiolysis of a solution of 0.3 moles/liter biphenyl in cyclohexane. The oscilloscope picture shows the rapid decay of biphenyl negative ions in the "spur." The abscissa represents time, with one small square being 100 nanoseconds, and the ordinate represents light absorption, with one small square being 5 percent absorption. The light absorption is proportional to the concentration of biphenyl negative ions.

tion of the activated complex. Such a result could yield a value for the partial molal volume of the electron of the order of 40 to 60 milliliters per mole, depending on the particular reaction involved.

At the AEC's Radiation Laboratory on the campus of the University of Notre Dame, certain aqueous solutions were chosen for study in which a particular radiolysis product might serve as an indicator of an effect of pressure (varied from 1 to 7,000 atmospheres) on the fate of hydrated electrons produced by gamma-irradiation. The first such solutions studied contained 0.01 *M* glucose and sodium bicarbonate at concentrations between 0.005 and 0.5 *M*. The hydrogen radiolysis yield, $G(H_2)$, was governed by a reaction between the hydrated electron and bicarbonate ion. As pressure was increased from 1 to 7,000 atmospheres, $G(H_2)$ increased from about 0.9 to about 2.4. Such data were interpreted to give for the electron a value of $\overline{V}$ in the range -6 to -1 milliliters per mole based on a value for the proton of $\overline{V}=-5$ milliliters per mole. Approximate equality of the values for the electron and proton is consistent with their having the same quantity of charge and negligible intrinsic volumes. In more recently completed work, the reaction between a hydrated electron and a water molecule was shown to accelerate with increase in pressure. The range of values obtained for $\overline{V}$ of the electron was in good agreement with the previous estimate.

Nanosecond Pulse Radiolysis

It is generally assumed that the action of high-energy radiation on liquids produces positive ions and electrons, and that the radiation energy is not deposited uniformly throughout the medium, but is lost in discrete amounts along the radiation track. Losses of this nature give rise to "spurs," i.e. high concentrations of ions in isolated regions. In the "spurs" the ions and electrons react together very rapidly. Some ions diffuse away from the "spur" and react in the bulk of the liquid with ions that have diffused from other "spurs." At Argonne, a Van de Graaff generator has been redesigned so that it produces nanosecond (one-billionth second) pulses of electrons with energies of 3 million volts and currents of about 2 to 5 amperes. These intense radiation pulses produce up to ten micromoles per liter of ions in a liquid. This concentration of a light-absorptive species is quite sufficient for the species to be observed directly by fast absorption spectroscopy. With this technique, species with lifetimes less than one-half a nanosecond can be observed. This is 1,000 times faster than previous measurements.

The results in water are illustrated in the left portion of Figure I–34, where the decay

of hydrated electrons in pure deoxygenated water versus time is followed. This oscilloscope picture is the first direct observation of reactions in a "spur." The XY portion of the trace defines the 100-percent transmission of the analyzing light by the water before the radiation pulse hits the solution at a time represented by Y. The hydrated electrons are produced at Y, and absorb a portion of the analyzing light moving the trace to A. The portion AB is the rapid reaction in the "spurs," while the slower portion BC is due to reaction in the bulk of the liquid. Addition of sodium hydroxide, which removes hydrated protons, eliminates about 50 percent of the "spur" decays while addition of ethyl alcohol removes hydroxyl radicals, eliminating the remaining 50 percent. Hence, the hydrated electrons must be reacting with hydrated protons and hydroxyl radicals in the "spur."

In pure ethyl alcohol similar results are obtained, but the addition of sodium hydroxide completely eliminates the "spur," indicating that the solvated electrons only react with the positive ion.

In a hydrocarbon such as cyclohexane, the reaction of the negative ion is observed by adding a solute such as biphenyl which reacts rapidly with an electron to give an observable negative ion. A typical decay curve is shown in the *right* portion of Figure I–34. In this case, the path of decay of the negative ion is entirely via decay with the positive ion. Here the "spur" reaction is much larger than in water; in keeping with the much lower dielectric constant of cyclohexane.

The above data illustrate that the model of the radiolysis of liquids described in the first paragraph is essentially correct, and the data will define exactly the size of the "spur" and the nature of the primary processes in the radiolysis of liquid.

OH, The Free Hydroxyl Radical

Free radicals or other reactive species may be produced from many gases under the influence of intense heat, energetic light, or beams of subatomic particles. Often in systems of practical importance the free radicals can undergo a variety of reactions with other molecules which may be present, so that the nature of the products formed depends on the relative rates of the different reactions. Hydroxyl (OH) radicals are produced, for example, in flames, explosions, polluted air, and water (H_2O) when exposed to ultraviolet or nuclear radiation, but little is known of the rates of reaction of OH in these systems. The reactions of OH with other gases are being studied at the Los Alamos Scientific Laboratory. OH radicals were produced in the presence of other gases by exposing the gases mixed with H_2O vapor to a short burst of ultraviolet light, which decomposed the H_2O into hydrogen (H) atoms and OH radicals. The number of OH radicals remaining at various times after their formation was determined by a technique known as absorption spectroscopy, which depends on the fact that the OH radicals selectively absorb light of certain known wavelengths. The rate of the reaction of OH with the added gas can then be deduced from the rate of disappearance of OH. The results show that OH radicals react much faster with the hydrocarbons-methane (CH_4), ethane (C_2H_6), propane (C_3H_8), and iso-butane (C_4H_{10})_ than do most other radicals at ordinary temperatures. This suggests that reactions of hydrocarbons with OH may be important in polluted air. Further studies of OH reactions may help show how planetary atmospheres behave under the influence of solar radiation, and how the various products of flames and explosions are formed.

Excited Molecules in the Liquid Phase

When materials are subjected to ionizing radiation, it is known that some of the molecules receive extra energy and thereby become excited. Thus, a knowledge of the chemistry of excited molecules is required in order to understand radiation effects in materials. At the present time, little is known about the reactions of these intermediates in the liquid phase. Work at Atomics International, Canoga Park, Calif., has suggested a new interpretation of radiation pro-

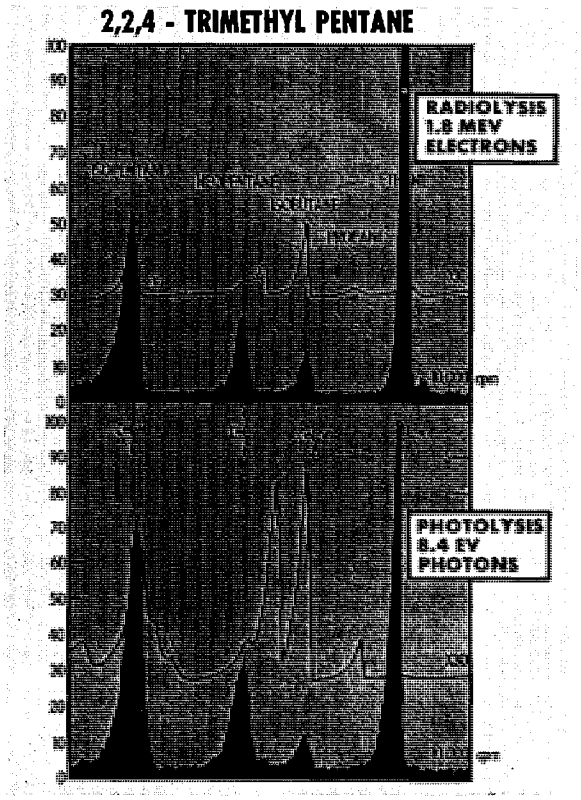

Fig. I–35. Excited Molecules in the Liquid Phase. Studies at Atomics International, Canoga Park, Calif., has shown that only certain fragmentation products formed in radiolysis of hydrocarbons can be accounted for by reactions of the excited molecules. The above are gas-radiochromatographs showing the products of radiolysis and photolysis of 2,2,4-trimethyl pentane. The *upper* curves show the total yields of products, *lower* (filled in) curves show the yields of radioactive products.

tection. It has been shown that only certain of the fragmentation products which are formed in the radiolysis of hydrocarbons can be accounted for by the reactions of the excited molecules. A radiochemical technique is used to compare the fragment radicals formed in radiolysis with those formed from excited molecules (see Fig. I–35). This technique is based on generating, in the liquid, a small number of radioactive free radicals which react with the other free radicals normally produced yielding radioactively labeled products. In essence, the radioactive free radical provides a means for the experimentalist to see what transient radicals are present in the system being irradiated. These studies showed that only certain of the fragmentation products formed in the radiolysis of hydrocarbons can be accounted for by the reactions of excited molecules. Also it was found that these excited molecules, although very short lived—they survive for only one one-hundredth nanosecond (10^{-11} of a second)—will react with excited aromatic solutes. This reaction can account for the known effect whereby the radiation decomposition of liquids is reduced by the addition of an aromatic solute to the liquid.

Photochemistry of Complex Ions

Coordination compounds comprise a class of substances formed between almost any metal ion and a variety of chelating agents or groups called ligands. These compounds are generally colored—often brilliantly—and the theory of the higher energy states whose presence is responsible for the colors is coming to be fairly well understood. Recent research shows that coordination compounds very often are photosensitive, *i.e.*, react chemically on absorption of light, and, moreover, that the nature of the chemical reaction can depend on the choice of wavelength of the light used.

Work at the University of Southern California (USC) Los Angeles, has led to the establishment of a set of rules for the behavior of trivalent chromium coordination compounds. In terms of these, it was predicted that the ion thiocyanate pentammine chromium (III) [$Cr(NH_3)_5(NCS)^{+2}$] in water solution, should release primarily ammonia (NH_3) rather than thiocyanate (NCS^-) when irradiated with visible light. This prediction, which is the opposite of what the compound does on heating, was confirmed.

Chromium compounds can also re-emit light, *i.e.*, as fluorescence of phosphorescence; in fact, the phosphorescent effect is closely related to the ruby laser, since ruby derives its color from a coordinated chromium "impurity" and the red light of the laser is that of the phosphores-

cence of the chromium. The USC work includes studying such light emission from various other chromium compounds, and with concurrent measurements of their photochemical sensitivity. Thus, the compound tetra thiocyanatodiaminechromium (III), $[Cr(NH_3)_2(NCS)_4]$, when dissolved in a mixed solvent "soup" which freezes to a glassy state on cooling, phosphoresces increasingly as the system is cooled; however, the light stimulating the phosphorescence also causes a chemical reaction, and it is found that at the "glass point", the phosphorescence increases strongly while the chemical change becomes less important. It could thus be determined that there was some third process which, while it interfered with the phosphorescence, led to a chemical reaction, and that this third process rapidly becomes less important as the system becomes rigid. The inference from this observation is that, contrary to a prevalent opinion, the energy state that reacted chemically is not the same as the energy state responsible for the phosphorescence.

Radiolysis of Liquids

At the University of Delaware, Newark, studies have been conducted in an effort to identify the excited molecular species formed when ionizing radiation, such as X-rays or gamma rays, pass through liquid organic matter. The manner in which a significant portion of this energy is imparted to the organic molecules is in some aspects very similar to the manner in which organic matter absorbs high energy photons of light in the ultraviolet region of the spectrum (photochemistry). It was found that the nature of the excited molecular states produced by the absorption of light photons and those produced by gamma rays were quantitatively the same in at least two different organic systems and lead to a common decomposition product.

These results suggest the possibility that at least part of the energy absorbed by molecules irradiated with gamma radiation is low enough so that those additives which are successful in reducing the energy of the molecules excited by ultraviolet light would also be successful in preventing decomposition of these molecules when they are exposed to ionizing radiation. It may be possible that certain radiation damage, either in reactors moderated by organic materials or in other liquid materials exposed to ionizing radiation, may be minimized or possibly even eliminated completely.

The systems investigated have been the benzene-cyclopentanone (the latter compound is a cyclic ketone) and the cyclopentanone-1, 3-butadiene (a compound which is polyunsaturated, *i.e.*, has two C=C bonds) systems. In both instances, the cyclopentanone molecule is either electronically excited directly to an energy rich state or receives energy through molecular collisions to be excited to the same state. The decay of this state has been investigated both in photo-chemical and radiation chemical studies and both approaches have shown quantitatively that this excited molecule is a common precursor to a known photo and radiation decomposition product in both systems, namely, 4-pentenal (an unsaturated aldehyde). This is believed to be the first time there has been reported a quantitative identification of an electronically excited state which is the direct precursor to a radiation decomposition product.

THEORETICAL AND STRUCTURAL

Both theoretical and experimental research are conducted under AEC sponsorship to seek a better understanding of the molecular structure, properties, and processes that control chemical changes in substances.

Characterization of Orbitals

The chemical behavior of molecules is determined by the character of the orbital clouds over which electrons are distributed, and guessed-at qualitative orbital features have been used for some time for intuitive chemical reasoning. Recently, Ames Laboratory succeeded in the first quantitative theoretical calculation of the actual character of such orbitals for a

series of molecules by determining localized self-consistent field molecular orbitals, which furnish a rigorous and precise foundation for future use of corresponding chemical concepts (see Fig. I–36).

The wider application of quantum chemical calculations requires extreme accuracy in order to furnish a quantitative understanding of binding energies and relative stabilities of atoms, molecules, and crystals. The development of methods yielding such accuracy depends upon the resolution of various theoretical difficulties, such as the problem of electron correlation. This research has led to an approximation whereby it is possible to calculate the energies of the beryllium atom and ions of seven other elements, each having the same number of electrons, to within three parts in ten thousand, corresponding to an accuracy of a few kilocalories, which is near the energies of significance to chemical differences.

Energy Transfer in Ion-Impact Mass Spectra

A new and much more precise method of exciting molecules in order to produce ions for mass spectrometry is now in prospect as the result of research at Brookhaven National Laboratory on the details of energy transfer for low velocity ions to target molecules. The amount and kind of excitation transferred during these collision processes is deduced from the relative yields of fragments which arise from the decomposition of the excited molecules.

Electron impact ionization is the present technique used to produce excited ions which decompose to yield mass spectra. Many closely related molecules yield very similar mass spectra if the electron impact ionization technique is used, because the excitation deposited is frequently sufficient to obscure subtle differences in molecular structure. Ion impact, however, provides a means of depositing energy in such a way that a more precise control of the magnitude of the excitation in the target molecule is accomplished.

If relatively low velocity ions are used as projectiles, the bulk of the energy deposited in an ion impact process comes from the recombination energy of the projectile ion. Additional

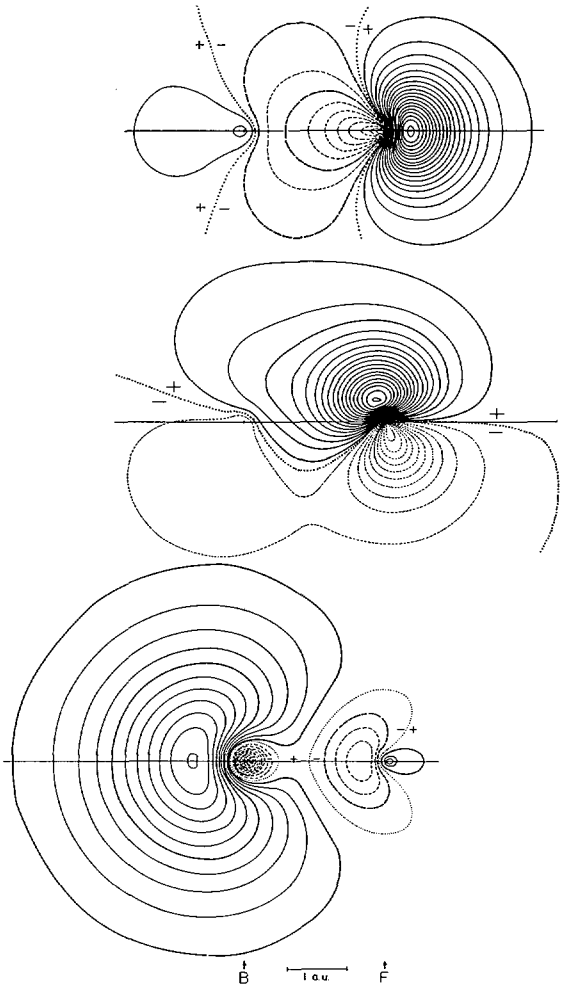

Fig. I–36. Characterization of Orbitals. With the use of a computer contour diagrams are prepared at the Ames Laboratory for a considerable number of localized molecular orbitals. The above are contour diagrams for the valence shell orbitals in the boron fluoride molecule. Cross sections in a plane containing the inter-nuclear axis are shown: (*upper* contours: lone pair on fluorine; *middle* contours: one of the three trigonally equivalent bond orbitals, with maximum in the plane of the paper; and *lower* contours: lone pair on boron). Fundamental theoretical calculations of this type are expected to be of great help to experimentalists in the prediction of properties of materials. At the bottom of the drawing the "*B*" stands for boron; the "*a.u.*" is for atomic unit (0.529 Angstrom); and "*F*" is for fluorine.

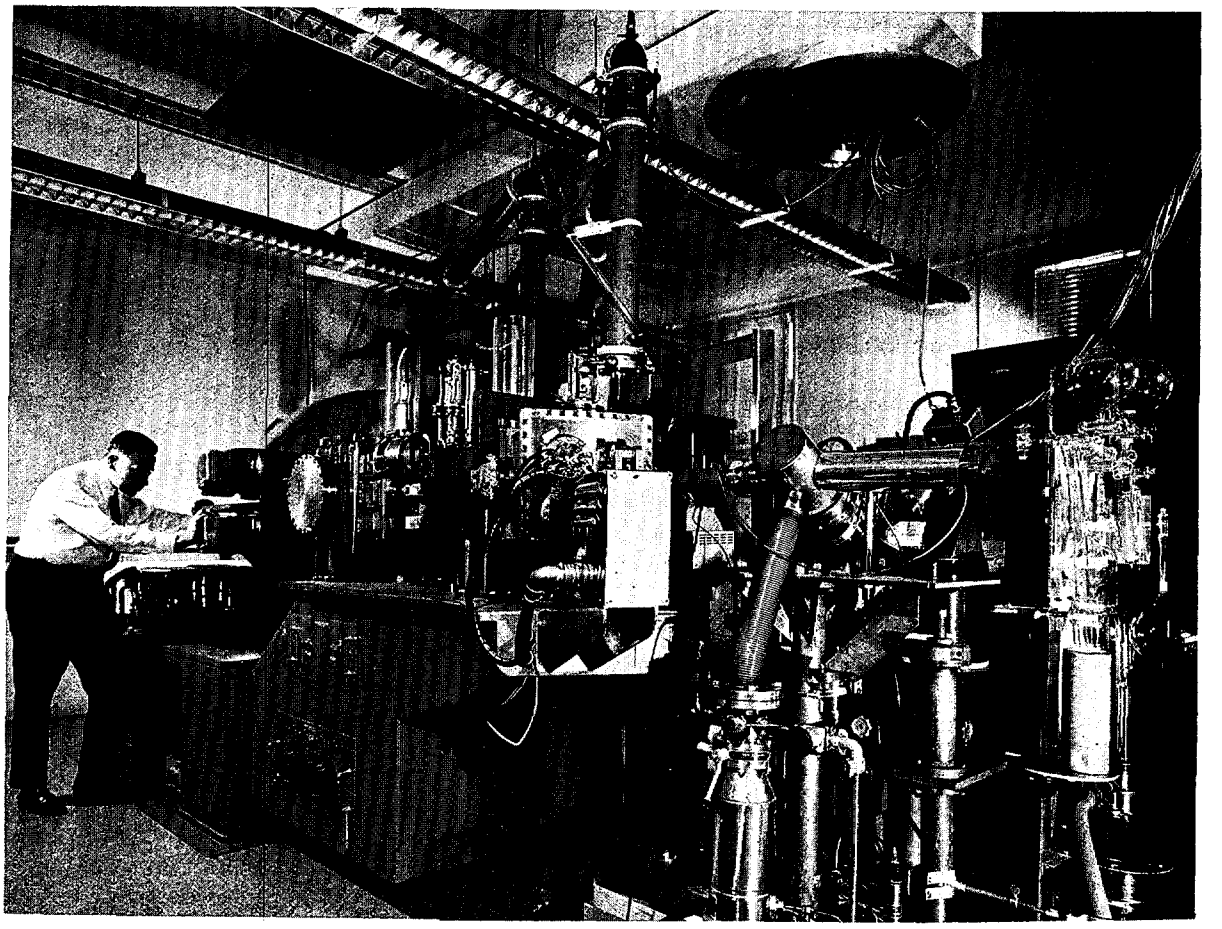

Fig. I–37. Energy Transfer in Ion-Impact Mass Spectra. The Brookhaven National Laboratory's electromagnetic isotope separator is being used to generate intense, low energy, mass analyzed beams of ions for research on ion-molecule collision processes. The beam of ions is brought out of the separator into the ion source of a small mass spectrometer (*front right* foreground) where collision processes take place with neutral gases introduced via the glass system on the right. The types of fragments produced by these interactions are collected and identified. The relative yields have provided valuable information dealing with energy conversion processes in isolated ion-molecule collisions.

energy can be deposited locally at the point of impact between the colliding molecules by conversion of the projectile ion's translational energy into internal energy of the target molecule. The Brookhaven isotope separator was used to produce an intense beam of ions with well defined and low velocities. The ion beam passed from the separator into a second mass spectrometer (see Fig. I–37), where it interacted with hydrocarbons such as isomeric butenes, propylene, and cyclopropane. The resulting fragments were collected and identified.

There are significant differences in the mass spectra obtained with 10 ev. ArD^+ ions,[20] for example, as compared with electron impact results. The process by which energy is transferred is believed to depend on the distance between the ion and molecule at the time of collision. If these distances are long, then parent molecule ions are formed. At shorter distances, a proton or deuteron may be transferred to form a new parent molecule ion which has little in-

[20] *ArD^+ ions*—The ionized form of the molecule formed by combining an argon atom with a deuterium atom.

ternal excitation energy. Decomposition of these slightly different ionic structures take place with significantly different rates and produce easily observed differences in the distribution of fragments. This technique of using rare gas hydride or deuteride ions to produce ion-impact mass spectra also provides a unique means of generating "protonated" molecules with very little excitation energy.

NMR Studies of Proton Exchange

Nuclear magnetic resonance (NMR)[21] studies at the Los Alamos Scientific Laboratory of hydrogen (proton) exchange in room-temperature solutions of water in liquid ammonia (NH_3) containing up to 50 percent water, have conclusively confirmed recent, less comprehensive work done elsewhere indicating that these exchange reactions take place much more slowly (10–1,000 times per second) than had previously been thought (100 million times per second). Proton exchange consists of hydrogen nuclei (protons) moving back and forth between the water and ammonia molecules in solution (see Fig. I–38).

Ammonia-water systems are of particular interest because they offer the opportunity for the study of exchange processes in systems involving hydrogen bonding, *i.e.*, where weak linkages between molecules occur through electron exchange interactions involving a hydrogen atom. Since water itself is a hydrogen-bonded liquid, the understanding of much of the solution chemistry of both inorganic and biological interest rests upon a basic knowledge of the role of the hydrogen bond in processes occurring in solution. The NMR technique lends itself well to such studies because the resonance absorption of radiofrequency radiation by nuclei depends upon the environment of the nucleus under observation, and this in turn is greatly altered if the nucleus is involved in an exchange process.

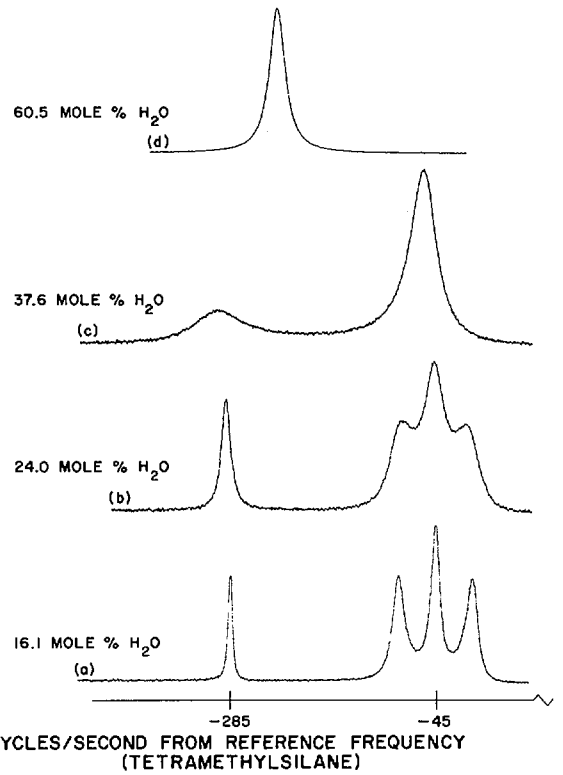

Fig. I–38. NMR Studies of Proton Exchange. Nuclear Magnetic Resonance (NMR) studies of water-liquid ammonia solutions at Los Alamos Scientific Laboratory show the increase in rate of proton exchange with increase in water concentration. Curve *a* shows a relatively low exchange rate. The protons remain in the H_2O and NH_3 molecules long enough (about 1 msec. or more) to produce sharp NMR peaks. The NH_3 resonance has three peaks because the nitrogen nucleus has three possible spin states producing three different nuclear magnetic fields. As the water concentration increases (curves *b* and *c*), this triplet becomes a singlet because the increase in the proton exchange rate causes the protons to "see" the N atom in an "average" spin state. When exchange becomes very rapid, a single peak characteristic of an average environment intermediate between NH_3 and H_2O is observed.

Sound Attenuation in He^3-He^4 Mixtures

Argonne National Laboratory has been carrying out experimental and theoretical investiga-

[21] *Nuclear Magnetic Resonance*—The nucleus of an atom, which has a positive electrical charge, spinning about on its axis behaves as a tiny magnet due to this spin. If a nucleus is placed in a constant magnetic field, it precesses (gyrates) about the direction of this magnetic field with a frequency which depends on the magnetic moment of the nucleus and its nuclear environment. This precession frequency can be found by measuring the resonance absorption of radiofrequency radiation by nuclei, that is, the resonance between the precession frequency of the nucleus and the frequency of an impressed radiofrequency magnetic field.

tions of helium-3 (He^3) and helium-4 (He^4), and He^3-He^4 mixtures. Such investigations are of continuing interest because of the pronounced manifestation of quantum mechanical effects in the macroscopic properties. For example, it has recently been shown experimentally that a 6-mole percent solution of He^3 in He^4 does not separate into two pure phases as would be expected from classical thermodynamics. Rather, for all concentrations lower than six percent the solutions remain homogeneous as a single phase, whereas more concentrated solutions do indeed separate out to a pure He^3 phase and a 6-mole percent phase. Theoretically, this is possible only because of quantum statistics.

These dilute solutions offer the possibility of investigating the interactions between fermions and bosons [22] and of supplying an experimental footing for many-body theories. Measurements of the sound attenuation, velocity, and the changes in these quantities with density are powerful microscopic probes in determining the interactions existing in these systems. At Argonne, an investigation has been made of the attenuation of sound in a 5-mole percent helium-3 and helium-4 solution. Experimental evidence has shown sound attenuation to take place. The observation of an excess attenuation in the dilute solution over that in a pure He^4 at low temperature arises because of an interaction of the sound waves with He^3 excitation. This is equivalent to thermion boson interaction. In addition, a theoretical explanation of the observed results has been developed. Work is being extended to understand further these interactions between fermion (He^3 excitation) and boson (He^4 excitation).

ANALYTICAL CHEMISTRY

Analytical chemistry makes use of a broad range of chemical and physical and nuclear techniques to measure the composition of matter. Today, it is frequently concerned with the detection of trace amounts of impurities as they may affect the specialized or critical properties of nuclear materials, or they may make use of newly developed methods, based on nuclear techniques, for the analysis of materials of chemical, geological, astronomical, biological, technological, or criminological significance, etc.

Fast Neutron Activation Analysis for O^{16}

As a part of the program to produce purer metals, Ames Laboratory is using fast neutron activation analysis as a reliable method for the determination of trace quantities of oxygen. The method uses the reaction of accelerated deuterons with tritium to produce 14 Mev. neutrons; the deuterons are accelerated to 150,000 electron volts and strike a titanium-tritide target. The nuclear reaction which is used to measure the amount of oxygen present is that oxygen-16 plus a neutron gives up nitrogen plus a proton ($O^{16}+n \rightarrow N^{16}+p$). The N^{16} is counted by its gamma radiation. Since the half-life of N^{16} is only seven seconds, the activation and counting are done very quickly and no residual radioactivity is left in the sample. A variety of materials have been analyzed for oxygen by this technique. In some cases, the oxygen levels as low as five parts per million (p.p.m.) were measured with an accuracy of one to two p.p.m. At higher levels, around 20 p.p.m., the accuracy is about two p.p.m. (approximately 10%) and the relative accuracy improves as the oxygen content increases. The method is of particular value in the case of volatile metals which cannot be analyzed by the standard vacuum fusion technique, and also is useful as a way of cross checking the other techniques used in the laboratory for oxygen determination.

Effects of Radiation in Chemical Analyses

During a chemical analysis of irradiated or originally radioactive materials, the effects of

[22] Statistics of the distribution of particles of a given type among the various possible energy levels take into account the quantization of the energy levels and the principle of the indistinguishability of the particles. Fermions (electrons, protons, He^3 atoms) obey *Fermi-Dirac* statistics: no more than one set of identical particles may occupy a particular quantum state. Bosons (light quanta, He^4 atoms, acoustical waves) obey *Bose-Einstein* statistics in which there is no limitation on the occupation number of any state.

radiation may be detrimental or useful, depending on the reactions involved. The nature of such effects in typical analyses is being studied at the Oak Ridge National Laboratory and ways to avoid or to exploit them, as the case may be, are being sought. For example, ammonium thiocyanate, which forms a colored complex with uranium, quickly decomposes when exposed to gamma radiation. It was found, however, that if stannous chloride is first added to the solution, the color is maintained for much longer periods of time.

Analyses for halide ions in aqueous solutions are frequently necessary in reactor technology. Gamma radiation has a deleterious effect on such aqueous solutions, thereby causing unreliable analytical results; possibly this is not the case for nonaqueous solutions. To check this possibility, the electroanalytical chemistry of the halide ions in dimethyl sulfoxide, a common nonaqueous solvent for inorganic substances, is being studied with a pyrolytic-graphite electrode.

Alizarin red S and similar hydroxyanthraquinone dyes have been used for the spectrophotometric determination of various metals. Zirconium (Zr) is one of the few metals that forms a colored complex with alizarin red S in highly acid solutions. The complex is very susceptible to radiation damage, because the quinone structure is readily attacked by reducing radicals. Therefore, a voltammetric method for determining Zr as the Zr-alizarin red S complex was developed. This method depends on the chemical reactivity of functional groups not readily affected by radiation.

Usually a concentrated (12 *M*) aqueous solution of hydrochloric acid will not attack gold, zirconium, tungsten, platinum, niobium or tantalum. However, under conditions of gamma radiation, five of these metals dissolve appreciably in this acid. Of the six metals, tantalum is attacked most slowly, and therefore, is shown to be the best of these metals for use as a container for highly radioactive acid chloride solutions. The increase in the dissolution rate results from the formation of chlorine during the irradiation. This effect of radiation can be exploited as a simple way to prepare dilute standard solutions of certain metals in acid chloride media. On the other hand, this same effect can be detrimental by introducing metallic interferences into analytical test solutions, for example, process solutions contained in inert metals or solutions in which inert metals are used as electrodes. Some alcohols (methanol, ethylene glycol, glycerol, phenol, catechol) scavenge the chlorine produced in gamma-irradiated chloride solutions and thus partly counteract the radiation effect.

Mössbauer Spectroscopy of Iron in Coal

Since the discovery of the *Mössbauer* effect,[23] emphasis has shifted from its use in studies of nuclear structure and transformations to its application as a tool in many areas of physics and chemistry. Carnegie-Mellon University, Pittsburgh, Pa., in collaboration with the Bureau of Mines of the U.S. Department of the Interior, has applied *Mössbauer* spectroscopy to the study of iron in coal. This work has provided information on the chemical state of the so-called "organic" iron present in some coals. Such information may conceivably enhance the nonfuel usefulness of this valuable mineral resource. (This use of the *Mössbauer* effect is another example of the widespread applications of advanced nuclear techniques in basic and applied research.)

Minerals identifiable in coals do not account quantitatively for all of the iron present, and it has been supposed that some sort of organic binding of iron in the coal is involved. Since the characteristics of the nuclear resonance absorption spectrum of iron-57, as revealed by the *Mössbauer* technique, depend on the oxidation state, nature of bonding, and environmental symmetry of the iron atoms, and because previous chemical studies had been unable to deter-

[23] *Mössbauer effect*—The recoil-free emission and absorption of gamma rays by nuclei bound in solids. In 1958, R. L. Mössbauer, a German physicist, found that if an excited nucleus which decays by gamma ray emission is embedded in a solid, it can give up its recoil momentum to the entire solid. Therefore, the emitted gamma ray will lose very little energy due to recoil and will thus have essentially the same energy as that of the excited state.

mine these properties of "organic" iron in coal, *Mössbauer* spectroscopy was attractive. By the *Mössbauer* technique, the iron can be observed without altering its chemical state or environment.

A number of samples of whole coal or vitrain, in rank from lignite (72% carbon) to anthracite (93% carbon), as free as possible from minerals, were selected for *Mössbauer* studies and chemical analyses. Several of the samples showed the well-known 2-line absorption spectrum of pyrite [iron (II) disulfide, FeS_2], a mineral known to occur frequently in coal. In addition, a widely-spaced 2-line component was shown by several of the spectra. This spectrum is different from the *Mössbauer* spectrum determined for any other iron compound. Since this sample also contained the highest content of "organic" iron according to the chemical analyses, its *Mössbauer* spectrum was probably that of "organic" iron in coal.

Interpretation of this spectrum was attempted through comparison of its quantitative parameters with those of known iron compounds. From the spectra, it was deduced that the non-pyrite iron in coal is in the iron (II) state, has four unpaired electrons, and is probably surrounded by six neighboring atoms. A few minerals and synthetic compounds of iron have *Mössbauer* parameters similar to those of the non-pyrite iron in coal, but these spectra are usually coupled with spectra of other forms of iron in the same materials. In addition, many of the similar spectra are unsymmetrical, in contrast to the symmetrical coal spectrum. These comparisons suggest that the iron is most likely bound in the coal to aromatic nitrogen atoms, though a clay-like silicate mineral or gel is also a possibility.

Mössbauer spectroscopy can be used as a guide in selecting coal samples for further studies of "organic" iron by chemical and other methods, and as an indicator of the stability or changes in the chemical state of the iron following various physical and chemical treatments of coal samples. Continuing *Mössbauer* studies of coal and known materials may eventually result in positive identification of the "organic" iron in coal.

PHYSICAL CHEMISTRY

The physical chemistry area of AEC-sponsored research is concerned with the relationship between chemical and physical properties of matter. New mathematical approaches as well as the use of computers form a vital part of this program.

Reactions of Gases on Metal Surfaces

Catalytic reactions are important in many chemical processes. In order to understand the fundamental nature of such reactions, the catalytic decomposition of ammonia has been investigated at the Ames Laboratory. The reaction was studied on a clean tungsten surface in a field emission microscope, an ultra-high vacuum device. The field emission microscope produces a million-fold magnified image of a metal single crystal and allows a direct observation of the surface layer of atoms. From such observations, it has been deduced that the accepted mechanism whereby gaseous nitrogen is produced by combination of adsorbed nitrogen atoms is incorrect. The production of adsorbed nitrogen atoms is the first step in the decomposition, but gaseous nitrogen is produced by reaction with more ammonia.

Surface reactions are also being investigated using the field ion microscope which has a sufficiently greater resolution than the field electron emission microscope so that adjacent atoms are resolved as shown in Figure I–39. On adsorbing acetylene new bright spots appear which are due to individual adsorbed molecules (shown in Fig. I–40).

Electrolysis at High Current Densities

Studies on the high-speed anodic dissolution of metals at the Lawrence Radiation Laboratory, Berkeley, have shown dependence of the

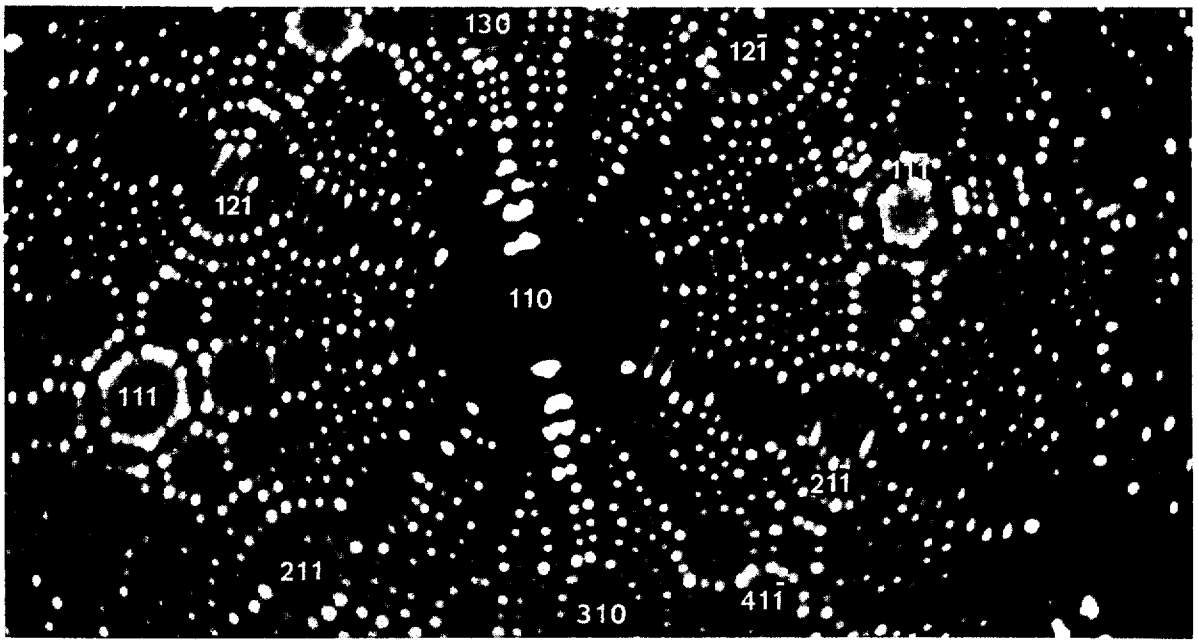

Figs. I–39 and 40. Reactions of Gases on Metal Surfaces. The *above* is an Ames Laboratory helium field ion micrograph of a clean tungsten emitter (radius about 300A) taken with the emitter at liquid helium temperatures. The (111) plane (spacings of 4.47A) is completely resolved with 23 atoms visible. Atom rows on the (211) and (121) planes are clearly separated (4.47A between rows) while adjacent atoms along atom rows are resolved on the (121) (distance between atom centers=2.74A). The helium field ion micrograph *below* is of the same tungsten emitter after exposure to acetylene. Several dozen new emission centers (indicated by *arrows*) are apparent on the (211) and (411) planes. Tungsten lattice atoms are missing on the (111) and (411) planes after the adsorption process.

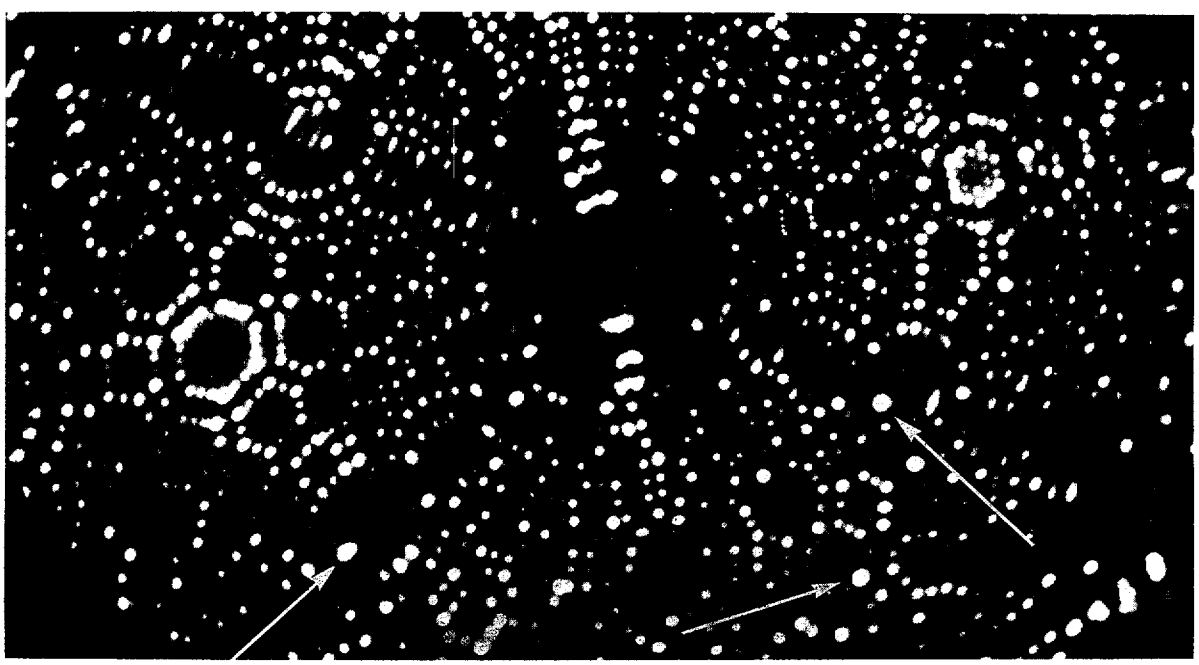

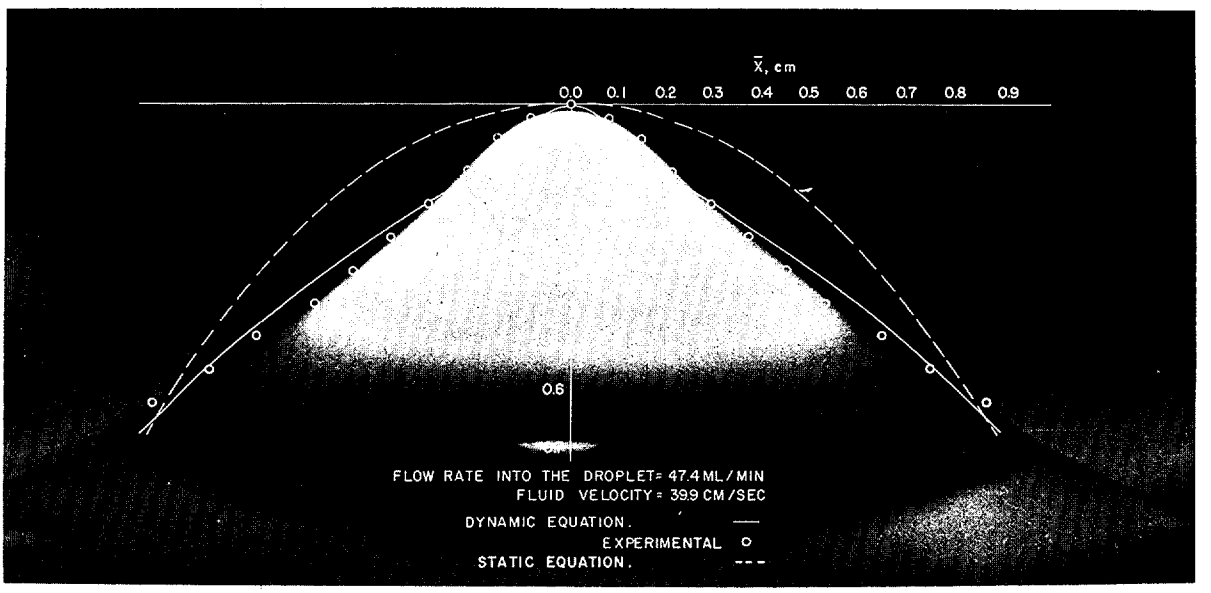

Fig. I–41. Formation of Liquid Drops. Extraction of uranium and other materials from solution, purification of metals by zone refining, heat transfer in steam generators, and transfer of oxygen in the lungs are examples of the broad range of applications in which the formation of drops is important. Recent work at the Ames Laboratory has produced a mathematical description of a forming liquid drop that is significantly more accurate than previous descriptions, especially when drops are formed so rapidly that the resulting train of drops approaches a continuous jet. A model has been developed which accurately describes the observable phenomena that occur during drop formation and makes it possible to study more subtle but equally important properties of drop systems which cannot be directly investigated by experimental techniques. Such properties would include, for example, oxygen transfer within drops of blood, and circulation of dissolved metal within the drops of a dispersed solution of metal ores. The graph shows a drop profile computed from this model. A photograph of the drop, in the process of formation, is superimposed on the profile.

nature of the dissolution process on hydrodynamic flow in the electrode gap, and on gas evolution from the cathode. It was also shown that the valence of the dissolution reaction, and thus the rate of dissolution, may strongly depend on current density and electrolyte composition. Electromachining techniques are relevant to the development of precisely controlled shaping processes for a large range of metals.

Influence of the electrolyte on the anodic dissolution reaction has been studied using copper and iron as anode material. The results show a marked influence of the current density on the apparent metal valence. This behavior may be understood by considering the change in anode potential with increasing current density, since both products found at higher current densities, namely copper^{+} (Cu^{+}) and iron^{3+} (Fe^{3+}), require a more anodic potential for their reversible formation from the metals than the alternate products Cu^{2+} and Fe^{2+}. Formation of a cuprous complex may explain the abnormalities observed in the copper-chloride system. Photomicrographs of the anode surface indicate a marked influence of the anodic dissolution reaction on surface structure.

INORGANIC CHEMISTRY

Under AEC-sponsored, broadly based inorganic chemistry studies, emphasis is placed on chemical compounds having extraordinary chemical bonding or structure.

Penta-Covalent Silicon

The element silicon, which lies below carbon in the Periodic Table, is capable of forming

275-845 O—68——6

compounds with structures similar to those of organic compounds containing carbon. Work by other inorganic chemists had suggested that there was something unusual about the chemistry and structure of a compound of silicon which can be formulated as silyldimethylamine $(SiH_3)(CH_3)_2N$. An X-ray diffraction investigation of this compound at Brookhaven National Laboratory provides the first firm structural evidence for the occurrence of silicon compounds in which silicon forms five covalent bonds. The molecule is actually a pentamer in the solid state, forming a 10-membered Si_5N_5 ring with three hydrogens and two nitrogens attached to each silicon atom. The discovery of this unusual bonding opens the way to a whole new area of inorganic chemistry which may have useful applications to polymer chemistry.

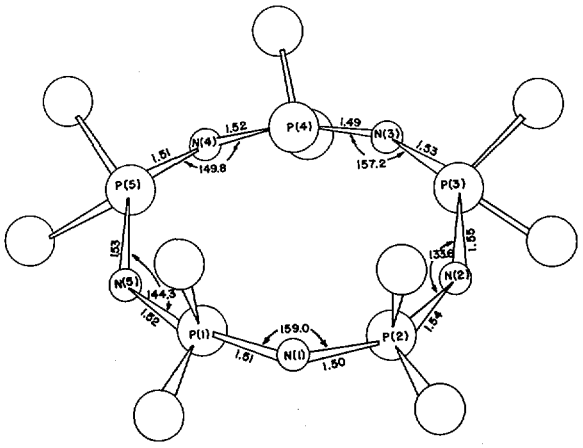

Fig. I–42. Structure of P–N Compounds. The molecular configuration of phosphonitrilic chloride $(PNCl_2)_5$, a structure determined at the Ames Laboratory. The compound exists as a 10-membered ring of alternating phosphorus and nitrogen atoms, with two chlorine atoms attached to each phosphorus. The presence of strong phosphorus-nitrogen bonds helps to explain the unusual stability of this type of molecule.

Structures of P–N Compounds

In recent years, plastics have come to be used in ever increasing amounts. However, at present almost all plastics are made from carbon-containing compounds and, therefore, have certain intrinsic deficiencies, such as poor resistance to heat. Increased attention has been focused on the formation of plastics and polymers which do not contain carbon. One series of compounds, involving phosphorus and nitrogen atoms, shows considerable promise. The diffraction of X-rays and the analysis of this phenomenon are presently being used at the Ames Laboratory to learn more about the atomic arrangement in these materials. Studies of a moderately large molecule of this type, phosphonitrilic chloride $(PNCl_2)_5$, show the presence of strong phosphorus-nitrogen bonds in this 10-membered ring (see Fig. I–42). Bonds between phosphorus and nitrogen that have been observed in other compounds in most of the earlier studies have not had this unusual stability.

Analytical Uses of Sodium Perxenate

The possible analytical uses of a relatively new chemical compound of the rare gas xenon, sodium perxenate (Na_4XeO_6), have been investigated at Argonne National Laboratory. The extremely powerful oxidizing properties of the higher valence states of xenon were used in several analytical applications. A rapid, simple qualitative test for manganese was devised, and analytical procedures involving the formation of highly colored solutions of manganese, chromium, and cerium were demonstrated. These experiments proved the feasibility of using xenon in its higher oxidation states as an oxidation reagent. The use of sodium perxenate rather than more conventional reagents results in considerable saving of time and effort, since the oxidation takes place instantaneously at room temperature thereby avoiding lengthy heating and cooling procedures.

The most convenient source of octavalent xenon is the white crystalline stable salt, sodium perxenate, which dissolves readily in water. In acid solution, perxenate oxidizes water, evolving oxygen, and yielding a solution of hexavalent xenon. The oxidation of manganous, chromous, and cerous ions in acid solution is rapid enough to compete favorably with the oxidation of water.

Manganous ion is oxidized to permanganate by perxenate at room temperature without the use of a catalyst. A rapid, simple qualitative test for manganese is carried out by observing the immediate appearance of the characteristic purple permanganate color when a few milligrams of solid sodium perxenate are added to a dilute acid solution of the unknown material.

This test can also serve as the basis for a quantitative determination of manganese. An aqueous solution of Na_4XeO_6 is slowly added, with vigorous mixing, to a dilute acid solution of the sample, and the absorption of the permanganate measured spectrophotometrically. This method has been used successfully to determine manganese in uranium and in magnesium metal.

HIGH TEMPERATURE STUDIES

Research in the high temperature chemistry area is concerned with physical and chemical properties of chemical compounds and chemical reactions at elevated temperatures (up to thousands of degrees) where their chemical and physical behavior differs appreciably from that at normal temperatures. The behavior of solutions of molten salts and oxides is emphasized because such studies yield fundamental thermodynamic data needed for the preparation of new materials.

Reaction of Graphite and Hydrogen

The reaction of graphite and hydrogen has been studied at Brookhaven National Laboratory at temperatures between 1,750° and 3,200° C. and at pressures from 1/100 to 1 atmosphere using resistively heated graphite filaments (see Fig. I–43). To carry out this work, an apparatus was built which can heat the filament at a rate of 50° C. per millisecond, measure the temperature continuously, and study the reaction for time periods of less than 1/10 of a second. The reaction rate increases both with temperature and pressure; in the ranges investigated, it changed 10,000-fold. At temperatures below 2,800° C., the reaction occurs on the surface

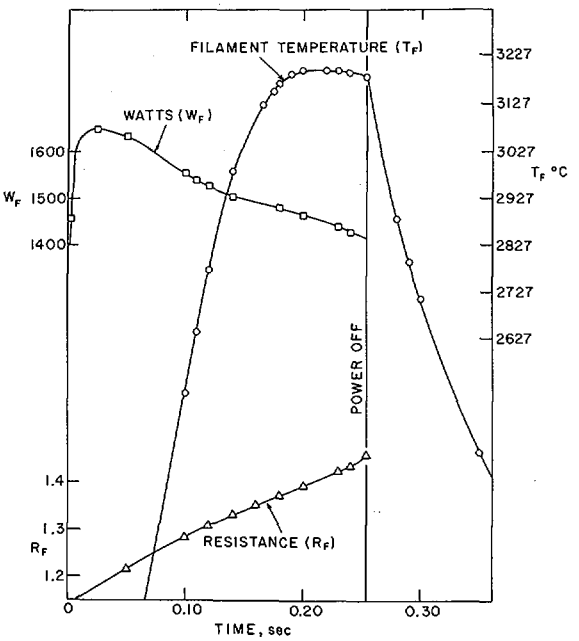

Fig. I–43. Reaction of Graphite and Hydrogen. Brookhaven National Laboratory graph showing the power, resistance, and temperature of a graphite filament when heated in 7.6 mm of hydrogen. This was obtained from an oscilloscope trace of the current and voltage across the filament, and the e.m.f. of the photoelectric pyrometer. In this run the hydrocarbon product formed was 99 percent acetylene, but two-thirds of the graphite evaporated, deposited on the wall, and did not react with the hydrogen. The heating rate in this run was 2.5×10^4 degrees centrigrade per second and the initial cooling rate 1.2×10^4 degrees centegrade per second; when thinner filaments were used, these rates were greater. Other similar runs were made at different filament temperatures and hydrogen pressures; in each case the rate of reaction was corrected for the amount of reaction that occurred during the heating and cooling periods.

of the graphite and depends on the atomic hydrogen concentration formed by dissociating molecular hydrogen at the graphite surface. The product from this reaction is mainly methane and ethane. Methyl radicals appear to be the intermediate product.

At temperatures above 2,800° C., graphite begins to vaporize significantly, forming polymeric carbon species. These react with hydrogen in the vapor phase surrounding the filament and at low pressure, yield acetylene as the only hydrocarbon product; at higher pressure, acet-

ylene and ethylene account 80 to 90 percent of the product. The rate of the reaction is proportional to the rate of vaporization of graphite. At 2,800° C., most of the energy supplied to the filament is lost by radiation. Above this temperature, the rate of vaporization increases rapidly, and as the temperature approaches within 100° C. of the sublimation temperature of graphite (3,525° C.),[24] more than 50 percent of the energy supplied to the filament goes into vaporization of the graphite. Thus, it is only at these high temperatures that the energy supplied to the filament can be used efficiently for the formation of acetylene.

At temperatures below 2,800° C., the rate of reaction between graphite and hydrogen is reduced as the product concentration increases. The equilibrium concentrations of the products formed increase with increased temperature.

Solutions of Metals in Molten Salts

Molten salts have been considered for use as engineering materials, and work is in progress at Atomics International, Canoga Park, Calif., to characterize some of their basic chemical and physical properties. Particular emphasis is being placed on fundamental studies of solutions of metals dissolved in molten salts. While carrying out *Soret*[25] effect measurements on the bismuth-bismuth halide systems to learn more about the mechanism of how the electric charge carriers are transported in the solution when a metal is dissolved in salt, it was discovered that thermoelectric force as high as 16 millivolts per degree were obtained. The figure of merit, a measure of the efficiency, is about 10 times better than the previous best thermoelectric substance and thus is of potential practical application in the conversion of heat to electricity.

In another study, electrical conductivities of molten salts are being measured at Atomics International to temperatures above their critical temperatures. (The critical temperature is the highest temperature at which a substance can exist as a liquid). This is the first time such measurements have been made for fused salts. The advantage of these studies is that the electrical conductivity can be studied over a much larger density variation in the super-critical fluid than in the case of liquids where the density range is limited. The results with bismuth trichloride ($BiCl_3$) and mercuric chloride ($HgCl_2$) showed that the conductivity undergoes a sharp decrease as the density decreases from that of the liquid. This confirms the earlier hypothesis made at Atomics International that the eventual decrease in electrical conductivity, that takes place as the molten salt is heated, is due to the density decrease which accompanies the heating.

Structure and Properties of Molten Salts

Investigations at the University of Pennsylvania, Philadelphia, are concerned with the structures of complex ions and the mechanism of ionic motions in molten salts at high temperatures and pressures. Since molten salts are liquids composed only of ions or their agglomerates, a knowledge of the structures of these ions and the nature of ionic movements is prerequisite to the formulation of an overall structural model for molten salts. Laser-excited *Raman*[26] spectroscopy has been under development in order to better understand complex ionic and molecular structures in fused salts through optical methods. Stannous chloride was found to possess a polymeric $(SnCl_2)_n$ structure in the pure fused state; the main species in mixtures with alkali halides is $SnCl_2^{3-}$.

Mixed molecular species such as mercuric iodo-bromide (HgIBr) exist in mixtures of mercuric dihalides. The *Raman* spectrum of intensely colored mercuric iodide (HgI_2) has been observed for the first time. The use of lasers allows systems to be studied at temperatures much

[24] The temperature at which graphite is transformed directly from solid to vapor without the intermediate step of liquification.

[25] The *Soret* effect is the partial demixing of a solution when it is exposed to a temperature gradient. This demixing can produce a voltage; this voltage per degree is the thermoelectric force.

[26] *Raman* spectra are composed of scattered radiation lines whose wavelengths reveal details about the vibrations of atoms composing the molecules giving rise to these spectra.

in excess of those previously possible. Such research is most important because molten salts now have many applications, *e.g.*, heat transfer media in nuclear reactors and liquid fuels in thermal breeder reactors.

Metal-Oxygen Systems

At Argonne National Laboratory, recent experiments with three different metal-oxygen systems at high temperatures (1,500° C.) and high pressures (60,000 atmospheres) have led to the synthesis of new crystal forms of known compounds and to the synthesis of other compounds which it has not been possible to prepare at atmospheric pressure. Some of the new high pressure compounds are thermodynamically unstable at atmospheric pressure. The three systems studied were: uranium-oxygen, transition metal-uranium-oxygen, and thallium-oxygen.

Two new compounds, nickel monouranate ($NiUO_4$) and zinc monouranate ($ZnUO_4$), have been synthesized in the transition metal-uranium-oxygen system at high pressure. The nickel compound has been prepared, at high pressure, in two different crystal modifications. The corresponding copper compound, copper peruranate ($CuUO_4$) can be prepared under ambient pressure; high pressure experiments have led to the synthesis of a new form of this compound.

An investigation of the thallium oxide system has shown that a new crystal form of thallic oxide (Tl_2O_3) is formed at high pressure. As reaction temperatures are increased, the oxide reacts with its platinum container to form the double oxide, di-thallic di-platinic heptoxide ($Tl_2Pt_2O_7$). The new oxide may be prepared more conveniently by reaction of thallic oxide with platinic oxide (PtO_2) at high pressure. The structure and properties of this compound have been determined. It has been possible to prepare an impure, poorly crystalline form of the new compound at ambient pressure, but the pure oxide has been prepared only by high pressure methods. An isostructural series of compounds with the formula $R_2Pt_2O_7$ (where R may be any trivalent rare earth atom) has also been prepared at high pressure.

Liquid-Liquid Immiscibility

Many liquids, usually consisting of an organic compound dissolved within certain concentration limits in water, are known to separate reversibly into two mutually insoluble (immiscible) liquids as the temperature of the solution is changed. At Oak Ridge National Laboratory it has recently been demonstrated that such immiscible liquids occur in molten fluoride mixtures containing the same materials (the fluorides of lithium, beryllium, and zirconium) as the fuel solvent used in the Molten Salt Reactor Experiment. By separation of the two liquids with a special high-temperature centrifuge (see Fig. I–44), the concentration-temperature dependence of liquid-liquid immiscibility of such mixtures has been studied in detail.

At 532° C. (the minimum temperature at which the phenomenon occurs), immiscible liquids are observed only in mixtures containing more than 45 moles of beryllium fluoride, less than 28 moles of lithium fluoride, and between (as extremes) 5 and 35 moles of zirconium fluoride per 100 moles of molten mixture. The composition region showing immiscibility becomes smaller as the temperature is increased; all mixtures of these materials exist only as a single liquid above 950° C.

The findings pose no threat to use of these fluorides as reactor fuels, which contain much more lithium fluoride and much less beryllium fluoride than those described above. However, such information does aid in understanding of the nature of the high-temperature liquid state, particularly in glass-forming systems.

ISOTOPIC GEOCHEMISTRY

Isotopic geochemistry research is concerned with the geologic history and behavior of uranium, thorium, and other radioactive mate-

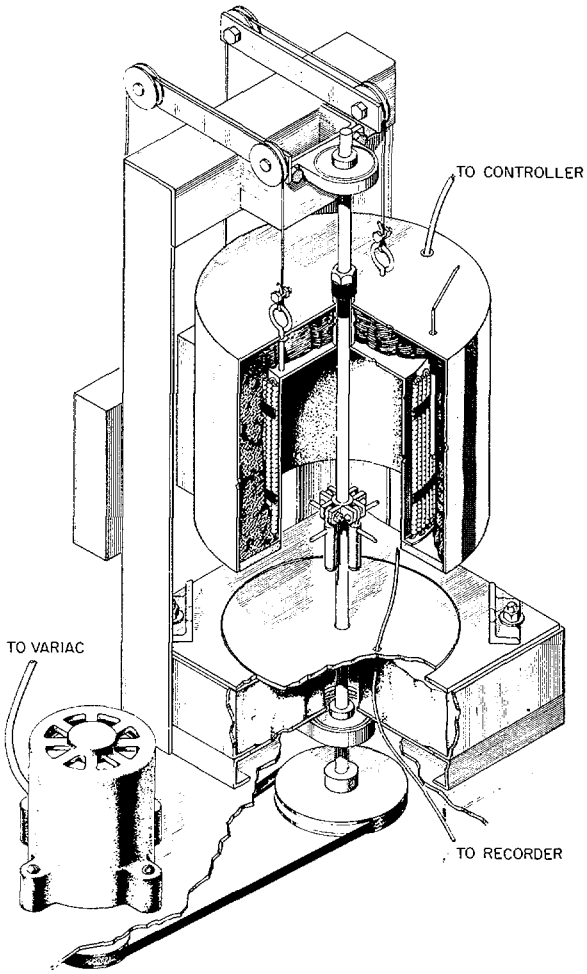

Fig. I–44. Liquid-Liquid Immiscibility. Drawing shows the high-temperature centrifuge constructed at Oak Ridge National Laboratory for the study of liquid-liquid immiscibility in molten salt systems. Only a few grams of material per sample are required. The small tubes attached to the central shaft (pre-loaded with the desired components in a glove box) are maintained at temperatures as high as 1,000° C. by the surrounding furnace assembly. Rotation of the shaft at 2,400 revolutions per minute produces a force of over 500 times gravity in the tube. After sufficient time for equilibration, the rotating shaft is brought smoothly to rest with the tubes hanging vertically, the furnace is quickly lifted, and the tubes are cooled with water, thus preventing any change in the composition or relative proportions of the liquids which might occur at intermediate temperatures. With this device, it was easy to separate the immiscible liquids at high temperature. The molten fluorides are analogous to the molten silicates in many respects, but melt at lower temperatures and are more tractable in experimentations.

rials and the application of isotopic technique to solve significant problems that cannot be answered in any other way.

Radiometric Age Dating

Isotopic geochemistry research at the Massachusetts Institute of Technology, Cambridge, has been concerned with testing the hypothesis of continental drift. This hypothesis states that North and South America were once joined to Europe and Africa, and that the Atlantic Ocean appeared only recently (in geologic time) as these large land blocks spread apart. The hypothesis has been tested through radiometric age dating in areas on both sides of the South Atlantic and it was shown that the pattern of ancient geologic terranes would fit together if the continents were returned to their former positions.

In Africa, an ancient province [27] 2,000 million years old, encompassing present-day Ghana, Ivory Coast, and westward, boarders a less-ancient province 600 million years old in present-day Nigeria. An almost straight boundary line between these provinces extends from Upper Volta in the north, through Dahomey, Togo, and southeastern Ghana, and reaches the continental margin close to Accra. If the continents had been together at that time, this line would have extended into northern Brazil close to the present coastal town of Sao Luis. Age studies of the ancient rocks underlying the sediments have shown that the line occurs exactly where predicted, with 2,000-million-year rocks on one side and 600-million-year rocks on the other, as in Africa. Other similar corresponding patterns are emerging as the work proceeds along the coast in both directions.

The research uses the radioactive breakdown of rubidium (Rb^{87}) to strontium (Sr^{87}) in the total rock material. If borne out by further investigations, this direct test of the earlier juncture of the continents will have important consequences not only in understanding the history

[27] An area throughout which geological history has been essentially the same or which is characterized by particular structural, petrographical, or physiographical features.

of the development of the earth's crust, but in practical ways such as the continuation of mineral belts between the two continents. It is already suggested that there may be one or more important mineral provinces in northern Brazil that have been relatively unexplored so far. Mineral deposits of particular interest in this prediction are iron, manganese, diamonds, tin, and gold. This research is of interest to the AEC because it applies highly advanced isotopic methods, such as precision mass-spectrometry, to obtain information on the structure, history, and probable origin of geologically and economically significant portion of the world.

Sources of Uranium

A problem of major concern to those interested in uranium mining is the source of the uranium now found in the sedimentary strata that contain the principal economic deposits of the five-state uranium province of the Colorado Plateau. A large number of the important ore deposits exist underground as isolated ore bodies in a porous stratum, showing no feeders above, below, or on the sides; how they got there is a geological mystery. One theory, among several that have been advanced to account for this phenomenon, pictures the original uranium ions as rising from deep in the earth's crust in naturally heated or hydrothermal solutions. These solutions rose along fissures and porous strata until they ultimately came into contact both with ground water and the organic environment of certain critical strata, where catalytic action caused the precipitation of uranium minerals. A few vertical uranium-bearing structures have been found that penetrate the plateau strata. These provide sites where evidence for upward migration may be examined critically. Among such sites studied by mineralogists from Columbia University, New York City, the veins of Kane Creek, South of Moab, Utah, provide unusually convincing evidence of hydrothermal activity (see Fig. I–45). Here, uranium-bearing vertical veins (age about 60 million years) penetrate much older strata (age about 225 million years). Closely associated with the uranium

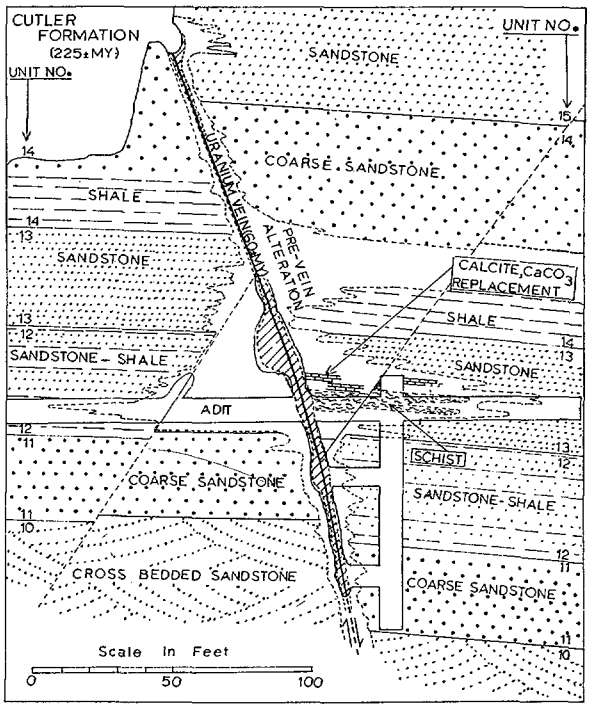

Fig. I–45. Sources of Uranium. Schematic drawing of Columbia University study of uranium-bearing vein penetrating Colorado Plateau strata, about 11 miles southwest of Moab in east central Utah. The vein (about 60 million years old) follows a fault (about 42 feet displacement) which cuts locally designated units of the Cutler Formation (Permean; about 225 million years old). Wall rock alteration both preceding and accompanying vein information indicates deposition of uranium from rising heated solutions.

minerals of the veins are chlorite (a magnesium silicate), and a local mica schist generally considered indicative of hydrothermal activity, in the range of 100° to 300° C. While several links are still missing in the interpretation of the chain of natural events, which would tie the vertical veins to deposits in horizontal strata, evidence in support of an original hydrothermal source for the uranium ions is strong. The examination of this concept and the extent to which it may be applicable in uranium exploration can very well have an important bearing on future uranium discovery.

Combined field and laboratory studies demonstrate that two periods of fluid invasion caused

mineral changes along fault lines in the Cutler Formation at Kane Creek. Normally, red and purple strata exhibit massive white areas up to 50 feet thick close to faults. These gradually taper away from the fault plane conduit and disappear a mile or more away. This early alteration change is followed by a localized greenish-gray alteration from a few inches to 20 feet thick that closely follows the fault plane. This forms the uranium-bearing vein, where uraninite (UO_2) is a principal mineral. It is the minerals of the veins that provide evidence of the temperatures which probably prevailed during the formation of the ores.

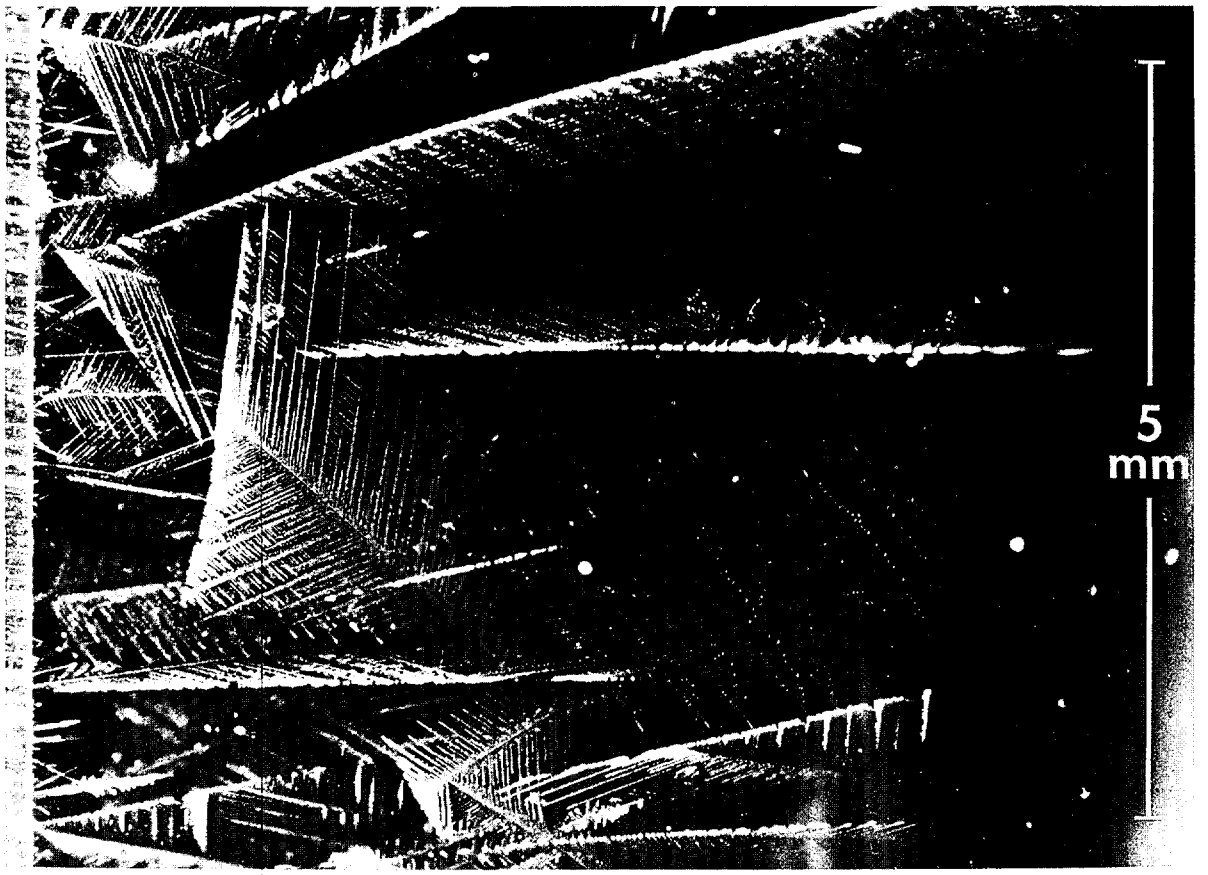

Fig. I–46. Glass-Metal Bonding. Lawrence Radiation Laboratory, Berkeley, photograph of dendrites of cobalt growing in a cobalt/glass composite from the interface. The interface is at the extreme *left* with cobalt to the *left* of it and glass on the *right.* For details see p. 91.

METALLURGY AND MATERIALS

Under the AEC's metallurgy and materials research program, studies are made to advance the understanding of the structure and properties of matter in the condensed state. These studies are primarily concerned with the relationship between structure and properties, what factors control them, how they are derived from the fundamental laws of nature, and what can be done to improve the properties. The program embraces both theoretical and experimental research using the disciplines of physical metallurgy, physical ceramics, and solid state physics. This research plays a vital role in the AEC's long range objectives by providing knowledge for maximum beneficial control and use of materials. Representative research carried out under this program includes radiation effects, temperature effects, superconductivity, research at high pressure, magnetic materials and properties, neutron diffraction, plastic deformation, and ceramic materials.

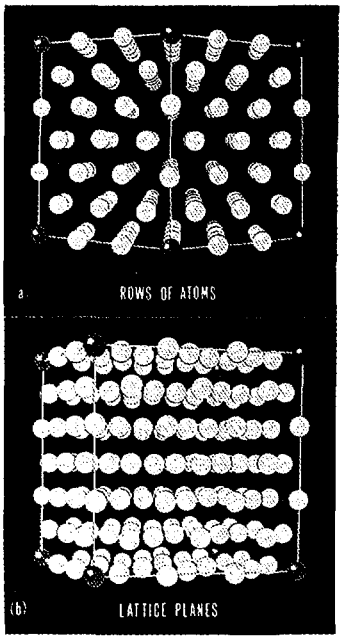

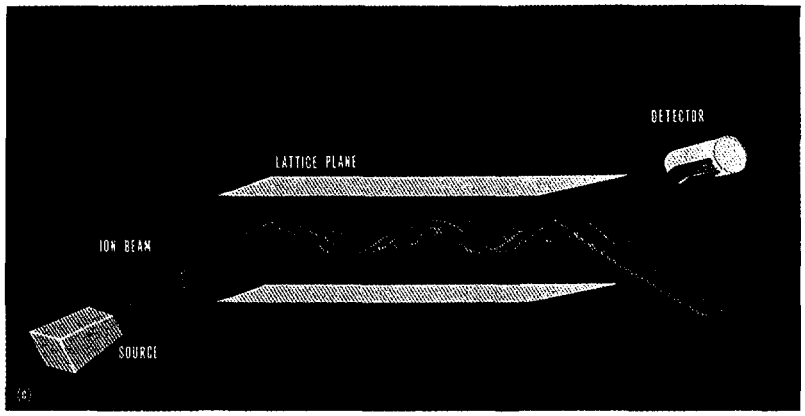

Fig. I–47. Channeling of Charged Particles. Studies at Oak Ridge National Laboratory have shown that when fast charged particles pass through a solid, those that emerge have discrete bands of energy. Measurement of the oscillating "wavelengths" of these particles can provide information on the electric fields that exist in solid crystals and which are related to the structure, binding forces, and electron densities within the material. Drawings (*a*) and (*b*) show crystal orientation of rows and lattice planes (sheets) of atoms. Drawing (*c*) depicts ray paths between sheets of a crystal to illustrate how the detection of only those ray paths having the right wavelengths to reach the detector is possible.

RADIATION EFFECTS

Interaction of radiation with matter is one of the most important areas of research under the metallurgy and materials research program. Although in many cases a deterioration of properties occurs when exposed to radiation, through increased understanding of this interaction, a number of beneficial new materials and processes have been developed, such as plasticized (hardened) wood and food preservation through irradiation processing. The materials within the pressure vessel [28] of an atomic reactor are, of course, subject to a great variety of radiations. Additional knowledge in the area of radiation effects will permit definition of more accurate material characteristics to predict and offset any damaging effects of radiation.

Channeling of Charged Particles

Normally, when fast charged particles pass through matter, they lose energy in numerous small steps, mostly as ionization energy. Thus, the average energy of the charged particles is reduced and also their energies spread over a wide range. However, Oak Ridge National Laboratory (ORNL) recently discovered that when fast particles, such as 50-Mev. iodine ions, pass through corridors or channels of a lattice of atoms in a perfect crystal of gold, the particles emerge with discrete bands of energy, a completely unexpected result. The explanation found for this phenomenon shows the way toward obtaining entirely new information about solids. The particles ricochet back and forth between the walls of the channel (see Fig. I–47). The number of times they ricochet depends on the thickness of the crystal, the angle of entry, and the exact position of the particle when it enters the channel. In the experiment performed at ORNL, the detector could only be reached by particles with certain values of "wavelengths" of these transverse oscillations, and thus with only certain values of energy losses. The "wavelengths" of these transverse oscillations were measured and with this new information it is possible to determine the

[28] See p. 111, "Nuclear Reactor Safety Research" of Part Two—Reactor Technology Programs.

strengths of the electric fields which repel the particles back toward mid-channel. These electric field strengths which exist inside a crystal lattice are related to the structure, binding forces, and local electron densities within the material.

Interactions With Crystal Lattices

In another investigation concerning channeling,[29] Brookhaven National Laboratory in collaboration with Bell Telephone Laboratories, Murray Hill, N.J., and Rutgers University, New Brunswick, N.J., studied directional effects of a number of various interactions of energetic charged particles with crystal lattices. Earlier investigations have established that electronic interactions (causing energy loss through ionization and excitation), as well as different types of atomic and nuclear interactions requiring close collisions between a particle and a lattice atom, are strongly dependent on the direction in which a well collimated beam enters the lattice. Related effects occur when charged particles are emitted from lattice sites in a crystal lattice or are scattered to large angles as they pass through the lattice. In any experiment where charged particles emitted by an impurity atom are detected outside and their energy and direction analyzed, it is possible to determine whether the emitting atom is in an interstitial position or on a lattice site. Such information is of great importance when attempting to decide where impurity atoms reside in such systems as salts containing rare gases or impurity-doped semiconductors. These effects—known as "blocking," because particle trajectories are blocked by atom rows and planes—have been simulated recently in computer calculations in silicon (see Fig. I–48). In one model, a large number of particle trajectories is followed after isotropic emission from a site and successive scattering by atoms of a row until deflection becomes negligible. The distribution of emergence directions compares well with that obtained in another model calculation in which the atomic row is replaced by an average potential. The thermal motion of the atoms is taken into account and the experimentally observed decrease of angular widths with increasing temperature has been confirmed.

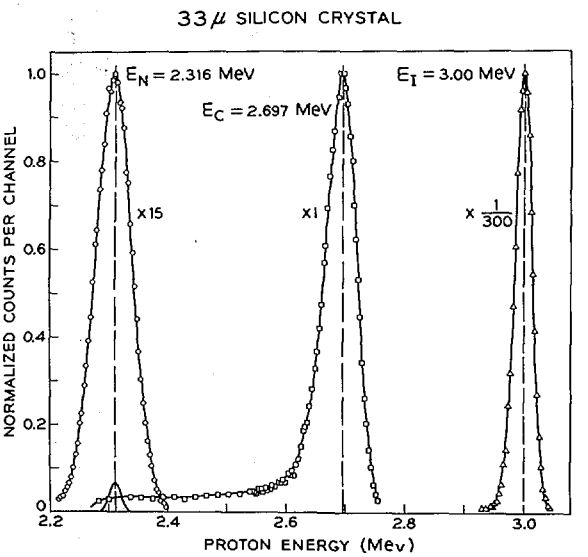

Fig. I–48. Interactions With Crystal Lattices. Brookhaven National Laboratory graph shows the effect of crystal orientation on energy loss of charged particles for the spectra of 3 Mev. protons after transmission through a 33-micron-thick silicon crystal. The detector has an aperature of 1 millimeter and is placed at 1 meter behind the crystal so that it accepts only the least deflected part of the beam. The spectrum on the left (scale is ×15) is obtained when the crystal is misoriented with respect to the beam. The *middle* spectrum (scale ×1) corresponds to channeling conditions, with the beam parallel to the 111 planes of silicon. The spectrum on the *right* (scale ×1/300 is that of the incident beam, taken without the silicon crystal.

Radiation Damage and Lattice Defects

At Atomics International, Canoga Park, Calif., the technique of high energy electron bombardment is being used to study the effects of radiation on pure metals and semiconductors. Earlier work had used the change in electrical resistance to measure damage; more recently the effects of the damage on the mechanical properties of metal crystals have been studied. In general, metals exposed to radiation become harder and more brittle.

[29] See also pp. 117–118, "Fundamental Nuclear Energy Research—1966."

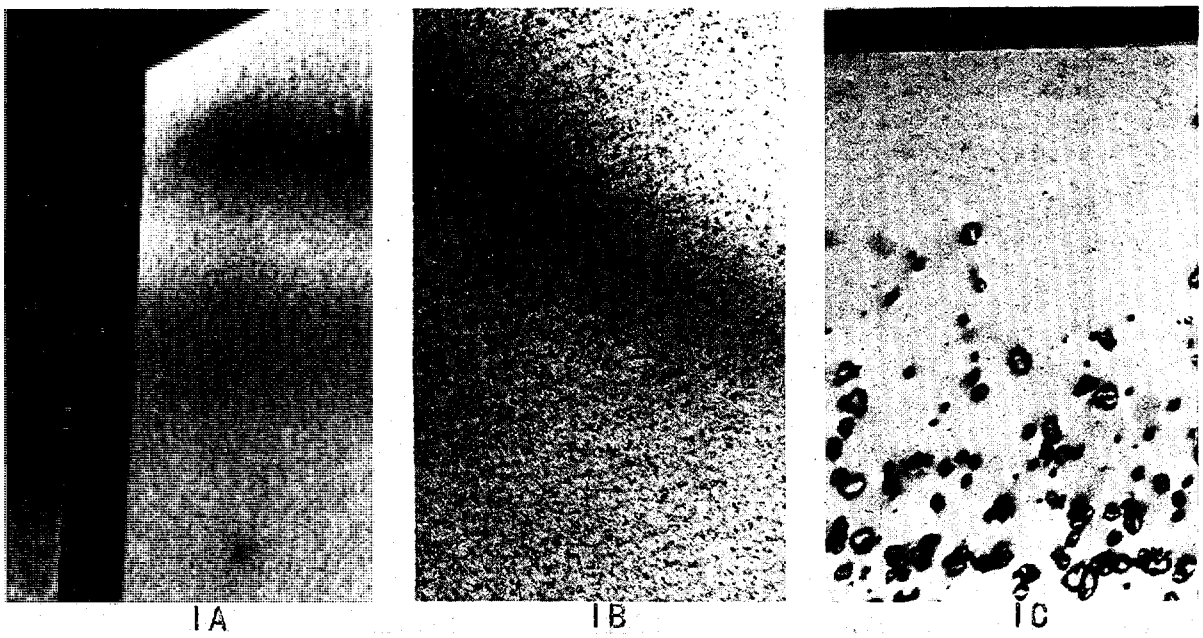

Fig. I–49. Radiation Effects in Molybdenum. Investigations at Pacific Northwest Laboratory are directed toward understanding the effects of nuclear radiation on metals such as the fact that metals become brittle after prolonged exposure to neutron radiation. To study this effect, samples are irradiated in a reactor for increasing lengths of time and subsequently examined at high magnification in the electron microscope. This latter technique makes it possible to "see" into the interior of a metal and to detect changes in the atomic arrangements. The figure (1A) on *left* is a photograph of nonirradiated modybdenum showing crystallites or grains separated by a boundary. The uniform contrast indicates perfect crystalline arrangements of the atoms. The center (1B) figure shows the effect of exposure to nuclear irradiation at 80° C. The black spots are due to atoms which have been displaced by the bombarding neutrons and which have then regrouped into clusters. This structure is representative of a material after moderate irradiation at relatively low temperatures. Because of these defect clusters, the ductility of the metal has been greatly reduced. Irradiating a metal in a nuclear reactor maintained at elevated temperatures (approximately 600° C.) produces a structure much different from that caused by irradiating at low temperatures, 80° C. Because of the increased mobility of the atoms at the elevated temperatures, the black spots or defect clusters are able to grow into large dislocation loops as illustrated in *right* figure (1C). With this type of defect structure, the material now has more ductility but less strength than that irradiated at the lower temperature.

The mechanical properties of metals are largely determined by the presence of imperfections called dislocations. Opposed to the localized point defects such as vacancies, dislocations are characterized by displacement of atoms along a line through the metal lattice. Motion and multiplication of these line defects are responsible for the ease with which a metal is permanently (plastically) deformed. Because of the lattice distortion which is present in the immediate vicinity of dislocations, vacancies and interstitials produced by electron irradiation are attracted to them since the vacancies and interstitials help relieve the distortion. Once interstitials or vacancies are associated with dislocations, considerable effort is required to separate them. In particular, if dislocation motion is to occur over large distances, the point defects must either be dragged along or the dislocations must break away from them. This produces a stiffening of the metal and an increase in the value of the elastic modulus. Studies of dislocation behavior can thus also be used to elicit information about the properties of point defects.

Recent modulus studies of electron irradiated

pure polycrystalline copper and gold have unexpectedly shown that the mode of defect production in the two metals is significantly different. In gold, relatively large numbers of vacancies and interstitials are created at dislocations during irradiation. These are created by a process called focusing, in which the energy imparted to a gold atom by an incident electron can be transmitted over large distances in the lattice. This transmitted energy can thus create defects far from the original electron encounter. On the other hand, focusing is much less prevalent in copper; those defects which are created at dislocations are produced by interaction of an incident electron with atoms very near the dislocations.

Radiation Damage in MgO

At Oak Ridge National Laboratory, the effect of radiation on magnesium oxide (MgO) is being studied by monitoring various color centers (defect centers which cause the transparent material to color because they absorb light of a particular wavelength) formed during irradiation. It has been found that ionizing radiation, such as gamma rays, causes very little intrinsic damage, but is effective in changing the valence states of various impurities. Magnesium oxide, because of its physical properties, is potentially very important in several areas of technology. Single crystals and hot pressed disks of MgO have high mechanical strength and are transparent in the visible range as well as in the ultraviolet and near infrared. Because the melting point is around 2,800° C., these crystals and disks are valuable for high-temperature optical applications. There are also potential uses for MgO in both reactor technology and space vehicles.

The studies have also shown that 1.5-Mev. electrons and high-energy neutrons are capable of producing oxygen vacancies which are observed as F centers (negative ion vacancies which have trapped electrons). These F-type centers absorb ultraviolet light of 2,500 A [30] wavelength at room temperature and their concentration can be determined simply by measuring the intensity of this absorption band. Fast neutrons are much more effective than electrons in producing vacancies, and it has been shown that impurities can also enhance vacancy production by radiation. For example, at a radiation temperature of 60° C. a dose of 1.4×10^{18} electrons per square centimeter yields an F-center concentration in relatively pure samples (10 parts per million of iron) of about 5×10^{16} centers per cubic centimeter, which is 50 times less than that obtained with a comparable dose of neutrons. This is what is predicted by the theory of atomic displacements or "knock-on processes" in solids.

Radiation Effects in Nickel

Recent studies on irradiated nickel showed that atoms displaced by neutron irradiation cluster into groups. The concentrations of these clusters vary greatly at different types of interfaces or boundaries within the metal. Two such interfaces of particular interest to these studies are normal grain boundaries [31] and twin boundaries.[32] Studies at Pacific Northwest Laboratory revealed that an unusual condition develops at twin boundaries when nickel is irradiated. When an atom is knocked out of its normal position by a neutron, it collides with other atoms before coming to rest and also displaces these other atoms. The displaced atoms prefer to travel in a direction where they strike the least number of neighboring atoms. The displaced atom, therefore, eventually moves through the lattice parallel to the closely packed rows of atoms. If this parallel path is suddenly blocked by a twin boundary, however, the displaced atoms collide or interact with atoms making up the twin. The energy of this collision will eject a large number of atoms on or near the boundary from their normal position. The displaced atoms form clusters along the twin boundary because there are no concentrations of empty lattice positions that can absorb the displaced atoms (see Figs. I–50 and 51).

[30] A is the abbreviation for an Angstrom unit, formerly abbreviated as Å; 10 billion angstroms equal 1 meter. The unit is used for measurement of wavelengths of light.

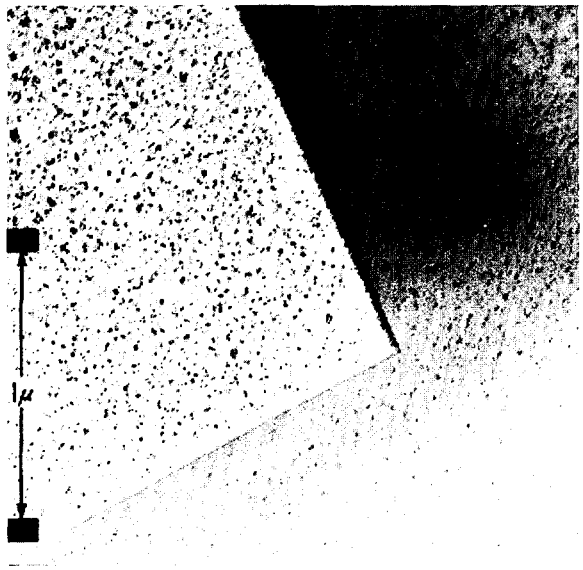

Figs. I–50 and 51. Radiation Effects in Nickel. Nuclear irradiation creates changes in atomic arrangements and the crystalline perfection within metals by displacing atoms. This may cause property variations, such as loss of ductility. At Pacific Northwest Laboratory, it has been discovered that in nickel, a material frequently used as an alloy or structural material in reactors, displaced atoms tend to cluster into groups. The 35,000× photo *above* shows that normal boundary areas (angled horizontal line) have many spaces which can absorb these displaced atoms. A "twin" boundary (angled vertical line) formed when the metal crystallized from the molten state, has "mirror image" atoms located on either side of the boundary. Because of this "twin" arrangement of atoms, there are few empty spaces which can absorb displaced atoms. Therefore, when atoms displaced by neutron irradiation collide with atoms making up a "twin," large numbers of "twin" atoms are affected and form a cluster along the "twin" boundary (black spots along angled vertical line). The localized displacement is graphically portrayed *below.*

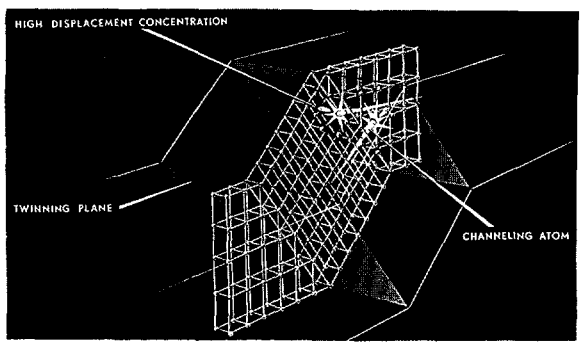

Interstitial Atom Behavior in Germanium

One of the obstacles to a clear understanding of the nature of the damage products in germanium (Ge) bombarded with energetic particles is the lack of knowledge of the ultimate fate of atoms driven into interstitial positions by elastic collisions. In view of the growing importance of germanium in the preparation of gamma-ray detectors and in various space applications, a more realistic appreciation of these damage processes and products is of practical as well as basic significance. Recent experiments at Oak Ridge National Laboratory have shown that interstitial germanium atoms produced by 1.5-Mev. electrons are able to move and interact with other imperfections even when the irradiation is carried out at liquid nitrogen temperature (−196° C.).

In germanium crystals containing small amounts of copper, substitutional copper atoms act as triple-level acceptors (they can remove three electrons from the conduction band in n-type crystals). However, a copper atom in an interstitial site acts as a single donor atom (it contributes a conduction electron on thermal ionization). Therefore, if a migrating interstitial germanium atom exchanges places with the substitutional copper atom, which in turn becomes lodged interstitially in the lattice, the result will be the addition of four electrons to the conduction band. Comparison of the radiation response of copper-doped n-type specimens with normal n-type germanium in a liquid nitrogen irradiation reveals that the rate of conduction electron removal by radiation induced acceptor states is significantly smaller in the former. In addition, upon warming the crystal into the range where lattice vacancies become mobile, the copper-doped crystals show a further decrease

[31] *Normal Grain Boundaries* are overlap regions or intersections of adjoining crystals. Such boundaries do not have an orderly arrangement of atoms within the grains. Also, the boundaries contain many empty lattice positions or vacancies. They can readily absorb displaced atoms in their vacancies.

[32] *Twin Boundary*—For every atom on one side of the boundary, there exists a second, equivalent atom on the opposite side that is related to the first atom by a mirror image through the boundary. This mirror image disrupts the uniform planar arrangement at a twin boundary and the atom planes undergo an abrupt rotation.

in conduction electron concentration (a reverse annealing) rather than normal recovery.

These results indicate that during irradiation, copper impurities are displaced into interstitial sites, presumably by moving germanium interstitial atoms, and during thermal annealing, vacancy-copper interstitial interaction returns these to substitutional positions, thereby restoring their acceptor behavior. It appears, therefore, that interstitial germanium atoms may migrate freely at temperatures at least as low as −196° C.

TEMPERATURE EFFECTS

In many applications, environmental temperature strongly influences the selection of materials used. In addition, because of the temperature dependence of most properties, temperature is a very important parameter in research. Consequently, the effect of temperature on materials is an active area of research.

Thermal Expansions at Low Temperatures

The thermal properties of solids often are understood more easily at very low temperatures where lattice vibration effects are relatively small. This is true also for thermal expansion effects. Ames Laboratory has developed a device for measuring temperature-induced length changes which are of the order of 1 percent of the average spacing between atoms in a solid (0.02 Angstroms) for 4-inch long samples. This is at least 10 times better than has been done before in any laboratory. Measurements have been made on the technically important (and theoretically understood) semiconductors such as germanium, silicon, and related compounds, indium arsenide (InAs), indium antimonide (InSb), gallium arsenide (GaAs), and gallium antimonide (GaSb). The results show that all of these solids first expand as they are warmed from absolute zero, then contract, and finally expand again as the temperature is increased towards room temperature. The initial expansions of InSb and InAs are only 0.4 A (one- or two-tenths of an atomic spacing) for the 4-inch long samples, and occur below −268° C.

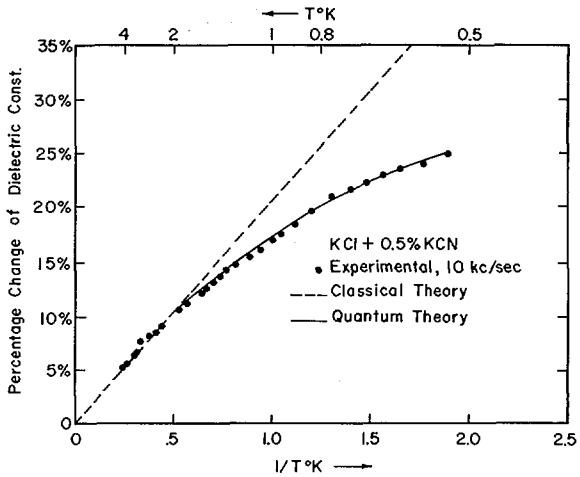

Fig. I–52. Low Temperature Mobility of Polar Ions. The low temperature mobility of CN– (cyanide) ions dissolved in KCl (potassium chloride) as measured at Cornell University by the change in dielectric constant are plotted above. The illustration shows the experimental data points follow a quantum theory (solid line) rather than the classical theory (dotted line).

Low Temperature Mobility of Polar Ions

Polar molecules [33] can orient when subjected to an electric field and contribute to the dielectric constant of the substance in question. For example, the high dielectric constant of water is caused by orientation of the water (H_2O) molecules. Thermal motion of the molecules counteracts this orienting effect, and therefore, the contribution to the dielectric constant from polar molecules decreases with increasing temperature. Heretofore, this temperature effect could not be verified at low temperatures because the molecules "freeze" in and cannot orient in the electric field. In experiments performed at Cornell University, Ithaca, N.Y., polar ions such as cyanide (CN^-) were "dissolved" in an appropriate ionic lattice such as potassium chloride (KCl). Such ions which maintain their mobility at temperatures as low as −273.11° C., were

[33] *Polar molecules*—Molecules that have a permanent dielectric moment because the centers of gravity of the negative and positive charges do not coincide.

studied and predicted effects were observed. The CN^- ion was found to rotate or orient by "tunneling," a quantum mechanical mechanism, rather than by the classical or thermally activated process (see Fig. I–52). The tunneling is very fast and the ions can, therefore, follow very high frequency electric fields, 10 billion cycles per second (10^{10} c.p.s.).

From an application point of view, these ionic crystals containing polar impurities exhibit very interesting properties at low temperature. The dielectric constant can be double that of the pure crystal with only a small concentration of such ions. Voltages of the order of a few volts may reduce this value to that of the pure crystal, and since these changes occur very rapidly, devices containing these substances are usable at very high frequencies.

SUPERCONDUCTIVITY

Some metals and a great number of alloys lose all their electrical resistance at very low temperatures. These materials possess a property known as superconductivity. The use of superconducting materials permits building electromagnets that consume negligible power. Materials with such properties are important for many areas of research and technology since these materials would be particularly useful for devices where power dissipation could be a major limitation.

Defect Studies in Superconductors

The possible technological applications of superconducting materials encompass many diverse areas, ranging from the generation of large volume magnetic fields at a minimum of expenditure of power to their use for computer elements. The characteristics of these materials may be altered by defects, such as dislocations and precipitates introduced during material preparation, or by defects which result from radiation damage in an energetic particle environment. At Oak Ridge National Laboratory, research has concentrated on the magnetic properties (which correlate with the performance in devices) of superconducters that contain defects introduced by radiation damage and by other methods. Systematic fast neutron irradiations of single crystals of niobium at room temperature have been carried out in the Oak Ridge Research Reactor with subsequent studies of the magnetic behavior of this material at low temperatures. Niobium has the highest transition temperature (the temperature at which the material becomes a superconductor) of all the pure elemental superconductors, and it has been found that the transition temperature remains essentially unchanged after intense doses of neutron irradiation. On the other hand, characteristic features of the magnetic properties, such as the magnitude and degree of reversibility of the mangetization in an applied magnetic field, are markedly altered by the irradiation. These investigations help clarify the nature of these radiation-induced defects and their effect on superconducting behavior.

Superconducting Currents

The strongest current that can flow in a superconductor without power loss has been the subject of studies at Cornell University. Of specific interest has been the current flowing in the main body of the superconductor and the current flowing in a layer close to the specimen surface. Below a critical magnetic field H_{c2} (in a type II superconductor,[34] a type that can retain superconductivity to relatively high magnetic fields) both components contribute to the total current flowing in the sample. Above H_{c2} and below a still high critical field H_{c3}, the only contribution comes from the surface layer. This study showed that the number and arrangement of dislocations (defects introduced into the crystal structure of the specimens by deformation) are important in determining the current carrying capacity of the bulk superconductor and that the surface condition and the orientation of the sample with respect to the magnetic

[34] See p. 280, "Fundamental Nuclear Energy Research—1965," and p. 120, "Fundamental Nuclear Energy Research—1966."

field were critical factors in determining the level of the surface current.

Static magnetization measurements were used to obtain values of the bulk current carrying capability of a series of niobium-titanium and niobium-tantalum alloys as a function of dislocation content, composition, temperature, and magnetic field. It is already established that crystalline defects generally increase the current carrying ability of superconductors, but in the present work, the surprising result found was that the current carrying capability is decreased if too many dislocations are introduced. A new model for the effectiveness of dislocations in high current superconductors was proposed and confirmed experimentally.

Values for the surface currents were obtained from measurements of the magnetic response to small low frequency alternating current (a.c.) fields superimposed on a direct current (d.c.) field above H_{c2} so that the only contribution came from the surface. The observations showed that all the characteristics of the magnetization behavior, including the nonlinear aspects, could be described by a simple model characterized by one parameter, the maximum current carried by the surface layer. The currents obtained from the data using this model were sensitive to the surface condition, the orientation of the sample and the frequency.

Tunneling Between Superconductors

At Atomics International (AI), part of the basic research effort is concerned with some unusual aspects of superconductivity, both to gain an understanding of basic phenomena and to delineate new applications and areas of research. A new superconductive phenomenon was recently discovered at AI as a result of sustained effort in the field of low temperature electronic tunneling.

The AI work involves determination of the electrical properties of tunnel diode structures consisting of two metal films separated by a very thin (about 20A) insulating layer. Under the influence of an applied voltage, electrons "leak" across the insulating layer by the quantum mechanical "tunnel" effect, thereby producing a current. The present discovery involves tunneling between a thin (about 500A) aluminum film and a thicker (2–30 microns) film of a second superconductor (indium, tin, or lead). In addition to the usual current observed when both films are less than two microns thick, a small oscillatory contribution is also observed. The voltage spacing of the oscillations is inversely proportional to the film thickness, suggesting the presence of a standing wave.[35] The effect can be successfully explained by the fact that in a superconductor, unpaired electrons (or quasiparticles) of a given energy can travel with two sharply defined velocities, instead of only one as in a normal metal. Consequently, a special sort of standing wave can be established across the thickness of the thicker film, one not possible in a normal metal. A knowledge of the voltage spacing and the film thickness allows the direct evaluation of the electron velocity in the direction normal to the plane of the film. This is an important result since other methods of measuring this velocity, the *Fermi* velocity, involve averages over nonequivalent directions. Mapping of the velocity surface as a function of crystallographic orientation is a basic goal which has yet to be attained in a practical sense. The present effect seems to offer considerable promise as a tool for achieving this goal. Beyond this, there is reason to believe that it will also prove to be a sensitive probe in the continuing effort to determine basic properties of the superconducting state.

Superconducting Transition Temperature

The variation of superconducting transition temperature (T_c) as a function of composition for the sodium chloride (NaCl)-type carbides, nitrides, and carbonitrides of the group IVa and Va elements in the Periodic Table (see p. XX) is being studied at the Los Alamos Scientific Laboratory. The systems studied to date include niobium-carbide (NbC), tantalum-carbide (TaC), hafnium-nitride (HfN), and hafnium-zir-

[35] *Standing wave*—A wave pattern that is stable and does not travel through the medium in which it exists.

275–845 O—68——7

conium nitrogen solid solution (Hf, Zr)N. The results of this investigation on well characterized samples have shown that the transition temperature varies sharply with composition within this class of compounds which explains the contradictory results attributed to these materials by other investigations. Since some of the higher superconducting transition temperatures are known to occur in this class of compounds, a more thorough understanding of the behavior of these materials is necessary for the development of useful superconductors.

All of the IVa and Va carbides and nitrides except tantalum nitride are readily prepared in the sodium chloride (NaCl)-type structure. An unusual property is that the lattice is preserved throughout a wide range of composition, varying from $MC_{0.5}$ to $MC_{1.0}$ for the carbides, and from $MN_{0.5}$ to $MN_{1.13}$ for the nitrides, where M represents the metal studied. Studies on the variation of the superconducting transition temperature, T_c, of NbC, TaC, HfN, and (Hf, Zr)N solid solutions as a function of composition show that T_c varies quite sharply with stoichiometry. For NbC and TaC, changes in T_c were found to range from a condition of no superconducting transition for measurements down to −272° C. (1° K.) for the lowest carbon content, to T_c values of −263° C. (9.7° K.) for $TaC_{0.987}$ and −262° C. (11.1° K.) for $NbC_{0.977}$ (see Fig. I–53). An opposite behavior was observed in the HfN system. The highest T_c, −264° C. (8.7° K.), was obtained for the lowest nitrogen content and no superconducting transition was found above −271° C. (2° K.) for the composition $HfN_{1.12}$. The transition temperature for the (Hf, Zr)N solid solution series increases smoothly as the composition becomes richer in zirconium and reaches its maximum value of −262° C. (11° K.) for $ZrN_{0.948}$.

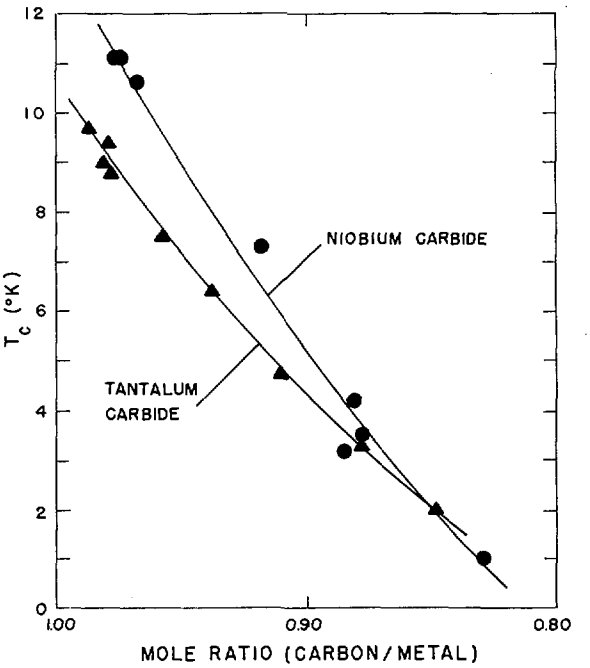

Fig. I–53. Superconducting Transition Temperature vs. Composition. The curves show the variation in superconducting transition temperatures (the temperature at which a substance becomes superconducting) for two of the compounds—niobium carbide and tantalum carbide—under study at the Los Alamos Scientific Laboratory.

Thin-Film Superconductors

Studies of thin films have already shown surprising increases in the temperature of the superconducting transition for films about 100A thick. Continuing work in these systems at Brookhaven National Laboratory has led to some other interesting discoveries about the magnetic fields at which the superconductor goes into the normal state (critical field) and the conduction mechanism. It has been found that the critical field in very thin aluminum films is higher than previous estimates for the upper critical field of superconductors. These estimates were based on energy arguments that compare the free energy of a superconductor of zero thickness to the loss in free energy of the normal state due to the electron paramagnetism. While the detailed mechanism for these critical fields is not clear, it appears likely that any explanation will involve a superconducting state that shows some paramagnetism. An understanding of the mechanism for the high critical fields in these systems may lead to a new class of high field materials.

Another interesting feature of these thin films relates to the method of electron conduc-

tion. In some of the films that were thinner than 100A, it was found that the resistance increased as the temperature decreased. This is in contrast to normal metallic conduction where the resistance decreases as the temperature decreases. The negative temperature coefficient of resistance usually indicates oxide between metallic particles and in this case, it appears plausible that electron conduction is accomplished by tunneling through the oxide. At some low enough temperature, it is found that the samples make a transition into the superconducting state. The transition temperature of these systems is from $-270.75°$ to $-270.25°$ C. compared to $-271.95°$ C. for the bulk material. Below the superconducting transition temperature (T_c), zero resistance is probably obtained by tunneling of superconducting pairs through the oxide. Theoretical work indicates that in this type of "granular" system, T_c can be enhanced. Hence, it is possible that this type of system will lead to new high temperature transition materials, as well as high field materials.

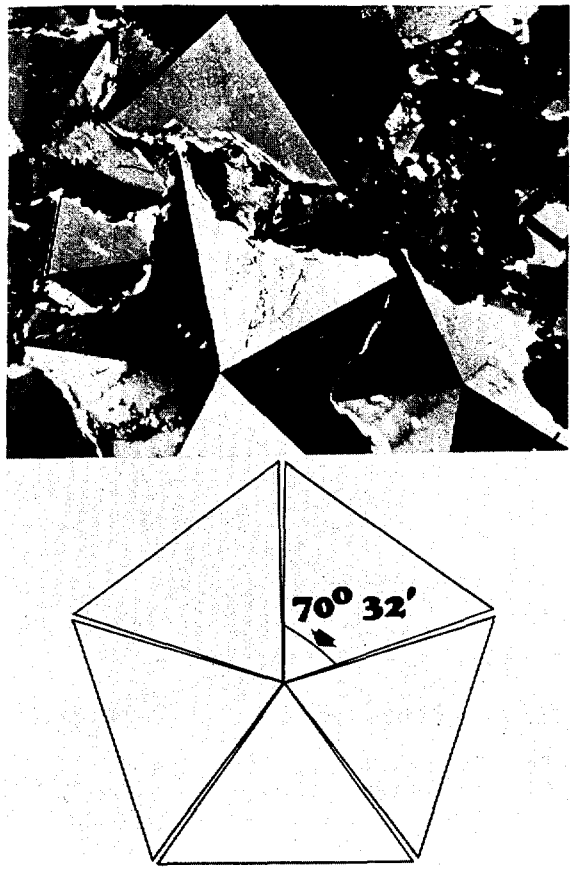

Fig. I–54. Crystalline Symmetry. The above Mound Laboratory transmission electron micrograph (enlarged about 15,000×) shows an unusual combination of nickel crystals. Groups of five crystals grew into pentagons in an unusual display of multiple "twinning." The drawing (*left*) clarifies the phenomenon, which is called "pseudo-fivefold symmetry" because the crystals do not mate perfectly. The interplanar angle of each twin crystal is 70°32′, just short of the 72° which would make perfect fivefold symmetry. These crystalline formations were discovered during the metallographic study of nickel, which had been plated by the thermal decomposition of nickel carbonyl.

MAGNETIC PROPERTIES

The most familiar magnetic property, ferromagnetism, is recognized by a metal's strong attraction to a magnet. The origin of this and other magnetic properties lies in the individual spinning electrons contained in the material and which act as elementary magnets. Magnetic properties and materials possessing unique magnetic properties are of interest in the pursuit of knowledge and also because of the possible applications in electrical equipment.

Magnetic Properties of Rare-Earth Metals

The absorption of very high frequency microwave radiation is being used at the Ames Laboratory to study the magnetic properties of the rare-earth metals. Long wavelength oscillations of the magnetic structure in the metal are set up when microwave power is absorbed. The absorption has been studied as a function of temperature and applied magnetic field in single-crystal high-purity terbium metal. The very high microwave frequency of 100,000 megacycles (3 mm. wavelength) was used (see Fig. I–55). Because of anisotropy (having different properties in different directions in the crystal) in the arrangement of the atoms in the

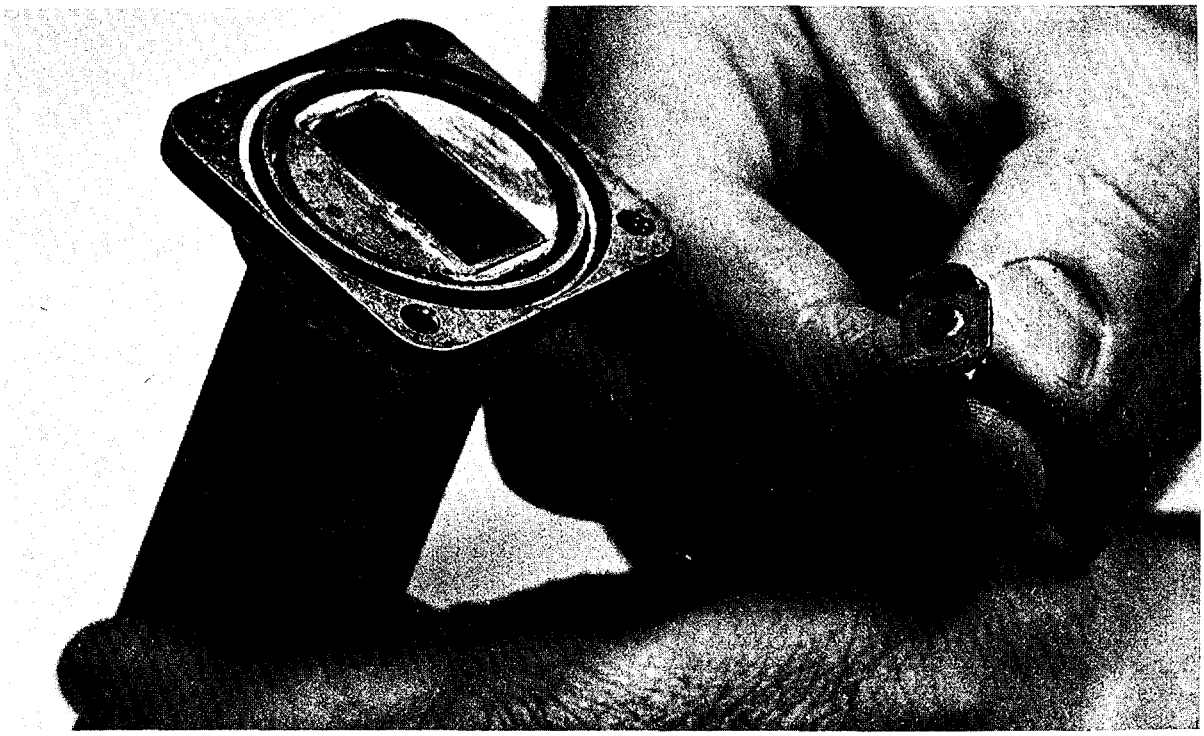

Fig. I–55. Magnetic Properties of Rare-Earth Metals. Photograph of a section of the high frequency waveguide, (3 mm. wavelength) shown at *right*, which is used in the Ames Laboratory study of the magnetic properties of the rare-earth metals by the microwave technique. A more standard microwave waveguide section (3 cm. wavelength) is shown at *left*.

metal crystal structure, it is very difficult to force the internal magnetization of terbium out of the "basal" plane, a crystallographic plane perpendicular to the main crystal symmetry axis. From the microwave absorption studies, it was found that at the temperature of liquid helium (−268.95° C.), the anisotropy in terbium is equivalent to the unusually high magnetic field of 600,000 gauss.

Further studies are being conducted to obtain information about the spectrum of oscillations in the magetic structure of the rare-earth metals. The microwave technique promises to be applicable in those heavy rare earths that absorb neutrons too readily to allow similar studies by neutron diffraction methods.

Nuclear Magnetic Resonance

At Argone National Laboratory the nuclear magnetic resonance (NMR) technique has been used as a research tool to examine bonding characteristics in metallic systems.

Nuclear magnetic resonance is a technique in which atomic nuclei are used as a "probe" for determining the electric and magnetic fields within a solid. In an NMR spectrometer, the device used to study this phenomenon, a sample is placed in a steady magnetic field. Those nuclei of the sample possessing a magnetic moment precess about this field with a frequency that depends upon the magnetic field exerted on the nuclei and the magnitude of their nuclear magnetic moments. In metals, the magnetic field exerted on the nuclei depends upon the strength of the externally applied field plus the polarization of the conduction electrons. Using NMR, accurate measurements of the conduction electron contribution to the magnetic field were made and this derived contribution related to the electronic structure of the system.

Intermetallic compounds of the Periodic Table's group VIII transition elements, iron, (Fe), cobalt (Co), nickel (Ni), ruthenium (Ru), rhodium (Rh), osmium (Os), and iridium (Ir), are known to form the ordered body-centered-cubic or cesium-chloride (CsCl) structures with aluminum. NMR studies have been made on these compounds to examine their electronic structure. The main attention has been focused on the aluminum nuclear sites as these nuclei are best suited for the resonance phenomenon. The position of the aluminum resonance line in these compounds relative to that of pure metallic aluminum is such that there appears to be little or no conduction electrons distributed symmetrically about the aluminum atoms and that charge is transferred from aluminum to the transition metal sites. Thus, for these intermetallic compounds the distinction between metals and ionic crystals appears to lose its clearcut character. This implies that intermetallic compounds may possess bonding of a type intermediate between ionic and metallic. Correlation of these results with specific heat, X-ray diffuse scattering,[36] and optical properties, leads to information on such topics as solution strengthening mechanisms, and order-disorder transformations.[37]

Magnetic Ordering

Magnetic ordering originates in the interactions among atoms, which themselves behave as elementary magnets. One question of interest in the theory of magnetism for both insulators and metals is the way ordering interactions change with the separation between magnetic atoms. Brookhaven National Laboratory developed a new method of determining this spatial dependence. It involves measuring the distribution of the magnetization per atom in the vicinity of the magnetic transition temperature for materials in which some of the magnetic atoms have been replaced by nonmagnetic atoms.

If the range of the interaction is large, then many atoms take part in the ordering process. In this case, statistical fluctations in the density of magnetic atoms are relatively unimportant and the ordering will be relatively uniform. If the range of the interaction is short, the opposite will be true.

A theory has been formulated from which the relative contributions of neighboring atoms to the ordering process can be calculated. The calculated magnetization distributions are then compared with the distribution of magnetic fields at the nuclei of magnetic atoms determined directly by using the *Mössbauer* effect. The most detailed comparisons have been made on ferromagnetic alloys of iron in palladium where excellent agreement was found.

Electron Spin Resonance

A recently completed project at Cornell University is the development of a technique to study the electron spin resonance (ESR) of the excited states of impurity atoms in crystals. This technique was applied to investigate a number of properties of the first excited state of chromium atoms and vanadium atoms which are intentionally added as impurities to magnesium oxide crystals. The fundamental process in the operation of a solid state laser is the emission of light from an impurity atom in a crystal. For instance in the ruby laser, chromium in a crystal of aluminum oxide emits light during a transition from an "excited state" to its "ground state." Understanding the detailed action of lasers and the ability to control the properties of lasers depends upon knowledge of the nature of these ground and excited states. The very powerful tool of electron spin resonance has long been applied to the study of the ground states of various impurity atoms and has given a very detailed picture of how impurities are incorporated in crystals.

But this is only half the story in understanding the properties of lasers, since it is also necessary to know something about the excited

[36] Analogous to the scattering of light by dust particles or the selective scattering of white light by the atmosphere that causes the sky to appear blue.

[37] In which the configuration of atoms in a compound changes from one in which there is a degree of ordering (preferential location of different atomic species) to one that is random, or the reverse.

state as well. The difficulty with applying the spin resonance technique in the excited state is that after the atoms are excited to that state, they remain there only a few-thousandths of a second. This is not very much time in which to perform an experiment which normally requires about 10 minutes. This newly developed technique was originally suggested at the Bell Telephone Research Laboratories, Murray Hill, N.J. It involves the simultaneous irradiation of the sample with light and with microwaves while the sample is in a large magnetic field and is immersed in liquid helium a few degrees above the absolute zero. The results of this difficult experiment imply the need to modify the conventional theoretical picture of the influence of the static host crystal upon the properties of the excited state. However, the results tend to confirm a conventional picture of the effects of the atomic motion of the host crystal. Finally, the experiments show the strong influence of interactions among the impurities much more clearly than conventional experiments using the ground state spin resonance, and make clear the need for understanding these interactions in more detail.

Magnetic Susceptibility of Alpha-Uranium

The magnetic properties of polycrystalline and single-crystal alpha-uranium [38] have been studied in detail at Argonne National Laboratory. The susceptibility (the magnetization per unit intensity of applied magnetic field) of the polycrystalline samples was constant at all temperatures. The three principal crystallographic directions had slightly different susceptibilities but the differences showed little change between −271° C. and 26° C. These results indicate that the atoms in alpha-uranium have no magnetic moment and that there is no magnetic order in this form of the element. These results contribute to the understanding of the unusual properties of uranium.

Ferromagnetic Films

The magnetic properties of ferromagnetic thin films are of considerable interest in the area of computer technology. One continual problem with such films is the characterization of the structure of the films, *i.e.*, the size and orientation of the small crystals composing the films. Electron microscopy and electron diffraction have been extensively used in studies of the structure. Work at Cornell University on ferromagnetic films was initially directed towards the magnetic properties but became focused on the structure of the films because of difficulty in fabricating specimens with the requisite magnetic properties. Electron diffraction at very small angles to the incident beam showed that the problems with the films arose from small discontinuities which were not readily detectable with high resolution electron microscopy. The small angle scattering technique has not been extensively used with films and shows great promise as a means of detecting discontinuities and of obtaining statistical data on particle size and separation in thin films.

Initial studies were made with permalloy, a technical alloy of iron and nickel. Further studies with improved techniques were carried out with pure nickel, palladium, chromium, and gold. The films were produced by condensing the hot vapor on a cold surface. Under the conditions of the experiment, the rate of condensation of the film was the critical factor. Those films deposited at a fast rate were continuous whereas those deposited at a slow rate were discontinuous, *i.e.*, they consisted of small particles about one millionth of an inch in diameter separated by vacuum or very thin layers, one or two atoms thick of foreign material such as oxide (see Fig. I–56).

NEUTRON DIFFRACTION

One of the many useful purposes of nuclear reactors is to serve as neutron sources for research. Beams of neutrons from special research reactors are used to probe the structure of matter. The unique properties of the neutron permit a variety of diffraction and scattering experiments resulting in information generally unattainable by any other means.

[38] *Alpha-uranium*—That allotropic modification of uranium metal which is stable below 660° C.; it has an orthorhombic crystal structure.

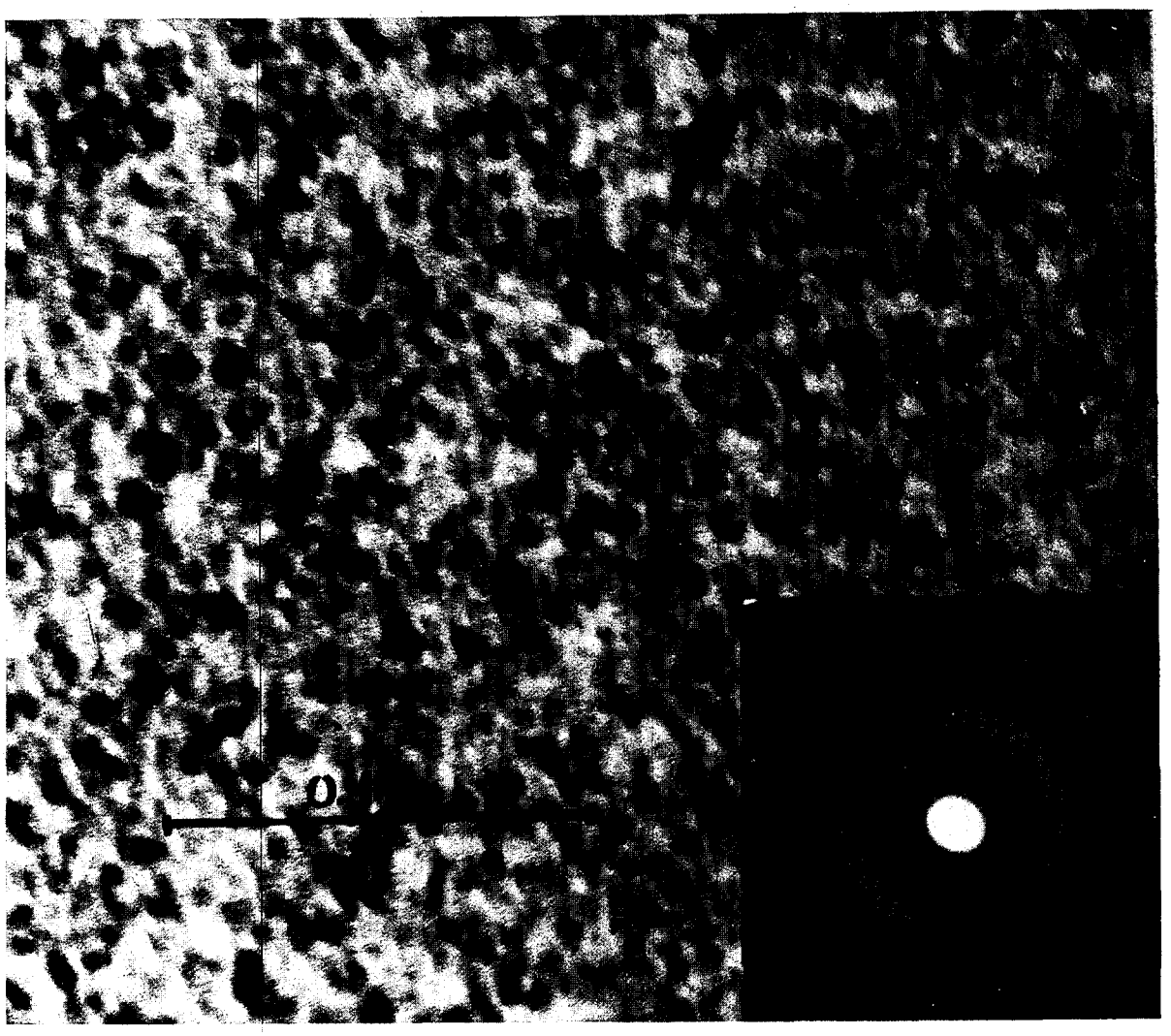

Fig. I–56. Ferromagnetic Films. An electron micrograph and the corresponding small angle diffraction pattern (*lower right*) from a vacuum deposited thin film of nickel are shown in this Cornell University, Ithaca, N.Y., photo. The ring around the central spot indicates that the film has gaps in it, a conclusion difficult to draw from the electron micrograph. The scale mark, 0.1 μ is equivalent to one hundred-thousands of a centimeter.

Atomic Vibrations in Diamond

At the Los Alamos Scientific Laboratory, the 253.7-carat gem-quality Oppenheimer diamond, which was borrowed from the Smithsonian Institution, Washington, D.C., has been used in neutron scattering studies. This is part of a continuing program of basic research using thermal neutrons as probes to increase our understanding of solids and liquids. In this experiment, the relationship between frequency and wavelength of atomic vibrations was determined for diamond. This relationship, called the dispersion relationship, serves as an identifying pattern or fingerprint for forces between atoms in the crystal. Before the experiment, little was known about the atomic vibrations of diamond, but it was expected that they would be very similar to those in germanium and silicon, which have the same crystal structure. This experiment showed that there are qualitative differences between the dispersion relationship in

diamond and the other two substances. This information helped indirectly to understand the way diamond absorbs infrared light and it has also illuminated the electronic structure of diamond.

The crystal structure of diamond has a complex three-dimensional pattern as illustrated by the enlarged model shown in Figure I–57. The balls represent carbon atoms, and rods holding them together represent strong electrical forces.

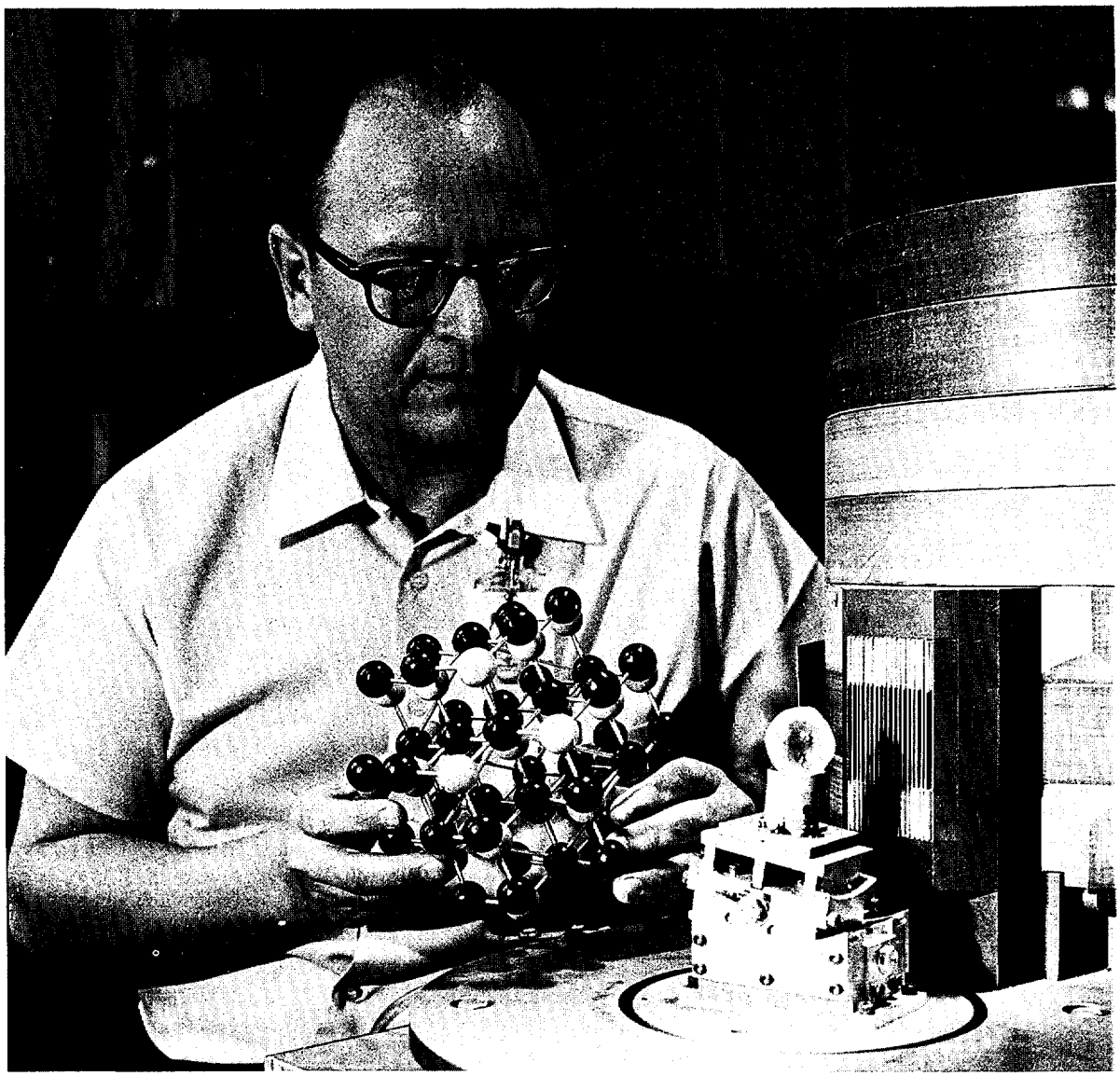

Fig. I–57. Atomic Vibrations in Diamond. A scientist at the Los Alamos Scientific Laboratory is shown holding an atomic model of a diamond crystal beside the 253.7-carat "Oppenheimer" diamond (borrowed from the Smithsonian Institution) mounted in position for a neutron scattering experiment. In the experiment, a beam of thermal neutrons from the Los Alamos Omega West Reactor excited atomic vibrations in the diamond and entered the neutron spectrometer (shown at *right*) to be counted and analyzed for changes in direction, energy, and momentum. Data from the spectrometer provided new information about the electronic structure of diamonds and the atomic vibrations produced in the scattering process.

Shaking the model will give some idea of the strength of the rods. Similarly, shaking the atoms in a crystal will give information about the forces holding it together. A good way of shaking the atoms is to bounce neutrons from them. A beam of neutrons from the Los Alamos Omega West Reactor with fixed energy and momentum was directed at the diamond. As neutrons emerged from the sample, the changes in energy and momentum incurred during passage through the crystal were detected by a neutron spectrometer set up to detect neutrons scattered at a given angle. These quantities in turn tell much about the motion of the atoms caused by the neutrons. These motions are vibrations with frequencies in the range of 10-trillion cycles per second. The experiment was not possible with a diamond of smaller size because of the sensitivity of the measurements.

Polarized Neutron Beam Research

Experimental studies with polarized beams of slow neutrons at Massachusetts Institute of Technology, Cambridge, Mass., yielded new information on two basic problems. The first problem deals with the determination of the spin state scattering amplitudes for the cobalt nucleus. It has been known for a long time that nuclear forces are spin dependent, *i.e.*, they depend upon the relative orientation of the spins of the interacting particles or nuclei. One result of this spin dependent interaction is the characterization of nuclear scattering by two distinct spin scattering amplitudes corresponding to parallel and antiparallel orientation of the neutron spin relative to the nuclear spin. By studying the scattering of polarized neutrons by polarized cobalt nuclei (maintained at a temperature of −271° C. with a large applied magnetic field), these spin scattering amplitudes have been found to differ greatly in magnitude and in algebraic sign. Prior to the cobalt work, such information has been available for only two other nuclei, namely hydrogen and vanadium.

A second problem under study at M.I.T. seeks to answer the question as to whether a neutron possesses an electric dipole moment. This neutron property is closely related to questions about the validity of various conservation laws in fundamental interactions and hence there is theoretical interest in the experimental results. The approach at M.I.T. has been to search for the extra scattering that should exist in the scattering of polarized neutrons by atoms if the neutron possessed this property. Since this scattering is known to be very weak (about 10,000 times smaller than normal nuclear scattering amplitudes) it must be sought in special cases, notably in *Bragg* scattering by carefully selected crystals. Experiments were initiated at the M.I.T. Research Reactor and extended at Brookhaven National Laboratory's High Flux Beam Reactor (HFBR), where there is a very sizeable intensity gain. At Brookhaven's HFBR, a beam of neutrons with aligned spins is scattered by a cadmium sulfide crystal, chosen in part because it has no direct magnetic interaction with the neutron spin. Interaction of the electric fields of the crystal with the assumed electric dipole moment of the neutron should give a difference in intensity of the scattered beam when the direction of the neutron spin is reversed. The new results indicated that the dipole moment is at least 25 times smaller than the upper limit obtained in an earlier experiment performed at Oak Ridge National Laboratory in 1950.

Uranyl Nitrate Dihydrate Structure

A neutron diffraction study carried out at Argonne National Laboratory resulted in a picture of the atomic arrangement in crystalline uranyl nitrate dihydrate, $UO_2(NO_3)_2 \cdot 2H_2O$ (see Fig. I–58). Although broad structural features had been obtained by infrared studies, the exact locations for the nitrogen and oxygen atoms were not known. Likewise, an indication of the hydrogen positions and their role in the structure was not available. Neutron diffraction was chosen, because this technique has a large advantage over X-ray diffraction in the study of such compounds. In neutron diffraction, all atoms are detected with about equal sensitivity

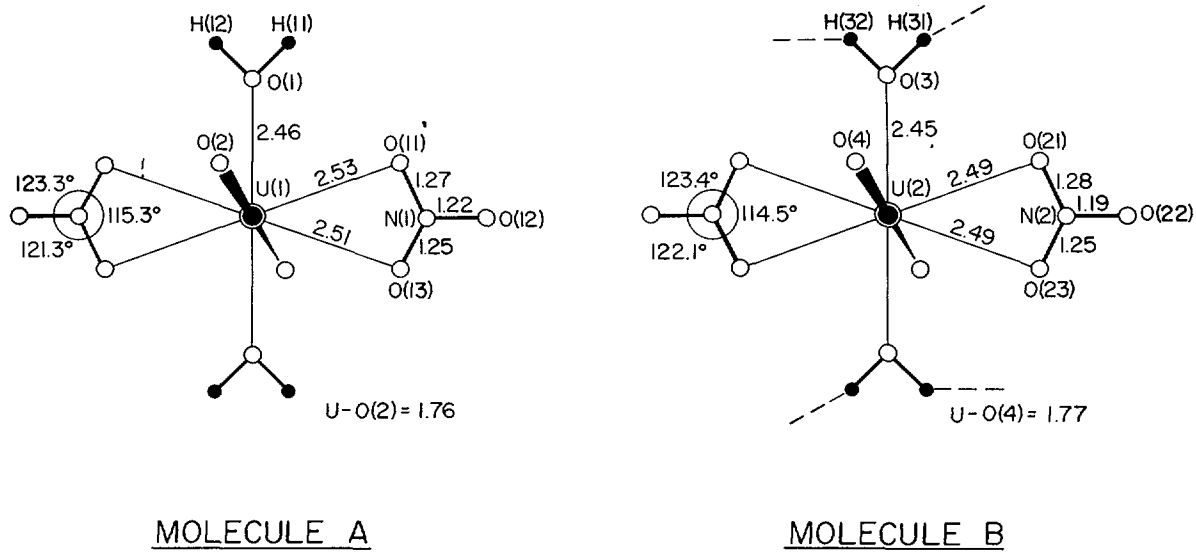

Fig. I–58. Uranyl Nitrate Dihydrate Structure. Planar oxygen hexagon about uranium atom found in $UO_2(NO_3)_2 \cdot 2H_2O$ resulting from a neutron diffraction study at Argonne National Laboratory. In Molecule A, the nitrate group is shown as nitrogen-one, N(1), with its three associated oxygen-ones, O(11), O(12), O(13). In like manner, the water-one is shown as O(1) with its respective hydrogen-ones, H(11) and H(12). A similar scheme for oxygen and hydrogen designation is used for Molecule B. The two kinds of hexagon planes as shown in the figure are linked together in chains by rather weak hydrogen bonds (O——H - - - O) and cross linked by similar but even weaker bonds.

whereas in X-ray diffraction the ability to detect an atom is proportional to its atomic number. Therefore, in an X-ray study of the compound, the light nitrogen and oxygen atoms (atomic numbers 7 and 8) may be just detectable in the presence of uranium (atomic number 92), but the hydrogen atoms will go undetected (atomic number 1). It was found that the basic structural unit of uranyl nitrate dihydrate is a linear uranyl group (UO_2) with a nearly planar and perpendicular oxygen hexagon; four of these oxygens are from the nitrate groups (NO_3) and two are from the water molecules (H_2O).

Neutron Monochromators

Although perfect crystals are useful in many research applications, a technique has had to be developed to introduce imperfections into germanium (Ge) crystals so as to conduct neutron diffraction experiments. The imperfect crystals are 50 times better for such use than perfect ones. Methods for introducing imperfections into these crystals and thus improving the experimental beam intensity have been explored at Brookhaven National Laboratory and a satisfactory process involving deformation by hot-pressing has been developed. Deformed germanium crystals are now in use as monochromators at six of the HFBR (High Flux Beam Reactor)[39] neutron spectrometers.

With the advent of the HFBR at Brookhaven, considerable attention has been paid to the best use of the available neutron flux as determined by the choice of monochromating crystals[40] for use with neutron diffraction spectrometers. In principle, the element germanium is advantageous because it

[39] The High Flux Beam Reactor (HFBR) was put in operation October 31, 1965. It has an extremely high neutron flux (1.6×10^{15} neutrons per second per square centimeter). There are nine ports from which neutron beams can be drawn. See pp. 228–230, "Annual Report to Congress for 1964," and p. 240, "Annual Report to Congress for 1965."

[40] These are crystals which allow a beam of neutrons of a particular well-defined wavelength to be selected from the wide spectrum produced by the reactor.

eliminates the small but troublesome contribution from neutrons of exactly one-half the desired wavelength, which are invariably present with the usual monochromators (copper and lead). These unwanted half-wavelength neutrons are frequently a source of confusion in the subsequent data analysis. In practice, available germanium crystals are unsuitable because they are extremely "perfect," *i.e.*, free of appreciable numbers of crystalline imperfections and impurities of any sort. In such a case, the intensity of the monochromatic beam is drastically reduced.

The process consists of hot-pressing a flat cylindrical crystal of germanium about 2 inches in diameter and ⅜ inch thick at a temperature of 800° C. and an applied load of 4,000–6,000 pounds. The crystal is contained in a steel die, and the whole assembly is placed inside a vertical tube furnace standing between the jaws of a hydraulic press. Under these conditions, the germanium deforms quite plastically with a permanent contraction of about one to two percent. Evaluation of the crystal is based mainly upon its "rocking curve," that is, the variation of intensity of scattered neutrons as a function of the crystal's angular position. Such a curve should show a smooth, symmetrical peak, and for optimum use in most experiments, the angular width of this peak at the middle should be about 0.25 degree. A monochromator of this sort gives something like 50 times as much useful intensity as an undeformed perfect crystal.

PLASTIC DEFORMATION

Metals and other crystalline materials are capable of withstanding a particular level of stress below which they do not undergo any permanent change in dimensions. Ductile materials, such as most metals, do not fracture immediately upon reaching this level. It is this ability to deform without fracturing that is probably the single most important property of metals. Consequently, studies aimed at understanding the general topic of plastic deformation encompass an active area of research.

Dislocations in Ordered Alloys

The unique features presented by dislocations in ordered alloys hold out the possibility of obtaining high yield strength in these materials by a judicious choice of metallurgical variables. In a continuing effort to better understand what makes metals or alloys weak or strong, an extensive investigation of an alloy containing 75 percent iron and 25 percent silicon was made at the Ames Laboratory. By using electron microscopy techniques, single crystal specimens were studied with respect to temperature and crystal orientation. It was found that increased strengthening can be obtained by lowering the temperature or by orienting the crystals in a specified manner.

Observations made with the sample oriented for single slip and tested at room temperature showed it to contain pairs of dislocations (see Fig. I–59). It is the movement of these dislocations on the single slip plane that causes deformation. At somewhat lower temperatures the dislocations no longer travel in pairs but singly, leaving behind ribbons of "mistakes" (antiphase boundaries) (see Fig. I–60). As a result, the stress required to move these single dislocations is high which in turn causes the yield strength to increase markedly.

Superplasticity in Metallic Materials

Superplasticity is a term which refers to the unique capability of certain metallic materials to be stretched to great lengths before breaking, sometimes to more than 2,000 percent of their original length (see Fig. I–61). This behavior is typical of hot glass but highly unexpected in crystalline materials. At Stanford University, Palo Alto, Calif., studies of the microscopic structure in the interior of superplastic materials have revealed subtle but significant changes in the structure which take place during superplasticity processes. The originally sharp angular boundaries of the grains (grains are the individual crystals which make up a metal) become smooth and rounded in shape as shown in Figures I–62 and 63. This change in geom-

etry of the crystals is evidence that superplasticity is due to the continual appearance and growth of new grains and the constant motion of grain boundaries during stretching. These observations of structural changes in superplastic materials are important because the operative mechanisms must be understood before the superplasticity effect can be exploited effectively (for example, shaping difficult-to-form metals) in nuclear reactor technology as well as in other engineering fields.

Superplasticity is known to occur in certain steels, titanium alloys, brasses, aluminum alloys and in some other alloys of lesser engineering significance. Research at Stanford has centered on a study of the behavior of aluminum-zinc alloys and a mathematical treatment of the superplasticity phenomenon in these alloys is being formulated.

Hydrogen Embrittlement of Metals

Numerous metals are known to fail when subjected to stress at low temperatures if they contain even small amounts of hydrogen. In metals, such as iron, that do not react with hydrogen to form hydride compounds, this embrittlement,

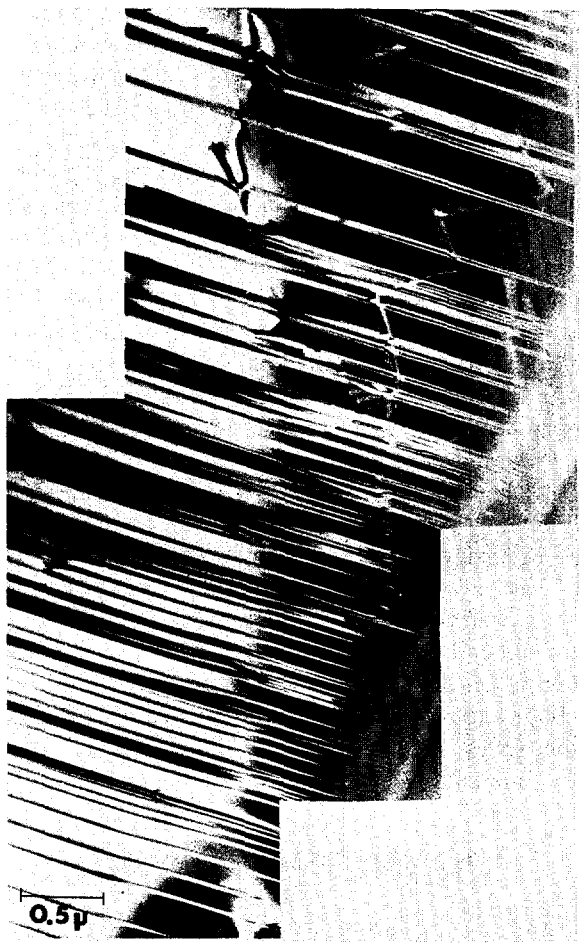

Figs. I–59 and 60. Dislocations in Ordered Alloys. Ames Laboratory micrograph on *left* shows nearly vertical dislocation pairs (double black lines) lying in the slip plane of the iron-silicon alloy that was oriented for single slip and deformed at room temperature. The scale at the left indicates 0.5 microns or 0.000020 inches. The dislocations are made visible since they represent a region of distortion in the crystal which interferes with and thus modifies the electron beam as it passes through these regions of the crystal in the electron microscope. On the *right*, a composite of several electron micrographs shows the nearly horizontal bands which are "mistakes" or antiphase boundaries produced by imperfect single dislocations generated during deformation at −30° C. of a single crystal oriented for slip on only a single-slip plane. The section from which the picture shown above was taken, unlike the previous figure, was inclined 60° to the slip plane. The antiphase boundaries being mistakes in the crystal are made visible by the electron beam from the electron microscope similar to the manner in which dislocations are made visible.

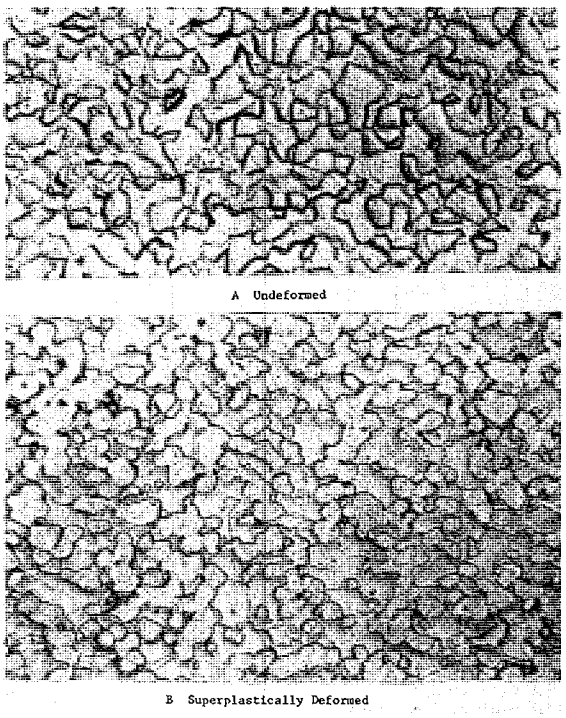

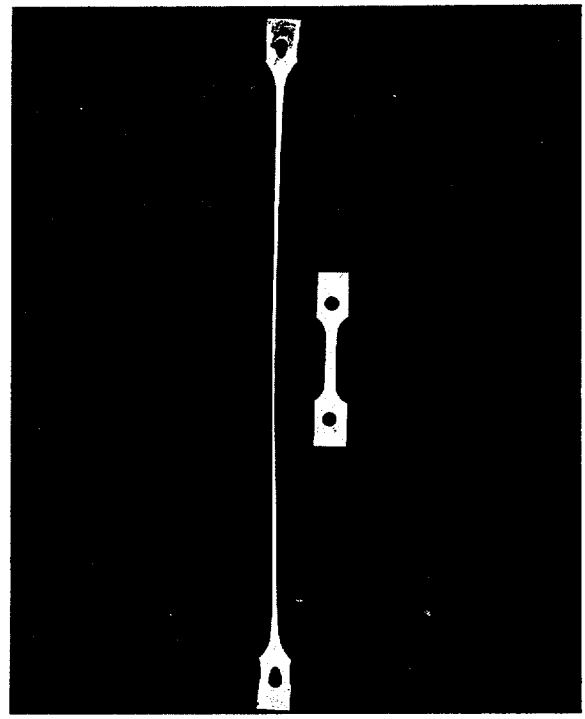

Figs. I–61, 62, and 63. Superplasticity in Metallic Materials. Photo *above right* is an example of an extraordinary degree of stretching in a superplastic zinc-aluminum alloy (78 weight % zinc). The specimen was stretched at a temperature of 257° C. at Stanford University, Palo Alto, Calif. Photomicrographs at *left* are of undeformed and superplastically deformed regions of the specimen shown above. In order to make these photomicrographs, the specimen was cross sectioned, polished, and etched with a chemical to reveal structural highlights. The magnification is 3,000×. Note how the original, sharp, angular boundaries apparent in Figure A have become more rounded and smooth during stretching as shown in Figure B. This change in structure suggests that the constant motion of boundaries leads to superplasticity.

or loss of ductility, has been attributed to the initiation of microcracks when hydrogen is precipitated from supersaturated solid solution in the form of bubbles. This phenomenon would not occur in a metal that does form a hydride, so the embrittlement mechanism in hydride formers must be different. At Argonne National Laboratory, transmission electron microscopy (a technique that allows observation of the interior of thin metal foils at very great magnification) has been used to demonstrate that in the case of zirconium-hydrogen alloys (hexagonal-close-packed crystal structure) the observed reduction in ductility can be attributed to the formation of small, zirconium-hydride particles finely dispersed in the atomic lattice. The ductility in metals is dependent on the movement in the lattice of line imperfections called dislocations. However, in the zirconium-hydrogen alloys, dislocation motion was found to be impeded by hydride particles and embrittlement resulted.

Effect of High-Pressure Hydrogen

In one of the applied metallurgy research programs at the Lawrence Radiation Laboratory, Livermore, it has been found that high-pressure hydrogen can embrittle stainless steel. This effect has very important implications, especially for the chemical process industry, because it has been widely assumed that stainless steel does not become brittle when exposed to high-pressure hydrogen.

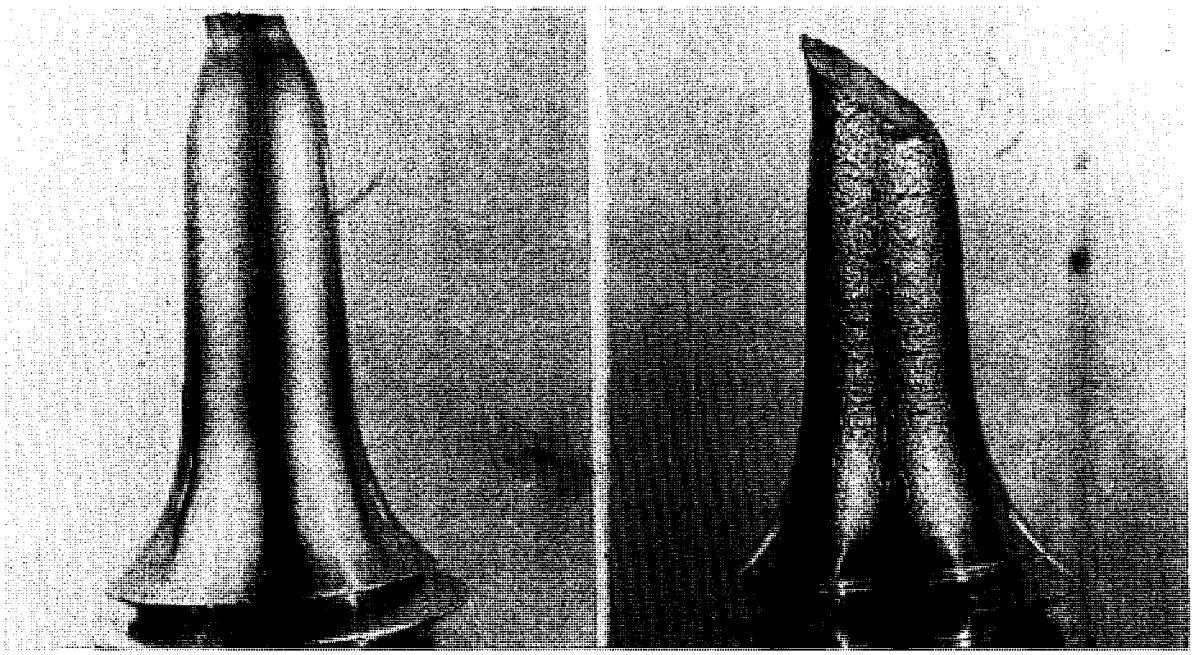

Fig. I–64. Effects of High-Pressure Hydrogen. Photos *above* show stainless steel specimens that were stretched until broken in high-pressure helium and hydrogen environments at Lawrence Radiation Laboratory, Livermore. The specimen at *left* was stretched until broken in an atmosphere of 10,000-p.s.i. helium; the specimen at *right* was given the same test in 10,000-p.s.i. hydrogen. The inception of permanent deformation (arbitrarily taken at 0.2% plastic deformation) occurred at a smaller load in hydrogen, indicating that cracks must have formed at low values of average permanent strain. Smoothly finished test specimens did not consistently show reduced mechanical properties in hydrogen; notched bars, such as those shown here, showed a more significant reduction in properties. (Magnifications are about 5×.)

Cylindrical specimens of type 304 stainless steel were stretched axially, in a 10,000 pounds per square inch (p.s.i.) hydrogen environment, until they broke (see Fig. I–64). The stretching (tensile) load was recorded as a function of displacement; thus, the load per unit cross-sectional area (stress) was determined for the onset of nonrecoverable or plastic deformation—where the elastic limit of the material is first exceeded—as well as for the breaking point, which occurs at a higher stress. Additional analyses of the influence of hydrogen were made by means of optical microscopy of polished sections of the stainless steel specimens and electron microscopy of Carlson replicas of the fractures. The results indicate that embrittlement requires a combination of three factors: (*a*) transformation, or rearrangement of metal atoms, during plastic deformation, (*b*) a threshold load much higher than the load required for permanent deformation, and (*c*) the diffusion of hydrogen to the region of threshold stress. The first requirement is met in many metastable stainless steels; the second may be obtained in the presence of a notch or scratch, which locally intensifies the load. The introduction of hydrogen into the metal should be enhanced by high pressure.

Ductility of Polycrystals

Most engineering materials are polycrystalline, *i.e.*, aggregates of many crystalline grains. When polycrystals are deformed, all the grains deform. The atomic mechanisms of deformation within a grain are often the same as they are in a free single crystal where they are more easily studied. This is true for many materials under many conditions, for example in high purity iron at room temperature, and in aluminum and

copper at all temperatures. In these cases, a quantitative relation can be established between the stress-strain behavior of single crystals and polycrystals.

In many other cases, however, such as in zinc and beryllium at low temperatures, and in alpha-zirconium and alpha-uranium (alpha forms of these elements being the room-temperature allotropic form) at all temperatures, the grains in a polycrystal would not fit together after deformation, if they deformed as they do when they are free. This should lead to fracture after a few percent deformation. In some cases, such as in zinc and beryllium at low temperatures, this does in fact happen. In others, such as in alpha-zirconium and in alpha-uranium at all temperatures, the ductility of the polycrystals is comparable to that of the single crystals, although the strength is higher. The reason for this unexpected ductility is that, in addition to the normal deformation mechanism of crystallographic slip, the mechanism of crystal twinning contributes to deformation in the grains of a polycrystal, whereas in single crystals it does so only under special circumstances. In alpha-zirconium and alpha-uranium the twinning occurs in enough crystallographic directions to accommodate all possible deformations of a grain.

In yttrium, hafnium, and the rare earth elements—gadolinium, dysprosium, holmium, and erbium—the ductility of polycrystals is larger than 10 percent and similar to alpha-zirconium. However, it was observed at Argonne National Laboratory that the number of slip and twinning modes occurring in these materials, although they have the same crystal structure as alpha-zirconium, is not large enough to allow the accommodation of every grain to the deformation prescribed by its surroundings as is the case with alpha-zirconium. This observation has led to a reconsideration of the theoretical criterion generally used for judging the ability of accommodation. It sugggests that an increase in the ductility from 10 to 100 percent, which would be an important achievement for the workability of materials, may be obtained by developing an alloy with a larger number of independent, full deformation modes. Also, it suggests that the difference between brittleness and a ductility of a few percent, which is important for structural applications of a material, has no relation to the number of independent modes, but, is probably controlled by the sensitivity of a material to stress concentrations.

TRIP Steels

The urgent need for stronger, more ductile alloys has become increasingly evident in recent years. Of particular interest for advanced design applications is the yield-strength range between 200,000 and 400,000 p.s.i. A study of the deformation characteristics of ultrahigh-strength steels strongly suggests that high values of elongation along with yield strengths above 200,000 p.s.i. are not to be expected in materials that depend upon dislocation interactions for strain hardening. The strain-hardening rate due to dislocation interactions is considered to be too low at high stress levels to prevent instability at low strains. At the Lawrence Radiation Laboratory, Berkeley, a process for substantially increasing the strain-hardening rate, and consequently the uniform elongation in steels has been developed which employs the strain-induced transformation of one crystal structure to another to enhance strain-hardening and has resulted in a new form of steel, called "TRIP" (transformation-induced plasticity).

During tensile testing of this type of alloy, martensite, a tetragonal crystal structure, was formed in a very finely divided state. This fine martensite formed barriers to dislocations, and these barriers were evidently substantially stronger than those formed by dislocation interactions. The work-hardening rate was found to be much higher than that of heat-treated low-alloy steels, and the plastic instability was displaced to significantly higher strains. Elongations in the range of 20 to 40 percent were obtained for alloys having yield strength between 290,000 p.s.i. and 220,000 p.s.i., respectively.

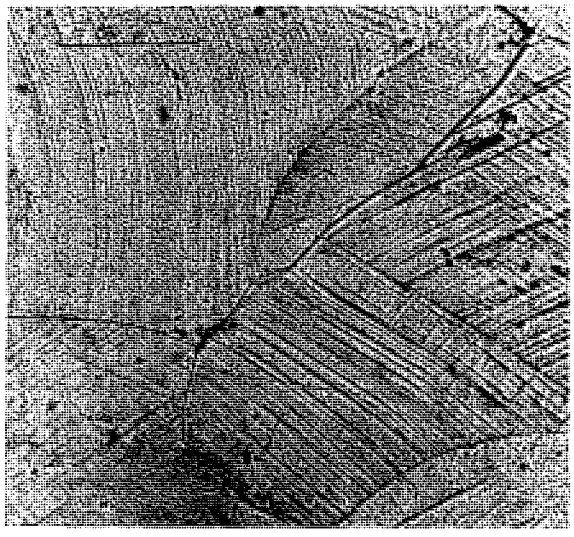

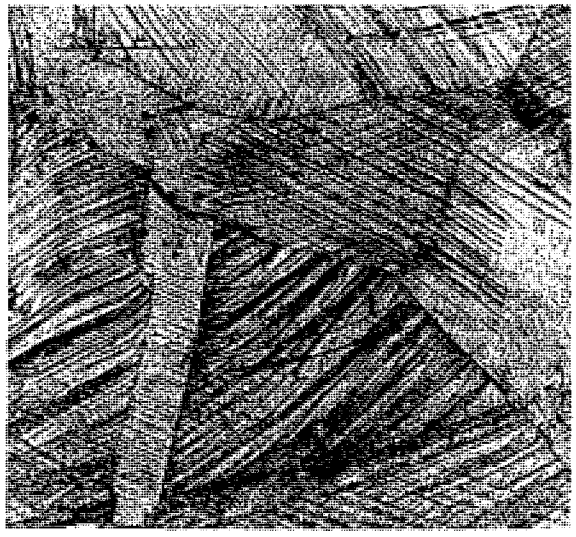

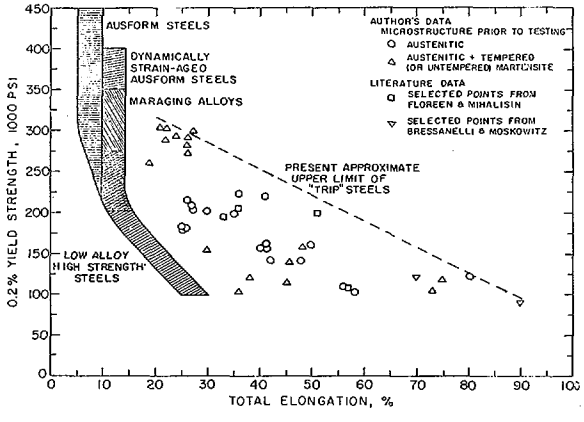

Figs. I–65, 66, and 67. TRIP Steels. Photomicrograph above *left*, shows the microstructure of TRIP steel, developed at Lawrence Radiation Laboratory, Berkeley, after thermomechanical deformation (reduced 20% at 449° C.). Photomicrograph, above *right*, shows the microstructure of a thermomechanically treated (reduced 20% at 449° C.) TRIP steel after a tensile test at room temperature. The area photographed was near the fracture surface. The material has undergone further transformation to martensite during the room temperature plastic straining, but the martensite plates are too small to be seen readily. Magnification of both 1,000×. At *left*, is a plot of elongations of various classes of steels versus yield strengths. In this plot, bands representative of the range of elongations at each yield-strength level are plotted for quenched and tempered low-alloy steels, for ausform steels, for maraging alloys, and for ausform steels that have been dynamically strain-aged. The band for TRIP alloys is displaced relatively far out on the strain scale as compared with the bands for other high-strength alloys.

The microstructures of alloys exhibiting the TRIP phenomenon have been examined at various stages of processing. The great advantage of augmenting the work-hardening characteristics of steels through the TRIP phenomenon is evident from a comparison of the curves in the graph of elongation versus yield strength (see Figs. I–65, 66, and 67).

Creep at High Pressure

In research carried out at Cornell University the pressure dependence of creep (deformation with time under load) in aluminum and indium has been studied. Results in aluminum indicate that the expansion of the lattice is outward when a vacancy is formed, whereas the results for another trivalent metal, indium, indicate a contraction. The nature of this lattice relaxation around vacancies is related in turn to their interaction with other defects such as dislocations and can be of importance in describing deformation processes in solids.

A new creep theory has been developed for the temperature range between one-quarter and one-half of the material melting point. This theory has been shown to be consistent with several experimental facts and critical tests of this theory are now under way. Most creep ap-

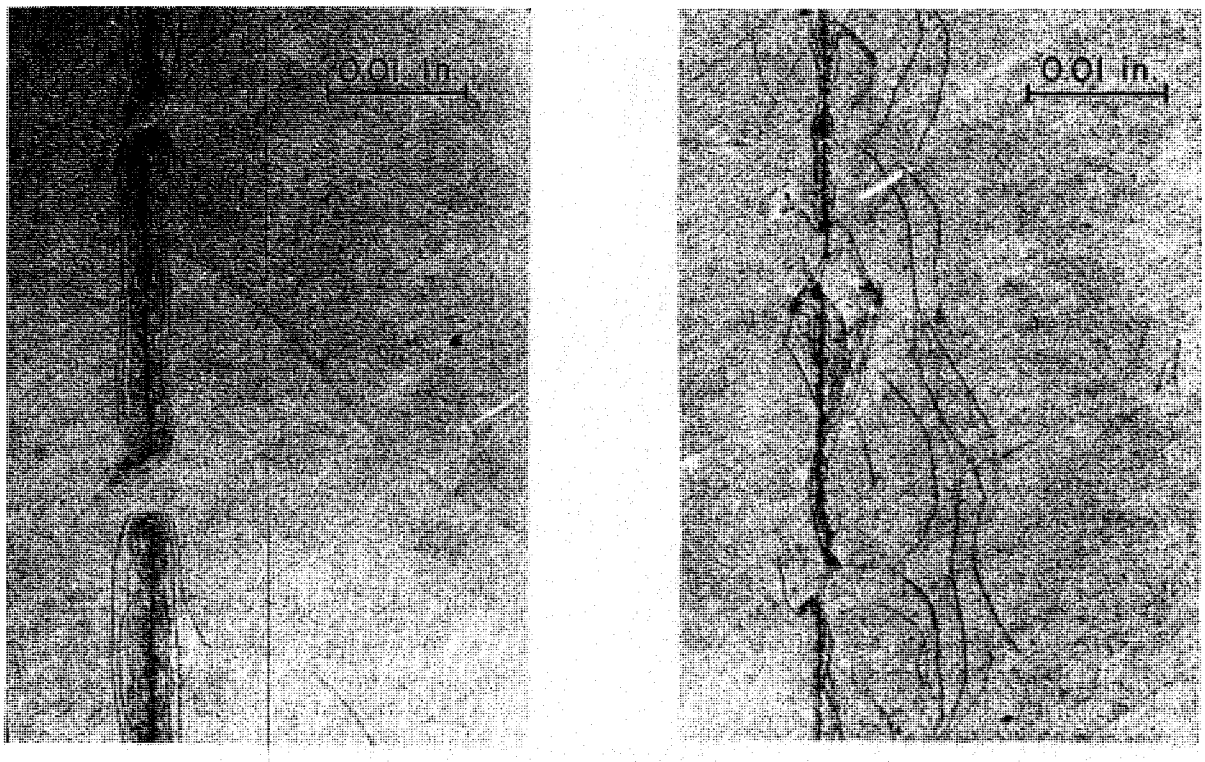

Fig. I–68. Dislocations in Metallic Crystals. These X-ray micrographs from the California Institute of Technology, Pasadena, Calif., illustrate the displacement of dislocations which is produced in a crystal by an applied stress. Dislocations are imperfections in the atomic structure and they are revealed as dark lines in the micrographs. The *left* picture shows the dislocations produced by scratching the surface of a zinc crystal. The *right* picture shows the dislocations after the application of a short duration stress pulse. Dislocation motion causes planes of the crystal to slip past one another. Slip by the movement of dislocations is analogous to the slip of a rug on the floor by the movement of wrinkles as shown in the schematic diagrams *below* each micrograph. The wrinkles to the left of the scratch move to the scratch, and the wrinkles to the right move further away from the scratch. Stress was applied to the surface of the crystal, in the direction of motion of the dislocations, for a period of 50×10^{-6} (50 millionths) of a second. Such observations provide information needed for prediction of the plastic response of crystalline materials subjected to applied forces.

plications (in turbines, reactors, etc.) involve temperatures less than half the melting point and, therefore, an understanding of the creep process in these lower temperature ranges is necessary.

CERAMIC MATERIALS

Nonmetallic materials with good high temperature stability properties generally fall into the category of ceramics. The most familiar of these materials probably are the metallic oxides. Applications for ceramics are widespread, ranging from electronic devices to refractory coatings. In the atomic energy field, ceramic fuel elements are being used in nuclear reactors. As a result, a greater understanding of this class of materials is an important goal for the research program.

Nonstoichiometric Oxides

In the investigation on defect structures in nonstoichiometric oxides conducted at Mar-

275-845 O—68——8

quette University, Milwaukee, Wis., the electrical conductivity of sintered ceramic cerium dioxide (CeO_{2-x}) [41] specimens was measured as a function of temperature, composition, and oxygen partial pressure. Based on the comparison between the theoretically derived relation and the experimental conductivity data, the nonstoichiometric defect structure of CeO_{2-x} was rationalized in terms of a defect model involving quasi-free electrons and both singly and doubly ionized oxygen vacancies.

An understanding of the defect structures, *i.e.*, the various types and concentrations of atomic and electronic defects present in nonstoichiometric oxides, is important because of the important role these defects play in determining the properties of an oxide (ionic conductivity, electronic conductivity, diffusion coefficients, etc.) and the stability limits of the oxide. A basic understanding of these properties and stability limits in terms of the defect structure in the oxide are necessary, for example, in order to better understand and thus better control the stability of nuclear fuels under various environmental conditions.

Microstructure in Ceramics

Effect of micromechanical stress-concentration on the strength of brittle ceramic materials has been demonstrated at the Lawrence Radiation Laboratory, Berkeley. Variations of the strength of a glass with uniform spherical pores as a function of pore size and volume has now been predicted on the basis of stress concentration and the size of flaw responsible for brittle failure. These determinations were made in a research effort directed towards understanding the effect of microstructure on the physical and mechanical properties of single and polyphase ceramic materials.

Methods are under development for ceramic materials with quantitatively definable microstructural features. Unique fabrication techniques have been employed to produce two-phase systems with controlled parameters such as volume fraction of dispersed phase, shape and size of dispersed phase particles, interfacial bonding between phases, and known internal stresses.

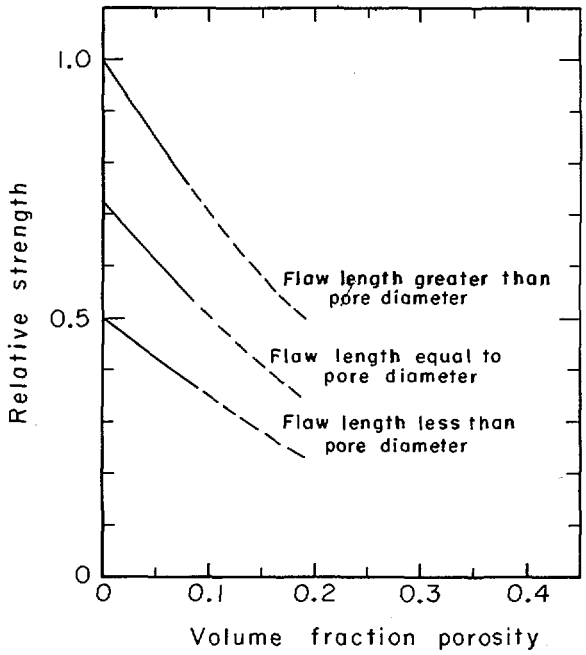

Fig. I–69. Microstructure in Ceramics. The relative strength of a matrix failing by flaw-induced brittle fracture as the porosity varies is shown in the Lawrence Radiation Laboratory, Berkeley, chart. The porosity was produced by dispersing nickel microspheres in a glass matrix by hot pressing and allowing the spheres to shrink away from the glass on cooling. No precipitous drop in strength was observed with the increased porosity.

Investigations have been made on stress concentration effects in porous glasses and predicting the effect of porosity on strength as the pore size and volume varied. On the basis of the hypothesis, only a monotonic decrease in strength with porosity should be observed, with no precipitous drop. Once the effect of stress concentration around pores reduces the tensile strength, further decreases in strength should be determined by the amount of material in the porous body available to carry the load. In general, the experimental results (see Fig. I–69) for uniaxial and biaxial strength of glass specimens containing spherical porosity agree very well with those predicted. The porosity was pro-

[41] In CeO_{2-x} the "2-x" indicates that the oxygen (O) to cerium (Ce) ratio varies from 2 to 2-x.

duced by dispersing nickel microspheres in a glass matrix by hot-pressing and allowing the spheres to shrink away from the glass on cooling from the hot-pressing temperature. With very small particle sizes, treatment with isopropyl alcohol was necessary to prevent bonding of spheres to the glass.

Glass-Metal Bonding

Presence of an oxide-like layer has been found essential for chemical bonding, which is responsible for adherence, at glass-metal interfaces. The establishment of such thermodynamic equilibria by Lawrence Radiation Laboratory, Berkeley, has emphasized the electrochemical nature of the processes involved and points the way for fundamental studies of importance to glass-metal seals, ceramic coatings, micro-composites, and cermet materials.

Electrochemical reactions tend to be initiated at a glass-metal interface if thermodynamic equilibrium, represented by saturation of the glass with the low-valance oxide of the substrate metal, is not present at the interface. In iron coupled with sodium disilicate glass, with or without cobalt oxide, atmospheric oxidation of the metal occurred, when heated in platinum crucibles which provided a path for electrons from the metal to oxygen at the glass surface. With glasses containing transition metal ions, whose oxidation potential is lower than that of iron, electrochemical reactions also caused oxidation of iron at the interface coupled with reduction of transition metal ions in the glass resulting in the formation of dendrites (see Fig. I-46). The composition of a precipitating dendrite was in all cases found to be determined by the adjoining glass in accordance with the equilibrium constant for the reaction.

Defects in Plutonium Oxide

The ratio of oxygen to metal atoms in plutonium dioxide (PuO_2) need not be exactly two to one. Instead of being limited to the normal, simple whole-number ratios, this compound can exist with ratios as low as 1.6 or 1.7 to one. A low ratio might reflect the fact that oxygen atoms are missing from the crystal structure leaving some sites vacant. Alternatively, the crystal might contain an excess of plutonium ions in normally unoccupied or interstitial sites. Which of the two possibilities actually occurs can be resolved by measuring the density of the compound: vacancies should lower the density relative to the compound $PuO_{2.00}$, and interstitial plutonium ions should increase it. Unfortunately, density measurements cannot be performed at room temperatures because compounds of the type $PuO_{1.8}$ are stable only above 650° C. To overcome this problem, an apparatus was developed at Argonne National Laboratory that relates small pressure changes of helium gas to the volume occupied by a plutonium oxide sample. Density measurements were carried out at 750° C. and it was found that the density decreased appreciably as the oxygen to plutonium ratio was made smaller. These results, favor the conclusion that vacant oxygen sites rather than interstitial plutonium ions are the predominant defects.

Also, an investigation was made to find theoretical relations between the concentration of vacant oxygen sites and the properties of plutonium oxide and compounds like it. The most satisfactory relations were derived on the basis that the defects tended to repel each other and as a result, were forced into partly ordered patterns (rather than being distributed randomly). A computer program has been developed to solve the complex equations involved in the theoretical model and the calculated results are in good agreement with experimental data for cerium dioxide and uranium dioxide. Agreement is not as good for plutonium dioxide, and this has stimulated additional experimental investigation of that compound.

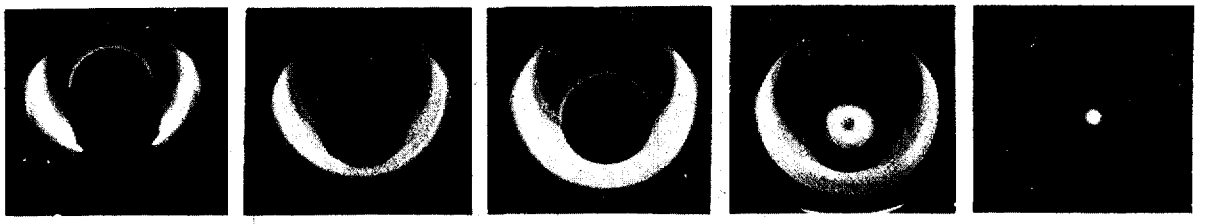

Fig. I–70. Dense Plasma Focus. The series of photos show (from *left* to *right*) the current sheath (the glowing collar around the inner electrode) of ionized deuterium gas as it accelerates down the electrode and compresses into the dense plasma focus in a Los Alamos Scientific Laboratory experiment. Details on this controlled thermonuclear reaction—which also holds promise for other scientific and industrial uses—are on page 98.

CONTROLLED THERMONUCLEAR RESEARCH

The goal of the AEC's controlled thermonuclear research program is to develop a controlled thermonuclear reactor which uses hydrogen isotopes, readily available from the ocean, to produce power for useful purposes. If successful, such a reactor could have very desirable features. First, its fuel would be readily available and inexpensive. Its reaction products would be non-toxic and non-radioactive. There would be no danger of a runaway reaction, since only small amounts of fuel would be in the reactor at any time. Finally, there is the long-term possibility of conversion directly from plasma energy to electricity. In addition, there are compelling interests of a more basic nature for studying the behavior of plasmas. More than 99 percent of the universe is in the form of highly ionized plasma. Yet, the study of such plasmas has received little attention until now.

FUSION REQUIREMENTS

To achieve a controlled thermonuclear reaction, certain requirements must be satisfied. The fuel must be deuterium, or a mixture of deuterium and tritium. The temperature of the ions must be between 100,000,000° and 1,000,000,000° C. (corresponding to between 10,000 and 100,000 electron volts). The plasma density must be about one ten-thousandth of an atmosphere (the density of air at sea level). Finally, the confinement time at these densities and temperatures must be of the order of a tenth of a second. If the density is higher, the confinement time can be shorter; if lower, it must be longer.

Two of the most critical problems have been solved. Methods have been found to achieve the desired temperatures, and plasmas consisting mainly of pure deuterium have been produced in the laboratory. The key remaining problem is the confinement of this exceedingly hot plasma within a limited region. Despite a number of alternative suggestions, the only promising mechanism of confinement still involves the use of strong magnetic fields.

Present research on plasma confinement schemes is oriented toward developing a configuration that does not exhibit instabilities.[42] A major ingredient of a confinement scheme is that of stability: in the absence of stability, the plasma escapes rapidly across the magnetic field to the vessel wall.

Plasma Confinement Experiments

Low-Beta, Open-Ended Systems

"Low-beta" refers to a plasma in which the particle pressure is small compared to the magnetic pressure. An "open-ended" magnetic field

[42] See p. 219, "Fundamental Nuclear Energy Research—1966."

system is one in which the magnetic lines of force leave the plasma confinement zone and lead outward into space as opposed to a "closed" system in which the lines of force close on themselves within the plasma confinement zone.

Low energy injection and compression. In pulsed experiments conducted at the Lawrence Radiation Laboratory, Livermore, low-energy ions are injected into a magnetic mirror configuration when the confining field is weak. As

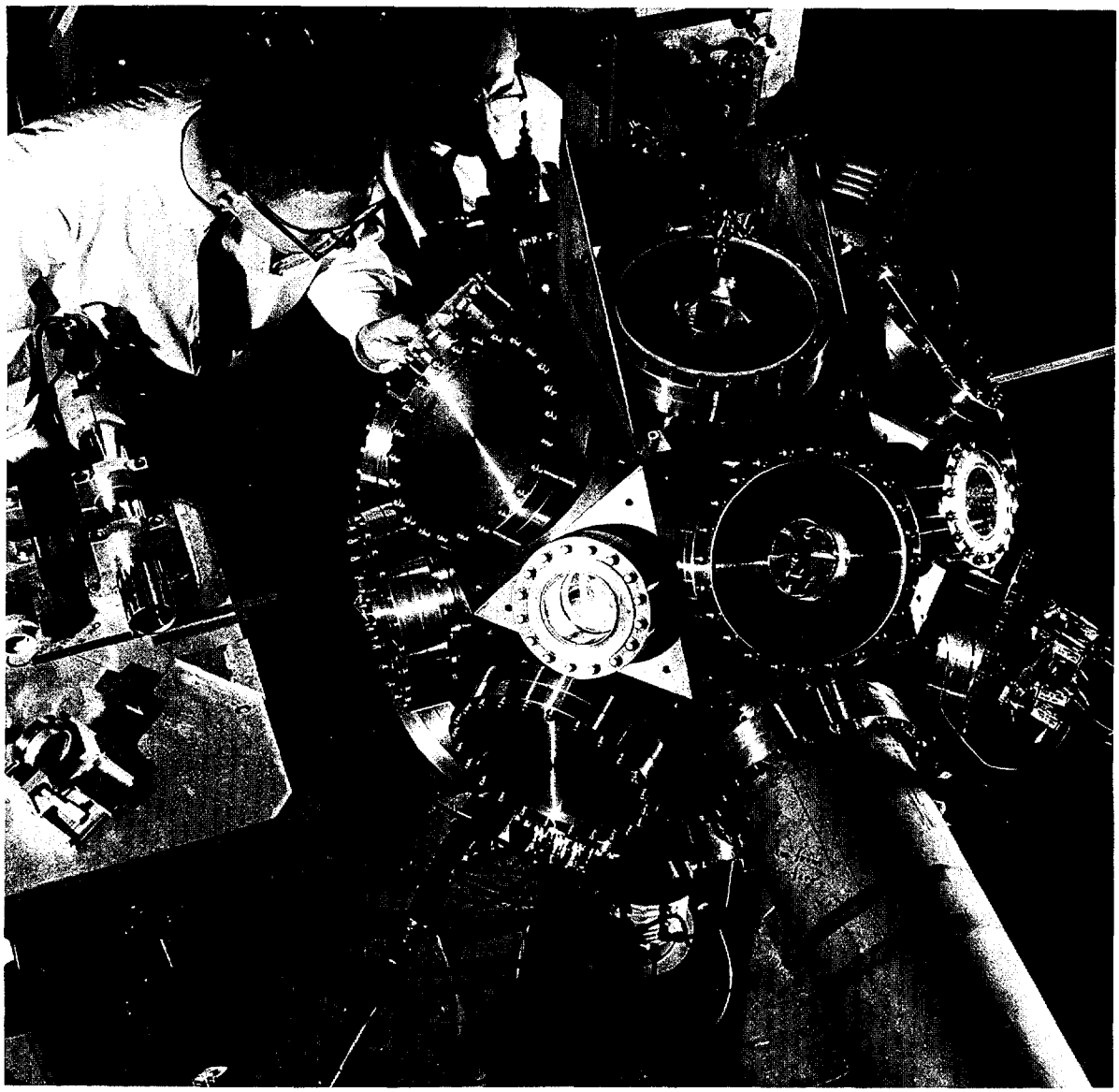

Fig. I–71. Multiport Vacuum Chamber. Single solid particles of lithium hydride within a multiport vacuum chamber are electrically suspended in vacuum free of material supports and irradiated with a focused high intensity laser beam to produce a free plasma at the United Aircraft Research Laboratories, East Hartford, Conn. The interaction of this radially expanding plasma with magnetic fields is being studied using confinement fields of mirrors, cusps, and minimum-B geometry. This is part of the specialized research effort performed at other than AEC laboratories for the controlled thermonuclear research program.

the field strength is increased, the ions are trapped and heated by magnetic compression. The 2X [43] device produces plasma densities and temperatures of thermonuclear interest. Specifically, it produces ion temperatures of 8 Kev. (thousand electron volts) and densities one one-hundred-thousandth of atmospheric density. The recent addition of a special field configuration generated by "*Ioffe bars*" [44] (quadropole windings) to this device has eliminated the interchange instability, and confinement is now apparently limited by microinstabilities.

Vacuum conditions have recently been improved to the point where the decay of the hot plasma is no longer caused primarily by the presence of contaminants. The lifetime of the plasma as a result has been increased to within a fraction of that to be expected for a perfectly stable plasma due to scattering of ions out along the field lines.

Molecular ion injection. In contrast to low-energy injection and heating by compression, an alternative approach is to inject energetic ions into a steady-state magnetic field, to trap them by one means or another, and attempt to build up the density to values of interest. One method, which has been pursued at Oak Ridge National Laboratory in the so-called DCX experiments,[45] involves the injection of a 600 Kev. molecular ion beam into a magnetic mirror configuration and trapping it by dissociation. In the DCX–2, the densities have been built up to values of typically 5 billion fast trapped particles per cubic centimeter. This is perhaps the highest value achieved in any high-energy-injection experiment. Microinstabilities are present, but they are due at least in part to an insufficiently good vacuum. Efforts are being made toward a still further increase in the plasma density in DCX–2.

Energetic neutral injection. Instead of molecular ion injection, another method being used at the Lawrence Radiation Laboratory, Livermore, and more recently at Oak Ridge National Laboratory is to inject an energetic beam of neutral particles and trap them within the reaction chamber by *Lorentz* ionization (a process by which electrons are torn from the atoms by magnetic force). In the Alice facility at the Lawrence Radiation Laboratory, Livermore, a magnetic well has suppressed the interchange instability. This offers a promising method of studying the residual microinstabilities under closely controlled conditions. In particular, such experiments will provide control over density gradients within the plasma, velocity distribution of trapped particles, and other parameters important for theory comparison.

Electron resonant heating. Oak Ridge National Laboratory is using still another approach in that the creation of hot-electron plasmas is achieved by Electron Cyclotron Resonant Heating (ECRH) techniques (see Fig. I–72). In these experiments, the hot-electron plasma shows evidence of remarkable stability, even in the absence of a minimum-B configuration. One interesting avenue which is being explored is the intermarriage of the last two techniques: the injection of an energetic neutral beam into the highly-stable plasma produced by electron cyclotron heating. This exploits a trapping mechanism called charge-exchange trapping which is about 100 times as efficient as *Lorentz* ionization.

Closed Line Systems

In closed line, low-beta systems, there is no end loss problem, but the problems of equilibrium and stability are appreciably more severe.

Stellarator. The first in this grouping is the stellarator, involving an axial magnetic field in a figure "8" or racetrack configuration. By supplementary coils, it is possible to provide not only a rotation of the lines of force, which is required for plasma equilibrium, but also a degree of "shear" in the magnetic field to help stabilize the plasma. (A shear field is one in which the amount of field rotation is a function

[43] See pp. 222–223, "Fundamental Nuclear Energy Research—1966."

[44] A major advance in the controlled fusion field occurred when the Soviet physicist Ioffe during 1963 showed that by modifying a simple mirror configuration by a set of current-carrying bars (*"Ioffe* bars") a true potential well can be produced.

[45] See p. 221, "Fundamental Nuclear Energy Research—1966."

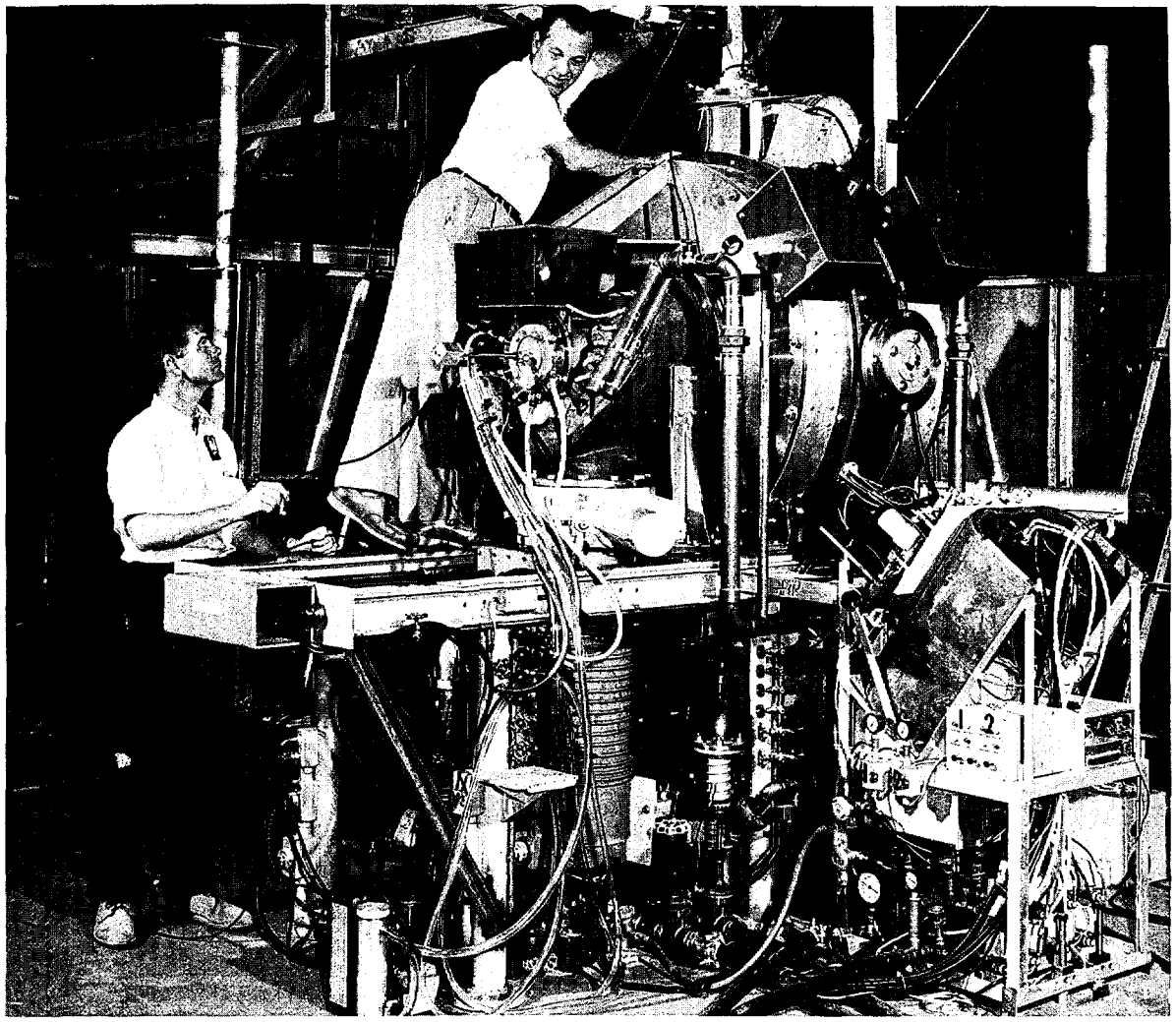

Fig. I–72. "Elmo" at ORNL. One of the Electron Cyclotron Resonant Heating facilities, called "Elmo" at Oak Ridge National Laboratory is shown above. The photograph was taken when the lead X-ray shield wall was partly removed, and shows the magnet coils, vacuum plumbing, microwave power supply (on floor to the right of the apparatus) and some of the instrumentation. With this flexible apparatus, plasma stability studies have been carried out in five different magnetic field configurations.

of radius.) The true behavior of hot plasmas in the stellarator was long masked by impurities flooding in from the walls. At the Princeton Plasma Physics Laboratory's Model-C Stellarator, ultra-high vacuum techniques and a new device called a divertor made it possible to reduce the impurity level to negligible values, thereby permitting a detailed study of plasma confinement and its parametric behavior over a wide range of operating conditions. Experimentally, the rate of plasma loss to stellarator walls is found to be much faster than predicted by classical diffusion, due apparently to certain specific instabilities. The problem is, how to suppress them? According to theory, the three most important parameters are: (*a*) high shear fields, (*b*) strong average minimum-B configuration, and (*c*) short "connection length", (that is, a short distance between the regions of good and bad curvature). High-shear effects

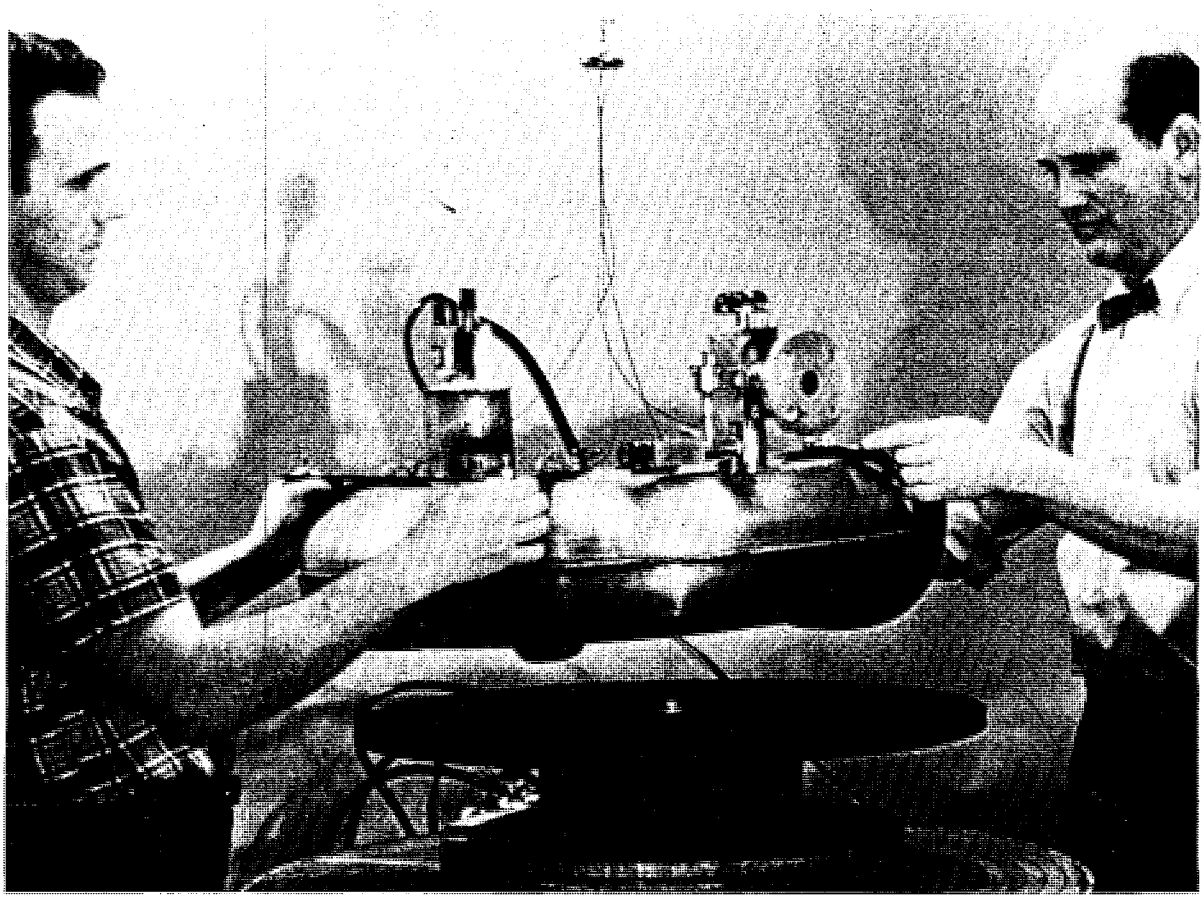

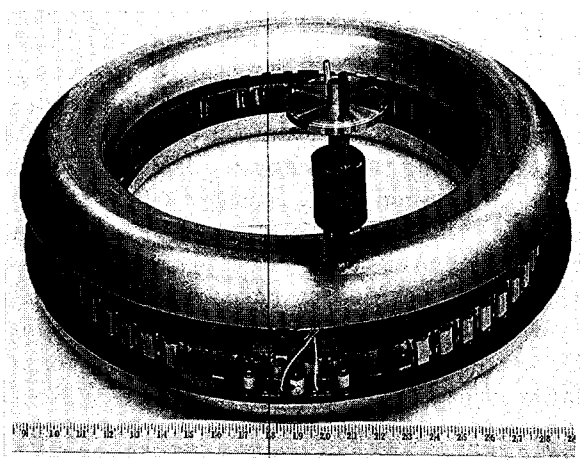

Figs. I–73 and 74. Toroidal Multipole. The superconducting ring shown in *above* photo from the Princeton University Plasma Physics Laboratory is floating freely about a foot above the table, supported by magnetic forces alone. The whole structure weighs about 70 pounds and has been successfully levitated for several hours. It is expected that similar coils will be used in future toroidal multipole devices. No equivalent experiment is known to have been performed to date. The photo at *left* shows the interior coil structure. The rectangular bundle at the core is made up of 3,300 turns of copper-clad niobium-zirconium wire of 0.014 outside diameter. When in operation, the core is surrounded by a double-walled chamber containing liquid helium at −268.9° C. The top half of the inner chamber is shown in a raised position.

are now under active investigation on the Etude and Model-C Stellerators with encouraging results.

Toroidal multipoles. There has recently been considerable emphasis on internal conductor multipole devices, linear or toroidal in shape, in which important stabilizing features are readily achievable. In these systems, current-carrying bars or rings are levitated or suspended within the discharge chamber. Simplest of these de-

vices is the Levitron at the Lawrence Radiation Laboratory, Livermore, involving a single levitated ring. At Princeton, a large linear multipole has yielded valuable information on heating methods suitable to such devices, and in a developmental project a superconducting ring has been levitated for several hours (see Figs. I–73 and 74). A complex device, possessing a number of advantages, is the toroidal octapole developed at General Atomics, La Jolla, Calif., and at the University of Wisconsin, Madison, in which four rings are suspended in the chamber. Preliminary experimental results are encouraging.

Astron. The Astron device at the Lawrence Radiation Laboratory, Livermore, possesses some unique properties for the confinement of hot plasmas. Its confining field is produced by two oppositely-directed currents. Specifically, currents flowing through an externally wound set of coils will produce an axial field within the straight tube. A beam of relativistic electrons is then injected and trapped in this field to produce a concentric layer of electrons (or E-layer, as it is called). If the current in this counterstreaming E-layer can be built up to a sufficient value, so that the net magnetic field in the center actually reverses in direction, the resulting magnetic configuration will have closed lines of force surrounding the E-layer. Moreover, the presence of the electron current sheet within the plasma produces a true minimum-B field (rather than the average-minimum-B attainable in other systems having closed lines of force). In the present facility, pulses of electrons from a linear induction accelerator have been successfully trapped in the central tube to form a weak E-layer of several percent. Up to the present time, no evidence of destructive instabilities has been found and steps are being taken to increase the E-layer toward the desired conditions of field reversal.

High-Beta Plasma Research

Experiments in another area are concerned with high-beta plasma, *i.e.*, high-temperature, high-density plasmas in which the outward plasma pressure is comparable to the inward pressure of the magnetic confining field.

Theta pinch. An important method of producing high-beta plasmas—called a theta pinch system—is under study by the Los Alamos Scientific Laboratory, General Electric Co. at Schenectady, N.Y., and the Naval Research Laboratory, Washington, D.C. This is a fast-pulsed experiment in which a very large current is abruptly impressed on a single-turn loop surrounding the plasma, thereby compressing and heating the plasma rapidly to high densities and temperatures. In the Scylla IV at Los Alamos Scientific Laboratory, plasma densities of 10 thousand trillion particles per cubic centimeter (10^{16}/cc) and temperatures of several thousand electron volts are routine. True thermonuclear reactions are observed. However, the short confinement times of just a few microseconds are caused by rapid loss of the plasma out of the ends. Careful studies carried out over the past 2 years show no evidence of instabilities during the brief confinement time. The next logical step is to increase the confinement time of the system—first by going to a much longer linear experiment, and subsequently by converting the system into a toroidal theta pinch. Engineering design for such a toroidal theta pinch, 15 meters (49.2 feet) in circumference called Scyllac, is underway at Los Alamos supported by experiments on the present 1-meter (3.2 foot) long theta pinch Scylla IV.

Dense plasma focus. Another effort at Los Alamos Scientific Laboratory has resulted in the development of the dense plasma focus device. (This device also has possible potential benefits as a compact, inexpensive, and very intense pulsed neutron and X-ray source for a large variety of applications in research and industry, such as pulsed neutron studies of nuclear reactor fuel and flash radiography). The neutrons and X-rays result from the thermonuclear reactions taking place in the high-density plasma formed at the end of two concentric, cylindrical copper electrodes. These are mounted inside a glass vacuum chamber filled at a

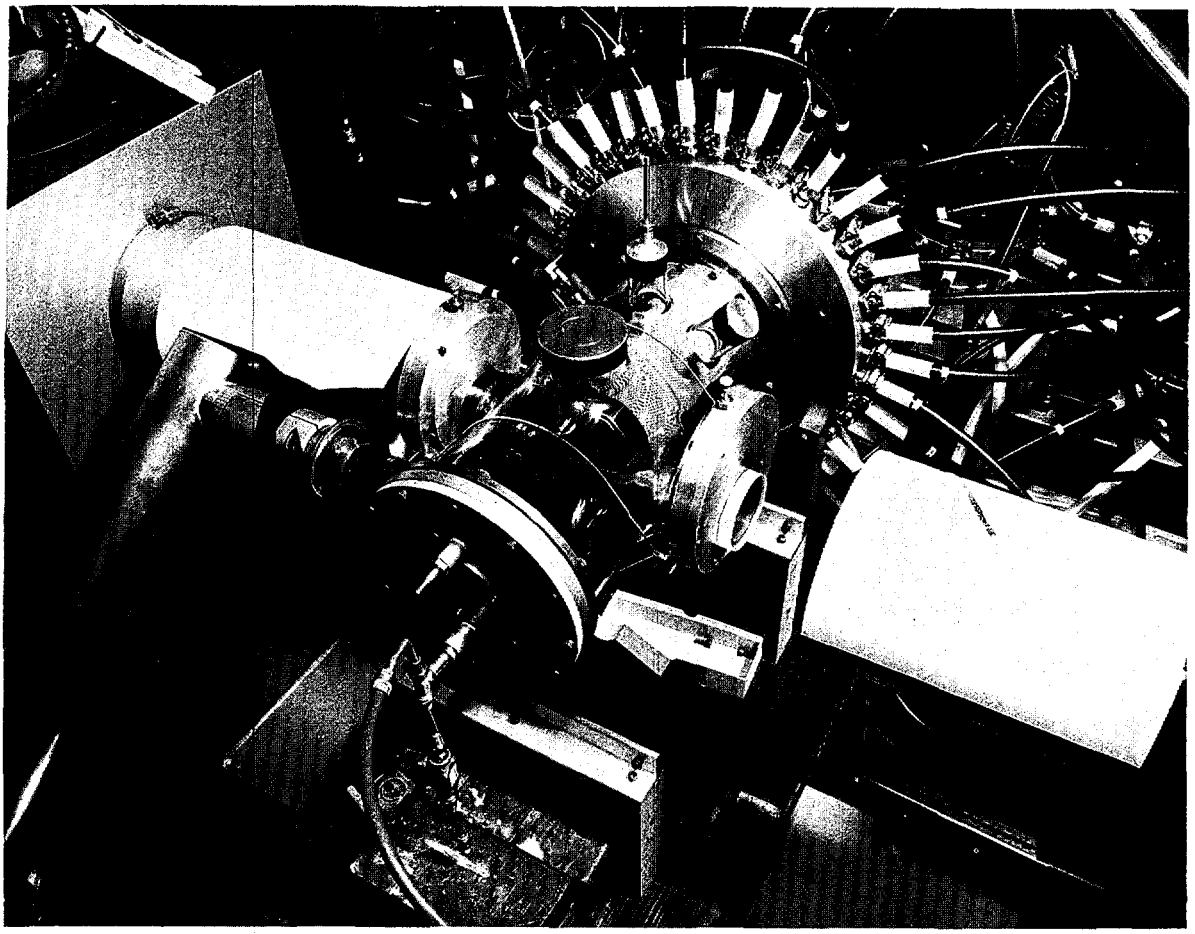

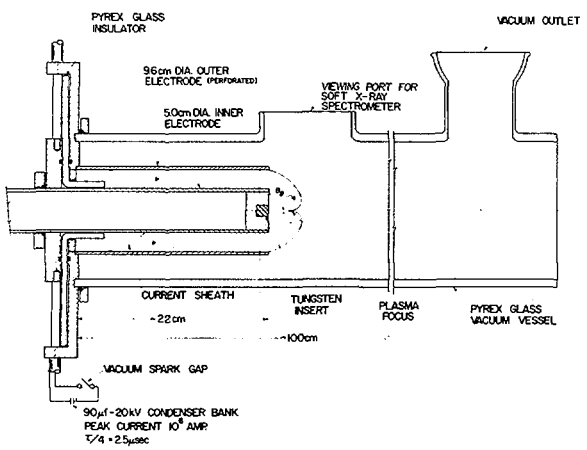

Figs. I–75 and 76. Dense Plasma Focus Pulsed Neutron and X-ray Source. Schematic drawing at *left* is of the dense plasma focus device developed at the Los Alamos Scientific Laboratory. In this device, a current sheath of ionized deuterium (D) or deuterium-tritium (D–T) gas is accelerated between concentric cylindrical electrodes to their open end where a fast Z-pinch effect compresses it into a dense plasma in which thermonuclear reactions take place producing an intense burst of neutrons and X-rays. This current sheath is produced by the application to the electrodes of 20,000 volts of electrical potential from a 90-microfarad condenser bank. The electrodes are mounted in a glass vacuum chamber filled with the D or D–T gas at a pressure of 0.1 lb./sq. in. Photo *above* shows the dense plasma focus device. The two concentric electrodes (the outer one is perforated to allow observation of the luminous current sheath) can be seen mounted inside the glass chamber which contains the D or D–T gas. The circular array of leads to the outer electrode and some of the condensers can be seen at the rear.

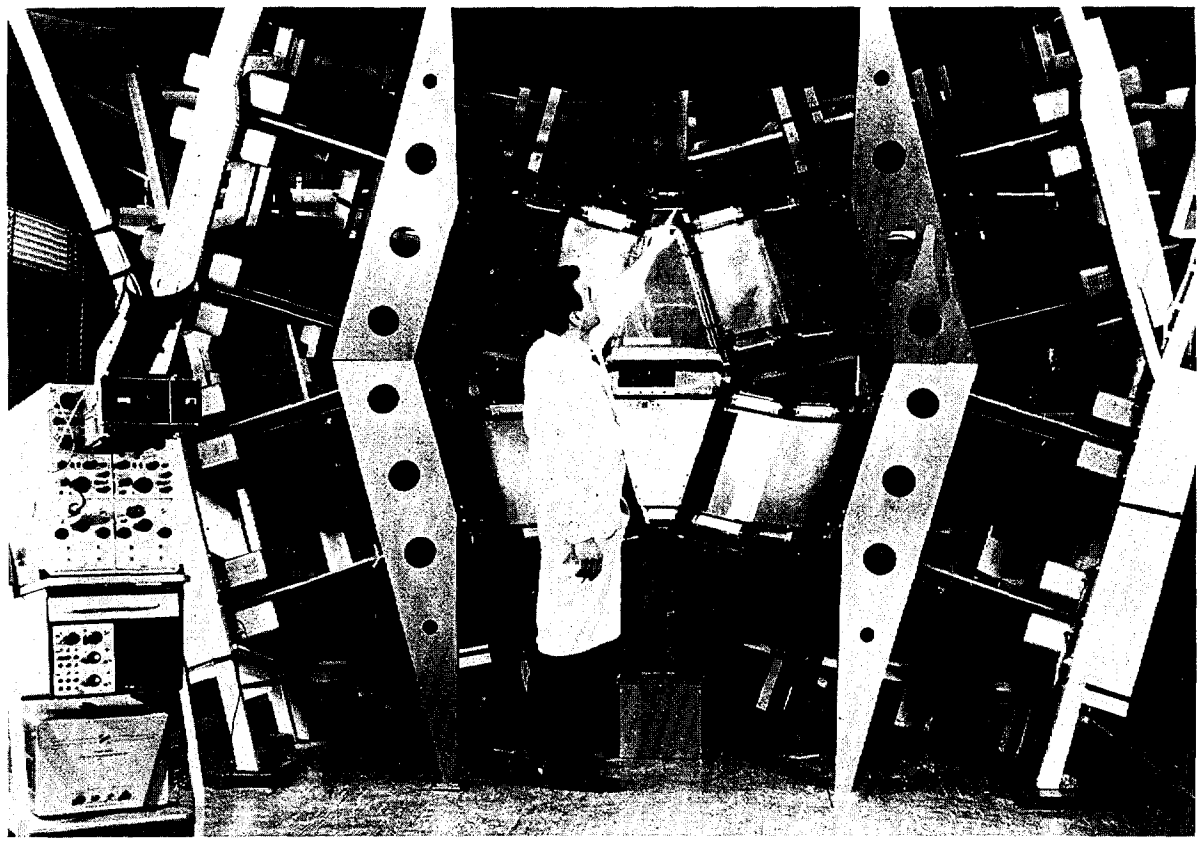

Fig. I–77. High-Temperature, High-Density Device. The Chalice experiment at Stevens Institute of Technology, Hoboken, N.J., is a combination theta-pinch and cusp experiment. Two theta-pinches both squeeze and heat plasma rapidly. It is then displaced into the cusp region formed by the magnetic fields of the two theta-pinch coils. The plasma is now confined in this cusp region. Difficult engineering problems have been overcome in building the Chalice experiment, and now the experimental program is underway. Of importance is the quantitative study of the plasma without disturbing it. The main tool for this is a delicate optical instrument built at Stevens Institute of Technology and called the Mach Zehnder interferometer (not shown in photo). It measures accurately and quantitatively what goes on within the plasma. The interferometer is so sensitive, however, that the shaking of the building due to wind or trucks passing by affects the instrument. (Chalice is located on the sixth floor.) This tough problem was solved by suspending the instrument with rubber bands. The resulting stability of the system is quite remarkable. It is now possible to measure the length of time that the plasma stays in the cusp region (confinement problem). If the cusp is too leaky, serious steps must be taken to counteract the leak.

pressure of 0.1 lb/sq. in. with deuterium (D) gas or a deuterium-tritium (D–T) gas mixture. The inner electrode, whose end is closed, and the outer electrode, which is perforated to allow observation of the space between the two, are both connected to a 90-microfarad, 20,000-volt condenser bank which stores 18,000 joules of electrical energy and which can produce a current of 1,000,000 amperes within 2.5 microseconds. When this electrical potential of 20,000 volts is applied to the two electrodes, the gas in the space between them is ionized and becomes conducting (see Fig. I–70, and Figs. I–75 and 76). This ionization, which begins at the base of the electrodes, produces a highly conductive annular current sheath which is accelerated to, and collapses off, the end of the center electrode to be rapidly compressed and heated by a fast

Z-pinch effect [46] to form a high-density plasma in which the thermonuclear reactions occur. Final plasma densities of about 20 billion billion (2×10^{19}) particles/cc, plasma temperatures of about 50 to 70 million degrees C., and minimum plasma radii of about 0.5 mm. have been obtained. Production rates of 20 billion (2×10^{10}) neutrons/pulse and 200 billion (2×10^{11}) neutrons/pulse have been observed with deuterium and deuterium-tritium mixtures, respectively.

SUPPORTING RESEARCH

Research on specialized problems is performed not only at AEC laboratories, but also at many other sites, mostly at universities.

Recent Noteworthy Advances

Three noteworthy recent results are reported here.

[46] The Z-pinch produces a radial force on a conductor resulting from the self magnetic field produced by a current flowing through the conductor. This force tends to squeeze the conductor radially toward its axis, the Z coordinate in a cylindrical coordinate system.

At Stanford University, near Palo Alto, Calif., studies are in progress aimed at understanding the newly discovered electron cyclotron echo effect in plasmas. This effect is a new tool for studying basic effects in a plasma. Collision times and plasma oscillations have been measured using this effect.

At Stevens Institute of Technology, Hoboken, N.J., research is in progress on Chalice, a high-temperature, high-density theta-pinch device (see Fig. I–77). Experiments are being performed on a reproducible basis and the plasma confinement properties of a cusp geometry are being studied.

At New York University, New York City, N.Y., an ambitious theoretical program is underway to investigate the containment, stability, and heating of plasmas. Special emphasis is placed on wave propagation (including shock waves), equilibrium, sheaths, orbit theory, and development of numerical methods. Recent calculations indicate the existence of new classes of toroidal plasma equilibrium conditions.

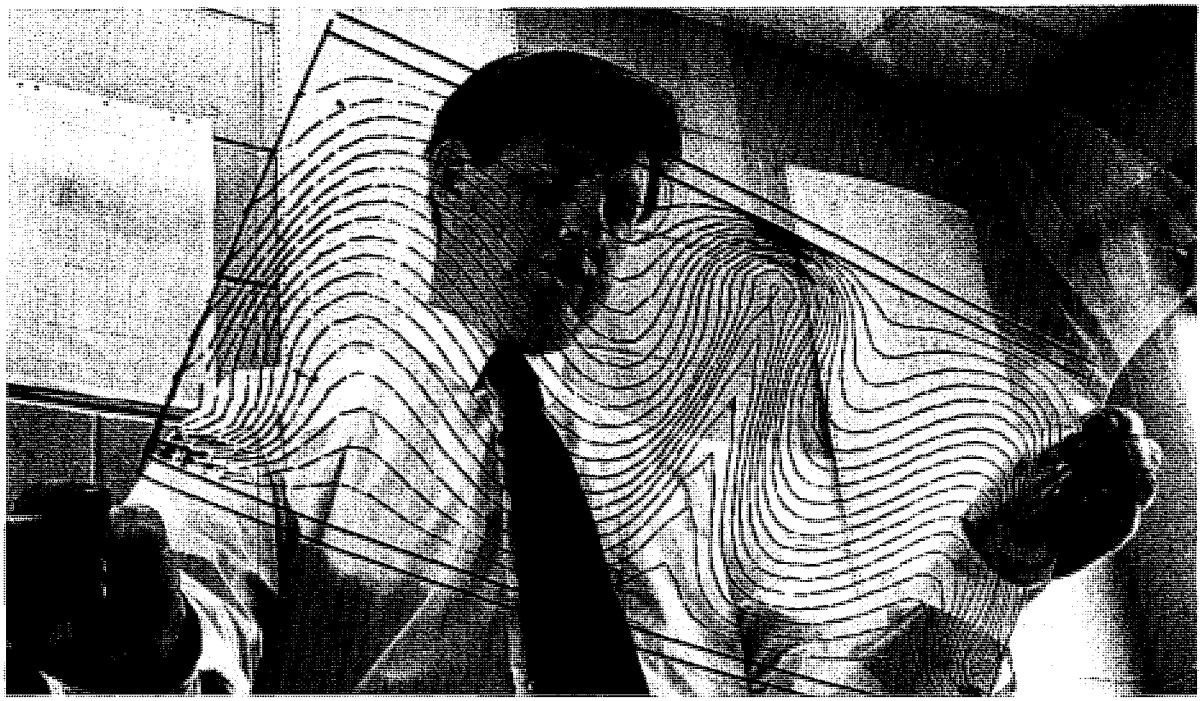

Fig. I–78. Fluid Dynamics. An Argonne National Laboratory mathematician inspects an enlarged picture of a computer-produced isotherm of a two dimensional-connective flow produced by heating the bottom of the liquid during fluid dynamics studies (see also p. 107).

MATHEMATICS AND COMPUTER RESEARCH

Modern high-speed computers and mathematical techniques are utilized extensively in the various technical programs of AEC. For example: (*a*) design of nuclear reactors, (*b*) development of improved atomic weapons, (*c*) analysis and control of experiments involving nuclear facilities, and (*d*) theoretical calculations to aid in a better understanding of the fundamental atomic and subatomic forces and particles. Recognizing the importance of this area of research to the effective prosecution of future nuclear energy programs, the AEC has supported three related but separate areas of research in the science of mathematics and computers: (*a*) computer research and development, (*b*) mathematics research, and (*c*) programing research. Projects are selected on the basis of their excellence and their potential contribution to the AEC mission, with emphasis on those areas of research which are not adequately supported by industry or other non-government institutions.

COMPUTER DEVELOPMENT

Computer research and development is concerned with the development of basic principles useful in the design of modern computers and their components. This work comprises an important support effort to the AEC's needs in theoretical computation, data analysis and automation of nuclear facilities.

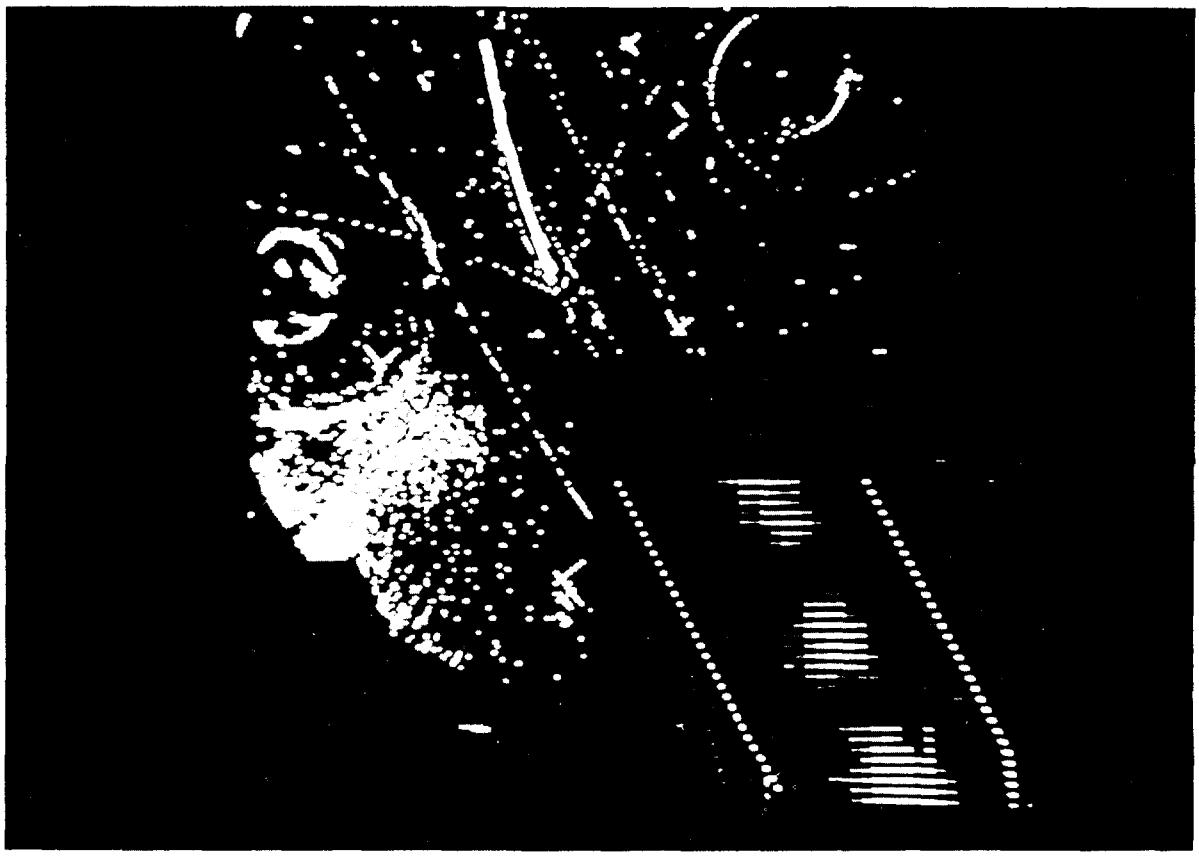

Fig. I–79. Automatic Bubble Chamber Measuring. An automatic bubble chamber film measuring system developed at Argonne National Laboratory uses a cathode ray tube to generate a spot whose motion is under computer control. The entire system is designed to allow an operator to directly assist the machine whenever a possible difficulty is sensed. The resulting flexibility is great enough to allow easy incorporation of those automatic measuring techniques which have been shown to be particularly powerful, such as the track filtering programs used by the mechanical flying spot devices. This same flexibility, coupled with human-computer interaction, will allow orderly progression of the system capability as increasingly complex subproblems can be solved by the computer. High energy bubble chamber events have been successfully measured, and a high speed machine for large volume automatic measuring is being assembled. In the photo, the track being measured appears as a heavy line (*top center*); a magnified view of the scanned region appears in the *lower right* quadrant of the picture. Experience gained in the earlier design and construction of CHLOE, a flying-spot device for reading spark chamber film, contributed to the success with which this development was accomplished.

Processing of Pictorial Information

The results of scientific experiments are in many cases most readily and naturally recorded by photography. These pictures must then be processed to obtain the information which the experiment was intended to develop. For example, an important area of AEC interest is the processing of bubble chamber photographs in high energy physics.

Current methods of picture processing by computers require that a digitized version of the picture be first produced. This is done by subdividing the picture into a large number of small squares, numbered according to some convenient scheme, and recording the numbers of those squares which contain a portion of the picture. Processing of this information—for example, the filling in of gaps, the thinning out of cloudy portions, or the reduction of the picture

to a standard size or position—is then done by a sequence of mathematical operations performed by a digital computer. The computer codes which cause the execution of these operations are apt to be time-consuming.

The precision that is needed in much picture processing is not particularly high: a fraction of one percent will generally suffice. Analogue computing circuits which operate upon quantities represented by continuously varying voltages, are capable of such precision, though not much more, and have advantages in speed of operation. At the University of Illinois, it has been found possible to design picture processing equipment which incorporates digitally controlled analogue computing circuits. This technique provides precision adequate for all practical purposes and has sufficient processing speed to give a continuous flicker-free display of the result. Two experimental devices have been successfully built and operated. They permit the preliminary picture processing operations to be performed off-line without tying up a digital computer. The cleaned-up and standardized output can be transmitted to a digital computer for analysis when convenient.

MATHEMATICS RESEARCH

A portion of the mathematics and computer program deals with the branches of mathematics which can solve problems in the physical sciences relevant to the AEC's overall program.

Algebraic Study of Stopping Variables

In many experimental situations sequential observations of some random phenomenon must be made. The experiment should only be continued until adequate information is obtained, as further effort will add little to the results but will obviously increase the cost. Indications of when to stop are given by so-called "stopping variables," which depend at any instant upon the observations recorded up to that instant. Past studies of stopping variables have been carried out entirely in terms of probability theory. It has recently been shown at the Brookhaven National Laboratory that by a suitable definition of the product of two stopping variables, the class of stopping variables becomes a semi-group of idempotent elements (when multiplication of an element by itself yields the same element it is said to be idempotent). This semi-group is further shown to be what is called in modern algebra a "lattice." This result makes available for exploitation in statistical investigations the very extensive modern literature on semi-groups and lattices.

Monte Carlo Method

With the advent of more advanced computer systems with increased speed and capacity, the solution of complex problems involving large numbers of particles has altered dramatically. At the AEC's Computing and Applied Mathematics Center, New York University, Monte Carlo [47] methods for the direct numerical integration of the *Schrodinger* [48] equation for systems of many particles have been developed. The basic approach is similar to that employed in the solution of diffusion equations, utilizing directly what is known as *Green's* [48] function. An exploratory series of calculations has already been carried out, with the aim of testing certain ideas proposed by *Bogoliubov* for calculating the energy of a fluid of identical particles exerting simple forces on each other. The study of the theory of fluids contributes to knowledge of the behavior of matter under conditions encountered in nuclear applications.

Linear Programming-Integer Problems

Linear programming is a relatively new and difficult mathematical field which had its origin in this country during World War II. Its pur-

[47] *Monte Carlo method*—A method for solving physical problems by means of a series of statistical experiments.

[48] *Schrodinger* equation: The *Schrodinger* equation is the basic mathematical expression of wave mechanics used to calculate the properties of atoms and nuclei. *Green's* function: In this context, *Green's* function is the average result for the diffusion of a number of particles all started in the same place.

275-845 O—68——9

pose is to minimize a specific factor in a large complex operation, such as its cost. A simple example is what is known as the transportation problem, where it is desired to minimize the total cost for transporting all the required items from each of a number of warehouses to each of a group of destinations. The AEC is interested in this area of research in order to enable it to increase the effectiveness of its various programs. A large class of problems in this field require solutions which are integers. A procedure was developed at Brookhaven National Laboratory by applying a mathematical technique, which is well developed for use of the solution of other types of problems, to integer linear programming problems. This is the method of generating functions. A nonlinear version of the transportation problem was worked out to demonstrate that a class of nonlinear integer problems can also be dealt with through the use of generating functions.

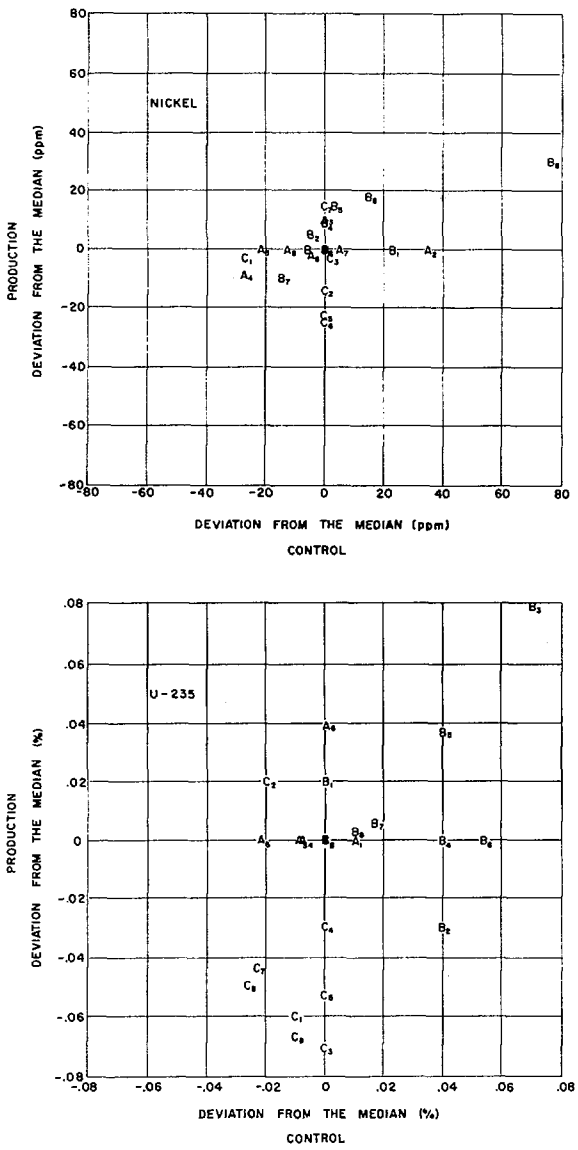

Fig. I–80. Computer Printout of Impurity Analysis Data. The two graphs show some of the results of a monthly uranium-235 sample exchange program between Los Alamos Scientific Laboratory and two other AEC laboratories (Union Carbide Corp., Y–12 Plant; Dow Chemical Co., Rocky Flats Plant) to compare and improve impurity analyses. The computer, using a Los Alamos-developed program, compiles and analyzes impurity determination data from the three laboratories, and produces graphs like those shown. The *top* graph, giving the results for nickel, shows good agreement except for one point. The *lower* graph, giving the uranium-235 results, indicates very small (hundreths of a percent) differences between the results from the three laboratories. The points on the graphs (one for each laboratory for each month) show the deviation of each laboratory's results from the median value of all the laboratories' results for that month for the production of uranium-235 (distance from the horizontal zero line) and for the control of material (distance from the vertical zero line). In some cases two points coincide, and therefore some points are not shown. Discrepancies have been found to exist when the three laboratories' results are compared. This has led to a restudy and re-evaluation of the methods and, indeed, of some basic chemical procedures used in determining the impurities in uranium-235, which for many applications in the nuclear field must have very high purities.

Fuel Cycle Model

Solution of a reactor fuel cycle model is now being incorporated as one of the Argonne Reactor Computation System computation modules. The fuel cycle model requires consideration of the following main features during the operational phase of the cycle: (*a*) enrichment and control adjustment to maintain desired criticality conditions over the operating period; and (*b*) adjustment of the length

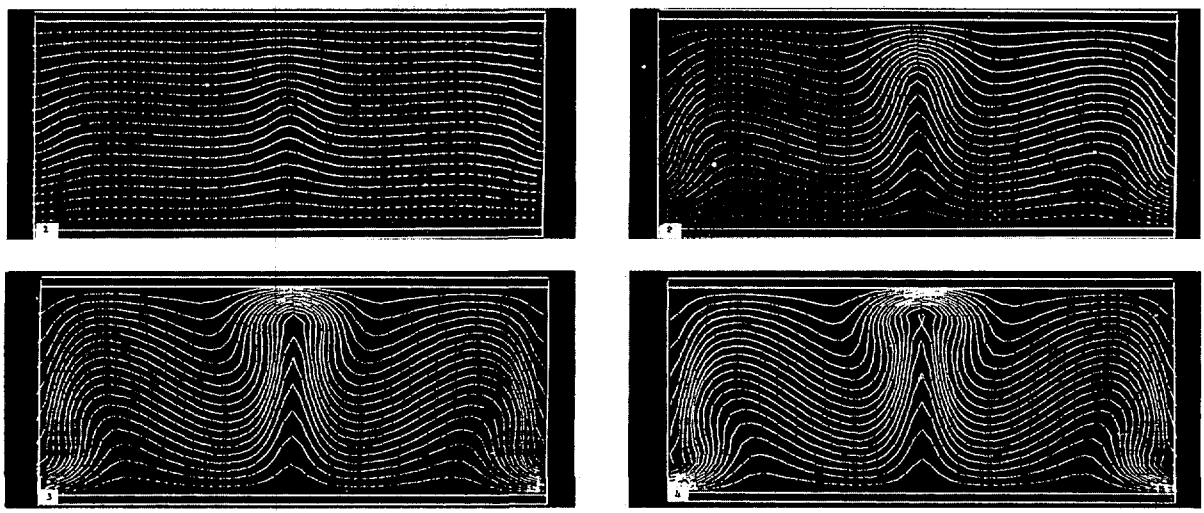

Figs. I–81, 82, 83, and 84. Fluid Dynamics. When a layer of any compressible heat-conducting viscous liquid is heated from below, at first the heat is conducted without any motion in the liquid. However, if the temperature gradient is too high the viscosity is not strong enough to counteract the instability caused by the greater buoyancy of liquids at higher temperatures. This causes the onset of a steady circulating motion in which part of the heat is transferred by conduction, another part by convection. The AEC's Computing and Applied Mathematics Center at New York University has developed a numerical scheme for calculating this motion. Also, at Argonne National Laboratory a program to study convective fluid flow has been conducted. This work has application in the design of bubble chambers, in the design of liquid-cooled reactors, and in many other fields. The above are Argonne computer produced isotherms showing four stages of a two-dimensional convective flow produced by heating the bottom of a liquid.

of the period so that the discharged fuel burnup remains within metallurgical or specified limits. Given fixed fuel management policies and external conditions, the equilibrium state must also be determined.

An equilibrium calculation specifies: (*a*) an internal fuel management policy giving the physical path and the number of stages that each material undergoes from loading to discharge; (*b*) an external fuel management policy giving the recovery factors, supply and demand priorities, and external feed components; and (*c*) the burnup of a given set of materials in the last stage before discharge. Also the value of the unpoisoned reactivity is specified at a given fraction of any burn step. The object of an equilibrium calculation is to find an initial isotope density and an operating period such that the following conditions are met: if fuel with given initial density is loaded and allowed to pass through the internal fuel stages (each passage lasting through one operating period) and is then discharged and passes through the external fuel scheme, then the fuel so recovered is required to have density identical to that of the original fuel.

A nonequilibrium calculation involves fuel management policies and external conditions which may vary with time. It is necessary to find an operating time and an initial charge density having a certain enrichment ratio so that the burnup at the end of the operating period reaches a given value while the unpoisoned value for the reactivity at a given fraction of the operating time takes on another given value.

Erythron Behavior

The kinetics of iron in the human may be studied with the help of radioactive tracers. By devising a mathematical model, the scope of

such studies has been extended to include the quantitative determination of the maturative and proliferative behavior of the red blood-cell and its precursors (erythrons). Important new information obtained at the Lawrence Radiation Laboratory, Berkeley, includes the rates of iron uptake for each generation of erythrons and the length of the total maturation period (about 6.5 days which is longer than previously believed). This study showed that significant intramedullary death (hemolysis) of nucleated erythrons does not occur in the normal human.

Age Distributions

Radioactive tracers are widely used for the study of the metabolic behavior of cellular populations. In these studies, almost no attention has been given to the distribution of cell-age in the populations, although metabolism depends heavily on age. Thus, at the Lawrence Radiation Laboratory, Berkeley, determination of the expected age distribution and the variance of the actual age distribution as functions of the cell's stochastic, age-dependent birth and death schedules give important information to an area of investigation which for the most part has been overlooked. In every case, the mean age distribution tends to a limit in time, but the behavior of the variance differs according as the subject population is contracting, stable, or expanding. More precise analysis of metabolic experiments may now be made on the basis of these statistical results, with the invocation of a fictitious steady state or the neglect of age distributions.

PROGRAMMING RESEARCH

Research in programming is concerned with improving the techniques of program writing for digital computers. As computers become more powerful, more sophisticated and more costly, they must also become easier to use so that they can be used most effectively.

Interactive On-line Computation

A group of programs have been developed in the interactive on-line computation program at the Lawrence Radiation Laboratory, Berkeley, which allow the user to display reasonably arbitrary graphic and alphanumeric output on a cathode ray tube console. The goal of this research is to create systems that will increase the productivity of computer users by permitting rapid interaction between themselves and computers. The hardware so far used on this project is a commercial display system which is attached to the CDC 6600 computer. These programs allow the user to interact with his executing program by selecting points on his display with a lightpen, drawing curves with a lightpen, or inserting digital input via a keyboard. One particular application has been developed and successfully used in accelerator magnet design.

The best possible use of systems using disc and extended core devices has been studied using several simulation models which have been built. These studies have led to a disc control system which has increased the rate of data handling by two or three times compared to standard CDC systems.

Part Two

REACTOR TECHNOLOGY PROGRAMS

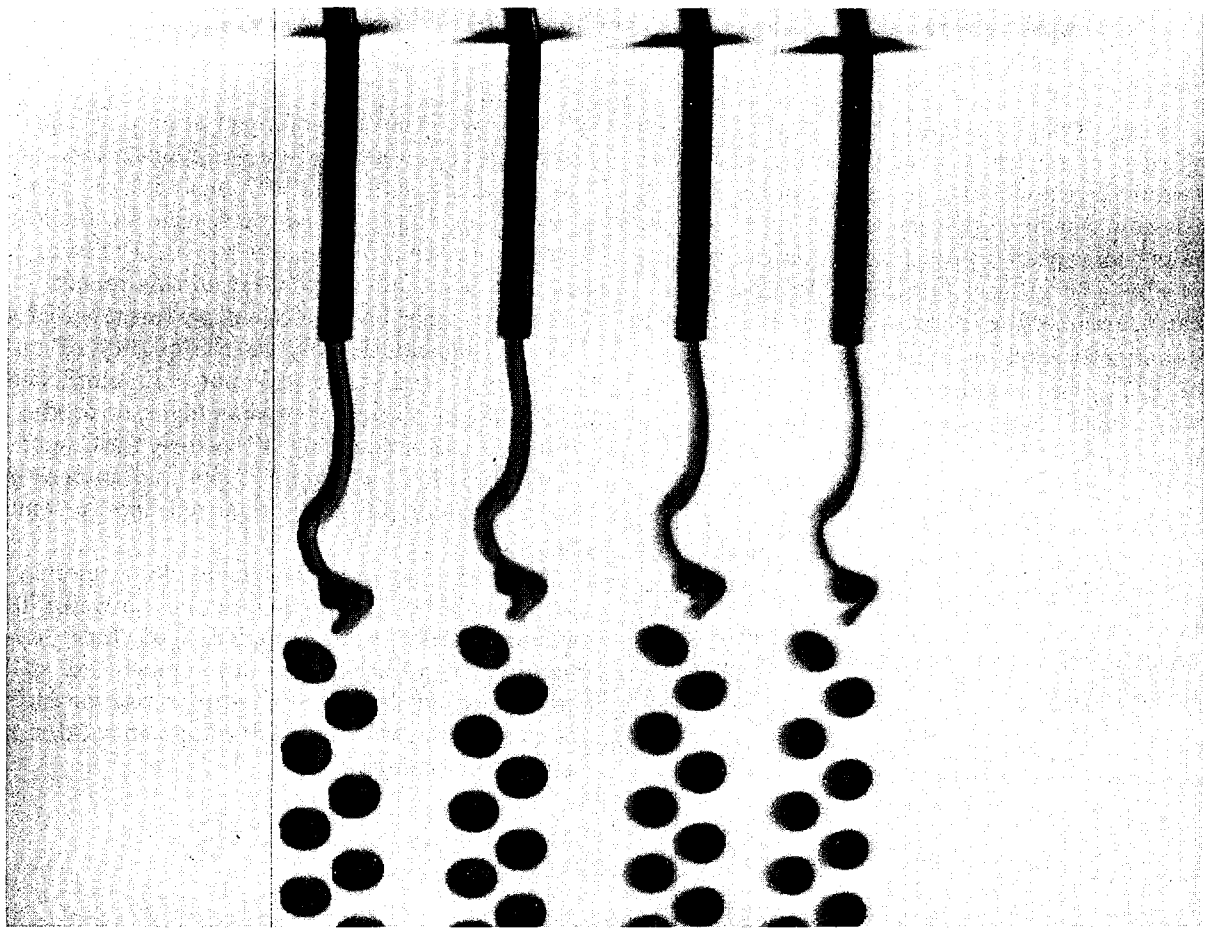

Fig. II–1. Microsphere Forming. This photo illustrates one of the techniques employed at Oak Ridge National Laboratory in making microspheres for use in reactor fuels from plutonium and uranium oxide gels. An aqueous stream of gel, flowing through the four vibrating nozzles, is released as droplets into an organic liquid during each phase of the vibration cycle; thus, each nozzle produces two groups of spheroidal particles which quickly form into microspheres having nearly equal diameters and masses. The microspheres lose water by diffusion to the surrounding organic liquid. They are later dried and calcined at 1,200° C. to form spherical oxide particles having near-theoretical density (see p. 199).

NUCLEAR REACTOR RESEARCH AND DEVELOPMENT

The AEC's program in reactor research consists largely of applied research and exploratory development, with little or no basic research *per se*. It is often referred to as nuclear technology and applied to work oriented to the overall reactor program rather than to specific reactor projects.[1]

Since 1965, a remarkable upswing of the growth of nuclear power has taken place. Between then and now, plans for approximately 60 new nuclear powerplants have been announced, representing a total electrical capacity of about 48 million kilowatts. Another significant factor is the increase in size of the newly announced reactors, which up to the beginning of 1966 were averaging about 500 megawatts and since then have averaged over 800 megawatts.

In addition to applications in electricity generation for civilian power, new and improved reactors are being developed for maritime and space applications and for specialized use in remote areas. Likewise, methods are being developed for the direct conversion of atomic energy to electricity.

In view of the burgeoning civilian power program and the upswing in use of nuclear reactors for other needs, special emphasis is now being placed by the AEC on research in nuclear safety. For this reason, nuclear safety research is given a prominent position in this report.

On the other hand, efficient performance of a reactor depends largely on the quality of nuclear fuels and structural materials employed in it; likewise, on its neutron budget, or production and use of neutrons. Therefore, AEC-sponsored research in reactor fuels and materials and in reactor physics is reported here in some depth.

Other aspects of nuclear technology summarized in this report include research in reactor instrumentation, heat transfer, and fluid dynamics. In addition, the development of still better methods for processing spent reactor fuels is discussed as well as the development of direct energy conversion.

[1] Project-oriented work is reported upon in the AEC's "Annual Report to Congress for 1967."

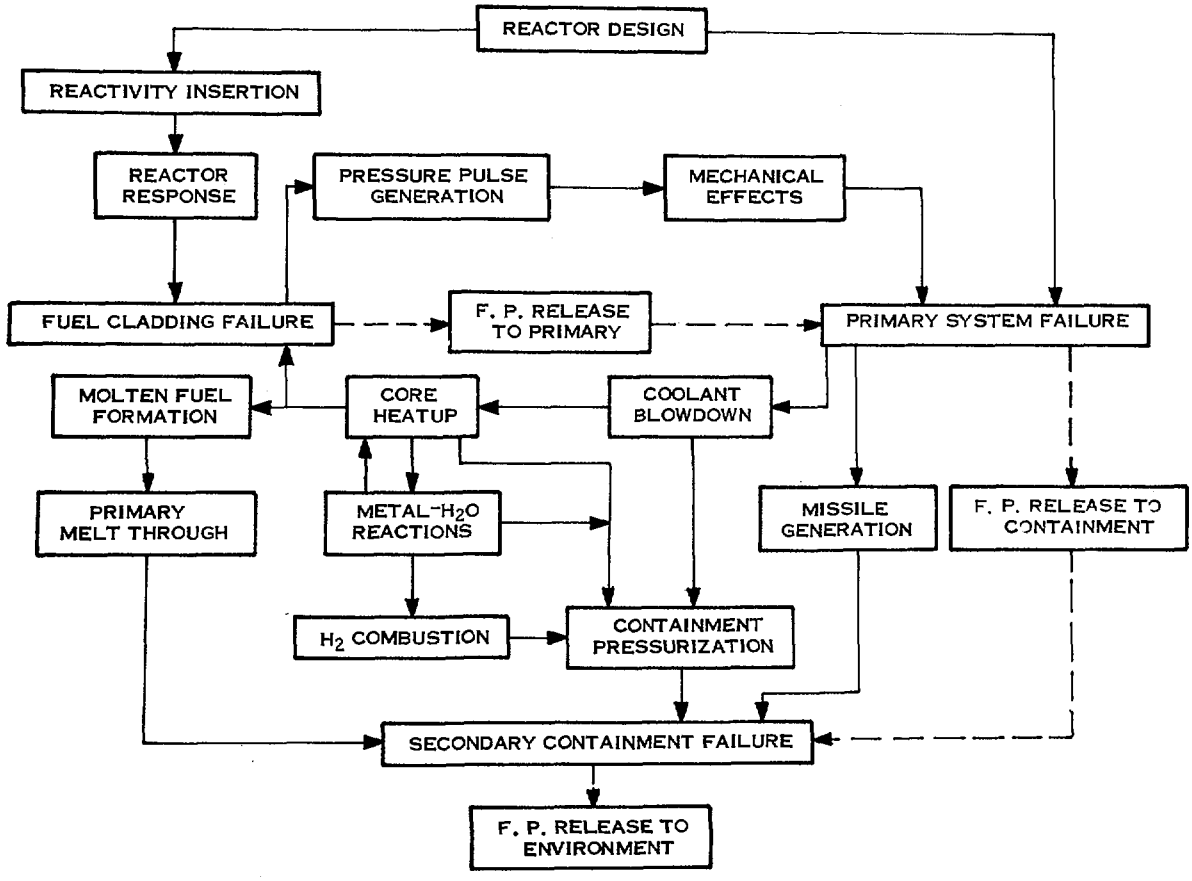

Fig. II–2. Accident Sequence Diagram. This diagram presents the major factors and the sequence and interrelationships of events which must be considered in the course of a potential nuclear reactor accident. Although the diagram applies specifically to water-cooled power reactors, it also demonstrates the basic principles used in the safety analysis of any nuclear system.

NUCLEAR REACTOR SAFETY RESEARCH

The recent emergence of the nuclear reactor industry as a major factor in supplying electrical power needs has placed a premium on nuclear safety research, particularly as applied to nuclear reactors. In addition to individual investigations already underway and reported previously,[2] further studies have become necessary in order to develop a more detailed understanding of reactor accident phenomena and the prevention and control of potential accidents through the use of engineered safety systems.

FUNDAMENTAL OBJECTIVE

The fundamental objective of the nuclear safety research program is to provide the AEC and industry with the safety-related information required to develop and regulate the safe application of nuclear energy. The program, sponsored and directed by the AEC and performed by industrial contractors and national

[2] See pp. 294–311, "Fundamental Nuclear Energy Research—1966."

laboratories, accomplishes this objective through the following activities:

(*1*) Safety-oriented design and fabrication of reactor plant systems;
(*2*) Development of safe operating procedures;
(*3*) Designing and engineering and safety systems to prevent or arrest potential accidents and limit the consequences to acceptable levels;
(*4*) Development of plans and equipment to provide the capability for recovery from the consequences of an accident, if it should occur;
(*5*) Assessment of the adequacy of safety margins by regulatory agencies; and
(*6*) Audit, inspection, and testing of reactor and plant systems to ensure that adequate safety margins are maintained.

Theoretical Accident Sequence

In developing the needed information, the safety program follows the theoretical accident sequence shown in Figure II–2 as a useful program planning aid. Although this diagram was generated specifically for water-cooled reactors, the basic principles can be extended to any system. It shows the course of an accident, the major factors which must be considered, and the interrelationship of these factors. At many points in this sequence of events, engineered safety systems can be applied to either interrupt the course of the accident, *i.e.*, accident prevention or to limit its consequences to acceptable levels.

Because nuclear power reactors have established and maintained an outstanding safety record, there is essentially no real accident experience upon which to base safety research. For this reason, analytical and experimental programs in nuclear reactor safety arise from theoretical and analytical considerations of the possibilities of accident initiation, system response, and the eventual consequences of various situations.

Dual Approach

The proper implementation of such a safety program requires two separate, but interrelated, types of investigations. One type involves relatively long-range studies of fundamental principles and phenomena which have safety implications. These studies yield a basic understanding of reactor accident behavior, so that a limited amount of data can be applied to a broad spectrum of problems. The other type of investigation is short-range and involves scoping tests to define problem areas, *i.e.*, tests of the performance of specific designs of engineered safety systems, and programs for the purpose of providing information on specific limited areas of concern. The best possible safety program involves a balance between these types of investigations, with continual readjustment as the needs of the industry evolve.

While water-reactor safety projects comprise the major efforts thus far undertaken in the reactor safety program, additional attention will be given to fast-reactor and gas-cooled reactor safety as these concepts continue to mature and design concepts become better established. Furthermore, much of the safety technology developed for water reactors is directly applicable to these advanced concepts.

Fission-Products Release

The intrinsic feature which distinguishes safety considerations of nuclear plants from those for equivalent fossil-fueled installations is the possibility of an accidental release of the fission products generated in the core. Control of these fission products is thus basic to reactor safety and is accomplished by means of three successive, sequential barriers to their accidental release: (*a*) the fuel cladding, (*b*) the primary reactor system, and (*c*) the secondary containment structure which includes the reactor shielding and the containment shell (see Fig. II–3). The fuel cladding, or sheath surrounding the fuel, presents the initial barrier to fission products. It is designed to retain its integrity under all normal operating conditions and for a wide range of possible abnormal events. Fission products can escape from the core only

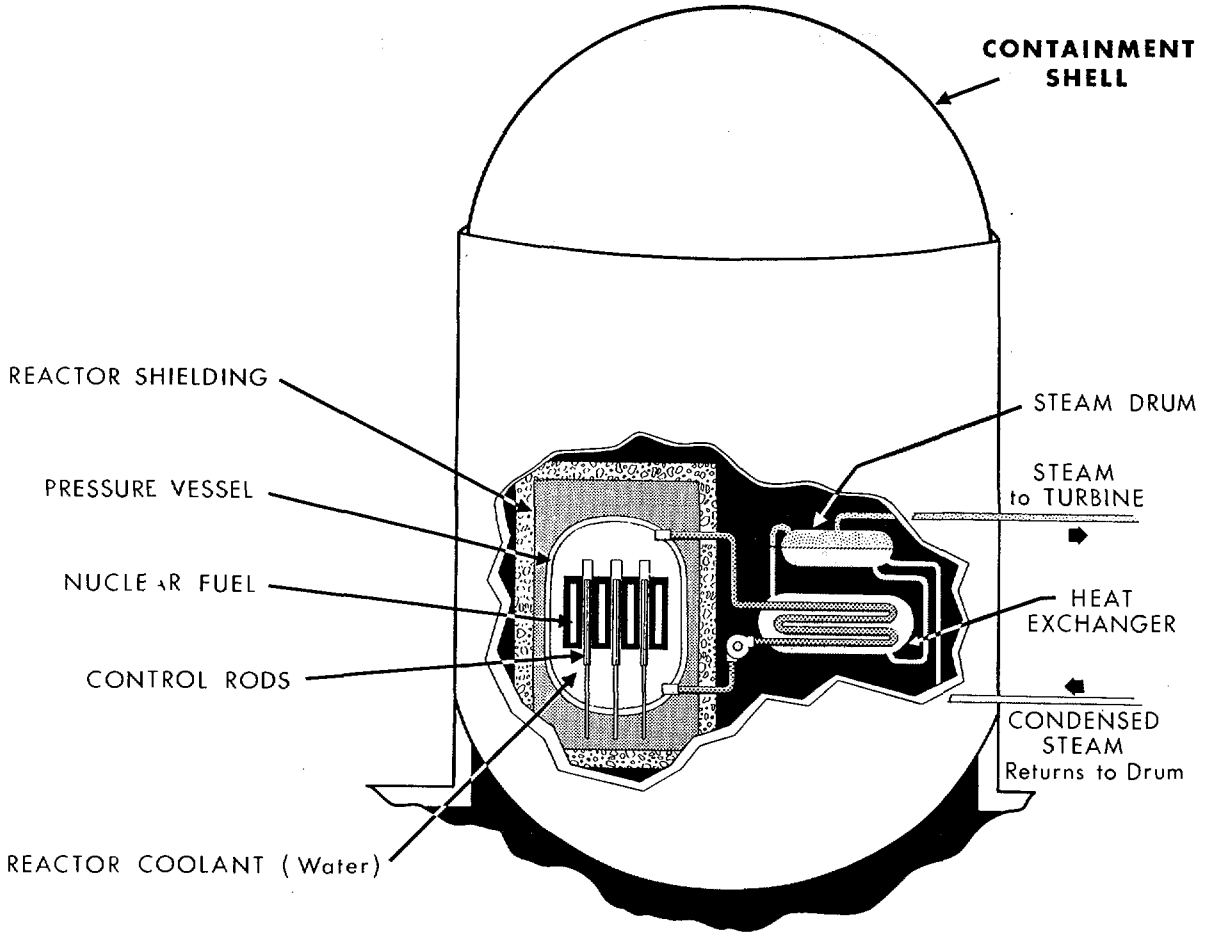

Fig. II–3. Power Reactor Shielding and Containment. Of primary concern in the AEC's nuclear reactor safety research program is prevention of an inadvertent release of the fission products generated in the core of an operating power reactor. The artist's concept of a typical light water power reactor shows the sequential barriers to such a release. The barriers include the cladding of the nuclear fuel, the pressure vessel, the reactor shielding, and the overall containment shell. Since the Nation's nuclear power reactors have an outstanding record for safety, there is little, or no, actual experience on which to base the AEC-sponsored safety research and development; potential accidents and their consequences must be theorized and then small-scale experiments conducted to prove or disprove the theoretical considerations.

upon the loss of fuel cladding integrity. The core and its controls, the coolant, and a number of reactor internals are enclosed within the pressure vessel which, combined with coolant piping and external coolant and heat exchange components, comprises the second barrier to the escape of fission products, the primary reactor system. The third barrier, *i.e.*, the secondary containment system, is provided to control the release of radioactive materials in the unlikely event of primary system failure. Release of fission products to the environment can thus take place only through sequential failure of these three barriers.

From a safety standpoint, the principal difference between a water-cooled thermal reactor and a sodium-cooled fast reactor lies in the possible mechanisms which may cause these barriers to fail. Accordingly, the entire safety program is focused both on the prevention of accidents and on the effective maintenance of these barriers to fission-product release.

WATER REACTOR SAFETY

The phenomena which are of most concern in water reactor safety are strongly influenced by the enthalpy, or stored energy, and the physical characteristics of the water coolant. One major problem area is the possibility of a rupture causing major violation of the integrity of the primary system, which could lead to depressurization and resultant loss of coolant; in turn, the loss of this cooling capacity could lead to fuel clad melting, with release of fission products and generation of high pressures. A second major problem area is the potential for overheating of the fuel in the event of a reactivity accident or uncontrolled power excursion. The consequences of such overheating are also influenced by the physical characteristics of water.

Primary System Integrity Studies

The most commonly hypothesized event initiating a loss-of-coolant accident is the sudden failure of some component member of the reactor's primary coolant system. The prevention of such a failure depends primarily on good system-design standards to be applied in the design, construction, testing, operation, and inspection of primary system hardware.

Criteria, codes, and standards. Several programs are underway, or planned, to upgrade and develop design and construction codes applicable to reactor primary systems. These standards will be made available to industry as examples of high-quality design practice. Currently, collection and upgrading of existing codes and standards is in progress at Oak Ridge National Laboratory; where these are not adequate, new codes will be developed. Nuclear piping codes, for example, will be upgraded to place stress analysis for pipes on the same basis as those provided for vessels in Section III of the ASME (American Society of Mechanical Engineers) Pressure Vessel Code. The Pressure Vessel Code, itself, will also be examined and modified, if necessary, to assure its adequacy as a standard for high-quality nuclear reactor vessels. Welding specifications will be developed as required. The development of a technical basis for criteria, codes, and standards is a vital reactor safety program element.

Primary vessel integrity. Although pressure vessel failure is considered highly unlikely, additional knowledge of design safety margins is needed. The degree of conservatism used in vessel design is not fully known, particularly when considering vessel failure due to sudden brittle fracture (as opposed to gradual strain failure). This was demonstrated in a recent test performed at the National Reactor Testing Station (NRTS) in Idaho on the PM–2A[3] reactor vessel. The highly irradiated vessel was subjected to a series of pressure tests at low temperature with artificial defects machined into the other wall of the vessel. The vessel did not fail until subjected to conditions that were much more severe than those predicted by prior analysis. Calculations had indicated that vessel failure was likely with a defect size of 1¼ inches deep by 9½ inches long, and at a temperature of —29° C. and a pressure of 3,540 p.s.i.g. ±885 p.s.i.g. Actual vessel failure occurred at 4,475 p.s.i.g. and —29° C. with a 1¾-inch deep by 11-inch long defect, which had been aggravated by hydrochloric acid etching (see Figs. II–4 and 5). Metallurgical examinations of sections of the vessel are being conducted to obtain additional information on the strength of the vessel material.

A heavy-section steel technology program, under the direction of Oak Ridge National Laboratory, is seeking information on materials properties, fracture characteristics, irradiation effects, and nondestructive testing techniques for the heavy-section (12-inch thick) steel proposed for use in future reactor pressure vessels. Other projects are providing supplementary information and analytical methods related to stress and fatigue considerations and to nozzle design. The results of investigations on reactor structure materials, particularly pressure vessel

[3] The PM–2A (Portable Medium Power Plant, No. 2A) was used to supply power at the Camp Century, Greenland, Army Research Center, for almost 3 years before being dismantled in 1963, after the vessel had been irradiated to its full dose limit.

Figs. II–4 and 5. Pressure Vessel Integrity. The Idaho Nuclear Corp., which took over certain NRTS operations, has continued the series of tests (begun by Phillips Petroleum Co., in 1965) on the irradiated Portable Medium Power Plant No. 2A (PM–2A) reactor pressure vessel to determine the extent of radiation-induced embrittlement which an actual reactor vessel has undergone. (The PM–2A supplied power to the Camp Century, Greenland, research center for almost 3 years before being dismantled in 1963 when the center was closed. The pressure vessel had been irradiated to its full dose limit during Camp Century operation.) In the tests, defects of varying depth and length were intentionally machined into a section of the pressure vessel. The vessel was then subjected to a variety of progressively more severe internal pressure and temperature conditions to observe the exact temperature-pressure combination at which, and the exact manner in which, the vessel would fail. Data obtained from these tests will be useful in establishing operating limits to prevent brittle fractures of pressure vessels. Calculations indicated that failure might occur with a defect 1¼ inches deep and 9 inches long at 3,540 p.s.i.g. ±885 p.s.i.g. and at a temperature of —29° C. (20° F.). The vessel eventually failed at 4,475 pounds per square inch and —29° C. The failure came only after an acid bath formed very sharp cracks at the base of the 1¾-inch-deep notch. Photo at *left* shows the failure cracks; on the *right* is a close-up view of part of defect area after rupture.

steel, being conducted by Brookhaven National Laboratory (BNL) and Pacific Northwest Laboratory (PNL) are described in the "Reactor Fuels and Materials" section (see p. 131).

Piping rupture studies. A better understanding of modes of cracking and rupture of piping is being sought, in order to further improve techniques for the design, fabrication, and inspection of nuclear piping systems. Current studies by the General Electric Co., at San Jose, Calif., and Schenectady, N.Y., and by Battelle Memorial Institute, Columbus, Ohio, on piping failure include: (*a*) fatigue effects, (*b*) stress concentrations in complicated piping configurations, (*c*) conditions under which cracks of various sizes may propagate to rupture, (*d*) rupture times and associated system forces, and (e) possible effects of in-service changes on the basic material properties of piping systems. The General Electric study is devoted to reliability engineering in piping systems to provide insight into the complete history of piping components from the conceptual-design stage through the entire oper-

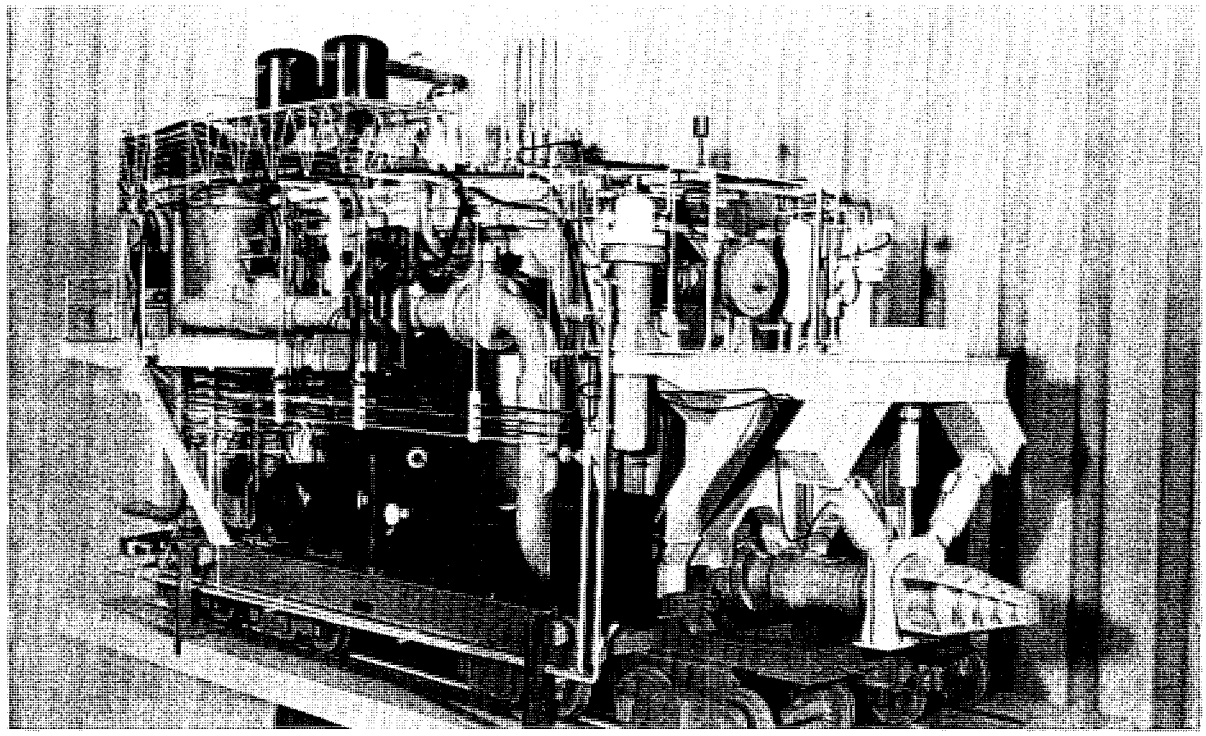

Fig. II–6. LOFT Dolly-Mounted Test Reactor. Scale model of the complete Loss-of-Fluid Test (LOFT) 50 megawatt (thermal) reactor experimental rig shows the reactor and test equipment mounted on the four-track railroad flatcar. The transportable system will permit remote assembly, disassembly, and maintenance of the experimental equipment at the NRTS. The first experiments are scheduled for 1970. The large plug at the front of the model represents a pipe rupture device for deliberately initiating the maximum credible (though highly improbable) accident postulated for a pressurized water reactor, namely, rupturing of a major coolant line. Top center are the reactor control rod drive mechanisms. A principal reason for building and operating LOFT is to evaluate the safety of water cooled power reactors by deliberately subjecting it to the damage caused by rupture of a major coolant pipe. LOFT is part of the safety test engineering program conducted for the AEC by the Phillips Petroleum Co.

ating life-time. This study should provide a basic understanding of the mechanisms involved in hypothetical pipe-rupture accidents, which will be important in preventing possible accidents and in designing and building safeguards.

The complete in-place inspection of nuclear powerplant piping is difficult because of the inaccessibility of the pipes. A monitoring system, therefore, is being developed at the Pacific Northwest Laboratory which could be in continuous operation to detect the initiation and growth of flaws in the primary system by means of acoustic signals produced by flaws and cracks as they grow. Current work is directed to determining the emission source of these signals.

Loss-of-Coolant Accident Studies

The loss-of-coolant accident is a potential, albeit unlikely, accident of major consequences for boiling-water and pressurized-water reactors. Accordingly, the AEC's nuclear safety program is devoting much effort to: (*a*) improving loss-of-coolant preventive measures (as discussed above), (*b*) understanding the accident course and potential consequences, and (*c*) evaluating engineered safeguards for limiting the potential accident consequences. All phases of the accident, including depressurization of the primary coolant system, core heat transfer, nuclear and chemical heat sources, core damage,

fission-product transport and deposition, and associated engineered safeguards, are being studied. Both analytical and experimental studies are being pursued to provide the information needed by industry and the AEC.

Experimental programs. The Loss-of-Fluid Test (LOFT) project[4] (see Fig. II–6), being conducted by Phillips Petroleum Co. at the National Reactor Testing Station will include a field-scale loss-of-coolant test on an operating 50-megawatt thermal (Mwt.) reactor and its containment system. Initial experiments are scheduled for 1970. The test program will provide an opportunity to study the performance capability of selected engineered safeguards and to assess the adequacy of analytical models for predicting the course and consequences of a loss-of-coolant accident in a real reactor system.

The LOFT project has for several years been a focal point for the reactor safety program, providing a basis for the definition, integration, and continuity of efforts on many related projects. A great deal of valuable information has been and will continue to be provided prior to the completion of the LOFT facility as a result of these supporting studies and experimental efforts. They have already provided much insight into potential problems, identified new problem areas, and developed analytical models and experimental data for use in power reactor safety analysis and design. Supporting experimental studies of metal-water reactions, fuel-pin heat transfer in a steam environment, physical properties of clad uranium dioxide (UO_2) fuel, and system depressurization phenomena are being conducted by various contractors.

A number of programs have investigated the complicated depressurization, or blowdown, phenomena. Large-scale blowdown experiments are being performed by the Containment Systems Experiment (CSE) by the Pacific Northwest Laboratory at the AEC's Hanford, Wash., plant, and LOFT Semi-Scale Blowdown (see Fig. II–7) projects. The United Kingdom Atomic Energy Authority (UKAEA) is also studying blowdown phenomena and provides information that complements U.S. programs.

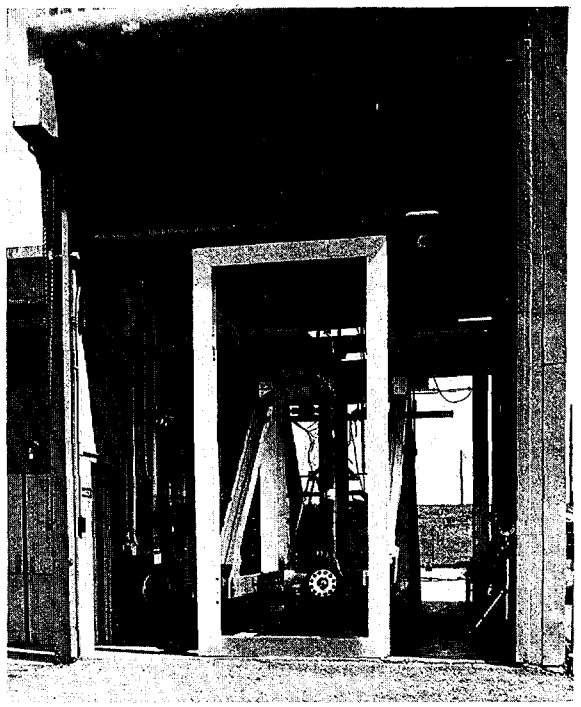

Fig. II–7. LOFT Semi-Scale Blowdown Rig. The LOFT semi-scale blowdown experiments are providing essential pretest data for evaluation of analytical methods in the determination of test pressure and heat transfer conditions, and for proof-testing of LOFT test components and instrumentation. The apparatus for the semi-scale blowdown experiments is shown mounted in test position. The 8.2-cubic foot vessel has provisions for simulation of a top or bottom break. The vessel will approximate blowdown conditions to 2,400 p.s.i.g. and 540° F. (280° C.).

Analytical effort. Major analytical efforts to describe the loss-of-coolant accident are being conducted, both in support of the LOFT project and in the evaluation of the applicability of existing data to analytical description of reactor accidents. Battelle Memorial Institute, (BMI) Columbus, Ohio, has developed new or improved computer programs such as the core heat transfer code, "Nurloc." Argonne National Laboratory has developed the "Chemloc" code which treats both core heatup and metal-water reactions, while the LOFT project has developed several computer codes for analysis of pri-

[4] See pp. 306–307, "Fundamental Nuclear Energy Research—1966."

mary system depressurization (blowdown). These analytical models have successfully predicted experimental results in the LOFT semi-scale blowdown experiments.

Emergency core cooling. The importance of emergency cooling to arrest a loss-of-coolant accident has led to extensive planning and supporting analysis at BMI to develop a program for obtaining additional information on emergency core cooling systems and to establish experimental tests which can be performed under conditions representative of advanced reactor designs. In addition, an in-plant testing program to be conducted by Phillips Petroleum will obtain data on a number of existing emergency core cooling systems. Experimental equipment has been designed to study details of emergency core cooling heat-transfer for both boiling-water and pressurized-water reactors.

The LOFT program has been somewhat reoriented to emphasize testing of emergency cooling system performance. An extension of the LOFT semi-scale blowdown supporting project is planned to study the effects of emergency core cooling injection.

Power Excursion Phenomena

A "power excursion accident" refers to a rapid increase in the amount of heat generated by nuclear fission resulting from the inadvertent sudden addition of positive reactivity [5] to the reactor. If the increased heat and its rate of production are sufficient, the event may be accompanied by fuel melting, metal-water reactions, and damaging pressure pulses. The programed research activities associated with power excursion phenomena may be divided into four general problem areas: (*a*) initiation and prevention, (*b*) reactor kinetics, (*c*) fuel pin failures, and (*d*) generation and propagation of pressure pulses.

Initiation and prevention. Nuclear powerplant operating and safety experience are analyzed to determine equipment and operator reliability, and to evaluate causal mechanisms for initiation of potential power excursion accidents. Included in this effort are projects examining standards and criteria for system components design, anti-seismic design, and protection and safety system instrumentation design.

Reactor kinetics. The Special Power Excursion Reactor Test (SPERT) oxide-core kinetics program, conducted by Phillips Petroleum at NRTS, performs self-limiting power excursions (in the SPERT–III reactor facility [6]) to evaluate the effects of various initial system conditions on the kinetic behavior of low-enrichment UO_2 cores. Excursions from low initial power have been performed with coolant conditions up to 500° F. (260° C.), 1,500 p.s.i.g., and 24 feet per second forced flow through the core. Good agreement between results from these tests and calculated results from a comprehensive reactor kinetics model, the "Paret" computer program (developed by Phillips Petroleum Co.) has been achieved. Additional excursion tests to be initiated at high (20 Mw.) power levels and with shorter reactor periods will be performed in 1968.

Analytical studies are underway at the University of Florida and at General Electric under subcontract to Phillips Petroleum to examine the adequacy of conventional (space-independent) kinetic formulations for analysis of the transient response of large cores typical of present power reactors, and to determine whether large-core power excursion experiments will be necessary. Results to date have partially defined the range of validity of small-core analytical methods, and have illustrated the need for spatially dependent kinetics calculations in dynamic analyses of large reactor cores.

Fuel pin failure. Data on fuel-pin failure mechanisms in power excursions are being obtained from tests in the Capsule Driver Core (CDC) [7] currently installed in the SPERT–IV facility as part of the SPERT subassembly

---

[5] Reactivity is a measure of the capability of the reactor to sustain a chain reaction. An increase in reactivity, or addition of positive reactivity, causes an increase in the rate of rise of power. Power is steady at a reactivity of one.

[6] See p. 89, "Fundamental Nuclear Energy Research—1965."

[7] See pp. 294–295, "Fundamental Nuclear Energy Research—1966."

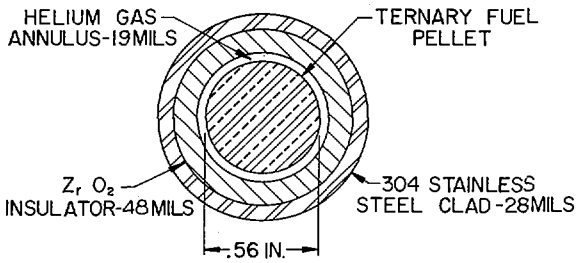

Fig. II–8. Power Burst Facility Fuel Rod Concept. The fuel for the Power Burst Facility (PBF) will consist of sintered pellets composed of a ternary mixture of urania, calcia, and zirconia. The PBF, at the National Reactor Testing Station, is being designed for power excursion tests with reactor periods as short as 1 millisecond. During such tests, the fuel will reach temperatures of approximately 2,350° C.; therefore, calcia-stabilized zirconia insulator sleeves surround the fuel pellets to keep the stainless steel cladding from melting. The helium gas annulus is provided between the fuel and insulator sleeves to allow for fuel expansion upon heating. Proof tests in the TREAT reactor and during other destructive tests have demonstrated the feasibility of using this type of fuel rod at energy densities and energy generation rates comparable to those expected during PBF operation. Additional proof tests will be performed in TREAT and in the SPERT-IV Capsule Driver Core to demonstrate that this type of fuel rod can withstand many repetitive excursion tests (100 tests in TREAT) at the maximum PBF design condition without damage.

testing program by Phillips Petroleum. Both the CDC and the higher-performance Power Burst Facility (PBF), scheduled for completion by 1969, provide experimental facilities for determining the manner in which fuel pins fail under various abnormal conditions; also, the energy thresholds for fuel damage and failure under accident conditions (see Fig. II–8). Studies conducted in the Transient Reactor Test Facility (TREAT) at NRTS on metal-water reactions have also provided data on thresholds and failure modes.

Generation and propagation of pressure pulses. Information on the pressures which might be generated in a power excursion accident will evolve from the SPERT–CDC subassembly tests and from the more extensive tests to be conducted in the PBF beginning in 1969. Experimental results obtained with the Capsule Driver Core thus far have indicated that approximately two percent of the nuclear energy contained within the fuel is converted to mechanical energy following the failure of encapsulated, water-logged fuel rods during a power transient (see Fig. II–9). This result is essentially the same as that obtained from integral-core destructive tests previously performed [8] in SPERT–I and, therefore, lends support to the application of capsule test results to integral-core problems. Forthcoming experiments will investigate pressures generated by other modes of fuel failure.

Additional information on generation and propagation of pressure will be obtained from integral-core limited-damage tests planned for performance in the SPERT–III facility following the current series of nondamaging tests. A project investigating acoustic wave propagation

[8] See pp. 155–156, "Fundamental Nuclear Energy Research—1964."

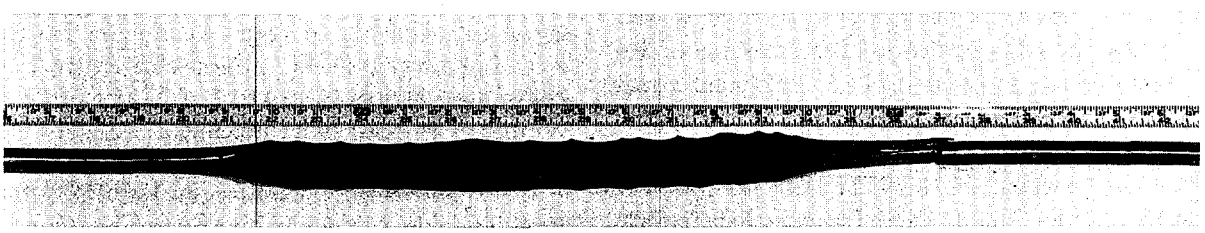

Fig. II–9. Generation of Pressure Pulses. Photo shows a fuel rod that failed during a 3.1-millisecond-period power excursion test in a Capsule Driver Core (CDC) test conducted by Phillips Petroleum Co. at the National Reactor Testing Station. The fuel within the rod had been intentionally water soaked prior to the test. The rapid heating of the water during the test caused a steam explosion inside the rod that ruptured the rod and expelled the uranium dioxide (UO_2) fuel into the containment capsule. The energy density in the rod at the time of failure was approximately 50 calories per gram of UO_2. Previous integral-core test results have shown that this type of fuel rod failure can cause damage, in the form of bowing or shearing, to adjacent fuel rods.

in a variety of homogeneous mixtures of water, steam, and gas is nearing completion.

Fission-Product Behavior

A broad program of studies of the behavior of fission products during the potential accidents described above has also been pursued. The objectives of the program are: (*a*) to learn what fission products would be released to secondary containment systems during the course of hypothetical accidents, and (*b*) to develop and test methods and equipment specifically designed to "trap", or place released fission products under control, so that in the event of secondary containment failure the fission products could not escape to the outer environment.

In the Transient Reactor Test Facility (TREAT) at NRTS, experimental studies have been made of the release and transport behavior of fission products from fuel samples severely overheated by short (½ sec.), but very large, energy releases, such as might occur during an extraordinary nuclear reactor excursion.

Mathematical models. At Oak Ridge National Laboratory (ORNL), construction of a new research tool, the Containment Research Installation (CRI), has been completed and the unit is now in operation. In the CRI, highly irradiated fuel samples are heated by electrical induction to simulate overheating of reactor fuel by fission-product decay after a loss-of-coolant accident. A careful and comprehensive experimental investigation of the factors controlling fission-product release has been started, as well as experimental studies of the behavior of released fission products in the containment vessel mockup which is part of the CRI. The extensive experimental data on fission-product behavior being generated in the CRI, and the Nuclear Safety Pilot Plant (NSPP), a larger facility at ORNL, are being incorporated into mathematical models and computer codes under development at Oak Ridge National Laboratory and at Battelle Memorial Institute (Columbus, Ohio) for application to large-scale power reactor accident analyses.

A simple model for fission product plateout in containment vessels was postulated and fairly well substantiated by NSPP and CRI results. For the dry air-iodine case, the effect of size sealing predicted by using the model is shown in Figure II–10. A prediction of iodine plateout in a condensing steam atmosphere has also been substantiated for a limited range of conditions. Although approximate in nature, these models are an important first step toward predicting fission-product behavior in full-scale containment vessels.

Filtration efficiency. The use of high-efficiency filters for control of particulate fission products released to secondary containment systems and the use of charcoal adsorbers for trapping the several chemical forms of released iodine are being thoroughly investigated at ORNL. Generally, elevated humidities are somewhat detrimental to the control of both particulate aerosols and organic iodides. By lowering the humidity and/or using specially treated charcoals, the satisfactory control of organic iodides can be effected. Continued study of the application of high-efficiency filters in highly humid systems is needed to adequately define the magnitude of this problem.

Factors affecting the efficiency of filtration-absorption equipment have been carefully studied, and limitations of such devices established. An important aspect of the work has been the development and testing of chemically impregnated charcoals for absorption of methyl iodide, a chemical form in which a small fraction of the released iodine occurs and which is especially difficult to trap. At Pacific Northwest Laboratory (PNL), the use of hydrazine-containing sprays for control of fission-product iodine in secondary containment systems has been investigated. The Containment Systems Experiment (CSE) facility at the PNL has been completed and put into operation. One of the objectives of this large containment facility is to investigate the performance of equipment for controlling fission products, *e.g.*, filters, charcoal traps, and containment sprays, which have been tested in small-scale facilities at ORNL.

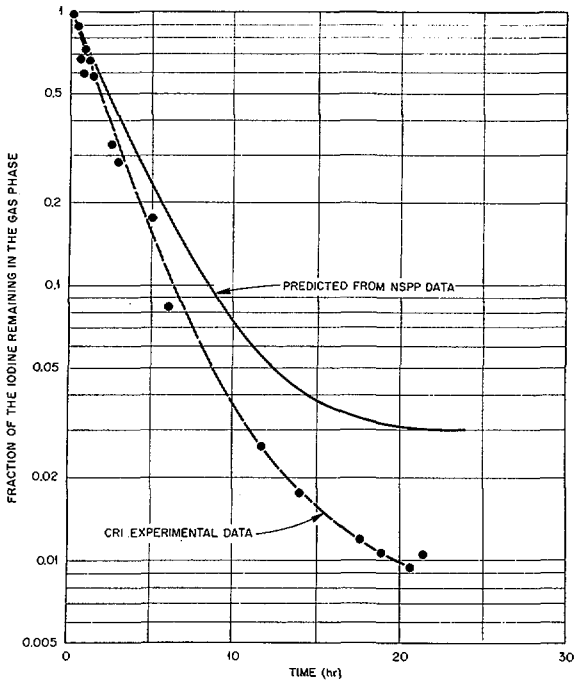

Fig. II–10. Fission Product Behavior. A simple mathematical model for fission product plateout in containment vessels has been postulated at Oak Ridge National Laboratory and fairly well substantiated by Nuclear Safety Pilot Plant (NSPP) and Containment Research Installation (CRI) results. For a dry air-iodine concentration case the effect of size scaling predicted by using the model is shown above. The solid line is the behavior predicted for the CRI by using the model and NSPP data only. The dotted line shows the actual CRI data. The initial slope substantiates the hydrodynamic aspects of the model quite well, while the curvature in the curve, which may be due to surface absorption and/or nonreactive forms of iodine (methyl iodide), is predicted within the same order of magnitude.

In the CSE, tests of the removal of fission products in large containment vessels have begun, and results on removal by deposition of these fission products on to surfaces and by the action of steam condensing on surfaces have been as predicted by analytical models developed in smaller scale experiments. Large scale tests of spray nozzle systems for washing fission products from the air inside containment vessels have shown the benefits of such systems in removing airborne fission products as well as reducing the pressure in the containment.

275–845 O—68——10

Fission-product concentration. Another project, for control of the fission-product noble gases, xenon and krypton, has been initiated at the Oak Ridge Gaseous Diffusion Plant (ORGDP) and the Oak Ridge National Laboratory (ORNL). These chemically inert gases, which are not trappable by methods used for other fission products, have to be removed from containment vessels and concentrated for storage in steel cylinders for later disposal. Two approaches to the problem are being pursued, the one at ORGDP involving concentration by the process of fractional distillation of liquefied fluoro-carbon-noble gas mixtures, and the other, at ORNL, by the process of selective permeation of the xenon and krypton through silicone rubber membranes.

In the ORGDP work, an absorption-stripping process employing a fluoro-carbon as the solvent will be used. According to the current flow sheet, the absorption column is expected to operate at about −94° F. (−70° C.) and 14 atmospheres. The loaded solvent is then fractionated in a second column operated at about 32° F. (0° C.) and 3 atmospheres to increase the fraction of krypton and xenon in the dissolved gases by preferentially removing oxygen, nitrogen, and argon. The noble gases are then stripped from the solvent in a third column which operates at 10° F. (−10° C.) and 2 atmospheres, and the solvent is recycled to the absorber. Several heat exchangers are needed, and interchange between warm and cold process streams has been used wherever possible to minimize the need for supplementary low-temperature refrigeration. The possibility of operating at higher temperatures is also being considered for decreasing cooling loads.

Contamination-decontamination experiment. The Contamination-Decontamination Experiment (CDE), shown in Figures II–11 and 12, at the National Reactor Testing Station, provides high-level fission product aerosols for the LOFT support studies. Four runs using short-cooled fuel pins containing 7,000 to 35,000 curies of fission products per run have been completed in the CDE. The aerosols are generated in the

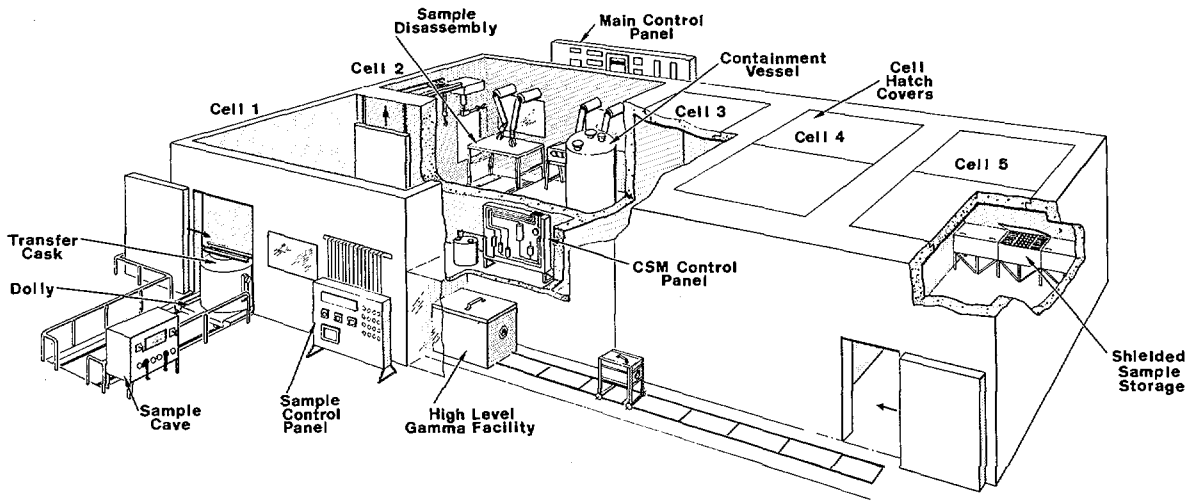

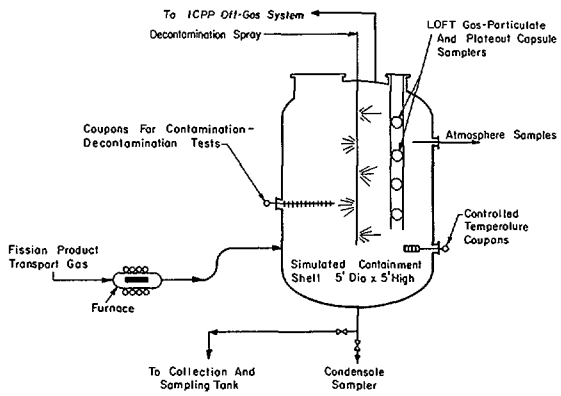

Figs. II–11 and 12. Contamination-Decontamination Experiment. Cutaway drawing of the Hot Pilot Plant containing the Contamination-Decontamination Experiment (CDE) facility (in cell 2) at the National Reactor Testing Station in Idaho. CDE is part of the Loss-of-Fluid Test (LOFT) support studies. The facility is being used to investigate the relative susceptibility to radioactive contamination and the ease of decontamination of various protective coatings (such as paints) which could be used inside reactor containment buildings. CDE is also used for testing the LOFT fission product sampling devices. Drawing at *left* is a schematic diagram of the sampling procedure. The CDE is operated for the AEC by Idaho Nuclear Corp.

CDE by induction melting of a small, highly irradiated fuel capsule in the presence of steam. The fission products released from the molten fuel are transported by steam to the 86-cubic-foot, stainless steel containment vessel. Environmental conditions and the atmospheric composition in the CDE furnace and containment vessel are controlled to match anticipated LOFT conditions.

The high-level aerosols generated in the CDE are being used to evaluate the contamination and decontamination of numerous types of protective coatings, to test the LOFT sampling devices, and to provide samples for development of analytical methods required to analyze the LOFT samples.

Environmental testing of LOFT samplers. Since the LOFT samplers will be used to establish the magnitude of the fission product release, determine the behavior of the fission products, and characterize the aerosol present in the LOFT containment building, satisfactory operation of these samplers is essential to the LOFT program. The LOFT samplers are being tested, in both the CDE and in the laboratory, under environmental conditions closely simulating the anticipated LOFT conditions. Testing at the NRTS has resulted in some mechanical design changes which have significantly improved the operation of the samplers. The tests also indicate that although the sampler orientation, location, and environmental conditions do exert varying influences on data from the samplers, the fission product distributions obtained from the LOFT samplers are generally representative when operated at specified conditions.

A Continuous Sampler-Monitor (CSM) is being developed and tested at the NRTS to continuously determine the fission product concentrations in the LOFT containment atmosphere (see Fig. II–12). This system separates the inlet sample stream into two fractions—a gas stream containing the rare gases and a liquid stream containing essentially the balance of the fission products and particulates—using a small spray scrubber. The liquid and gas stream fractions are amenable to rapid analysis by gamma-ray spectrum stripping techniques. Preliminary tests conducted in the laboratory and in the CDE on the CSM show that the scrubber effectively separates the I_2 and HI forms of iodine and particles larger than 0.2 micron from the gas stream. Evaluation of the scrubber performance on organic iodides and particles smaller than 0.2 micron is underway.

Containment Integrity

Reactor containment systems are basically large pressure vessels designed to control the release of radioactive materials to the outside environment in the unlikely event of failure of the reactor primary system. The primary concern for safety is the assurance that not only will the structure withstand high internal pressures without failure, but that the leak rate through the shell and its various penetrations will remain small under these conditions. Attention must also be given to other forces which might affect containment integrity, such as earthquakes and ejected missiles.

The determining factor for the maximum pressure transient that the containment structure must withstand is, for water reactors, the stored energy in the coolant and core, plus contributions from metal-water reactions and decay power. Blowdown (depressurization) of water and steam from small pressurized vessels in the LOFT and CSE projects is now providing confirmation of the analytical methods for determining this pressure transient. Experiments conducted by Oak Ridge National Laboratory and Argonne National Laboratory on small samples of metal-clad fuel are providing basic data on the amount of additional energy which might be expected from this source under accident conditions. Reinforced and prestressed concrete[9] is now extensively employed, as it yields a biological shielding benefit in addition to its containment function.

Engineered safety systems for rapidly reducing the pressure in the containment have commonly taken the form of water sprays or pools for steam condensation. Further information on the performance of these safeguards will be obtained from the CSE program, carried out by PNL, and the advanced engineering safety systems tests being conducted by General Electric at San Jose, Calif.

Considerable effort is now in progress to determine methods for testing and demonstrating the strength, tightness, and reliability of the containment in the plant application and engineering test project at the Carolinas–Virginia Tube Reactor, Parr, S.C., containment system. Oak Ridge National Laboratory is also studying the instruments, controls, and devices that operate to close all penetrations into the containment structure if an accident should occur.

Fission product analysis techniques. In following the release, transport, and deposition of various fission products from an experimental fuel meltdown such as in LOFT, conventional radiochemical procedures are too slow and cumbersome. Idaho Nuclear Corp. is developing a computerized spectrum stripping method for the gamma ray spectra of gross fission products. Precise gamma ray energies are being measured with a lithium-drifted germanium detector and assigned to the corresponding fission products. Using a Ge (Li) spectrometer having a resolution (full width at half maximum) of about

[9] The design principles of the containment structures (including concrete) to withstand accident-derived pressures were reviewed in the two-volume "Summary of U.S. Reactor Containment Technology" (ORNL–NSIC–5) by ORNL in 1965, and the specific application of prestressed concrete for these structures was examined intensively by ORNL and the Franklin Institute in 1964 in the "State-of-the-Art of Prestressed Concrete Pressure Vessels for Nuclear Power Reactors" (ORNL–TM–812). These documents are available at the Clearinghouse for Federal Scientific and Technical Information, National Bureau of Standards, U.S. Department of Commerce, Springfield, Va. 22151, $3.00 per copy.

750 ev. at 100 Kev. and a 4,096-channel pulse-height analyzer, it is possible to determine gamma ray energies to about ±0.2 Kev. over an energy range from 50 Kev. to 2.5 Mev. Preliminary spectrum stripping methods have been successfully applied to a variety of gas and plateout samples from experimental meltdowns of irradiated fuel.

Design for seismic loading. The design of large containment structures to withstand seismic loadings has been reviewed by Oak Ridge National Laboratory, and a program has been initiated to develop improved antiseismic designs of four different designs.

In addition to simply strengthening the structure, several concepts are being developed for limiting the forces that can be transmitted from the ground to the reactor foundations. These include the use of a layer of weak material under the foundation and partial or total flotation in water or aqueous muds. These designs describe reactors which can withstand a range of severe vibration and displacement loads due to earthquakes combined with loads which may be caused by reactor accidents. The designs are aimed at preserving the containment structural and leakage integrity, as well as the functioning of its associated engineered safeguards systems.

Further work will be concerned with model testing of seismic parameters to assure the adequacy of critical parts of antiseismic designs. Also, screening tests with simplified lumped-parameter-system simulators will be investigated. Rigorously accurate mathematical or experimental models for vibration systems are often difficult or impossible to set up and to work with because, at every point in the model, all parameters such as density, elastic modulus, and internal friction or damping coefficient must match the parameters at the corresponding points in the real system. A frequently useful approximation is to set up a model in which the mass is assumed concentrated at a few points, flexibility exists only in specified regions, and frictional forces act only on a finite number of points in the system. When applicable, these "lumped parameter" models permit accurate analysis at much less cost than would use of the rigorous model.

Earthquake geology study. The AEC is also sponsoring investigations by the U.S. Geological Survey to acquire basic data on earthquake geology to aid in selecting safe reactor sites. A study of the phenomena associated with ground rupture due to faulting is being accomplished by an extensive review of the geological literature, by direct field examination of surface manifestations in regions effected by earthquakes, and by correlation with instrumental records of earthquakes that were attended by faulting. This work will summarize the present knowledge in order to develop parameters for evaluating the likelihood of occurrence, the potential magnitude, and the effects of faulting in specific geologic settings. In connection with this program, the AEC sponsored part of the Geological Survey's intensive investigation of the engineering geology aspects of the 1966 Parkfield-Cholame (about 150 miles north-northwest of Los Angeles) earthquakes.

A regional environmental map of part of the Los Angeles Basin is being prepared by the Geological Survey to indicate areas that have special geologic and seismologic problems relevant to siting reactors. A prior knowledge of areas in which geologic-seismologic problems exist will facilitate the selection of safe reactor sites. Experience has shown that knowledge of the regional geologic environment is particularly important in areas of high seismicity, such as California, because the earthquake potential of faults and other zones of earth deformation cannot always be determined from investigations in small areas.

FAST REACTOR SAFETY

In the field of fast breeder reactor[10] safety, the major effort has been oriented to meet the

[10] A breeder reactor is one that will be capable, by extremely careful design for highly efficient use of the available neutrons, of producing more fuel than it burns. A therman breeder reactor will use the thorium-uranium-233 cycle, whereas a fast breeder reactor, or "fast reactor", will use the uranium-plutonium-239 cycle.

needs of the sodium-cooled liquid metal fast breeder reactor (LMFBR) program, in accordance with the establishment of this breeder concept as the one of highest priority in the AEC's civilian power program. Because safety considerations enter into all aspects of the LMFBR program, it has been important to initiate, at an early stage, a comprehensive, long-term program of safety research to ensure timely development of the requisite safety technology.

Fast reactors now envisioned for producing electrical power and "breeding" their own fuel use only slightly diluted fissionable material as fuel in a compact, unmoderated core. Hence, they will operate at extremely high power densities relative to other types of power reactors. The principal concern for fast reactors—to a much greater extent than for water reactors—is, therefore, the nuclear excursion accident. This is due to the different neutronic characteristics (shorter neutron lifetime and smaller delayed neutron fraction) of the fast reactor system and because of its potential for large reactivity additions from core geometry changes which may result from accident situations.

Much attention is being given to the *Doppler* coefficient [11] and the high-temperature cross-section data for the fuel to determine whether or not the excursion is self-limiting. Work on sodium-cooled reactors, but not necessarily fast reactors, has been going on for more than 10 years, but the new emphasis on fast breeders demands a coordinated safety program.

Fast-Reactor Meltdown Program

The core-meltdown problem is an important consideration in fast-reactor safety. Basically, a meltdown is a multistage accident in which some operating abnormality occurs and produces fuel failure and movement. This, in turn, leads to a reactor excursion (sudden burst of neutrons and the consequent excessive heat). In recent years, the movement and production of vacuities in the sodium coolant has been added to fuel failure and movement as a cause of possible excursions with resultant destruction of the core and release of fission products. This added cause applies especially to reactors fueled with plutonium, since they tend to have a positive sodium-void coefficient (the excursion is heightened by vacuities in the coolant). AEC research into the meltdown problem is keyed to considerations of the maximum hypothetical accident, studying it theoretically and experimentally—seeking ways to prevent it, and looking for ways to restrict the consequences to close quarters to protect the operators and public.

Research into the meltdown accident includes several parallel approaches. First, controls and instruments are being improved to maximize the extent to which the initiating mechanism can be prevented or limited. Also, as experience is gained, confidence in the reliability of components is generated, and operational data is compiled so that the design of handling equipment, pumps, etc., can be improved. Next, material with specific *Doppler* coefficients are being designed into the system as aids to the control systems. These are called "negative coefficients" and may be built into the reactor, for example, by using one-piece metallic field elements and relying on their axial expansion to "dilute" the fuel and make the excursion self-limiting. Another approach to the meltdown accident is that of studying core failure itself, including the movement mechanism, in order to provide data for a realistic safety analysis and guidance to designers so serious meltdowns can be avoided. For example, the designer must be able to determine, for a specific core, whether movement can occur with a sufficient degree of coherence over the core so that idealized excessive rates of reactivity additions can actually occur. Finally, the core-destruction phase of meltdown must be understood (see Fig. II–13). This includes knowledge of such items as equations of state for high-temperature reactor materials, the amount of energy available to do work on the

[11] A term used to describe the change in absorption of fission rate due to changes in the relative motion of a neutron and its target atom. This effect is temperature dependent, since the amplitude of the vibrational motion of the target materials increases with temperature.

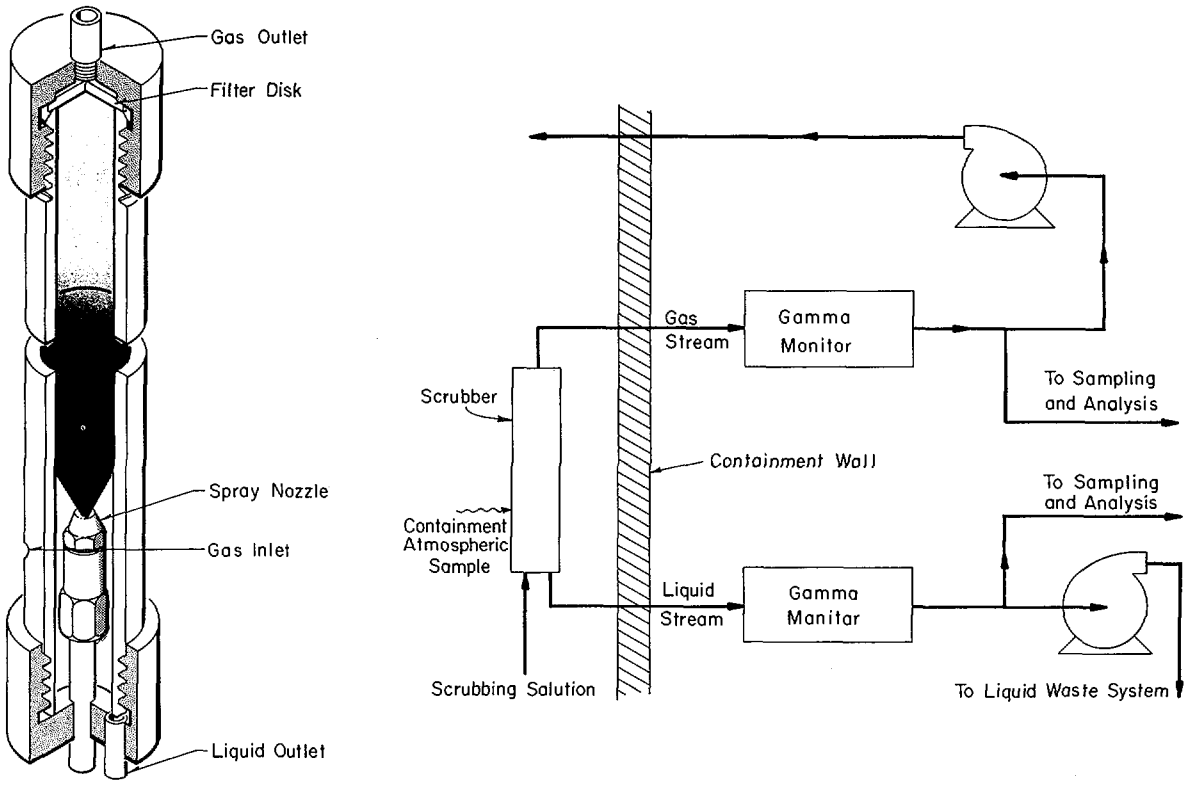

Fig. II–13. Environmental Testing of LOFT Samplers. The Continuous Sampler-Monitor schematic flow sheet, *above right*, and cutaway drawing *above left*, of a spray scrubber are being developed and tested at the National Reactor Testing Station in Idaho for the Loss-of-Fluid Test (LOFT) program. The CSM is being designed for the AEC by Idaho Nuclear Corp. to continuously determine the fission product concentrations in the LOFT containment atmosphere following the reactor safety experiments scheduled to be conducted in the early 1970's by Phillips Petroleum Co. for the AEC at NRTS.

core surroundings, etc. Much of the work on fuel meltdown is being done at Argonne National Laboratory.

Research on Sodium Fires

A small sodium fire (0.2-square-foot) was conducted in a sealed chamber with an initial oxygen concentration of 4 volume percent. Pressure-history data were collected during the Atomics International, Canoga Park, Calif., test, and the burning rate of sodium was measured as a function of the oxygen concentration and found to be proportional to the amount of oxygen. A smaller sodium fire yielded data on the concentration of airborne sodium, its plateout, and the fallout of sodium aerosols with time (see Fig. II–14). The deposition due to plateout and fallout showed that an automatic, remotely operated sampler could be operated successfully. The aerosol concentrations and the amounts deposited were consistent with the simple material balance.

Fission Product and Contamination Control

Atomics International recently developed curves to indicate the approximate relation between noble-gas production and its solubility in liquid sodium. The curves represented an extrapolation of similar data for argon and krypton and their solubility in liquid sodium. Also, a radiation index was prepared to determine a relative listing or ranking of those fission prod-

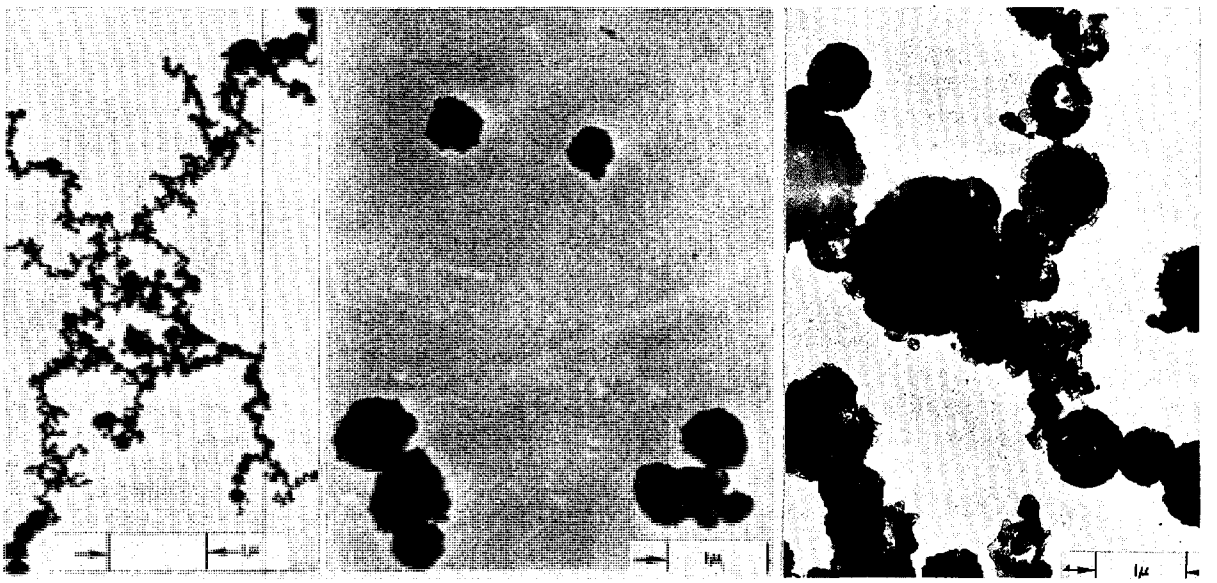

Fig. II–14. Research on Sodium Fires. Studies are being conducted at the Atomics International, Canoga Park, Calif., to characterize, predict, and develop appropriate engineering safeguards for the energy and effluents (sodium oxide, fission product, and fuel aerosols) generated during potential large sodium fires in a liquid metal-cooled fast breeder reactor (LMFBR). Experiments conducted to date have shown that in potential accidents in which fission product (iodine-131) and/or fuel (uranium dioxide-plutonium oxide) aerosols are released in the presence of sodium oxide "smoke" (aerosol) from a sodium fire, the sodium oxide scavenges the other airborne particles. This behavior indicates that the sodium oxide aerosols will provide an inherent mechanism for controlling and significantly reducing the release of airborne contamination following potential major accidents in the LMFBR. On the *left* are uranium dioxide particles, *center* shows sodium dioxide particles, and on the *right* are sodium dioxide and uranium oxide particles scavenged after 5 minutes.

ucts that contribute to the radiation level after shutdown.

In an initial experiment on the removal of cesium from sodium by cold-trapping, sodium containing 104 parts per million of cesium was circulated over sodium oxide at 538° C. and through a cold trap at 149° C. for 16 hours. Results showed appreciable trapping.

Chemical Reactions in Fast Reactors

Part of the reactor safety work at Argonne National Laboratory includes the assessment of potential problems by investigating the chemical and physical interactions between liquid sodium and the fuel and its cladding. This includes such features as the transient heat transfer associated with such interactions, the high-temperature physical properties of fast-reactor materials, migration and segregation of fuel in mixed uranium-plutonium compounds, and the reaction of sodium with air. The work on fuel migration and segregation is important in assessing the extent to which *Doppler* broadening can be decreased as a shutdown mechanism in an operating reactor.

Transient Testing of Fuel

One objective of recent work at General Electric Co., San Jose, Calif., was to examine a transiently irradiated fuel specimen that had already been subjected to a high burnup of the uranium and plutonium. The cladding deformed to the extent of 0.9 percent, compared with the predicted one percent; the inner surface of the cladding cracked a little because of the deformation. Metallography showed clear evidence of crack propagation due to grain-boundary precipitation at the inner surface. The major

conclusions were: (*a*) the fission gas released from fuel that is melted during a transient can be one of the primary causes of cladding failure; (*b*) the fission gas so released is a large factor in redistributing the uranium and plutonium oxides; (*c*) there was no sign that the melted fuel had foamed; and (*d*) there seems to be a considerable margin between the demonstrated performance limit (about 1% of cladding deformation and more than 50% molten fuel) and the postulated credible accidents in a fast, ceramic-fueled reactor, inasmuch as current design criteria and safety analyses do not result in any fuel becoming completely molten.

GAS-COOLED REACTORS

Studies directed to gas-cooled reactor safety include the chemical reactions that may occur between normal and accidental coolant contaminants and various materials, together with the emission, transport, deposition, and behavior of fission products within a gas-cooled reactor.

Steam-Graphite Reaction Studies

The primary chemical reaction of concern in gas-cooled reactor safety is the steam-graphite reaction, which can cause the release of carbon dioxide and potentially explosive hydrogen and thus enhance the release of fission products to the primary system. Safety programs involved with the study of this reaction at Oak Ridge National Laboratory include small-scale laboratory studies of steam-graphite reaction kinetics, analytical and engineering-scale steam-graphite reaction studies performed with such parameters as varying flow conditions, temperatures, and specimen geometry; and in-pile experimental studies of the steam-graphite reaction.

The release of fission products from irradiated fuel during a steam-graphite reaction is also being measured at ORNL by both in-pile and laboratory experiments. These fission-product studies include: (*a*) small-scale laboratory experiments to examine fission-product release and transport due to steam oxidation of carbon-coated fuel; (*b*) in-pile experiments to determine the amounts, characteristics, and forms of released fission products; (*c*) experiments to measure and characterize nongaseous fission-product release from irradiated fuel; and (*d*) experimental study of the chemical and physical properties of gaseous fission products and the mechanisms by which the fission products are transported. The in-pile experiments are just getting underway but the laboratory experiments, including those with trace fission isotopes (see Fig. II–15), have demonstrated both the release and high-temperature behavior of fission products removed from oxidized fuels.

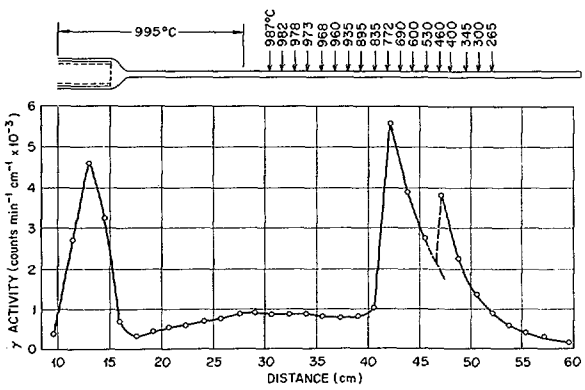

Fig. II–15. Steam Graphite-Reaction Studies. The primary chemical reaction of concern in gas-cooled reactor safety is the steam-graphite reaction, which can cause the release of carbon dioxide and potentially explosive hydrogen, thus enhancing the release of fission products to the primary system. In-pile experiments at Oak Ridge National Laboratory have demonstrated both the release and high-temperature behavior of fission products removed from oxidized fuels. Charted above is the separation of fission products evaporated from contaminated graphite by use of a thermal gradient tube. The peaks due to cesium-134, cesium-137, and silver-110 were obtained by exposure of the specimen at 1,000° C. to a helium-steam mixture having a partial pressure of steam of 250 torrs.

Experimental Site Study

In addition to these established programs, the suitability of several facilities for conducting experimental physics measurements is under study at ORNL. Reactivity transient tests to illustrate the effects of transient heat flux on

reactivity feedback may be possible at the UHTREX (Ultra-High Temperature Reactor Experiment at Los Alamos), EBOR (Experimental Beryllium Oxide Reactor in Idaho), or HTLTR (High-Temperature Lattice Test Reactor at Hanford) installations; and these facilities are being evaluated by their respective operating organizations for such tests. Test reactors with burst input capabilities, *e.g.*, TREAT and General Atomic's TRIGA, will be considered by General Atomic, San Diego, Calif., for examining the behavior of HTGR (High Temperature Gas Reactor) fuels under severe temperature transients. In tests accompanying the decommissioning of a large graphite production reactor at the Hanford site, Douglas United Nuclear, Inc., will conduct measurements to determine the usefulness of this reactor class in interpreting the space-dependent kinetics behavior of HTGRs.

OTHER SAFETY ACTIVITIES

The AEC sponsors a continuing research and engineering development program for the treatment and disposal of all types of radioactive wastes. Included in this program is an associated environmental research program, involving geohydrologic, geoseismic, and meteorologic studies related to nuclear facility site evaluation and to the safe control of all radioactive waste handling operations. So that full use can be made of the nuclear safety program output, information developed under the various program activities is being collected, interpreted, and disseminated in a useful form.

Information Dissemination

The Nuclear Safety Information Center (NSIC) [12] at Oak Ridge National Laboratory serves the industrial and scientific community by collecting, storing, evaluating, and disseminating nuclear safety information generated throughout the world. Information is disseminated by issuance of quarterly indexed bibliographies containing abstracts of the Center's acquisitions, by preparation of reviews of the literature in select subject areas, and by operation of a program of Selective Dissemination of Information (SDI). This is a program under which workers in the nuclear field periodically receive summaries of literature in their field of interest. Abstracts of the Center's acquisitions are stored in the memory banks of a digital computer. Codes have been developed which expedite computerized preparation of the quarterly bibliography, permit retrospective searches of the Center's acquisitions for special bibliographies, and answer specific technical inquiries.

ORNL also prepares the bimonthly technical progress review journal Nuclear Safety, which covers significant developments in the field of nuclear safety.[13]

---

[12] NSIC's services are available without charge to governmental agencies, research and educational institutions, and the nuclear industry. The Center's reports and quarterly indexed bibliographies may also be purchased for a nominal sum from the Clearing House for Federal Scientific and Technical Information, Springfield, Va. 22151. Requests for information, special bibliographies, and SDI should be addressed to: Nuclear Safety Information Center, Oak Ridge National Laboratory, P.O. Box Y, Oak Ridge, Tenn. 37830.

[13] *Nuclear Safety* is available by subscription from the Superintendent of Documents, U.S. Government Printing Office, Washington, D.C. 20402. The cost is $3.50 per year.

Fig. II–16. Fabrication of Refractory Metals. Economical fabrication methods are being developed under a study of refractory metals (niobium, molybdenum, tantalum, and tungsten) and their alloys at Oak Ridge National Laboratory (ORNL). Photo shows a 2,000° C. tungsten billet being loaded into an extrusion press. The white hot billet, during the transfer from the furnace to the press, reacts with air to form a molten oxide layer, which lubricates the extrusion. This self-lubricating technique is under development at ORNL (see p. 148).

REACTOR FUELS AND MATERIALS

Since, as described in the introduction, the reliability and efficiency of nuclear reactors are closely connected with the fuel materials and structural materials used in them, the AEC is sponsoring a vigorous program of research and development in the field of reactor fuels and materials. Representative investigations on metallic and ceramic reactor fuels, the effects of radiation and corrosion on reactor structural materials, fabrication techniques, and methods of nondestructive testing of materials are reported in this chapter.

METALLIC FUELS

Alloys of thorium, uranium, and plutonium with zirconium and titanium have been under continuing investigation for use as reactor fuels.

Thorium-Uranium-Zirconium Alloy

Pacific Northwest Laboratory has demonstrated the superior in-reactor performance of prototype thorium-uranium-zirconium fuel elements. Exposures to as much as 18,000 megawatt days per ton (MWD/T),[14] in excess of two atomic percent (a/o) burnup, have been successfully attained without altering the engineering characteristics or capabilities of the elements.

These elements have readily withstood the rigors of nearly 30 irradiation test cycles, with the attendant interim handling and evaluations

[14] *MWD/T*—megawatt days per ton. The extent of reactor fuel burnup which has taken place in a reactor; the term is also used to express the extent of irradiation of a sample in radiation damage studies.

during 4 years of testing.[15] Fuel swelling amounted to only three percent, which is the minimum value required to accommodate the new atoms that are formed by the fissioning reaction. A detailed examination of one of the elements in the electron microscope, at magnifications as high as 20,000 diameters (20,000×), revealed no tearing, cracking, or fission gas porosity, the metallic structure retaining its pre-irradiation appearance.

EBR–II Fuel Surveillance

A continuing evaluation of the irradiation performance of the EBR–II [16] fuel, conducted in the Fuel Cycle Facility (FCF) at the National Reactor Testing Station in Idaho, has led to a method of determining the amount of fuel pin swelling.

The basic fuel element used in EBR–II (see Fig. II–17) consists of a cylindrical fuel pin fabricated from uranium-235 with five weight percent of fissium alloy [17] encapsulated in a thin-walled stainless steel tube. A thin annular space around the fuel pin is occupied by metallic sodium, which is an excellent heat-transfer medium. When the fuel element is fabricated, a

[15] See pp. 7–9, "Fundamental Nuclear Energy Research—1965."

[16] Experimental Breeder Reactor-II, operated by the Argonne National Laboratory at the National Reactor Testing Station (NRTS), Idaho. See p. 57, "Fundamental Nuclear Energy Research—1965."

[17] An alloy of uranium and the elements molybdenum, ruthenium, technetium, rhodium, palladium, niobium, and zirconium, deliberately added to the initial fuel to provide an equilibrium alloy for melt refining.

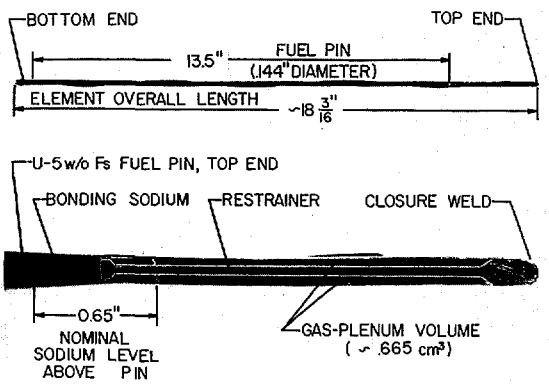

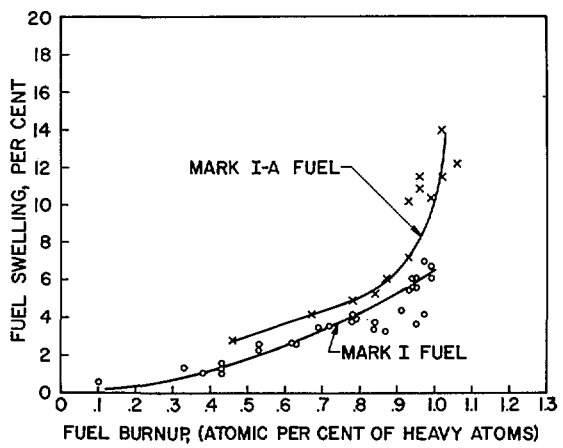

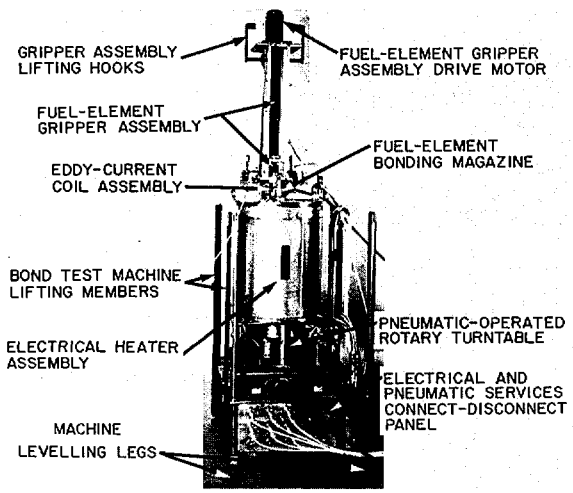

Figs. II–17, 18, and 19. EBR–II Fuel Surveillance. Argonne National Laboratory has developed a technique of remotely measuring the change in volume of sodium in EBR–II fuel elements. A Mark 1A-Type fuel element is shown *above left*. The sodium-level measuring device, *above right*, employs a pulsed eddy-current system, consisting of a high-frequency coil which applies an electromagnetic field at the surface of the metal cladding as the sodium-filled element passes lengthwise through the coil. Whenever the wave encounters a discontinuity, an echo is produced as a peak on an associated strip recorder. The machine has proven capable of long periods of sustained operation within the high gamma radiation environment of a hot cell. The chart at *left* summarizes several thousand measurements made on the Mark I and Mark IA fuel elements. These measurements have enabled the setting of a maximum irradiation limit and the continued monitoring of fuel-element performance. By the end of 1967, more than 38,000 EBR–II driver fuel elements will have been irradiated to established burnup levels up to 1.2 atom percent without any failures.

sufficient quantity of sodium is added to fill this annulus and submerge the top end of the fuel pin below a column of sodium of specified length.

During fissioning of fuel in the reactor, solid and gaseous fission products accumulate in the microstructure of the fuel pin and cause it to increase in volume. The swelling displaces sodium from the thin annulus separating the pin from the stainless steel capsule, and causes the top end of the fuel pin to become submerged below a column of sodium longer than that originally present. The change in length of the sodium column is a measure of the swelling of the pin as a result of irradiation in the reactor. This is important, because excessive swelling of the fuel may develop sufficient pressures to rupture the cladding in the fuel elements. Routine surveillance of fuel performance, thus, is an important operating consideration.

CERAMIC FUELS

Ceramic fuels, composed of the oxides, carbides, nitrides, and similar compounds of uranium and plutonium, have the capability for high burnup at high operational temperatures. Hence, they are of particular interest for use in fast breeder reactors.

Stoichiometry Effects in Oxide Fuels

Environments experienced by nuclear fuel materials are uniquely severe. A typical uranium-plutonium fast reactor fuel, for example, operates for thousands of hours at temperatures up to 5,000° F. (2,750° C.) and with temperature gradients approaching 4,000° F. per inch (2,200° C.). Since the operating behavior of these materials is predicted largely from data gathered in the laboratory where such strenuous conditions cannot even be approached, discoveries frequently arise from carefully conducted "in-reactor" experiments. Such was the case in tests recently performed by Pacific Northwest Laboratory to study effects of changing the oxygen content in uranium dioxide (UO_2) fuels.

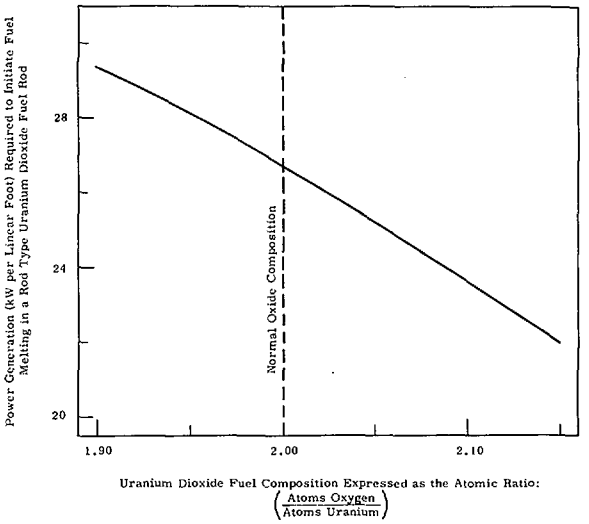

Fig. II–20. Stoichiometry Effects in Oxide Fuels. The variation in fuel power rating required to achieve incipient uranium dioxide fuel melting for various fuel compositions is shown in the Pacific Northwest Laboratory chart. Note that the addition of oxygen causes a continuous decrease in the power rating required for melting, *i.e.*, in the "thermal efficiency." All fuel specimens operated with 900° F. (483° C.) oxide surface temperatures, and contained less than 1 percent porosity.

Ten cylindrical UO_2 specimens with various controlled oxygen or uranium contents were irradiated at power densities sufficient to cause melting of more than 50 percent of the fuel (melting point=5,100° F. or 2,800° C.). Following irradiation, segments were cut from the specimens. Measurements were made of the extent of melting which had occurred, and a correlation worked out between the average fuel composition and the maximum power density achievable without fuel melting. This showed that reducing the oxygen content resulted in a higher fuel thermal efficiency (see Fig. II–20).

Migration of impurities. Even more interesting was the fact that the excess oxygen or uranium was not uniformly distributed after irradiation. Migration of these excess atoms to the central portion of the fuel, which was molten during irradiation, had occurred while the composition of the solid approached that of uncon-

taminated UO_2. Such a migration is desirable because impurities (oxygen, uranium, fission fragments) concentrated in the fuel center have relatively little effect on thermal efficiency or dimensional stability of the fuel. Since operating a fuel with a molten center results in the movement of impurities to the center, such operation may provide a built-in mechanism for purification of the fuel, thereby permitting longer lifetimes and reduced fuel costs.

High-Temperature Conductivity of UO_2

Because the temperature of uranium dioxide (UO_2), a widely used reactor fuel, often approaches 4,500° F. (2,480° C.) during reactor use, a knowledge of its high temperature properties is important. One such property is the electrical conductivity which, it has been shown at the Pacific Northwest Laboratory, increases greatly as the temperature of the UO_2 rises.

The electrical conductivity of UO_2 was determined from room temperature up to 4,250° F. (2,340° C.) (see Fig. II–21). Near room temperature, UO_2 is an electrical insulator. However, unlike metals which show a decrease in conductivity as the temperature increases, the conductivity of UO_2 increases. At about 1,600° F. (870° C.), the conductivity begins to increase very rapidly as the temperature increases, and the UO_2 behaves much like a conductor. Near the melting point—about 4,400° F. (2,425° C.)—the conductivity is more than 100,000 times greater than at room temperature.

Most important, this analysis of the high-temperature electrical data has provided a better understanding of the electronic structure of UO_2 at high temperatures and how it may be related to other properties of direct importance in design of nuclear fuel systems. The relatively high electrical conduction may contribute significantly at these higher temperatures to an increase in thermal conduction, a very important property in predicting fuel performance. Because of the high electrical conductivity and other favorable electrical properties, UO_2 may also have promise as a fuel for the direct conversion of nuclear energy to electrical energy.

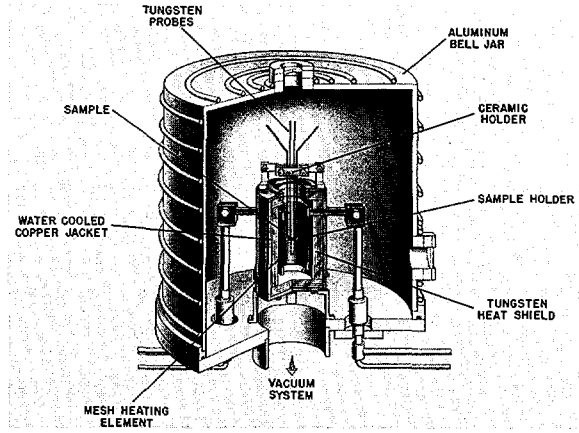

Fig. II–21. Electrical Conductivity Furnace. This high temperature furnace is used to measure the electrical conductivity of refractory ceramics at Pacific Northwest Laboratory. The refractory metal, mesh-type heating element can be heated from room temperature up to as high as 5,400° F. (2,980° C.) by a high direct current—this is 900–1,200° F. higher than the capability of other known apparatus. The internal parts of the furnace, likewise heated to high temperatures, are also made of refractory metals. The ceramic sample is positioned in the hot zone and electrical measurements are made with tungsten probes. Measurements can be made in inert gas, hydrogen, or vacuum.

Coated-Particle Fuels

The fuel for high-temperature gas-cooled reactors consists of uranium oxide or carbide particles in graphite. To prevent escape of gaseous fission products, each fuel particle is coated with a layer of dense impervious carbon, deposited on it from a hot decomposing hydrocarbon gas. At Oak Ridge National Laboratory (ORNL) two notable advances in coated-particle fuels have recently been made. A mathematical model relating irradiation performance of coated fuel particles to their physical characteristics has successfully predicted particle stability in use. Also, substitution of propylene for methane as a coating gas has markedly reduced the required coating time and temperature.

The mathematical model permits a computer calculation of the fission burnup that a fuel particle can withstand based on the nature of fission and the dimensions, densities, and struc-

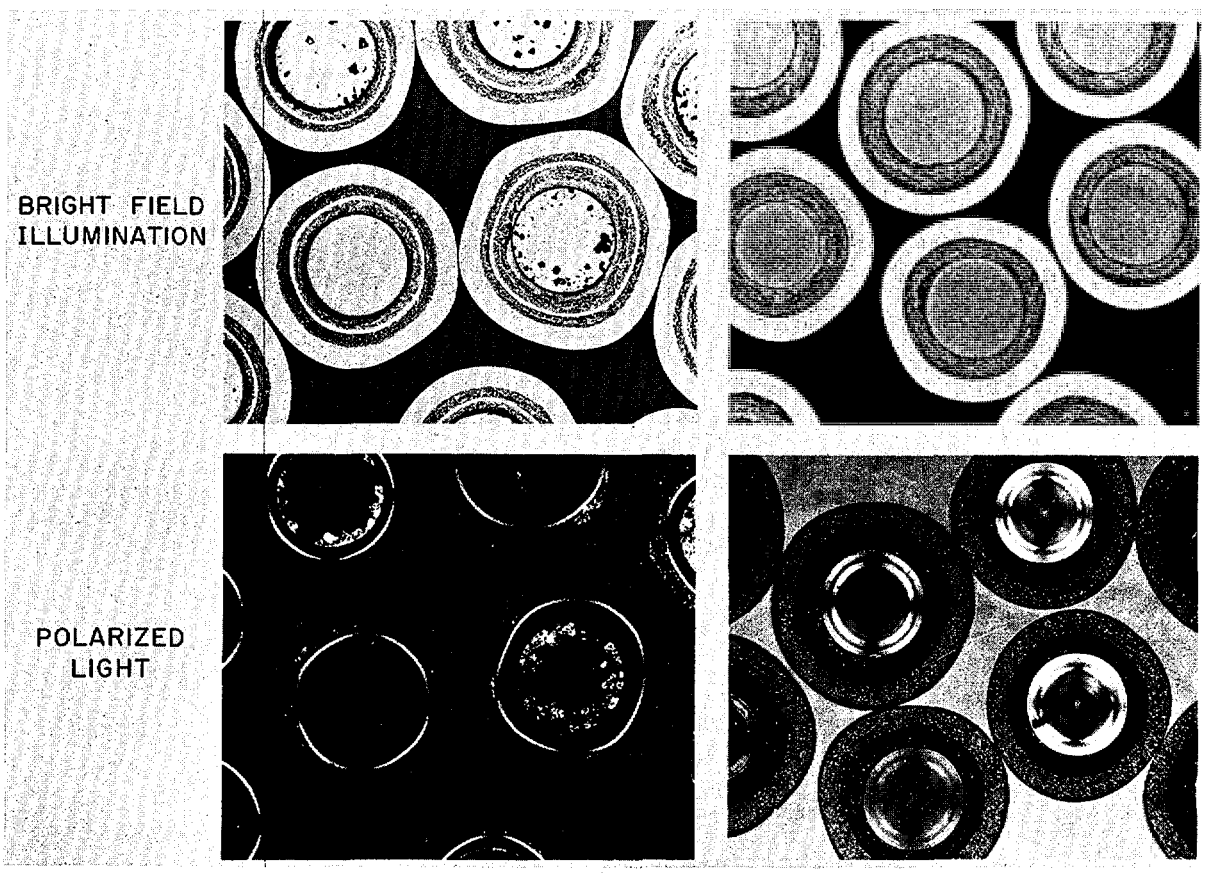

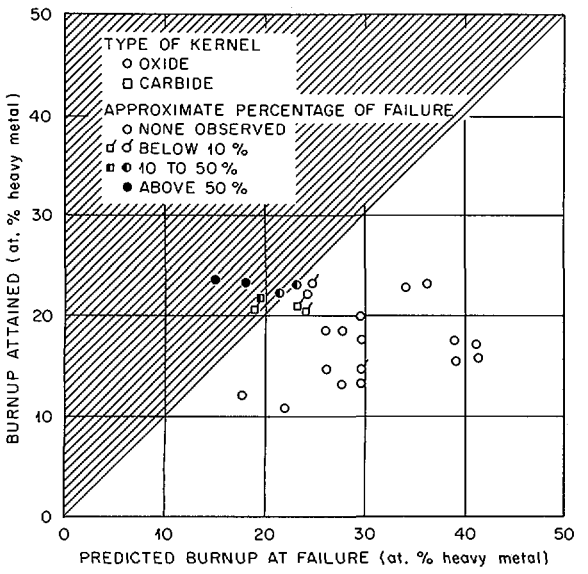

Figs. II–22 and 23. Coated-Particle Fuels. Photos (magnified 100× *above* show structures of pyrolytic carbon coatings on thorium-uranium oxide particles. In the *left* photos, the coatings were deposited from methane, requiring 1 hour and temperatures up to 2,000° C.; the outer layer density was 1.9 grams per cubic centimeter. The *right* photos show coatings deposited from propylene by a new Oak Ridge National Laboratory method. An outer coating density of 2.0 was achieved with only 10 minutes total coating time and a maximum temperature of 1,200° C. Chart, at *left*, is a comparison of mathematical model predictions with coated-particle failures observed in an irradiation experiment at ORNL. The shaded area represents burnups higher than predicted for failure; that is, the calculated stress from the accumulated fissions is sufficient to break the coating and let fission gases escape. The predicted burnup was based on: 30,000 p.s.i. rupture stress, 100% release of fission gas from kernels, 25% of total inner coating porosity available as free volume (except 50% for porous inner coatings).

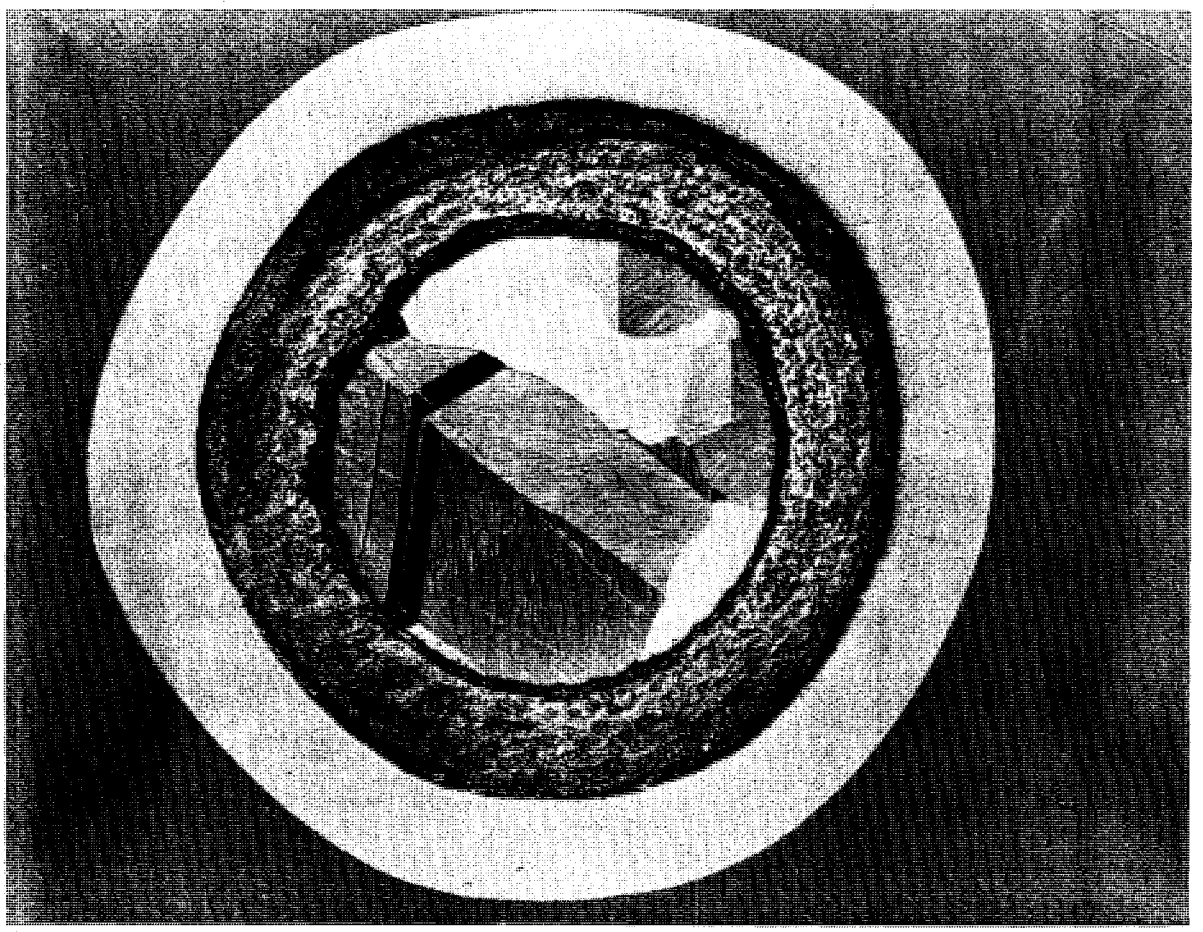

Fig. II–24. Miniature Fuel Element. A coated nuclear fuel particle is shown in cross section, magnified 250×. Actually no larger than a grain of common table salt, these miniature nuclear fuel elements contain a core or kernel of fissionable fuel in the form of uranium and thorium dicarbide coated with two or more layers of carbon or graphite. The coatings, referred to as pyrolytic carbon because of the high temperature processes used in their preparation, serve to protect the fissionable material and contain fission products formed as the uranium is consumed in the nuclear fission process. The use of carbon and graphite (with the highest melting point of any element) rather than metal claddings permits this unique fuel, as shown in this Gulf General Atomic photo, to operate at very high temperatures, thus increasing the efficiency of electric power generation.

tures of the particle and the coating layers. When several batches of coated fuel particles were irradiated to various burnups, the incidence of failures matched the predicted behavior strikingly (see Fig. II–22).

For irradiation stability, the outer layer of the carbon coating must be very dense and have structure and properties that show no directional variation. On particles of mixed thorium-uranium dioxide, $(Th,U)O_2$, a sufficient coating of this type normally requires heating for at least an hour in methane (CH_4) at 2,000° C. or above, which is costly for large-scale production. A similar coating is formed in one-tenth the time at only 1,250° C. by the ORNL-devised process using propylene (C_3H_6) as the source of carbon (see Fig. II–23). Irradiation tests of this type of coating thus far indicate excellent performance.

General Atomic development. Coated particle fuels of outstanding performance characteristics have also been developed by General

Atomic Division (now Gulf General Atomic, Inc.) of General Dynamics in San Diego, Calif. Spherical particles of fissionable fuel and fertile material (uranium and thorium), about one-hundredth-of-an-inch in diameter, are clad with multilayer coatings of carbon, graphite, or metal carbide only a few thousandths-of-an-inch thick (see Fig. II–24). Because of their small size (about the size of a grain of table salt), spherical shape, and outstanding high temperature properties, these coatings maintain their integrity during long periods of operation at high temperatures while under intense irradiation by neutrons and fission fragments.

New Uranium Mononitride Nuclear Fuel

A cooperative study between Oak Ridge National Laboratory and Battelle Memorial Institute, Columbus, Ohio, is rapidly providing detailed knowledge of the properties of uranium mononitride (UN), a potential new reactor fuel particularly for fast breeder reactors and compact space reactors. Uranium mononitride possesses much better dimensional stability than uranium metal, higher uranium density and thermal conductivity than uranium dioxide (UO_2), and better stability toward water and air exposure than uranium carbide. Sufficiently pure UN had not previously been available. However, a method has been developed for producing material with about 200 parts per million each of oxygen and carbon as the only significant impurities.

The availability of high-purity UN and a unique technique for measuring gas-solid interactions at high vacuum have permitted measurement of the stability of UN at the operating temperatures of high-temperature power reactors. Heated in vacuum, UN decomposes to molten uranium metal and nitrogen gas. In excellent agreement with theoretical predictions, measurements at 1,300° to 1,500° C. show dissociation pressures down to less than one ten-billionth of atmospheric pressure. With these results (see Fig. II–25) added to others, the dissociation pressure is known over a range of more than 10 decades.[18]

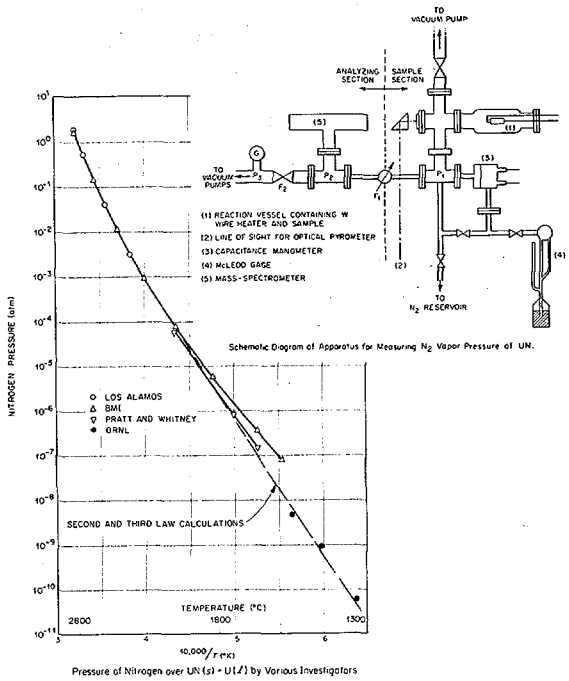

Fig. II–25. Uranium Mononitride Fuel. The graph shows the dissociation pressure of uranium mononitride. It combines the results of several studies, showing the wide range of pressures enabled by Oak Ridge National Laboratory measurements of extremely low pressures. Values predicted from thermodynamic theory are also shown. The ORNL apparatus, diagrammed in *upper right*, can measure differences in gas volume of one-billionth of a cubic centimeter under equilibrium conditions and can detect under transient conditions, gas flows of ten-trillionths of a cubic centimeter per second. The technique is useful for studying many gas-solid interactions; solubility and rate of solution of nitrogen in refractory metals and alloys has been one application. The apparatus uses a mass spectrometer (T-shaped (5) in *left* part of drawing) to measure total pressure and individual gas pressures down to one-trillionth of atmospheric at temperatures as high as 1,800° C.

Electronic Structures and Properties

The fissile elements thorium, uranium, and plutonium combine with the nonmetal elements of Groups IV to VI (of the Periodic Table of Elements; see Fig. I–1) to form compounds with the cubic sodium chloride-type crystal structure.

[18] A decade is a 10-fold variation in a numerical value; *e.g.*, 6 decades would be a million-fold (10^6) variation.

275–845 O—68——11

Some of these compounds, the monocarbides, mononitrides, monophosphides, and monosulfides, have high melting points, high thermal conductivities, and suitable densities, all of which make them attractive as fuels for fast high-energy neutron breeder reactors. For this reason, these materials are being prepared, fabricated, and studied at Argonne National Laboratory.[19] This group of actinide compounds is also of theoretical interest because their common crystal structure provides a basis for comparison of the changes in properties associated with systematic changes in electronic configuration.

Recent measurements have shown that the electrical resistivities of the plutonium compounds increase as the nonmetal component changes from Group IV to VI. Plutonium monosulfide (PuS) was found to be a low-resistance semiconductor up to 425° C. Above this temperature, it exhibits metallic-type conduction as do the other compounds. This unusual dual behavior, only observed in PuS, has been helpful in the interpretation of the electronic configuration of this and other actinide compounds. Resistivity values of the plutonium compounds have been combined with data for other actinide compounds in Figure II–26.

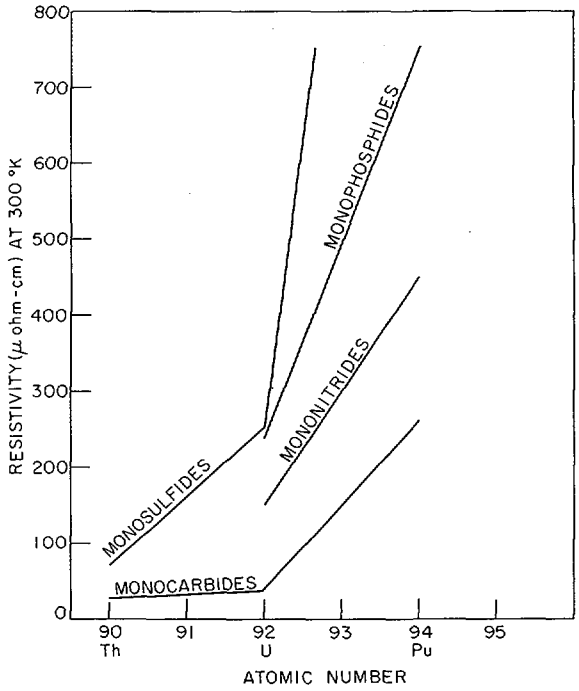

Fig. II–26. Electronic Structure and Properties. This Argonne National Laboratory chart shows room-temperature resistivities of the actinide compounds plotted against the atomic number of the actinide component. All these compounds have low electrical resistances characteristic of metals. The study showed that thorium and uranium compounds exhibit a similar increase in resistance with change in nonmetal components, as was found with the plutonium compounds. In addition, the resistances of compounds with common nonmetal components increase as the atomic number of the actinide member increases. Systematic changes of this nature have previously remained unnoticed. These changes are now relatable to the electronic structures of the actinide compounds, and the electrical properties of all the Group IV to VI (Periodic Chart of the Elements) nonmetal compounds are predictable.

REACTOR MATERIALS

The effects of radiation and of corrosion on reactor structural and component materials must be known if reactors of assured safety and durability are to be designed and built. Hence, the AEC is sponsoring studies in these areas; also, in the area of new fabrication techniques and improved methods for nondestructive testing of materials.

Radiation Effect on Materials

Radiation Embrittlement of Iron

The embrittlement of reactor structural steel by fast neutron irradiation is being investigated at Brookhaven National Laboratory by a fundamental study of the fast neutron embrittlement of iron itself. It has been observed that the tensile yield strength of iron increases with exposure to fast neutrons at 70° C.; and that above a critical exposure level of approximately 2×10^{18} fast neutrons per square centimeter, the iron undergoes a transition from ductile to brittle behavior when tensile tested below −145° C.

[19] See pp. 233–236, "Fundamental Nuclear Energy Research—1966."

(125°–130° K.).[20] Heating to 250° C. for 4 hours is required to remove this latter effect.

It has been found that highly purified iron, or iron containing an element which will combine with carbon and remove it from solid solution, does not undergo this embrittlement. Other investigators have shown that interstitial impurity atoms, such as carbon, and radiation-induced defects begin to migrate and anneal out or combine with each other at specific temperatures. For example, displaced iron atoms (interstitials) are able to move freely at −200° C. A complex formed by these iron interstitials and carbon atoms dissociates at −30° C. Carbon and nitrogen atoms begin to move rapidly in the iron lattice around room temperature. A carbon lattice vacancy complex probably dissociates near 200°–250° C., while vacancies are believed to be mobile at 350°–400° C.

Accordingly, iron samples containing 30 parts per million by weight of carbon were irradiated at −70° C. and at 0° C. to an exposure of 2×10^{18} fast neutrons per square centimeter and tensile tested below the ductile to brittle transition temperature. No embrittlement was observed and only an increased yield strength was produced, as shown in Figure II–27. However, a higher carbon iron (200 p.p.m. carbon) has shown brittle behavior below −155° C. after an irradiation at 0° C.

If the irradiated iron is warmed up to room temperature or up to 150° C. immediately after the irradiation but before the tensile testing, the embrittlement cannot be introduced. Therefore, the defects which cause embrittlement after a 70° C. irradiation cannot be produced by allowing the defects created at subzero temperatures to move.

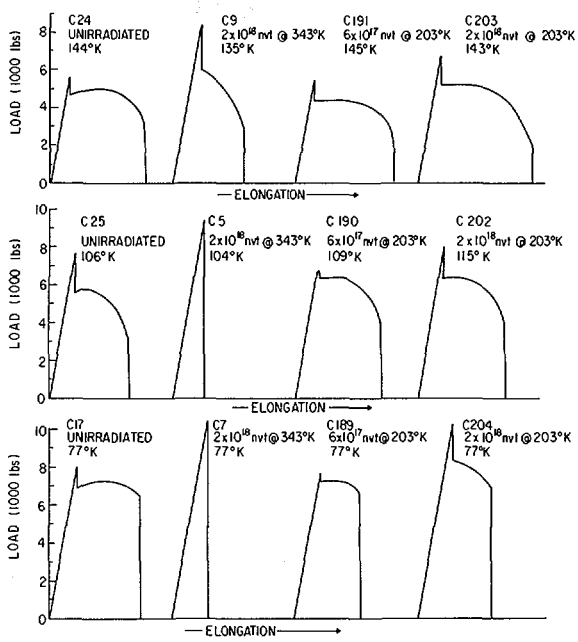

Fig. II–27. Radiation Embrittlement of Iron. The effect of low temperature on the radiation embrittlement of iron is shown in the Brookhaven National Laboratory chart, as well as load *vs* elongation charts of iron before and after irradiation at +70° and −70° C. When tested below −145° C. (128° K.), iron is brittle after an irradiation of 2×10^{18} at 70° C. (see specimens C5 and C7) while similar specimens irradiated to exposures up to 2×10^{18} at −70° C. retain the normal low temperature ductility. Note tensile testing temperature listed below irradiation temperature.

Radiation Effects on Stainless Steels

The effects of neutron irradiation on the mechanical properties of stainless steels at temperatures to 1,400° F. (760° C.) are being studied at Pacific Northwest Laboratory. Emphasis is being placed on the combined effects of metallurgical structure and neutron environment on strength and ductility. A series of in-reactor creep tests on type AISI 304 [21] stainless steel over the temperature range 750°–1,400° F. (400°–760° C.) have been conducted. It was discovered that neutron flux had little effect on dynamic creep rate at these temperatures, but consistently reduced the time to failure compared with out-of-reactor behavior.

[20] *K scale*—In recent years, scientists have used the absolute or Kelvin (K) scale for low-temperature studies. On this scale, the degrees are the same size as on the centigrade scale, but the 0 point is at −273.15° C. Water freezes at 273° A (absolute) and at 0° C. (centigrade). The boiling point of water on the absolute (or Kelvin scale) is 373°. Therefore, the absolute temperature can be obtained by adding 273° to the centigrade temperature. Absolute 0 temperature on the centigrade scale is −273°; on the absolute (or Kelvin scale) it is 0°.

[21] AISI 304 is a steel containing 18 percent chromium and 8 percent nickel by weight, which is the basic composition for stainless steels commonly used in nuclear reactor applications.

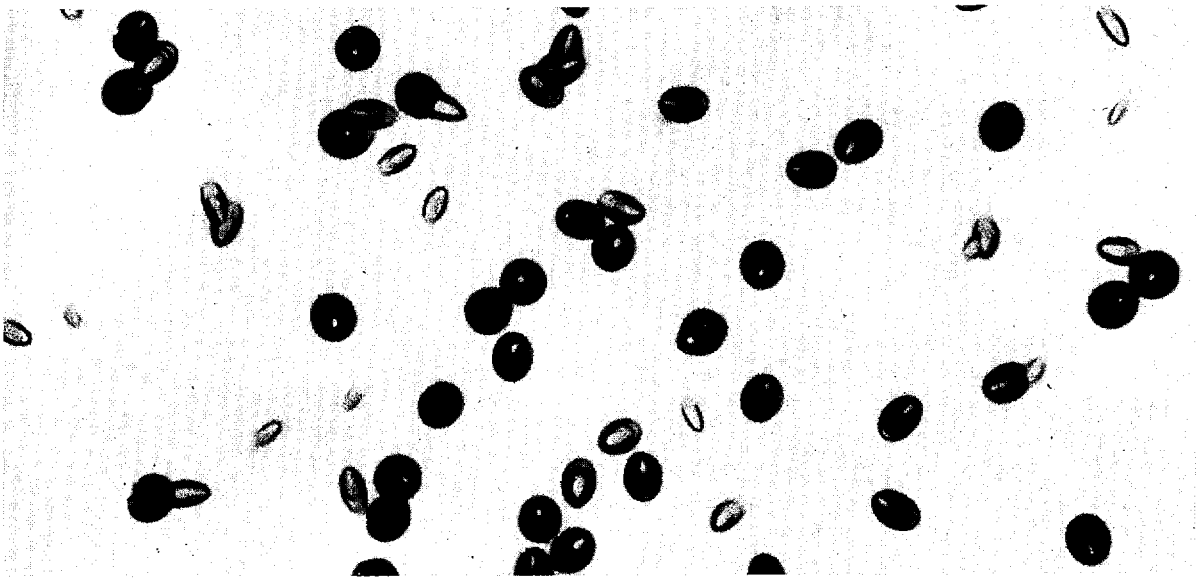

Figs. II–28 and 29. Fission Tracks. Photo above resulted from a Pacific Northwest Laboratory study of fission tracks and shows an irradiated sample of ordinary glass microscope slide coated with a thin layer of fissionable uranium. These tracks are actually trails of disrupted material caused by the passage of the fragments from the fissioning uranium. After irradiation, the glass was etched in hydrofluoric acid to enlarge the tracks for viewing in an optical microscope, as shown here with a magnification of 500×. *Photo below* is of fission tracks in irradiated mica due to the fissioning of the natural-uranium impurities. This figure illustrates a technique developed at PNL to facilitate track counting. The right side of the figure shows the effect of coating a thin film of aluminum on the surface of the mica after etching. Tracks only on one surface are visible. The long track on the left side of the figure shows the full length of the track as it penetrates each layer of mica. The tracks are defined more clearly on the side coated with aluminum and, therefore, much easier to count.

Extensive investigations of the microstructure of stainless steels of various compositions and irradiation histories were made to determine the causes for mechanical degradation after elevated temperature irradiation. Some investigators have attributed the loss of ductility under these conditions to the presence of helium generated during the irradiation process. Although this is probably an important contributing factor, careful examinations with the electron microscope by PNL investigators have shown that certain features, such as surface pits, metallic carbides, and cavities can produce contrast effects similar to those produced by helium bubbles and lead to erroneous conclusions.

Furthermore, it has been demonstrated that carbide formation can be promoted by neutron irradiation and possibly by radiation-induced gas atoms. This knowledge is being used to develop a more consistent model of non-recoverable irradiation damage to these alloys and to develop thermal-mechanical treatments to improve strength and ductility for elevated temperature reactor service.

Fracture Mechanics Studies

Investigations being performed at Pacific Northwest Laboratory (PNL) using a specially designed specimen to determine the effect of reactor environments on the brittle fracture characteristics of reactor structural materials, have shown that neutron irradiation promotes propagation of cracks, once they are initiated. Primary emphasis has been placed on radiation effects on zirconium alloys used for pressure tubing and on pressure vessel steels. The PNL-developed double cantilever beam (DCB) specimen provides valid measurements of plane-strain fracture toughness and yet is compact enough to be accommodated in the core and test positions of most current reactors. Furthermore, several measurements of the fracture toughness parameters can be made from a single specimen.

The versatility of the specimen has been demonstrated by applying it to fatigue crack propagation studies, fracture-toughness profile measurements across weld and heat-affected zones, hydrogen embrittlement studies, and irradiation effects studies. An eddy-current method for measuring dynamic crack velocities and advanced mathematical models for treating complex stress states near flaws were developed.

It was discovered that a principal effect of neutron irradiation at water reactor temperatures is to reduce the ability of A302–B, the principal pressure vessel steel in general commercial use, to resist the growth of moving cracks. That is, a crack once initiated in the brittle temperature region will propagate in a more catastrophic manner in an irradiated vessel than in an unirradiated vessel.

Creep in Vanadium-Base Jacket Alloys

The jacket material surrounding the nuclear fuel in a fast reactor fuel element can greatly prolong the useful life of the fuel if it possesses sufficient creep strength to resist the tendency of the fuel to swell. In addition, the jacket material must be chemically compatible with the fuel and the liquid-metal coolant. This combination of properties is not usually found in a single commercially available structural material, and therefore must be obtained through new alloy development. Strong jacket materials that are compatible with metallic fuels and liquid sodium are being developed at Argonne National Laboratory for use in liquid-metal-cooled fast breeder reactors (LMFBR). Since it is not unusual for the creep strength to be adversely affected by such variables as temperature, strain rate, material composition, metallurgical condition, and the operating environment, the effects of these variables are studied over a sufficiently broad range to simulate reactor operating conditions. Under these conditions, vanadium (V)-titanium (Ti) alloys containing an addition of chromium (Cr) exhibit the most promising creep behavior.

Vanadium-20 weight percent (w/o) titanium (V-20 w/o Ti) has a much higher creep strength than stainless steel and responds to heat treatment. The V-15 w/o Ti-7.5 w/o Cr and V-5

w/o Ti-5 w/o Cr alloys, developed at Argonne, have been heat treated to attain creep strengths more than 10 times as great as that achieved in V-20 w/o Ti. Furthermore, their creep strengths are not appreciably decreased over the range of temperatures and strain rates that are of interest to reactor operation. Exposure of V-20 w/o Ti at 650° C. to liquid sodium containing 20 parts per million by weight of oxygen (20 p.p.m. O_2) results in a significant decrease in creep strength; however, similar exposure to sodium containing a more likely reactor concentration of 10 p.p.m. oxygen has only a slight effect. Preliminary tests on V-15 w/o Ti-7.5 w/o Cr indicate that its creep strength is even less affected by exposure to sodium containing 10 p.p.m. oxygen than is V-20 w/o Ti.

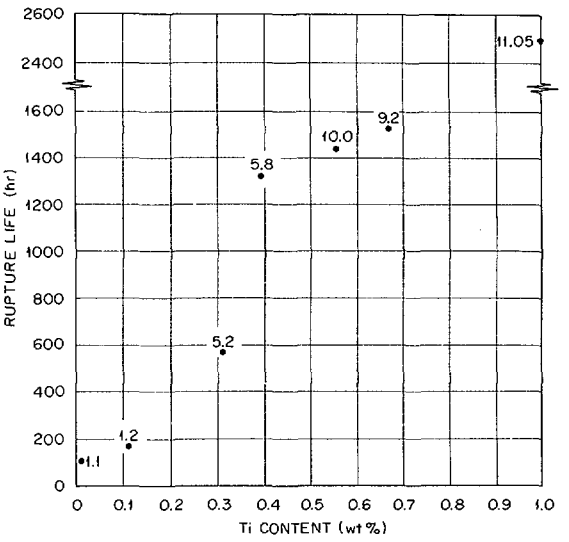

Influence of Ti on the Post-Irradiation Creep Properties of Ni-12 Mo-7 Cr-0.05C.

Fig. II-30. Post-Irradiation Creep Properties. Oak Ridge National Laboratory graph shows the effect of titanium content on the creep of irradiated modified Hastelloy N. Nickel-base alloys containing 12% molybdenum, 7% chromium, 0.05% carbon, and the indicated titanium contents were annealed 1 hour at 1,177° C., irradiated at 650° C. to a dose of 2.5×10^{20} (250 quintillion) neutrons/cm², and stressed at 650° C. with 32,350 pounds per square inch. The plot shows the time to failure. Above each point is the percent elongation; this is the increase in length at failure and is a measure of the ability of the material to deform to accommodate in-service dimensional changes. Unirradiated normal Hastelloy N, similarly tested, has a rupture life of 800 hours and an elongation of 12.5%.

Helium-3 Surface Activation Analysis

Oxygen and carbon, common impurities in metals, can have large effects on the properties of metals. These properties are important in applications where high reliability is necessary, as for instance, in nuclear reactors and spacecraft. A method of analysis has been developed at the Los Alamos Scientific Laboratory in which the distribution of oxygen and carbon in metals can be observed, and their concentrations can be estimated. A metallographically polished sample is bombarded with singly charged positive ions of helium-3 (He^3) accelerated to an energy of 6 million electron volts (Mev.) in a Van de Graaff accelerator, and the sample is then autoradiographed; that is, it is placed in contact with a photographic emulsion so that the radiation emitted can expose the emulsion. The He^3 ions activate the oxygen and carbon by the reactions $O^{16}(He^3,p)F^{18}$ and $C^{12}(He^3, He^4)C^{11}$. The fluorine (F^{18}) and carbon (C^{11}) both emit positrons (positive electrons), so the most exposed (blacker) parts of the emulsion indicate the areas of highest oxygen and carbon concentration. Since the activation products decay at different rates, a time sequence of autoradiographs indicates which areas were caused by which element (see Fig. II-32).

Although there is some difficulty in obtaining a uniform bombardment, a focusing method has been developed which partially overcomes this problem. The target apparatus is shown in Figure II-33. After the beam is focused, the sample is irradiated for about 30 minutes. The He^3 ions penetrate into the sample to a depth of less than one-thousandth (0.001) of an inch; however, in many samples the surface distributions of oxygen and carbon are typical of the overall distributions. While the autoradiographs are being taken, the activity of the sample is also recorded electronically. The data taken in this way are later analyzed on a computer to determine which element caused the

primary exposure and how much of each element was present. This method can be used to measure oxygen and carbon distributions in metals containing as little as 25 parts per million oxygen or carbon, something that cannot be done by ordinary chemical analysis (see Fig. II–34). If the distributions of these elements and how they affect the properties of metals are known, the characteristics of the metals can be improved.

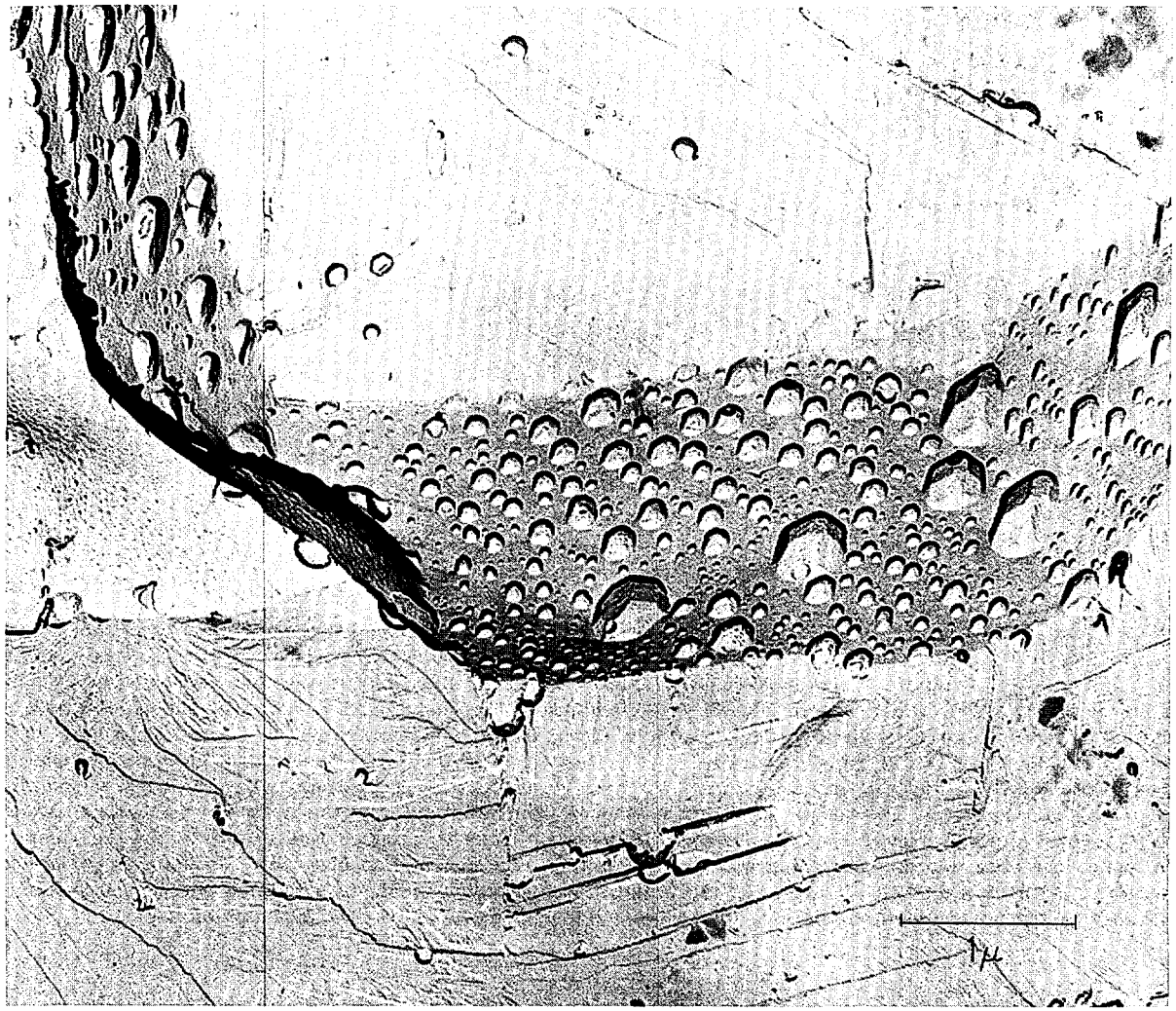

Fig. II–31. Helium Bubbles in Irradiated Beryllium. Though formation of gas bubbles in irradiated materials has important effects on structural strength, theories of gas diffusion are not yet adequate to explain all that occurs. This fractograph photo, made by Idaho Nuclear Corp. at the National Reactor Testing Station, Idaho, was taken through an electron microscope at 16,000 diameters magnification to show the surface of a beryllium sample that had been fractured by compression. The sample had previously been irradiated for 3,560 hours at 600° C. to an exposure of 1.08×10^{21} neutrons/cm^2 above 1 Mev. energy. The helium gas appears to diffuse to the grain boundaries and migrate to the specimen surface. The gas bubbles are more numerous and larger in the grain boundaries than on the cleavage planes in the fractograph. Beryllium is an important reactor material because of its high ability to scatter and slow neutrons and its low affinity for absorbing them. Thus, it is used as a neutron reflector and moderator, and current studies indicate it may be useful as a fuel cladding material (see pp. 240–241, "Fundamental Nuclear Energy Research—1966").

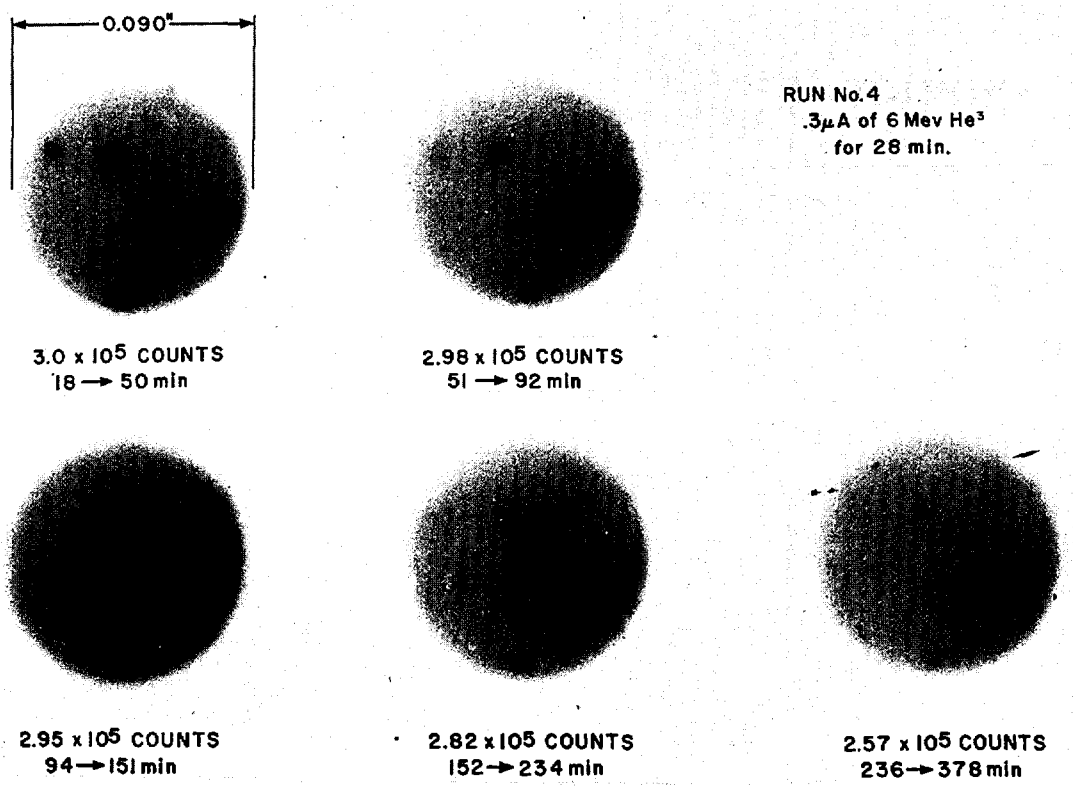

Figs. II–32, 33, and 34. He^3 Surface Activation Analysis. The autoradiographs *above* are from a tantalum sample irradiated with helium-3 (He^3) ions. Times of exposure are indicated below each spot, in terms of the number of minutes after irradiation. The darker spots (about 0.008-in. in diameter) in the first two exposures result from carbon-11 (C^{11}), which has a half-life of 20.4 minutes. The background results from fluorine-18, which has a longer half-life (112 minutes) and therefore shows up in the autoradiographs for a longer time. The diagram, below *left*, is the target apparatus used in the LASL method. The quartz disc fluoresces when the He^3 beam strikes it, and the operator adjusts the beam to make the spot uniform when the beam current is about 0.3 microamperes. The quartz disc is then removed from the beam, and the sample is bombarded. Below *right* shows a metal sample that was bombarded with He^3 ions to produce radioactive C^{11} in the sample. Although the beam for this activation was uniform (circle), the distribution of carbon (darker area) was not uniform. Without a method of regulating the beam, it would be impossible to determine whether the nonuniformity of the autoradiograph was due to the beam intensity or to the carbon distribution.

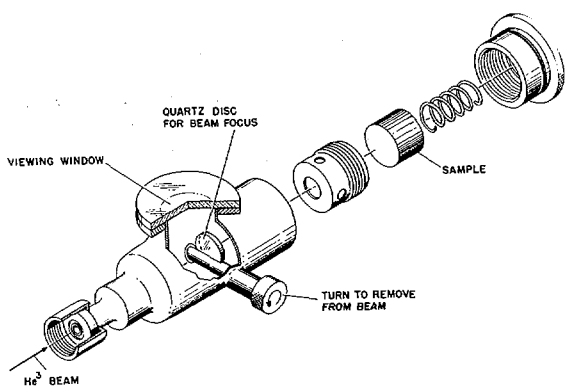

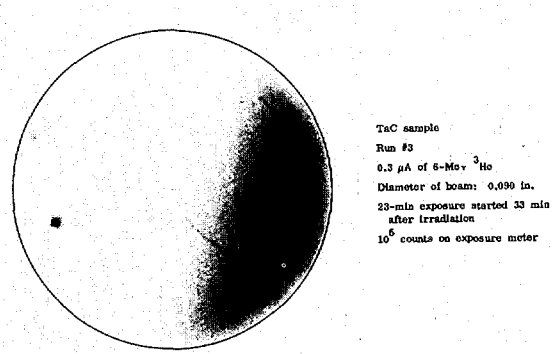

Thermal Conductivity of Graphite

Thermal conductivity is of great interest in any reactor, particularly high temperature heat-producing reactors. At the Los Alamos Scientific Laboratory, as part of the Rover nuclear rocket program, the thermal conductivity of a commercial "hot-worked" graphite (ZTA grade) has been measured over the temperature interval −100° to 2,700° C. The "hot-working" process results in a graphite with a higher density than the starting material and one which has a much greater preferred orientation than did the starting material. Preferred orientation means that the basal planes of the grain lie (on the average) in planes which are perpendicular to the direction of the applied "working" force. The thermal conductivity is enhanced in the direction parallel to the basal plane, and at room temperature is equal to 1.81 watts per centimeter per degree centigrade (w/cm° C.), but the thermal conductivity perpendicular to the basal plane remains relatively unchanged at 1.00 w/cm° C.

Three different measurement methods were used to cover the temperature intervals considered: a transient technique (−100° to 400° C.), a series comparison method (250° to 900° C.), and a radial heat flow method (1,100° to 2,700° C.). The data obtained appeared to be internally self-consistent regardless of the technique employed. Deduction of the thermal conductivity by the radial heat flow method for specimens wherein the basal planes paralleled the axis of the cylindrical samples required a numerical solution for the appropriate two-dimensional heat flow problem. This was generated by the fact that in this case, the heat flow in one radial direction is along the layer planes, whereas in a radial direction perpendicular to the first direction, heat flow is across the planes. Since the solution does not appear in the literature, the analysis and coding was done at Los Alamos. Thermal conductivity results were considered in terms of current theories of heat conduction in single crystals. Since the two major modes of heat conduction (in-plane and across-plane) are not experimentally separable in polycrystalline graphite, application of current theories has not proven to be particularly successful at this time. Measurements of thermal expansion and the irreversible dimensional changes which occur in this particular graphite when heated beyond 2,300° C. have been investigated and analyzed.

Corrosion Effects on Materials

High Temperature Corrosion in Helium

The corrosion of metals and alloys in high temperature helium gas environments is being studied at Pacific Northwest Laboratory (PNL), in support of the design and operation of the gas-cooled loop in the Advanced Testing Reactor.[22] One of the important reasons for using helium in a gas-cooled loop or gas-cooled reactor is that this gas does not react chemically with materials having cobalt or nickel as a base, even at high temperatures. Impurities in the helium, however, can react with such materials and degrade their properties and performance. Corrosion studies in both laboratory and engineering scale systems show that even at temperatures up to 2,100° F. (1,150° C.), selected nickel-base and cobalt-base alloys are not destructively oxidized at the low oxygen concentrations which can be maintained in the helium gas by the PNL-developed purification system. Evaporation of alloy species from the nickel-base and cobalt-base alloys at temperatures above 2,000° F. (1,095° C.) is significantly reduced in pressurized, high-velocity helium relative to a vacuum.

Corrosion in Liquid Metals

Several significant advances have been made by Argonne National Laboratory in the area of chemistry and corrosion in liquid sodium, which is used as coolant for fast breeder reactors. They include the development of a vanadium-base alloy with improved resistance to

[22] Now under construction at the National Reactor Testing Station in Idaho.

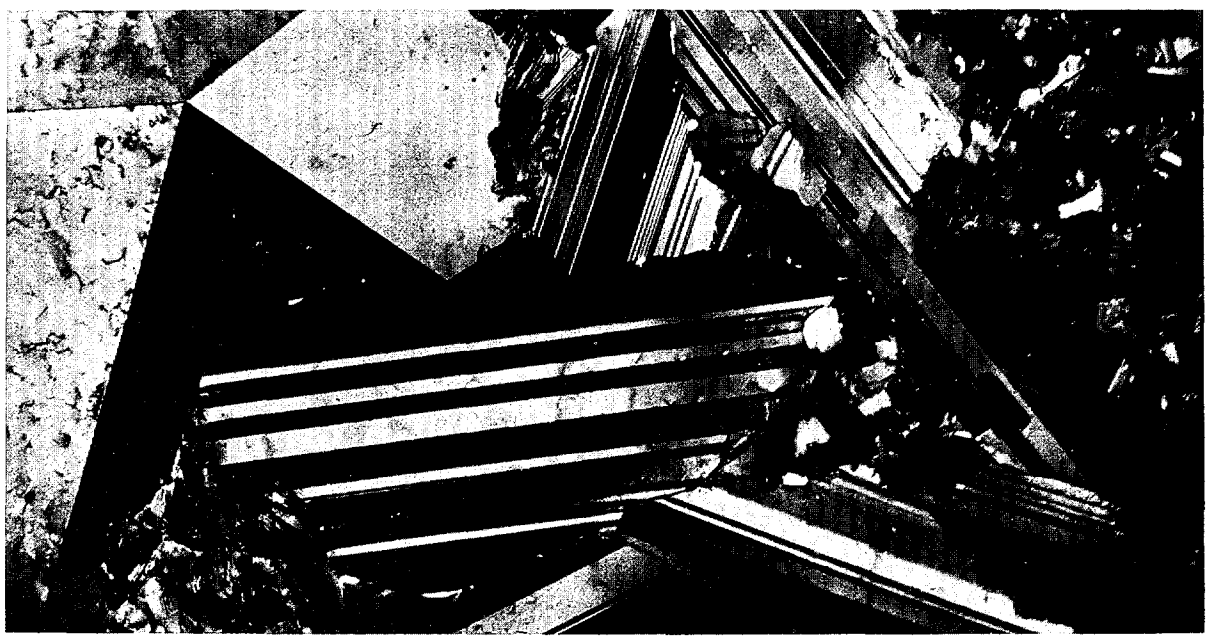

Figs. II–35 and 36. Pseudo-Fivefold Symmetry in Carbonyl Process Nickel. At Mound Laboratory, the effect of impurity gases on nickel coatings deposited by the thermal decomposition of nickel carbonyl [$Ni(CO)_4$] is being studied. A transmission electron micrograph (40,000×) revealed grains which have apparent fivefold symmetry (shown *above*). These are nearly perfect, fivefold twinned grains. The normal to the observed plane is the < 110 > direction; the boundaries are parallel to (111) planes. The (111) planes of adjacent twin grains are separated by low-angle "tilt" boundaries. Five such boundaries account for five 1°28′ mismatches. The angle between the (111) planes, which intersect along the < 110 > direction, is 70°32′, instead of the 72° needed for perfect fivefold twinning. *Below* is a transmission electron micrograph (50,000×) showing the general structure of a nickel coating made with a small quantity of hydrogen present in the carbonyl plating gas.

corrosion in reactor-grade sodium, and the application of a theoretical model to a technique for distinguishing types of liquid-solid reactions.

Vanadium alloys have been of great interest as fuel cladding materials for fast reactors because of favorable nuclear, high-temperature mechanical, and metallurgical properties. However, in common with other refractory metals, commercially available vanadium alloys suffer unacceptably high corrosion rates (material loss) in sodium at practical reactor operating conditions. Argonne has now developed and demonstrated refractory metal alloys with potentially acceptable corrosion behavior in systems of practical interest. Among the alloys of interest are vanadium-20 weight percent titanium, vanadium-15 weight percent titanium-7.5 weight percent chromium, and vanadium-5 weight percent chromium.

In the investigation of a technique for studying liquid-metal corrosion, the tin-tantalum system has been used to demonstrate successfully the applicability of a rotating-disc technique and the convective-diffusion model for mass transport to high-temperature liquid-metal systems (see Fig. II–37). Of particular importance is the ability to distinguish between reaction types when liquid and solid interact, and to identify the controlling process as a function of system variables.

Graphite Sublimation in Reactors

The loss of structural graphite from a high temperature (900°–1,700° C.) reactor by the corrosive action of oxidant impurities in the helium coolant has been under experimental study at the Los Alamos Scientific Laboratory. The reaction rate at which the reactor structure would be corroded away has been determined as a function of temperature and oxidant concentration (1 to 100 parts per million), while the coolant flow rate, geometry, and pressure were maintained constant. It was determined that gas purification techniques are adequate for maintaining oxidant concentrations at a sufficiently low level to permit presently planned gas-cooled reactors to meet their requirements. However, if operating temperatures are extended above 1,700° C. the carbon reaction is observed to increase much more than

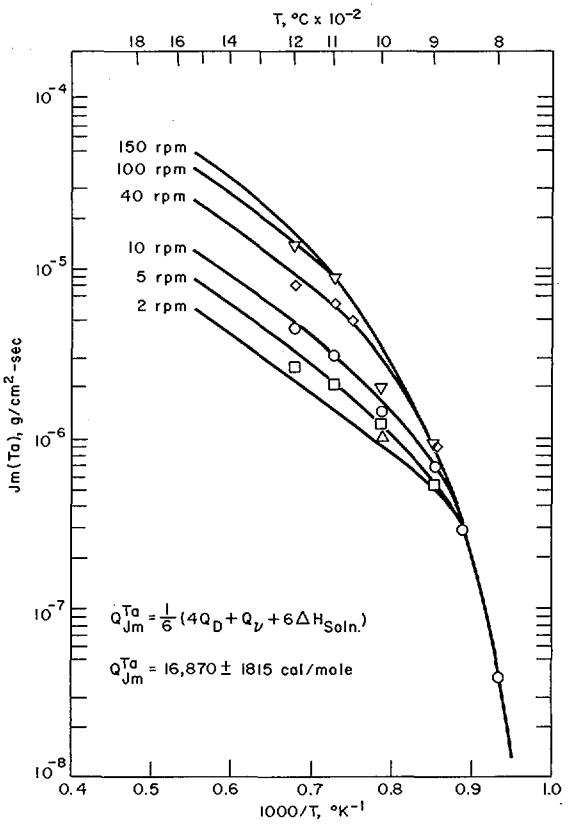

Fig. II–37. Corrosion in Liquid Metals. The Argonne National Laboratory chart shows the effects of temperature and speed of rotation of a tantalum disc in molten tin on its maximum dissolution flux, J_m, in units of g/(cm²-sec). At the higher temperatures the mass transport data points were found to be in good agreement with predictions based upon a model involving liquid convection and diffusion in the liquid near the surface of a rotating disc. The activation energy (temperature dependence) for the dissolution process, Q_{Jm}, at the higher temperatures was related to the activation energy for tantalum diffusion in liquid tin, the activation energy for the viscosity of liquid tin, and the temperature dependence of the solubility of tantalum in liquid tin. The decrease in the temperature dependence of the dissolution flux with increasing temperature is indicative of a transition from control by a reaction at the surface of the tantalum to liquid-diffusion control.

would have been expected from extrapolation of the data obtained at temperatures below 1,700° C. The new data correlate with a theory that carbon sublimation (or evaporation) begins to play a part in the oxidation process at higher temperatures. It is well known that at temperatures below 1,700° C., with low oxidant concentrations and reasonably low flow rates, the rate of reaction is limited by the rate of diffusion of the oxidant through the relatively stagnant gas film on the surface of the carbon structure. Since this diffusion rate is only very slightly dependent on temperature, it might be assumed that only slight increases in reaction rate would result from a rather extensive temperature increase. It now appears that the carbon from the structure is diffusing into the gas stream where it reacts with the oxidant. Since the rate of carbon sublimation is very highly dependent on temperature, the rate of carbon loss is greatly accelerated by small increases in temperature above 1,700° C. (see Fig. II–38).

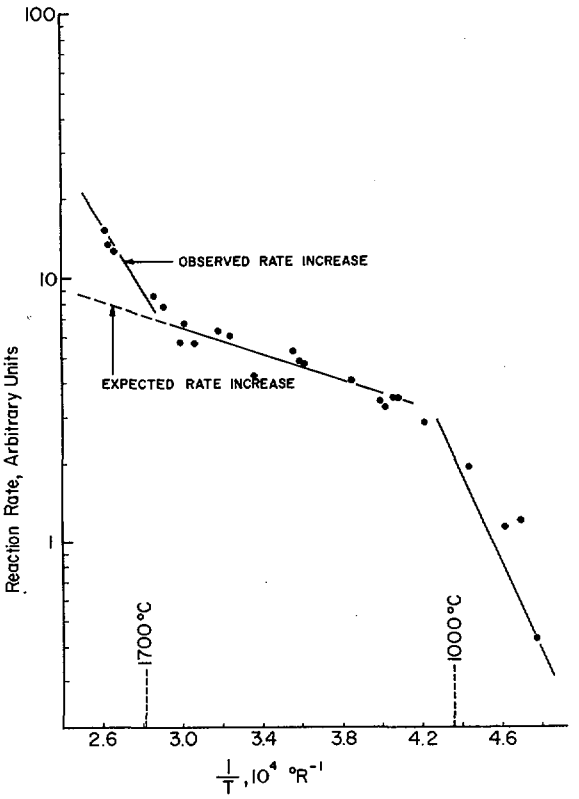

Fig. II–38. Graphite Sublimation in Reactors. The rate of graphite corrosion in reactors has been studied at the Los Alamos Scientific Laboratory and found to increase unexpectedly at temperatures above 1,700° C. This high corrosion rate has great significance to the design of high-temperature gas-cooled graphite reactors. The increased rate of graphite oxidation, with parts-per-million quantities of carbon dioxide in helium at very high temperatures, is shown on the above curve, where the observed reaction rate deviates from that expected. It is theorized that carbon sublimation places carbon in the gas phase adjacent to the solid carbon surface. Carbon dioxide then reacts with the sublimed carbon as well as the carbon surface. The increased rate agrees closely with calculations on the rate of graphite evaporation.

Fabrication Studies

Fabrication and Study of Refractory Metals

More economical fabrication methods are emerging from the Oak Ridge National Laboratory (ORNL) study of refractory metals (niobium, molybdenum, tantalum, and tungsten) and their alloys. A corollary to their strength at very high temperatures is high strength and brittleness at customary metalworking temperatures. This is particularly true of tungsten, the metal with the highest melting temperature. The work at ORNL includes both extension of conventional techniques to higher temperatures and deposition of metals from gases reacting at a heated surface.

Self-lubricating extrusion. Several recent advances center around the ORNL self-lubricating extrusion [23] technique, in which tungsten and molybdenum are lubricated during extrusion by a film of molten oxide which later evaporates. This method was extended to alloys that oxidize too slowly and to niobium and tantalum, which do not form suitable oxides, by applying a chemical-vapor-deposited coating of pure tungsten or molybdenum to the billet before extrusion. Thin-walled tungsten tubes of about an inch in diameter were produced by reextruding a tungsten tube shell fabricated into a duplex

[23] Extrusion is the forming of a material by forcing it through an opening—similar to squeezing toothpaste from its tube. It is widely used for metallic, ceramic, and plastic materials.

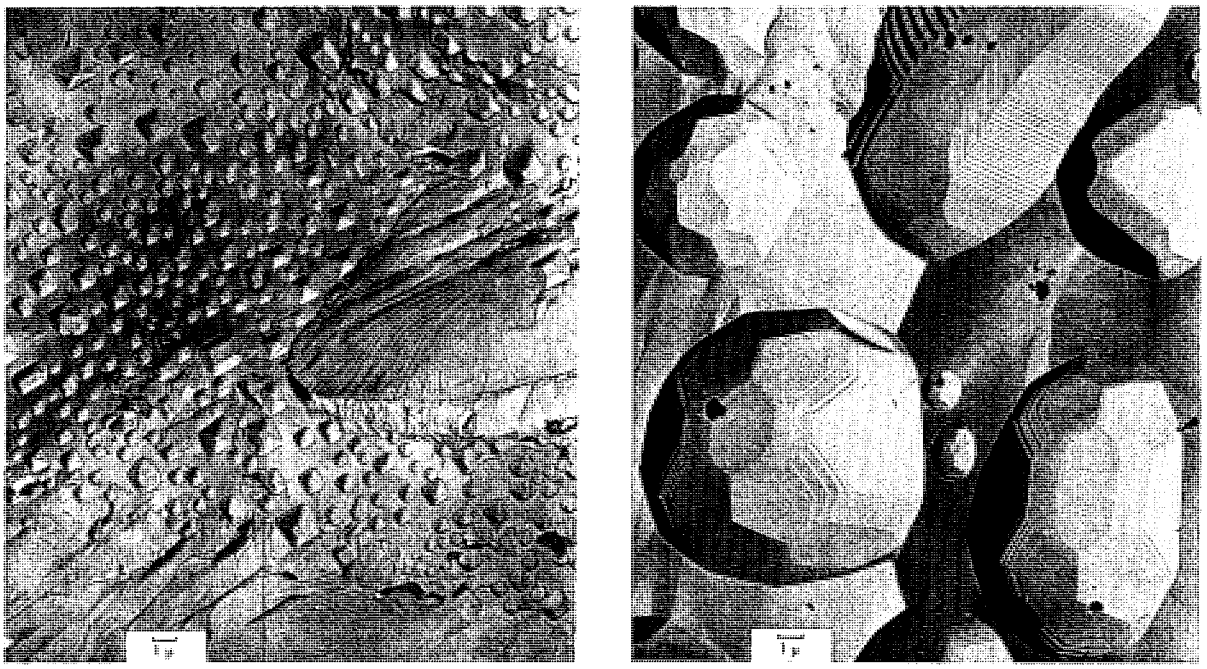

Figs. II–39 and 40. Chemical Vapor Deposition. Electron micrograph on *left* shows gas bubbles that had developed along boundaries between grains (separate crystals) in chemical-vapor-deposited tungsten. Such bubbles develop upon heating if sufficient fluorine is present. They inhibit grain growth and may affect mechanical properties. This photograph shows bubbles in material annealed 2 hours at 2,500° C. Their polyhedral shape is a result of movement of tungsten atoms along the surface to maintain equilibrium between the internal gas pressure and the surface tensions of the more prominent crystal faces. On *right*, the electron micrograph shows gas bubbles that developed along boundaries between grains in chemical-vapor-deposited tungsten (as compared with photo on left). This photo shows bubbles in material annealed 5 hours at 2,500° C.; they are larger than the bubbles shown in left photo. These two photos, as a pair, won the Best-in-Class award for electron micrographs using replicas at the 1966 American Society for Metals Metallographic Exhibit in Chicago.

billet with molybdenum, which is subsequently removed. Also, advancements in tube drawing [24] techniques permit fabricating thin-walled tubing from the extruded tube shells. Higher drawing temperatures, achieved in part by the use of zirconia (ZrO_2) dies, enabled successful production of molybdenum tubing. Similar drawing of tungsten awaits furnace modification.

Chemical vapor deposition. The technique of chemical vapor deposition is a very economical and convenient way of preparing various shapes, particularly tubing, from refractory metals. Oak Ridge National Laboratory has developed techniques for depositing many complex shapes that would be impossible to form by conventional techniques. It has also made considerable progress in optimization and understanding of the chemical-vapor-deposition process, and has determined the mechanical properties of the deposited tungsten in comparison with the values for tungsten prepared by conventional techniques. The deposited tungsten has a characteristic columnar structure that is stable at annealing temperatures up to 2,500° C. The columnar structure would be detrimental for some applications, because of its effect on strength, ductility, and fabricability. However, it was demonstrated at ORNL that the alignment of individual crystals, which governs mechanical behavior, is the same in deposited tungsten as in wrought tungsten after both have been rolled to one-fifth their original thickness.

[24] Drawing is the forming of wire or tubing by pulling the material over dies.

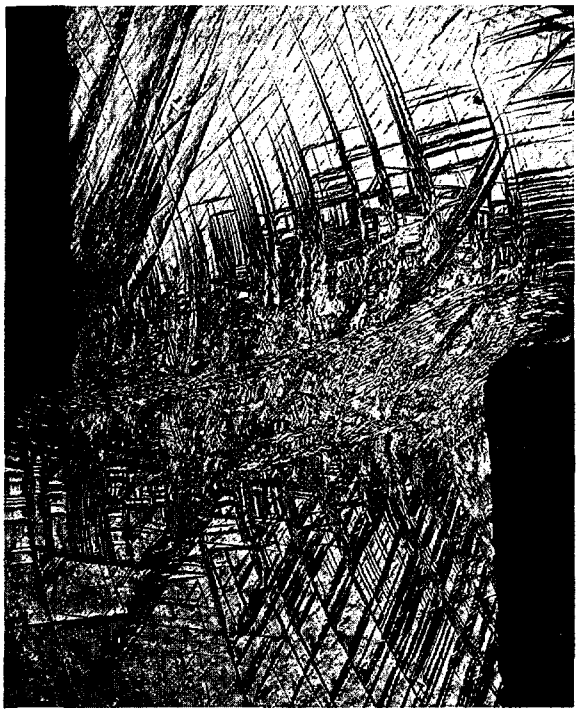

Fig. II–41. Deformation in Zirconium. This Oak Ridge National Laboratory photo (magnified 60×) shows the deformed region of a single crystal of zirconium. A portion of the specimen has been forced to move past another in a direction with very high resistance to relative motion of planes of zirconium atoms. The very complicated structure is the result of several deformation mechanisms, including a remarkably high order of "twinning"—in which portions of the grain deform by shifting into an atom arrangement that is a "mirror image" of the rest of the grain.

Furthermore, the vapor-deposited tungsten can be rolled at temperatures as low as 400° C., a very low fabrication temperature for tungsten.

Vapor-deposited tungsten containing from 1 to 30 parts per million fluorine shows impairment of mechanical properties that increases with fluorine content. At temperatures in the range of anticipated use, this impurity forms bubbles whose volume depends on temperature, time at temperature, and fluorine content. These bubbles can be conveniently studied by electron microscopy of replicas of fractured surfaces (see Figs. II–39 and 40). Their polyhedral shape provides information on the surface energy of different tungsten crystal surfaces. Also, initiation and growth of the bubbles under stress may give clues to how irradiation-produced gases embrittle metals.

Deformation in Zirconium

The plastic deformation of metals permits them to assume desired shapes during fabrication and to absorb strains that occur in service. Preparation of high-quality single crystals of zirconium at ORNL is contributing to the understanding of deformation in this important metal for nuclear reactors. For metals to deform, the individual crystals or grains must change shape; this happens in two ways. The usual mechanism is "slip," in which planes of atoms move past each other. When suitable directions for slip are unavailable, "twinning" occurs, in which portions of the grain deform by shifting into an atom arrangement that is the mirror image of the rest of the grain. Single crystals can be oriented to force deformation on certain planes in specified directions. When a zirconium crystal is aligned so that slip is difficult and then is forced with high stress to deform, unusually high degrees of twinning occur (see Fig. II–41). These results, along with other study of deformation behavior of zirconium, will lead to improved fabrication and utilization of zirconium alloys.

Sintered Aluminum Products

Sintered aluminum products (SAP) material is aluminum fabricated from partially oxidized powder; the resulting dispersed oxide strengthens the aluminum and extends its usefulness in reactors to higher temperature ranges. Oak Ridge National Laboratory has extensively investigated the characteristics of this material and its processing parameters for preparation with sufficient uniformity and reliability for reactor use. The work has led to production of a uniform material. Previously available SAP exhibited erratic behavior in the form of poor process yield, structural inhomogeneity, gas fissuring and blistering, properties dependent on direction, premature fracture, and poor ductility under prolonged load.

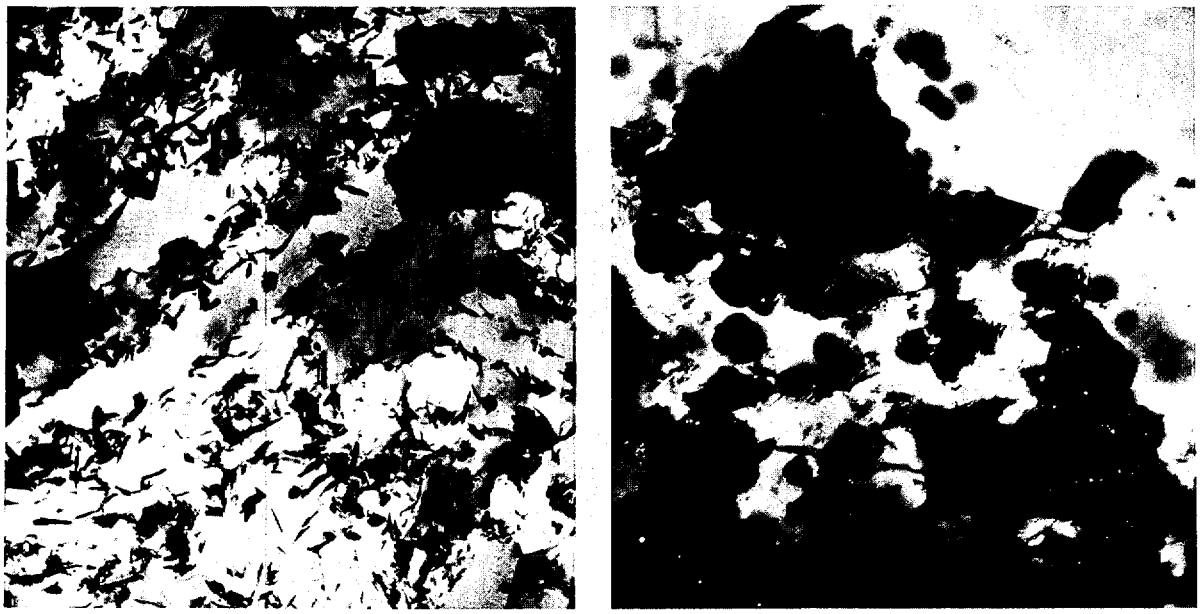

Fig. II–42. Sintered Aluminum Products (SAP). Electron micrographs comparing Oak Ridge National Laboratory SAP and a typical commercial SAP (ISML–930). The ORNL material on the left shows the finely dispersed oxide particles; dark patches are differently oriented aluminum grains. The commercial material on the right contains inclusions of impurities introduced during milling. Both photos are magnified 25,000×. The high magnification of electron micrographs has permitted ORNL to study the inhomogeneties that cause the lack of reproducibility in commercial SAP and to improve the fineness of the dispersion.

The ORNL study has resulted in a process that eliminates the nonuniformity of SAP (see Fig. II–42). The form of dispersed oxide and the identification of inclusions, such as iron and aluminum carbide (Al_4C_3), have led to a better understanding of the effect of processing variables on the properties of SAP. Finally, the mechanical properties were found to be very sensitive to testing conditions, so much of the reported variation could be traced to differences in testing procedures.

Coextrusion of Fuel Elements

An improved coextrusion technique, utilizing unique billet and extrusion tool designs, for fabricating integral-ribbed, tubular fuel elements has been developed at the Savannah River Laboratory (see Figs. II–43 and 44). With this technique, the metal needed to form the ribs on the tubular elements is supplied from ribs on the outer sheath of the composite billet. The ribbed billet is extruded from a grooved steel container that matches the shape of the billet and prevents circumferential flow of metal during extrusion.

In previous billet designs, the outer sheath was cylindrical, and the billet was extruded from a round container. This design produced two undesirable characteristics: (*a*) uncontrolled core thickening beneath the ribs which can limit reactor power due to excessive heat generation in the rib area; and (*b*) thinning of the clad at the base of the ribs which increases the possibility of fission product release at this point. The new ribbed billet co-extrusion technique eliminates both of these detrimental characteristics.

Because no thinning of the cladding occurs at the root of each rib, the technique allows manufacture of elements with thinner nominal cladding. In addition, elements can be extruded with greater ratios of rib height to wall thickness and with the more uniform distribution of

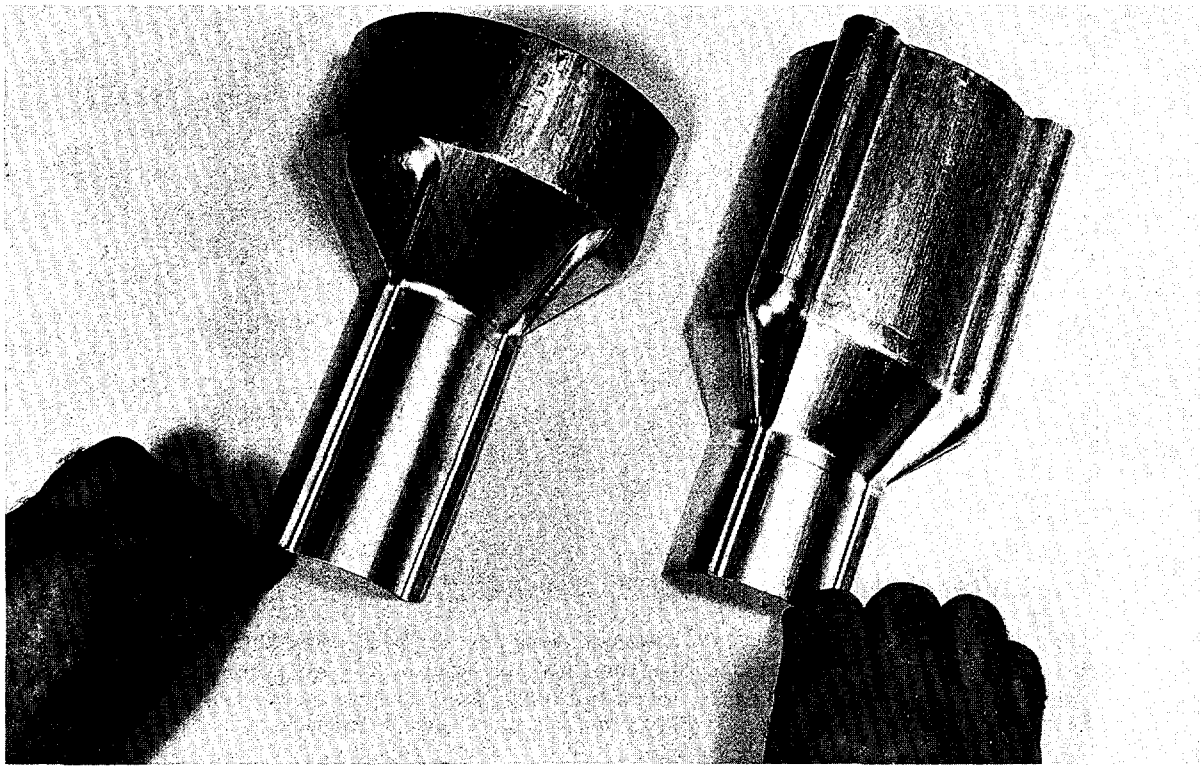

Figs. II–43 and 44. Coextrusion of Fuel Elements. Ribbed billets developed at Savannah River have eliminated the upset of the fuel core beneath ribs in extruded fuel tubes. The photo *above* shows a section of a composite tubular billet as it enters a die (broad portion) and a section of the ribbed fuel tube (small portion) that emerges. A round billet is shown on the left and a ribbed billet is shown on the right. The photo *below* shows a cross section of the rib area of a fuel tube. The core is a uranium-aluminum alloy, while the cladding is aluminum. The tube on the left was extruded from a round billet and shows the core upset. The tube on the right was extruded from a ribbed billet and has no upset. Reactor power can be increased by eliminating local temperature gradients, or fuel hot spots, caused by such core upsets.

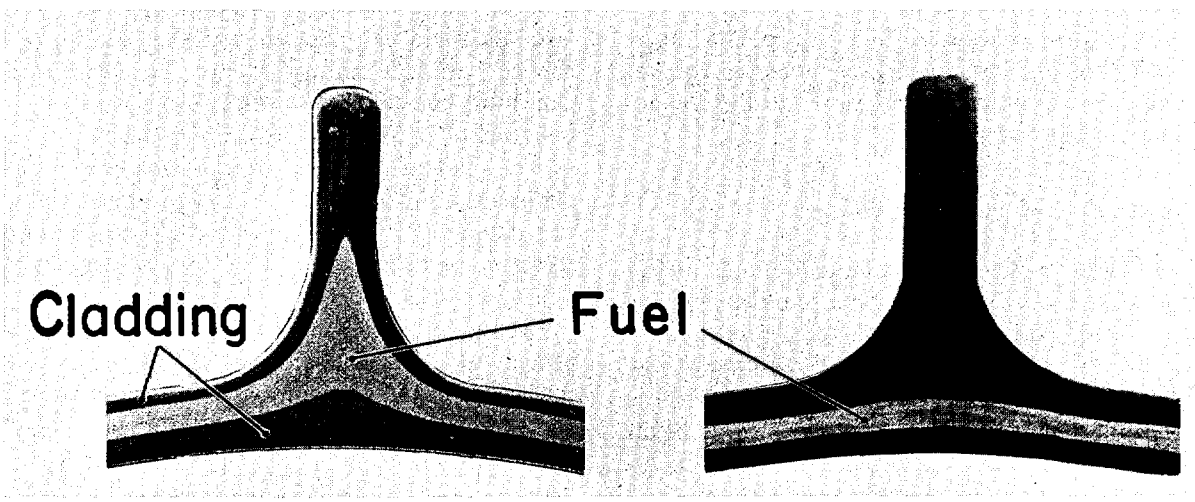

fuel. These improvements are expected to allow operation of fuel elements of the current design at higher power levels and will permit manufacture of the extremely thin elements for future operation at higher neutron flux. Thinner cladding will also provide increased neutron economy during irradiation and decrease the cost of chemical separation and waste storage following irradiation.

Nondestructive Testing

Ultrasonic Testing

Pacific Northwest Laboratory is actively developing a research program to conduct ultrasonic nondestructive tests on nuclear reactor critical components directed toward providing a better understanding of the way in which

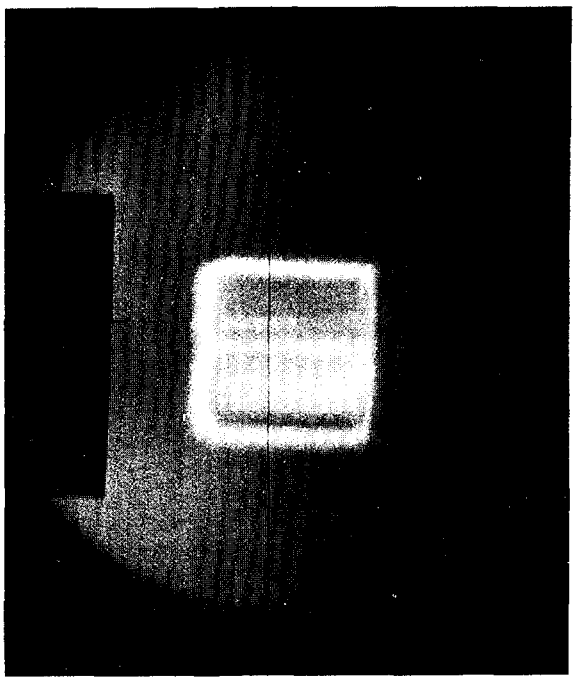

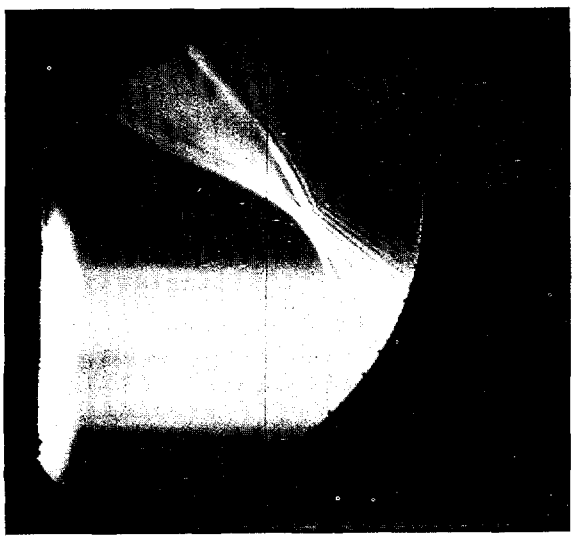

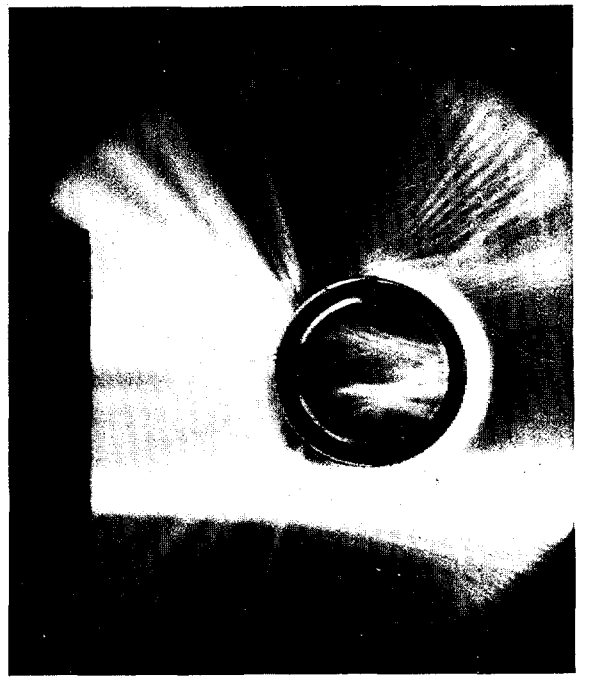

Figs. II–45, 46, and 47. Schlieren System for Study of Ultrasonic Phenomena. In regions of abrupt density changes in transparent media, light is diffracted just as it is by objects of size comparable to the wavelength. This phenomenon is used by ballistics students in the *Schlieren* optical technique for observing shock waves. Oak Ridge National Laboratory nondestructive test engineers have adapted the technique to study the transmission of ultrasonic waves through various media. The *Schlieren* pattern reveals the path of a pulse of ultrasonic energy through a tank of water (*upper left*), while the change of the pattern (*upper right*) when a solid object, such as a piece of tubing, is placed in the tank shows the nature of the interaction of ultrasound with the solid object. Photo at *left* shows how ultrasound can be focused by a curved surface. The understanding gained from these experiments will improve the interpretation of ultrasonic test results and should open possibilities for a new ultrasonic inspection method.

275-845 O—68——12

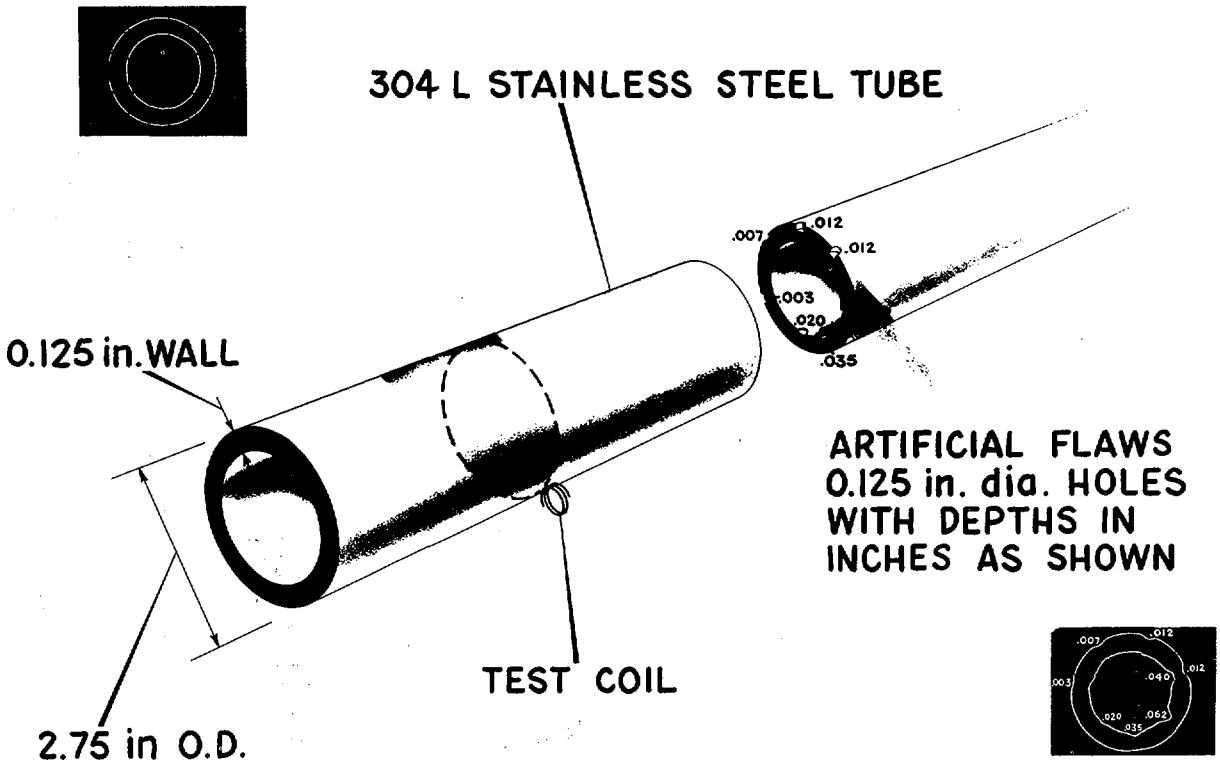

Fig. II–48. Nondestructive Electromagnetic Testing. The figure illustrates a display scheme used with an eddy current (electromagnetic) tubing tester being developed at Pacific Northwest Laboratory. Two extreme cases are shown. First, when a tube with no defects is rotated beneath an eddy current test coil, two smooth concentric circles representing the inner and outer tube diameters appear on a cathode ray tube (*upper left*). The defective tube case is illustrated by the display produced by a tube with known defects (*lower right*). Indentations distort the smooth circles whenever flaws are encountered. The location of the indentation on the display corresponds to the flaw location in the tube, while its depth indicates the flaw size. Note that the device is sensitive enough to simultaneously detect flaws on both the inner and outer surfaces.

ultrasonic energy travels through liquid and solid media. Studies are currently in progress to provide a suitable model to mathematically describe this phenomena.

When pulsed ultrasonic methods are used to detect flaws in metals, the shape and frequency content of the received signals are affected by normal attenuation and diffraction effects, as well as by flaw size and orientation. To date, several different mathematical functions have been examined and discarded because they were unable to predict, with sufficient accuracy, the wave forms which are experimentally observed.

Quite recently, however, a new mathematical function has been found which shows excellent promise for reducing the discrepancy between calculated and experimental results. This model consists of a series of damped sinusoidal functions, generally referred to as *Kautz* functions. Recent work, consisting of analyzing *Kautz* functions under various conditions of simulated materials properties using a large digital computer, indicates that good correlation between the experimentally observed and the mathematically predicted pulse shapes is now possible. *Kautz* functions offer potential for mathematically describing ultrasonic wave forms, and also may be applied in other areas where mathematical models are needed to analyze similar experimental data.

Electromagnetic Testing

The multidimensional nature of the eddy current, or electromagnetic, test signal constitutes a sound technical basis for the development of a multiparameter eddy current testing system. Experiments have been conducted at Pacific Northwest Laboratory to evaluate, in depth, this test concept so that maximum benefit is derived from its unique characteristics. One of the primary uses for such a testing system is in examining the many miles of tubing in a nuclear reactor plant. A significant new development has been the demonstration of a technique for simultaneously displaying flaw location and size on an oscilloscope (see Fig. II–48).

This technique, similar to a radar display of a cross section of the tube, indicates the relative magnitude and positions of the flaws. Previous eddy current displays had been in the form of blips on an oscilloscope which, in turn had to be interpreted to determine the exact size and locations of the defect. It is expected that this new type of equipment will ultimately result in improved quality assurance methods at decreased cost. The additional information which is made available by this system also permits greater ability to identify and classify signals in terms of actual tubing quality.

Fig. II–49. Zero Power Reactor—No. 3. In developing the designs for reactors, zero power reactors (ZPR) are used to determine the critical size (ability to sustain a fission reaction) and other physics characteristics, such as neutron flux distributions, fuel configurations, control features, and to test design calculations. These experimental "mock up" reactors are operated at such low levels of radioactivity that a liquid coolant and heavy permanent shielding are not needed. Photo shows Argonne National Laboratory's ZPR–3, which is located at the National Reactor Testing Station in Idaho. Since 1955, it has been used for studies on 50 different types of reactors; currently, it is being used for studies on fast (breeder-type) plutonium-fueled reactors. For tests, the two halves are slowly brought together by worm gears; the ramp is raised to deflect stray radiations that are set up between the halves (see p. 158).

REACTOR PHYSICS RESEARCH

Such parameters as neutron population and neutron use in reactor cores, as well as the manner and rate of neutron interactions with reactor materials, are essential to the design and construction of safe, dependable nuclear reactors. In view of the importance of these parameters, the AEC is sponsoring a broad program of research in the field of reactor physics.

INTEGRAL MEASUREMENTS

Measurements of neutron cross sections, neutron scatter, *Doppler* effect, and other parameters, using the entire spectrum of neutron energy levels rather than just one energy level are termed integral measurements. These are distinguished from differential measurements (see

next section), which use only one neutron energy level.

ZPR–3 Assembly 48

Most important physics characteristics of fast breeder power reactors can be measured at room temperature and low power, thus eliminating the need for associated large, complex, liquid-metal coolant systems such as are required when large quantities of power are the objective. Argonne National Laboratory's Zero Power Reactor-3 (ZPR–3) at the National Reactor Testing Station in Idaho has, for the past 22 years, been providing the majority of this information through studies of more than 50 different types of reactors. Included in this series have been studies of mockups of a number of proposed or existing fast reactors. These include studies of the Experimental Breeder Reactor-II (EBR–II), the Argonne Fast Source Reactor (AFSR), the Experimental Breeder Reactor-I (EBR–I), the Enrico Fermi Power Reactor, the Argonne Fast Reactor Test Facility (FARET), the Southwest Experimental Fast Oxide Reactor (SEFOR), and the French Fast Reactor (Rapsodie). The results of ZPR–3 studies have aided in the design of these reactors and have established numerous operating characteristics. Currently, the ZPR–3 is being used for first-of-their-kind physics measurements on plutonium-fueled breeder reactor designs. (See footnote 10 for definition of fast breeder reactors—often referred to as "fast reactors.")

Other work on ZPR–3 has firmly established the neutronic characteristics of a wide variety of small and intermediate size, uranium-fueled fast reactors containing a number of specific combinations of uranium-235 and 238, sodium, and structural materials. The ZPR–3 is shown in Figure II–49.

More recently, ZPR–6 and ZPR–9 [25] have been operated at Argonne National Laboratory in Illinois as fast critical facilities for the same purposes.

ZPR–3 is the first of these facilities to perform reactor physics studies of unmoderated plutonium-fueled reactors, *i.e.*, "fast" plutonium-field reactors. A plutonium-fueled critical experiment of special interest to fast reactor physicists, a large plutonium-fueled assembly of simple composition and geometry designated "assembly-48," has been constructed in ZPR–3. The reactor core was designed to be similar to that of a very large power reactor in its neutron energy spectrum, yet simple enough in the arrangement of its constituents to allow detailed analysis.

International aspects. At an International Conference held in 1966 at Argonne, 11 fast reactor design groups from the United States, United Kingdom, France, and West Germany, compared their detailed theoretical results obtained from studying this reactor. The success and failures in computing data measured from this assembly showed where improved methods and better nuclear data were needed and thus more clearly established the areas of future fast reactor physics research. The basic physics studies were continued in 1967 by studies in other cores, altered to shift experimental emphasis to other important regions of the fast neutron spectrum. The core compositions were kept simple to continue the assembly-48 philosophy of ease of analytical interpretation.

An international intercomparison of methods of measurement in fast critical experiments, initiated in 1966, began to assume a broader base in 1967, the participants including the United Kingdom, France, and the United States, with Sweden and West Germany to follow. Measurements thus far have shown that while most instruments were in good agreement, some recalibration will be necessary. The continuing intercomparison will result in increased confidence in the validity of measurements to be made throughout the world.

Heterogeneity investigations. The ZPR–3, and the fast critical facilities ZPR–6 and 9 at Argonne National Laboratory, are constructed of drawers containing plates of various basic materials such as enriched uranium, depleted uranium, steel, aluminum, sodium (encapsu-

[25] See pp. 263–264, "Fundamental Nuclear Energy Research—1966."

lated in plate-shaped steel cans), and graphite. One important difference between such a critical facility and a power reactor is that the power reactor fuel element is typically a pin of small diameter, for which heterogeneity (local neutronic perturbations due to a nonhomogeneous mixture of core materials) effects are small. The heterogeneity effects due to the plates are considerably larger; hence, it is necessary to understand these effects and to correct experimental data for them, if subsequent extrapolations of the data to power-reactor designs are to be reliable. Analyses and experiments have been carried out at Argonne to study the effects of these plate heterogeneities upon pertinent quantities such as critical mass and the sodium reactivity coefficient.

The heterogeneous critical assemblies have been calculated to have critical masses smaller than that of the more homogeneous power reactor from a few percent to as much as 30 percent. The effect of varying the heterogeneity has been studied, and agreement between calculation and experiment for various degrees of heterogeneity has been good.

Analysis of Fast Fission Cross Sections

The rate at which fission occurs in a reactor depends upon the probability of fission (cross section) and upon the average neutron energy in the reactor (neutron energy spectrum). These values vary for different types of fuels and structural materials, and also depend upon the way the fuels and materials are arranged in the reactor. The relative rates of fission in isotopes of plutonium, uranium, neptunium, and thorium are measured in fast reactors, and such information as rates of breeding and heat generation are determined. An understanding of the fission events in a reactor depends in part upon an accurate knowledge of the variation with neutron energy of the fission cross sections of fuels and fertile materials. Measurement of these cross sections is a fundamental aspect of nuclear physics, but the results obtained by many different experiments over a period of years were often not evaluated carefully

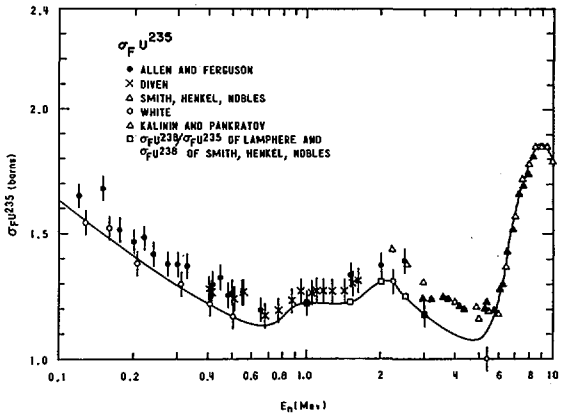

Fig. II–50. Analysis of Fast Fission Cross Sections. The fissioning rate in a reactor depends upon several variables, such as the probability of fission occurring (cross section), the neutron energy spectrum, the types of fuels and materials and their arrangement. The Argonne National Laboratory chart shows the difference between several typical measured data for uranium-235 (U^{235}) and the "best data" curve obtained through careful evaluation.

enough to permit their direct use in accurate reactor calculations. The fission cross sections of thorium-232, uranium-233, 234, 235, 236, and 238, neptunium-237, and the plutonium isotopes 239, 240, 241, and 242 have been evaluated at Argonne National Laboratory's ZPR-3 to obtain more consistent, accurate data for fast reactor physics anaylsis. The study showed that a careful examination of source data and methods is vital and that, in particular, the cross section of uranium-235 must be well known, since it is the yardstick used to measure other cross sections. This study has helped stimulate interest in additional precise measurements of fission cross sections. Figure II–50 shows differences between typical measures data and the selected "best data" curve.

Inelastic Neutron Scattering Measurements

Knowledge of the probability of collision of a neutron with reactor materials (with resultant marked loss of energy) is important in fast reactors because better breeding ratios are achieved if these inelastic scatterings are minimized and the neutron energy is kept as high

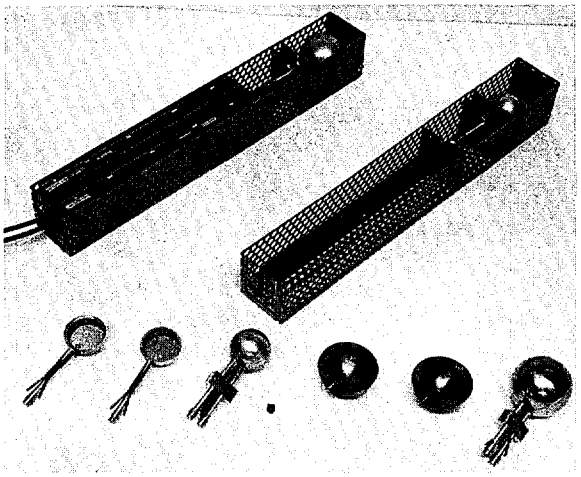

Fig. II–51. Inelastic Neutron Scattering. A method for measuring the wide range of neutron energies present in a fast reactor has been developed at Argonne National Laboratory. The method involves measuring the rate of fission in a material whose fission cross section varies strongly with neutron energy, with and without spherical shells of reactor fuels and materials surrounding the fission detector. Photo shows counters, shells, and positioning drawers used in these inelastic scattering measurements conducted with the ZPR–3.

as possible. Because of the wide range of neutron energies present in a fast reactor, these measurements are difficult. A method of performing these measurements in a fast reactor itself has been developed with Argonne's ZPR–3. This consists of measuring the rate of fission in a material whose fission cross section varies strongly with neutron energy (threshold fissile and material), with and without spherical shells of various reactor fuels and materials around the fission detector. Inelastic scattering in the shell reduces the fission rate; thus, the probability (cross section) of scattering can be found.

These measurements can be performed conveniently in the center of a fast reactor core in a critical facility, such as ZPR–3, to provide checks upon the accuracy of reactor calculations. Careful control of the fission-rate measurements is needed because the changes produced by the shells are small—only a few percent. An initial experiment performed in ZPR–3 has shown that certain cross section sets have serious errors in some inelastic scattering cross sections. The specially developed detectors and shells for this experiment are shown in Figure II–51.

Zoned Core Concepts

The study of large fast breeder reactors can be accelerated if some of the physics parameters of very large reactors can be studied in smaller experiments. The feasibility of zoned cores for this purpose has been investigated on ZPR–6 and 9 at Argonne National Laboratory. It has been found that such reactor parameters as the *Doppler* effect [26] and the spectral component of the sodium-void effect, both of which are important for reactor safety, can be measured with zoned cores.

A zoned core is one composed of concentric cylindrical regions, the innermost of which has the same material composition as that of a large fast power reactor. It is important to determine the smallest central zone that is useful, since materials for this zone may involve the higher isotopes of plutonium, which are difficult to obtain. It has been verified, by comparing measurements in zoned and full-sized cores, that a central zone as small as 192 liters (about 6¾ cubic feet) is adequate to give acceptable accuracy, while on the other hand, a 125-liter (about 4½ cubic feet) zone is definitely too small. For comparison, the volume of a full-size mockup (see Fig. II–52) of a carbide-fueled fast reactor, with uranium-235 as fissile material, was 2,600 liters (about 90 cubic feet). While the exact size of zone needed will vary with core composition, these experiments provide a valuable check of theoretical methods.

Doppler Effect Measurements

Accurate calculation of the *Doppler* effect is one of the more important problems in fast reactor physics because the rapid reactivity re-

[26] *Doppler* effect—A shift in the measured frequency of a wave pattern caused by movement of the receiving device or wave source. Since, in a reactor fission cross sections depend on the relative velocity of the neutrons and the uranium atoms (neutron movement can be considered wave motion), vibration of the uranium atoms in a fuel element due to the increased operating temperature leads to the *Doppler* effect. This can vary the reactivity of the reactor.

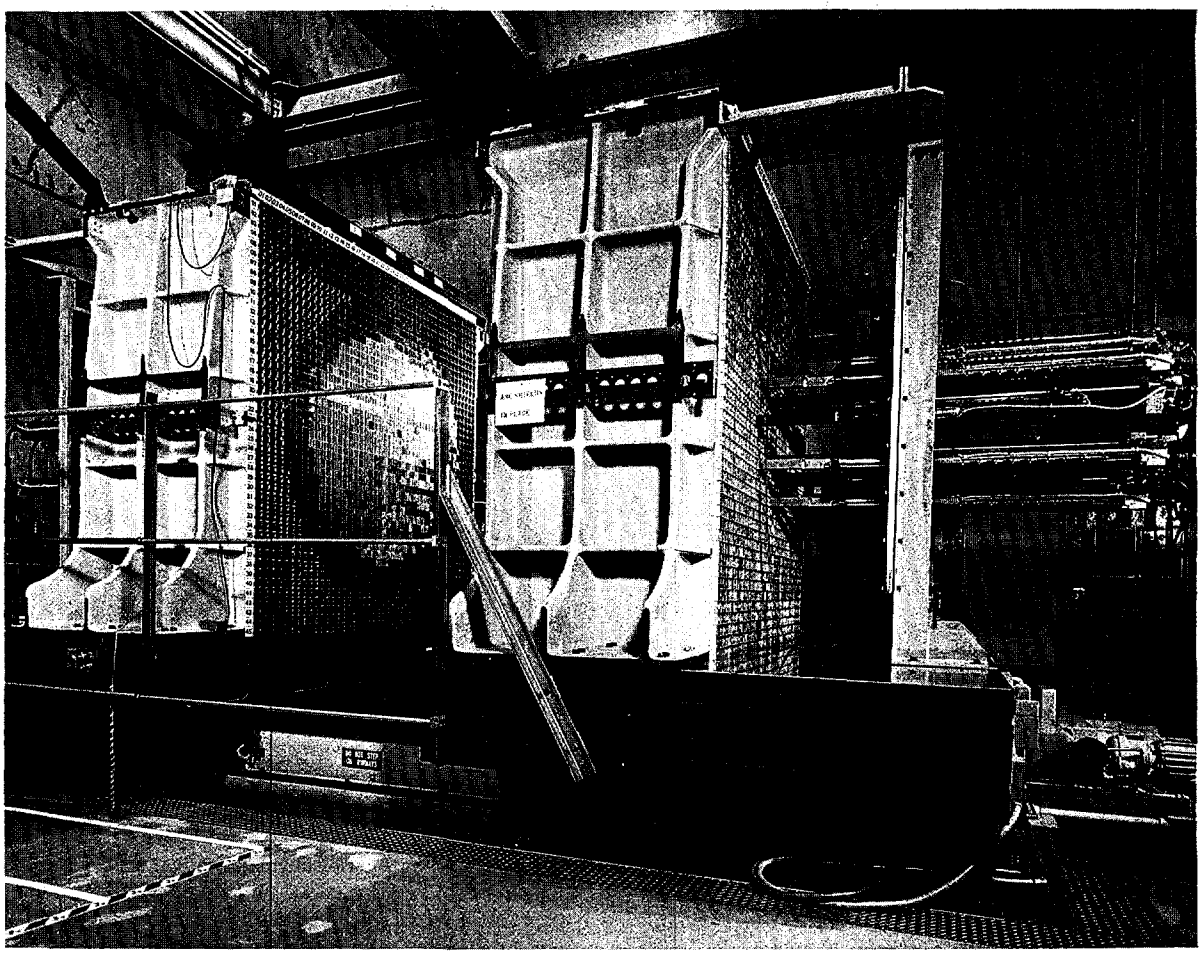

Fig. II–52. Assembly No. 5 in ZPR–6. ZPR–6 is one of Argonne's split bed-type critical facilities used in support of the fast power breeder reactor development program. Assembly 5 is a depleted uranium reflected core having a composition representative of a large, dilute-uranium carbide-fueled fast breeder reactor. The 2,600-liter (about 90-cubic feet) core contains 1,600 kilograms of uranium-235, the largest quantity of fissile material ever used in a single critical assembly.

duction provided by this effect as reactor power rises is an important safety feature. Likewise, direct measurements of the *Doppler* effect are necessary to check theory, and a detailed program of such measurements is underway in the fast critical assemblies ZPR–6 and 9 at Argonne National Laboratory using both zoned and uniformly loaded cores. Comparison of recent measurements with current analytical techniques has confirmed the adequacy of these techniques for prediction of several important facets of the *Doppler* effect. The uranium-238 *Doppler* effect, which is the major contributor to the overall negative reactivity effect, has been predicted quite well by theory.

The *Doppler* effect occurs because a change in the thermal velocity distribution of the fuel atoms with temperature changes the width of the cross-section resonances and changes the amount by which one atom can shield a neighboring atom of the same isotope. When the fuel temperature rises, the increase in thermal velocity of the fuel atoms leads to an increase in the rates of both fission and capture, which are proportional to the product of the cross section and the flux. In a large fast breeder reactor, the

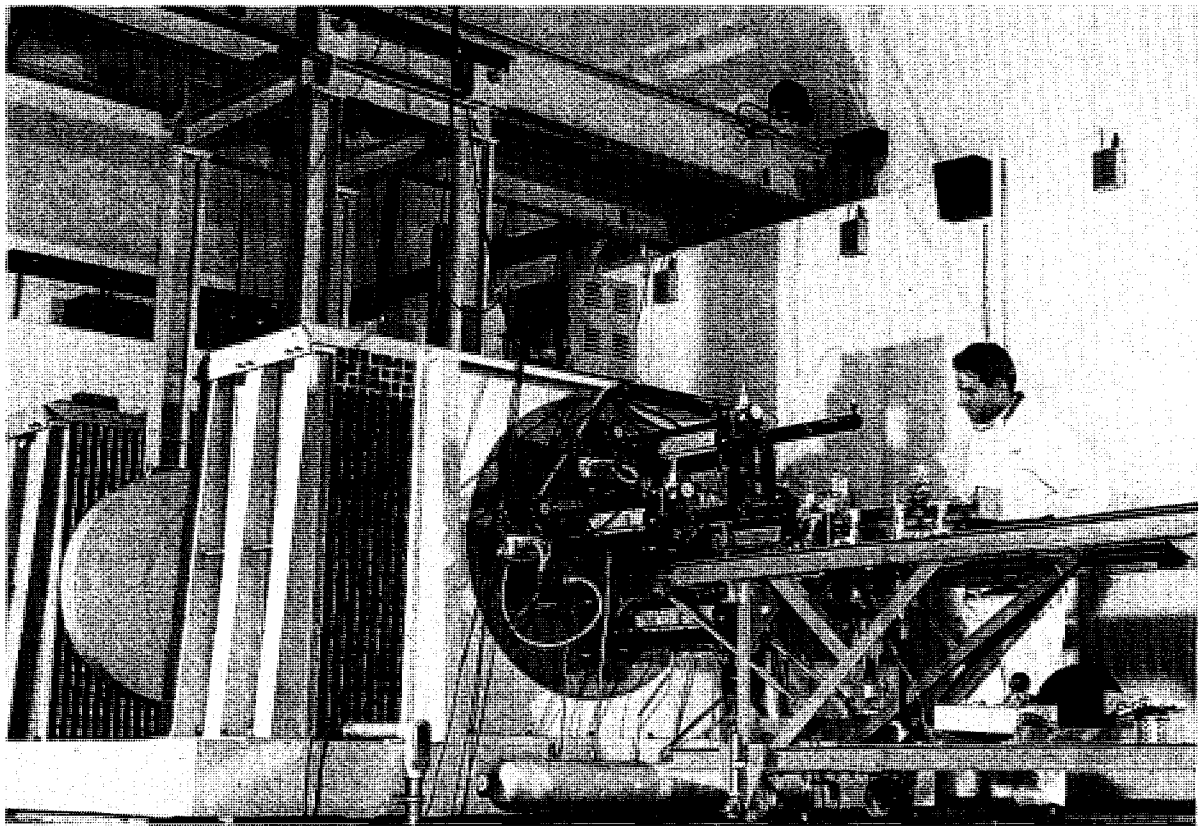

Fig. II–53. Research at Atomics International. A zoned critical assembly at the Epithermal Critical Experiments Laboratory at Atomics International, Canoga Park, Calif., is being used to investigate the *Doppler* effect in the plutonium isotopes by means of heating small samples that contain various ratios of the different isotopes. The samples are placed in a test zone in which the neutron energy distribution simulates that which would exist in a proposed fast power-producing reactor. Studies are being conducted over the temperature range from −253° to +900° C. in a wide variety of neutron spectra.

increase in capture outweighs the increase in fission, producing an overall negative reactivity effect with increasing fuel temperature.

Sodium Void Effect on Reactivity

The reactivity effect associated with the possible sudden loss of the sodium coolant is of great interest in analyzing the safety of large sodium-cooled fast breeder reactors. Should boiling of the sodium in a reactor excursion lead initially to a gain in reactivity, the power tends to rise, making the excursion more difficult to cope with. Therefore, it is important to know accurately what the magnitude of the sodium void effect [27] on reactivity is, and studies have been underway at Argonne National Laboratory for some years on this problem. Measurements made in both the ZPR–3 and ZPR–6 fast critical experiment facilities have helped to reduce the considerable uncertainties in calculations of this effect. Measured values of the "leakage" component of the sodium void effect have been found to agree with calculated values to within about 10 percent. This indicates that there are no serious errors in the calculation methods or data involved in calculating this component.

Neutrons at lower energies in a fast reactor tend to be less important in maintaining the chain reaction than those at higher energy. When sodium is removed from the reactor, neu-

trons do not undergo collisions with the sodium nuclei and the average neutron energy rises, leading to a gain in the effectiveness of the neutrons in maintaining the chain reaction. However, neutrons simultaneously have a greater chance of escaping (or "leaking"), thereby losing effectiveness. The net algebraic result depends on the difference between two relatively large numbers, so that large percentage uncertainties in the total effect are produced by relatively small uncertainties in the components.

The "leakage" component, which corresponds to the retarding effect that collisions between neutrons and sodium nuclei have on leakage of neutrons from the reactor, is not sensitive to choice of fissile isotopes; extensive measurements of the leakage component, of direct applicability to plutonium-fueled reactors, have been made with uranium-235-fueled critical experiments. The measured leakage component has been carefully compared with theory, and the discrepancies that exist are not major.

Detailed measurements of the reactivity component caused by changes in the neutron energy spectrum are underway in both uranium-235- and plutonium-239-fueled critical experiments. It has been found, as expected, that this "spectral" component in uranium-235-fueled reactors is relatively small. There are disagreements between theory and experiment which are probably from improper choices of fission and capture cross sections of uranium-235. For plutonium-239-fueled compositions, the measured spectral components are, again as expected, more positive (corresponding to a larger reactivity gain on removal of sodium) than in the case of uranium-235.

While the available results have been of some assistance in checking cross sections, the data uncertainties, particularly in fission and capture cross sections of the plutonium isotopes, are so large that many more measurements of this type are needed.

Resonance Integral Measurements

A program of experiments aimed at the measurement of resonance integral cross sections of reactor materials has recently been expanded by the addition of equipment to make radioactive sample measurements. Previous measurements have been limited to samples that could be physically handled by the personnel involved. Now, however, a radioactively "hot" sample changing device is in operation in the Advanced Reactivity Measurement Facility-II, operated by Idaho Nuclear Corp. for the AEC at the National Reactor Testing Station, Idaho.

The new apparatus, shown in Figures II–54 and 55, allows a "hot" sample to be loaded into a drum under water. The drum has means for drying the sample, one of the requirements in this kind of experiment, and handling the sample remotely. The new device offers the possibility of determining resonance integrals of radioactive nuclides which have been long sought after by reactor designers.

In addition, the new sample changer is also ideally suited for making temperature dependent resonance integral measurements. In the past, such measurements have been difficult because the heat loss by the heated sample contributes to the overall temperature of the reactor core, and leads to serious errors in data interpretation. Now, however, this heat loss can be removed from the system by the drying gas passing around the sample. Measurements of this type are needed in designing high temperature reactors, in study of reactor safety, and in breeder reactor cores.

Eta of Plutonium-241

Continued operation of a nuclear reactor depends on producing at least as many neutrons as are consumed. The quantity "*eta*" refers to the number of neutrons produced on the average for each neutron absorbed by the atomic fuel material. This important quantity has been measured for plutonium-239 (Pu^{239}) and 241 in the low power test reactors—Advanced Reactivity Measurement Facility (ARMF–I and ARMF–II)—at the National Reactor Testing Station in Idaho. These reactors measure with

[27] *Sodium void effect*—A term used to describe the changes in the power level of a fast reactor that occur upon loss of sodium coolant.

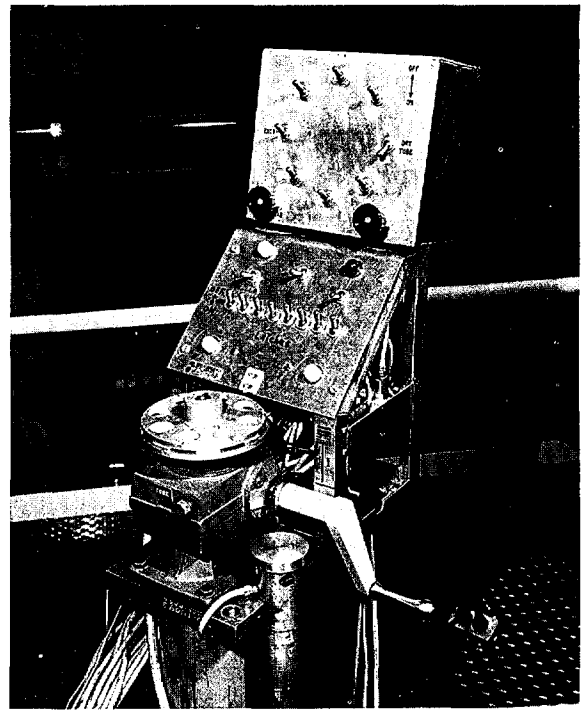

Figs. II–54 and 55. Resonance Integral Measurements. The "hot" sample changer used by Idaho Nuclear Corp. for measurements of resonance integral cross sections of reactor materials, is shown on the *left* as it is being lowered into position in the ARMF–II at the National Reactor Testing Station. The rotating drum has room for eight samples. These are loaded under water and then dried inside the apparatus by flowing gas through the compartments. The reactor core shown covered by about 3 inches of water is normally under 15 feet of water during operation. Photo on *right* shows the control "console" for the "hot" sample changer. It is located 18 feet above the sample drum and consists of a crank for mechanical rotation of the drum, and toggle valves to control gas flow to the pneumatic clamps and water purging system. Samples may also be inserted directly through the plugged 2-inch tube in the foreground.

great precision the changes in neutron population; thus it is possible to determine *eta*. A small sample of the material is placed in solution and measured under standard fixed conditions.[28] Similar measurements are made on known materials, such as uranium-235 (U^{235}) and boron, for comparison. The results showed that whereas plutonium-239 produces nearly the same net number of neutrons as uranium-235, plutonium-241 furnishes about five percent more under normal low temperature conditions. Since both of these plutonium isotopes are present (though in varying proportions) in any plutonium fueled reactor, *eta* for each one is needed in calculations of these new reactor types. The ratios of *eta* of Pu^{239}/U^{235} equaled 1.0117 ± 0.0077, while for Pu^{241}/U^{235} it equaled 1.0574 ± 0.0081 for fissions by neutrons in the thermal range. In other words, plutonium-239 and -241 produce slightly more neutrons upon fission than does uranium-235 under the same conditions.

[28] Conditions standard for flux distribution and temperature, the latter at 20.44° C.

High Burnup Studies of Pu^{241} and U^{233}

Irradiations of the fissile isotopes uranium-233, uranium-235, plutonium-239 and plutonium-241, and measurements of the resulting changes in reactivity (a measure of the ability to sustain a chain reaction), are continuing by Idaho Nuclear Corp. at the National Reactor Testing Station. Such reactivity changes are due

to the depletion of the fissile isotope in question and to the production of neutron absorber atoms (fission products) during the fission process. These fission products are radioactive and decay to other atoms (daughter products) that may, or may not, have different neutron absorption characteristics (cross section). Depletions ranging between 10 and 80 percent of the original fissile isotope contents have been obtained and reactivity measurements, extending over periods in excess of one year following termination of irradiation, have been made. During the first 50 hours following irradiation the reactivity changes are due primarily to the decay of the two isotopes, iodine-135 and xenon-135 (I^{135} and Xe^{135}). Between 50 and 500 hours the changes are due primarily to the decay of promethium-149 to samarium-149 (Pm^{149} to Sm^{149}). Beyond 500 hours and up to about 13 months, no changes have been detected. The fission products are known to be decaying because of the gamma rays they emit. Hence, the conclusion is that on the average the cross sections of the daughter products do not differ by a measurable amount from the cross sections of the original fission products present at 500 hours after termination of irradiation. After 500 hours no significant change in reactivity was observed and decay times of samples before measurement of reactivities of up to 12,000 hours produced no further change. The reactivities of the samples are controlled not only by the U^{233} or U^{235} present but also by the amounts and cross sections of specific fission products.

Delayed Photoneutrons

Virginia Polytechnic Institute, Blacksburg, is doing research on the production of "delayed neutrons" in reactors. After fission occurs, neutrons are emitted for some time from the fission fragments. These are called "delayed neutrons," and are important for the control of both fast and thermal reactors. In addition, when heavy water or beryllium is present in a reactor, gamma rays from fission products produce additional delayed neutrons by the photoneutron process. Research on delayed neutrons, in particular the abundance and lifetimes of the delayed photoneutron groups, was suggested to aid the design of new reactors. Results to date include verification of previously reported delayed neutron groups and the identification of two previous unknown short-lived delayed photoneutron groups.

Delayed neutron data has been obtained by a "chopped beam" method, which permits investigation of the delayed neutron groups in time ranges of from milliseconds (1 millisecond = 1/1,000th of a second) to minutes. Thus far, data have been obtained for delayed photoneutron groups with half-lives of 4 and 74 milliseconds and delayed neutron groups with half-lives of 0.46, 2.32, and 7.31 seconds. The method employed has the advantage over previous techniques of examining in detail the time range of the order of milliseconds after fission.

Neutron Diffusion in Light and Heavy Water

High energy neutrons injected into a good moderator, such as light water (H_2O) or heavy water (D_2O), are slowed by collisions with the moderator molecules and then behave as a diffusing gas in thermal equilibrium with the moderator. In designing a nuclear reactor it is important to know the rate at which these neutrons migrate (or diffuse) from one location to another in the moderator; work at the Savannah River Laboratory (SRL) has determined these diffusion rates with new reliability and precision. The diffusion of neutrons is complicated by the fact that, unlike ordinary molecules, the neutrons can be absorbed or even leak out of the system as they move about. These effects lead to a decreasing neutron density as neutrons diffuse away from the vicinity of the source, and the decrease is characterized by a "die-off coefficient," K, which can be measured directly.

Two methods are commonly used to measure neutron diffusion coefficients. In the "static" method, the neutron population attenuation is measured as a function of distance from a source of continuously supplied neutrons. The absorb-

ing properties of the medium are varied by adding strong neutron absorbers such as boron. These absorbers preferentially absorb the slower, lower energy neutrons. In the "pulsed" method, the decay of the neutron population is measured as a function of time after the injection of a burst of neutrons into the sample. The leakage properties of the medium are varied by altering the size of the sample. Since the faster neutrons leak from the sample more easily, reducing the sample size will produce an abnormal abundance of the lower energy neutrons. This is the opposite of the effect that is obtained when strong absorbers are added in the static experiment. Therefore the pulsed measurement can be analyzed as if it were the equivalent of a static measurement in which neutron multipliers (or negative absorbers) are added to the sample.

Previous measurements in heavy water seemed to indicate that the value of K at "zero" absorber concentration depended slightly on the method of measurement, static or pulsed. Combination of pulsed method and static method experiments were performed on both heavy and light water at SRL. The results for heavy water are shown in Figure II–56. The fact that these results are joined by a smooth curve at "zero" absorption demonstrates for the first time that the die-away coefficient, K, has been found independently of the method of measurement. Similar results were found for light water. These measurements furnish a direct comparison for the various diffusion theory models.

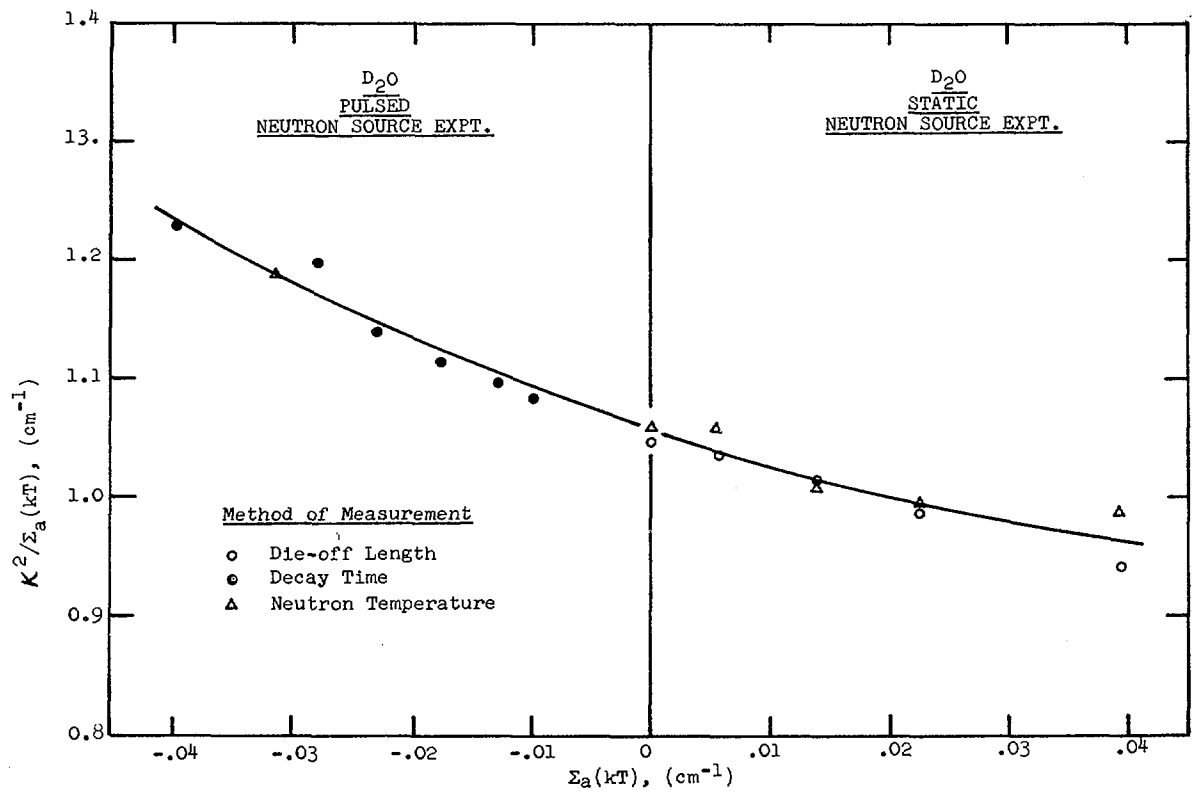

Fig. II–56. Neutron Diffusion in Heavy Water. The Savannah River Laboratory chart shows the variation of die-off coefficient, K, with the amount of neutron absorbing boron (proportional to ξ_a) mixed in heavy water (D_2O). Both pulsed and static methods of measurement were employed. In previous measurements a small discrepancy existed between the results of these two types of experiments in D_2O. The fact that these results are joined by a smooth curve at "zero" absorption removes this discrepancy and allows an overall test of the diffusion theories.

Capture and Fission Cross Sections

An experiment in which the neutron capture and fission cross sections of uranium-233 were measured simultaneously over the neutron energy range from 0.5 to 100 electron volts (ev.) was successfully performed in a cooperative effort by the Oak Ridge National Laboratory (ORNL) and Rensselaer Polytechnic Institute (RPI), Troy, N.Y., yielding the first direct measurements of the capture cross section ever made. The technique used was essentially the same as the one applied in earlier uranium-235 measurements,[29] except that modifications were required to circumvent a severe background problem resulting from the isotope's high specific activity of alpha particles.

As was the case for uranium-235, the sample was fabricated at ORNL in the form of a fission chamber which was centered in a large tank of liquid scintillator that was sensitive to gamma rays. A high-intensity pulsed-neutron source was obtained from a target placed in the beam of the electron linear accelerator at RPI, and the time-of-flight technique was used to deduce the energies of the neutrons from the flight time between the target and the sample. Gamma rays were emitted by the sample following both fission and capture events, the fission events being distinguished from the capture events by accompanying fission chamber pulses. Thus, the measurements yielded not only values of the capture and fission cross sections themselves, but also values of the parameter α, the ratio of the capture cross section to the fission cross section, which is important for establishing the feasibility of breeder reactors. Breeder reactors will be possible only if the average value of α is considerably less than 1.

A sample of some of the data is shown in Fig. II–57, in which the parameter α ($\alpha=\sigma_c/\sigma_f$) is shown to vary between 0.02 and 0.9 for the energy range from 0 to 25 ev. Extension of these measurements to higher energies gives an average epithermal value of α of about 0.18, which agrees with direct integral measurements and contradicts evaluations based on earlier cross-section measurements.

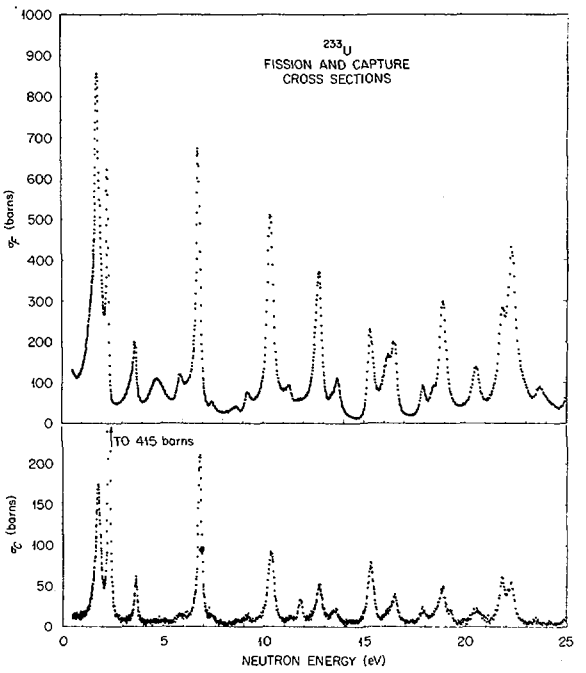

Fig. II–57. Capture and Fission Cross Sections. The measured values of the neutron fission and capture cross sections for uranium-233 are shown above. These, derived by Oak Ridge National Laboratory and Rensselaer Polytechnic Institute, and similar measurements for other energy ranges are needed to determine the feasibility of breeder reactors. The parameter α ($\alpha=\sigma_c/\sigma_f$) is shown to vary between 0.02 and 0.9 for the energy range from 0 to 25 ev. Extension of these measurements to higher energies gives an average epithermal value of α of about 0.18, which agrees with direct integral measurements and contradicts evaluations based on earlier cross-section measurements.

Scattering Cross Sections

Oak Ridge National Laboratory (ORNL) is engaged in a long-range program to develop nuclear models for calculating neutron scattering cross sections, with the current emphasis on inelastic scattering cross sections. Inelastic scattering is a neutron-nucleus interaction which proceeds as follows: the neutron joins the nucleus to form an extremely short-lived compound nucleus; the compound nucleus ejects a neutron of lower energy; and the nucleus rids

[29] See p. 112, "Fundamental Nuclear Energy Research—1964."

itself of the excess energy by emitting gamma radiation. Such reactions are commonly referred to as n,n′ or n,n′γ reactions. To date, 12 elements have been measured for various incident neutron energy.

The experiments consist in the measurement of the spectra of neutrons scattered at various angles from samples of the elements. The incident neutrons are obtained from the D(d,n) reaction [30] in a deuterium gas target. With the accelerators available at ORNL, the neutron energy can be varied between 3.8 and 8.5 million electron volts (Mev.). The energies of the scattered neutrons are determined from the time interval between the production of the primary neutrons and the detection of the scattered neutrons.

The samples are fabricated in the form of small cylinders and are located 8 to 11 centimeters (3.4–4.33 inches) from the neutron source. Thus far, measurements have been made for the following elements and incident neutron energies:

Neutron energies	*Elements*
4.5 Mev.	Carbon, iron.
5 Mev.	Carbon, sodium, aluminum, silicon, potassium, calcium, vanadium, iron, cobalt, yttrium.
5.6 Mev.	Carbon, silicon, iron.
6.2 Mev.	Iron.
6.6 Mev.	Iron.
7.6 Mev.	Carbon, magnesium, aluminum, silicon, sulfur, iron, cobalt, yttrium.

Below 5.6 Mev., the angular range was between 20 and 140 degrees from the incident neutron beam, while for higher energies it was between 25 and 114 degrees. The data are in various stages of reduction; however, most of them are in the form of "raw" cross sections which still require corrections.

Cross Section of Promethium-147

One of the more important reactor-produced isotopes is the fission product, promethium-147, which acts as a reactor poison (neutron absorber) in reactors and also has possible by-product use as an energy source for space applications. The total cross section of promethium-147 has been measured as a function of neutron energy by the Idaho Nuclear Corp. with the Materials Testing Reactor (MTR) Fast Chopper at the National Reactor Testing Station, Idaho. The sample was obtained from a stock of fission-product promethium which had been separated for use as a space energy source and was further purified at the MTR. The cross sections were also measured as a function of time; hence, the cross section caused by the daughter product, samarium-147 (Sm^{147}), being formed by decay of the promethium could be distinguished from the promethium-147 (Pm^{147}) cross section.

Both promethium-147 and samarium-147 contain many resonances, as do a great number of isotopes. Since the distribution and size of the resonances is characteristic of each isotope, they can be used to identify or determine the amount of one isotope in another or in a mixture. For example, the growth of Sm^{147} can be followed in a sample of Pm^{147} by observing, with the MTR fast chopper, the increasing effect of the samarium resonances [31] with time. Neutron transmissions through a Pm^{147} sample over the neutron energy region from 23 to 2.5 electron volts, corresponds to a neutron time of flight varying from 300 to 900 microseconds.

A fast chopper, such as the one at the MTR, can resolve resonances only up to moderate neutron energies. Furthermore, it can only measure total cross sections of radioactive materials, whereas the cross sections of absorption of neutrons is of more direct importance to the reactor program.

The absorption cross section of 2.7-year half-life promethium-147 was measured in February 1967 at the Nevada Test Site using an underground nuclear explosion (the Persimmon scientific-study event of the AEC's Plowshare program) as the source of neutrons. The intense

[30] A deuteron, d, hitting a deuterium gas target, D, results in the emission of a neutron, n.

[31] A resonance occurs when the neutron interaction probability becomes much larger at a certain energy.

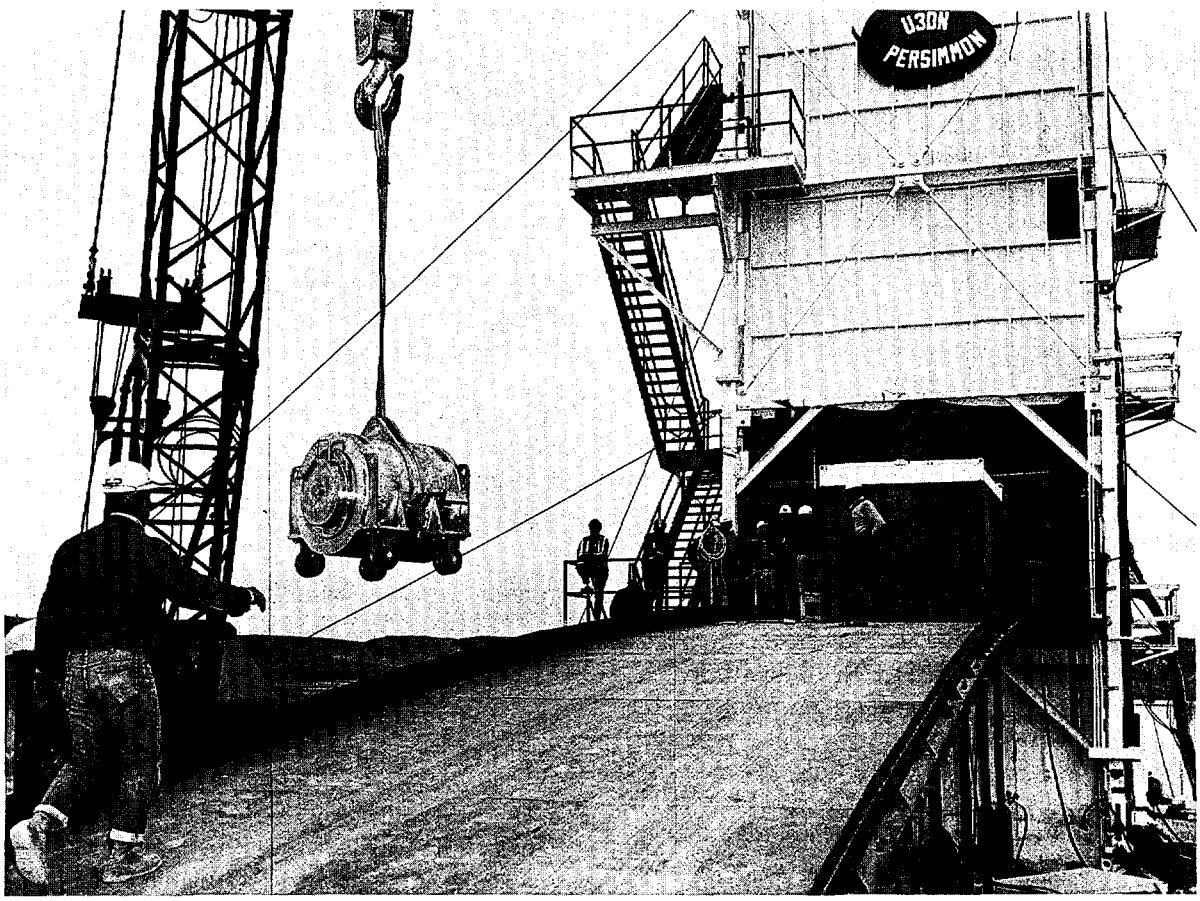

Fig. II–58. Promethium-147 Cross Section Measured. The 1,000-curie sample of Pm^{147}, enclosed in a massive lead shield is shown arriving at the experimental area of the Nevada Test Site for the Plowshare Program's "Persimmon" event in early 1967. A nuclear explosive, detonated deep underground below the tower, provided an intense beam of neutrons used by the Idaho Nuclear Corp. and Los Alamos Scientific Laboratory to measure the neutron absorption cross section of Pm^{147} as well as for a large number of other nuclear physics measurements.

beam of neutrons from the nuclear explosion allowed direct measurement of neutron absorption despite the intense radioactivity of the 1,000-curie Pm^{147} sample (see Fig. II–58). The Pm^{147} cross section was measured over a very wide range of neutron energies. This experiment, the first of a series of measurements on very radioactive materials to be made at the Nevada Test Site, was a cooperative effort of the Idaho Nuclear Corp. and Los Alamos Scientific Laboratory. Analysis of these data, a laborious process, is now being carried out.

275–845 O—68——13

EVALUATION CALCULATIONS

The AEC sponsors research into improved methods for calculating various reactor parameters and for evaluating sets of data obtained from these calculations.

Fission Product Yields

The yields of fission products from the fission of plutonium-239 in a fast reactor are being studied at the Los Alamos Scientific Laboratory.

In the design and safety evaluation of a nuclear power reactor it is necessary to know, among other things, the yields of the radioactive products produced by fission. These fission products emit beta and gamma radiations and have half-lives which range from a fraction of a second to several thousand years. Much information exists on fission product yields for fission of uranium-235 by thermal neutrons (0.025 electron-volt energy). However, little experimental information is available on yields from fast neutron (energy of about 1 million electron volts) fission of plutonium-239. Because fast fission of plutonium-239 is basic to the operation of power breeder reactors, a theoretical approach was employed to calculate yields of approximately 200 selected radioactive nuclides which result from this type of fission. The calculated yields, together with the known radioactive properties of the nuclides studied, have been incorporated into an existing computer code to determine the quantities or inventory of fission-products for any specified reactor power, operating time, and time after shutdown. Calculations indicate that the total fission-product inventory, for similar reactor conditions, is roughly the same for thermal fission of uranium-235 as for the fast fission of plutonium-239. The inventories of individual nuclides, however, do vary.

Reactor Cross Section Evaluation

The Cross Section Evaluation Center (CSEC) at Brookhaven National Laboratory (BNL) evaluates neutron cross section data.[32] During 1967, it acted as the hub of a large scale national effort by the AEC to obtain an evaluated set of basic data for use in reactor calculations. The other national laboratories, and most of the private companies involved in the design and construction of nuclear reactors, have contributed to this effort.

This set of data, designated as ENDF/B (Evaluated Nuclear Data File, Version B), was compiled on an automated magnetic tape format as a cooperative venture by some 18 U.S. laboratories. After thorough checking and testing during 1967 by these laboratories, the data will be used in reactor design studies. The availability of a standardized and well-tested set of cross sections for reactor design studies will greatly aid the U.S. nuclear energy program by providing reliable and readily comparable calculational results.

The evaluation work of the CSEC and compilation work of the Sigma Center, also at BNL, have been combined to form the National Neutron Cross Section Center effective July 1, 1967. The automation requirements of evaluated and compiled cross sections are similar, and greater efficiency will result by coordinating this work within the new Center.

Argonne Reactor Computation

The Argonne National Laboratory is developing a digital-computer code system, called the ARC (Argonne Reactor Computation) system, which will facilitate the solution of complex reactor theory and design problems. Intended for use on modern, high-speed digital computers such as IBM's System/360 or CDC's 6600, it represents a break with traditional computer methods in that individual operations, rather than being performed by free-standing codes with their own input and output routines, are carried out instead in highly specialized computation units called modules, which operate under the direction of a central operating system in a unified and automated manner. The ARC modules are simply specialized codes written in a programming language called "Fortran." The automated nature of the system eliminates the human errors that in the past have been common in the solution of complex reactor problems. Also, the ability to link various ARC modules in an arbitrarily complex manner permits attacking problems not previously possible.

The system uses a "Datapool," or storage library, which contains all user-supplied input data, the ARC modules, and the data generated by any of the modules during an ARC run. The "Datapool" is kept on a magnetic disc for rapid

[32] See pp. 255–256, "Fundamental Nuclear Energy Research—1966."

access and permanent storage. The user is able to designate which data are to be stored away into the "Datapool" from the current ARC run and which previously generated data are to be retrieved for use during the current run. This capability facilitates the rerunning of previous problems with slight changes in input data, or the running of new problems requiring the results of previous computations, and is one of the most powerful aspects of the ARC system concept.

Transport Theory Burnup Code

A one-dimensional, transport theory [33] burnup code, "DTF-Burn," has been written at the Los Alamos Scientific Laboratory for use on the IBM 7030 computer. This program, which could be readily adapted for use on the IBM 7094, makes use of the variable dimensioning feature of Fortran-IV,[34] so that any problem whose dimensions do not exceed the total available core storage may be run. The code was written especially for fuel depletion analyses of reactor systems, such as large-scale fast power reactors, which require multi-group transport theory for an accurate computation of the neutron flux. For each burnup time interval, the code computes the neutron flux distribution as a discrete ordinates solution of the *Boltzmann* transport equation. With this flux distribution, the code then computes the change in isotopic composition during the interval. Permissible burnup isotopes include uranium-235, 236, and 238; neptunium-239; and plutonium-239, 240, 241, and 242; as well as fission products.

Neutron Absorption Code

The central problem in the design of a nuclear reactor is the calculation of the ultimate fate of neutrons produced by the fission reaction. One of the neutrons produced in each fission must be absorbed in the fuel in fission capture to sustain the chain reaction. The excess neutrons are either absorbed in the reactor components in nonfission capture reactions or escape from the reactor. The equations describing the competing reactions are exceedingly complex; in the past, they have been dealt with piecemeal by a variety of techniques embodied in several computer codes. The "Hammer" system of computer codes, developed as a joint effort of the Savannah River Laboratory and Brookhaven National Laboratory, is a collection of the best of these codes available, linked together with a significant amount of new coding to produce a consistent, complete treatment of the neutron balance equations. Use of the new system requires significantly less effort on the part of the reactor designer, and gives him greater confidence in the results.

THERMAL NEUTRON SCATTERING

In order to accurately predict the nuclear characteristics of a reactor, it is necessary to be able to calculate the neutron population as a function of energy and position inside the reactor. Such calculations require that fundamental data on neutron reaction cross sections with the reactor materials be known. Using these data with a theoretical model, the neutron reaction rates with the various reactor materials can then be calculated.

Rotating-Crystal Neutron Spectrometer

An important part of a thermal reactor, in which most of the fissions and neutron captures take place at low neutron energies (below one electron volt), is the moderating material, which slows down and diffuses the energy of the neutron by virtue of inelastic scattering. From studies at Pacific Northwest Laboratory (PNL) using a new spectrometer developed at PNL (see Figs. II–59 and 60), a better understanding has been obtained of neutron scattering with such moderator materials as light water (H_2O), heavy water (D_2O), beryllium, graphite, and zirconium hydride.

[33] Two types of programs are used for reactor burnup calculations: diffusion theory and transport theory. Diffusion theory is the more approximate and is suitable only for certain types of reactors, while transport theory is more generally applicable.

[34] Special computer programming language.

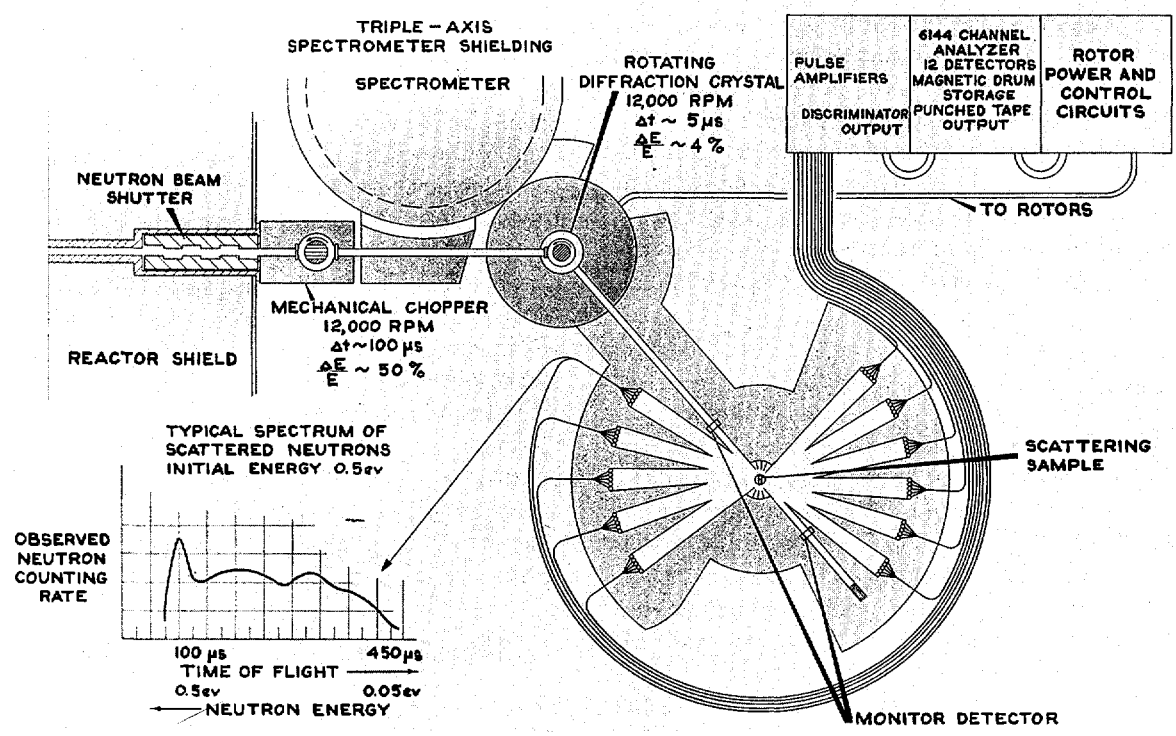

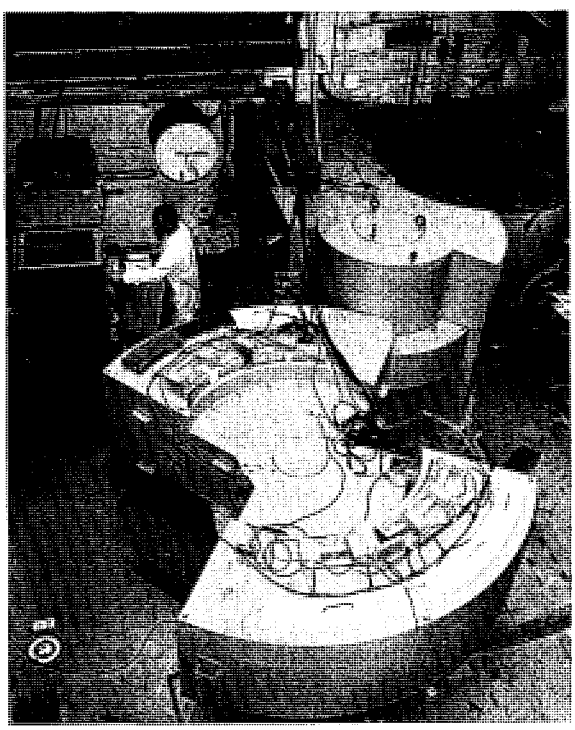

Figs. II–59 and 60. Rotating-Crystal Time-of-Flight Spectrometer. Schematic diagram *above* describes the operation of the rotating crystal spectrometer developed at Pacific Northwest Laboratory. In photo *left*, the spectrometer, which is used to obtain a beam of neutrons of one energy from a source having a wide range of energies, is shown. In the *foreground* is the movable, shielded scattering chamber which contains nine banks of neutron detectors placed around the central sample position. The chamber pivots about the axis of the (shielded) rotating crystal. Data recording and control equipment are in the *left background.*

The neutron spectrometer is a device for obtaining a beam of neutrons of essentially one energy from a source of neutrons having a wide range of energies. This is accomplished by using a crystal that scatters the neutrons of a particular energy or wavelength (monoenergetic neutrons) in a particular direction—scattering neutrons in such a manner from a crystal is called *Bragg* diffraction. In the PNL spectrometer the crystal is rotated, causing it to produce short bursts of monoenergetic neutrons by diffraction. A mechanical device called a chopper

rotates in phase with the crystal to eliminate (chop) virtually all neutrons from the beam except those with the desired energies. The source of neutrons entering the spectrometer is a Hanford production reactor.

The bursts of neutrons from the sample of moderating material under investigation and the scattered neutrons are detected in 12 detectors which cover the range of scattering angles from 15 to 165 degrees. The energy of the scattered neutrons, and hence the energy loss of scattering, is determined by measurement of the scattered neutrons' velocity by time-of-flight.

This spectrometer has proven to be practical from a standpoint of resolution and intensity. It has been used in high resolution studies of neutron scattering from D_2O and H_2O at room temperature, H_2O at –5° C., and zirconium hydride at room temperature. While the interpretation of these measurements in terms of the fundamental energy modes of the systems is still in progress, the significance of the system has been demonstrated in the first clear observation of the first molecular vibrational level of the H_2O molecule at an energy of 0.2 electron volts.

Dispersion Relations of BeO

The slow neutron inelastic scattering program [35] of the Idaho Nuclear Corp. at the Materials Testing Reactor (MTR) in Idaho is directed toward determining the relative numbers of neutrons at different energies in reactors (usually called the neutron energy distribution). This distribution is important because the efficiency of the fission process, and therefore of reactor design and operation, depends on how the neutrons are distributed in energy. Recently, experiments have been conducted in which neutrons are scattered from samples of beryllium oxide (BeO), a promising reactor moderator. These experiments have provided information about the motion of the beryllium and oxygen atoms within the beryllium oxide. Since this motion determines the slowing down rate of the neutrons and the final energy distribution, a better definition of the neutron moderating, or slowing down process, in beryllium oxide is being evolved. From the physicists' point of view, the motion of the atoms are determined when the dispersion relations of the waves moving through the crystal are measured.

The theory which explains the dispersion relation data has evolved from other theories which have been developed at the MTR to explain the motion of the hydrogen and carbon atoms in simple hydrocarbon molecules. The atoms in the crystal of beryllium oxide were divided into molecules of two beryllium atoms plus two oxygen atoms. Then, these beryllium oxide "molecules" were joined to other beryllium oxide "molecules" to form the crystal. This new method of describing crystals as if they are joined molecules has not only been successful for beryllium but for diamond also, and shows great promise for explaining the motions of atoms in other valence-force crystals.

Linear Accelerator Experiments

In a cooperative effort, a Rensselaer Polytechnic Institute (RPI)-Knolls Atomic Power Laboratory (KAPL) team, using a very high resolution scattering analyzer at the RPI linac laboratory, has been conducting continuing studies [36] of thermal inelastic neutron scattering in various reactor moderator materials, including water, metal hydrides, and polyethylene, using incident neutrons in the energy range of 0.1 to 2 ev. The scattering data are corrected for multiple scattering effect (the effect of multiple neutron collisions in the moderator rather than one collision only), and scattering laws for the various materials are then derived from the corrected data. Preliminary scattering measurements also have been made on uranium oxide which extend the phonon frequency spectrum beyond that previously known. It is expected that further careful measurements of this type will be required for the calculation of tempera-

[35] This work was originally started by Phillips Petroleum Co. (see pp. 26–27, "Fundamental Nuclear Energy Research—1965") ; on July 1, 1966, Idaho Nuclear Corp. (a joint venture of Aerojet-General and Allied Chemical Corp.) took over some of the contractural work previously done by Phillips at the National Reactor Testing Station.

[36] See p. 27, "Fundamental Nuclear Energy Research—1965."

ture coefficients, particularly in fast reactors, caused by *Doppler* broadening of nuclear cross section resonances.

The General Atomic Division (San Diego, Calif.) of General Dynamics is also continuing its studies [37] of thermal inelastic scattering of neutrons in moderator materials, using its electron linear accelerator to produce short bursts of neutrons and using a neutron flight path to measure the speed, hence the energy, of the neutrons. Using this technique, General Atomic has measured the scattering from polyethylene at room temperature and zirconium hydride at 420° C., and then used the data to check the accuracy of calculations based on theoretical models. The agreement of measurements and calculations was found to be reasonable except for small scattering angles.

In addition, General Atomic has also studied several experimental measurements of the scattering law for water, from which it has been ascertained that some of the data were strongly affected by multiple scattering and should be corrected accordingly. These studies have determined the circumstances under which meaningful corrections can be made, using theoretical models, and have shown how existing scattering law data can be used to guide the improvement of theoretical models even when the correction for multiple scattering cannot be carried out accurately.

ADVANCED FACILITIES

Research and test reactors of advanced design are required to provide intense neutron sources for neutron beam research and for testing various reactor fuels and materials.

ETR Flux Stabilization

The Engineering Test Reactor (ETR), operated by Idaho Nuclear Corp. for the AEC at NRTS, provides high neutron densities for irradiating specimens for reactor fuel development. To achieve maximum information from these irradiations it is essential that the neutron density remain almost constant throughout an ETR operating cycle (6 weeks, including shutdown time). A program to develop methods of limiting neutron density variations to plus or minus 10 percent is currently being carried out. Recently, a fuel loading with new specifications for uranium and boron was tested in the ETR. The test showed that increasing the uranium (U^{235}) and boron content from the current values of 400 grams and 2.8 grams to 500 grams and 3.8 grams, respectively, will reduce the control rod motion by approximately 60 percent (see Fig. II–61). Since control rod motion is the principal cause of neutron density variations during reactor operation, these variations will be significantly reduced when fuel with the new specifications is used routinely. The new specifications in conjunction with new control rod designs or control methods should make it pos-

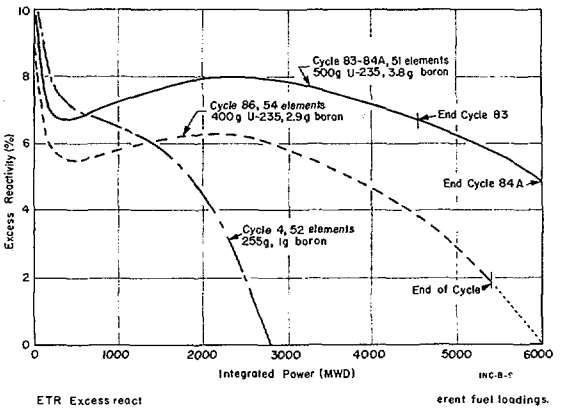

Fig. II–61. ETR Flux Stabilization. To achieve maximum information on specimens being irradiated by the high neutron densities of the Engineering Test Reactor (ETR) at NRTS, it is essential that the neutron density variations be as constant as possible. The Idaho Nuclear Corp. has been testing different fuel loadings for the ETR that will limit the neutron density variation, caused by control rod motion, to plus or minus ten percent during a 6-weeks cycle of operation. The graph shows the ETR's excess reactivity as a function of integrated power for three different loadings. The solid line, at *top*, represents a loading of 500 grams of uranium-235 and 3.8 grams of boron which reduces control rod motion by 60 percent.

[37] See pp. 27–29, "Fundamental Nuclear Energy Research—1965." In October 1967, the Division was purchased by Gulf Oil Corp. and renamed Gulf General Atomic, Inc.

sible to restrict neutron density variations to the desired limits.

When ETR operation began in 1956, the fuel elements contained 255 grams of uranium-235 and one gram of boron. Core loadings of these elements experienced neutron density variations of 100 percent in some cases and would operate for only 16 full-power days. In order to reduce the number of refuelings thereby improving operating efficiency, and to further reduce rod motion, the U^{235} and boron contents were increased to the current values of 400 grams and 2.8 grams. Fuel loadings of these elements experience neutron density variations of around 25 percent and operate for approximately 28 full-power days. The present effort to maintain neutron density variations within plus or minus 10 percent of a specified value by loading with 500 grams of U^{235} and 3.8 grams of boron, was made necessary by the increasing sophistication of the test programs in the ETR.

Proposed Euratom Research Reactor

The Critical Experiments Facility (CEF) at Oak Ridge National Laboratory is being used in a cooperative program with Euratom (European Atomic Energy Community) to fix the design of a pulsed fast research reactor (SORA) which the Ispra, Italy, laboratory of Euratom has proposed for construction. The requirements for SORA—its name is derived from a combination of the first two letters in each of the two Italian words meaning "source" and "rapid"—are that it be able to produce bursts of neutrons of about 50 microseconds duration and that about 50 bursts be produced per second.

The SORA core will consist of closely spaced rods of uranium (or a uranium alloy) arranged so that the cross section of the assembly is hexagonal. Five sides of the hexagon will be surrounded by an iron reflector. The sixth side will be left open so that a separate piece of reflector material (probably beryllium) mounted on a wheel can be rotated at high speed next to the core. As the reflector sweeps by the core face, the reactor will be made supercritical and a neutron burst will occur. The average power of the reactor is expected to be one megawatt, and cooling will be provided by liquid metal circulating through the core.

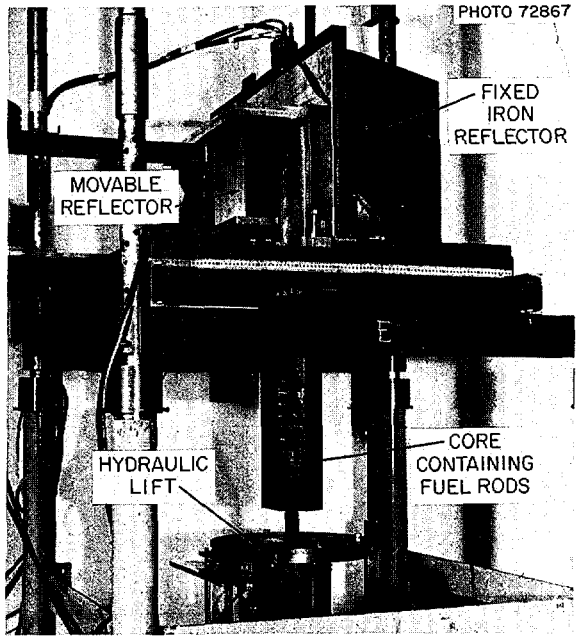

Fig. II–62. Proposed Euratom Research Reactor. The mockup of the proposed SORA pulsed fast research reactor tested for Euratom at Oak Ridge National Laboratory's Critical Experiments Facility has a hexagonally shaped core of iron containing closely spaced uranium rods. Criticality is achieved when the core is raised by a hydraulic lift into the fixed iron reflector on the table above. The iron reflector surrounds five sides of the hexagonal core. In the proposed reactor it is expected that the core will be repetitively "pulsed" by rotating a separate reflector piece at high speed next to the sixth side of the core, causing bursts of neutrons to be emitted. The reactivity effect of this reflector has been measured in the mockup experiments by moving the piece of beryllium (or iron) attached to the end of the arm shown at the *left center* of the photograph.

ORNL's participation in the SORA program consists in performing tests on the mockup of the core and reflector shown in Fig. II–62. The iron components were machined in Italy, and the fuel rods (uranium enriched to 93% in the U^{235} isotope) were supplied by ORNL.

The iron core block used in the mockup can accept as many as 95 of the rods, each of which

is 1.4 centimeters in diameter and 24 centimeters long. In one experiment 58 kilograms of uranium resulted in a critical loading which was very near that predicted by the Reactor Physics Department at Ispra.

Other experiments have shown that the movable reflector will be adequate to produce the desired bursts. Information gained from the tests has included the time behavior of the neutrons; the pulse characteristics of the system; and the effect on the reactivity of varying the size, position, and composition of the movable reflector.

Pulsed Research Reactor Studies

Concepts for high-performance pulsed fast research reactors are under study at Brookhaven National Laboratory. Engineering work and fuel development studies indicate that a fast, liquid metal-cooled reactor developing 60-microsecond bursts with a peak power of the order of 20,000 megawatts (Mw) may be feasible, based on the first fatigue-life tests of a molybdenum matrix cermet fuel. At a repetition rate of 22 bursts per second, the average-out power in such a system would be about 30 Mw. The neutrons generated during the power bursts would provide an intense source for neutron physics research.

Two modes of operation are possible in the pulsed system. In an accelerator-injected pulsed reactor, neutrons are injected in short bursts into the reactor core by an electron-accelerator-driven neutron source, *i.e.*, an accelerator booster, while the reactivity of the core is simultaneously pulsed to a near-critical condition (near critical on prompt neutrons). The magnitude of the burst in a system of this type is limited by the output of the accelerator-driven source.

In the second mode of operation, the reactivity of the reactor could be pulsed to a supercritical condition without injection of neutrons from an accelerator. However, the pulse would be longer in duration, and some kinds of experimental use would be more difficult. In this mode of operation, the burst magnitude would be limited by thermal shock to the fuel element, a result of the sudden increase in temperature experience during a burst.

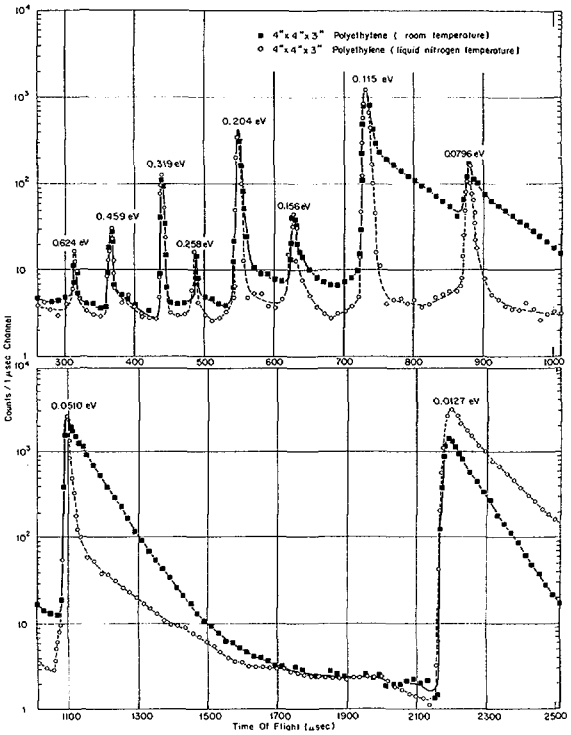

Fig. II-63. Pulsed Test Reactor Studies. Experimental neutron time distribution, as observed with a neutron diffraction spectrometer in an Idaho Nuclear Corp.-Rensselaer Polytechnic study. These distributions were obtained from the surface of a 4″×4″×3″ polyethylene sample and have an equivalent time resolution of 3 to 12 microseconds (μsec). The (0002) planes of a beryllium crystal set at an angle of 45° to the neutron beam were used to select the neutron energies. Time of flight was then used to separate the different energies. A neutron flight path of 3.398 meters was used and 10 energy peaks were observed. The energies of these various orders are labeled at the diffraction peaks. It is of interest to note the dramatic effect on the time distributions when the sample was cooled to liquid nitrogen temperature (—190° C.).

Studies by NRTS and RPI. Studies of the design of pulsed reactor systems for thermal neutron sources are being conducted by the Idaho Nuclear Corp. in collaboration with Rensselaer Polytechnic Institute (RPI), Troy, N.Y. For

time-of-flight neutron spectroscopy, two requirements exist—that the pulse width be narrow and that the average neutron intensity be high. Because of these requirements, experiments have been performed, using the RPI electron linear accelerator, to investigate the design of moderators for optimizing the thermal neutron intensity and pulse width from pulsed fission neutron sources. The results show that pulses as narrow as 11 microseconds of 0.0510 ev. neutrons can be obtained from moderators with peak neutron intensities comparable with any other system tested to date.

Important improvements are gained by maintaining the sample at very low temperatures, as shown in Fig. II–63, where a comparison is made of the intensity-width functions for polyethylene at room temperature and at −190° C. The improvement in pulse width is marked for the cold sample because the room temperature system yields background from one energy to the next.

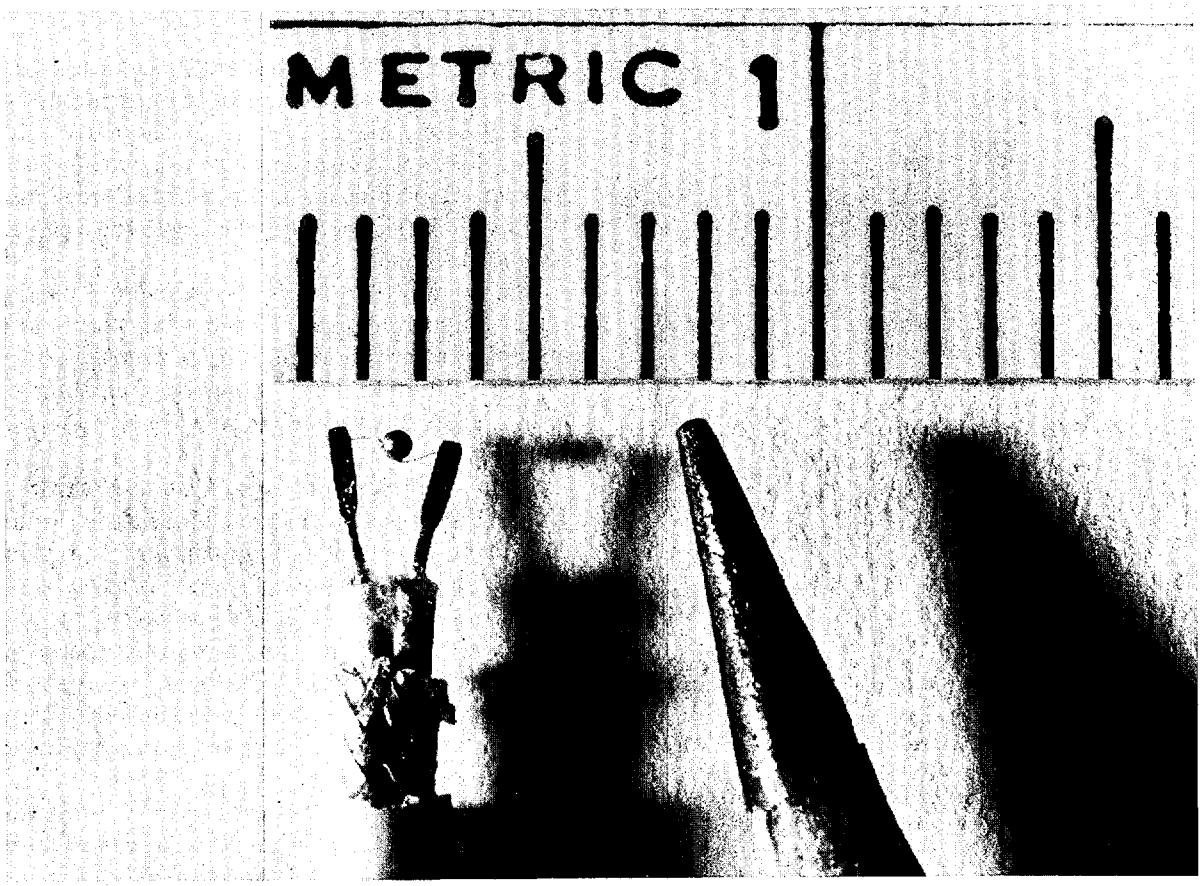

Fig. II–64. Fission Couple. Called a fission couple, a device has been developed at the Los Alamos Scientific Laboratory for measuring very fast neutron flux changes in a reactor at temperatures as high as 1,650° C. without perturbing the flux by the device itself. Shown with a pencil point for size comparison, the fission couple consists of a small bead (about 0.020" diameter) of uranium carbide fissile material attached to the junction of a minute thermocouple. As the neutron flux changes, the fission rate in the bead and, therefore, the heat output of the bead changes correspondingly, causing a change in the output of the thermocouple. (See Fig. II–65 also.)

REACTOR INSTRUMENTATION

Instruments for neutron detection; for the determination of temperature, pressure, and flow rate of coolant fluids; for detecting the presence of chemical impurities in the coolant fluids; and for determining other parameters are essential to the safe and efficient operation of nuclear reactors. The AEC, therefore, sponsors continuing investigations in the field of reactor instrumentation.

NEUTRON DETECTORS

Since knowledge of the intensity of neutron fluxes and the range of neutron energies is needed in the operation and control of nuclear reactors, adequate instrumentation for measuring these parameters must be developed.

Criticality Alarm Systems

A criticality alarm system which meets the most stringent requirements for neutron sensitivity, yet can be used in areas where there are high levels of gamma radiation present, has been developed by Pacific Northwest Laboratory.

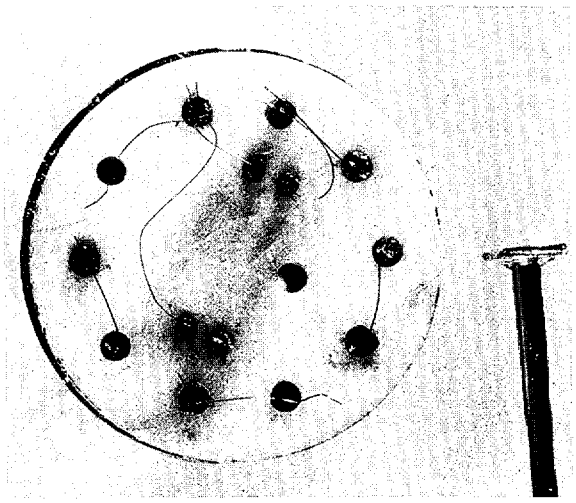

Fig. II–65. Fission Couple for Use in UHTREX. The beads used in the fission couple array shown *above* are "smaller than the head of a pin" shown at *bottom left.* This device, for use in the Ultra High Temperature Reactor Experiment (UHTREX) at Los Alamos Scientific Laboratory, measures neutron flux changes as the uranium-235 beads are heated by fission. The extremely small thermocouples attached to the beads give a fast-response to the change in temperature. Inert beads, placed in series with the uranium beads, eliminate the undesired fraction of the signal generated by the thermal environment and gamma heating.

The total system contains a detector and an electronics package consisting of two alarm circuits and an audit circuit. The detector is a boron trifluoride tube which is made sensitive to a wide range of neutron energies through proper moderation of incident neutrons. The pulses from the detector are amplified and properly shaped for analysis by the alarm circuitry. The primary alarm circuit has an adjustable level so that an alarm can be activated at any pre-set point in the measurement range. The secondary alarm circuit (backup) is not adjustable and is set to alarm at 1½ times the minimum required level. A recorder outlet also is provided for measurement of the neutron levels experienced in case of a criticality incident.

The audit circuitry determines that the total criticality alarm system is functioning properly. Environmental neutrons generated by cosmic rays are continually being counted by the detector. The audit circuit requires that such a background event be registered within a specified time period to prove proper functioning of the criticality alarm system. If the alarm circuitry does not register a pulse within the specified period of time, an instrument failure signal is given. This signal is distinct from the criticality alarm signal.

The capabilities of this instrument are particularly important in fuel processing plants and hot cells, where there may be momentary high gamma radiation levels from the handling of fissile material which could cause a chain reaction.

Fission fragment damage. Pacific Northwest Laboratory has also developed a neutron dosimeter using the fission fragment damage principle. The dosimeter permits neutron dose evaluation in mixed radiation fields, around reactors, accelerators, and plutonium operation and handling facilities. The dosimeter is small, can be easily attached to personnel or equipment, and requires no electrical or other utilities for operation.

Figure II–66 illustrates a typical multifoil dosimeter with four fission foils to provide both dose and neutron energy spectrum measurement. The fission fragments, which are formed when neutrons strike the foil of fissile material, enter the plastic material and cause a damage area or track that can be seen using a microscope after etching with hot caustic solution (6-normal sodium hydroxide at 70° C.). Freedom from track fading, environmental influences, and insignificant beta and gamma radiation sensitivity are major assets of this neutron dosimeter.

Spark Counter Neutron Detector

A neutron detector capable of operating in large neutron flux and at fairly high temperatures is being developed at the Georgia Institute of Technology, Atlanta. The work, which is only in the initial stages, is intended to provide a simple, mechanically rugged neutron detector which can be used in nuclear reactors and in reactor-powered space vehicles. It is based simply on the counting of spark discharges in a series of concentric spark gaps in a compact,

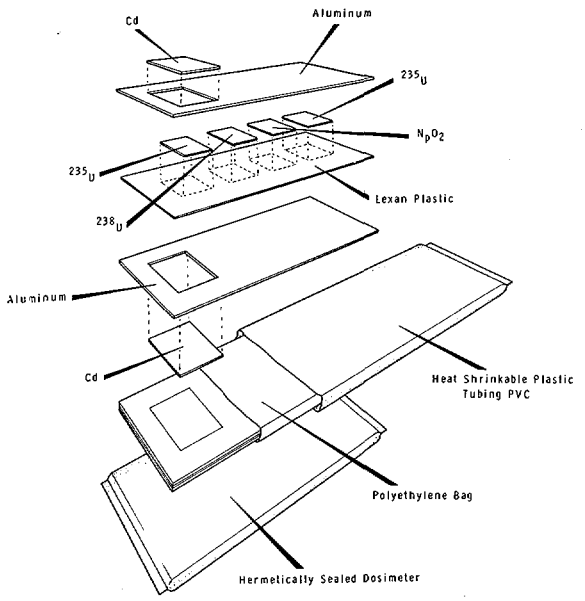

Fig. II–66. Prototype Neutron Dosimeter. A small, pocket-size, ¼-inch thick dosimeter has been developed by Pacific Northwest Laboratory to permit neutron dose evaluation in mixed radiation fields. The dosimeter, which is 3¼ inches long and less than an inch wide is sealed in heat-shrinkable plastic tubing. The four foils contain small amounts of fissile material and are attached to the aluminum plate with epoxy resin. The shrinkable plastic tubing prevents any leakage from the foils.

gas-filled cylindrical assembly which is designed for ultimate insertion into a reactor. Such a detector will provide a valuable means of monitoring neutron fluxes under conditions where most alternative detectors are unreliable or inadequate.

Neutrons interact weakly with most gases, but if they impinge on a boron-containing material they cause the ejection of alpha particles that are capable of creating ions in any surrounding gas. The detector under development consists of a cylindrical tube containing a series of parallel spark gaps, ⅛- to ¼-inch wide, formed between a row of concentric large and small metal washers. Between each pair of washers are disks of boron nitride to convert passing neutrons into alpha-particle emission which will trigger the passage of sparks across the neighboring spark gap formed by the nearest pair of washers. The whole counting assembly is filled with an inert gas, such as helium or argon, with a small organic additive to facilitate spark formation at moderate applied voltages.

Such a system is very rugged and provides large output pulses which can be counted without further amplification; it is expected that it can be operated at fairly high temperatures. In addition, its sensitivity is low enough that it may be used in regions of high neutron density, such as inside a nuclear reactor, without suffering serious overloads.

Two types of detectors have been constructed and tested in a neutron flux of about 10 million (10^7) neutrons per square centimeter per second and an efficiency of 10^{-7} counts per incident neutron has been obtained under varying experimental conditions. Tests of the performance at elevated temperatures are in progress.

Fast Reactor Neutron Spectrometers

Two unique neutron spectrometers for measuring the energy of neutrons are being developed at the IIT Research Institute in Chicago, Ill. These devices are capable of measuring the energy spectra of neutrons from fast reactors with substantially greater accuracy than other existing devices. In the development of fast reactors, much more detailed knowledge of the neutron spectrum is required than for the slow, or thermal,[38] reactor.

The first of these two neutron spectrometers is intended to operate over a range of neutron velocities from 280,000 to 2,800,000 meters per second (1,000 to 100,000 electron volts in energy). This instrument has demonstrated an ability to operate in an environment in which the ratio of gamma rays to neutrons is 10 times greater than that which can be tolerated by other instruments.

The second instrument operates over the range of neutron velocity from 2,800,000 to

[38] The operation of a thermal reactor depends on the presence of neutrons whose velocity is 1,400 meters (4,593 ft.) per second, in contrast to the greater than 280,000 meters (918,624 ft.) per second velocity for the neutrons in fast reactors.

28,000,000 meters per second (from 100,000 to 10,000,000 electron volts in energy). It offers an even greater improvement—100 times better—in the ability to measure neutron spectra without distortion from gamma rays.

It is expected that these two instruments will play a substantial role in the accurate measurement of neutron spectra in fast reactors, and hence will contribute significantly to their development.

Proton-recoil neutron spectrometer. An in-core neutron spectrometer based on observation of the readily detected recoil of protons (hydrogen nuclei) bombarded by the neutrons has also been under development at Argonne National Laboratory for some time. This instrument successfully discriminates between gamma rays and neutrons, and its development has reached a point where it is yielding quite useful information about neutron energy spectra, such as shown in Figure II–67.

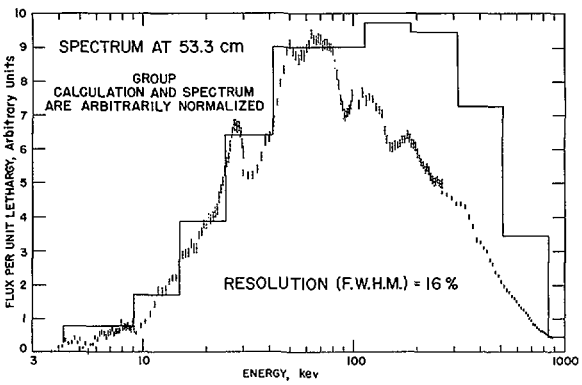

Fig. II–67. Proton-Recoil Neutron Spectrometer Results. The number of neutrons crossing a fixed area in a fixed time and having a fixed (percentage-wise) interval of energy is shown *above* in terms of energy. Argonne National Laboratory has developed an in-core neutron spectrometer that successfully discriminates between gamma rays and neutrons. The solid line in the chart is a calculated result; the points are measurements obtained with the neutron spectrometer that operates on a proton-recoil principle. The resolution (full-width at half maximum) refers to the spread in energy of the spectrometer. Details of the measured spectrum extending over an energy region that is small compared to 16 percent of the energy in question cannot be resolved.

PROCESS INSTRUMENTATION

Because of inability to withstand high temperatures and pressures, irradiation, and corrosive conditions, conventional instruments cannot be used for measuring operating variables inside liquid metal reactors. However, acoustic energy can be generated by transducers outside the radiation shield and transmitted into hot areas through solid acoustic probes which are insensitive to the extreme conditions. Probes can be hermetically sealed into pressurized vessels by means of special mounts, while read-out of acoustic effects can be made at locales removed from the prohibitive conditions.

Incipient Boiling Detector

Liquid metals such as sodium and potassium, are prone to superheat, *i.e.* to become heated above the boiling point without release of vapor. Any of several circumstances can promote sudden release of the superheat energy as an explosive vaporization. This can cause erratic operation of the reactor, whose design assumes that the core-coolant channels are always filled with molten metal—a much better heat-exchange medium than its vapor. Resultant local overheating can cause core burnout.

An instrument which will indicate the proximity to boiling is being developed by Aeroprojects Incorporated, West Chester, Pa. This instrument, the incipient boiling detector, whose sensing probe is placed in a typical critical location in the reactor, gives a readout signal which combines local conditions of pressure and temperature. After proper calibration, the readout information indicates proximity to boiling in degrees F. The difference between this temperature and that shown by the usual temperature indicator (which does not integrate pressure) is a measure of the degree of superheat. A test instrument has been calibrated in molten metal, and preparations for testing in a dynamic loop, simulating actual operating conditions, are in progress.

The operation of the instrument is based on the fact that when a liquid is irradiated with ultra-high frequency sound waves, cavitation will occur in the liquid. Cavitation is the rapid expansion and contraction of minute vapor bubbles in the liquid resulting from the alternate rarefactions and compressions produced by the passing ultrasonic wave.

The collapse of these bubbles produces a white noise[39] which may be detected by suitable microphone-type sensors placed at suitable remote positions on the acoustic system which transmits the ultrasonic power to the liquid. Since the boiling process itself consists of the production of vaporous bubbles, the ultrasonic power required to produce cavitation is theoretically zero at the boiling point. If the power required to produce cavitation threshold conditions (as shown by zero cavitation noise) is measured at various temperatures, a calibration curve can be made, and since the threshold varies directly with local pressure as well as indirectly with temperature, this curve represents the proximity to boiling as a function of two variables simultaneously.

Flowmeter for Molten Metals and Salts

The use of molten metals and fused salts in nuclear reactors has pointed up the necessity of development of an ultrasonic instrument for measuring the flow rate of molten liquid through conduits of these systems. Such a flowmeter is being developed by Aeroprojects, Inc., West Chester, Pa. Conventional instrumentation is automatically precluded by design and safety requirements such as hermetic sealing, fabrication of the instrument from the metal used in the reactor, non-restriction of the flow channel, and operation at high temperatures.

Sealed-in acoustic transmitters and receptors capable of withstanding the severe conditions can be mounted by means of side entries which permit unrestricted flow. The operating concept involves transmission of an ultrasonic signal from the transmitter probe through the moving liquid. This signal is received by two receptor probes placed equidistantly upstream and downstream from the transmitter. By determining the time interval between reception of the signal by the downstream and by the upstream receptors, the rate of flow may be calculated. A prototype instrument has shown the feasibility of flow measurement in a test loop using water as the simulant liquid.

[39] Noise which covers very wide frequency bands, *i.e.*, has constant power per unit band-width.

Fluidic Temperature Sensor

The efficiency, lifetime, and, to some extent, safety of nuclear power sources which use gases and/or vapors as the working fluid, are dependent upon temperature control of the working fluid. The temperature of this fluid is a critical factor in the operation of the nuclear powerplant. Conventional temperature sensors, such as thermocouples and resistance thermometers, are susceptible to radiation effects and high temperature environments. Thus, the recent development of a new, highly accurate and reliable temperature sensor capable of operating with high temperature fluids is of vital interest to the AEC.

The Marquardt Corp., Van Nuys, Calif., has successfully demonstrated the operation of a new concept in fluid temperature sensing, a fluidic temperature sensor. This sensor was specifically designed for operation in a high radiation environment and with high temperature gases and/or vapors. This highly reliable temperature sensor has no moving parts (fluidics) and employs no electronics. It senses the temperature of the fluid and generates an output pressure signal proportional to the fluid temperature (see Figs. II–68 and 69). The fluidic elements are similar to electronic elements except that the temperature sensing functions are accomplished by the flow of gas or vapor in small passages rather than by electrons in electrical conductors.

The fluidic temperature sensor consists of an oscillator, a beat frequency detector, a frequency converter, and a power stage with an integrator. All of these functions are performed

by gas or vapor flowing in fluidic elements. The oscillator is a sophisticated type of whistle based on acoustic resonance principles, and is used as the temperature sensitive element to generate a frequency which is a function of the fluid temperature (gases and/or vapors). The beat frequency detector compares the oscillator output frequency to a reference frequency to generate a frequency difference signal. The output of the beat frequency detector is filtered to eliminate noise and is then converted to an analog output pressure signal in the frequency converter. The operation of this sensor concept was demonstrated with air as the working fluid and exhibited an error of less than $\pm 1/2$ percent.

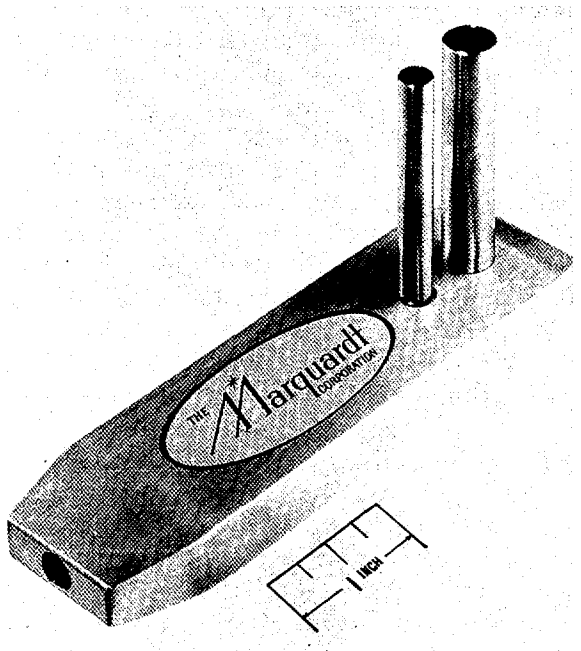

Carbon Meter for Liquid Metals

United Nuclear Corp., Elmsford, N.Y., has developed a meter to provide a continuous measure of carbon activity in flowing sodium. Changes in the carbon activity of the sodium are reflected in the rate of carbon delivery by the probe within less than 1 minute. The meter is expected to be used in liquid metal-cooled fast breeder reactors and also in laboratory studies of carbon transfer by liquid metals. The subject is of practical importance because sodium can change the carbon content of the structural materials it contacts sufficiently enough to impair their mechanical properties, particularly the ductility. The work has progressed far enough to show that the meter responds quickly and positively to small increases in carbon activity at a level low enough to give a sodium system operator ample warning before significant carburization of stainless steel components can occur.

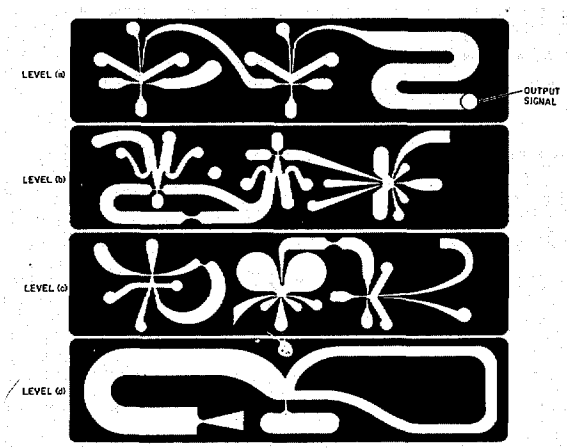

Figs. II–68 and 69. Fluidic Temperature Sensor. The fluidic temperature sensor developed by The Marquardt Corp., Van Nuys, Calif., is designed for installation inside a high temperature nuclear gas or vapor line. The sensor can be used in high nuclear radiation environments. A sample of the fluid whose temperature is to be measured is extracted by the inlet port (opening at the left) of the sensor shown in *left* photo. The fluid sample flows through the temperature sensor and back to return (larger tube on the right). As the sample flows through the sensor, a pressure signal is generated by the temperature sensor which is proportional to the fluid temperature. This pressure signal is supplied by the readout tube (smaller tube). No other source of power except the energy in the fluid itself is being used in the operation of this device. The internal construction of the sensor, as shown above *right*, is analogous to a solid state electronic circuit. The sensor consists of four layers (levels) of active fluidic elements and three interconnection manifolds (not shown). The heart of the sensor is an acoustic oscillator or whistle whose resonance frequency changes with fluid temperature. The fluidic elements operate on gas flow to various functions such as frequency generating, beat frequency detection, integration, etc., necessary to generate the output pressure signal.

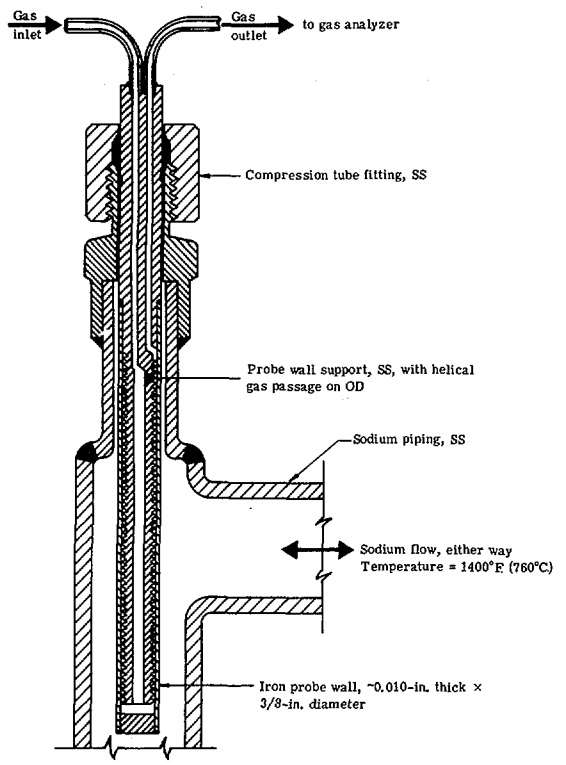

Fig. II–70. Carbon Meter Probe. Shown is the sensing element of a meter, developed by the United Nuclear Corp. at Elmstford, N.Y., which continuously measures the carbon activity (carburizing potential) of a sodium stream. Decarburizing gas maintains a very low carbon activity at inner surface of the iron wall. Carbon from the sodium diffuses through the wall, reacts with the gas, and is carried to a remote gas analyzer. The carbon content of the gas stream is proportional to the carbon activity in the sodium.

The meter sensing element, shown in Figure II–70, is a thin-walled iron tube, no larger than a cigarette. Carbon from the sodium diffuses through the wall at 1,400° F. (760° C.) and reacts with a decarburizing gas (argon +½% water vapor +5% hydrogen) inside the tube. The carbon content thus produced in the gas stream is first converted to methane; it is then continuously measured with a flame ionization detector and related to the carbon activity in the sodium.

The detector is stable and extremely sensitive. It can readily measure carbon arriving in the gas at the rate of eight billionths (8×10^{-9}) of a gram per minute. A typical carbon meter probe immersed in clean sodium circulating in a stainless steel loop delivers carbon to the detector at the rate of 70×10^{-9} (70 billionths) gram per minute. If this rate is increased to 2.4 micrograms (2.4 millionths of a gram) per minute by bleeding a little carbon activity into the sodium, type 304 stainless steel adjacent to the probe carburizes at the rate of 55 micrograms per square centimeter in 2.5 hours. This amount of carburization is not detectable with a microscope and does not significantly impair the structural integrity of the steel. In high carbon sodium, the rate of carbon delivery by the probe is in excess of 30 micrograms (30 millionths of a gram) per minute. Stainless steel surfaces exposed to such sodium are heavily carburized and completely embrittled in a few hours. One probe has been operated at 1,400° F. (760° C.) in high carbon sodium for 2 months, during which it passed more than two carbon atoms for each iron atom in the probe wall.

Digital Computer for the UHTREX

An important step toward reducing the probability of human error in reactor systems has been taken at the Los Alamos Scientific Laboratory by incorporating a digital computer in the Ultra High Temperature Reactor Experiment (UHTREX) system, a gas-cooled graphite reactor operating at 2,400° F. (1,300° C.). The computer has been programmed to automatically perform a variety of recordings, checking, calculating, and operating functions. It records some 80 system temperatures and pressures each hour and makes other special logs on demand from the operator, as well as checking over 600 system temperatures and pressures every 15 seconds. If any one of these temperatures or pressures is too high, a complete record of the event is typed and an alarm is sounded. The computer checks the position of all valves in the system each second. It types a record of all valve position changes and will sound an alarm if a valve position changes in such a way as to endanger any part of the system. The computer is also in charge of the fuel loading process. It opens and

275–845 O—68——14

closes valves in a prescribed sequence to load fuel when requested to do so by the operator, and keeps a complete fuel history. Provision has been made for computer control of reactor coolant flow rates, temperatures, and power. Thus far, the computer has been quite reliable; it is felt that the system will contribute significantly toward the recording of better data from the reactor experiment and will help to operate the reactor system smoothly, efficiently, and safely.

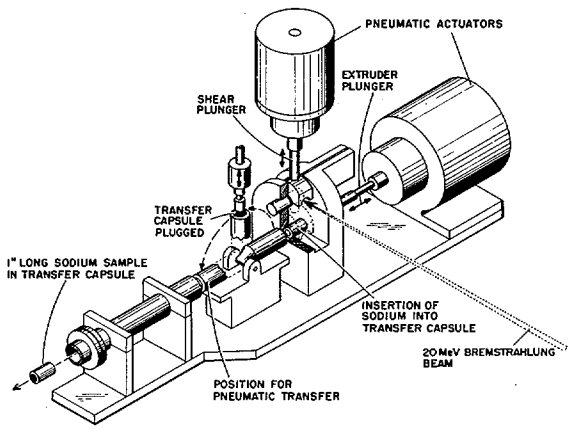

SODIUM EXTRUDER FOR GAMMA-N ACTIVATIONS

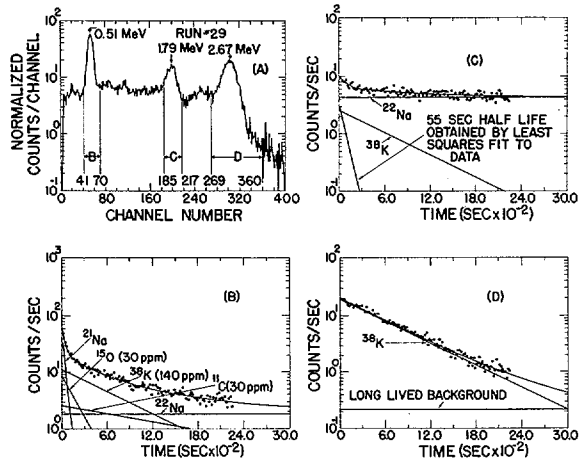

Figs. II–71 and 72. Photon Activation Analysis for Oxygen and Carbon in Sodium. At the Los Alamos Scientific Laboratory, techniques have been developed for detecting oxygen (O) and carbon (C) impurities in sodium (used as a coolant in some nuclear reactors) down to one part per million by photon activation analysis. The O^{16} (γ, n) O^{15} reaction is induced in the sample shown in the apparatus at *left*. Radiation emitted by O^{15} is detected to measure the amount of O present in the sodium (Na) sample. Immediately after the termination of the 5-minute irradiation, the sample is sheared out of the sealed tube and extruded into an unactivated plastic capsule, and counting is started within 40 seconds. The charts *above* show the results of a photon activation analysis of impurities in sodium by measuring the decay products of radioactive O^{15} and C^{11} produced by irradiating the sample with gamma-ray photons. The gamma-ray spectrum of an activated sodium sample is shown at *A*. Unfolded decay curves for peaks *B*, *C*, and *D* are given in the corresponding charts. Peak *B* results from O^{15} and C^{11}, although Na^{22} and potassium (K^{38}) also contribute to it. Peak *C* results from Na^{22}, and peak *D* results from K^{38}. The intercept of each line at zero time (the end of the irradiation) is proportional to the amount of that isotope present in the sample.

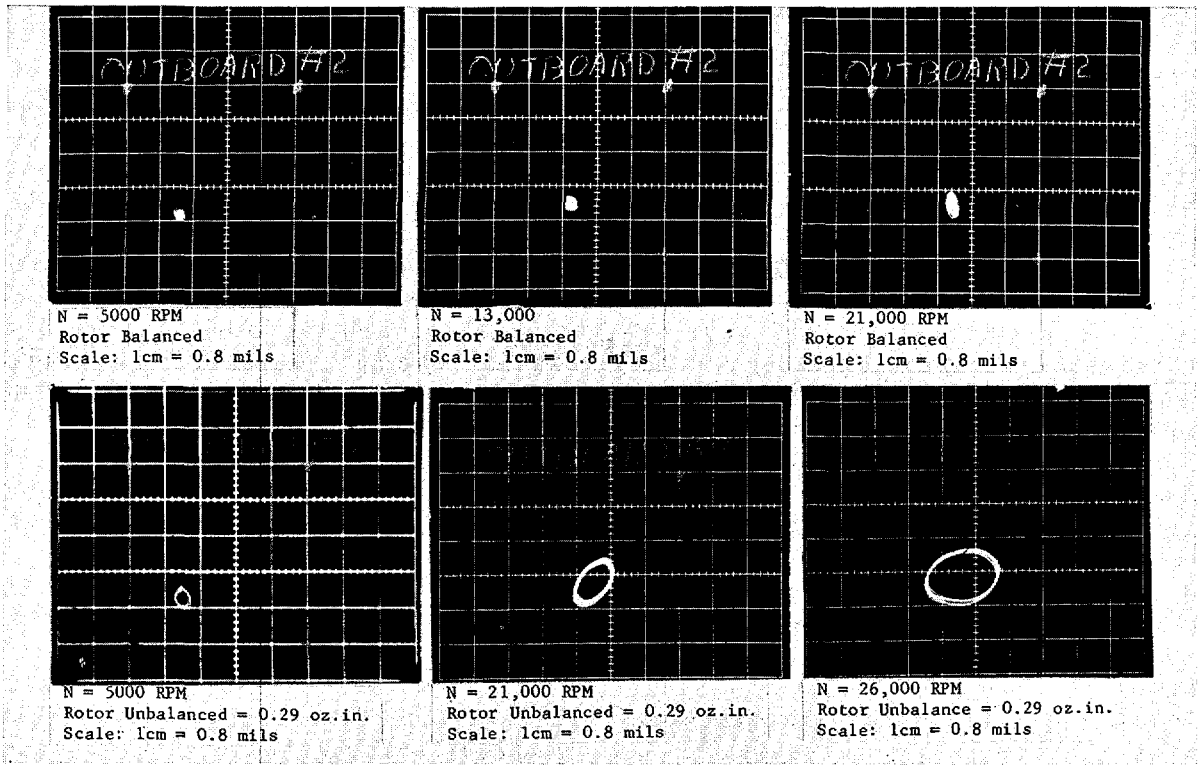

Fig. II–73. Liquid Metal Bearing Test Results. These Mechanical Technology, Inc., photos show the motion of a liquid metal (sodium-potassium) bearing-rotor as measured by a pair of orthogonally mounted capacitance probes. The probe signals are amplified, linearized and transmitted to the x and y axes of a dual beam oscilloscope. The three top panels show the very small motions of the rotor center at different speeds, when the rotor is fully balanced. The three bottom panels show the orbit of the rotor center at various speeds under the indicated mechanical unbalance. At the top speed of 26,000 r.p.m., the rotor unbalance used in this case (0.29 oz. inches) is equivalent to a rotating force of approximately 174 lbs. on each 2-in. diameter × 2-in. long bearing, *i.e.*, to a unit load of 43 p.s.i. Under this load and speed, the rotor whirls in the bearing, with an orbit whose major diameter is approximately 0.0016 inch (1.6 mils). These tests were conducted in sodium-potassium (NaK) with a bearing diametral clearance of 4 mils (see p. 196).

HEAT TRANSFER AND FLUID DYNAMICS

Intimate knowledge of the laws governing heat transfer and fluid dynamics is essential to the design and construction of nuclear power reactors. Hence, the AEC has a continuing interest in research in these important fields.

HEAT TRANSFER STUDIES

Since nuclear power reactors basically are heat engines intended to convert heat from fissioning atomic nuclear energy into electric power by means of turbines, investigations are being conducted to add to the body of knowledge on transfer of heat in fluids and solids.

Nonuniform Heat Generation Program

Because nuclear reactors are such a compact source of power, more knowledge about the limitations on the rates of heat transfer from channel walls to flowing liquids is necessary for efficient design. This limitation is called critical heat flux, and its predictability is based upon

experience rather than theory. The Babcock and Wilcox Co., Lynchburg, Va., has contributed to this experience by operating electrically heated, water-cooled channels at sufficiently high rates of heat transfer to determine the limitations for several pressures, flow rates, and water temperatures. The principal interest in this particular work was the distribution of the heat transfer rate along the length of the channel, which was varied so as to be similar to that found in nuclear reactors. In addition to a uniform distribution of heat transfer rate (tested for reference), three other distributions were tested with maximum heat transfer rates: (*a*) near the middle of the channel, (*b*) near the entrance of the channel, and (*c*) near the exit of the channel. It was found that the heat transfer performance of the channel was lowest when the maximum rate was near the exit of the channel. The relative performance of the other distributions depended upon the various combinations of pressure, flow rate, and water temperature.

The channels with the various heat-transfer rate distributions previously described were tubes with an inside diameter of 0.446 inch and a length of 6 feet. Following these, there were experimental annular channels of the same length, constructed so that the annular flow channel had an inside diameter of 0.607 inch and an outside diameter of 1.053 inches. The heat rate distributions here were uniform on the inside diameter, and either uniform or distributed with the maximum near the middle of the length on the outside diameter. The fluid conditions in all these tests covered the power reactor ranges from the BWR (boiling water reactor) to higher pressure PWR (pressurized water reactor) types. The pressures were 1,000, 1,500, and 2,000 pounds per square inch absolute; the flow rates, expressed as mass velocity, were 0.5, 1.5, and 2.5 millions of pounds per hour per square foot; and the water temperatures at the channel inlet ranged from 200° C. to 325° C.

Two-Phase Flow in Multirod Geometries

An investigation of two-phase flow (flowing mixture of vapor and liquid) in complex coolant channels is being conducted by the General Electric Co., San Jose, Calif.[40] One result of the investigation is the revealing of patterns of redistribution of the liquid phase during boiling.

The coolant channels used in this investigation are characteristic of many current nuclear reactors. The nuclear fuel is in the form of square arrays of rods, arranged in parallel assemblies and held apart from one another by means of "spacers." The coolant flow is parallel to these rod assemblies in the spaces between the rods, and is bounded on the outside of the assemblies by channel walls. In the process of cooling, boiling of the coolant takes place and the coolant becomes a mixture of liquid and vapor.

One important question to which an answer is being sought is: how does the liquid phase redistribute itself during the boiling process? The results of tests run with steam-water at 1,000 p.s.i.a. in a 9-rod channel show that when the quality, *i.e.*, the ratio of steam mass rate to total mass rate, is less than about 20 percent, then the local quality in the corner of the channel is less than the channel average. For example, if the average channel quality is 15 percent, the local quality in the channel corner is about 5 to 10 percent. On the other hand, if the channel's average quality is greater than 30 percent, the local quality in the corner is greater than the average; *e.g.*, at an average quality of 31 percent, the local corner quality is 35 to 40 percent. These results are particularly significant since, in the case of square arrays of uniformly heated rods being tested for critical heat flux,[41] the critical heat flux is known to occur first in the corner of the channel.

Heat Transfer Through Rod Bundles

In conventional liquid-metal, shell-and-tube heat exchangers, there are regions on the shell side where the liquid metal flows at various angles across the tube bundle (see Fig. II–76). Years ago, heat transfer measurements were

[40] See pp. 289–290, "Fundamental Nuclear Energy Research—1966."

[41] Limit of heat transfer under boiling conditions.

made for 90° cross-flow of liquid metals, where only the test element was heated. However, it has been a controversial point among design engineers as to whether the results were representative of a commercial exchanger where all tubes are heated or cooled equally. A study was recently completed at Brookhaven National Laboratory, from which it was concluded that, in general, the results can indeed be applied to a commercial exchanger where heating or cooling is equal for all tubes. The investigation was carried out in the low-flow range, where any differences would be magnified. The test section consisted of a bundle of ½-inch o.d. (outside diameter) electrically heated rods enclosed in a rectangular shell. The rods were arranged vertically in an equilateral triangular pattern and NaK (sodium-potassium alloy) flowed through them in the horizontal direction.

Figure II–74 shows the experimental results when only the test rod was heated, while Figure II–75 shows them when all the rods were heated. In the figures, the *Nusselt* number [42] is proportional to the heat transfer coefficient and the *Peclet* number [42] is proportional to the flow rate. The spread in the curves in each figure is normal and shows the effect of rod location on the heat transfer coefficient. A comparison of the two sets of curves shows that, at the higher flow rates, the heat transfer coefficient is not dependent on whether all the rods are transferring heat to the flowing NaK. On the other hand, at the

[42] *Nusselt* and *Peclet* numbers are dimensionless groupings of system parameters in heat transfer and fluid dynamics used for correlation and characterization purposes.

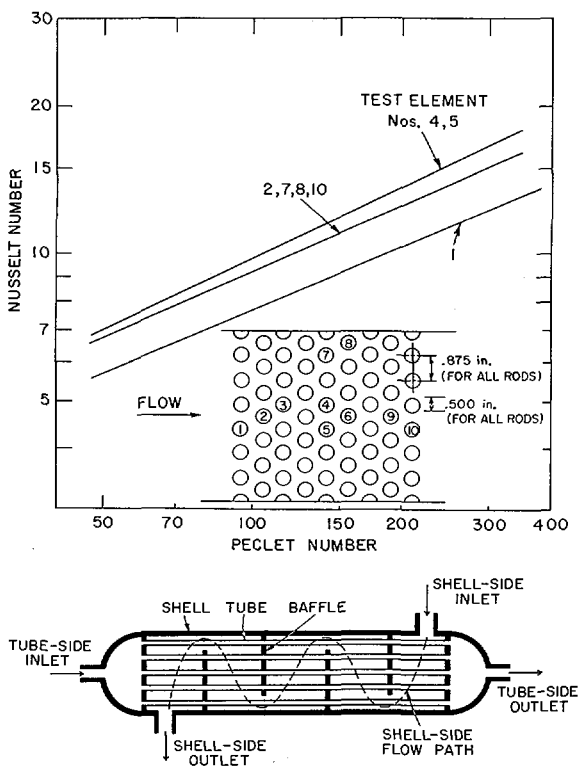

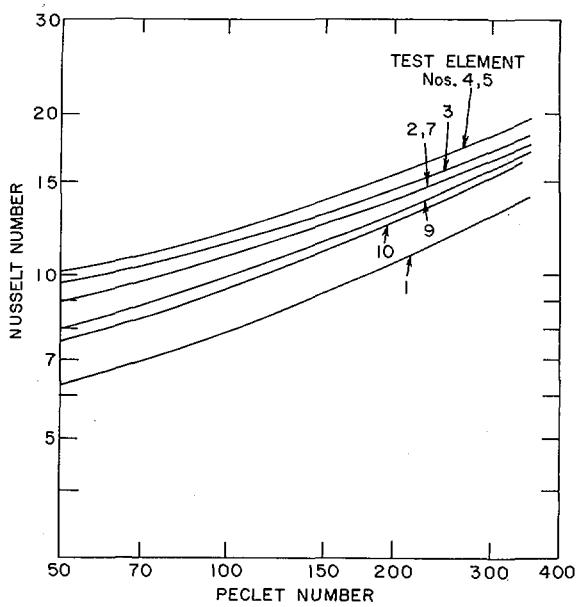

Figs. II–74, 75, and 76. Heat Transfer to NaK Flowing Through Rod Bundles. Chart, *above left* shows the heat transfer characteristics of sodium-potassium (NaK) for a flow 90° across a staggered rod bundle with only the test element heated. Chart *above right* shows same information for the condition of equal heat rates on all rods. Test element locations for the Brookhaven National Laboratory experiment are also shown in *left* figure. Comparision of these two figures shows that as the flow rate is increased, heat transfer coefficients obtained under condition where only the test rod is heated approach those obtained under condition where all the rods are heated until, at a sufficient flow rate they are both the same. This means that experimental data obtained under the first condition can often be used to design commercial heat exchangers. The schematic diagram *at left* is a conventional liquid-metal shell-and-tube heat exchanger; the dotted line shows the shell-side flow path.

lower flow rates, the coefficients are significantly higher when all the rods are heated. However, for the flow rates normally encountered in liquid-metal heat exchangers, it may be concluded that experimental results, obtained where only the test rod is heated, are directly applicable to commercial exchangers, where all tubes in the bundle are transferring heat.

In a related study, it was found that when the liquid metal flows through the rod bundle at 45° rather than 90° the heat transfer coefficients are reduced by about 25 percent.

Boiling-Inception Superheats

In the operation of fast breeder reactors which use alkali metals as coolants, it is of prime importance to know the conditions under which the coolant might inadvertently boil, should there be a flow stoppage or sudden insertion of reactivity. Preliminary tests with pool boilers and small loops have shown that alkali metals sometimes attain very high superheats (above saturation temperature) before inception of boiling. The subsequent vaporization then tends to occur "explosively" with sudden generation of large amounts of vapor, accompanied by large oscillations in fluid temperature and pressure. Brookhaven National Laboratory is currently studying this phenomenon of inception superheat.

A large-scale pumped loop has been used to measure boiling-inception superheats in potassium. The test section used for these first experiments was a 12-inch-long nickel tube, 0.300-inch i.d. (inside diameter). Fluid temperatures were measured at inlet, within the test section, and at the exit. Absolute pressures were measured at inlet and exit. Results showed that substantial superheats (of the order of 17° to 90° C.) were indeed required to initiate boiling. There appeared to be a slight but noticeable time (or history) effect. In a series of sequential runs under the same condition, boiling initiation superheats appeared to increase with time. In a series of runs with decreasing pressures between runs, the measured superheat increased as pressure decreased. This is in agreement with theoretical predictions. These data are shown in Figure II–77. No effect of inlet subcooling could be detected. The measured superheat stayed essentially constant (within experimental accuracy) while inlet subcooling increased from 1° to 55° C.

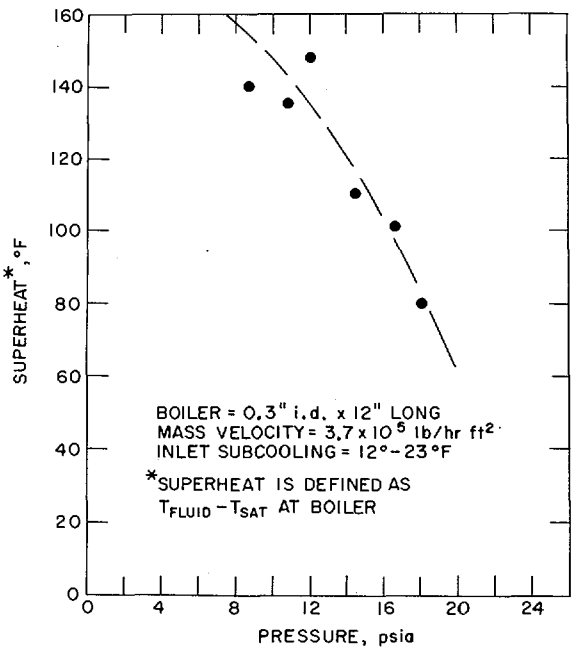

Fig. II–77. Boiling Inception Superheats. Chart shows Brookhaven National Laboratory's experimental measurements of boiling-inception superheats for forced-convection flow of potassium. The experiments were performed in a Haynes-25, pumped loop. Inception points were obtained at pre-set flow rates, pressures, and inlet subcoolings by incremental increases in heat flux in test section. The results agree with theoretical predictions that boiling can be initiated more easily (with lower superheat) at higher operating pressures.

Superheat research at ORNL. Experimental studies on the characteristics of boiling alkali metals are also continuing at the Oak Ridge National Laboratory (ORNL) with emphasis on the superheat (temperature in excess of the boiling temperature) required to initiate bubble formation with potassium on various surfaces (see Fig. II–78). Knowledge of the superheat is pertinent to the prediction of design performance and safety of alkali-metal-cooled nuclear reactors for space-power systems or for fast breed-

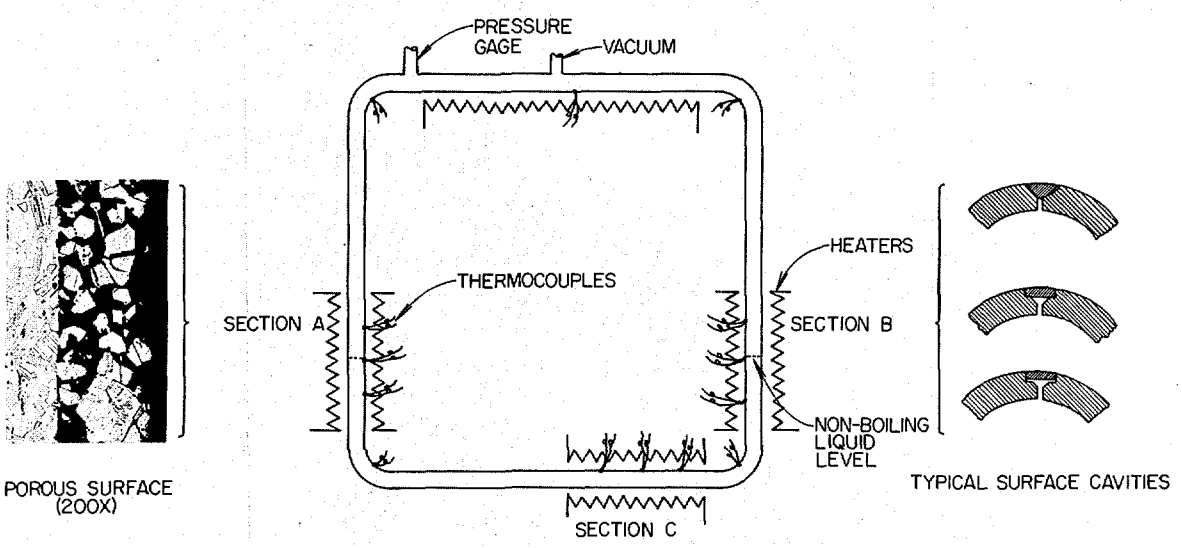

Fig. II–78. Superheat Boiling Initiation Experiment. A natural-circulation loop in which the test fluid is boiled in one vertical leg and condensed in the opposed vertical leg has been used at the Oak Ridge National Laboratory to determine the superheat (excess of the wall temperature over the boiling temperature) required to initiate boiling with sodium and potassium. This apparatus is so arranged that the surfaces labeled *A*, *B*, and *C* can be independently studied. Thus, the characteristics of *Section A* (a porous surface, with an average pore size of 0.002 in., shown at 200× in the *left* inset) can be examined by heating this region while cooling the opposite leg. In turn, the performance of *Section B* containing surface cavities (0.006-in. diameter cylindrical holes, of shapes shown in the right inset, arranged at 1-inch separation in two diametrically opposed rows of four holes) can be determined by reversing the situation—*i.e.*, by heating *Section B* while cooling *Section A*. *Section C* (a smooth, as-received tube) can be tested by rotating the loop 90 degrees so that this leg now assumes a vertical orientation. Heat fluxes up to 20,000 B.t.u. per hour per square foot can be achieved.

ing. Earlier results on smooth surfaces showed superheats to be so high (130° to 240° C.) as to cause explosion-like release of the stored energy when a bubble finally forms, with attendant severe oscillations in tube wall temperatures and boiler pressures. This, in turn, may lead to the introduction of voids through coolant expulsion from the channel and cause severe thermal and/or nuclear transients with subsequent core damage. Modification of the surface (either with a thin, porous coating or with discrete, small-diameter holes) results in 10- to 40-fold reductions in the superheat (see Fig. II–79) and also significantly diminishes the magnitude of the wall temperature oscillations (see Fig. II–80). Some instability in the performance of the porous surface suggests that the use of discrete holes in the surface is preferable to the use of a porous surface.

Boiling-Sodium Heat-Transfer Facility

Fluid flow and heat transfer characteristics of boiling-sodium coolants are being investigated in a new 2,100° F. (1,150° C.) experimental facility designed at Argonne National Laboratory. Test data acquired with the metal liquid-vapor mixtures in this loop are essential for designing efficient and safe cooling systems for central station fast-reactor power plants, as well as for *Rankine*-cycle[43] systems for generating power for use in space. Except for nuclear radiation, the new test facility simulates the conditions (pressures, temperatures, and heat flows) that eventually will be attained in a single fuel channel in such advanced reactors.

[43] In the *Rankine* cycle, the liquid metal is converted to vapor by heating and the vapor used to turn a turbogenerator to produce electricity.

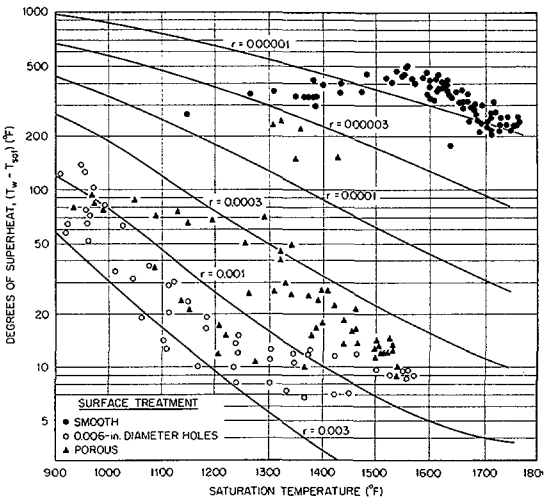

Figs. II–79 and 80. Superheat Boiling Initiation Measurements. The superheats required for boiling initiation with liquid potassium in natural circulation on treated surfaces (porous or 0.006-inch-diameter holes) are compared in the *above* Oak Ridge National Laboratory chart with earlier data for smooth surfaces (solid dots on chart). While the porous surface (*triangles*) was less effective than the surface with discrete holes (*open circles*), both surfaces cause substantial reductions in the superheat. Over the temperature range of these experiments, the superheat data correlate reasonably well with predictions (*solid lines*) based on a model involving a spherical vapor bubble (of radius equal to the pore size of the test surface) in thermal equilibrium within a liquid pool of uniform temperature. The charts *below* compare the temperature patterns observed at the outside surface of the treated tube sections A and B with results previously obtained for a smooth surface; the saturation temperature (boiling temperature at the existing system pressure) was in all three cases about 1,460° F. (790° C.). The amplitude of the temperature oscillations, which was about 150° F. (66° C.) on the *smooth* surface, was significantly reduced when either a porous coating or small-diameter holes were present on the inside surface.

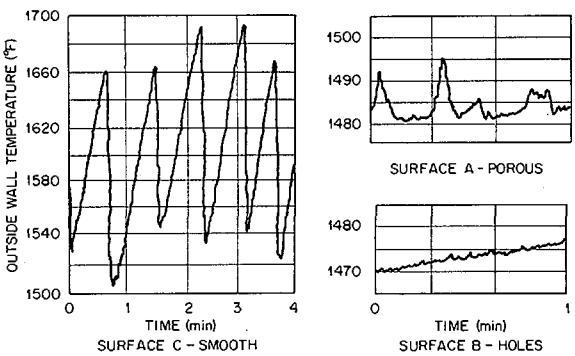

The new test loop, made of niobium-zirconium alloy for high strength at the high operating temperatures of interest to researchers, is housed entirely in a vacuum chamber to protect the refractory alloy from oxidation by air (see Fig. II–81). The vacuum chamber is approximately 10 feet high and 4 feet in diameter. In the loop, a pump circulates 5 gallons per minute of liquid sodium through a preheated section, then into the heated boiler and test section, and then to a condenser where the vapor is cooled back to liquid form. The condenser, which radiates heat to the chamber walls, consists of a coil of niobium-zirconium tubing having a ½ inch diameter and a 0.035-inch thick wall. Of the 150 feet of tubing in the loop, 120 feet are in the condenser coil itself. The pump, of a type called helical induction, circulates the molten sodium by electromagnetic force rather than by means of moving mechanical parts. Loop construction has been completed and, during the numerous shakedown and instrument calibration test runs, sodium temperatures, circulation, and pressures have been as high as 1,000° F. (540° C.), 25 ft./sec., and 200 p.s.i.a., respectively.

FLUID DYNAMICS STUDIES

The AEC is also supporting studies in fluid dynamics. Recent advancements include development of techniques for turbine-erosion and liquid-bearing studies.

Turbine Blade Erosion Studies

The Aeronutronic Division of Philco-Ford, Newport Beach, Calif., has: (*a*) proven the feasibility of a novel technique for measuring the size of condensate droplets formed by expansion of a saturated vapor through a supersonic nozzle, and (*b*) obtained turbine blade erosion data by running a supersonic turbine for 96 continuous hours in wet potassium vapor. These investigations are related to the development of reliable, long-duration *Rankine* cycle space powerplants using liquid metal working fluids and nuclear reactor heat sources.

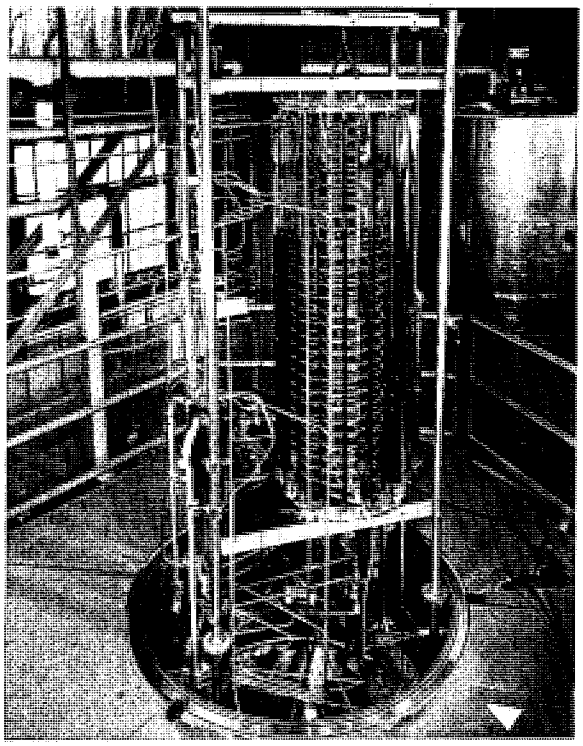

Fig. II–81. Boiling-Sodium Heat-Transfer Facility. A new niobium-zirconium test loop is being used at Argonne National Laboratory for studying the flow and heat-transfer performance of boiling-sodium liquid-vapor mixtures at temperatures and pressures as high as 2,100° F. (1,150° C.) and eight atmospheres. The thermal-radiation heater is at the *left foreground;* the shutter-controlled coil condenser is on the right side of the loop (*center of photo*). The upper half of the vacuum chamber (in background at *right*) is sealed over the loop before a test is run.

Since many of the two-phase flow phenomena responsible for turbine erosion are not yet understood, even in a common fluid such as steam, it is necessary to determine such basic parameters as condensate droplet size and turbine blade erosion due to impingement of these droplets in order to acquire basic design data.

The unique droplet-size measuring technique developed by Aeronutronic uses a supersonic nozzle with a wedge placed immediately downstream of the nozzle exit plane. The shock at the leading edge of the wedge turns the vapor flow parallel to the wedge surface. However, the condensate droplets formed in expanding through the nozzle pass through the shock and, depending on droplet size and interaction with the vapor, may or may not impinge on the wedge. By using appropriate wedge materials, the erosion length resulting from droplet impingement becomes a sensitive measure of particle size.

The turbine blade erosion test was run with a supersonic turbine in wet potassium vapor having average nozzle inlet temperature of 675° C., inlet pressure of 5.6 p.s.i.a., and exhaust pressure of 0.81 p.s.i.a. The average rotational speed was 17,800 r.p.m. over the 96-hour test period. The turbine wheel was constructed of TZM [44] material, was 5.0 inches in tip diameter,

[44] 0.5 percent titanium, 0.1 percent zirconium, and the balance molybdenum.

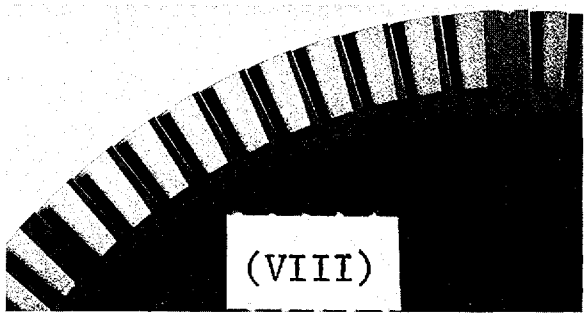

Figs. II–82 and 83. Erosion of Turbine Blades. Photo *above* shows typical appearance of turbine blades before testing at Aeronutronic Division, Newport Beach, Calif., and photo *below* shows the appearance of turbine blades after endurance test, 25° blade angle. The turbine blade erosion test was run with a supersonic turbine in wet potassium vapor having average nozzle inlet temperature of 675° C., inlet pressure of 5.6 p.s.i.a., and exhaust pressure of 0.81 p.s.i.a. The average rotational speed was 17,800 r.p.m. over the 96-hour test period conducted as a part of the study on turbine blade erosion from impingement of potassium droplets.

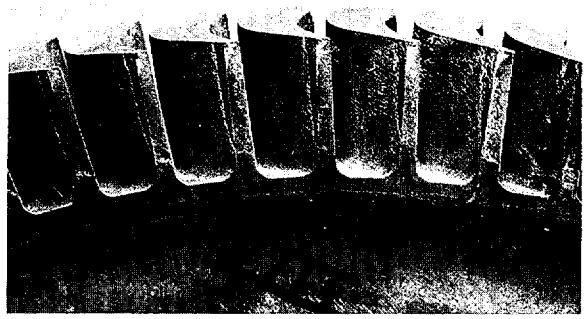

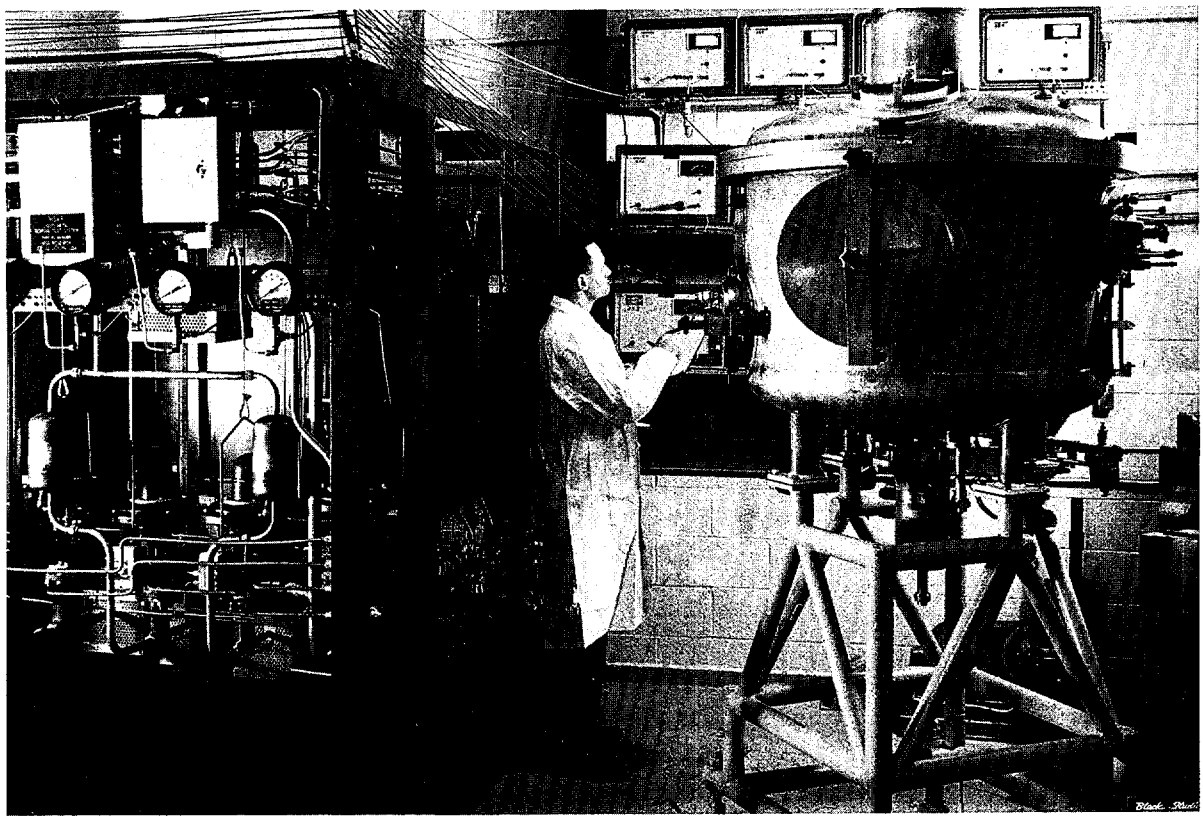

Fig. II–84. Liquid Metal Bearings Test. The sodium-potassium (NaK) circulation assembly for the liquid metal bearing test at Mechanical Technology, Inc., Latham, N.Y., is shown at the *left*. It contains a 40 p.s.i. electromagnetic pump and flowmeters, cover gas purifier (not shown), cold-trap, sump-tank, and cooler, as well as pressure, temperature, flow controls. There are two separate flow circuits, one of which provides the lubricant to the test rig bearings, while the second is a closed loop bearing coolant circuit. The test rig is mounted in the container vessel shown at the right of the figure. (The connecting piping between the circulation assembly and the vessel are omitted.) A bank of 12 amplifiers is panel mounted at the rear. Each amplifier linearizes and amplifies the signal from one of the capacitance probes mounted in the test rig to measure the small motions of the rotor within the bearing clearance. The amplified signals are then transmitted to oscilloscopes for monitoring and recording.

and had 0.29 inch high-impulse type blades. The wheel was divided into eight sections having blades of four different geometries. Figures II–82 and 83 are close-up pictures of the before and after test appearance of a blade section having 25° blade angles. It was noted that: (*a*) some erosion and corrosion of the test turbine blades does occur; (*b*) damage was not of sufficient magnitude, however, to cause more than minor performance degradation of the turbine; (*c*) all blades had the same definite damage pattern; and (*d*) variation of the turbine blade angle had no effect on the blade erosion pattern or on the amount of material removed from the blades.

Liquid Metal Bearings

Frequently in nuclear applications the level of radioactivity, high temperatures, and the intolerance of some nuclear components to contamination preclude the use of conventional oil bearings, making it necessary to lubricate machinery bearings with the process fluids.

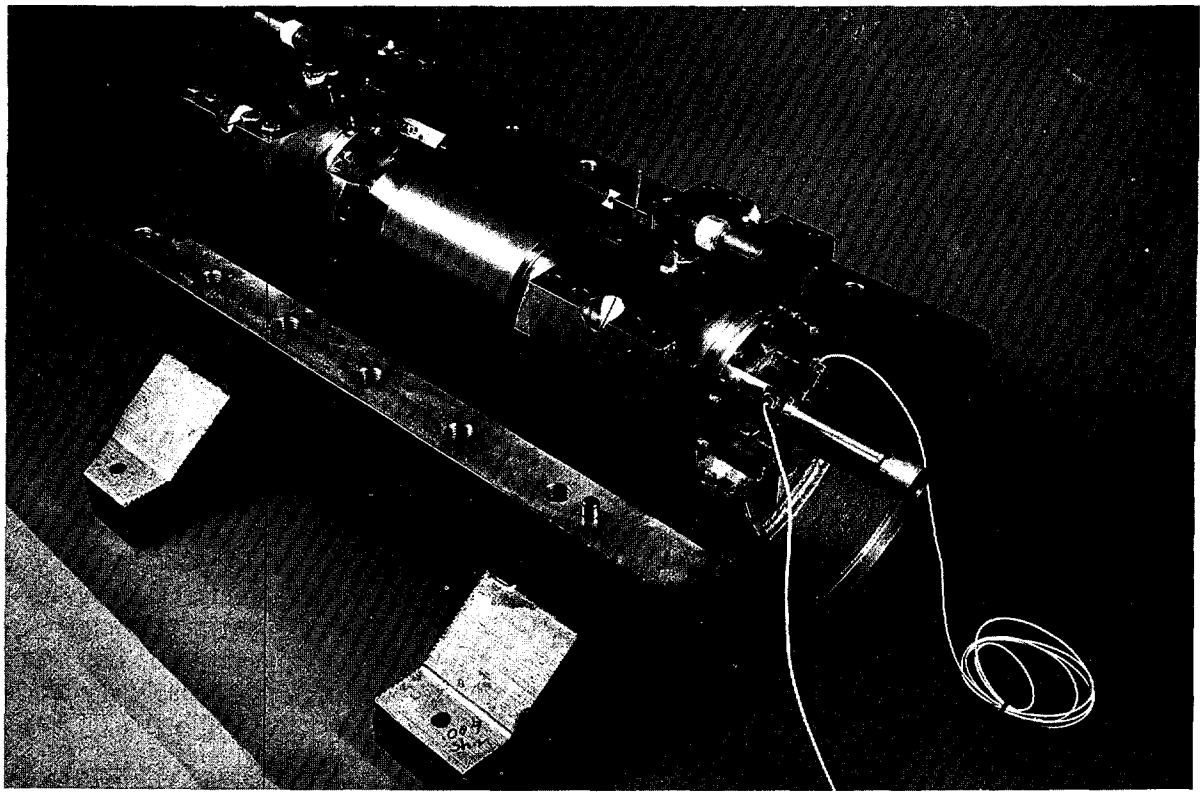

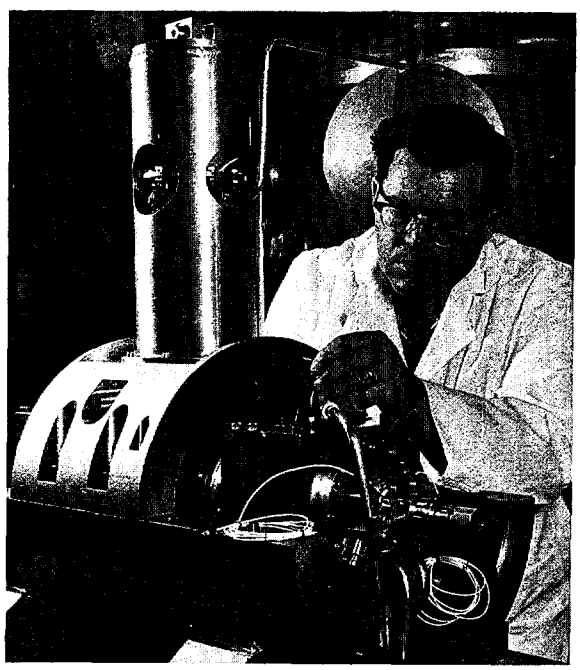

Figs. II–85 and 86. Liquid Metal Bearings. Photo *above* shows one of the Mechanical Technology, Inc., liquid metal bearings test rigs partially disassembled. Tilting pad bearings are used in the test program because of their inherent stability and self alignment capability. Each bearing has four pads which are individually supported on spherical-seat pivots. Photo *above* shows the rotor supported in the two liquid metal bearings. One of the two pairs of capacitance probes used at each bearing is shown at the left hand side. One of the capacitance type probes and its lead wire is shown at the right hand side. These probes measure the shaft motions that occur within the bearing clearance as functions of load and speed. Photo at *left* shows the fully assembled test rig. The vertical cylinder contains a pneumatic load cylinder and spring bank which apply the static load to the rotor through a floating, hydrostatic gas bearing. Dynamic loads are imposed by inserting known unbalance weights in the rotor.

Under a technology program in progress [45] at Mechanical Technology, Inc., Latham, N.Y., in which bearing design data and procedures are being evolved for use in development of nuclear turbomachinery where the cycle (process) fluid lubricant is a liquid metal, it has been found that consideration of fluid inertia cannot be overlooked in lubrication studies. One important example where this technology is needed is in the development of sodium circulation pumps for the liquid metal fast breeder reactor, now considered necessary to conserve the nuclear fuel resources in an expanding nuclear economy. In these large pumps, at least the journal bearings immediately adjacent to the impellers must be lubricated by liquid sodium. The bearing size (20″ diameter or larger), as well as the low viscosity of sodium at about 1,000° F. (540° C.), result in highly turbulent bearing films, exceeding previous lubrication experience.

The theory of turbulent lubrication was derived analytically and verified experimentally using a low viscosity fluid to achieve high bearing film turbulence. Bearing performance charts were calculated from the theory, and their accuracy is currently being checked in bearing tests using the sodium-potassium eutectic alloy, or alloy with the lowest melting point ("NaK 78") as the lubricant. This eutectic alloy, being liquid at room temperature, permits extensive bearing data to be obtained directly in a liquid metal. The NaK circulation assembly and the test rig container vessel used in the program are shown in Figure II–84. Some of the early test data is shown in Figure II–73 on page 187, and the test data is shown in Figures II–85 and 86.

In the current series of tests, a 57-pound rotor supported on 2-inch diameter bearings has been operated through and above its 24,000 r.p.m. design speed. The fluid film *Reynolds* [46] number is 11,000 and the bearings are subjected to static and dynamic loading, each up to 75 lbs. per square inch. A significant result to date has been an indication that fluid inertia, normally neglected in lubrication, appears to be important in liquid metal bearings, particularly at surface discontinuities.

[45] See pp. 282–283, "Fundamental Nuclear Energy Research—1966."

[46] *Reynolds* number—A dimensionless unit used to describe fluid flow.

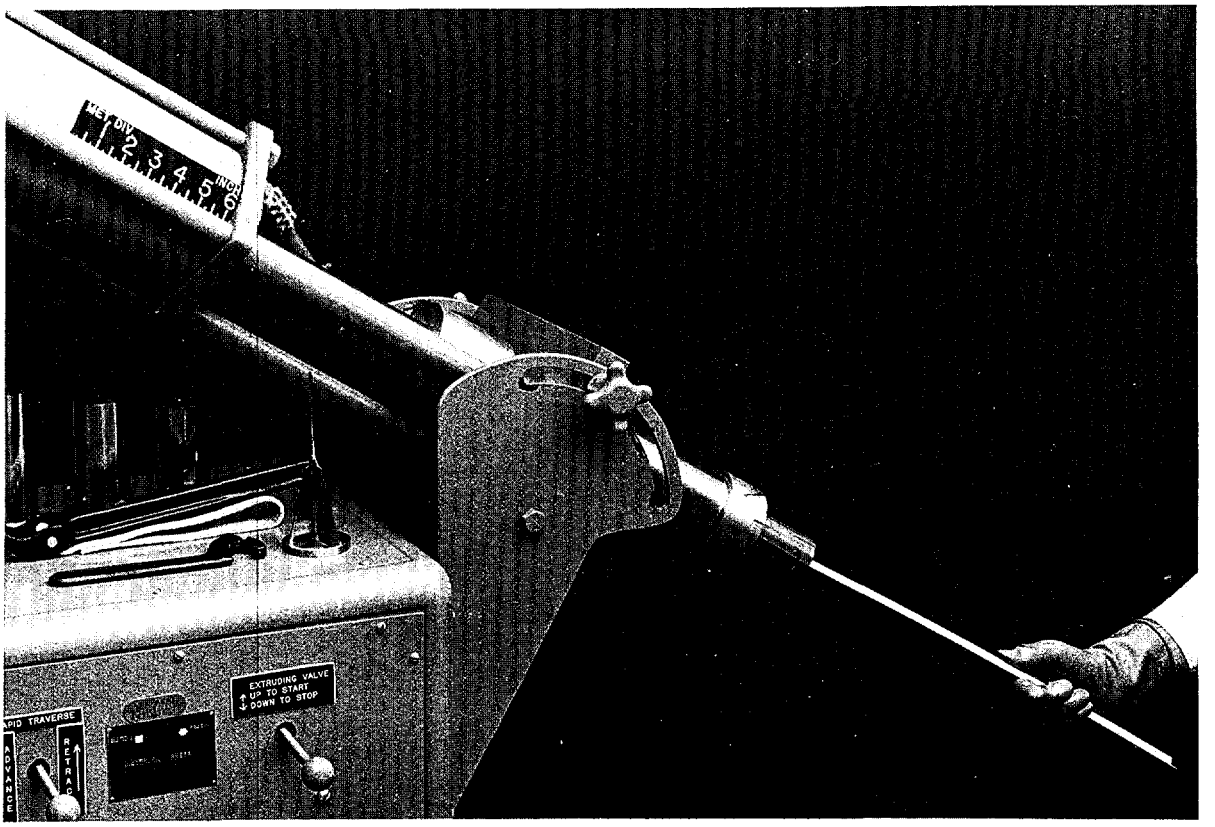

Fig. II–87. Sol-gel Extrusion. This photo shows sol-gel thoria being extruded in the form of a ¼-inch-diameter fuel rod; note the rigidity and straightness of the "green" extruded piece. After drying and calcination at 1,200° C., the densified fuel rod is ready for easy insertion into long tubes or for preparing pellets. This method, alternatively using sol-gel-derived UO_2-PuO_2 fuel material from the fuel reprocessing cycle, also appears promising for use in fast reactor fuel refabrication. Oak Ridge National Laboratory is investigating the processing of spent fuels as a part of the AEC's fast breeder reactor development (see p. 199).

FUEL PROCESSING DEVELOPMENT

Investigations have been continuing [47] on the processing of spent nuclear reactor fuels. The goal of this work is to develop improved methods of salvaging the remaining fissionable and fertile material [48] for use in fabricating new fuel elements, preparing the hazardous radioactive wastes for safe storage and long-term disposal, and recovering useful fission products and other byproduct radioisotopes for applications in research and technology.

AQUEOUS PROCESS DEVELOPMENT

At present, recovery of the fissionable and fertile materials that remain in spent nuclear reactor fuels is accomplished by their chemical removal from aqueous solutions obtained through dissolving the fuel elements in strong acids. The removal is accomplished either by the solvent extraction method, using an organic solvent that contains TBP (tributyl phosphate), or by the ion exchange method. Al-

[47] See pp. 48–56, "Fundamental Nuclear Energy Research—1965."

[48] The *fissionable,* or fissile, materials, uranium-233, uranium-235, and plutonium-239, undergo nuclear fission upon absorbing thermal neutrons. The *fertile* materials thorium-232 and uranium-238, undergo conversion to fissionable materials when their atomic nuclei capture neutrons; *e.g.,* thorium-232 to uranium-233 by addition of a neutron to each thorium-232 nucleus, uranium-238 to plutonium-239 by addition of a neutron to each uranium-238 nucleus.

though these aqueous processes are currently in use on a plant scale, research and development studies are being continued in order to improve their effectiveness and increase their versatility.

Centrifugal Extractor

Centrifugal extractors of a new design are now separating plutonium and uranium from radioactive fission products at the Savannah River Plant. The new extractors have replaced conventional mixer-settlers, in which the two phases are separated by gravity. Because the centrifugal separation is so much faster, the holdup time of the process solutions in the extraction equipment is 50 times shorter than before. This significantly shorter holdup time has decreased radiolytic degradation of the solvent. The use of smaller equipment for the same throughput has also improved nuclear safety by making it more difficult to accumulate a critical mass of fissionable material. The extractors, originally developed by the Savannah River Laboratory, are fabricated of stainless steel, are 10 inches in diameter, have a flow capacity of over 60 gallons per minute (g.p.m.), have a speed of 1,750 revolutions per minute (r.p.m.), and develop a centrifugal field of about 300 times the force of gravity.

In the new extractors, the steps of pumping, mixing, separating, and decanting are all performed in a single device having a single rotating shaft. The extractor is a cylinder having three chambers, as shown in Figure II–88. In the bottom chamber an impeller on the end of the drive shaft serves as a pump and mixer. In the central chamber, vanes attached to the shaft force the liquid to rotate as a body so that the chamber serves as a liquid-liquid centrifuge (similar to a dairy cream separator). In the chamber on the upper end, a combination of circular weirs serves as a continuous decanter.

A particular feature of the new extractor is the application of air pressure in the weir chamber to remotely regulate the interface position in the centrifuge. By this means compensation can be made for changes in the relative density of the feed streams. By maintaining the interface radius at a midpoint between the outlet weirs, clean separation of phases can be obtained at maximum flow rates.

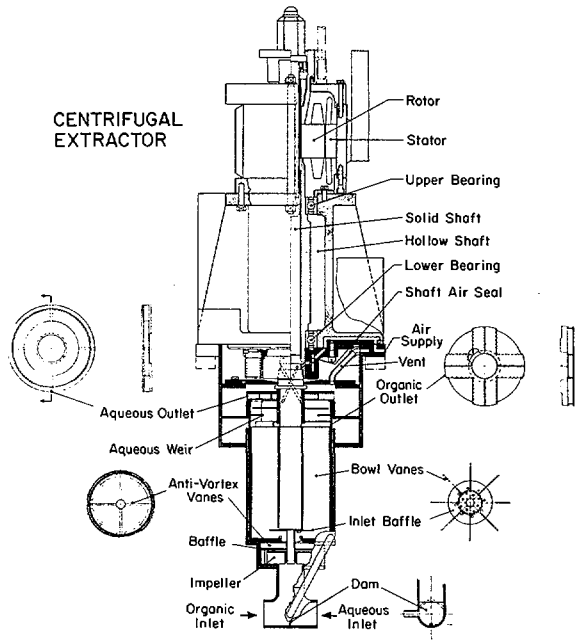

Fig. II–88. Centrifugal Extractor. Diagram shows the major components of the centrifugal extractor developed at Savannah River for separating radioactive materials. The extractor (shown in cross section) is an integral unit having a pump mixer (at the *bottom*), centrifugal separator (above the pump), and motor drive (at the *top*), all mounted on one vertical shaft. An assembly of 18 such units is separating plutonium and uranium from fission products by continuous counter-current solvent extraction. Radiolytic degradation of the solvent is minimized by short contact times.

Ion Exchange Method

The Savannah River Laboratory and the University of South Carolina, Columbia, are jointly studying the design processing equipment to demonstrate the use of ion exchange membranes to continuously concentrate and purify aqueous solutions of metal ions. The process uses a difference in acid concentration to force the metal ions out of a dilute solution through the ion exchange membrane (cation type), and into a more concentrated solution. It may also be used with a different type of membrane (anion type) to remove acid from a

solution. No electric or pressure potentials are used. Specifically, the first design is one for the concentration of uranium solutions from spent reactor fuel elements or from uranium ores. Several small concentrating units have been built and successfully tested to determine design data.

Use of ion exchange membranes provides some distinct advantages over other methods of separation and concentration. Because the membranes do not require regeneration, they can be used continuously for long periods of time. A wide range of flow rates and concentrations can be processed. Also, operation of membrane systems can be made rather simple, and application to many chemical separations appear to be possible.

Fast Breeder Process Development

The limited lifetime of the stainless steel clad fuel elements used in fast breeder reactors may be expected to have a significant effect on the rate of discharging and the methods for reprocessing the spent fuel. Currently, the goal for such fuels is 70,000–100,000 megawatt-days per ton (MWD/T). Investigations are underway at Oak Ridge National Laboratory (ORNL) to determine if existing plants, using well established solvent extraction methods, can be modified for processing the spent fuels; also, if the sol-gel process for fuel refabrication can be readily adapted to remote operation.

Recycle buildup of neutron-active isotopes of plutonium may require remote reconstitution or refabrication of the fast reactor fuels, and it appears that the sol-gel process can be readily adapted to perform this remote reconstitution. Uranium and plutonium sols can be separately formed from their nitrate solutions and then blended in desired proportions. The mixed gel can then be converted into oxides and formed into rods (see Fig. II–87) or pellets, microspheres (see Fig. II–1), or ceramic shards by drying and crushing. Calcining at the relatively low temperature of about 1,150° C. provides mixed urania and plutonia in the form of a homogeneous refractory ceramic of almost theoretical density (density of pure materials with no voids) that can be loaded into fuel tubes.

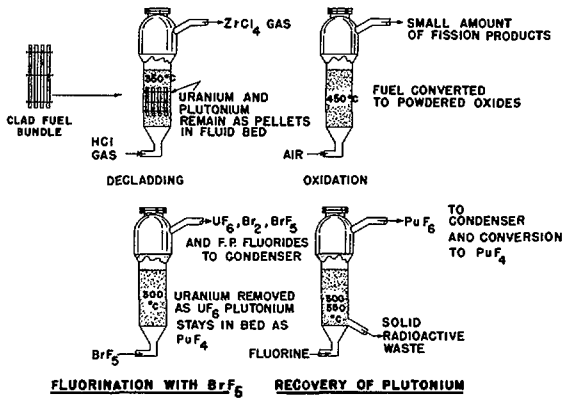

Fig. II–89. Bromine Pentafluoride Process. The processing steps employed in recovering uranium and plutonium from nuclear reactor fuel materials using the bromine pentafluoride (BrF_5) fluid-bed volatility techniques are illustrated in the Argonne National Laboratory sketch. All operations involving chemical separation of uranium and plutonium from fission products and cladding materials are carried out in a fluid-bed reactor. The principle of fluidization involves the passage of a gas upward through a bed of solid particles at a speed sufficient to allow the particles to move with an apparent random motion and acquire certain characteristics of a liquid. Since the solids mix within the bed and transfer heat rapidly to walls of the reactor, it is possible to carry out the highly exothermic (heat emitting) reactions in the volatility process under nearly constant temperature conditions.

FLUORIDE VOLATILITY PROCESS

Extensive programs aimed at developing methods for the recovery of uranium and plutonium from partially spent reactor fuels by fluoride volatility techniques are being carried out at several laboratories. These methods are based on the ability of certain fluorinating agents to convert uranium and plutonium to volatile hexafluorides (UF_6 and PuF_6) which are readily separated from associated less-volatile fuel materials, such as cladding and radioactive fission products. The primary objective of the fluoride volatility program is to develop the technical data for the design of a commercial reprocessing plant for power-reactor fuels.

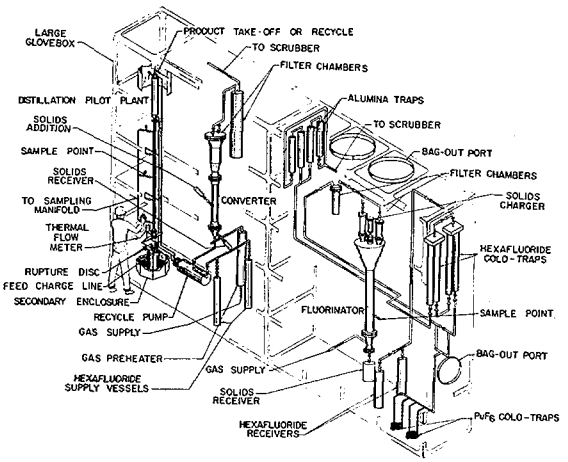

Fig. II–90. Plutonium Hexafluoride Recovery. Drawing is of an engineering-scale facility being operated at Argonne National Laboratory to demonstrate the various steps in the fluid-bed fluoride volatility process. The large glovebox contains equipment used for processing unirradiated plutonium-containing fuel material. In the fluorinator, uranium dioxide-plutonium dioxide fuel is reacted with bromine pentafluoride to form uranium hexafluoride (UF_6) and then with fluorine to produce plutonium hexafluoride (PuF_6), which is collected in refrigerated traps. The conversion of PuF_6 to plutonium tetrafluoride by thermal decomposition of PuF_6 has been demonstrated in the converter reactor. In this operation, PuF_6 is introduced at the bottom of the reactor and passed upward through a fluidized bed heated to 300° C. Under these conditions, PuF_6 decomposes to solid PuF_4, which deposits on the bed particles. Purification of UF_6 from small quantities of volatile fission-product fluorides will be studied in the distillation pilot plant located adjacent to the converter reactor.

Bromine Pentafluoride Process

Argonne National Laboratory has discovered that uranium can be separated from plutonium by the use of bromine pentafluoride (BrF_5) as a fluorinating agent (see Fig. II–89). In this process, the fuel material is first converted to a powdered oxide by reaction with oxygen. The powdered oxide is then reacted with BrF_5 gas to convert uranium oxide to gaseous UF_6, while plutonium oxide is converted to solid plutonium tetrafluoride (PuF_4). Plutonium is then recovered separately as gaseous hexafluoride (PuF_6) in a subsequent step using fluorine at high temperatures (300° to 550° C.) as the fluorinating agent. This process (see Fig. II–90) offers a distinct advantage over the earlier fluoride volatility process based on the production of UF_6 and PuF_6 together by the direct reaction of the fuel material with fluorine.

Plutonium hexafluoride is a rather unstable compound, readily undergoing decomposition to PuF_4 and fluorine. Therefore, special steps are required to recover the decomposed plutonium from process equipment in which PuF_6 has been

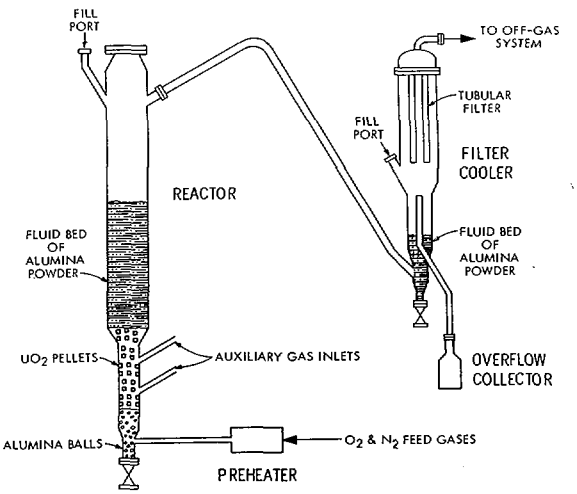

Fig. II–91. Semiworks Reactor System. The semiworks reactor system at the Oak Ridge Gaseous Diffusion Plant is being used to solve operational and engineering problems in applying fluid-bed fluoride volatility techniques developed in the laboratory to a full-scale processing plant recovering fissionable materials. The schematic drawing indicates how tests on the oxidation of the uranium dioxide (UO_2) pellet fuel to convert it to powdered urano-uranic oxide (U_3O_8) are conducted. The reactor is charged with ½-inch diameter alumina (Al_2O_3) balls, powdered alumina (Al_2O_3), 48 to 100 mesh, and the reactor grade uranium dioxide (UO_2) pellets. The alumina (Al_2O_3) balls position the pellet bed above the oxygen (O_2) entry point at the bottom of the reactor for optimized gas distribution. Satisfactory operation has been obtained when the reaction takes place only at the top of the pellet bed so that the urano-uranic oxide (U_3O_8) powder is readily carried up into the fluidized alumina (Al_2O_3) in the upper 10-inch diameter reactor section, and the relatively high superficial velocity of 3 ft./sec. is maintained in the smaller 5-inch diameter section of the reactor to aid in conveying the powder. The reactor system will soon also be used for decladding and fluorination experiments. The two major components of the system are shown in Fig. II–92.

handled. The principle advantages of the new process employing BrF_5 are: (*a*) that a separate step is not required for the separation of UF_6 from PuF_6, and (*b*) the number of processing steps involving PuF_6 are reduced to a minimum. Thus, the handling of the delicately stable PuF_6 is simplified.

Process Feasibility Studies

Technical and economic feasibility studies are being conducted at the Oak Ridge Gaseous Diffusion Plant (ORGDP) [49], Oak Ridge, Tenn., on the fluid-bed [50] fluoride volatility process. The purpose of the studies is to translate the results of basic research and development, conducted primarily at Argonne, Oak Ridge, and Brookhaven National Laboratories,[51] into conceptual plant designs necessary for components development and plant scale-up work.

[49] The ORGDP is an AEC production facility at Oak Ridge, Tenn., operated by Union Carbide Corp.

[50] A fluid-bed (synonymous with "fluidized-bed") is composed of small, solid particles of an inert substance, such as alumina (Al_2O_3). A gas stream is passed through the bed, thereby agitating the inert particles and imparting the characteristics of a fluid to the particles. The fluid-bed serves as a heat transfer medium which provides good control of temperature during a reaction.

[51] See pp. 305–307, "Fundamental Nuclear Energy Research—1962" also pp. 355–359 "Fundamental Nuclear Energy Research—1963"; pp. 133–134, "Fundamental Nuclear Energy Research—1964"; and pp. 50–51, "Fundamental Nuclear Energy Research—1965."

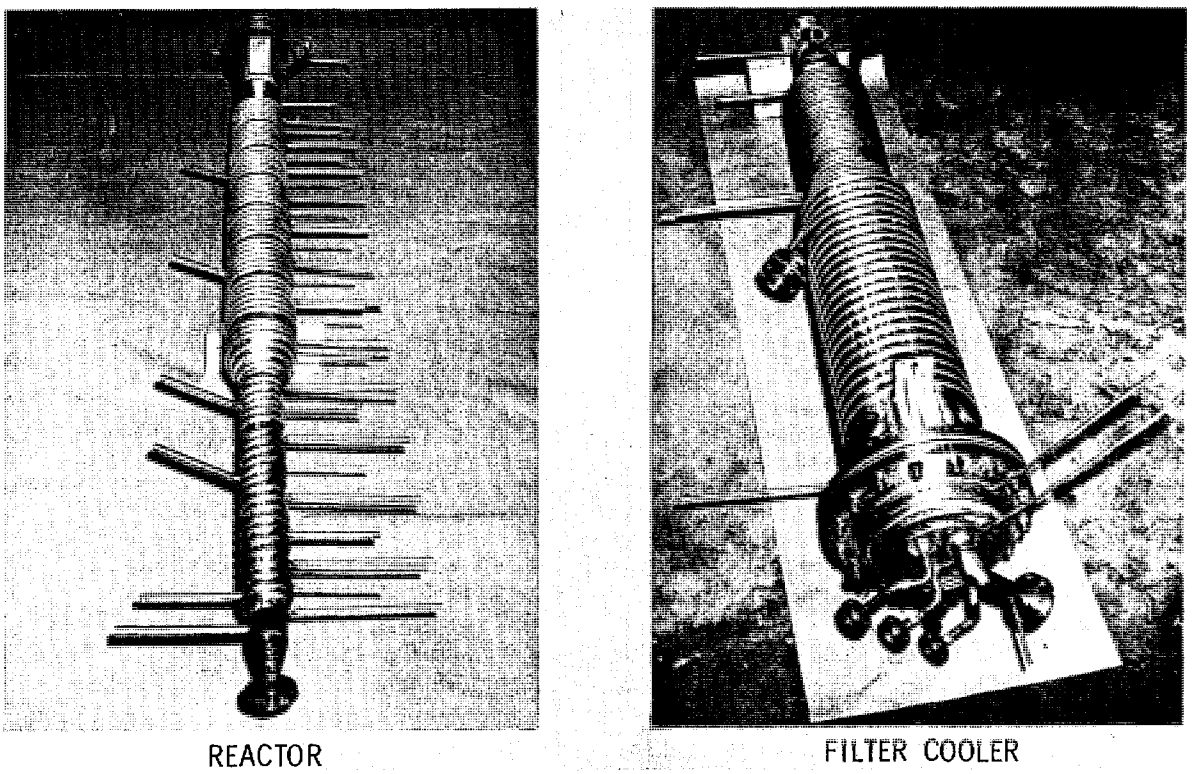

Fig. II–92. Semiworks System Components. The Oak Ridge Gaseous Diffusion Plant semiworks fluid-bed reactor has a 10-inch-diameter upper section and a 5-inch-diameter lower portion. It is constructed of low carbon nickel because the operating temperature may be as high as 600° C. For increased corrosion resistance, special procedures, employing low carbon nickel wire, were used to weld the low carbon nickel to itself and to the Duranickel flanges. Cooling coils are welded to the walls, and the vessel is provided with gas inlet nozzles at several elevations. The filter cooler was fabricated in a similar manner, using so-called commercially pure nickel and standard weld material. The enlarged upper section is designed for the installation of tubular-type filters. A diagram of the system is shown in Fig. II–91.

275–845 O—68——15

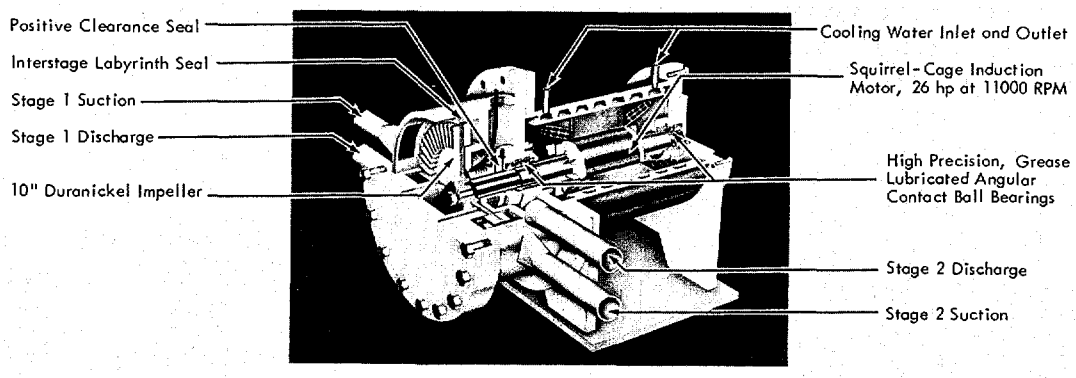

PERIPHERAL COMPRESSOR

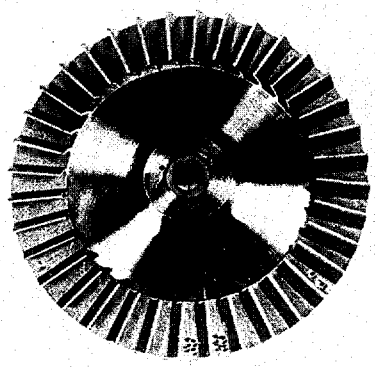

10" DURANICKEL IMPELLER

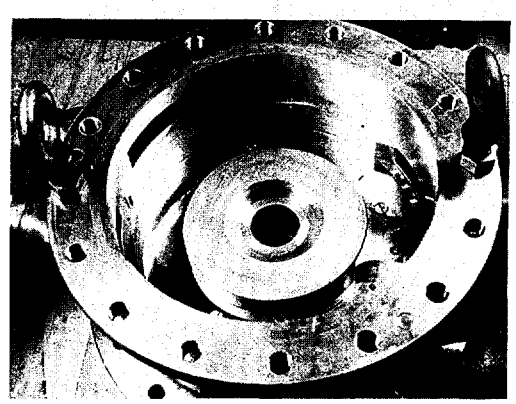

IMPELLER HOUSING

Fig. II–93. Peripheral Compressor. Recycle of reactant gases is required to reduce reactant usage and, consequently, to lower overall reprocessing costs of a fluid-bed volatility process. The novel two-stage peripheral compressor shown above, developed at the Oak Ridge Gaseous Diffusion Plant was adapted to meet the volatility process requirements. The compressor operates at a speed of 11,000 r.p.m. and is capable of delivering over 75 c.f.m. of fluorine (F_2) and 150 c.f.m. of hydrogen chloride (HCl) at a discharge pressure of 14.7 p.s.i.g. with atmospheric suction. As shown in the lower pictures, the inside nickel surfaces of the compressor were unaffected after 2,000 hours of operation on mixtures of 20 to 75 percent fluorine (F_2) in nitrogen (N_2). The minute scratches and pits on the parts are machine marks made during fabrication and balancing.

Special equipment and components for the fluid-bed fluoride volatility process are being developed. Operation of the semiworks fluid-bed reactor,[52] designed to provide scale-up data for a larger, plant-size system, and completion of a 2,000-hour test in fluorine (F_2) service of the ORGDP-designed peripheral compressor have been accomplished.

The semiworks reactor (see Fig. II–91) has been employed in pellet oxidation studies with 35 and 65 kilogram (kg.) charges of uranium dioxide (UO_2). By way of comparison, a plant-scale reactor is expected to have a maximum diameter of about 2½ feet and to contain a batch charge of about 1,500 kg. of uranium dioxide (UO_2). The 65 kg. charge is, however, about 15 times as big as previously used in smaller scale flow sheet tests.

A plant-size peripheral compressor, designed at ORGDP using experience gained in a basic compressor research program (see Fig. II–93), has now been tested. After 2,000 hours in fluo-

[52] In this case, not a nuclear reactor but a vessel containing the chemical reaction.

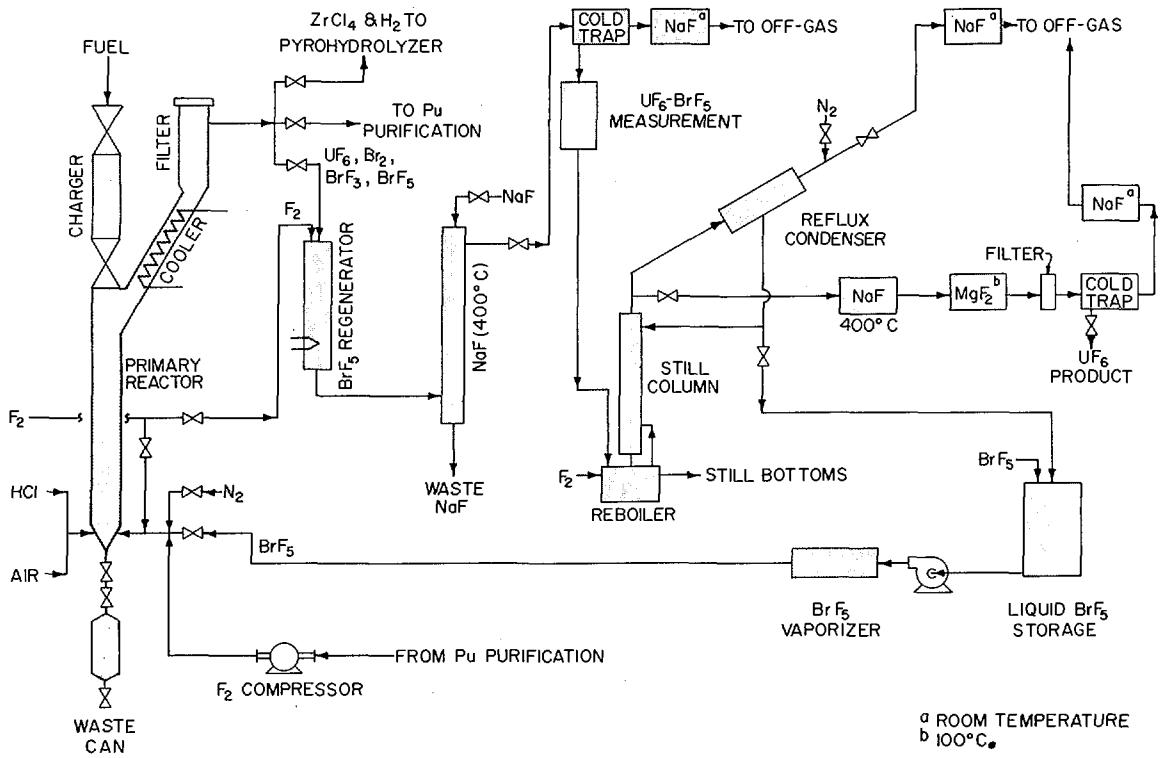

Fig. II–94. Fluid-Bed Volatility Pilot Plant (FBVPP). The above is a partial flowsheet for the hot pilot plant that is being installed at Oak Ridge National Laboratory to demonstrate the recovery of uranium and plutonium from spent oxide power-reactor fuels. Fuel is introduced into the primary (chemical) reactor that contains an inert fluidizing medium, alumina (Al_2O_3). The zirconium cladding is removed by converting the metal to volatile zirconium tetrachloride ($ZrCl_4$). The oxide fuel pellets (UO_2) are contacted with air to form uranium oxide (U_3O_8) powder, then bromine pentafluoride (BrF_5) is used to form volatile uranium hexafluoride (UF_6). The volatilized UF_6 is trapped and finally separated from BrF_5 and volatile fission product fluorides by a batch distillation system and use of a hot sodium fluoride (NaF) trap and a magnesium fluorine (MgF_2) bed. The plutonium remaining in the bed in the primary reactor is reacted with fluorine to produce volatile plutonium hexafluoride (PuF_6) that is swept from the reactor and collected in a cold trap prior to further purification and conversion to plutonium tetrafluoride (PuF_4).

rine service, operating at about 10,000 r.p.m., and compressing about 50 cubic feet per minute (c.f.m.) of gas from 1 to 2 atmospheres, the unit was removed and disassembled for inspection. All metal surfaces were in excellent condition.

Molten Salt Breeder Reactor Processing

Continuing studies and tests revolving around the successful operation of the Molten Salt Reactor at Oak Ridge National Laboratory are expected to lead to the development of an efficient thermal breeder reactor.[53] Such a reactor would burn fuels contained in circulating molten fluoride salts and would be capable of converting thorium into enough fissionable uranium-233 to supply its own fuel needs, as well as enough extra uranium-233 to equal its fuel inventory, or capacity, every 10 to 20 years. To achieve the neutron economy needed for a molten salt breeder reactor requires that the fission product poisons[54] be continuously removed from the fuel; therefore, separation processes are being developed at ORNL to accomplish such a purpose.

[53] See footnote 10 for definition.

[54] These poisons, resulting from the nuclear fissioning of the reactor fuel, act as neutron absorbers and reduce the efficiency of the breeder, or the extent of the "breeding gain."

One class of poisons includes certain isotopes of the noble gases, which can be easily separated from the circulating molten fuel salts by using a gas separator.

Another important class includes nuclides of the rare earth elements, the fluorides of which exhibit solubility in the molten salts, as well as relatively low volatilities. Processes now being studied will provide for the more difficult separation of this class of poisons from the fissionable uranium-233 and from the valuable carrier salt by use of a well-established flouride volatility method, followed by a low-pressure distillation method. In the first step, the uranium can be separated from the fuel salt by contacting the salt with elemental fluorine (F_2) to convert the uranium tetrafluoride salt (UF_4) to the volatile hexafluoride (UF_6), then collecting and purifying the UF_6 gas. In the second step, the remaining carrier salt, which is principally a mixture of lithium-7 and beryllium fluorides, can be separated from the rare earth fluorides, as well as several other fission-product fluorides, by low pressure (1 mm. of mercury) distillation (1,000° C.) of the more volatile lithium and beryllium salts. The purified carrier salt and the uranium are then used to reconstitute fuel for return to the reactor.

PYROCHEMICAL PROCESS

High-temperature pyrochemical processes are being developed for the recovery and purification of high-plutonium-content ceramic and metal fuels from fast breeder reactors. Lower fuel-reprocessing costs are expected to result from pyrochemical methods because they are simple, compact, and capable of handling fuel shortly after discharge from the reactor. This capability of handling fuel after only a short cooling period makes possible a reduction in the quantity of fuel awaiting processing and a rapid reuse of fuel, largely because inorganic reagents are employed which are stable under irradiation. Other economic advantages of pyrochemical processes are small process volumes, which require a minimum of shielded space, and the direct production of solid wastes. These characteristics make pyrochemical processes highly suitable for a fuel-reprocessing plant designed to serve one or several reactors.

Salt Transport Process

Laboratory and engineering investigations at Argonne National Laboratory have been directed toward the development of a new pyrochemical procedure known as the salt-transport process. Good results have been obtained in the recovery of uranium nearly free from fission-product elements. In this process, uranium or plutonium is purified and recovered by selectively transferring it from one liquid-metal solvent (donor solution) to another liquid-metal solvent (acceptor solution) by passing a molten salt back and forth between the two metal solvents. From a process standpoint, this method of separation has the advantage that only small solution volumes are required, since not all the uranium or plutonium need be in solution at one time.

Chemical studies have been conducted to provide basic data for the development of the salt-transport process. In these studies, binary alloys of magnesium with zinc, cadmium, or copper, and salts consisting of magnesium chloride ($MgCl_2$) alone or in combination with other chlorides (alkali and alkaline-earth chlorides), were investigated to determine their relative effectiveness as solvents in salt-transport separations. Liquid copper-magnesium alloys were found to be suitable donor solvents and liquid magnesium-zinc alloys were found to be suitable acceptor solvents. A furnace used in these studies is shown in Figure II–95.

Engineering studies have been carried out to develop the technology required for plant-scale applications of pyrochemical processes. The feasibility of the salt-transport separations was successfully demonstrated in pilot-plant tests with unirradiated uranium to which fission-product elements had been added. In this work, high uranium recovery (99%) and excellent separation of uranium from the fission-product

elements (ranging from 99.9% for zirconium to 99.999% for niobium) were achieved. Plans are in progress to conduct similar experiments with plutonium. Installation of equipment to carry out these experiments has been completed.

Fuel Cycle Facility

Continued operation of the Fuel Cycle Facility[55] (FCF) by Argonne National Laboratory in conjunction with the Experimental Breeder Reactor (EBR–II) at the National Reactor Testing Station (NRTS), Idaho, has confirmed feasibility of the completely remote processing and refabrication of the fast reactor fissium alloy fuel currently being used. All of the fuel in the reactor has been recycled at least once, with some in its third cycle. In other words, it has been removed from the reactor after irradiation, melt refined,[56] and reenriched in uranium–235 in the FCF, recast into fuel pins, and then refabricated into fuel subassemblies which are returned for reuse in the reactor.

Significant information relating to the sustained operability and to the maintainability of pyrochemical fuel processing and remote fabrication equipment in an inert atmosphere (pure argon) and high radiation fields (10,000 to 100,000 roentgens[57] per hour) has been gained from FCF operations. Further, it is indicated that this type of processing will be feasible for other types of fast reactor fuels. Little difficulty has been encountered which could be attributed to gamma irradiation effects on the equipment designed for this purpose.

ASSOCIATED RESEARCH

The AEC also sponsors chemical research in other areas. Two important such areas deal with fuel burnup analysis and with chemonuclear development.

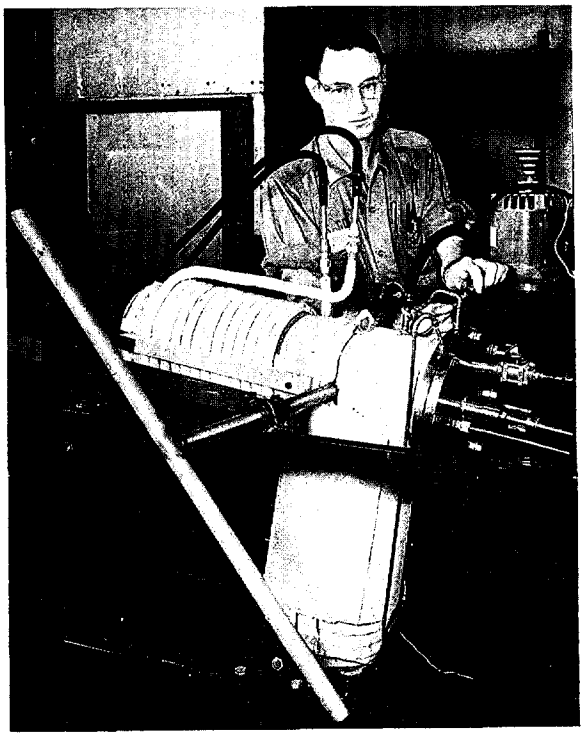

Fig. II–95. Tilt-pour Furnace Used in Pyrochemical Processing. In the high-temperature pyrochemical processes being investigated at Argonne National Laboratory for the reprocessing of fuels from fast breeder reactors, liquid metals and molten salts are used as reagents. Experimental studies of process reactions involving these reagents are being conducted in an induction-heated tilt-pour furnace, which has general versatility for pyrochemical work. The furnace shown in the photo is in the "pour" position. The material is first heated in the section having the induction heater coiled on the outside (*left* of photo). This section is kept in an upright position during heating and then tilted for pouring the contents into a crucible contained in the other section (*bottom* of photo). Here the material is allowed to solidify and is later removed for study. The furnace allows heating under a vacuum or an inert atmosphere.

Thermal Fuel Burnup Analysis

More accurate methods for measuring the percentage of uranium and plutonium which has fissioned in a spent nuclear fuel element are being developed by the Nucleonics Laboratory

[55] See pp. 82–85, "Fundamental Nuclear Energy Research—1965."

[56] In melt refining, the fuel material is melted at about 1,400° C. in a zirconia crucible; then, certain fission-product impurities are removed by volatilization, while others are removed by selective oxidation reactions with the crucible material.

[57] *Roentgens*—An exposure dose of X- or gamma-radiation such that the associated corpuscular emission per cubic centimeter of air at standard conditions produces ions carrying one electrostatic unit of charge of either sign.

of the General Electric Co. at Pleasanton, Calif. It has been demonstrated that this burnup value can be determined most accurately by measuring the amount of a fission product produced within the fuel. While the number of possible fission products is large, few satisfy all the requirements for the ideal burnup indicator, which are: (*a*) the fission product should be non-volatile, so that it is not lost from the fuel by distillation; (*b*) it should have a low cross section, so that it is not destroyed by neutron absorption; (*c*) it should be subject to simple accurate analysis; and (*d*) its fission yield should be well known and should be constant for all fissioning species. The fission product neodymium-148 (Nd^{148}) has been found to meet all these requirements.

The basic method of measurement of this burnup indicator (see Fig. II–96) requires the dissolution of fuel and, after chemical separation, the measurement of the relative concentrations of neodymium isotopes to those of the heavy elements. The anion exchange chemical procedure developed for the separation of neodymium is highly specific and integrates well with the methods previously developed for the separation of uranium and plutonium. The mass spectrometric data obtained are processed by a computer code, developed in conjunction with this program which yields the nuclear fuel burnup as well as the uranium and plutonium isotopic compositions.

The development of this mass spectrometric method increases the accuracy of the burnup measurement by a factor of seven over the cesium-137 radiochemical measurement formerly employed by industry. Furthermore, the largest remaining source of error in the measurement of burnup, *i.e.*, uncertainty in the fission yields, has been reduced by measurement of these nuclear constants. The new method has been proposed as a standard method for adoption by the American Society for Testing and Materials.

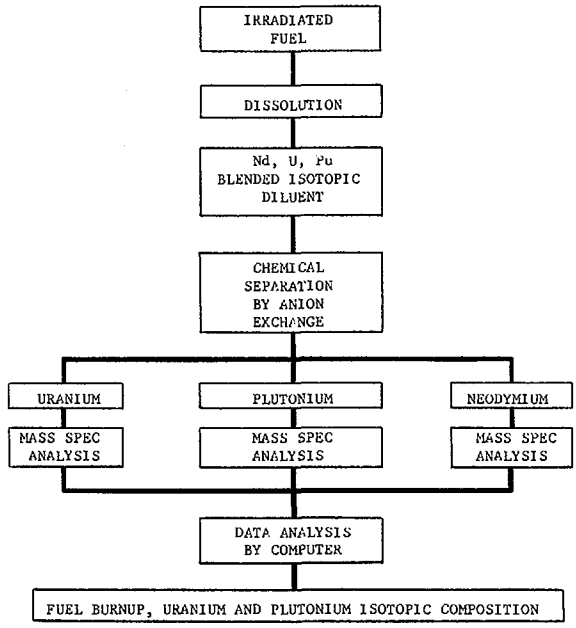

Fig. II–96. Thermal Fuel Burnup Analysis. More accurate methods for measuring the percentage of uranium and plutonium which has fissioned in a spent nuclear fuel element are being developed by the Nucleonics Laboratory of the General Electric Co. at Pleasanton, Calif. It has been demonstrated that this burnup value can be determined most accurately by measuring the amount of a fission product produced within the fuel. The diagram shows the analysis scheme.

Chemonuclear Development

Rensselaer Polytechnic Institute (RPI), Troy, N.Y., in studying the peaceful uses of nuclear energy, has helped to pioneer in chemonuclear development[58] where nuclear energy is used directly for chemical synthesis. The energy of the fission fragments (83% of the approximately 200 Mev. available) of the fissioning of uranium-235 can be absorbed in a surrounding gas media producing chemically reactive species which, on interaction, can produce commercially valuable chemicals. A particularly interesting development in the basic studies of the irradiation of carbon monoxide has been the isotopic enrichment of the isotope carbon-13 in carbon monoxide by the use of a very sharp ultraviolet light emitted from excited iodine. Isotopic enrichment and separation by the use of photochemical methods, in this manner, had never been accomplished before.

[58] See pp. 54–56, "Fundamental Nuclear Energy Research—1965," for description of previous work by RPI, Brookhaven National Laboratory, and others.

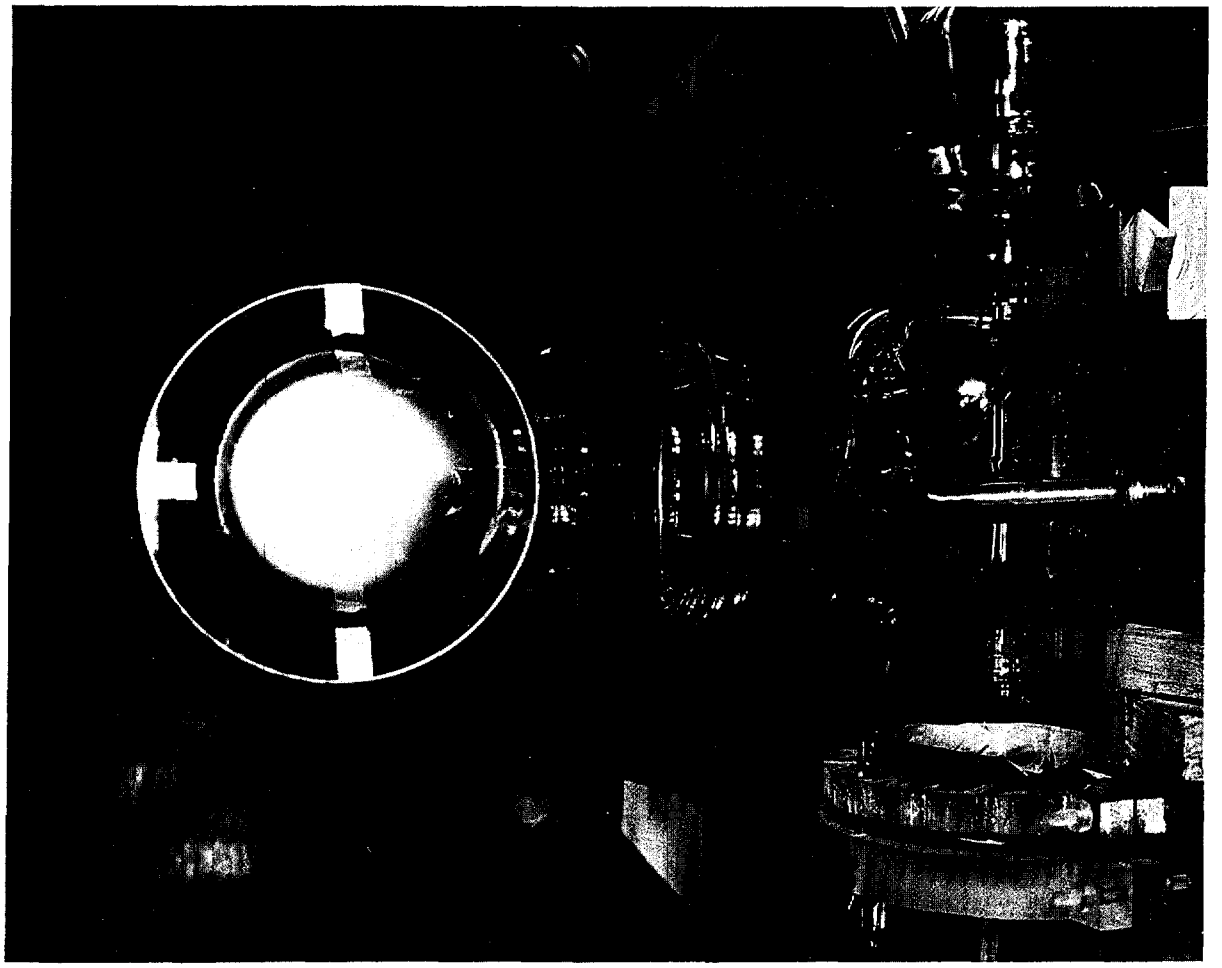

Fig. II–97. Plasma Magnetohydrodynamics. Several approaches are being studied for the direct production of electricity by passing an electrically conductive working fluid between the poles of a magnet. At Brookhaven National Laboratory, the concept of such a magnetohydrodynamic (MHD) power generator involves the use of a gas (plasma) seeded with vaporized metal to make it electrically conductive. Unexpectedly, the studies have led to the production of plasmas having the characteristics of natural ball lightning phenomena. These plasma balls have a relatively long lifetime, ½ to 1 second, after production in a radiofrequency (RF) discharge. They range in diameter from 6 to 12 inches and can be produced in air, oxygen, and nitrogen at one atmosphere (see p. 213).

DIRECT ENERGY CONVERSION

The direct conversion of nuclear energy to electrical energy without following the steam turbogenerator cycle is the subject of a vigorous research and development program sponsored by the AEC. Much of this program is directed toward the development of compact generators for use in space power systems.

THERMIONIC SYSTEMS

The basis for thermionic systems of direct energy conversion is the thermionic generator, or converter. Basically, this consists of two electrodes contained within an evacuated enclosure. One electrode, the "emitter," is heated, whereupon electrons "boil off" from the surface.

Some of these electrons impinge on the other electrode, the "collector," which is maintained at a temperature lower than that of the emitter. If an external circuit is then connected between the electrodes, the excess electrons deposited on the collector can flow through this external circuit, producing electrical power. If the converter is so constructed that the emitter electrode is also the cladding for a quantity of nuclear fuel and is placed into a nuclear reactor, the emitter can be heated by the fissioning of the fuel. If a sufficient number of such converters are then assembled into a compact array, the converter fuel can form a critical mass and serve as the core of a thermionic reactor. In this case, the emitter and collector electrodes of the individual converters would be electrically connected in a series-parallel arrangement to produce a higher voltage and current.

Thermionic Reactor Development

The General Electric Co.'s Nuclear Thermionic Power Operation, near Pleasanton, Calif., is carrying out research and development in nuclear thermionic reactor technology for ultimate application to supply electric power for use in space and remote terrestrial locations.[59] Major emphasis is continuing on the development of essential fuel, cladding, and insulator materials, and on proof test irradiations of thermionic converters. The results of further high temperature testing of fuel and cladding in the laboratory, in combination with earlier results from 10,000-hour furnace tests, have demonstrated the basic compatibility of uranium dioxide fuel with tungsten clad under anticipated thermionic fuel element conditions. Ten thermionic converters have been irradiated in test reactors, including prototype multi-cell thermionic fuel elements.

In addition to these basic investigations of the thermionic fuel element, attention has also been given to the entire thermionic reactor. A mathematical model has been developed which describes the operating electrical characteristics of the thermionic converter in good agreement with laboratory experimental data. This model has been incorporated in a comprehensive computer calculational program, so that for the first time it has been possible to examine in detail the performance of a thermionic reactor made up of hundreds of thermionic fuel elements, with thousands of individual thermionic cells comprising the fuel elements.

Fuel Element Development

The experimental program in nuclear thermionics at Gulf General Atomic, San Diego, Calif. (see footnote 37), is directed toward the development of in-core thermionic reactors. Work on the development of a unit cell thermionic fuel element has progressed to the point where stable performance at suitable power levels for reactor operation has been achieved in both in-pile and out-of-pile converters. Lifetimes for both tests are in a range consistent with anticipated space applications. As part of the fuel element development, technology programs are in progress on fuel fabrication development, tungsten cladding development, high temperature fuel-cladding interactions, high temperature insulator seals, sheath insulators, and integral cesium reservoirs. Integration of fuel elements into a reactor concept is underway to determine the effects of liquid metal cooling and inter-connection of fuel elements.

Cesium Plasma Studies

Successful thermionic converters, whose usefulness as long-lived, reliable power supplies for space or remote terrestrial applications has been proven by years of exhaustive and rigorous testing, depend upon the use of a cesium plasma (a gaseous mixture of electrons, cesium ions, and neutral atoms) between the converter electrodes. Because of the important role the plasma plays in converter operations, the physical properties of cesium plasmas have been under study at the Los Alamos Scientific Laboratory [60] and experimental spectrographic techniques for

[59] See pp. 268–269, "Fundamental Nuclear Energy Research—1966."

[60] See p. 273, "Fundamental Nuclear Energy Research—1966."

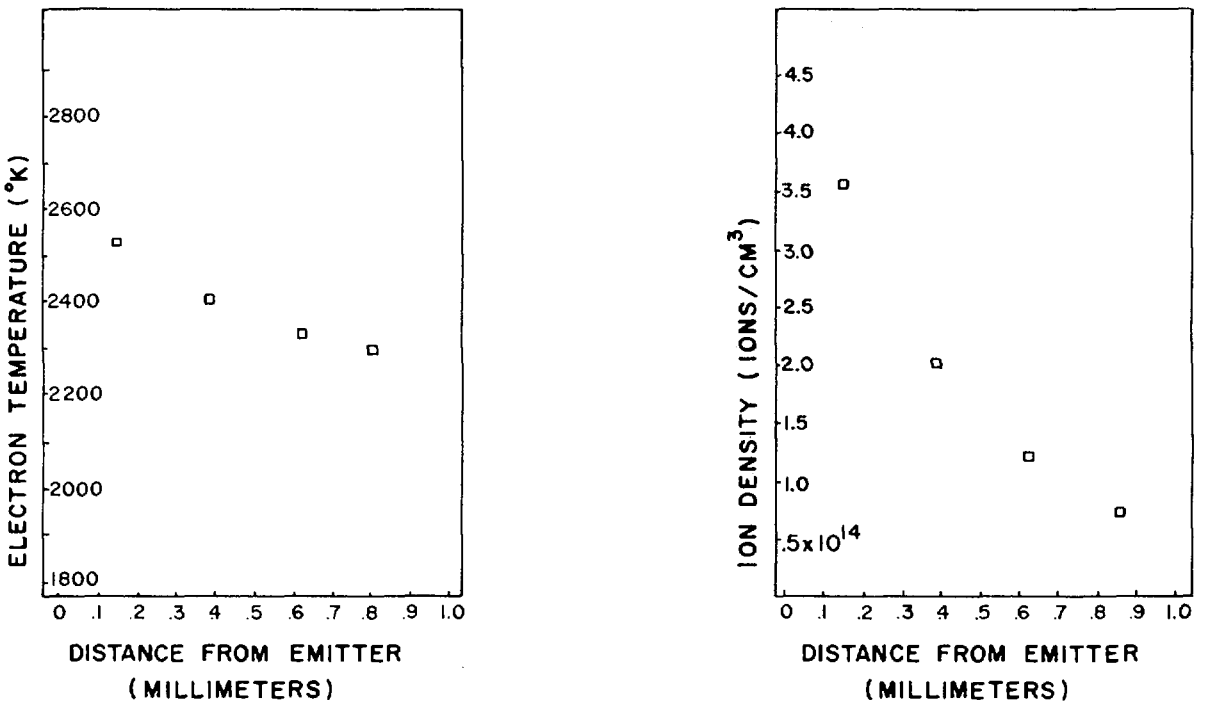

Fig. II–98. Cesium Plasma Studies. Because of their importance to the operation of practical thermionic converters (which use the electrons boiled off from a hot metal surface to convert heat energy directly to electrical energy), cesium plasmas have been studied extensively at the Los Alamos Scientific Laboratory where spectrographic techniques for their analysis have been developed. Using these techniques, the light given off by the plasma can be analyzed to show how the electron temperature and ion density vary as a function of the distance from the emitter (the electrode from which the electrons are boiled off) in the interelectrode gap of an operating thermionic converter. For the data shown, the converter had an emitter temperature of 1,637° C. and a cesium pressure of 1.9 torr (mm of mercury). The current output of the device was 7.0 amp/square cm. of emitter surface, and the spacing between the electrodes was 1.0 millimeter.

thermionic plasma analysis have been developed. Accurate spectrographic determination of some of the fundamental radiative properties of the cesium system have been made recently in special ovens under known, carefully controlled plasma conditions. The properties (for example, radiative recombination cross sections, which are a measure of the probability that an electron and an ion will recombine) have been used to determine the values of the electron temperature and ion density in operating thermionic converters where plasma characteristics are unknown. The data have been used by many investigators to create theoretical models which aid in understanding converter operation. When analyzed, the light given off by the cesium plasma is seen to consist of spectral lines and bands. Both spectral lines and bands can be used to yield electron temperatures and ion densities, quantities important in the theoretical analysis of converter operation. The experimental technique permits the determination of these quantities at particular points in the interelectrode gap, yielding a temperature and density profile. A typical profile with pertinent information is given in Figure II–98. An important feature of the data is that the temperature and density are not constant across the gap.

Several independent methods exist for the determination of the temperature and density. Comparisons of the electron temperatures ascertained by various methods indicate that a state of equilibrium (local thermodynamic equilibrium) exists in the main body of the

plasma. When the ion densities, as determined by the different methods are compared, it is concluded that the atomic ion is the dominant species rather than the heretofore-speculated molecular ion.

Development of an Adsorption Cesium Reservoir

An adsorption cesium reservoir,[61] developed by the Radio Corporation of America (RCA), Lancaster, Pa., marks a significant advance in thermionic energy converters used to generate electricity from nuclear fission and radioisotope heat sources. The development makes possible the generation of electric power without the necessity of any external control systems for the converter.

The thermionic converter employs cesium plasma to increase the conversion efficiency. In the past, cesium, an active alkali metal, was retained in a liquid reservoir externally attached to the converter. This type of reservoir requires precise control and must be held at a lower temperature level than the rest of the converter. These requirements impose severe control and cooling complications for outer space applications of thermionic converters.

RCA has developed a high-temperature reservoir that can be included within the thermionic converter. In the new reservoir, designed to employ the principle of adsorption, atoms of cesium "stick" to metal surfaces. Because it consists of a multiplicity of small elements that provide a large "sticking" area, the reservoir contains a relatively large amount of cesium in a small volume.

An important characteristic of the adsorption reservoir is its ability to supply cesium to the converter in just the right quantities for all operating conditions. The reservoir is thermally coupled to internal structures in the converter so that, for any change in heat input to the converter, the reservoir change is in the correct direction to maintain the cesium pressure at the optimum value for full power output of the converter.

The resulting self control of cesium pressure has increased versatility of the thermionic converter, making it a more practical device for converting heat to electricity for both space and terrestrial power systems.

Curium-244 Heat Sources

Regardless of whether the power system being developed is a thermionic system or a thermoelectric[62] system, a heat source is required to activate it. One possible source of heat is from the radioactive decay of certain heavy-element isotopes. At the Savannah River Plant, curium-244 (Cm^{244}) is being produced for evaluation as such an isotopic heat source. The isotope generates 2.6 watts of heat per gram largely by emission of alpha particles. Recent studies indicate it can be a prime candidate for use in either thermionic or thermoelectric power systems for space applications.

Heavy elements are produced in Savannah River reactors by irradiation of targets initially containing plutonium-239. The plutonium is converted to heavier elements by successive neutron captures. In a program to produce 4.5 kilograms of curium-244, target elements were irradiated for about 2 years at high neutron flux and are now cooling by radioactive decay. The chemical process for separating the curium-244 from the target assemblies has been successfully demonstrated on a laboratory scale. Larger scale processing facilities for recovery of the 4.5 kg. of curium are currently under construction.

Curium sesquioxide as heat source. A form of curium has been found at the Savannah River Laboratory (SRL) that appears to be suitable for heat sources. Monoclinic curium sesquioxide (Cm_2O_3) is stable both in chemical composition and in crystal structure when exposed to heat and to self-radiation. The Cm_2O_3 also exists in two, or possibly three, other crystallographic forms. The monoclinic structure is formed when the oxide is heated in the temperature range of

[61] See pp. 269–270, "Fundamental Nuclear Energy Research—1966."

[62] In the thermoelectric method of energy conversion, two conductors are joined together at both ends so that an electric current will flow when there is a difference in temperature between the two junctions; see pp. 149, 155, "Fundamental Nuclear Energy Research—1964."

about 1,000°–1,600° C. The structure is retained even on cooling to room temperature, and is not altered appreciably by radioactive decay of the curium-244 (see Fig. II–99).

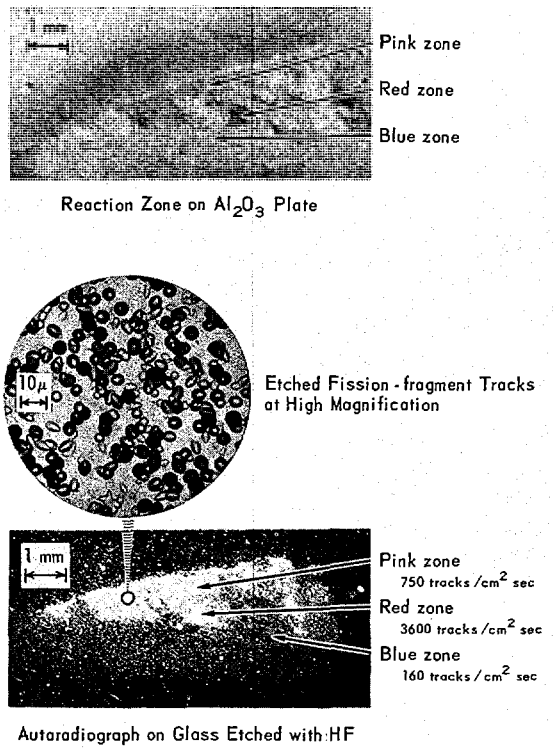

Fig. II–99. Curium Sesquioxide as Heat Source. At Savannah River Laboratory (SRL), studies are being made on the potential use of curium as heat sources for direct energy conversion, as well as other uses. The work has produced the above fission fragment autoradiograph of curium-244 (Cm^{241}) in an alumina plate. The distribution of Cm^{244} in cermet pellets and the penetration of Cm^{244} into refractory container materials is conveniently determined by a new technique developed at SRL. A glass slide exposed to a specimen containing curium and then etched in hydrofluoric acid (HF) reveals an image of the specimen consisting of etch pits in the glass at the sites of individual fission tracks. The *top* photo shows an alumina (Al_2O_3) plate that had been heated to 1,600° C. in contact with a pellet of curium sesquioxide (CM_2O_3), forming complex oxide compounds that appeared in red, pink, and blue fluorescent zones. The *center* photo is an enlargement of a portion of the autoradiograph showing the individual etch pits in the glass slide. The *bottom* photo is an autoradiograph of the alumina plate showing different concentrations of Cm^{244} in the various fluorescent zones.

Metallurgical examinations at SRL of pressed-and-sintered compacts have established the excellent compatibility of tungsten with the $Cm^{244}{}_2O_3$ fuel as a potential container metal. No interaction was observed between the oxide and tungsten at temperatures up to 1,850° C. for about 6 hours, or for shorter periods of time up to the melting point of the oxide, 1,950° C.

MAGNETOHYDRODYNAMICS

A magnetohydrodynamic (MHD) power generator is a device for the direct production of electricity by passing an electrically conductive fluid between the poles of a magnet. In liquid-metal MHD, the working fluid is a molten alkali metal; in plasma MHD, the working fluid is a gas seeded with a vaporized metal to make it electrically conductive.

Liquid-Metal Magnetohydrodynamics

An experimental and analytical study of liquid-metal magnetohydrodynamics is being conducted at Argonne National Laboratory to explore the relative merits and potential of the concept as an advanced power-conversion system,[63] particularly for generating electricity for use in space vehicles. Recent analytical studies show that the two-component (lithium-cesium) two-phase generator cycle originally proposed by ANL has a realizable over-all efficiency of 10 percent, which makes this cycle superior to other liquid-metal MHD power cycles proposed for space power (see Fig. II–100). However, to achieve this efficiency, generator electrical end-losses must be reduced by at least 80 percent.

Performance of the condensing injector, a key component of an alternate MHD power cycle, has been studied experimentally. Pressures were measured at the outlet as vapor-liquid conditions were varied to conform to actual cycle parameters. The inlet vapor flow was supersonic in the condensing-injector MHD cycle, the condensing injector converting the thermal energy from the reactor into kinetic energy. The accelerated stream then passes

[63] See pp. 271–272, "Fundamental Nuclear Energy Research—1966."

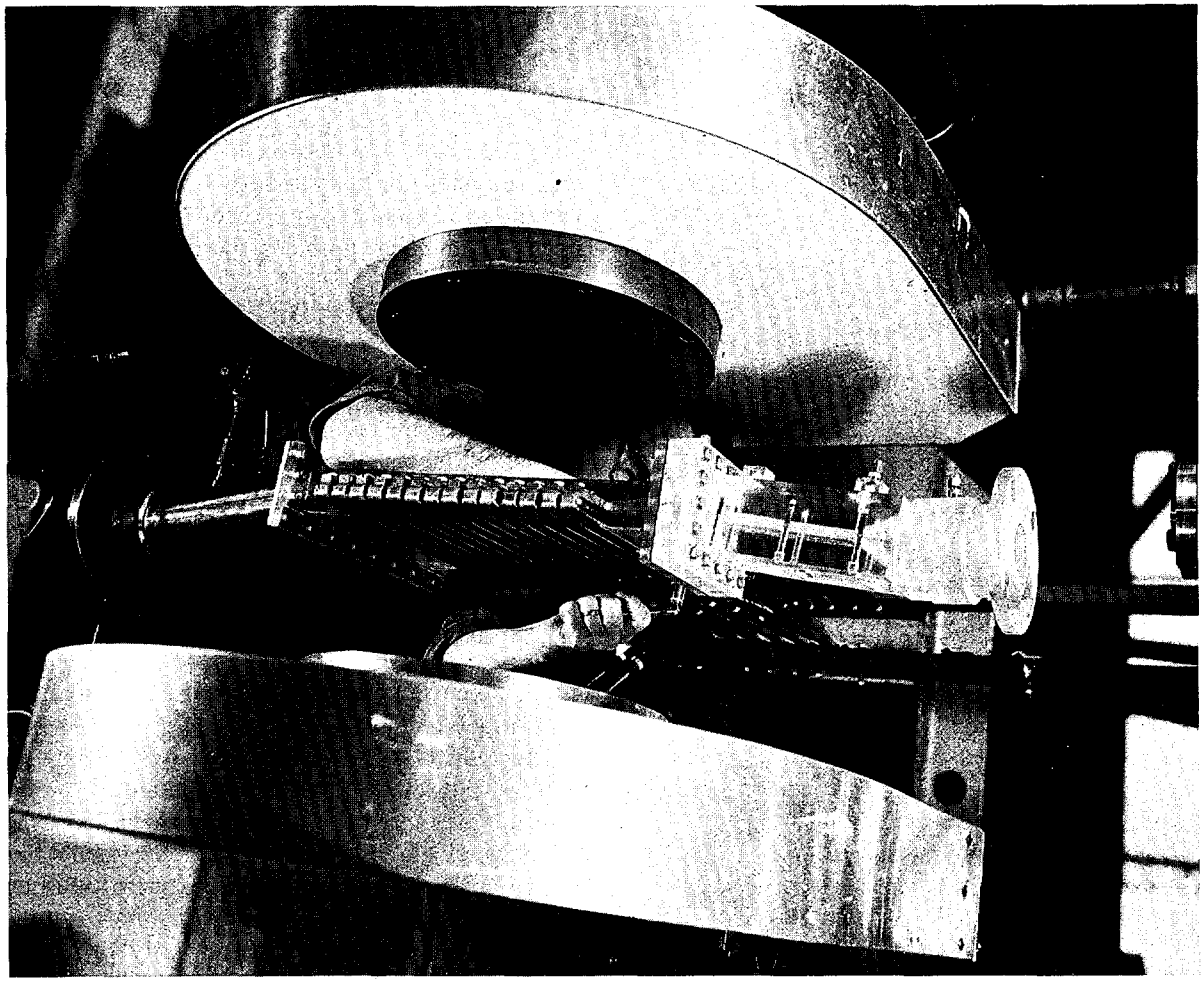

Fig. II–100. Liquid-Metal Magnetohydrodynamics. Analytical studies at Argonne National Laboratory, where the liquid-metal magnetohydrodynamic (MHD) concept for direct power generation is being studied, have shown that a two-component (lithium-cesium) two-phase generator cycle holds good promise. Photo shows a two-phase liquid metal MHD generator being installed between the poles of an electromagnet.

through a magnetic field within the generator to produce electricity.

As experiments with MHD components lead to a better understanding of actual performance, analytical studies will be able to realistically define the technical and economic potential of MHD power systems.

Plasma Magnetohydrodynamics

Studies have continued at Brookhaven National Laboratory [64] on a new system of non-equilibrium ionization in which metastable electronic states of nitrogen, excited by fission fragments in a gas-cooled nuclear reactor, keep the gas ionized as it flows through a magnetohydrodynamic (MHD) generator. Spectrographs show that excitation and ionization of such atoms as copper, calcium, sodium, aluminum, and others is maintained for approximately 200 milliseconds after the metastable electronic state is initially formed. Only about 10 milli-

[64] See pp. 273–275, "Fundamental Nuclear Energy Research—1966."

seconds is needed for the MHD generator. Unexpectedly, the studies have led to the production of plasmas having the characteristics of ball lightning phenomena (see Fig. II–97).

Nitrogen gas containing a large concentration of metastable electronic states was produced by a 75 MHz RF [65] discharge. The RF was then shut off, and the gas allowed to mix with a sodium-argon mixture. There was a much brighter glow as the gases mixed, indicating a rapid transfer from the metastable electronic nitrogen states to electronically excited sodium atoms.

[65] *MHz RF*—Megahertz radiofrequency; one megahertz is the equivalent of 1 million cycles per second.

Ionized gas measurements. Methods of measuring the conductivity of ionized gases at relatively high pressures (several atmospheres) have been developed so that measurements of significance in MHD work could be made. In one method, use is made of the fact that any ionization present in a resonant microwave cavity will tend to shift the resonant frequency of that cavity in a manner such that the conductivity due to that ionization can be readily determined. The microwave cavity is basically in the form of a hollow metal cylinder. The ionization in the cavity is induced by an electron beam from a Van de Graaff accelerator passing along the axis through whatever gas it

Fig. II–101. Plasma Magnetohydrodynamic Studies. Plasma conductivities must be measured to efficiently design magnetohydrodynamic nuclear reactor power systems. In the experiment shown here, the electrical conductivity of an uranium iodide-neon gas plasma (the lighted area within glass tubes) is being measured at Brookhaven National Laboratory. Other experiments have measured conductivities of plasma excited by metastable states of nitrogen. The measurements are made at relatively high pressures (several times that of normal atmosphere). Figure II–97 is another photo of the Brookhaven studies.

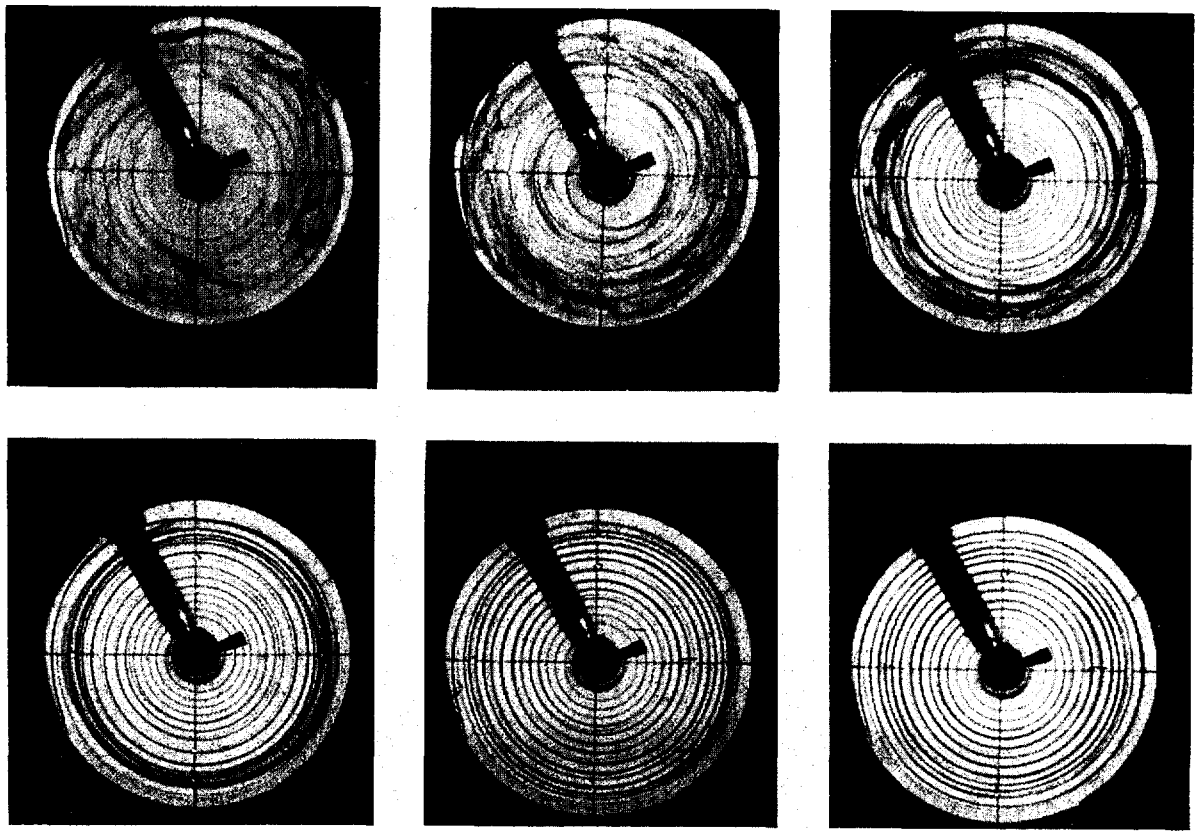

Fig. II–102. MHD Studies of Vortex Flow. These photographs of dye traces taken through the transparent endwall of a vortex tube fed by an electrically conducting liquid strikingly reveal the stabilizing influence of an applied magnetic field parallel to the axis of the tube. The unstable flow with no magnetic field, as seen in the frame at the *upper left*, is characterized by large amplitude fluctuations in the dye trace. The effect of increasing the magnetic field in 15,000-gauss increments to a maximum of 75,000 gauss is seen in subsequent frames from left to right. At 75,000 gauss, the flow is completely stable, as made evident by the spiral dye rings which the *lower right-hand* frame reveals. Whereas, under the conditions of this experiment the magnetic field extended the range of stable operation by about tenfold, a greater increase might be expected for the case of a plasma-core nuclear reactor to which these studies are applicable.

is desired to study. The shift in resonant frequency of the cavity is then studied as a function of time after the electron beam is turned off. In this manner, the conductivity, and also the time it takes for the ionization to decay, can be studied in gases at pressures many times higher than heretofore possible (see Fig. II-101).

Ball lightning studies. An unexpected result of plasma MHD studies at Brookhaven National Laboratory has been the first experimental production of plasmas approaching the reported characteristics of natural ball lightning. These are floating glowing balls 6 to 12 inches in diameter, lasting on the average about 3 to 5 seconds. They usually appear after a conventional lightning stroke, near the point of impact. Until the present, there has been no satisfactory explanation of these phenomena. The plasmas produced by the 75 MHz discharge last about a half to one second after the RF has been cutoff, and can be produced in nitrogen, oxygen, or mixtures thereof, *e.g.*, air with and without water vapor. It has been definitely established that they are caused by metastable electronic states in both oxygen and nitrogen.

In addition, if these balls are produced inside a large (8 ft. cube) cavity resonator fed by a 75-MHz oscillator they last for 10 or more seconds before finally hitting the wall. An analysis shows that DC fields of the same magnitude (about 1,000 volts per centimeter) as the RF field in the cavity exist after lightning strokes, and that current flow is sufficient to maintain the ball for several seconds instead of the approximate 1 second it would last if there were no electric field (see Fig. II–97).

Magnetohydrodynamic Studies of Vortex Flow

The exploratory study of confined flows of a vortex (tornado-like) nature for possible application to advanced energy conversion systems is continuing at the Oak Ridge National Laboratory. One such system would use an ultra-high-temperature reactor in which the nuclear fuel is permitted to vaporize and then ionize so as to become an electrically conducting gas (plasma). Rotation of this plasma as a vortex results in a centrifugal (outward) force on the heavy fuel atoms which causes them to be concentrated near the wall of the containing tube, thereby effecting holdup of the fuel within the vortex tube. A strong magnetic field parallel to the axis of the vortex might be used to stabilize this flow in order to reduce turbulent frictional losses and mixing. That such magnetohydrodynamic stabilization is possible was predicted analytically and verified experimentally in what is believed to be the first quantitative investigation into the stability of confined, jet-driven vortex flows (see Fig. II–102).

The possibility of developing a unique means for generating electrical power using a magnetically stabilized, vortex plasma-core reactor is suggested by the fact that there will be voltage developed radially across the tube as a consequence of rotation of the plasma in the magnetic field. If this voltage can be fed through appropriate electrodes to an external load, an electric current will flow. Preliminary analysis of this concept suggests that it may be of interest for future space missions having very large power requirements.

Part Three

BIOLOGICAL, MEDICAL, AND ENVIRONMENTAL RESEARCH PROGRAMS

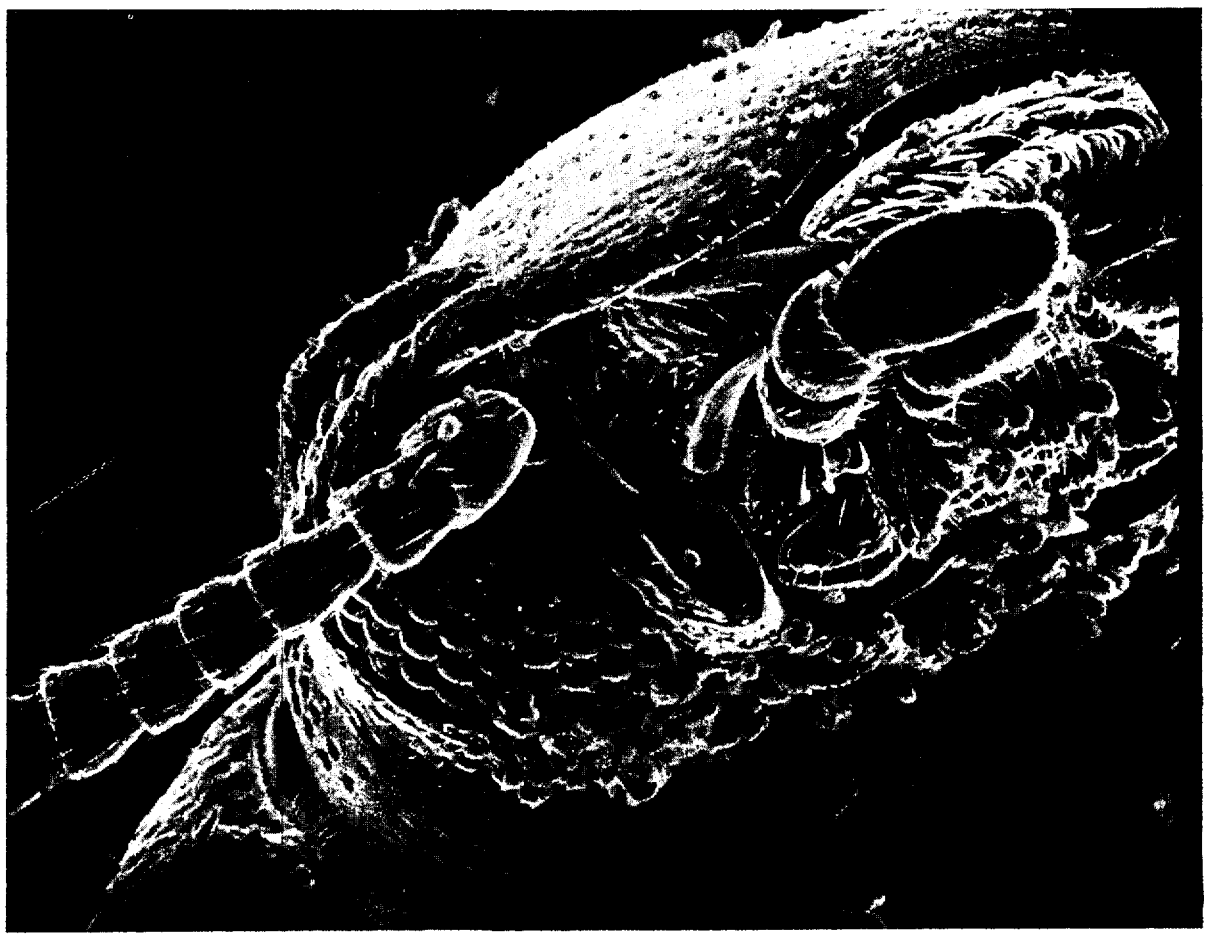

Fig. III–1. New Magnification Technique. At Lawrence Radiation Laboratory, Berkeley, a relatively new scanning electron microscope is being used for systematic studies of biological materials. The above is a living flour beetle, magnified about 260×, as seen in the scanning electron microscope. This is one of the first pictures of a living specimen taken with an electron microscope. See page 230 for details.

275-845 O—68——16

BIOMEDICAL AND ENVIRONMENTAL RESEARCH

The goal of the AEC's biological, medical, and environmental research program is to develop the scientific knowledge needed for full comprehension of possible short- and long-term consequences of the interaction of radiation with biological systems. Special emphasis is given to overcoming the attendant hazards of nuclear energy and developing the useful potentialities of radiation in the life sciences.

The AEC, through the fostering of biomedical research, has set forth the following objectives of the biomedical research program:

1. In areas of basic research—

(*a*) to formulate concepts of principles, mechanisms, and implications of the interactions of radiations with biological systems;
(*b*) to solve selected problems of importance in the life sciences that may be subject to resolution through the use of radiations and by-product materials; and
(*c*) to provide data to extend and refine existing scientific guidance for the control of exposure to radiation.

2. In areas of specialized problems of health and safety—

(*a*) to devise procedures for ways to apply new data toward the evaluation of biological consequences for man of all nuclear energy programs and devices; and
(*b*) to develop means for improving health and safety in nuclear operations.

3. In areas of beneficial applications—

(*a*) to discover and promote beneficial uses of special nuclear and radioactive materials and accelerator radiations in the treatment of cancer and other diseases; and
(*b*) to discover and promote unique uses of these nuclear materials and radiation for beneficial purposes in practical medical, biological, agricultural, and food processing applications.

The following pages summarize some of the current findings emanating from these efforts. The subject matter is arranged in sections that take in broad areas of the biomedical research program.

This year's report also describes in some depth two areas of specialized study: Atmospheric Sciences, and Semiconductor Detector Applications. These follow the sections devoted to other aspects of the basic research program, including highlights of outstanding progress and achievements in the AEC's program of biological, medical, and environmental research.

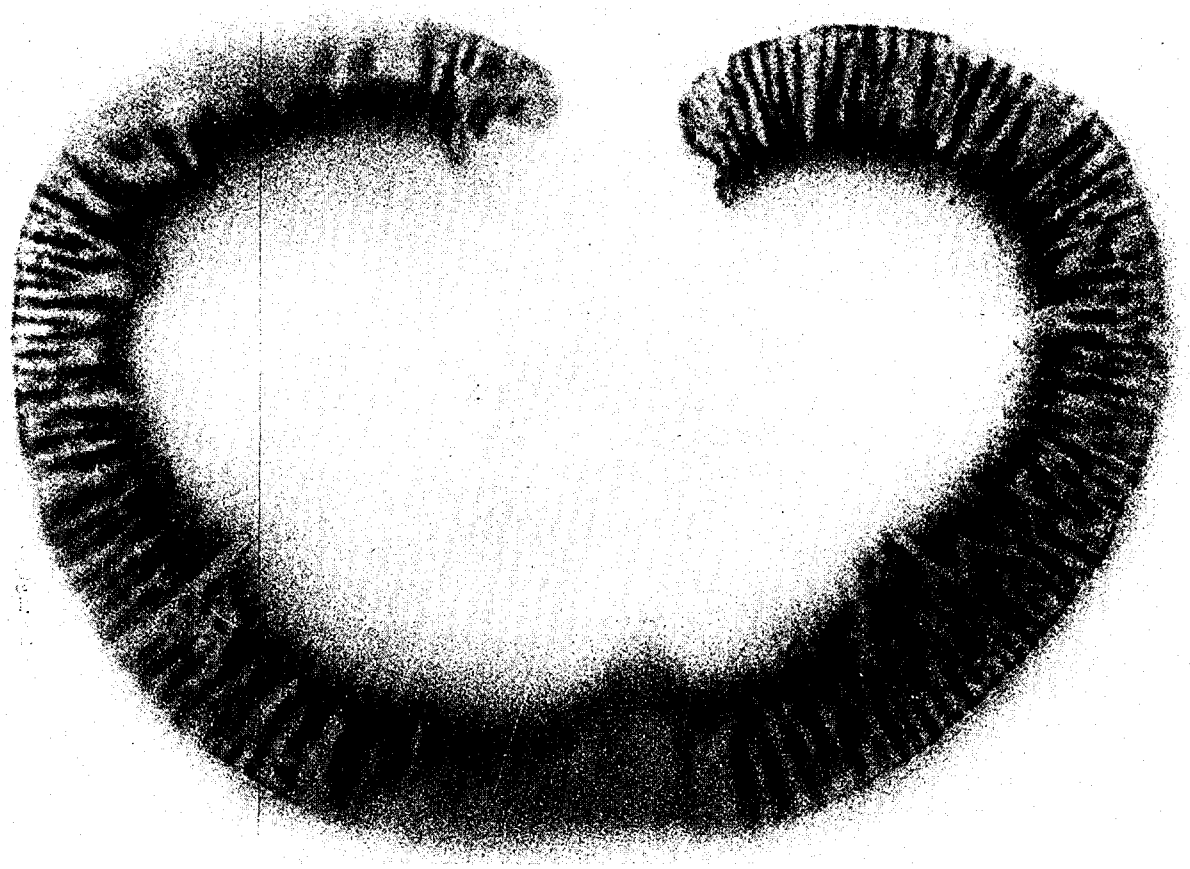

Fig. III–2. Localization of Technetium-99^m. Argonne Cancer Research Hospital radioautograph from technetium-99^m in rabbit kidney (5 millimeter slice) showing localization of radioactivity in the cortex 45 minutes after intravenous injection of the technetium-iron complex. See page 222 for expanding uses of the technetium-99^m radioisotope in diagnostic studies of diseases.

SELECTED BENEFICIAL APPLICATIONS

AEC-sponsored projects are currently underway to foster and encourage new and unique applications of radiations and radioisotopes in medicine, as in the diagnosis and characterization, treatment, and control of diseases other than cancer (which is summarized in another area of biomedical research) and in basic studies of organs and organ systems in health and disease. Projects are also in progress in agriculture to control and eliminate insects, weeds, and diseases, and to improve farm-animal productivity and increase knowledge of animal diseases.

MEDICAL RESEARCH

The medical research program of the AEC consists of studies on applications of radioisotopes and special radiation sources in diagnosis and therapy and includes such projects as: (*a*) treatment and control of diseases other than cancer; (*b*) diagnosis and characterization of disease states such as those of the circulatory and endocrine systems; (*c*) basic biological studies on metabolism and synthesis as related to disease and better understanding of the transportation of metabolites across intracellular spaces, cells, organs, and organ systems in

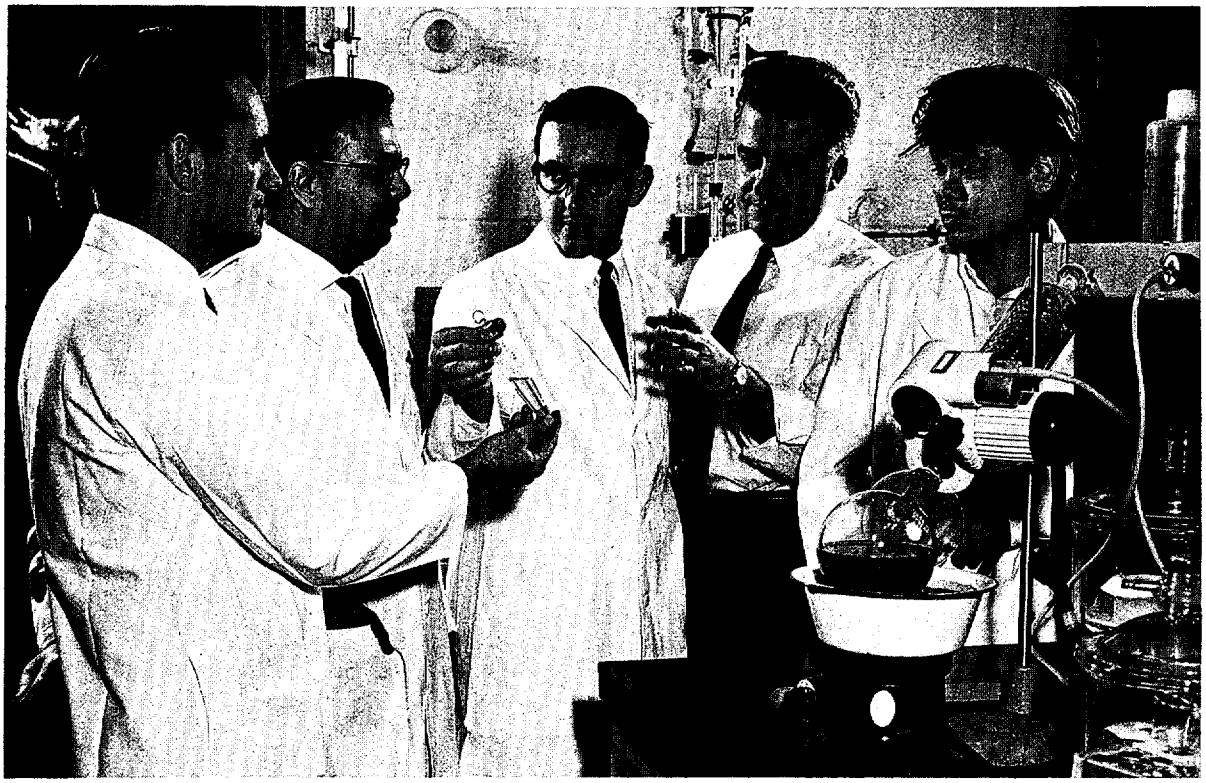

Fig. III–3. Synthesis of Human Insulin. Medicine was given an invaluable research tool in the study of diabetes when a Brookhaven National Laboratory Medical Department research team synthesized human insulin for the first time. The vial (*left* of center) contains the first human protein ever made in a laboratory. In the United States, 2 percent of the population suffers from diabetes and is kept alive only by periodic shots of the hormone insulin which keeps their blood sugar from rising to lethal levels. These regular injections of insulin, obtained from the glands of cattle and pigs, substitute for the natural human insulin that is lacking in the diabetic due to some malfunction of body activity. At present, diabetes cannot be cured; only controlled. The perfection of the techniques to construct human insulin is an important event in the efforts to understand the body processes and opens whole new avenues for research on diabetes. It is now within the limits of possibility that insulin could be manufactured commercially. This human insulin would not cause the toxic rejection in the body that animal insulin does. The synthesized insulin can be altered into analogs—altered forms of the insulin molecule—with the possibility of producing an artificial insulin that would have natural insulin's assets without its liabilities. Insulin molecules can be built with radioactive tracers included in the structure and perhaps provide answers to the questions of how the insulin stimulates the oxidation of blood sugar, and what biochemical reactions are involved.

health and disease; and (*d*) development and use of whole body counting facilities and scanning devices for study of metabolic processes having diagnostic potential. A few notable recent advances in the treatment of diseases, other than cancer, using unique applications of radioisotopes and special radiation sources are described below. For studies in the cancer research program, see p. 235.

Treatment of Diseases

Lymphocytes and Organ Transplantation

One of the more interesting and relatively recent developments in physiology and medicine is the recognition that the lymphocyte plays an important role in the immunological rejection of tissue transplants. It has long been known

that the first observable effect of total-body irradiation of a few hundred rads [1] is a precipitous drop in the level of circulating lymphocytes. The physiological role and cytological properties of the lymphocyte are still far from being unraveled. At the University of California at Los Angeles (U.C.L.A.), attempts are being made to develop new methods to measure physical properties of lymphocytes and separate them into different types while maintaining their viability. It has been shown that there is a similarity in their behavior observed after irradiation, both *in vivo* and *in vitro* [2] and after immunological stimulation.

The lives of many human beings with incurable diseases could be prolonged if it were possible to replace certain disease-affected organs, *e.g.*, kidneys and liver. Unfortunately, grafts from individuals other than identical twins are often rejected because the patient's own lymphocytes (one of the cell types present in blood and lymph) "recognize" the foreign graft and destroy it. At Brookhaven National Laboratory, studies on the role of the lymphocytes in causing this rejection have resulted in partial success with skin graft implants in animals.

Circulating blood or lymph of calves is shunted outside the body of the animal and is exposed to radiation from a gamma ray source consisting of radioactive cobalt or cesium. The irradiated blood or lymph is then returned to the animal (see "A" in Fig. III–4). Lymphocytes are far more sensitive to radiation than are other cells in the blood or lymph and it has been observed that in animals whose lymphocytes are destroyed by this method, skin grafts implanted from unrelated donors survive longer than animals not so treated.

This technique of irradiating lymph or blood outside the body has one distinct advantage. Significant and sustained reduction of circulating lymphocytes is accomplished without producing any harmful effects on the rest of the

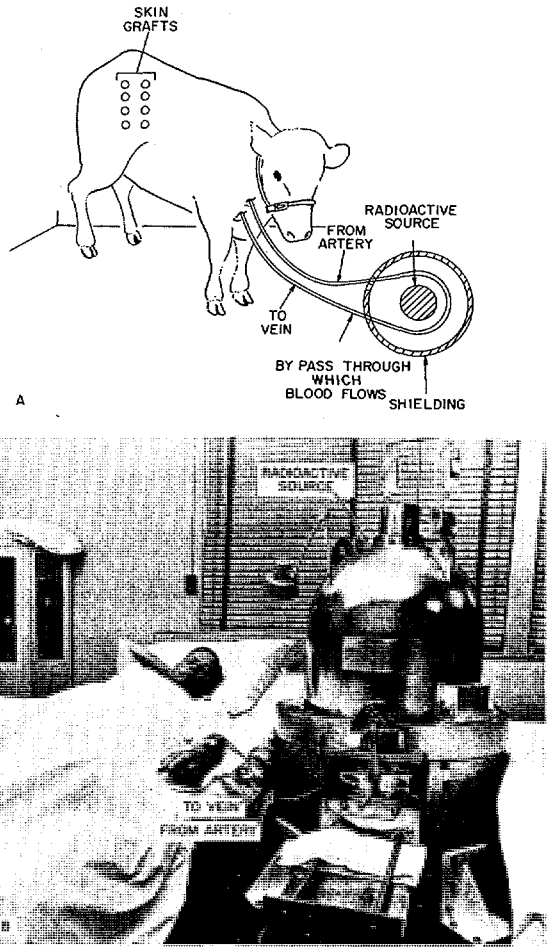

Fig. III–4. Studies to Aid Organ Transplants. The Brookhaven National Laboratory diagram (at *top*) shows a calf whose blood is being irradiated. Blood entering the bypass from a neck artery passes the radiation source and returns to the calf via a neck vein. The photo (at *bottom*) shows a patient whose blood is being irradiated. The procedure is similar to that of the calf except that a forearm artery and vein are used.

body. When irradiation of lymph was combined with skin grafting at certain selected sites of the body, the grafts survived up to 61 days (the maximum duration of the treatment so far). Skin grafts in untreated animals survived from 8 to 11 days. These results suggest that the fraction of the lymphocytes responding to the presence of a graft returns via lymphatics and can be destroyed by radiation before the

[1] *Rad* is an acronym for *r*adiation *a*bsorbed *d*ose; the basic unit of absorbed dose of ionizing radiation. One *rad* is equal to the absorption of 100 ergs of radiation energy per gram of matter.

[2] *In vivo*—in the living body; *in vitro*—not in the living body.

lymphocytes enter the blood and can attack the graft. The graft survival can probably be prolonged for as long as lymph irradiation can be continued.

These observations have resulted in studies on human beings in collaboration with Peter Bent Brigham Hospital, Boston. Irradiation of the blood is employed to prepare patients for kidney transplantation and to help in the treatment of patients in whom transplanted kidneys are rejected (see "B" in Fig. III–4). Initial results indicate that irradiation is helpful in controlling episodes of kidney rejection.

Diagnosis of Diseases

Diagnostic Uses of Technetium-99^m

The search for radioisotopes that can be used as a scanning agent for diagnosis of diseases has been advanced by the finding that technetium-99^m [3] (Tc-99^m), a decay product of molybdenum-99, is a very versatile agent. It has been used successfully in different forms for diagnosis of several conditions and is becoming increasingly useful in nuclear medicine because of several favorable physical characteristics (see Fig. III–5). Technetium-99^m is readily supplied through a molybdenum-99 (67-hour half-life) generator system (see Fig. III–6) previously developed at Brookhaven National Laboratory to overcome the lack of availability of Tc-99^m because of its 6-hour half-life. For this reason, and because of the virtual absence of beta particle emission, very little radiation energy is deposited within the patient. Its low energy gamma emisson of 140 kev., (thousand electron volts) is detected very efficiently. The chemical form of technetium-99^m, as it is obtained from the generator, is the pertechnetate.

A survey by the Stanford Research Institute, Menlo Park, Calif., for the National Center for Radiological Health (U.S. Dept. of Health, Education, and Welfare) in 1966 indicated that technetium-99^m was the most common agent used for brain scanning at diagnostic centers and that 48 percent of the patients were being examined with this agent. This percentage is increasing rapidly.

[3] The superscript "m" stands for metastable; indicating that the isotope is unstable and decays without particle emission to a more stable form of the element.

Technetium-99^m in Thyroid Studies

At Brookhaven National Laboratory (BNL) the evaluation of technetium-99^m as a tracer to study thyroid gland physiology has shown that this isotope is as useful as iodine-131 in the diagnosis of abnormal conditions of the thyroid gland. A primary advantage is that the disease may be studied as well as with radioactive iodine, but with less than one one-hundredth the radiation dose, as compared with iodine-131.

Using the pertechnetate chemical form of technetium-99^m, about 0.5–4.0 percent of the administered material was found to localize in the thyroid within 15 to 30 minutes after intravenous injection. Iodine-131 normally concentrates in the thyroid to the extent of 20–50 percent in 24 hours. The degree to which the technetium is localized in the thyroid is an indication of the action of the "trapping mechanism" of the thyroid, that is, of the ability of the thyroid to extract iodine from the blood prior to the formation of the thyroid hormone. In this case the extraction of technetium parallels the extraction of iodine. However, following extraction from the blood, iodine is "bound" in the form of thyroid hormone, whereas technetium-99^m is not bound. Suppression or stimulation of the thyroid trapping mechanism by administration of either synthetic thyroid hormone (triiodothyronine) or thyroid stimulating hormone (TSH) has similar effects on thyroid uptake of technetium and iodine.

In addition to being useful in the assessment of thyroid physiology, excellent scintillation scans which outline the thyroid anatomy can be obtained with technetium-99^m. Because rather large amounts can be safely administered, the accuracy of the scans is improved and better resolution is possible because of the low energy of its gamma rays.

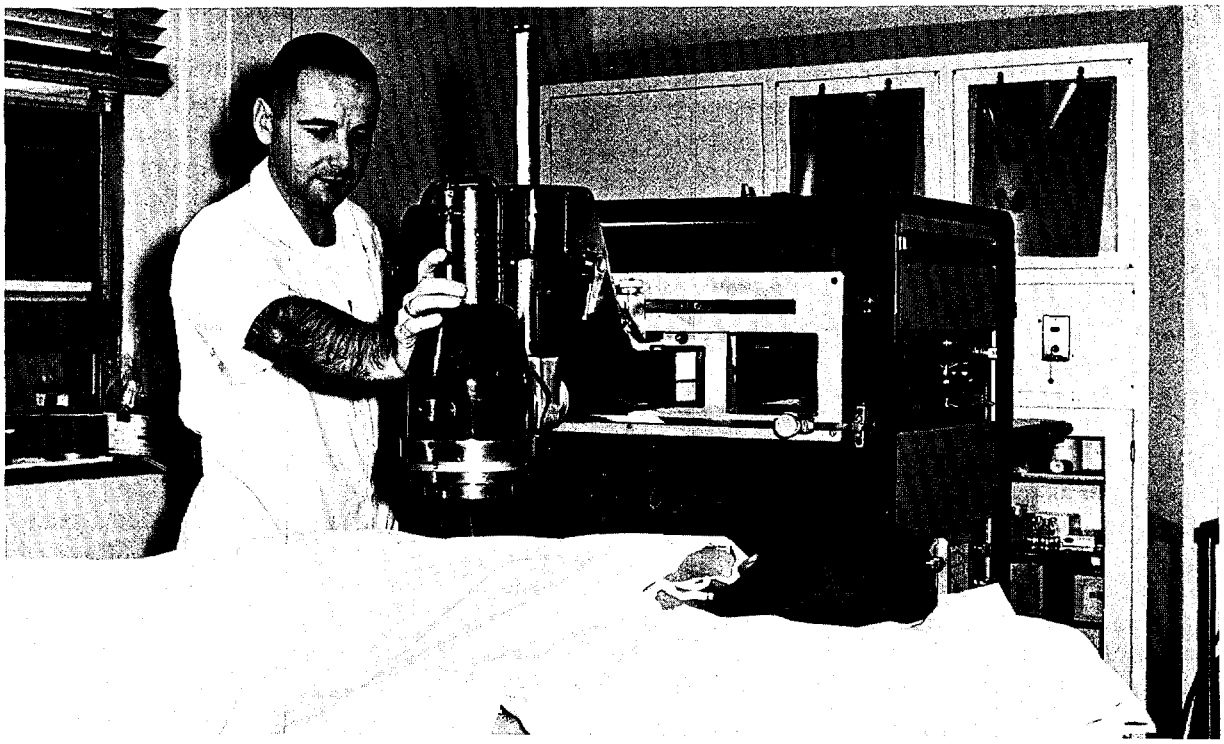

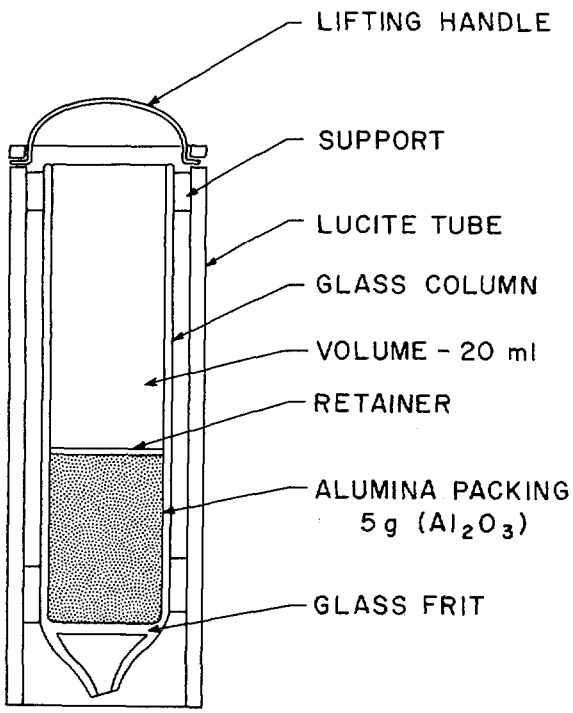

Figs. III–5 and 6. Diagnostic Uses of Tc^{99m}. Low energy gamma rays from radioactive technetium-99^m, which was concentrated in the patient's kidney after having been injected intravaneously in the form of technetium-iron ascorbate, are detected by a scintillation crystal (photo *above*) which is moved back and forth in a precise pattern over the patient. The signals from the detector are converted by the plotter, to which it is connected, into a "picture" of the kidney by means of a moving stylus activated by the pulses from the detector. This representation of the kidney provides important information for diagnostic purposes. The use of Tc^{99m}, developed at Brookhaven National Laboratory and elsewhere, is an important advance in the field of diagnostic scanning. The gamma rays from Tc^{99m} are easily detectable outside the body; yet its short half-life (6 hours) and the absence of charged particle radiation (alpha particles or electrons) or high-energy gammas, means that a sufficiently large dose of Tc^{99m} can be administered to insure good detail and high contrast in the scans and at the same time subject the organ being scanned and the patient's whole body to a much lower dose of radiation than was possible with isotopes used earlier. The Tc^{99m}, which is prepared by a method (diagram at *left*) developed at BNL is an almost ideal isotope for liver, spleen, and kidney scanning. It has already been applied in thyroid studies, and is widely used in brain tumor localization.

Technetium Iron Complex for Diagnosis

At Argonne Cancer Research Hospital, a technetium-99^{m} iron complex has been developed that can be used as a kidney scanning agent.

When an acid solution of the pertechnetate ion is reduced with ascorbic acid in the presence of ferric chloride and then neutralized, an iron complex is formed. A large portion of this agent is promptly excreted in the urine after intravenous administration, but a significant amount remains fixed in the kidney. In laboratory animals, radioautography shows that the nuclide is localized in the kidney 45 minutes after injection (see Fig. III–2). In humans, of the approximately 40 percent remaining in the body 24 hours after administration, about half (20% of the original dose) is retained by the kidneys. Whole body counts show a two-phase elimination curve with an intial half-time of about 1 hour and a second half-time of 5.7 days.

The retention of this material in the kidney makes it a good renal scanning agent. Two methods of diagnostic examination have been used: (*a*) one millicurie is administered intravenously, and scintiphotography or scanning is started 1 hour later, or (*b*) four millicuries are injected and the examination is started 18 hours later. The second method has the advantage of primarily showing the nuclide fixed by the renal parenchyma, since urinary excretion is essentially complete by that time.

The radiation dose to the kidney is only 500 *millirads* [4] per millicurie. A one-millicurie dose gives about 15,000 counts per minute on the gamma scintillation camera 1 hour after injection. This gives excellent renal scintiphotographs in 4 minutes. The four-millicurie doses give about 10,000 counts per minute at 18 hours, which permit scintiphotography in 6 minutes. Considering that the conventional renal scan done with mercury-203 Neohydrin gives a minimum of eight and a maximum of 20 *rads* to the kidney, and takes about 30 minutes, the efficacy of this new agent is apparent.

[4] A *millirad* is one-thousandth of a *rad*.

"Scatter Counting" of Radioisotopes

A technique for "scatter counting" has been shown at Oak Ridge Associated Universities (ORAU) to be highly accurate for measuring the total amount of a radioisotope present in a human being or when unevenly distributed in a biological sample. This procedure is particularly applicable to low level whole body counting.

The older, conventional, counting technique was to adjust the electronic instrument to record only the "photopeak" energies coming from the patient, thereby counting only those radiations that have not scattered or "bounced" and thus have not lost any of their energy. The "photopeak" is the major high-energy gamma emission and it varies with different radioisotopes. Photopeak counting is of great value in the separate detection of mixed radioisotopes, and in localizing radioisotopes by scanning. Because of these facts, the belief has developed that it is always better and more accurate to count the photopeak.

The ORAU studies have shown that photopeak counting is often very inaccurate when the task is to measure quantitatively the total amount of a single known radioisotope in a person. The radioisotope is practically never uniformly distributed in the patient and the pattern of its distribution affects the efficiency with which the radioactivity is detected. Thus, if the radioisotope shifts from a single deep location, for example, in the stomach after a dose by mouth, to a more general distribution when it has entered the blood stream, the number of radiations measured by a photopeak instrument may increase, even though the total amount of radioactivity is the same. On the other hand, if the electronic settings are chosen so as not to record any of the high energy photopeak radiations, but rather to record a certain selected band of lower energy "scatter" radiations, the total number of counts recorded will be truer whatever the distribution of the isotope in the body may be.

This new technique was tested first by measuring point sources of iodine-131 at many sites

in a water phantom which simulated a patient's body. Computer analysis suggested that detection of scatter radiation is much less affected by source distribution changes than the conventional "photopeak energy" methods. Accordingly, this system of "scatter" analysis was tested and compared to "photopeak" analysis in nine patients (see Figs. III–7 and 8). The average of the maximum errors in these patients was 1.8 percent using "scatter" and 22 percent using "photopeak" analysis. The data also show that the efficiency of detection in the "scatter" method is also independent of body size and shape. The "scatter" system of whole body counting makes it possible to measure the amount of iodine-131 present in a living person with a precision not previously available. This will be of value in clinical diagnosis and research applications as well as in health physics. Early results of experiments with radioisotopes other than iodine-131 indicate that the scatter method is applicable to nearly all, if not all, gamma-emitting radionuclides.

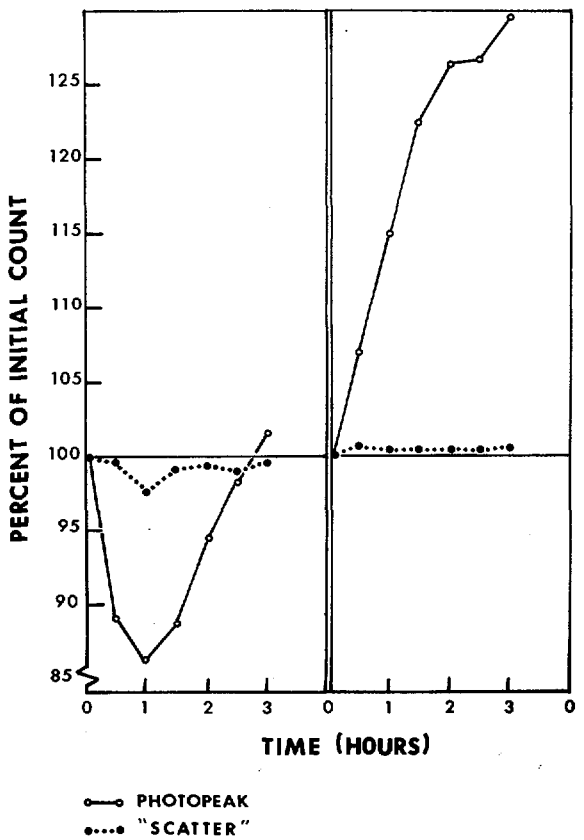

Iron Absorption in Hemochromatosis

Research at Lawrence Radiation Laboratory, Berkeley, has provided evidence that a rare disease called hemochromatosis—caused by the body's inability to control iron absorption—probably exists from birth and is very likely hereditary. These findings have improved understanding of the disease and have contributed to an explanation of how iron absorption occurs and to the treatment of anemias.

Hemochromatosis is characterized by an excessive amount of iron in the patient's body,

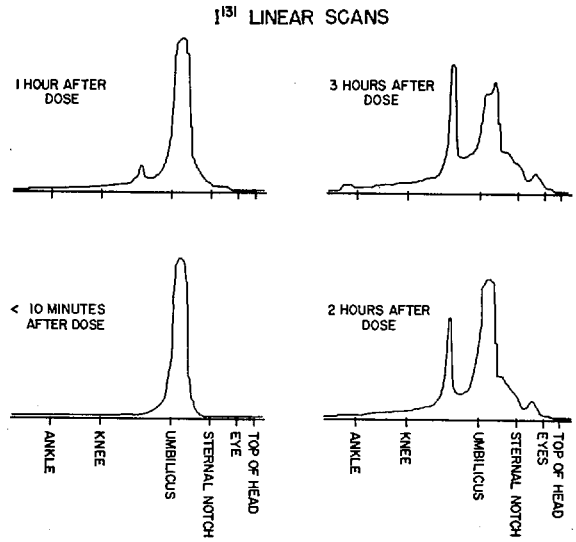

Figs. III–7 and 8. "Scatter Counting" of Radioisotopes. Examples of "scatter" and "photopeak" whole-body counting results in two patients at the Oak Ridge Associated Universities medical facility are shown in graph *left above*. The patients had a constant amount of iodine-131 (I^{131}) present during the period of study. Note the small variation during the first 3 hours after oral administration in the "scatter" counting data and the unpredictable variation in photopeak data due to changes in the bodily distribution of the I^{131}. The *above* right shows serial linear scans of the iodine-131 distribution in a patient given I^{131} orally. These changes are responsible for the increase in scattered radioactivity and photopeak error.

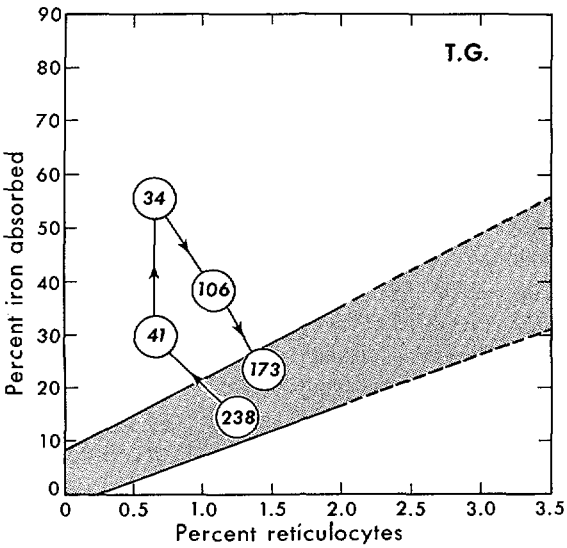

Fig. III–9. Iron Absorption in Hemochromatosis. The stippled region in the chart represents the range of the relationship between oral iron absorption and the percent of circulating reticulocytes in normal subjects. The points shown are those of a series of tests at Lawrence Radiation Laboratory, Berkeley, on a typical hemochromatotic patient before, during, and after phlebotomy (bleeding) therapy. The numbers inside the points are the serum iron (SI) concentration (SI; normal 70–170) at the time of the test; 238 before therapy; 41 and 34 after therapy; 106 (normal SI) 1 year after therapy; and 173 2 years after therapy (SI above normal again.) The abnormally high absorption when the SI was a normal 106 implicates an inborn defect of control of iron absorption as a primary factor in the etiology of hemochromatosis.

causing damage to organs such as the liver, heart, and pancreas. Untreated, it is usually fatal. Some researchers have contended that patients with the disease have eaten high-iron diets all their lives; others have held that patients have eaten regular diets, but absorb too much of the iron in those diets.

In studies at Berkeley in the past 6 years, techniques have been refined and tested for measuring iron absorption with a whole-body counter, using both healthy persons and patients with various diseases. Radioactive iron-59 is given to the subject by mouth; 2 weeks later, the amount remaining in the body, as measured by the whole-body counter, indicates the amount adsorbed (see Fig. III–9).

A group of seven patients with hemochromatosis was studied before and after a year's treatment. This treatment consisted of removal of 50 to 100 pints of blood from each patient, thus, removing 12 to 25 grams of iron. The patients' absorption of iron was found to be within the normal range before treatment, while after treatment, when they no longer contained large amounts of iron, their iron-absorption rate was greatly increased. This increased absorption undoubtedly existed during the patient's entire life and is considered, therefore, to be the basic cause of the disease.

Metabolic Studies

Trace Metals and Parkinson's Disease

The importance of trace metals to health and disease has been appreciated by investigators for a number of years; however, these investigators were handicapped by the deficiencies of their analytical tools, primarily analytical sensitivity. This has been particularly limiting in studies of the trace metal, manganese. Methods developed at Brookhaven National Laboratory—namely, isotopic techniques and neutron activation analysis of tissues—have provided better sensitivity and specificity at the sacrifice of analytical speed. The importance of manganese as an essential element lies in its extensive participation in both catalytic and noncatalytic biochemical processes for which this metal is specific. Among recent investigations on manganese have been those involving studies of melanin-producing tissues. It was found that melanosomes concentrate this metal actively. Since melanin formation is defective in the brains of patients with the neurological disease, *Parkinsonism*, efforts were initiated to effect melanogenesis and determine whether this affects the disease. These studies are as yet incomplete in the sense that it is not yet known whether the maneuvers which have indeed improved the disease have done so by means of improving formation of melanin.

One of the agents investigated was the melanin-precursor Di-hydroxyphenylalanine

(DOPA), but this is also a precursor of several biogenic amines. This material had been tried by several investigators and variable reports have accrued. At Brookhaven, the method used consisted of: (*a*) slow chronic increase of DOPA given to in-patients; (*b*) extensive documentation of the neurological status; and (*c*) extensive monitoring of vital organs for toxicity. In about three out of four patients treated with as large a daily dose as was deemed tolerable, marked improvements of signs and symptoms was induced. Several side-effects of this treatment have been observed, which have made it mandatory to increase the vigilance exercised over the patients. During administration of D–L DOPA a redistribution of manganese among the tissues was observed. During the present investigations with L–DOPA, the significance of this redistribution is being evaluated.

PLANT RESEARCH

Plant research in the AEC-sponsored program includes studies on: (*a*) means for the control and elimination of insects, weeds, and diseases of plants; (*b*) mineral nutrition and metabolism in plants; (*c*) radiation induced mutations for enhancing productivity and resistance to diseases and environmental stresses in plants of economic importance; and (*d*) radiation sensitivity of plants. In this section, as examples of the above, the next few pages summarize studies on survival of seedlings and their growth after exposure to gamma and neutron irradiation. A feature section on this area of research was included in "Fundamental Nuclear Energy Research—1964", entitled "Radiation Effects in Plants and Seeds."[5]

Survival and Growth After Irradiation

Sensitivity of seeds to different types of radiation can be assessed by measuring different seedling responses. Responses after exposure to

[5] Reprints may be obtained by writing to the Director, Division of Biology and Medicine, U.S. Atomic Energy Commission, Washington, D.C. 20545.

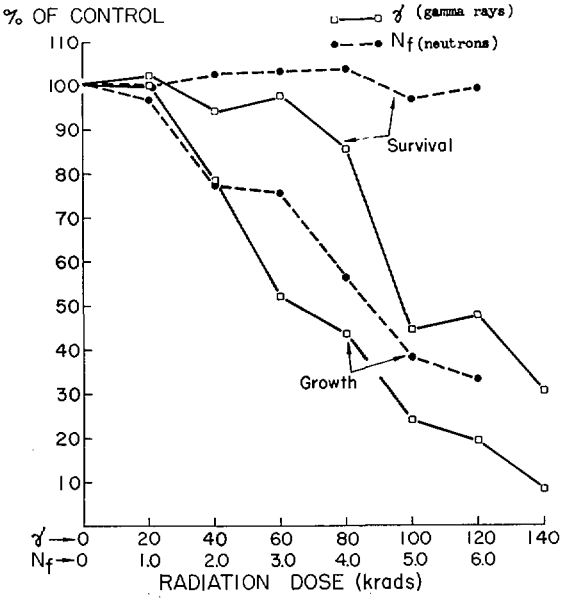

Fig. III–10. Irradiated Seed Survival and Growth. Chart shows seedling survival and growth of okra, *Hibiscus esculentus*, following irradiation with gamma rays (γ) and unmoderated fission neutrons (N_f). Note that for equivalent dose (rads), the neutrons caused a greater reduction in seedling growth without affecting survival. The study was made at the University of Tennessee-AEC Agricultural Research Laboratory at Oak Ridge.

different types of radiation (gamma and neutron) can provide information pertinent to the sensitivity of the processes involved.

In multicellular organisms, such as higher plants, survival and growth are two responses that can be studied to measure the effect of a treatment such as irradiation. Some processes may contribute to both responses, yet seedling survival and growth are not necessarily a cause and effect relationship. For example, a surviving seedling might or might not show growth. Seedling survival and growth are affected adversely by exposure to different types of radiation. If survival and growth truly involve different processes and the two responses do not necessarily show a cause and effect relationship, it is possible that interactions may be observed when different types of radiation are used.

At the University of Tennessee-AEC Agricultural Research Laboratory, experiments were made to determine whether seedling survival

and growth at an intermediate stage of the life cycle show relative differential sensitivity (interaction) to gamma and neutron irradiation. Seeds of okra, *Hibiscus esculentus* L. cv. "Clemson Spineless," were exposed to gamma rays from cesium-137 and unmoderated fission neutrons. Control (non-irradiated) and irradiated seeds were sown in the greenhouse. Seedling survival and true growth (dry weight of plant parts above the cotyledonary nodes) were determined 1 month after planting. A range of doses (0–140 kilorads of gamma rays and 0–6 kilorads of neutrons) was used.

Seedling growth and survival are plotted in Figure III–10 as a function of gamma rays and neutrons. The gamma-irradiated seed showed a reduction in seedling survival and growth indicating that the processes contributing to each response have similar radiosensitivities. However, the neutron-irradiated seeds showed a reduction in seedling growth but no reduction in survival, indicating that the processes contributing to each response have differential sensitivities to unmoderated fission neutrons.

There is an apparent interaction between the two types of radiation and the relative sensitivity of the processes (metabolic and/or physiologic) that contribute to seedling survival. The exact nature of this interaction (differential sensitivity) is not known.

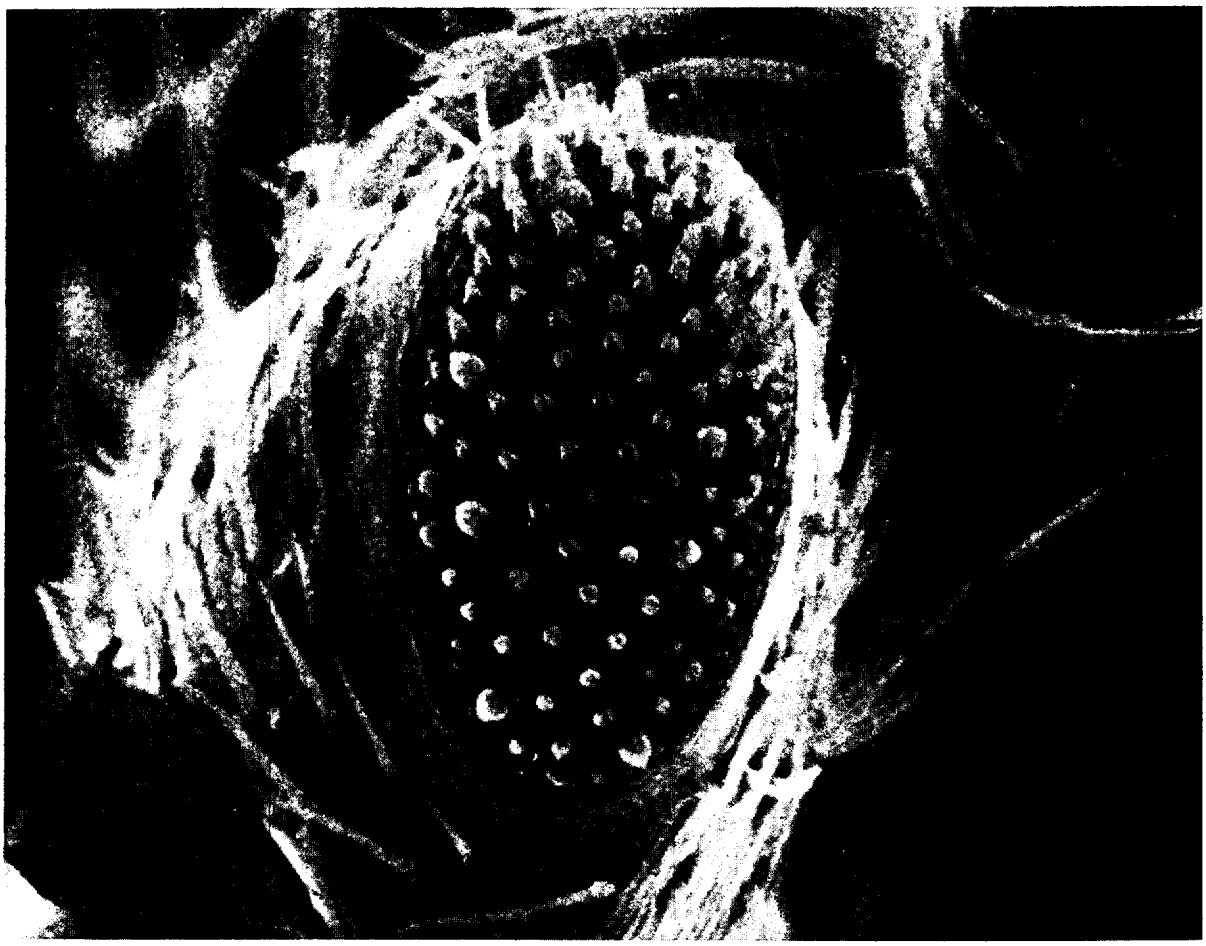

Fig. III–11. Tip of Feeler. Photo shows the tip of a palp (feeler) of a living flour beetle at about 1,160 × magnification. A new scanning electron microscope technique developed at Lawrence Radiation Laboratory, Berkeley, can be used as a microprobe to study the effects of radiation on a developing system and since the specimen is viewed while it is alive its response to the electron beam can be better studied.

INSTRUMENTATION AND RADIOLOGICAL PHYSICS

AEC-sponsored instrumentation research and development contribute to advances in radiation protection techniques and biomedical research by developing new and improved instruments. As new instruments and techniques are developed, studies in the area of radiological physics are enhanced. Detailed knowledge of the physical processes which precede radiobiological change is prerequisite to the interpretation of radiobiological effects, to the design of radiobiological experiments, and to the formulation of improved radiobiological dosimetry.

INSTRUMENTATION

Development of advanced instrumentation is based on studies that discover and develop new methods and techniques for improving the observation and measurement of important biomedical phenomena. Investigations are carried out on material, systems and special components, and special techniques.

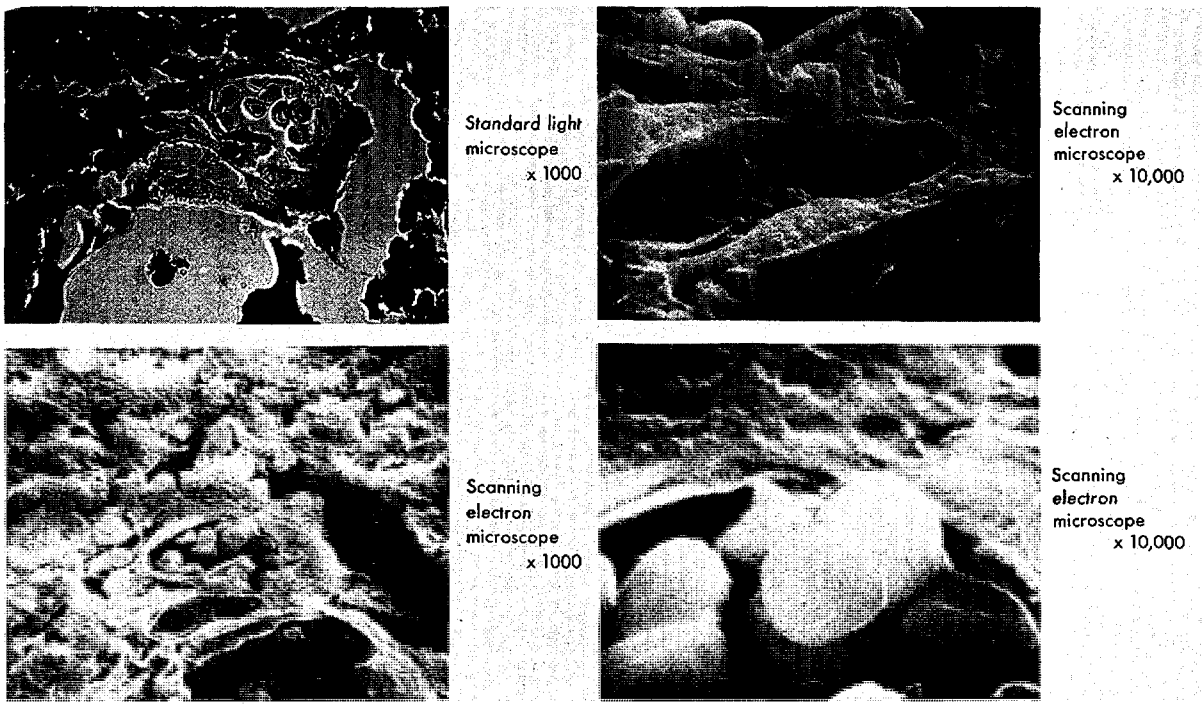

Fig. III–12. Irradiated Brain Section. The series of photos show comparison of sectioned irradiated brain tissue as seen in light microscope (*upper left*) and scanning electron microscope (*lower left* and on *right*). Note the three-dimensional appearance and higher magnification possible with the new scanning electron microscope. Technique now in use at Lawrence Radiation Laboratory, Berkeley.

Scanning Electron Microscope

At Lawrence Radiation Laboratory, Berkeley, the relatively new scanning electron microscope—a variation of the conventional transmission electron microscope—has been applied to the systematic microscopic study of biological material. One achievement of this technique is a series of photographs of living flour beetles (see Figs. III–1, and III–11). This appears to be one of the first times living organisms have been visualized by electron microscopy.

Photographs of other specimens show the surfaces of tissues in three dimensions at magnifications 100 times greater than has been possible with the stereoscopic light microscope (see Fig. III–12). The result is a direct visualization of the submicroscopic surface features of tissues at magnifications of up to 5,000 times. Magnifications of 20,000 are considered feasible.

Image from secondary radiation. The stereoscopic light microscope allows the scientist to see a tissue surface directly in three dimensions up to a useful magnification of only about 100; this barely reaches down to the cell level, leaving fine detail out of reach. At higher magnifications—up to 1,000—the light microscope is useful only for looking at thin sections or slices. Highly magnified direct visualization of surfaces has awaited the present application of the scanning electron microscope.

The new scanning electron microscope also offers significant advantages over the conventional electron microscope. Such microscopes are capable of high magnifications—100,000 being common—but they cannot "see" the surfaces of specimens satisfactorily. Normally, the electron microscope directs a stream of electrons through a thin slice of chemically treated tissue and focuses the electrons on the other side, forming a shadow image of the specimen.

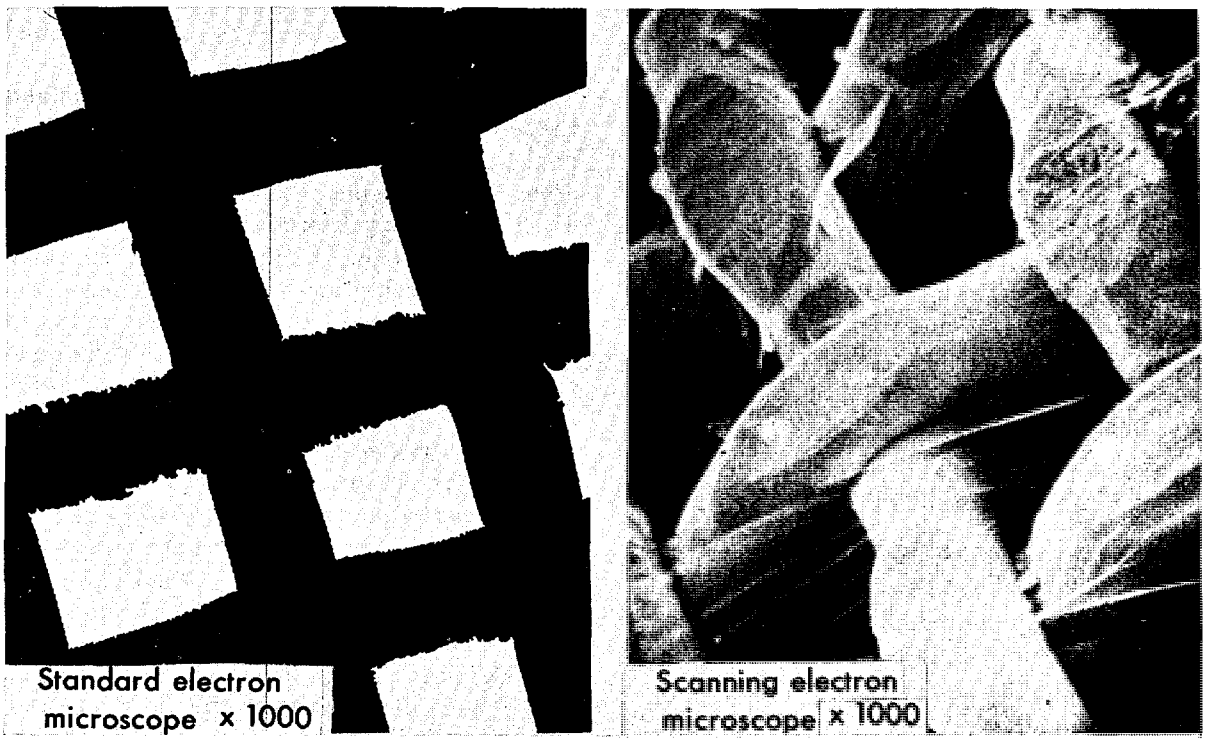

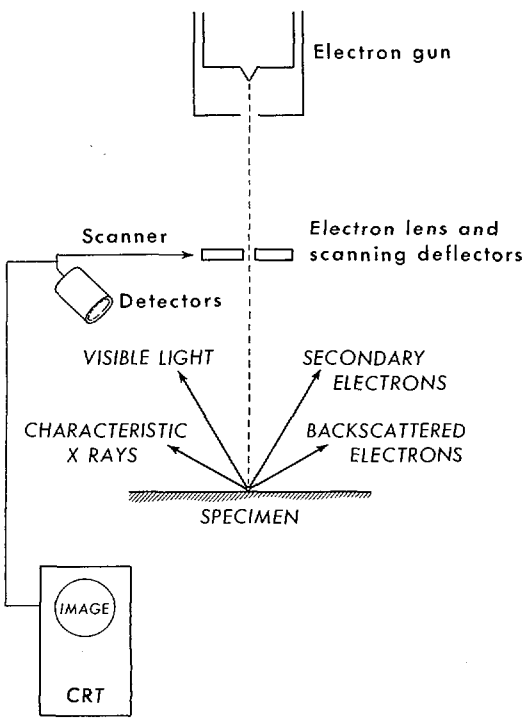

Figs. III–13 and 14. Scanning Electron Microscope. Photos *above* are a comparison of standard electron microscope (*left*) and scanning electron microscope (*right*) images showing how a steroscopic view is possible with scanning electron microscope. Note that qualities such as the stainless steel 200-mesh woven grid being covered with a thin layer of plastic (Formuar) can be perceived with the scanning electron microscope. Schematic drawing on *left* shows basic scanning electron microscope system used in the new technique employed at Lawrence Radiation Laboratory, Berkeley, which can produce high-magnification, three-dimensional pictures.

In the scanning electron microscope, however, a microbeam of electrons sweeps over the surface of a specimen that can remain unmodified by slicing or chemical preparation. The electrons cause secondary radiations to emerge from the specimen's surface; these are collected by a detector and translated into an image in a system similar to television (see Figs. III–13 and 14).

Living specimens helpful. There are several advantages, moreover, to viewing a living specimen. Morphologically, sample preparation

is simpler and more accurate. Physiologically, it is an advantage to be able to observe the ongoing life processes.

At Donner Laboratory, scientists for years have used a flour beetle, *Tribolium confusum*, for studies in radiation biology, both with accelerators and in space. This insect has a shell-like covering with which it is able to seal off its vital organs, protecting it from the loss of water that normally occurs when living organisms are exposed to a vacuum; even eggs and larvae of the beetle usually survived the exposure and continued to develop.

RADIOLOGICAL PHYSICS

Research in radiological physics seeks to achieve a detailed understanding of the fundamental physical and chemical processes, whereby ionizing radiation interacts with matter, and to determine the underlying principles, both theoretical and experimental, by which the effects of ionizing radiation can be quantitatively formulated.

Low Energy Electron Studies in Matter

When nuclear radiation strikes matter, be it in the gaseous, solid, or liquid form, one of the principal results is the generation of low-energy electrons. These electrons diffuse through the irradiated material and interact very strongly with atoms and molecules of the material. An effective understanding of the details of the absorption of these electrons by the irradiated material involves, first of all, a knowledge of the number and energy of the electrons so generated and, secondly, an understanding of the particular interactions which occur. Measurements of the number of electrons have been carried out for the last several years at Oak Ridge National Laboratory with the "Keplertron," an electron energy analyzer, together with very strong radioactive sources irradiated in the ORNL reactors. These have shown a large buildup of low energy electrons below 100 electron volts (ev.) in energy in all irradiated media.

Electron interactions. In order to understand the second step in the radiation damage process, namely the interaction of such electrons with atoms and molecules, studies are underway at experimental and theoretical levels of the interaction of electrons with matter in its three states of condensation—the gaseous form, the solid form, and the liquid form. For studies in the gaseous state, new experimental techniques have been developed for the investigation of the interaction of low-energy electrons (below 20 ev.) with molecules. Detailed and pioneering results were obtained on negative ions formed by low-energy electron capture. Of particular importance are the results on capture cross sections, temporary negative ion states of aromatic molecules, and the measurement of temporary negative ion lifetimes.

Theoretical studies have led to the finding that a molecule having an electric dipole moment can capture an electron only when its moment is greater than a certain critical value. The critical value of a dipole moment lies, for example, between those of the water and ammonia molecules. This finding is important for the interpretation of experiments in which electrons interact with molecules having a permanent dipole moment.

Laser employment. The development of the laser has opened up new possibilities for studying the interaction of light with matter, particularly in the condensed or solid phase. Consideration of the laser as a probe to study collective excitations in solids has shown that certain nonlinear interactions between photons, electrons, and collective modes should occur with relatively high probability. Experimental investigation along these lines may reveal new characteristics of matter in the condensed phase.

An ultraviolet laser has been employed by Argonne National Laboratory to provide excitation of sensitive photoluminescent dosimeters. With this system it is easy to measure quantitatively 1 milliroentgen of cobalt-60 exposure.

Further improvements in this system should make it possible to do track visualization and *in vivo* biological microdosimetry with a spatial resolution on the order of 10 microns.

Photoelectric effects. Additional information on electron interactions in solids is being obtained through study of the photoelectric effect, *i.e.*, the emission of electrons from the surface of the solid when the solid is irradiated with light. New details of energy losses suffered by very low-energy electrons in solids are being obtained from studies of the energy distribution of photo-electrons excited by photons in the vacuum ultraviolet region of the spectrum. These studies give evidence of selective absorption of energy in solids from electrons with energies as low as 5–15 electron volts, and may help to delineate one phase of the complex process of transfer of energy from incident radiation to biological materials.

Ultraviolet radiation studies. Although matter in its liquid state most nearly resembles human tissue, almost no information is available on electron interactions with liquids. A program, initiated in 1966, represents a first attempt to study electron interactions in liquids directly. Details of radiation damage to water are being revealed by a new technique discovered at ORNL. Optical experiments with very damaging ultraviolet radiation have proven unexpectedly easy and promise to give new insight into the exact mechanisms by which nuclear radiation interacts with the aqueous environment. In these experiments, ultraviolet radiation is reflected off a water surface. The way in which this reflection depends on the light energy and angle of reflection is determined by the behavior of electrons within the liquid. For example, enhanced reflection at 1,000 angstroms (12.5 ev.), 1,700 angstroms (7.3 ev.), and 2,100 angstroms (5.9 ev.) has tentatively been attributed to ionization, singlet excitation, and triplet excitation, respectively, while a peak at 1,250 angstroms is unidentified. These peaks are similar to those found in water vapor in absorption experiments and indicate that condensation of water vapor to liquid water does not profoundly influence the electrons in the water molecules. Health physics calculations based on these results should lead to improvements in estimates of radiation dose and, hence, better calculations of radiation safety.

275-845 O—68——17

Dosimetry in Cell-Sized Volumes

At Pacific Northwest Laboratory, experiments are underway to measure how radiation deposits energy which can directly cause injury in tiny volumes the size of living cells. Measurements in sample targets (ten-millionths of a centimeter thick) indicate that a maximum of 100 to 110 thousand electron volts (ev.) of energy can be deposited by energetic protons in a cell one ten-thousandth of a centimeter in diameter. This is about 20 percent more than previous estimates.

The targets used for investigation of energy transferred from the incident protons to cell-sized volumes, originally developed at Columbia University, consist of relatively large cavities filled with a low-pressure gas formulated to represent soft tissue. The large gas-filled cavity can be shown to accurately represent absorption sites of greatly reduced size. Scaling factors of 100,000 to 1 million (10^5 to 10^6) are obtainable. The energy lost in the gas by the passage of each proton can be inferred by measuring the resulting ionization of the gas.

Such information is important not only to fundamental studies of the biological effects of radiation, but also to the health physicist concerned with the welfare of individuals exposed to radiation. Neutron radiation, which is a component of cosmic radiation in the atmosphere and a significant radiation in the nuclear industry, deposits in soft tissue about 90 percent of its radiation dose through energetic protons. These protons result when uncharged neutrons collide with the hydrogen component of tissue. Since the proton is a charged radiation, it rapidly deposits energy along tracks which are typically less than one one-hundredth of a centimeter.

At Argonne National Laboratory, experiments with mice are underway to measure the radiation exposure to mouse testes from the strontium-90 taken up in the pelvic region. Tiny photoluminescent dosimeters have been employed with improved reproducibility and calibration accuracy to provide a quantitative measure and good spatial resolution.

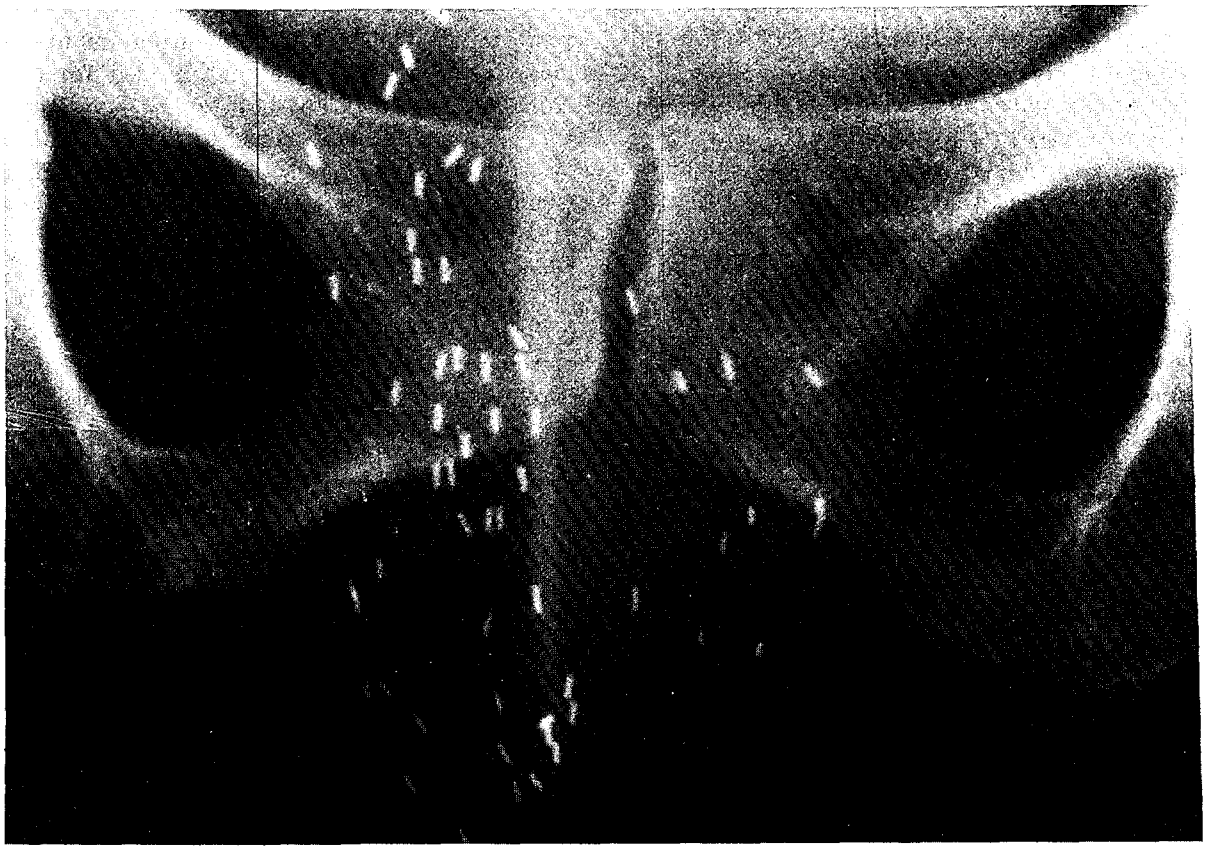

Fig. III–15. Radioactive Chromium Wire. A new technique for cancer therapy, using small pieces of chromium-51 wire, has been developed at Argonne Cancer Research Hospital. Photo shows an X-ray of the pelvis of a patient with cancer of the anus showing implanted "seeds" of radioactive chromium wire which can be left in the body permanently.

CANCER RESEARCH

Cancer research in the atomic energy program seeks to discover, develop, and perfect unique means of diagnosis and therapy of cancer and to acquire additional knowledge for these purposes from studies on the metabolic patterns of malignant diseases and the affected host. An investigation of the use of radioactive chromium wire for implant into cancerous tissue is discussed below. New insight into tumor formation has been obtained from the discovery of a fatty substance found to occur in a variety of animal and human tumors. The role of enzyme synthesis in the liver in transformation of normal liver into cancerous liver is being studied.

CANCER THERAPY

Radioactive isotopes have been used extensively as sources of internal radiation in treating cancer.

Radioactive Chromium Wire

New radioactive sources are constantly being evaluated for their potential applicability for treating cancer patients. Recently, radiothera-

pists at Argonne Cancer Research Hospital (ACRH) have become interested in the use of high-purity chromium wire for this purpose. This wire was first produced at the Bureau of Mines Research Center, Albany, Oreg., about 10 years ago, but at that time the AEC's regulations restricted the use of radioactive chromium in cancer therapy. However, recent changes in these restrictions have led to renewed interest in the technique.

Other radioactive metals have been used as cancer therapy implants, but chromium wire is unique among these because it may be left permanently in the body. Radiochromium has a convenient half-life (the time needed for the radiation level to fall by half) of 27 days. Such a half-life is sufficient to ensure an effective dose of radiation, but not so long that the metal would have to be removed to prevent an overdose.

At the ACRH, the wire is cut into $\frac{3}{16}$-inch long pieces and then irradiated in an Argonne National Laboratory reactor to convert some of the chromium atoms into the isotope form, chromium-51. These small pieces or "seeds" are introduced into the body using a special radio-

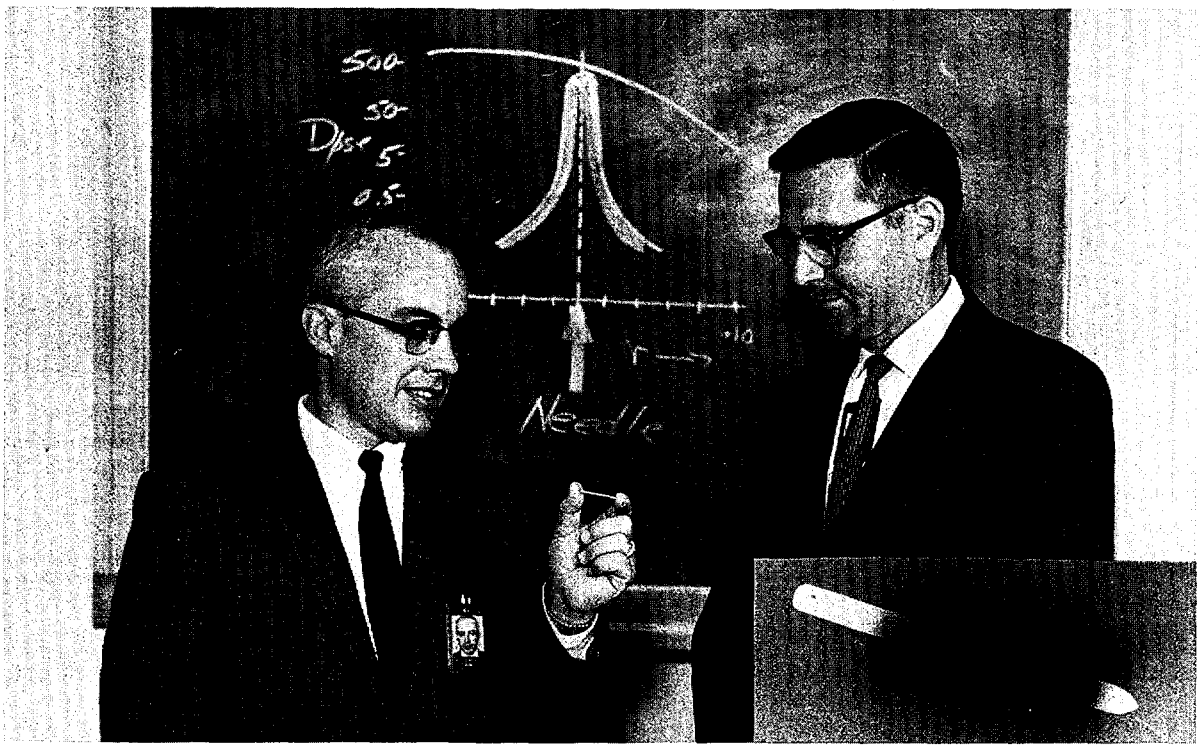

Fig. III–16. Californium-252 for Cancer Therapy. Ten needles containing californium-252 (Cf^{252}) are being prepared at the Savannah River Laboratory for use in radiation experiments at Brookhaven National Laboratory. Californium-252 emits neutrons that may be more specific against oxygen-deficient cancer cells than X-rays and gamma rays. Dose measurements in tissue equivalent material and animal studies will precede any future treatment of human patients with the needle. Only about a microgram of californium-252 is needed to give a radiation dose equivalent to a conventional radium needle. A needle (*center* of photo) is shown prior to being loaded with the radioisotope. The inset photo (*lower right*) was made by laying a Cf^{252} loaded needle on a photographic film; the dark area shows the exposure of the film by radiation from the californium-252. The outline of the needle was obtained by exposing the film and needle to X-rays. The possible use of an internal isotopic neutron source in cancer therapy would be a major advancement since, heretofore, neutrons have been applied in cancer therapy only from external sources such as nuclear reactors and cyclotrons. Neutrons from external sources have had limited use because of the damage done to healthy tissue surrounding the tumor.

isotope implantation gun. The seeds are placed in an array or distribution within the tumor. Under some situations the implantation is done through the skin and in other situations the implantation is done at the time of major surgery. Because of the relatively long half-life of this material, the radioactive sources are constantly available and ready for use by the radiotherapist. These sources have proved to be highly flexible and useful for a number of situations. Figure III–15 shows an X-ray of a chromium implant done deep in the pelvis for cancer of the anus.

Irradiation in Chronic Granulocytic Leukemia

At the Medical Division of Oak Ridge Associated Universities,[6] a study has shown how irradiation of the spleen may be of benefit in treating chronic granulocytic leukemia, a disease of middle-aged and elderly people. It has long been known that irradiation of the spleen improves the patient, but with little understanding of how or why the improvement comes about or the best use of the treatment. As a first step in this study, a careful comparison was made between spleen irradiation and radiation directed to the liver. Observation showed that the treatment of the spleen produced a highly predictable improvement in the condition of the patient's blood, while treatment of the liver produced variable results ranging from almost no effect to one similar to that produced by irradiation of the spleen. No explanation has been found for the variation in results of liver irradiation, although several hypotheses are being considered. Extension of this work will relate the dose, timing of treatments, and size of spleen to the effect produced.

Irradiation of the liver was not expected to be an advance in the treatment of the disease. Rather, the liver was used as an organ that could be compared to the spleen to see whether the spleen plays a unique role in chronic granulocytic leukemia. If the role of the spleen could be fully shown it would improve understanding of the disease and its treatment. The effects of irradiation of the spleen are also being compared with those of total-body irradiation in this disease.

New Total-Body Irradiation Facility

The Oak Ridge Associated Universities has constructed and equipped a facility that will allow prolonged total-body irradiation treatment of patients at low dose rates (see Figs. III–17 and 18). The new facility will make possible a reevaluation of the effectiveness of chronic total-body exposure to cobalt-60 gamma radiation in patients having chronic leukemias and other blood diseases characterized by overproduction of cells. This type of treatment has been found to be of some value in these diseases, but its administration has been complicated by lack of equipment designed especially for the purpose.

In some medical centers, exposure of such a patient to five roentgens (*R*) [7] per week from a conventional X-ray machine or cobalt-60 teletherapy source in one dose each week has produced remissions or amelioration of symptoms said to have lasted 5 to 15 years. These successes carry the implication that man can live for long periods of time in radiation fields of five to 10 *R* per week—above the occupational exposures considered permissible for normal persons.

The first patient to be treated in the new low-exposure rate total-body irradiation facility received a dose of approximately 100 *rads*, while he was exposed almost constantly in a 1.5 *R*/hr cobalt-60 gamma ray field for 100 hours during

---

[6] Previously known as the "Oak Ridge Institute of Nuclear Studies" (ORINS) the corporate name was changed to "Oak Ridge Associated Universities" (ORAU) in January 1966. The old ORINS—embracing the Medical Division, Information and Exhibits Division, and the Special Training Division—continues as a major operating unit of ORAU to serve as the avenue through which the sponsoring institutions (see appendix) of the Association participate in and support the nation's nuclear energy programs. Mention of Oak Ridge Associated Universities, or ORAU, in this part of the report refers to work done, or being done, by the Medical Division of ORAU.

[7] Roentgen (*R*), a unit of exposure dose of ionizing radiation; it is not a measure of the amount of energy actually absorbed. *R* has been recently adopted as the symbol for roentgen replacing the *r* previously used.

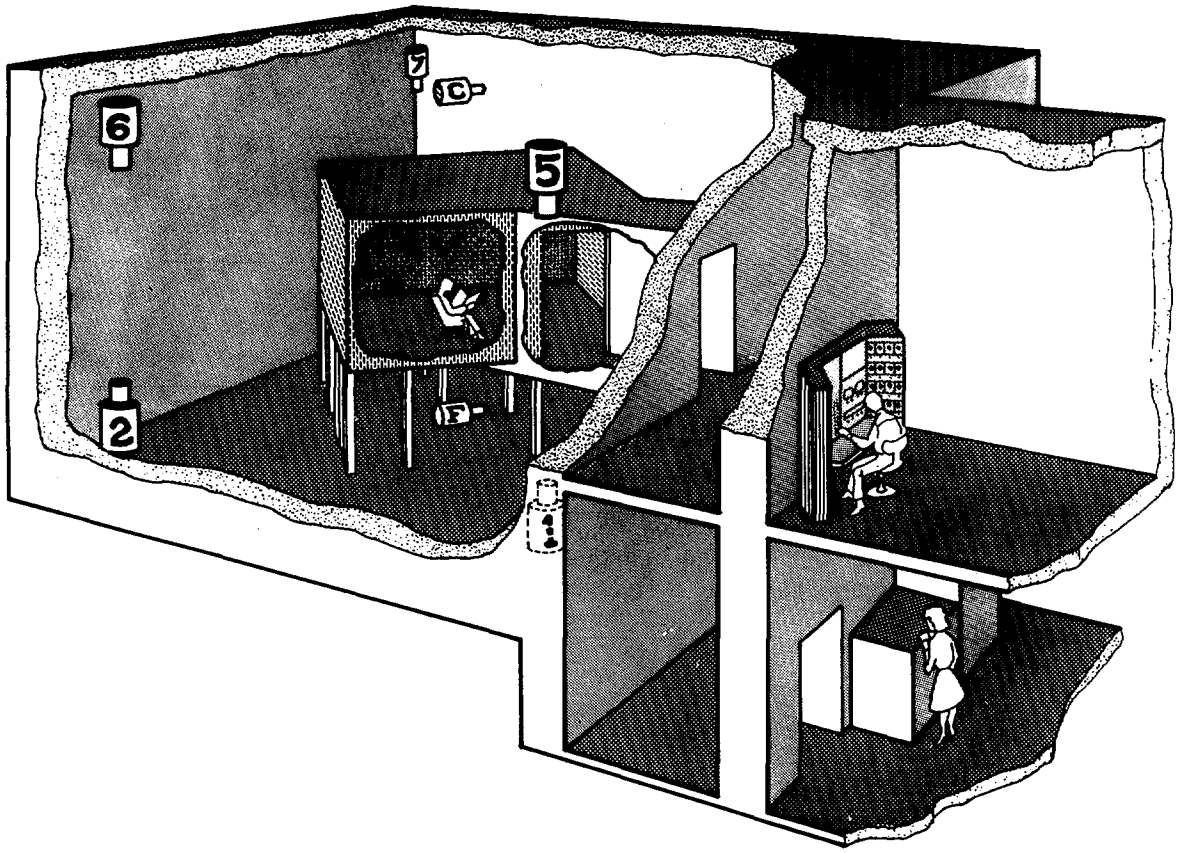

Figs. III–17 and 18. New Total-Body Irradiation Facility. The cut-away diagram *above* shows the inner irradiation chamber contained in the new low-exposure-rate total-body irradiation facility at Oak Ridge Associated Universities. The facility consists of a large (35×35×18 ft.) chamber, heavily shielded and made of cement, in which a 16×16×8 ft. parlor-bedroom is centered in the radiation field produced by 10 retractable cobalt-60 sources in the corners of the larger chamber. The exposure field in the inner room can be made to approximate one roentgen per hour or a selected lower dose rate and has a sufficiently uniform three-dimensional isodose pattern to permit the patient to move freely about the room even when being exposed. Automatically operated devices protect the patient from being excessively exposed during any pre-determined time period and allow nursing personnel to enter the room routinely or as needed. Surveillance by "intercom" and closed circuit TV is provided to detect unexpected trouble during exposure. The photo *below* is an exterior view of the facility. The irradiation room is in building at *right* of photo.

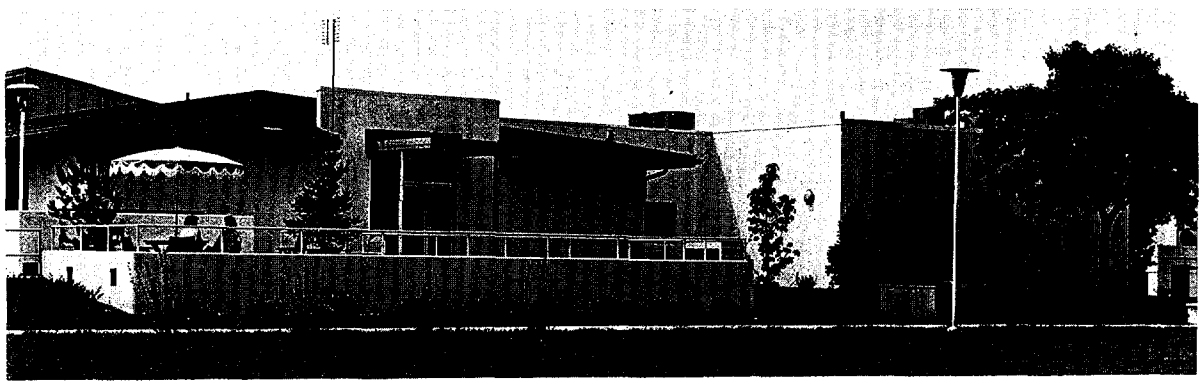

5 consecutive days. He averaged 20 hours of exposure out of each 24 hours (30 *R*/day; average whole-body dose was about 20 *rads* in 1 day). He experienced no ill effects and slept and ate well during his entire stay in the facility. At intervals his cardiac and pulmonary functions were monitored remotely by electronic devices to detect any signs of physiologic disturbances. None were found. Since termination of the radiation exposure, his blood platelets, which were about four times too abundant (idiopathic thrombocythemia), have declined gradually to about normal levels (from 1.6 to 0.4 million/cubic millimeter). His other cellular blood components have shown no clinically significant depression.

A retrospective study of past clinical experience with irradiated workers has redefined the chances of bodily damage from single doses of much larger amounts of radiation, but it has not been possible to predict how these probabilities of injury might be changed when the same doses are given over long periods.

The new radiation facility not only will be useful in studying therapy of chronic leukemia, but also will provide opportunity to test if low radiation doses at such slow delivery rates have any direct effect upon digestive, circulatory and neural physiology.

DIAGNOSIS

It is known that radioisotopes are taken up by malignancies in a concentration that is different from the concentration in the surrounding normal tissue, and this feature is used in detecting cancers.

Respiratory Distortion Problem in Diagnosis

To detect cancers, a patient is given a radioisotope in a suitable form and is then "scanned" with a radiation detector which measures the amount of radioactive material over each point, the heaviest concentrations being in the diseased organs. In modern scanners, each detected gamma ray produces a small dot on a film and the whole scan provides a picture of the distribution of radiation in the organ and, hence, of the location of lesions. Studies at the Argonne Cancer Research Hospital (ACRH) are leading toward solution of a major problem in scanning techniques—that of obtaining distortion-free pictures. Suitable radioisotopes and detectors for diagnostic scanning are being developed to accomplish this.

A recent study at ACRH considered the best way to obtain satisfactory scans of organs such as the liver and spleens, which are usually distorted by respiratory movements. In preliminary work, three types of scanners were used to make scans of a moving phantom and to assess the loss of resolution in each. The detectors were: a variable speed research scanner designed at ACRH; a conventional rectilinear scanner; and a gamma scintillation camera. The final resolution with motion was found to be best with the gamma scintillation camera; intermediate with the variable-speed research scanner; and the poorest with the conventional rectilinear scanner.

The problem of respiratory distortion was then attacked by using the scintillation camera in conjunction with technetium sulfur colloid, a preparation of technetium-99^{m} that is routinely used for liver, spleen, and bone marrow scanning at ACRH. The dose of sulfur colloid for liver scanning is two to three millicuries.

The scintillation camera takes less than 1 minute to record a satisfactory scan, during which 400,000 disintegrations can be recorded. A cooperative patient can hold his breath for this interval, thus completely preventing motion. When a patient cannot cooperate for so long, an alternative method is used. The patient is asked to hold his breath in full expiration and the exposure is started immediately. When the patient desires to breathe again, he signifies this by a hand signal and the exposure is stopped. When the patient is comfortable, he again holds his breath and the exposure is continued. This procedure is repeated until the desired number of dots has been accumulated on the scintiphotograph. The method can be used with all but ex-

tremely ill patients. Since it takes 30 to 45 minutes to obtain a single view of the liver with a conventional scanner using the radioactive tracers previously available, and since control of respiratory motion is impossible for this length of time, the method represents a significant advance. More views of the liver can be taken, and less cooperation from the patient is required—a very important consideration in dealing with the critically ill patient. In addition, by controlling respiration, the quality of the examination is improved. The alternative procedure for controlling respiration is to paralyze a phrenic nerve by giving a blocking injection of a local anesthetic in the back, an undesirable and painful operation.

A program of fast section scanning, directed toward the accurate determination of the positional coordinates of brain tumors, is being pursued at the University of California at Los Angeles (UCLA).

CARCINOGENESIS

Investigations are being made in an attempt to more closely define the conditions under which irradiation of tissues gives rise to cancer, by using different conditions of exposure and by studying the early processes that occur before tumors are seen.

Fatty Substance in Malignant Tumors

Investigations at the Oak Ridge Associated Universities have led to a significant discovery that substantial quantities of a previously unidentified lipid (fatty substance) occur in a wide variety of animal and human tumors but not in normal tissues. This lipid has now been found to be a glyceryl l-ether diester (GEDE). The determination of its nature has been possible by means of modern technical procedures including thin layer chromatography, gas liquid chromatography, identification of chemical derivatives, infrared spectra and nuclear magnetic resonance spectra. The data so far demonstrate that: (*a*) the quantities of GEDE found in normal tissues are minute compared to those found in tumors, and (*b*) a critical part of the chemical structure (the ether bond) can be formed in the tumor cell. The relatively high concentrations of this material in the many tumors examined suggest that it is closely associated with the cancer process.

In vivo and *in vitro* studies with experimental mouse tumor cells (*Ehrlich* ascites tumor) on the incorporation of precursor materials (acetate, glycerol, glucose, fatty acids, fatty alcohols and triglycerides) into this substance have demonstrated that the fatty acids, fatty alcohols and triglycerides can be incorporated into the ether hydrocarbon chain. Investigation of the intracellular distribution of this lipid in mouse tumor cells studied has shown that a large proportion of the ether-containing lipid is in the mitochondria. Mitochondria are structures in the cell cytoplasm that function in energy production. Experiments with the cells grown in tissue culture have shown that tumor cells can produce the substance in the tissue culture medium. These data indicate that tumor cells do not simply concentrate the substance from dietary sources but are capable of synthesizing the lipid ether bond in the absence of other tissues.

Metabolic Control and Carcinogenesis

Recently, at Argonne National Laboratory, it was discovered that liver tumors could be produced in rats which are quite similar to normal liver except that the control of adaptive enzyme synthesis in the tumors is defective. These findings suggest that a careful analysis of changes in the control of adaptive enzyme synthesis in the liver during the experimental production of liver cancer may reveal key events associated with the transformation of normal liver into cancerous liver. A study is underway at Argonne to correlate structural (morphological) changes with changes in the capacity for enzyme adaptation in the liver cell during exposure to tumor-producing agents (carcinogens).

Rats are fed small amounts of carcinogens in the diet. Other rats are fed these carcinogens

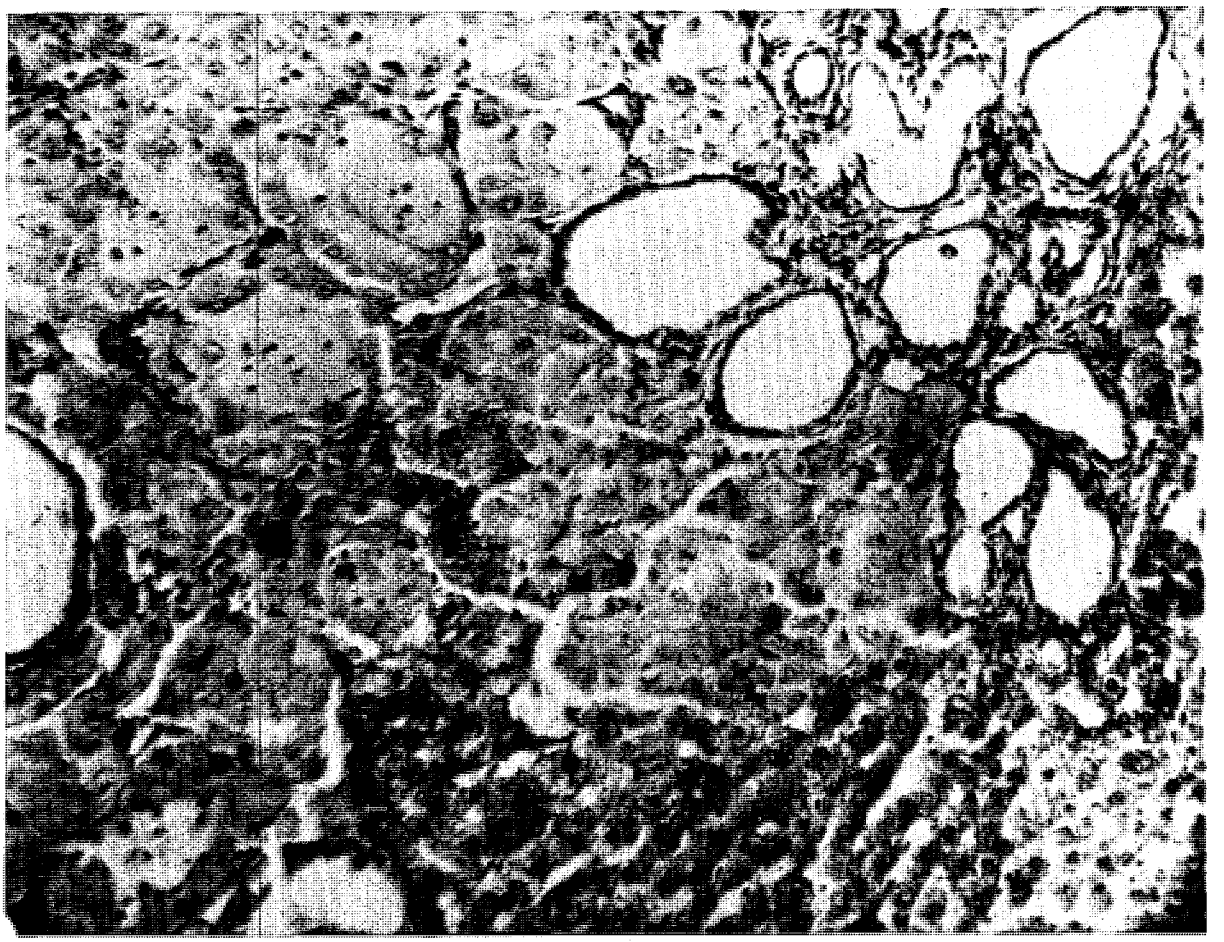

Fig. III–19. Metabolic Control and Carcinogenesis. The above is a light photomicrograph of a liver specimen from a rat given a carcinogen, diethylnitrosamine, at Argonne National Laboratory. The *lower-right* quadrant of the picture shows normal liver parenchymal cells. In a stained specimen, the glycogen has a reddish appearance and the nuclei appear blue. The *upper-left* quadrant contains tumor cells which have arisen from liver parenchymal cells. Glycogen is absent and the cells have a disorganized appearance. In the *upper-right* quadrant, a tumor can be seen that consists mainly of abnormal bile ducts. These abnormal bile ducts appear as large spaces lined by small cells.

in combination with selected agents such as phenobarbital, which are known to affect liver metabolism and morphology but which do not produce tumors. Still other rats are given both types of agents in addition to low doses of ionizing (gamma) radiation (which also affects the structure and function of the liver without producing tumors). Specimens of the liver from rats on each treatment are examined by means of light microscopy. (see Fig. III–19) and electron microscopy for structural changes in the cells. Adaptive enzymes are analyzed to detect possible changes in the functional capacity (metabolism) of the liver. Changes in structure are correlated with changes in metabolism, if possible, and this information is related to the time of occurrence, frequency of occurrence and properties (both structural and metabolic) of tumors which arise in the different groups.

In a current experiment, a carcinogen (diethylnitrosamine) is fed in conjunction with

phenobarbital, a commonly used sedative which causes marked proliferation of intracellular membranes (endoplasmic reticulum) as well as the stimulation of drug metabolizing enzymes in the liver cell. Results obtained to date show that effects of the combined administration of diethylnitrosamine and phenobarbital on the synthesis of adaptive enzymes are substantially greater than those observed when either agent is administered alone. These effects do not appear to be altered when the rats are exposed to low doses of radiation. The combined treatment also produces more pronounced morphological changes than either agent alone, and these effects are exaggerated when the rats are exposed to radiation. Although the study is only in its initial stages, it appears that important insights into the mechanism of liver carcinogenesis may be gained through this experimental approach. A further extension of this study involves the feeding of the carcinogen N-2-fluorenylacetamide, with and without phenobarbital, and a comparison of the responses obtained with those using diethylnitrosamine.

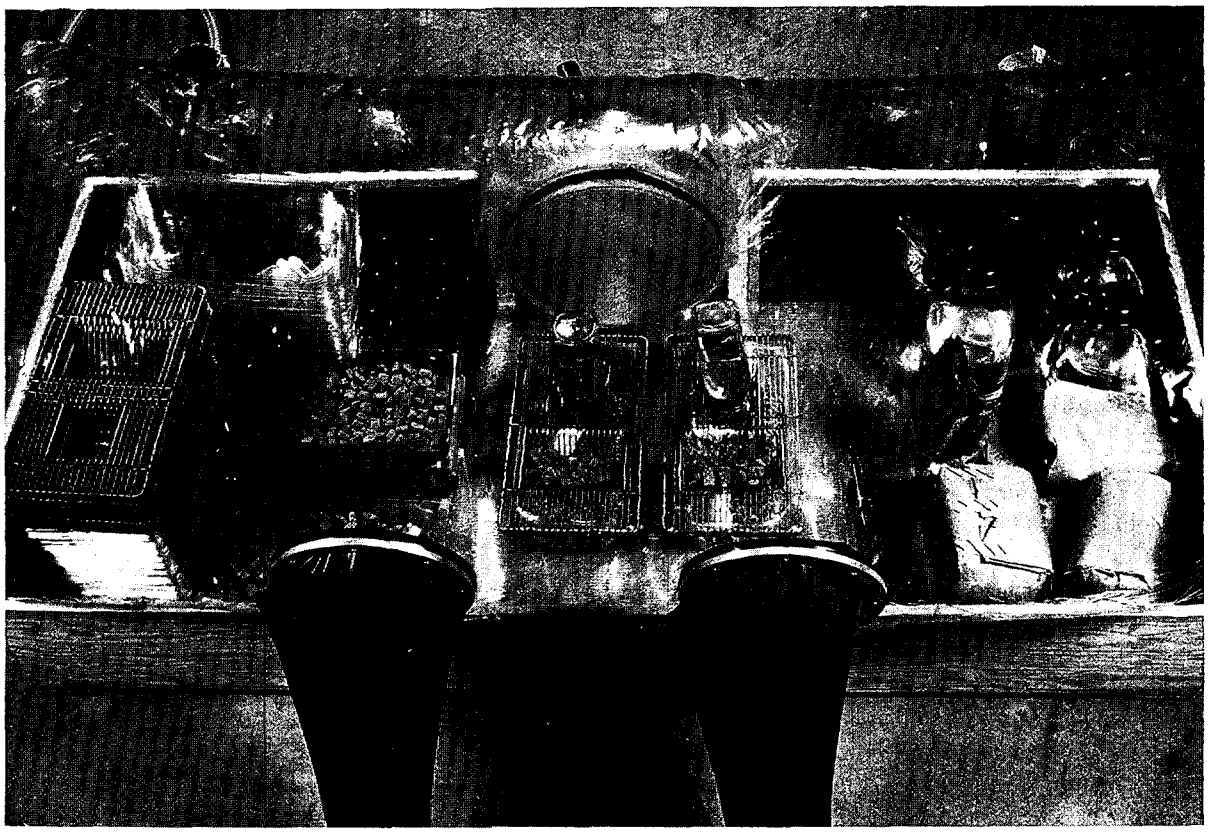

Fig. III–20. Rearing Germ-Free Mice. At Oak Ridge National Laboratory, flexible plastic "glove box" isolators are used in rearing germ-free mice for studies on aging and the late somatic effects of radiation. Such careful control of environmental conditions has resulted in the development of several strains of germ-free mice. Air for the mice is provided through the circular filter (*top center* of photo) and the airtight gloves (*bottom*) are used for human operations inside the isolator.

SOMATIC EFFECTS OF RADIATION

Research into the somatic effects of radiation seeks to identify and explain those biological mechanisms which give rise to both early and late radiation effects. Pathological, physiological, and cytological responses to irradiation of the individual organ systems, their relative radiosensitivity and their contribution to the response of the whole organism are all of interest. A special feature chapter on late somatic effects in mammalian species was included in the 1966 edition of this report.[8]

LATE EFFECTS OF RADIATION

Many studies continue to help understand better the late or delayed effects of large doses of radiation received in a relatively short period of time, where, in general, the survivors of single exposures have shown good clinical recovery from early effects. The irradiated human population groups in Japan and Rongelap Island, and certain experimental animal colonies are

[8] "Fundamental Nuclear Energy Research—1966." Reprints of the feature chapter may be obtained by writing to the Director, Division of Biology and Medicine, U.S. Atomic Energy Commission, Washington, D.C. 20545.

examples. Investigations are also carried out on somatic effects which result from continuous exposures of organisms to low dose rates over prolonged periods. Such studies encompass epidemiological work as well as change in incidence of tumors and leukemia, changed susceptibility to infectious diseases, change in time of onset of degenerative diseases, change in lifespan, and altered capabilities of living systems.

Aging in Germ-Free Mice

Several strains of germ-free mice have been developed at Oak Ridge National Laboratory (ORNL) for use in studies concerned with microbial influence on long-term changes in irradiated and nonirradiated subjects. In corollary tests with two such strains of mice (ICR and RFM), investigators have found that the absence of detectable micro-organisms does not increase the maximum length of life but does increase the number of mice reaching "old age." This suggests that aging cannot be prevented by exclusion of micro-organisms from the environment.

Germ-free colonies originate from mice aseptically removed from the sterile uterus of their dams at full-term fetal stage and then carefully reared in a sterile environment that is continuously monitored for contamination (see Fig. III–30). Although development of a few diseases is affected in such mice by the absence of micro-organisms (glomerulosclerosis, myeloid leukemia, and all infectious diseases), most other diseases (for example, lymphoid leukemia, solid tumors, and amyloidosis) occur with the same incidence and at the same relative time during the lifespan in germ-free mice as they do in mice raised conventionally.

The incidence of tumors does not seem to be different in germ-free and normal mice, except for radiation-induced myeloid leukemia, which is common in irradiated conventional mice of the RFM strain, but has not been seen in germ-free mice of the same strain.

Degenerative diseases, which have been thought to occur as a result of repeated infections, have been studied in germ-free mice where such infections do not occur. Many of the degenerative diseases (glomerulosclerosis, arteriosclerosis, polyarteritis, and amyloidosis) have now been observed in germ-free as well as conventionally raised mice, suggesting that infections are not required for the development of degenerative diseases. These results are consistent with an autoimmune mechanism also currently under investigation at ORNL.

Biosatellite Experiment

The National Aeronautics and Space Administration (NASA) has begun a series of in-flight experiments with unmanned satellites designed to test the effects of weightlessness and the space environment on biological systems. The first Biosatellite–A was lost in space in December 1966.[9] A second biosatellite was successfully launched on September 7, 1967, and recovered on September 9. A number of biological experiments on the biosatellite were funded by NASA and carried out by the AEC's Lawrence Radiation Laboratory, Berkeley, and the Brookhaven and Oak Ridge National Laboratories.

Analysis of data from the radiation experiments is underway. There are preliminary indications of significant differences between *Tribolium confusum* (flour beetle) irradiated during the flight and the ground controls. It is too early in analyses of the data from the experiments carried out by Brookhaven and Oak Ridge National Laboratories to determine whether or not there are any significant differences between samples, such as *Neurospora* (bread mold), *Habrobracon* (wasps), and *Tradescantia* (spiderwort—a wild flower) irradiated during the flight and the ground controls.

Since 1961, the AEC and its contractors have been cooperating with NASA in developing radiobiological information required for space

[9] See pages 26–28, "Fundamental Nuclear Energy Research. 1966." Reprints of a feature chapter, "Space Radiation Biology," are available from the Director, Division of Biology and Medicine, U. S. Atomic Energy Commission, Washington, D.C., 20545.

Fig. III–21. Neuropathological Effects of Heavy Ions. Electron micrograph (10,000 ×) of rabbit brain (sensory cortex) taken at Donner Laboratory 61 days after local alpha-particle beam irradiation with a single dose of 7,000 *rads*. Thickened capillary basement membrane passes transversely across the field. Areas of increased electron density can be seen where glial fibrils meet the plasma membrane adjacent to the basement membrane (*arrow*). At this point, the basement membrane is split and thickened to nearly one micron, whereas, normally, it is not over 0.1 micron in control areas of unirradiated brain. An endothelial cell is at the *lower left*, and phagocytic cell cytoplasm is in the center of the field.

mission planning. The studies, funded by NASA and conducted at the uniquely equipped AEC facilities, are, for the most part, extensions of investigations supported by the AEC.

Central Nervous Systems

Neuropathological Effects of Heavy Ions

Studies at the Donner Laboratory of Lawrence Radiation Laboratory, Berkeley, of delayed effects of radiation on brain tissues, both in humans and animals, and the influence of such factors as immunity indicate no relationship between late necrosis and immunization.

In one experiment, coagulation necrosis (killing of cells) was observed in the brain of a monkey 37 months after the monkey had received 5,000 *rads* in a single radiation dose to the pituitary. Such necrosis may appear years after irradiation with doses greater than 2,500 *rads* spread over a period of several days.

The electron microscope has shown the formation of vacuoles (spaces) in the brain's capillary endothelial cells 2 weeks after alpha-particle irradiation. Some similar changes were observed in certain capillary cells (pericytes). Later, the cytoplasmic vacuolation was less marked, but basement-membrane thickening of capillaries was noted 4 weeks after irradiation (see Fig. III–21).

A proton beam was used to irradiate two groups of six rabbits each; the objective was to determine if immunity may be a factor in delayed radiation necrosis of the brain. One to three days earlier, half of the animals had re-

ceived a subcutaneous injection of rabbit spinal cord and an adjuvant.[10] Two to three weeks following irradiation, the animals' brains were examined for lesions. No relationship could be found between the presence of delayed radionecrosis and immunization experience. Round-cell infiltration within the lesions of the immunized rabbits was less than in the nonimmunized. These findings indicated that delayed radionecrosis is unaffected by the subject's immunological status. However, experiments should be done in which immunization follows irradiation rather than preceding it.

Effects in Central Nervous System

A novel method has been used at the Donner Laboratory to measure dynamic impedance in monitoring radiation effects in neural tissue not detectable by conventional brain wave analysis. Conventional neurophysiological methods have stressed voltage measurements of neuronal activity with little regard for the contribution of other tissue elements such as glia. However, it has been shown that changes in cerebral impedance occur in response to a variety of environmental stresses or during different physiologic states. Suggestions have been made that impedance reflects changes occurring primarily in glial or extracellular components. This method uses extremely low signal levels (20 microvolts at 1,000 cycles/second) to measure continuing changes in resistive and reactive vectors of tissue impedance.

Following brain irradiation with 910-Mev. alpha particles, there is a sharp increase in impedance from baseline values of 20 kilo-ohms to peak levels of 60–80 kilo-ohms during the first 3 weeks after exposure (see Fig. III–22). Threshold doses are in the range of 10,000 to 15,000 *rads*. Studies performed elsewhere have shown that increases in impedance reflect local shifts in fluid from glial and extracellular compartments into the neuronal compartment.

A complimentary approach to the study of radiation-induced fluid shifts involves special

[10] A substance which aids another, such as an auxiliary remedy.

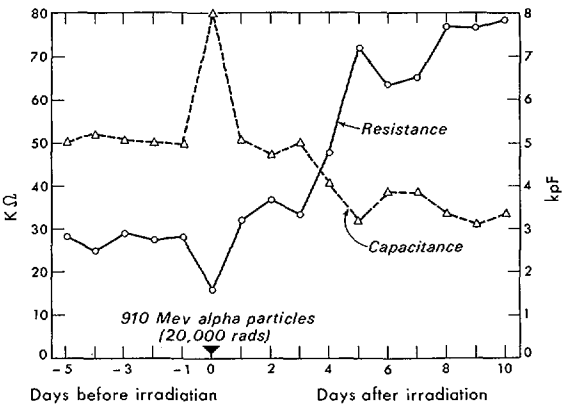

Fig. III–22. Effects in Central Nervous System. Donner Laboratory chart shows the relative changes detected in neural tissue following 20,000 *rads* of alpha irradiation to the brain. Resistance is measured in kilo-ohms (KΩ) and capacitance in kilo-pico-*Farads* (kpF). These changes are thought to reflect local fluid and electrolyte disturbances between neurons, glial cells, and extracellular spaces.

electron-microscopy techniques. Two methods are being used, both of which are designed to insure adequate preservation of extracellular spaces, which are generally difficult to render visible. One method involves glutaraldehyde-osmium tetroxide fixation perfusion; the other ultra-rapid freeze substitution fixation. Studies using these methods should help to clarify understanding of radiobiological mechanisms in the central nervous system's response to heavy particle irradiation.

As a part of studies on the radiation effects in central nervous system, resistive and capacitive components of cerebral impedance have been measured at the site of focal brain irradiation with 910-Mev. alpha particles. The changes are thought to reflect pathology in fluid and electrolyte distribution between neurons, glial cells, and extracellular spaces.

HEMATOPOIETIC SYSTEM

Studies of the hematopoietic (blood forming) system are directed toward determining the effects of partial or whole body irradiation, either acute or chronic, on the system, and toward determining the relationship of radiation modifi-

cation of the system to the health of the individual. Many tasks are undertaken in this category that are gradually adding to the fund of information about blood cell formation, different cell series, stem cell differentiation and proliferation, and kinetics of blood cell populations.

One of the first and most serious effects on the body of overexposure to radiation is the destruction or injury of the blood and blood-forming tissues.

Erythropoietin Studies

Argonne Cancer Research Hospital (ACRH) has several continuing programs devoted to studies on the blood. Recent advancements have included: (*a*) the further purification of erythropoietin—the hormone that stimulates red cell formation; and (*b*) a determination of some of the factors governing urinary concentration of erythropoietin in anemic patients. Additional information has been developed on: (*a*) the effects of male sex hormones on erythropoietin production; (*b*) increased uptake of iron by bone marrow cells exposed to erythropoietin; (*c*) the effect of erythropoietin on polycythemia vera through *in vitro* studies of the human bone marrow disease; and (*d*) changes in chromosome pattern after therapy in a case of a human blood disease.

Purification of Sheep Plasma

During the recent past, further progress has been made in purification of sheep plasma erythropoietin. This project was initiated in 1957 when the U.S. Public Health Service entered into collaboration with the University of Chicago and Armour and Co. on a joint project for the extraction, purification, and characterization of the hormone erythropoietin from the blood plasma of sheep rendered anemic by treatment with phenylhydrazine. By 1962, ACRH biochemists had obtained fractions of plasma with a potency of about 450 units per milligram of protein. This represented an enrichment factor of about 63,000 over the original starting anemic-sheep plasma. Unfortunately, quantities of the best fraction obtained in this range, *i.e.* 450 units per milligram of protein, were insufficient to carry the process any further. In part, this was because of extensive losses of activity in a particular step in the purification process. More recently, methods for coping with the difficulty have been developed and it is now possible to produce purified fractions of anemic sheep plasma with potencies of about 6,500 units per milligram of protein. This represents an enrichment factor of about 930,000.

The table below summarizes the various stages in the process of purification. It will be noticed that as the potency (units/mg) and purification factors are increased, the percent recovery from the plasma is reduced.

Fraction	*Units/mg*	*Percent recovery*	*Purification factor*
Anemic plasma	0.007	100	
Step III	2.7	35	388
Step IV	19	20	2,700
SES–5 [a]	133	10.4	19,000
CaP–2B [b]	6,500	2.2	930,000

[a] The SES-5 fraction is derived from Step IV by ion-exchange column chromotography.

[b] The CaP-2B fraction is derived from SES-5 by calcium phosphate gel adsorption.

When a pure sample of the hormone has been produced, it will be possible to make a detailed analysis of its chemical composition. This, in turn, may lead to synthetic production of the hormone, to be used, perhaps, in treatment of those blood diseases that are caused by insufficient amounts of erythropoietin in the blood. At the present state of technology, it has been estimated that plasma would be needed from a flock of 325 sheep to produce 10 milligrams of material with a potency of 6,500.

Erythropoietin in Anemic Patients

The low yield of the most pure fractions of erythropoietin that can be obtained from the blood plasma of anemic sheep has contributed to the long delay in final purification and characterization of this hormone, and it has become increasingly important to find an alternative

source of starting material. It appears that urine from anemic patients (which is known to contain erythropoietin) may prove to be the only feasible large-scale source.

The amount of urine that would be required would represent daily collection for about 3 years from a single patient, or one month's collection from 36 patients, which does not seem to be an impossible goal. As a result, there has been increased interest in the factors governing the amount of erythropoietin in the urine.

It has been noted at Argonne Cancer Research Hospital, as well as at other institutions, that although the urinary concentration of erythropoietin is usually several times smaller than the plasma concentration, there is great variability in the ratio of these concentrations and the amount in the urine does not appear to be in direct proportion to the severity of the anemia.

In a recent attempt to clarify one of the factors which may govern the amount of erythropoietin in the urine, a series of studies was carried out on anemic patients to determine the effect, if any, of increasing body alkalinity on the concentration of erythropoietin in the urine. The patients were given either ammonium chloride [NH_4Cl (3 grams 3 times a day)], or sodium bicarbonate [$NaHCO_3$ (6 grams 3 times a day)]. Administration of sodium bicarbonate increases the alkalinity of body fluids and of the urine; ammonium chloride has an opposite effect.

The concentrations of erythropoietin in the plasma and the urine were then estimated in the usual manner by injecting one milliliter of either urine of plasma into test animals.

The amounts of erythropoietin in the blood plasma varied only slightly in either case.

Administration of sodium bicarbonate increased the concentration of erythropoietin in the urine about 17 times in a patient with myelo fibrosis and about three and one-half times in a patient with hypoplastic anemia. Other possibilities having been excluded, it appears that, at least in these patients, more erythropoietin is excreted into alkaline urine. The exact renal mechanism by which this was accomplished is, as yet, unclear.

Effects of Male Sex Hormones

The stimulating effects of the male sex hormone, testosterone, on the production of erythropoietin as determined at ACRH[11] have suggested that testosterone stimulates red cell formation in mice by altering the kidney so that it can produce more erythropoietin in answer to an additional stimulus. Further experiments with anemic mice, having the genetic formula WW_v, have indicated that increasing the amount of erythropoietin in the blood by giving injections of testosterone may lead to a way of treating some of the human anemias. The plasma of these mice contains high concentrations of erythropoietin, yet the number of red cells in their blood remains below normal, and they do not respond to injections of erythropoietin unless it is given in repeated large doses. When WW_v mice were injected with 2.5 milligrams of testosterone every other day for 2 weeks, the volume percent of red cells in the blood rose from 40 percent to 52 percent, which indicated a significant reduction in the degree of anemia.

For the experiments, the erythropoietin concentration in the plasma of three different kinds of mice was compared by injecting 0.4 cubic centimeters of their plasma into assay mice and estimating the increase in red cell production (and, hence, the amount of erythropoietin present) by measuring the amount of radioiron present in a sample of the blood. The three different kinds of mice were: (*a*) normal mice of the CF_1 strain, (*b*) untreated anemic mice of the WW_v strain, and (*c*) anemic mice of the WW_v strain injected with 2.5 milligrams of testosterone on 2 successive days (see Fig. III–23).

The plasma of the normal CF_1 mice produced no increase in uptake of radioiron; the plasma of untreated WW_v mice produced an increase in uptake of 13 percent; and the plasma of WW_v mice treated with testosterone produced an uptake increase of about 25 percent.

[11] "Fundamental Nuclear Energy Research—1966" pp. 52–53.

These results suggest that the plasma of the anemic mice contains more erythropoietin than the plasma of normal mice and that this amount can be still further increased by injecting the anemic mice with testosterone. As a result of this, more red cells are formed and the anemia is alleviated.

It is possible that the same kind of situation may be present in some kinds of human anemia, *i.e.*, that sufficient numbers of red cells cannot be produced by the amount of erythropoietin normally present in the blood plasma (even if the amount is greater than is present in normal subjects).

It may be possible then to increase the production of erythropoietin to amounts that will be high enough to increase red cell production and thus relieve the anemia by giving injections of testosterone.

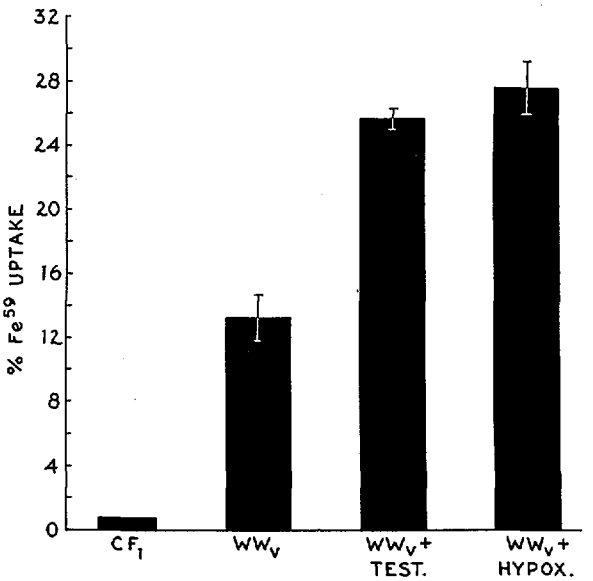

Fig. III–23. Testosterone Effect on Mouse Erythropoietin. The chart compares radioiron (Fe^{59}) uptake produced in test mice by: (*a*) plasma of normal CF_1 mice (no increase); (*b*) plasma of untreated WW_V mice (an increase of 13%); and (*c*) plasma of WW_V mice injected with 2.5 milligrams of testosterone on two successive days (an increase of 25%) at Argonne Cancer Research Hospital.

Iron Uptake by Bone Marrow

The hormone erythropoietin is known to regulate the production of red blood cells by acting on the stem cells of the bone marrow to direct their development into the red cell line. Exactly how the hormone acts to produce this differentiation is not known in detail, but recent experiments, using radioactive iron-59 as a tracer, on rat bone marrow cell cultures at Argonne Cancer Research Hospital have given important information on some of the steps in the processes.

It was shown that rat bone marrow cells in short-term *in vitro* cultures synthesize hemoglobin at a rate that is determined by the amount of erythropoietin added to the culture medium. For the first 4 to 5 hours after exposure to erythropoietin, little or no radioactive iron-59 is incorporated into the heme fraction of the hemoglobin, but there is a significant increase in the amount of iron taken up by the cells. This erythropoietin-stimulated increase in cellular uptake of iron precedes the stimulated increase in heme synthesis, and is dependent upon the amount of hormone in the medium.

The stimulated iron uptake could be inhibited by the addition of puromycin (in concentrations of 75 micrograms per milliliter) and actinomycin (in concentrations of 2.5 micrograms per milliliter), but not by dinitrophenol (in concentrations of 3/100,000 molar strength).

The data suggest that one of the early effects of erythropoietin in the induction of red cell differentiation is to facilitate entry of iron into marrow cells, and that this effect is dependent upon prior RNA synthesis and protein synthesis, but is independent of coupled oxidative phosphorylation.

Studies of Polycythemia Vera

The successful treatment of any disease is determined largely by an understanding of the physical and physiological factors that are its cause. In recent years, the study of many diseases has been made easier by the use of substances labeled with radioactive isotopes whose passage through the body, or accumulation in tissues, can be detected by instruments that are

275-845 O—68——18

sensitive to radiation, thus giving information on the different ways in which normal and diseased subjects handle these materials. Another technique that has also been of great value has been the cell culture system, which permits the removal of samples of tissue and culturing them alive in vessels outside the body—known as *in vitro* (literally, in glass vessels) tissue culture. It is particularly valuable because it pinpoints the activities and requirements of individual tissues, unaltered or screened by the actions of other body tissues.

Recently, at Argonne Cancer Research Hospital, both of these methods have been applied together to the study of the behavior of red blood cells and particularly to the study of red blood cell diseases.

A human blood cell disease that has been studied in this way is polycythemia vera, which is characterized by the overproduction of red cells, white cells, and platelets. The overproduction of red cells was the feature under special study, and experiments with bone marrow from patients having polycythemia vera have shown that this marrow (which normally gives rise to red cells in the adult animal) does not respond in a normal way to the hormone erythropoietin. Furthermore, this abnormal response to the hormone is not due to any factor in the polycythemia vera plasma, but to a defect in the marrow cells themselves.

The activity of the bone marrow was estimated by comparing the rate at which the cells took up radioactive-labeled iron (Fe^{59}) from the culture medium and used it to form the heme fraction of the hemoglobin molecule. The radioactive heme was extracted from the cells and "counted" in a scintillation counter. The culture system was subjected to a number of variations designed to give information on different factors.

Comparison of the effects of erythropoietin upon heme synthesis in a system with normal marrow and a system with polycythemia vera marrow, shows that erythropoietin increases heme synthesis by fivefold in the normal system, but by a very much smaller amount in the polycythemia vera system; even the highest concentrations of erythropoietin only increase heme synthesis by a factor of 1.5 in patients with polycythemia vera. It appears then that erythropoietin is not responsible for the increased red cell production.

It was considered whether the plasma of the polycythemia vera patient might contain some factor (or inhibitor) that served to block the normal effect of erythropoietin on the bone marrow. For this purpose, a culture system was set up that contained normal human bone marrow and polycythemia vera plasma. The addition of erythropoietin produced the normal increase in heme synthesis. It appears therefore that there is no inhibitor in the polycythemia vera plasma.

Other experiments have shown that the polycythemia vera marrow is very insensitive to even extremely high doses of erythropoietin, and that the erythropoietin in the polycythemia vera plasma is not of a peculiar type that acts only on its own cells. The disease appears to be caused by some defect in the marrow cells of the polycythemia vera patient. Further studies will continue from this standpoint.

Other Hematopoietic Studies

Chromosome Pattern After Radiation Therapy

The association of irregularities of chromosome number and form with malignant tumors was originally established in 1914. Since that time it has been found that about half the patients with acute leukemia have variable chromosome abnormalities in the leukemic cells, although the rest of the body cells are normal. It is not yet known though, whether the abnormal chromosome pattern is the cause or the consequence of the leukemia. The subject is one of interest to hematologists, since chromosome pattern in the bone marrow of a patient not suffering from overt leukemia might indicate that leukemia would eventually develop. In consequence, a close watch is kept on these "preleukemic" syndromes when they are detected in the hope of learning something more about the

cause of cancer. It has been observed that leukemia tends to appear in radiologists after the age of 40, whereas for U.S. male whites over 25 the proportion of deaths attributed to leukemia is highest before the age of 40. Whether this pattern can be linked to the occupational exposure of radiologists to X-rays is a matter for some speculation.

In a case recently studied at the Argonne Cancer Research Hospital, the patient was a 60-year-old woman with thrombocythemia (an abnormality characterized by overproduction of blood platelets). Samples of her bone marrow showed that most of the marrow cells (75%) had normal chromosome patterns, while the remainder (25%) had 48 chromosomes (that is, two more than normal). The two extra chromosomes belonged to the medium-size C type. She was treated with drugs and radioactive phosphorus-32 and in 3 months' time, all the abnormal patterns had disappeared. Marrow examinations have been continued at approximately 4-month intervals, and, after about 1 year, the abnormal patterns have begun to reappear. In the most recent sample, six percent of the cells had 47 chromosomes and 12 percent had 48 chromosomes, including the two extra C chromosomes. Although the abnormal cells are increasing in number, the platelet count has remained within normal limits. The case is interesting in its resemblance to those leukemias of childhood that respond temporarily to antileukemic drugs, the period of remission being characterized by a disappearance of the abnormalities of chromosomes.

Whether the emergence of some cells with abnormal chromosome patterns will be coupled with a rise in platelet count remains to be seen.

Recovery of Bone Marrow After Irradiation

The efficiency of high-dose irradiation for inducing long-term remissions, or even cure, in patients with localized *Hodgkin's* disease has generated great enthusiasm in the care of these patients. One of the major factors limiting extensive wide-field irradiation therapy for disseminated *Hodgkin's* disease is the possibility that the blood-producing tissues will be unable to recover from radiation directed to cancerous lymphatic tissue occupying the same region. Therefore, studies at the ACRH have attempted to clarify the kinetics of bone marrow repopulation in mice and in patients after partial-body irradiation.

Results of these studies indicate that primitive undifferentiated bone marrow cells emigrate from shielded leg marrow to repopulate distant marrow sites and the spleen in mice that have received a supralethal dose of X-rays. Radiobiological methods, morphological studies and experiments measuring the splenic uptake of iododeoxyuridine labeled with iodine-131 demonstrate a rapid proliferation of undifferentiated cells during the first 5 days after irradiation. During this proliferative phase, these stem cells cannot be induced to differentiate into red blood cells either by exogenous or endogenous erythropoietin. After 5 days, red blood cell production, estimated by the uptake of radioiron (Fe^{59}) in the spleen, proceeds rapidly. New red cells, white blood cells, and platelets appear in the peripheral blood during the second week after the irradiation.

The recovery of red blood cell production, estimated with radioiron kinetics and body-surface scanning techniques, was measured in a patient with recurrent *Hodgkin's* disease who had received extensive, but low-dose radiotherapy in the past. Localization of sites of active bone marrow permitted the rational design of X-ray treatment ports, and high dose radiotherapy was administered, preserving the remaining blood-producing tissue.

REPRODUCTIVE SYSTEM

Work on the reproductive system of animals involves studies of the cells, tissues, organs, and their functions necessary to the production of viable offspring, and observes the effects of radiation on these parts of the system and its function.

Reproduction in a Life Study Herd

A bovine herd is under a life-time study at Oak Ridge, Tenn., to observe the effects of irradiation on: (*a*) fertility; (*b*) growth and viability of the calves; (*c*) pathological response in the cows; and (*d*) performance of the offspring by sire groups. The herd, originally established in 1961 at the University of Tennessee-AEC Agricultural Research Laboratory, presently consists of 197 adult Hereford cows, 6 and 7 years of age, that were exposed when 18–20 months old to various doses of whole body irradiation in the large animal irradiation field. Data collected to date do not demonstrate that irradiation of these female cattle has an effect on the total reproductive performance of this herd. The irradiation was delivered as an acute single dose at 200, 300, 400, and 600 *R*. The 600 *R* was delivered in two separate exposures at about 8 weeks apart.

The cows are presently completing their fourth and fifth lactation. In 950 matings from all groups excluding the present year, there have been 839 pregnancies (an 88% conception rate). These pregnancies resulted in 831 full-term fetuses. This calving percentage in the irradiated groups (80–82%) did not differ from the controls (81%).

The viability and growth of the calves up to 200 days do not differ from the controls. The average daily gain from birth to weaning has been 1.68 pounds for the controls, as compared to 1.67 pounds for the irradiated groups.

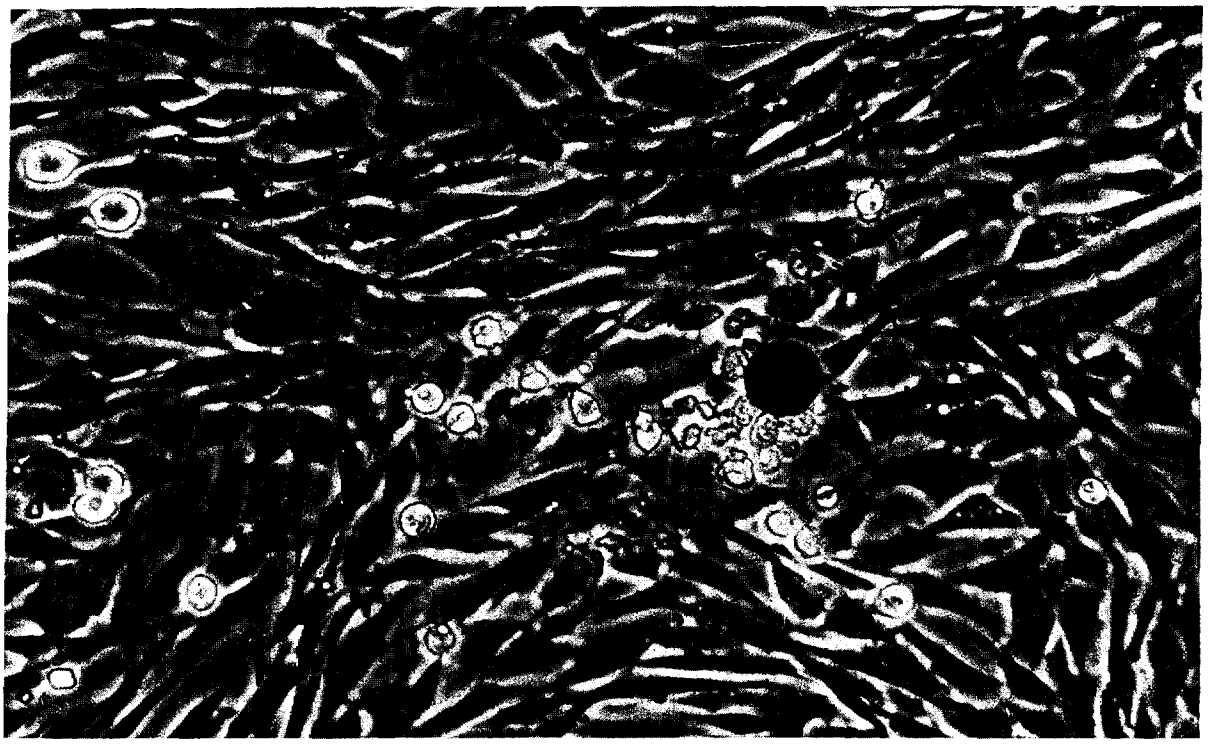

Fig. III–24. Plutonium Oxide Particle in Hamster Cells. The effect of alpha radiation from a microsphere of plutonium oxide on the growth of cells has been observed at Los Alamos Scientific Laboratory by means of time-lapse microphotography. The photo (1,300×) shows Syrian hamster cells growing around a 20-micron diameter sphere of plutonium-239 oxide. The cells normally grow in an organized fingerprint pattern. Although the cells within the range of the alpha particles emitted by the plutonium (inside the *dashed circle*) are killed, outside of the range the growth pattern is not disturbed and the cells appear to grow normally. See page 257 for details.

TOXICITY OF RADIOELEMENTS

Studies of the toxicity of radioelements [12] are concerned with determination of the quantitative aspects of uptake, distribution, retention and excretion of radionuclides in man and animals, the mechanisms of translocation that are involved and the radiobiological toxicity of these nuclides in man and animals. Comparisons are made through studies of several species to form a firmer basis for extrapolating results obtained in animals to man.

BIOLOGICAL EFFECTS

Research is underway to gather observations on the biological effects of radioisotopes which are administered, accidentally ingested, or inhaled, and the quantitative relationships between biological effect and radiation dose. Acute and chronic studies of the effects of plutonium, uranium, radium, strontium, iodine, and cerium administered to a variety of laboratory animals form an essential part of the program on biological effects. Also important are the problems of radiation dose *in vivo* and methods for determining dose in terms of biological effects.

[12] "Fundamental Nuclear Energy Research—1965" (pp. 152–169) dealt with the toxicity of radioelements at some length in a feature section. Reprints of the "Toxicity of Radioelements" section may be obtained from the Superintendent of Documents, U.S. Government Printing Office, Washington, D.C. 20402; price 20 cents.

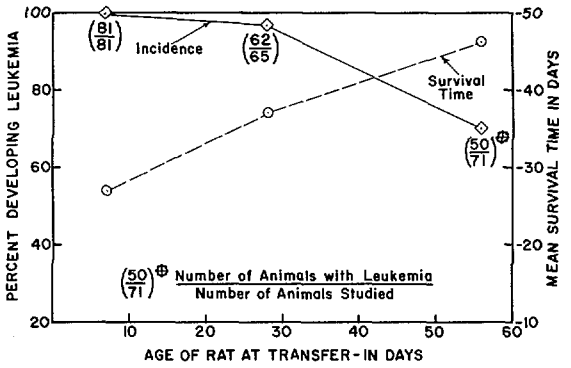

Fig. III–25. Successful Transfer of Leukemia. Rat leukemia induced by exposure to strontium-90 was successfully transferred to young rats by injecting leukemic rat blood at the Lovelace Foundation for Medical Education and Research, Albuquerque, N. Mex. The incidence of successful transfer of leukemia in rats decreased with age when three different age groups of rats received leukemic rat blood. Animals that developed leukemia survived longer when inoculated at older ages.

Strontium and Iodine Studies

Rat Leukemia

At the Lovelace Foundation for Medical Education and Research, Albuquerque, N. Mex., a continuing fission product inhalation program is investigating the biological effects of inhaled radioactive fission products. As a part of this overall program—which was started in 1960—rats have been exposed by inhalation to an aerosol containing soluble strontium-90 in an effort to determine resultant life shortening and the incidence and type of neoplasms attendant to such exposure. A number of cases of leukemia developed in rats that received strontium-90, either 100–200 or 500–1,000 microcuries per kilogram of body weight. The latent period between exposure and induction of leukemia appeared to be dose dependent and was found to be 7 months at the higher dose level and 11 months at the lower dose level.

Neoplasms in Miniature Swine

In studies on radiation induced neoplasms in swine, there have been some indications that there is possibly either a virus invasion or a loss of normal control over cellular proliferation in the damaged cells which causes these tumors. The biological effects of daily ingestion of various levels of strontium-90 in miniature swine have been under investigation at Pacific Northwest Laboratory since 1958. The miniature pig has continued to be the experimental animal of choice because of its relatively long lifespan and its size similarities to man.

Fifty-three cases of lymphopoietic (lymph-forming tissue) or hematopoietic (blood-forming tissue) neoplasms have been observed to date in animals ingesting 250 to 625 microcuries of strontium-90 per day. Four of these swine also had multiple bone tumors in addition to leukemic manifestations (see Figs. III–26 and 27). The preponderance of cases has been observed in animals ingesting 125 microcuries per day.

On a regimen of 25 microcuries per day, the pigs accumulate about 250 microcuries of strontium-90 in their bodies. This accumulation is more than 100 times greater than the limits set for workers in atomic energy industries.

Response of Chickens to Radioiodine

The high accumulation of iodine by thyroid tissue is the principal reason iodine-131 might be one of the most hazardous fission products to be considered in the event of a serious nuclear accident. Other investigations have shown that 6,000 microcuries [13] of iodine-131 per 100 grams of body weight injected into chicks destroy the thyroid gland. Pretreatment with a low-iodine diet and thiouracil (an anti-thyroid agent) reduced this to 1,500 microcuries of iodine-131 per 100 grams.

Experiments at the University of Tennessee-AEC Agricultural Research Laboratory have shown that 50 microcuries of iodine-131 administered to the embryo or the newly hatched chick or, 400 microcuries (300 microcuries per 100 grams) administered to a 2-week-old chick, would destroy its thyroid. The administration

[13] A microcurie is one-millionth of a curie.

of 100 microcuries or more of iodine-131 to embryos arrested their development to that of 18th- to 19th-day embryos (yolk sacs remained outside their bodies) even though they lived 8 days after they should have hatched. However, as little as two microcuries of iodine-131 given to a 16-day embryo reduced iodine-131 uptake by the thyroid of the 4-week-old chick while it required 50 microcuries to reduce growth rate. The chick thyroids receiving two microcuries of iodine-131, however, recovered their capacity to absorb iodine-131 by 6 weeks of age. The five-microcurie iodine-131 chicks exhibited permanent damage to the thyroid, while those that received 50 microcuries exhibited no appreciable uptake by the thyroid even at 15 weeks of age. The administration of iodine-131 to the hen at levels of up to 5,000 microcuries produced similar damage in their offspring. The effects are shown in Figure III–28.

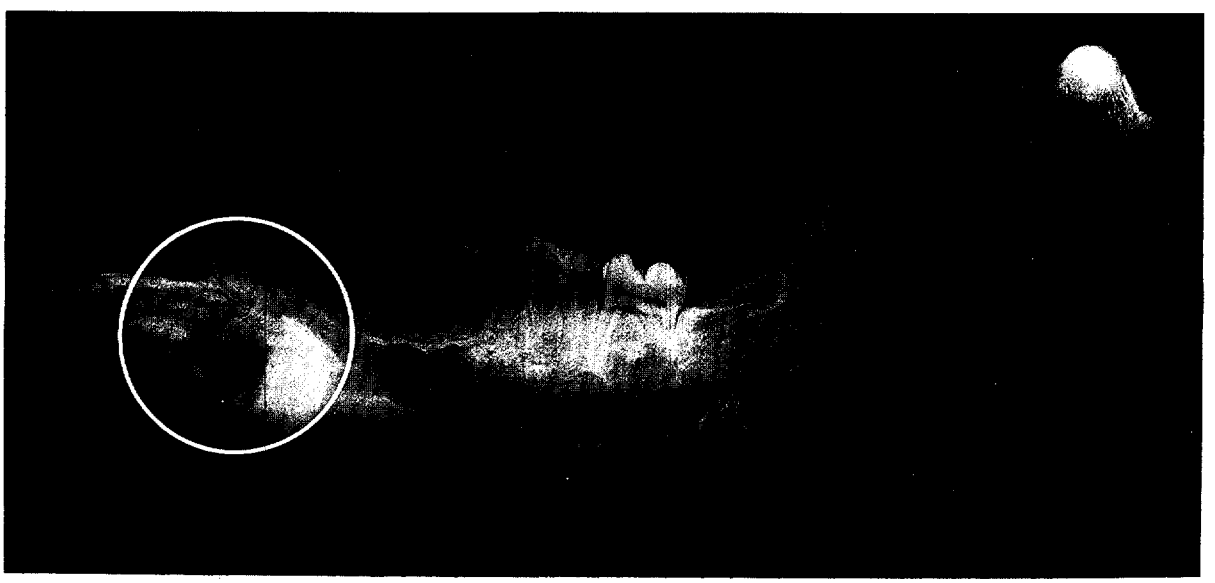

Figs. III–26 and 27. Neoplasms in Miniature Swine. These Pacific Northwest Laboratory radiographs of the skull (*above*) and mandible (*below*) of Hanford miniature swine show growth of bone tumors that developed in addition to leukemic manifestations in swine that have been on daily feedings of various levels of strontium-90. Circled area on mandible radiograph is a giant cell tumor; that on the skull is an osteosarcoma.

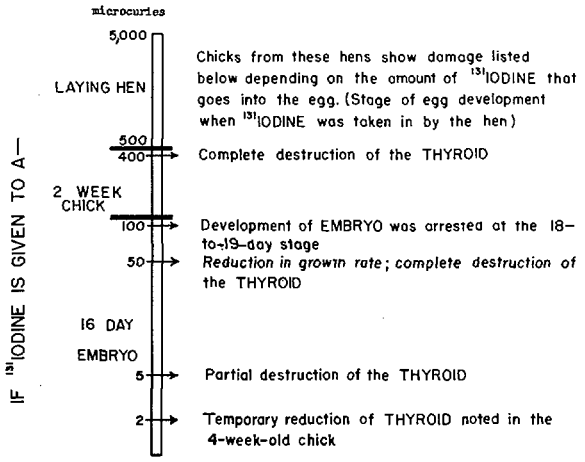

Fig. III–28. Response of Chickens to Radiation. Studies at the University of Tennessee-AEC Agricultural Research Laboratory have shown that iodine-131 accumulating in the thyroid tissue can have a destructive effect and may be a hazardous fission product in event of a nuclear accident. The effect of radioiodine (I^{131}) on the domestic fowl when given at different stages in its life span is shown in the chart.

Plutonium Studies

Excretion of Taurine

A study at Pacific Northwest Laboratory (PNL) in cooperation with the University of Washington School of Medicine, Seattle, has provided data which may help to explain the reduction in circulating lymphocytes—an effect consistently seen in dogs which have inhaled plutonium dioxide. (Lymphocytes are cells produced in lymphoid tissue and make up about 20 to 30% of the white cells in normal human blood.)

When human patients with chronic leukemia no longer responded to drug therapy, they were treated by a method of extracorporeal irradiation.[14] In the procedure used at the University of Washington, the blood is circulated through an irradiation device outside the body (in a manner shown in Fig. III–6) and irradiated daily for 6 hours over a period of about a week. Following irradiation, a marked drop in the number of circulating lymphocytes was observed in the blood. Urine samples from these patients analyzed at PNL showed that this lymphopenia was accompanied by a large increase in the level of urinary taurine, the end product formed from the metabolism of the essential sulfuramino acid, cysteine.

Continuing studies with Beagle dogs indicate that chronic lymphopenia may be the result of a true destruction of circulating lymphocytes rather than an inhibition of their production. This tentative conclusion is drawn from the high correlation between the decrease in the number of circulating lymphocytes and the increase of taurine in the urine. It was found that the levels of urinary taurine in dogs are elevated as much as six to eight times higher than the normal range (50–100 milligrams/24 hours)

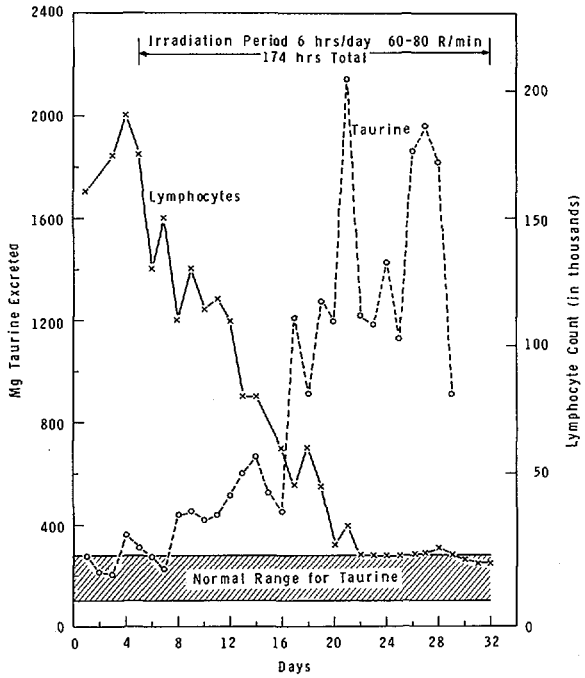

Fig. III–29. Excretion of Taurine. Chart shows the effect of extracorporeal irradiation of circulating blood in human leukemia patients on lymphocyte count and taurine excretion. It was shown at Pacific Northwest Laboratory that while the lymphocyte count drops rapidly after irradiation, the taurine excretion rises markedly. Continuing studies with Beagle dogs indicate that chronic lymphopenia may be the result of a true destruction of circulating lymphocytes rather than an inhibition of their production.

[14] See pp. 108–109, "Fundamental Nuclear Energy Research—1966."

depending upon the quantity of plutonium-239 dioxide deposited in the lungs and lymph nodes.

Drugs which produce a lymphopenia also cause a marked increase in urinary taurine excretion. Cortisone, for example, given to rats and Beagle dogs produces a rise in urinary taurine for 48 hours after administration. This taurine level may be as much as 10 to 20 times the normal values. Similarly, treatment with amethopterin, a metabolic antagonist of the B vitamin folic acid, also produces an immediate rise in urinary taurine during the first 24 hours after treatment.

While the experiments with plutonium dioxide and drugs are not conclusive, they do lend strong support to the hypothesis that elevated urinary taurine levels which occur following irradiation injury from either internal or external sources arise from the destruction of circulating lympocytes (see Fig. III–29).

Plutonium-238 Lung Deposition

The feasibility of using existing whole body counters to determine deposition of plutonium-238 in the human lung has been studied at Pacific Northwest Laboratory. It was concluded that the detection of a lung burden of plutonium-238 (0.016 nanocuries, or 16-billionths of a curie), could be detected with existing equipment and that with some equipment refinements, approximately one-half that amount (0.008 nanocuries, or eight-billionths of a curie) could be detected.

These values were obtained by first determining the energies of the gamma rays that are present in the plutonium-238 radioactive decay scheme by using a lithium drifted germanium detector. The two most prominent energies were sought with the large sodium iodide crystal employed with the whole body counter. The significance of this program lies in the fact that: (*a*) it is possible to detect plutonium-238 that is deposited in the human lung, and (*b*) this method can be used to verify the results of bioassay programs.

Radioactive Microspheres and Growth

At the Los Alamos Scientific Laboratory time-lapse motion pictures were taken (through the microscope) of the effect of the alpha radiation given off from plutonium oxide microspheres on the organized growth pattern of Syrian hamster cells growing in culture medium. Figure III–24 shows the growth pattern of the cells around a 20-micron[15] plutonium oxide sphere after 52 hours. The growth pattern is disrupted by the accumulation of dead cells only within the range of the alpha particles (about 30 microns). These and other similar observations indicate that the zone of damage from an intensely radioactive particle does not extend significantly beyond the range of the emitted radiation, even though the local radiation dose may be hundreds of thousands of *rads*. Studies of this type are carried out to evaluate the potential health hazards associated with the use of radioactive materials in the form of pellets or spheres (particularly the transuranic elements) as energy sources for radioisotope auxiliary power units.

Cesium and Cerium Studies

Toxicity of Cerium-144 in Dogs

At Argonne National Laboratory, cerium-144—a radioisotope produced in nuclear fission—has been shown to produce two distinct types of disease when given to Beagle dogs. Cerium-144 was studied because it represents a "biologically insoluble" radioisotope which localizes in both phagocytic cells and the bones. Because of this biological behavior the anticipated effects differ from the effects of "biologically soluble" isotopes which localize more or less uniformly throughout most mammalian tissues and organs.

Dogs were injected with 25–250 microcuries of cerium-144 per kilogram of body weight.

[15] A micron is one millionth of a meter.

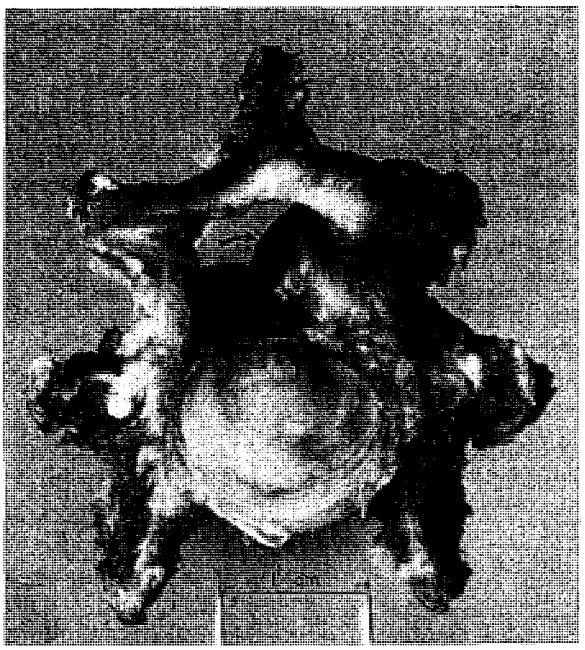

Fig. III–30. Toxicity of Cerium-144 in Dogs. Argonne National Laboratory studies have shown that higher doses (60–250 microcuries) of cerium-144 cause dogs to develop anemia and die within 100 days; those receiving lower doses, develop bone cancer from 3 to 5 years later. Photo shows a tumor (*arrow*) partially occluding the spinal canal of a vertebra from a Beagle that had received cerium-144, a fission product.

Those receiving the higher doses, 60–250 microcuries, died within 100 days after injection from anemia resulting from irradiation of the bone marrow by the cerium. In these animals, the time between injection of the isotope and death was related to the size of the dose given; as the dose was decreased the time required for anemia to develop lengthened.

Animals given lower doses generally did not develop anemia but died of bone cancer (osteogenic sarcoma). The sarcomas developed 3 to 5 years after injection of the cerium-144, at which time nearly all of the isotope had been eliminated from the body. Of the 11 sarcomas that developed, 10 were in the vertebrae (see Fig III–30). This portion of the skeleton, therefore, appears to be highly susceptible to the induction of tumors by cerium-144.

Influence of Solubility

Recent results have shown how the solubility of material can influence the biological effects of inhaled radioactive fission products. The studies are being conducted at the Lovelace Foundation in New Mexico. For the study, the metabolism of inhaled cesium-137 in Beagle dogs was compared for the very soluble compound, radioactive cesium chloride, and a quite insoluble form, which was encapsulated in fused clay particles.

Whole body retention data are shown in the Figure III–31. The curve for the insoluble form has two distinct phases, a sharp decrease during the first 3 days related to clearance from the upper respiratory tract and a second phase with very slow decrease in which over 90 percent of the radioactivity was found in the lung. In contrast, when the cesium-137 was inhaled in a soluble form, it was readily absorbed from the

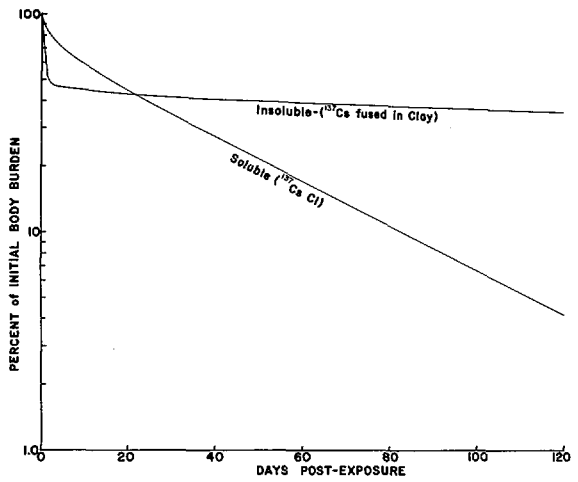

Fig. III–31. Influence of Solubility. Whole body retention of cesium-137 inhaled by Beagle dogs in either a soluble form, radioactive cesium chloride, or an insoluble form, encapsulated within fused clay particles is under study at the Lovelace Foundation. The long-term retention of cesium-137 in the insoluble form is the result of a portion of the inhaled activity remaining in the lung. In the soluble form, the cesium-137 was rapidly absorbed from the lung, distributed to other body tissues and excreted from the body at a much faster rate than that seen in the insoluble form.

lung, distributed throughout the body tissues, and eliminated from the body at a much faster rate. For equal initial total body burdens, the infinite radiation dose from the insoluble form to the lung, the critical organ, would be approximately 500 times the infinite radiation dose from the soluble form to the whole body which is in this case the critical organ. This results from the longer retention time for the insoluble form and its retention in a smaller tissue volume, the lung, as contrasted to shorter retention time in the whole body for the soluble cesium-137. Results of this nature are of great assistance in assessing the range of potential injuries which could occur in the event of a nuclear reactor incident where some of the fission products accumulated in the nuclear fuel may be released to the atmosphere in several different forms.

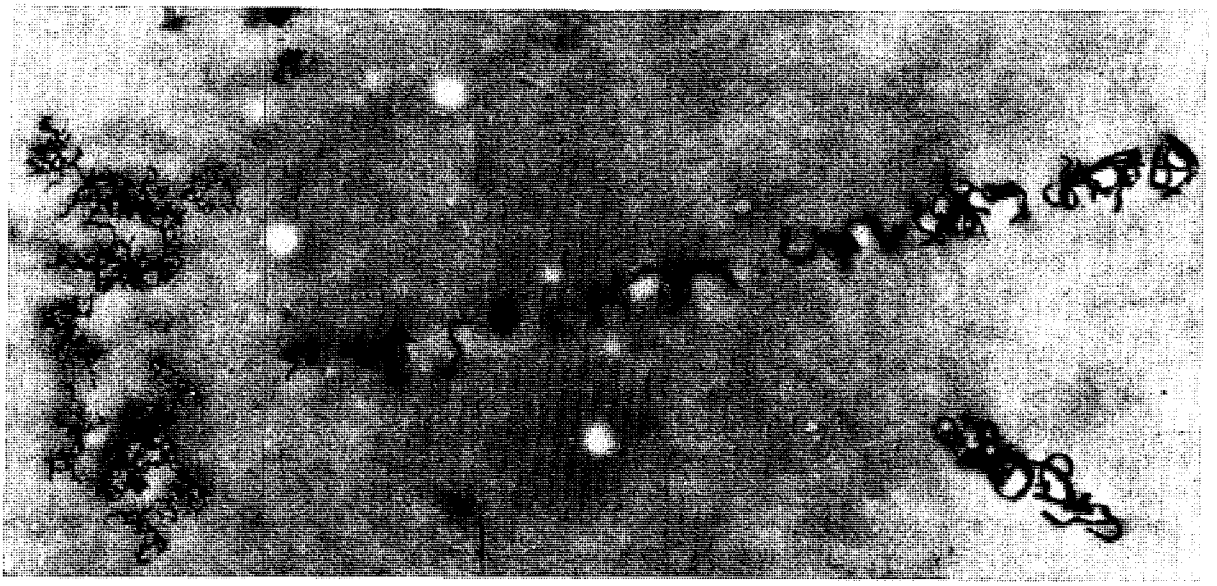

Fig. III–32. Plutonium Tracks. Plutonium alpha tracks as seen in animal tissue at high magnification (around 8,000 ×) by the techniques of electron microscopy combined with autoradiography at Argonne National Laboratory. Gradation in the structure of an alpha track may aid in determining the location of a submicroscopic mass of plutonium accidentally deposited in living tissues thus facilitating the removal of the highly toxic element.

COMBATING RADIATION'S DETRIMENTAL EFFECTS

Research into effective measures for combating radiation effects seeks a better understanding of the biological mechanisms involved. Studies are centered on the action and effects of drugs known to protect against radiation effects, materials and methods for treating radiation sickness, and removal of radioactive elements from the body.

PROTECTIVE AGENTS

Research on protective agents involves a search for: (*a*) cellular and subcellular location of the agent during optimum protection, (*b*) chemical nature of the target molecules and their interaction with the protective agent, (*c*) chemical, biological, and physical factors which influence the protective effects of the agent, including synergistic effects of other agents.

Chemicals To Protect Against Head Damage

Protection against radiation may be achieved by mechanical shielding with a metal such as lead, and it has also been found that certain chemicals, if injected before irradiation, can confer protection. Work on some of these chemicals is being carried out at Argonne Cancer Research Hospital.

Studies summarized below were designed to evaluate the degree of protection conferred by three specific chemicals on mice given lethal irradiation to the head while the rest of the body was protected by a lead shield. The mice were males of the C57BL strain. The chemicals were mercaptoethylamine (MEA), aminoethyl-iso-thiouronium (AET) and para-aminopropiophenone (PAPP), all of which are known to confer some protection against whole body irradiation. Chemicals were administered by intraperitoneal injection prior to irradiation. Aqueous solutions of MEA and AET were used at dosage levels of 225 and 400 milligrams per kilogram of body weight, respectively. PAPP,

in 50 percent propylene glycol in water, was given in dosages of 30 and 60 milligrams per kilogram body weight.

While all three chemicals produced appreciable reduction in dose factors for death after lethal irradiation to the head, MEA was particularly effective. The extent of protection, as measured by the dose reduction factor, was not as great, however, as is achieved with the same chemicals against whole body irradiation.

MEA-treated mice. In 243 mice treated with MEA, the amount of radiation necessary to produce an LD_{50}, *i.e.*, sufficient to kill 50 percent of the animals irradiated, was $2{,}159R \pm 13R$. Control animals given the same dose of radiation, but not injected with MEA, had an LD_{50} of $1{,}624R \pm 5R$. Thus, animals treated with MEA can survive a higher dose of radiation, and the dose reduction factor (DRF) for MEA is 1.33. In experiments in which the time between injection of the drug and irradiation was varied, it was found that the best results were obtained when the drug was given 5 minutes before irradiation and that there was a loss of protection when the interval exceeded 20 minutes.

AET-treated mice. In 174 mice treated with AET, the LD_{50} was $1{,}902R \pm 24R$, while the controls for this experiment had an LD_{50} of $1{,}626R \pm 19R$. The dose reduction factor for AET is therefore 1.16. The best effects were obtained when the interval between drug administration and irradiation was 5 minutes. There was a gradual loss of protection as this interval was increased to 20 minutes, after which there was no protection.

PAPP-treated mice. In 159 mice given PAPP at dosages of 30 mg/kg the LD_{50} was $1{,}880R \pm 20R$. The LD_{50} for 120 mice given 60 mg/kg PAPP was $2{,}049R \pm 23R$. Irradiated controls for these mice had an LD_{50} of $1{,}626R \pm 13R$. The dose reduction factor for $PAPP_{30}$ was therefore 1.16 and for $PAPP_{60}$ was 1.26. $PAPP_{30}$ conveyed a maximum protective effect when the interval between injection and irradiation was 15 minutes. There was a sharp decline after 20 minutes and a loss of protection at 30 minutes.

AIDING RECOVERY

Studies on aiding recovery include: (*a*) basic radiation recovery mechanisms, (*b*) collection, preservation, and transfusion of platelets and leukocytes, (*c*) attempts to identify and isolate bone marrow stem cells, (*d*) mechanism of control of hematopoiesis, including the physiology and chemistry of erythropoietin and other regulator substances, (*e*) control of immune response to donor tissue and rejection phenomena, and (*f*) control of infection, including studies with germ-free animals.

Hematopoietic Spleen Colonies in the Rat

At the Oak Ridge Associated Universities, it was found possible to extend a valuable research technique—that of growing hematopoietic cells—to a new and larger species of animals, the rat. This procedure, originally developed in Canada for studies with mice, is used to measure in a specimen of bone marrow or other hematopoeitic tissue the number of progenitor cells that are capable of giving rise, through repeated cell division, to large numbers of blood cells. A mouse is given a dose of total-body irradiation sufficiently large to destroy all blood forming tissue, and then is injected with a measured number of the cells to be tested for their generative capacity. After a few days the mouse is killed and carefully examined. Small white nodules will be found in the spleen, each nodule representing the offspring from one donated cell (see Fig. III–33).

This method has been of great value in studying quantitatively the potential of bone marrow cells after irradiation and other forms of injury. The successful extension of the technique to the rat required some special adaptations in procedure. It is proving of value because certain experiments can be done better in the larger animal.

Fig. III–33. Hematopoietic Spleen Colony in Rat. Rat spleen shown in photo has small white nodules which represent colonies of growing cells which have shown their capacity to generate additional new cells from a single implanted cell. The work at the Oak Ridge Associated Universities is aimed at growing hematopoietic cells in a larger species—the rat. Other studies done elsewhere have accomplished this in the mouse.

Formation of Antibody and Aging

Oak Ridge National Laboratory studies have shown that the secondary antibody-forming potential [16] of mice increases rapidly after antigenic priming, reaches a maximum, and thereafter declines exponentially at a rate comparable to that of the primary antibody-forming potential. In an attempt to gain better insight into the causes of age-related changes in the secondary antibody-forming potential per mouse and spleen, studies have been continued with mice of various age groups. Results thus far indicate that: (*a*) the factors responsible for decrease in the relative number of progenitor cells with age are not different in immunized and nonimmunized individuals; (*b*) during senescence (the period from maturity through old age) the functional lymphoidal (anti-body-producing) system is aging; and (*c*) during aging the ability to produce antibodies gradually returns to its embryonic level (see Fig. III–34). Future studies will concern the role of embryonic, juvenile, and adult environments on immunologically competent cells derived from juvenile and aged donors.

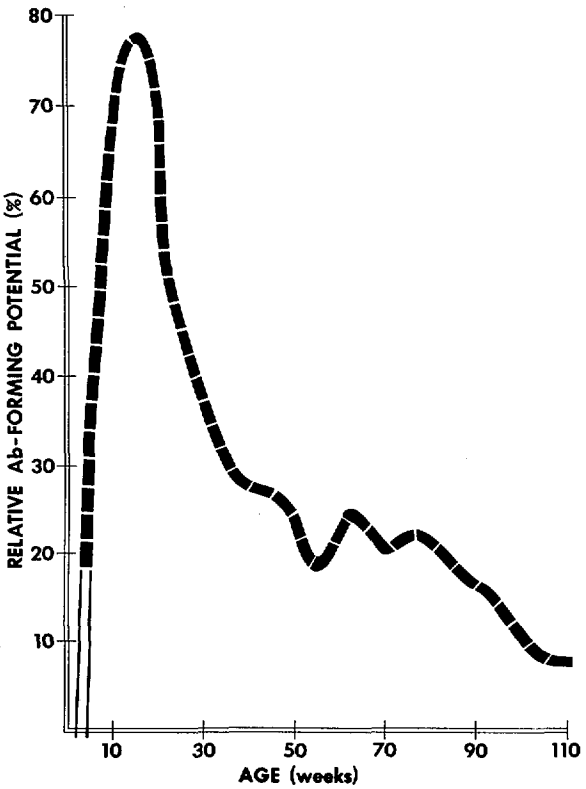

Fig. III–34. Formation of Antibody and Aging. Work at Oak Ridge National Laboratory has shown that the secondary antibody potential of mice increases rapidly after antigenic priming but, after reaching a maximum, declines rapidly. Chart shows the change with age in the relative immune competence of mice. Maximum response of 100 percent is equivalent to the highest observed response of one individual mouse.

[16] Primary antibody-forming potential is an animal's inherent ability to respond to a first administration of a given antigen.; if the same antigen is given to the same animal at a later time, the second response is called secondary antibody-forming potential.

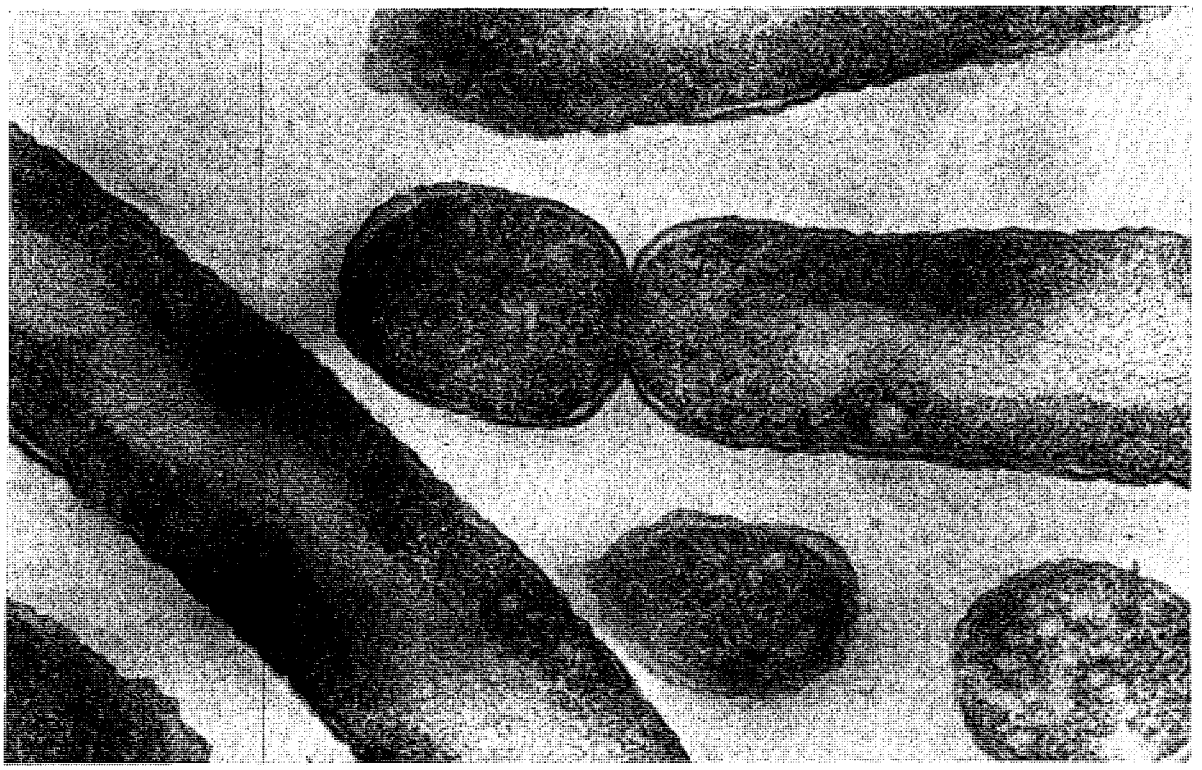

Fig. III–35. DNA-less "Minicells". A cell division mutant of the bacterium *Escherichia coli* that may be useful in various studies has been developed at Oak Ridge National Laboratory. In addition to normal cell division, the organism frequently has a secondary division that produces very small cells—"minicells"—that are chemically active but have no nuclei nor deoxyribonucleic acid (DNA). The electron micrograph shows bacterium dividing into a normal cell and a minicell. See page 268 for details.

RADIATION GENETICS

The research program in radiation genetics seeks to determine the mechanisms by which radiation induces changes in the genetic material of cells, the sequence of events by which such radiation-induced changes in the germ cells express themselves as altered characteristics in the individuals of succeeding generations, and the manner in which these genetic changes are incorporated into or eliminated from populations. An understanding of the fundamental physiochemical properties of genetic materials is prerequisite to understanding the way in which radiation and other mutagens act upon the genetic materials of humans, animals, plants and micro-organisms, and to the prediction of the genetic effects of radiation on individuals and populations. Studies to be described here cover the categories of cytogenetics, microbial and biochemical genetics and gene action, and human and mammalian genetics.

CYTOGENETICS

In vivo and *in vitro* studies are carried out in AEC-sponsored cytogenetics research for: (*a*) examination of the relationship of abnormal chromosomes constitutions to congenital malformations, sterility and lethality; (*b*) determination of the structure and function of chromo-

somes under normal conditions and subsequent to treatment with radiation and other mutagenic agents; and (*c*) determining mechanisms involved in protection and repair of chromosome breaks as a result of mutagenic action.

Chromosome Organization and Distribution

Studies at the Laboratory of Radiobiology of the San Francisco Medical Center, are aimed at gaining an understanding of chromosome structure and how genes and chromosomes react to ionizing radiation. It has been found that the number of aberrant chromosomes produced in plant cells by radiation from tritium incorporated into DNA in the form of tritiated thymidine, rises very quickly and then reaches a plateau so that no more are induced with the addition of more of the isotope. This seeming independence of yield to dose of radiation indicates that there are very few places (submicroscopic) within the nucleus of the cell where chromosomes come close enough to one another to rejoin abnormally after being broken.

The distance between chromosomes also seems to be important in determining the number of chromosome aberrations obtained after irradiation of cells in various stages of the mitotic cell cycle. Reports that a cell can be sensitized to a second dose of radiation following a first dose, in addition to producing its individual damage, only slows the progress of the cell through the mitotic cycle. Therefore, at the time of the second dose, the cell may be in a stage in which the chromosomes are packed so they can rejoin more easily to form aberrations following chromosome breakage. When cells in the same stage of the cycle were compared, it was found that a first dose of radiation did not affect the response to a second dose.

Other studies at the San Francisco laboratory suggest that X-rays may affect the way in which the units of the chromosome are reorganized at each cell division (see Fig. III–36). Broadbean roots were used because they contain many actively reproducing cells with large and easily observed chromosomes at the time of mitosis. Newly synthesized chromosomes were labeled with tritiated thymidine, and the cells were X-irradiated after the first mitosis. Upon reaching division for the second time, they were examined to determine the distribution of chromosome labeling. Normally, at this second division after marking of the chromosomes with tritiated thymidine, it is found that only one of the two chromatids (subunits) of the chromosome is marked. However, in this experiment, both were marked. This shows that the X-rays have altered the way in which the new chromosome subunits were formed. Experiments of this kind provide a means for studying the behavior of chromosomes at a time when they are not visible.

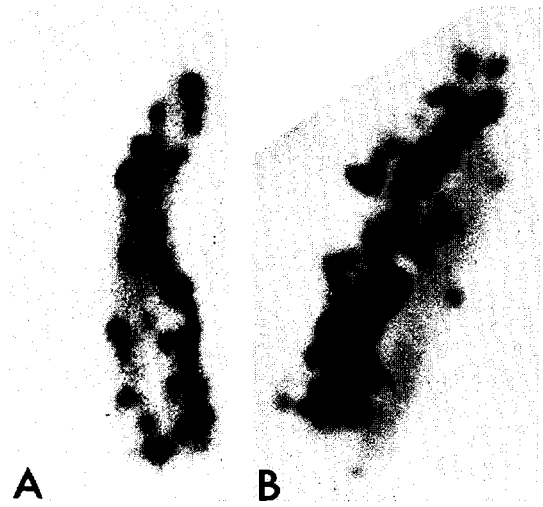

Fig. III–36. X-ray Effect on Chromosome Sub-Units. Chromosome *A* (*left*) is an example of a chromosome from a cell labeled with tritiated thymidine and later irradiated by X-rays. The black grains show both halves (chromatids) of the chromosome labeled at the second cell division. The normal pattern is exemplified by chromosome *B* (*right*) which has grains over only the left-hand chromatid.

Studies with Synchronized Cells

Methods of synchronizing mammalian cells in culture enable responses which vary as the cell "ages" between one division and the next. To

[17] DNA=Deoxyribonucleic acid, the chemical substance in the nucleus that serves as the repository of hereditary information in normal cells.

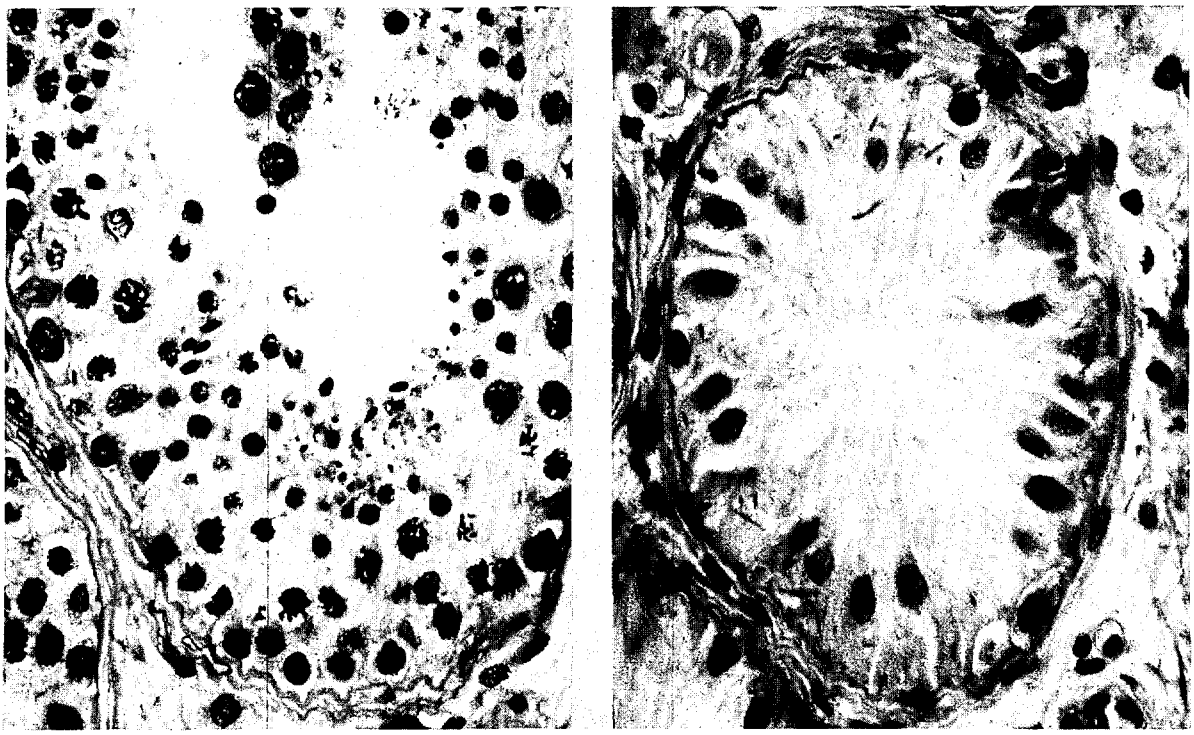

Fig. III–37. Radiation Response of Spermatogonia. Comparison of the radiation sensitivity of the human testis with that of the mouse indicates that each has the same general response to X-rays, but that spermatogonia in man appear to be more sensitive. Cytogenetic studies are being made at Oak Ridge National Laboratory, on material obtained by the Pacific Northwest Research Foundation in Seattle, from volunteers who were given local X-irradiation to the testes. Biopsies (removal of living tissue for examination) were taken at several intervals over a period of more than a year following the irradiation. The microphotos (1,200×) above show a normal human testis on *left* in which all cell types from spermatogonia to mature spermatids are present. On the *right* is an irradiated human testis, 195 days after a 100-roentgen dose. Only *Sertoli* cells and a few spermatogonia (stem cells) are present. In general, the data indicate that human spermatogonia had a slower initial rate of decrease, but that cellular degeneration persisted longer and that recovery came much later than had been expected on the basis of data obtained from experimental animals but not on the basis of data from accidental human exposures. However, this comparison must be evaluated in the context of species differences in the time sequences of events and in that of the relative importance of differing factors involved in both initial depletion and subsequent recovery of the spermatogonial population. This emphasizes the importance of checking, in humans, certain crucial findings from animal experiments.

the previous method of selecting cells at division, a further technique has been added to eliminate cells actively synthesizing DNA[17] and thus synchronize stages such as G_1 and G_2 (see definitions below) and mitosis much better.

X-ray responses have been examined in synchronous Chinese hamster cells in some detail at the Argonne National Laboratory. It has been shown that most responses vary greatly depending upon the stage of the cycle at which the cell is irradiated.

(*1*) Survival of cells after an X-ray exposure is greatest when the cells are in the latter stages of DNA synthesis (S), less just before DNA synthesis begins (G_1) and least when the cells have completed DNA synthesis (G_2) or are in mitosis (M).

(*2*) Cell division is delayed most when cells are in DNA synthesis at the time of X-ray exposure, less at other stages.

(*3*) Part of the division delay produced by X-rays is the result of a slowing down of DNA

synthesis which occurs most readily when the cells are actively in synthesis at the time of exposure.

(*4*) Other macromolecular syntheses, *e.g.*, RNA [18] and protein synthesis, are not affected by moderate X-ray doses.

(*5*) Chromosome aberrations differ in type and frequency according to the stage of the cell cycle at which the cells are irradiated. Before DNA synthesis, most chromosome aberrations are induced, whereas during synthesis and especially after it, (G_2), chromatid aberrations are induced. These results are consistent with and reinforce current ideas on the separation of chromatid units just prior to DNA synthesis.

(*6*) The radiation damage which results in retarded growth in colonies ("small colony formation") varies throughout the cell cycle in the same manner as does survival.

X-radiation responses. In addition to the above, Argonne's studies of X-radiation responses in synchronized cells in the presence of inhibiting drugs are being continued. The arrest of protein synthesis (with cycloheximide), messenger RNA synthesis (with Actinomycin D), and DNA synthesis (with hydroxyurea or excess thymidine) in synchronous hamster cells at different stages of the cycle, enable the X-radiation response to be correlated with particular cellular processes. Hydroxyurea makes an excellent synchronizing agent for Chinese hamster cells. It also enhances the sensitivity of inhibited cells to X-rays and may, therefore, be a useful practical radiosensitizing agent in addition to having other properties.

Radiosensitivity and chromosome volume. At Brookhaven National Laboratory, studies showed that a direct proportionality exists between the radiosensitivity of herbaceous plants and the volume of the chromosomes at the interphase stage of division in the cells of such plants. Continuing work, extended to other forms of life, ranging from viruses and bacteria to the higher animals, has now shown that: (*a*) similar relationships between chromosome volume and radiosensitivity exist; and (*b*) that these relationships can be used to classify all the forms studied thus far in seven distinct groups.

GENETICS AND GENE ACTION

Work in the fields of microbial and biochemical genetics and gene action encompass investigations of cellular and extracellular transfer of genetic information, mechanisms of recombination, fine structure gene analysis, and the biochemical basis of phenotype.[19]

DNA-less "Minicells"

At Oak Ridge National Laboratory, a mutant that affects cell division of the bacterium *Escherichia coli* has been isolated that may be useful in a variety of studies. In addition to undergoing normal cell division near the midpoint of the rod-shaped cell, cells of this organism frequently undergo a second division close to one pole (see Fig. III–35). This misplaced division results in the production of a class of very small cells, dubbed "minicells", that have some unusual properties. Although they respire and are chemically active, minicells cannot divide and therefore cannot reproduce.

These small cells may be separated from the bulk of the population and analyzed. They have normal appearing walls and membranes and contain reasonable amounts of vital cellular material such as ribonucleic acid and protein. However, they do not have nuclei, and consequently have no deoxyribonucleic acid (DNA).

Many cytoplasmic enzymes can be detected in these small cells, as well as in the parental population. However, the photoreactivating enzyme, although present in the parental cells, has not been detected in the minicells.

Studies are underway to determine other properties of DNA-less *E. coli* cells, particularly concerning a possible relationship with the mutant's unusual radiation characteristics, *i.e.*, it is resistant to X-rays but responds normally to ultraviolet light.

---

[18] RNA = Ribonucleic acid.

[19] Normal or modified appearance of the organism as a result of gene action.

Genes for Soluble RNA

A class of mutants exists in the yeast, *Saccharomyces cerevisiae*, which can be suppressed by other genes at other genetic loci in the same nucleus. Such mutations are referred to as being "super-suppressible," while the suppressors are called "super-suppressors." Mutational and genetic analysis of yeast at Oak Ridge National Laboratory has shown that the so-called "super-suppressor genes," unlike most genes, do not encode proteins, and are very likely the genes that act as templates for soluble ribonucleic acid. The soluble RNA's, vital components of the genetic translation system, transfer amino acids to the site of protein synthesis. Further progress in this system depends upon identifying which one of the 40–60 soluble RNA species is specified by a given super-suppressor gene.

Genetic Control of Enzymes

The genetic control of enzymes is being studied in the fruit fly, *Drosophila melanogaster*, at Oak Ridge National Laboratory. This insect has been studied from a genetic point of view for over 50 years. Thus, there is a large store of information about its genes and chromosomes. Until recently, no biochemical method provided a convenient way of studying the genetic control of enzymes in this organism. The development of gel electrophoresis (the migration of the enzyme through a gel in an electric field) provided such a method so that now the genetics of enzymes in a complex organism is readily subject to analysis (see Fig. III–38).

The enzyme on which most of the work has been done is alcohol dehydrogenase, a convenient enzyme to work with because it may be detected easily. Multiple forms of alcohol dehydrogenase are easily detected by gel electrophoresis. Single gene mutations affect the properties of all forms simultaneously. Thus, the multiple forms are products of one gene and not products of multiple independent genes. The molecular basis for the differences between the multiple forms is not known as yet. Most likely it reflects different three-dimensional configurations of the enzyme molecule or differential binding of other molecules to the enzyme.

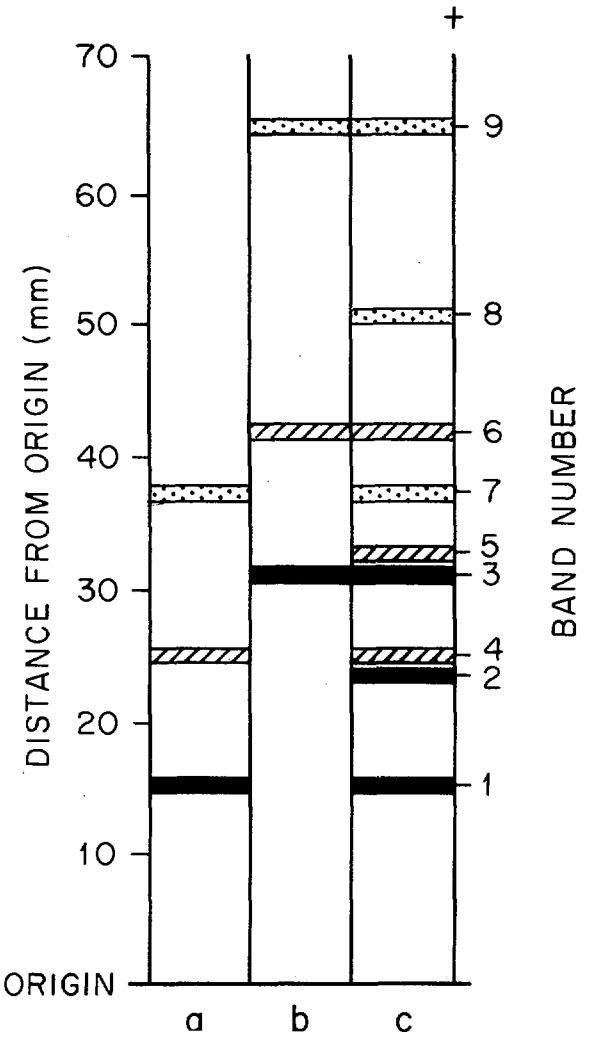

Fig. III–38. Genetic Control of Enzymes. Development of gel electrophoresis—the migration of an enzyme through a gel in an electric field and makes it possible to analyze the genetics of enzymes in a complex organism. The above is an electrophoresis pattern for alcohol dehydrogenase, an easily identified enzyme of the fruit fly, *Drosophila melanogaster*, being studied at Oak Ridge National Laboratory. Columns "*a*" and "*b*" are the parents; "*c*" is the hybrid.

Mutation Induction by Light

The first observations of mutations induced by visible light (4,000–7,500 A [20]) and near-visible light (3,200–4,000 A) have been reported at Argonne National Laboratory. These observations were made on continuous cultures of two different strains of a bacterium (*Escherichia coli* B/r). The mutation involved a change from sensitivity to the bacterial virus (T5) to resistance to it. Moderate, non-lethal, intensities of visible and near-visible light (much less than the intensity of light from the noonday sun) produced mutation rates more than 20 times the spontaneous mutation rate in the dark. The mutagenic potential of visible and near-visible light, previously unsuspected, is of concern because all higher plants and animals are exposed to light of these wavelengths. Identification of the chromophore (the compound in the cell that absorbs the light) should increase the understanding of the role which this compound plays in the living process as well as improve the understanding of how the genetic material (DNA) functions.

Preliminary measurements show that the effective wavelengths for mutagenesis lie between 3,200 and 5,000 A (see Fig. III–39). The efficiency for one strain is somewhat higher for the visible part of the spectrum than for the near-visible part. Direct absorption of the light by genetic material is not involved with visible light, but may play a role in the effects produced by near-visible light. In addition, oxygen is required for mutation with visible light, but not necessarily with near-visible light.

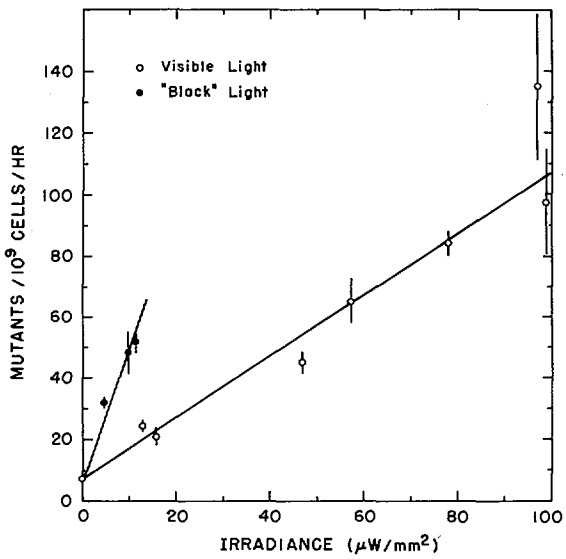

Fig. III–39. Mutation Induction by Light. Argonne National Laboratory plot of the mutation rate (from sensitivity to the bacterial virus T5 to resistance to it) in continuous cultures of the bacterium *Escherichia coli* in relation to intensity (irradiance) for both long-wavelength ultraviolet (black light) and visible light. In both cases the mutation rate is proportional to light intensity.

[20] A is the abbreviation for Angstrom unit, formerly abbreviated as Å; it is one hundred-millionth of a centimeter and is used for measurement of wavelengths of light.

Fig. III–40. Red Blood Cell Surface. At the Lawrence Radiation Laboratory, Berkeley, use of the electron microscope is producing new information on red blood cell surfaces. This is an electromicrograph (10,000×) of a platinum-shadowed, thin-sectioned rat erythrocyte. At the top of the photo, in the platinum shadowed region, can be seen what appear to be filaments at the surface in this oblique section of the membrane. See page 276 for other details.

MOLECULAR AND CELLULAR LEVEL STUDIES

Molecular and cellular level studies seek to identify and characterize in cellular and subcellular systems the critical macromolecules, organelles, and biochemical mechanisms which are affected by the absorption of ionizing radiation; the nature of the primary lesions which are thereby produced; the chain of aberrant physicochemical events which follow, eventually resulting in observable changes in cellular performance; and spontaneous cellular repair processes that are capable of correcting radiation-induced damage and restoring normal function. Interactions and responses of cells to visible, ultraviolet, and other nonionizing radiations, and the biological production of light are also included in this category of study. The subcategories of work include photobiology, radiation biophysics, nucleic acids and proteins, cell regulatory mechanisms, developmental biochemistry, and cellular organelles.

CELL REGULATORY MECHANISMS

Studies of cell regulatory mechanisms are aimed at the level of cellular processes or phenomena, such as the genetic control of cell processes, the biochemical basis of homeostasis and the dynamic steady state, regulation of cell activity by hormones and other agents, the molecular basis of the immune response, effects of radiations and other mutagenic agents on the replication and transcription of DNA, and the molecular basis of nerve function.

Cell Growth Rate and Population Size

The size of a population of cells in a given environment can be an important determinant of its rate of growth. This raises some intriguing questions about the nature of the population size-growth rate relationship which have a direct bearing on the interpretation and application of radiation effects. In autoradiographic studies with a mouse ascites [21] tumor conducted at the Laboratory of Radiobiology, University of California San Francisco Medical Center, it has been learned that the progressive retardation of growth rate with increasing tumor mass is due principally to: (*a*) prolongation of the time required for synthesis of deoxyribonucleic acid (DNA), and (*b*) a decrease in the proportion of cells in mitosis.

It is of interest that a pre-DNA synthesis period could not be detected in the ascites tumor cells whether the mitotic cycle was 8 hours during rapid growth or 22 hours during slow growth. This suggests that such a period is not obligatory for the assembly of necessary precursors, which apparently can take place concomitantly with DNA synthesis itself. The findings of the marked prolongation of DNA synthesis is contrary to the frequent generalization that this period is rather constant for mammalian cells and that a change in the duration of the mitotic cycle reflects mainly a change in the pre-DNA synthesis period. Cessation of mitosis in an increasing proportion of cells as the cell population enlarges may merely represent an extension of the mechanism responsible for prolongation of the DNA synthesis period. Such "out-of-cycle" cells can resume mitosis upon inoculation into a new host.

These findings provide a framework for further study of growth rate-controlling factors as well as of relationships between growth rate, population heterogeneity and radiosensitivity. For example, the response to a single exposure to radiation may be altered by changes in the age distribution of cells as the population expands. Moreover, the optimum spacing of repeated exposures as in radiotherapy may be determined by the shifting growth rate as the population contracts as a consequence of a prior exposure to radiation.

DNA Replication and Repair in Human Cells

In studies of the synthesis of deoxyribonucleic acid (DNA) in cultured human cells, a new technique has shown that after irradiation, synthesis of DNA occurs in a manner completely different from that in normal unirradiated cells. The technique resolves small changes in the density of biological molecules, by their relative position in a tube that has been centrifuged at high speeds for several hours. It has been used in DNA replication studies at the Laboratory of Radiobiology at the San Francisco Medical Center. Evidence is accumulating that this post-irradiation synthesis is part of a process that repairs some of the radiation-induced damage to the cells' genetic material, *i.e.*, DNA. Although a similar phenomenon is well-known in lower forms, such as bacteria, this is the first evidence for repair of genetic damage by human cells.

With the same technique, it has been found that the DNA in each chromosome is organized into about 100 units, each of which doubles once before the cell divides. Work is in progress to determine the relative sizes of these units, and their temporal patterns of replication. Previous work on the effects of ionizing radiation on the rate of DNA synthesis suggests that the targets of irradiation are these individual subunits of

[21] A tumor causing an accumulation of fluid in the peritoneal cavity.

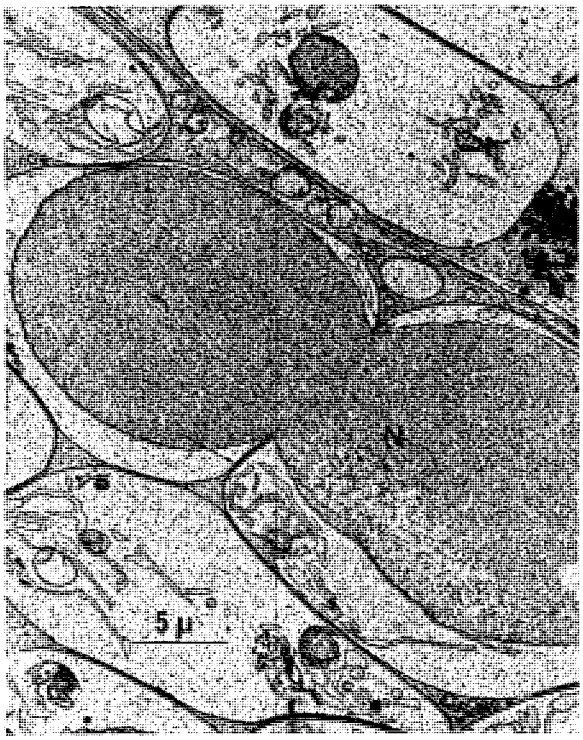

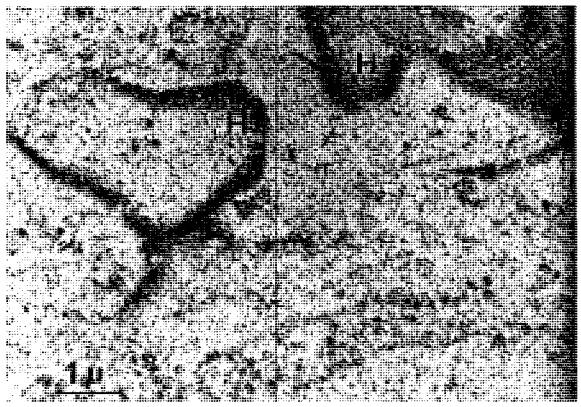

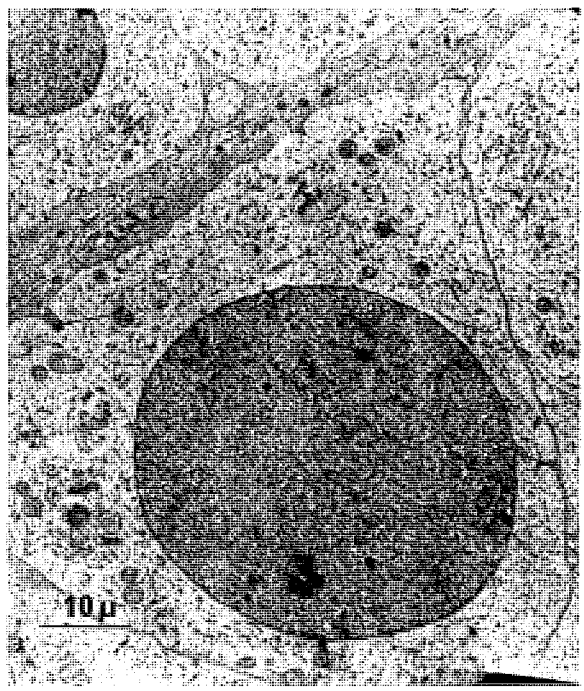

Figs. III–41, 42, and 43. Plasma Membrane Synthesis and Cell Division. Electron microscope observations at Argonne National Laboratory have shown that relatively low doses of irradiation (50 to 200 roentgen) are not lethal to the cells but do cause alteration of the basic biological events. Electron photomicrograph in *upper left* shows a magnification (18,500×) of cleavage furrows (arrows) pinching off the nucleus (*N*), which has failed to complete normal division in an X-irradiated (200*R*) grasshopper testis cell. At *upper right* the beginning (7,000×) of a cleavage furrow in a normal cell is shown at the arrows. The furrow is predetermined by the deposition of granules on the plasma membrane at this site. Photo at *left* (25,000×) is a tangential section of an advanced cleavage furrow showing numerous helices (H) polymerized from ribosome-like granules.

the chromosomes rather than the entire chromosomal DNA. The concept that the chromosomal DNA consists of subunits may be of importance in considerations of differentiation and of the radiosensitivity of differentiated relative to undifferentiated cells.

Plasma Membrane Synthesis and Cell Division

At Argonne National Laboratory studies on the effect of irradiation on differentiating cells have shown that relatively low doses, ranging from 50 to 200 *R*, do not kill the cells, but cause aberrations in morphology of the tissues so that basic biological events are altered. Thus, irradiation not only brings about morphological disturbances in development but also is a tool to study fundamental biological events.

It is generally known that irradiation doses at the biological level (50 to 200 *R*) upset synchronization during cell division. Both light- and electron-microscope techniques are able to

demonstrate the inhibition of nuclear mobilization and chromosome apportionment (mitosis or meiosis). The ability of the cell to divide into two bodies is not affected (see Figs. III–41 and 42). High resolution electron micrographs of grasshopper testes revealed the ribosomal mobilization and reorganization associated with cell division.

Since the discovery of the cell, biologists and physicists have been puzzled by the kinetics of cell division. Many types of models—sols, gels, and surface acting chemicals—were promulgated to explain how a cellular sphere separates into two.

Electron microscope observations of the macromolecular morphology of the plasma membrane revealed that ribosome-like granules are attached to the inner surface of the cell membrane, at the presumptive division furrow, in the form of a ring (see Fig. III–42). Ribosomes are capable of synthesizing proteins. It was demonstrated at Argonne—with autoradiographic techniques—that in a dividing protozoan, the proteins of the surfaces of the daughters adjacent to the division furrow are newly synthesized.

In the division process, not only is a mechanical pinching necessary but also there is required a 26-percent increment in surface area of the original sphere. The ultrastructure of the ribosomal belt at the division furrow reveals that ribosomal polymerization occurs. The polymerization (see Fig. III–43) causes the belt of ribosomes to form helices (coils) and it is believed the tightening of these coils causes a gradual diminution of ribosomal surface available for plasma membrane synthesis. The differentially diminishing rate of plasma membrane deposition causes the pinching process of cell division. The division process, rather than being dependent upon a physical alteration of the furrow, is accomplished by a localized decrease in the rate of chemical synthesis of new plasma membrane.

Present efforts are aimed at determining the nature of the material that appears to be of ribosomal origin by using tritiated uracil and thymidine as tracers.

Biochemical Effects of Radiation

Recent experiments at the Los Alamos Scientific Laboratory have permitted the accurate timing of several biochemical events in the life cycle of animal cells grown under artificial conditions. Observations show that cells grown under these conditions are capable of spontaneous repair of irradiation damage. The biochemical events mark the completion of ribonucleic acid and protein synthesis necessary for cell division and indicate that the several essential features of cell division involve the synthesis of large molecules late in the cell's life cycle. With these precise timing techniques, the immediate effects of radiation doses on cell growth have been investigated.

Cells growing under closely controlled conditions were exposed to small doses of X-rays, and

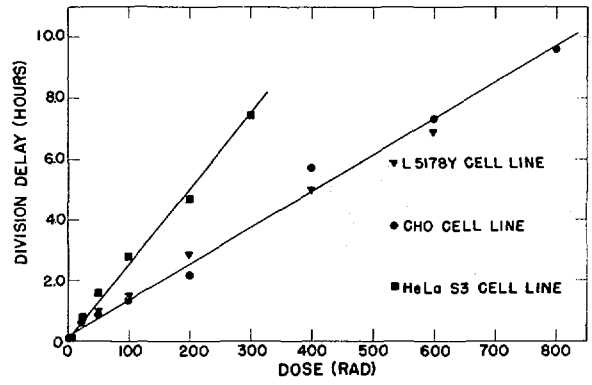

Fig. III–44. Biochemical Effects of Radiation. The immediate effects of irradiation on cell growth have been investigated at the Los Alamos Scientific Laboratory using techniques which allow the accurate timing of biochemical events in the life cycle of animal cells. The cells were given small doses of X-rays and their progress through their life cycle was observed. The graph shows the delay in cell division in three different cell lines grown in tissue culture after X-ray doses ranging from 25 to 800 *rads*. The fact that the data fit straight lines indicates that: (*a*) the different cells have typical radiosensitivities; (*b*) only a very few reactions are damaged (multiple injury data would tend to curve up or down); and (*c*) all cells recover, divide at least once, and may ultimately die of defects undetectable in the generation in which the damage is inflected.

Figs. III–45 and 46. Red Blood Cell Surface. Lawrence Radiation Laboratory, Berkeley, has been using the electron microscope to attain new knowledge about red blood cell surfaces. To obtain photos for study, the cells are fixed with osmium, freeze-dried, and shadowed with platinum. Above *left* is an electronmicrograph (25,000×) of a platinum-shadowed, thin sectioned rat erythrocyte (cell). This thin section, which is nearly perpendicular to the plane of the membrane in the region of the platinum shadowing, shows filaments both in the obliquely sectioned region (*upper right* corner) and at the terminator between the platinum shadowed region and the unshadowed region (*center of figure*). Electronmicrograph (9,000×) on *right* is also a platinum-shadowed, thin-sectioned rat erythrocyte showing the platinum deposited upon the surface which is mostly between two successive microtome cuts. The surface is viewed nearly normal to the plane of the membrane and shows a "pebbly" appearance.

the effects on their progress through the life cycle were measured. Cells which had successfully completed their final protein synthesis continued through the life cycle and divided on schedule. Younger cells in which terminal synthesis was not yet complete stopped as though injured and continued only after a delay during which injury was presumably repaired. Fig. III–44 shows that the higher the radiation dose, the longer the cells were delayed, although all susceptible cells originally stopped at the same time regardless of dose and regardless of the line of cells used for the experiments. This observation suggests that the same biochemical feature was affected in each case.

The similarity in stopping point noted for irradiated cells and cells poisoned by the reversible inhibitors of protein synthesis, cycloheximide (actidione), suggests that radiation delay as well as spontaneous repair of radiation damage involves essential protein synthesis. Cells stopped by radiation and then poisoned for periods of time up to 3 hours were released from effects of the poison by washing and the time to division was measured. In each case, the time to division was the sum of the time required for recovery by irradiated cells plus the time of exposure to the poison.

Thus, inhibition of protein synthesis prevents spontaneous repair from radiation injury, but does not impair the cell's capacity to recover once the inhibitor is removed. It now appears that the delay induced by radiation involves a temporary failure in capacity of the cell to synthesize certain essential proteins and that repair involves their eventual synthesis before progress of the cell through division can be resumed. Distribution of the cells in the replication cycle after recovery suggests that, when specialized protein synthesis ceases, other essential biochemical processes also stop. Thus, it appears that young cells are radiosensitive while older

cells are radioresistant from the standpoint of essential protein synthesis. However, when division occurs each older cell becomes two young cells which, if truly viable must be able to undergo repeated division for an indefinite period, and failure to continue suggests that there are changes in the genetic material rather than in protein synthesis.

Red Blood Cell Surface

The cell membrane is almost always observed in thin section as a "unit membrane" having a thickness of about 75 angstroms. In sectioned tissue blocks, however, an intercellular space about 150 angstroms wide is usually seen. These observations and the appearance of the red blood cell surface as seen by carbon replicas are indications that not all the membrane material is revealed in conventionally stained and sectioned membranes. Recent research at Lawrence Radiation Laboratory, Berkeley, has given new information on the outer surface architecture of the red blood cell based on electron photomicrography (see Figs. III–40, and III–45 and 46).

Cell specimens were fixed with osmium, freeze- or ethanol-dried, platinum-shadowed, and embedded in a plastic. In tangential or very oblique sections (relative to the membrane surface), a "pebbly" surface was observed, similar to that seen with the replica technique. In sections perpendicular to the plane of the membrane, the electron micrographs showed that the deposited platinum was in tight contact with the portion stained by osmium. It was also noted that the thickness of the metal is always several times greater than the known thickness of the deposited metal, and its appearance is often that of random filaments. This filimentary appearance and the unexpected greater thickness of the deposited metal layer can be explained in terms of the shadowed appearance of replicas or tangential sections. Such an explanation, however, must assume that there is a portion of the membrane outside the "unit membrane," and that this material is not smoothly or homogeneously distributed over the surface of the cell.

DEVELOPMENTAL BIOCHEMISTRY

The development of a complex organism from a single fertilized egg involves rapid cleavage into many seemingly identical cells, followed by the organization of the cells into diverse types which show increasing specialization of function and morphology. This process of cell divergence is called "differentiation." It appears certain that the ultimate control of the process of differentiation resides in the genetic material (DNA) in the nuclei of the individual cells. The ultimate expression of these genetic characteristics is the production, in the cytoplasm, of functionally distinct classes of proteins. Thus, differentiation must be viewed as a series of nucleocytoplasmic interactions during the development of the organism.

Protein Synthesis in Development

Work in progress at Argonne National Laboratory is concerned with the nature and control of protein synthesis in the frog embryo during the developmental stages prior to differentiation. This work has concentrated on: (*a*) the stimulus responsible for the initiation of protein synthesis during development, (*b*) the rate of protein synthesis as a function of stage of development, and (*c*) the role of the nucleus in the direction of this protein synthesis.

Although a number of invertebrate species have been shown to initiate synthesis at fertilization, the current work shows that protein synthesis in the frog egg is initiated by the influence of maternal hormones, while still in the ovary, and reaches its maximum rate well before the maturing oocyte is capable of fertilization. The rate of protein synthesis is not affected by the process of fertilization; thus, it appears that fertilization has no immediate quantitative effect on protein synthesis.

In addition, removal of the nucleus from the developing egg has no effect on the rate of protein synthesis. Thus, it has been concluded that, although the nucleus must provide the ultimate control of growth and synthesis, the expression

of the genetic characteristics coded in the nucleus does not necessarily occur as a simple, timed sequence of events. Obviously, the organism is capable of investing the cytoplasm with a programmed set of templates which allow the later expression of genetic characteristics without the direct participation of the genetic material.

Enzyme Activity in Rat Liver

Most of the cells in the liver are of one kind and are organized into small units called lobules, each with its own system of blood vessels and lymph and bile ducts. Differences have been seen between cells around the periphery of the lobule and cells near the center. One difference is the size of their mitochondria, structures concerned with the conversion of foodstuffs into energy and involved in many biosynthetic processes. Mitochondria in cells near the center of the lobule are considerably smaller than those seen at the periphery. At Argonne National Laboratory, mitochondria isolated from rat liver have been distributed according to size in a linear sucrose gradient by zonal centrifugation. The activity of 12 enzymes has been measured.

With the aid of mathematical techniques developed at Argonne, a consistent and significant displacement of the midpoints of the distribution of many enzyme activities (from each other and from the total protein) was found. These results suggest a relationship between the size of the mitochondrion and its enzyme complement. If the profile of enzyme activity in relation to the size of mitochondria reflects the profile of mitochondrial sizes across the lobule, these differences in enzyme complement indicate differences in the metabolic role of peripheral and central cells. Since some association of enzymes catalyzing sequential reactions was apparent, metabolic specializations in different regions of the lobule may be recognized by this technique.

The heterogeneous distribution of enzymes seen in this study raises the question of whether one or two populations of mitochondria are present in the liver. A computer analysis of the data gave the best fit for single, normally distributed populations of mitochondria. Their individual structural diameters may, therefore, be only coincidentally related to their location within the lobule. Their array of enzymes may be controlled by changes in the composition of the blood as it flows from the peripheral region to the central zone.

Other evidence, however, has indicated the presence of two populations of mitochondria, one composed of small, round particles, the other consisting of larger, oblong bodies. Each population has a size distribution that greatly overlaps the other and, from the present study, each could have a unique enzyme complement. While no direct evidence was obtained to support either hypothesis, assumption of the latter possibility has permitted interesting speculation concerning the internal organization of mitochondria in rat liver.

NUCLEIC ACIDS AND PROTEINS

Research on nucleic acids and proteins includes studies on the structure, function and physiocochemical properties of these marcromolecules and on the basic mechanisms of their biosynthesis and degradation.

"Helical Wheel" Models of Structure

Proteins are large complex molecules constructed of some 20 different amino acids. The structure and function of these molecules are determined in part by the linear arrangement (the sequence) of the constituent amino acids. The behavior of a protein molecule depends on its three-dimensional structure which is not under direct genetic control, but depends upon the amino acid sequence. This characteristic of proteins suggests that it may be possible to predict the three-dimensional structures from the sequences. Work at Argonne National Laboratory is leading to the development of "helical wheel" models of proteins to aid in predictions.

For proteins that can be crystallized, the three-dimensional structure can be directly ob-

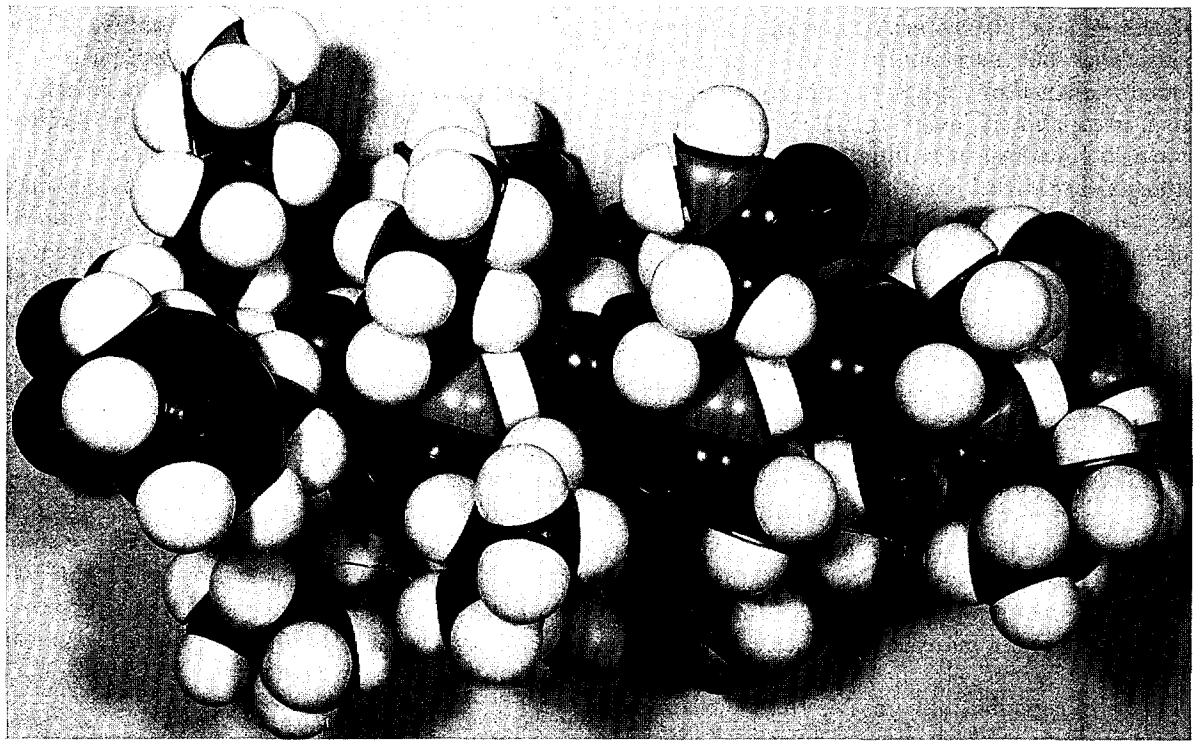

Figs. III–47, 48, and 49. "Helical Wheel" Models of Structure. Using the amino acid characteristics of proteins as a basis, Argonne National Laboratory is developing three-dimensional models of the molecules. Photo *above* is of a three-dimensional model of one of the alpha-helices of the protein *Myoglobin*. The models of the individual atoms are the so-called space-filling type. At *left below* is an end-on view of the model. Drawing, *below right* shows use of a two-dimensional model called a helical wheel to represent the three-dimensional model.

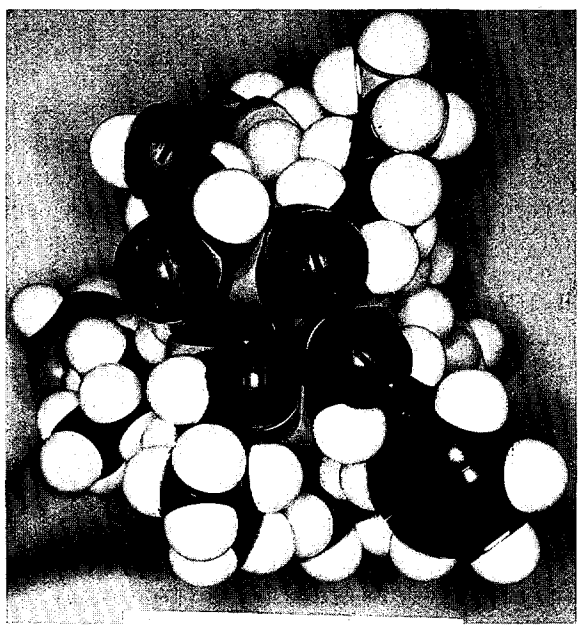

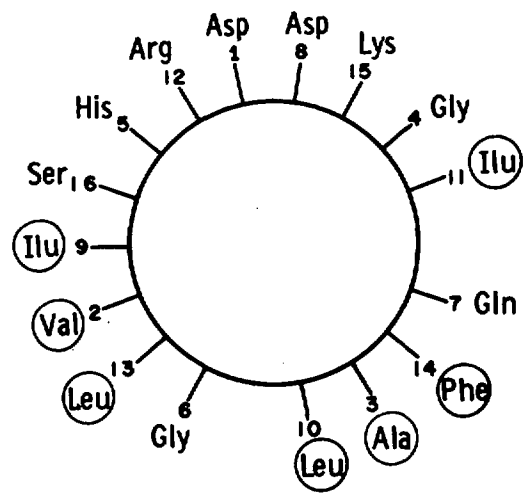

tained by X-ray and neutron diffraction. However, for non-crystallizable proteins, such as the *Bence-Jones* proteins from multiple myeloma patients, a new approach is needed. Since the sequence of amino acids can be readily obtained, a study is underway at Argonne aimed at predicting the three-dimensional structure of a protein from its amino acid sequence.

Many proteins are commonly coiled (at least in part) in the form known as an alpha helix. A three-dimensional model of an alpha helix in the muscle protein myoglobin is shown in Figure III–47. If the model is viewed "end-on," then the circular two-dimensional model looks like that shown in Figure III–48. The end-on view of the helical backbone (the polypeptide chain) can be represented as a circle, and the side-chains emerging from the backbone as external spokes. To simplify the model further, the groups of atoms making up the side-chains of the different amino acids are represented by three-letter abbreviations (Leu for leucine; Ala for alanine, and so forth). These models are called "helical wheels." In Figure III–49, the sequence corresponding to the same helix as that shown in the other two figures is plotted on a wheel.

The wheels can be used to represent structures of proteins and to separate sequences of proteins into two groups: (*a*) those likely to be helical in structure, and (*b*) those not likely to be helical in structure. This procedure markedly reduces the number of structural shapes that a protein can have. The number can be further reduced by using chemical and X-ray information. The next goal is to identify the amount of information necessary to predict a single and unambiguous three-dimensional structure for a given protein.

Purified Viruses for Vaccines

A technique has been developed at Oak Ridge National Laboratory in which newly developed zonal ultra-centrifuge rotors are used to obtain large amounts of purified viruses for use in the preparation of new vaccines. It has been possible to separate the virus easily from virtually all of the extraneous material that has been responsible for major side effects of "flu" vaccines, for example.

The zonal ultracentrifuge, under development at the laboratory since the early 1960's, separates particles of different sizes and densities by rotating them at extremely high speeds. Virus particles are separated by passing a virus-containing solution onto the surface of a density gradient in a high gravitational field. The virus particles settle into the gradient, and the virus-free solution passes out of the rotor. A purified virus is then recovered as a zone from the gradient solution.

Several common cold viruses, such as respiratory syncytial, ECHO 28, and adenovirus, as well as influenza virus, *Rauscher* and *Moloney* leukemia viruses, herpes simplex, and bacteriophages have been obtained in a highly purified state by this method. This work is jointly sponsored by the AEC and the National Institutes of Health.

PHOTOBIOLOGY

The AEC's research in photosynthesis is oriented toward understanding the details of the energy conversion process, beginning with the initial absorption by a living cell of a photon of radiant energy and ending with the formation of "energy-rich" metabolites. The process of photo-synthesis in plants is one of the most important of all biological phenomena; it provides the only known biological mechanism for the fixation of electromagnetic energy present in the visible light region of solar radiation and, as such, serves as the ultimate energy source for all living things.

"Isolated" Photosynthesis

It has long been recognized that research into photosynthesis could help advance agricul-

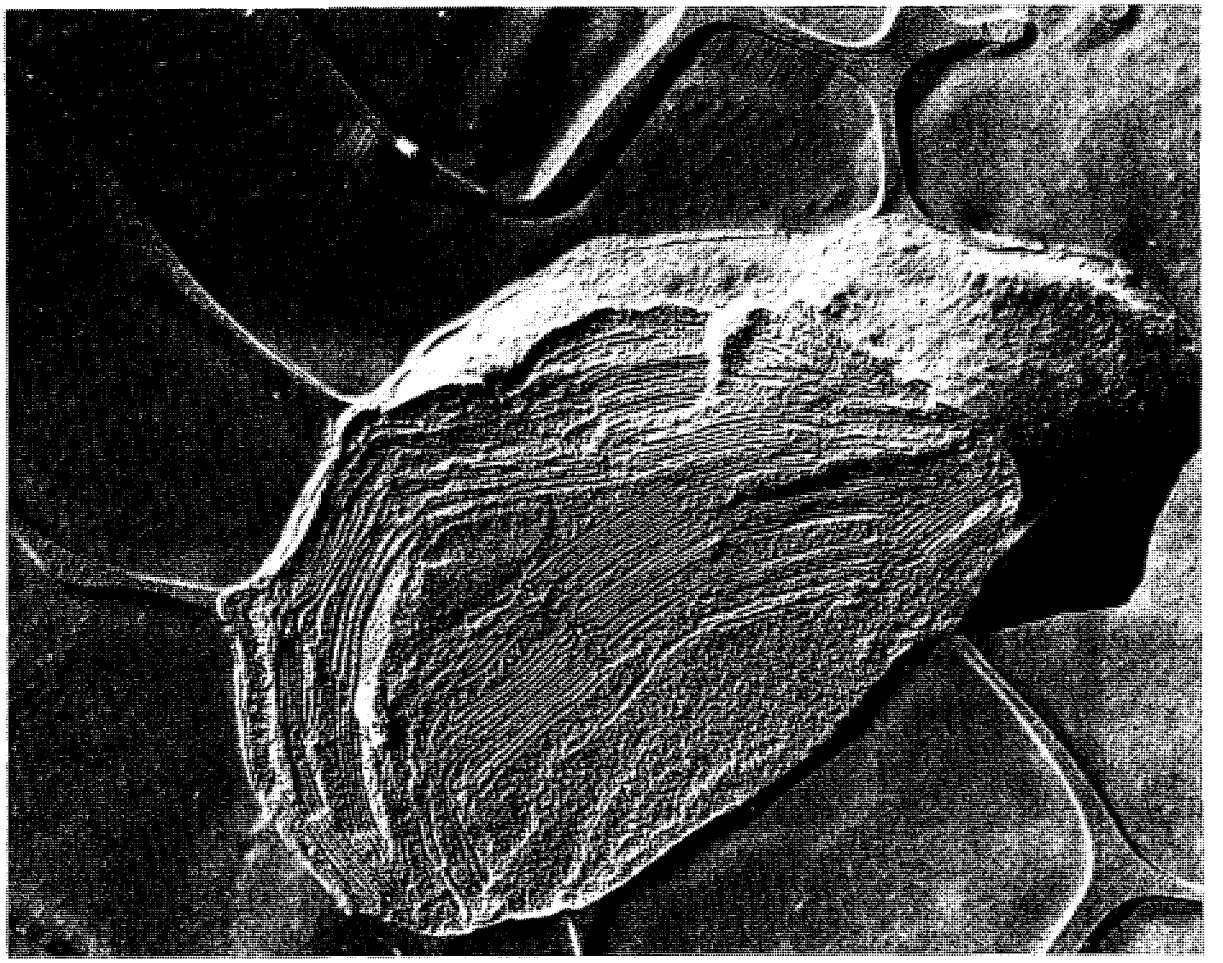

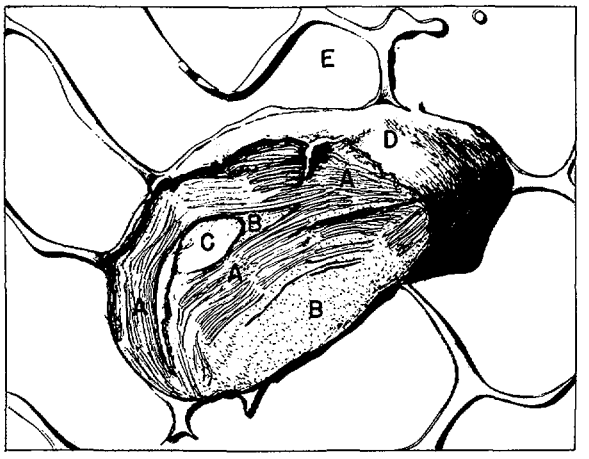

Figs. III–50 and 51. "Isolated" Chloroplast. Spinach chloroplasts have been isolated by methods which give good rates of photosynthesis at the Lawrence Radiation Laboratory, Berkeley. A suspension of these chloroplasts was quick-frozen, and the frozen block was cleaved with a very fine knife (microtome) to give a rough surface. In a vacuum, some ice was allowed to evaporate from this surface, which was then coated by a condensation of a vapor of carbon and platinum to give a mask. The mask was then photographed with an electron microscope as shown *above*. The chloroplast is approximately 2.5 by 5 microns, or 0.1 by 0.2 mills. The quick-freezing of the suspending solution produced the pattern seen outside the chloroplast. The diagram, *left*, shows the chloroplast structure; *A* is the lamellae—layers of lipid and protein with chlorophyll, other pigments, and enzymes and the site of light absorption and splitting of water to give oxygen and hydrogen. *B*, the stroma—soluble enzymes and site of conversion of carbon dioxide and hydrogen to sugars and other products. *C*, starch granule—one of the storage products of photosynthesis. *D*, is the surface of chloroplast—the double membrane split off reveals the surface of the inner membrane. *E*, the frozen solution in which chloroplast was suspended.

ture. A chemical biodynamics group at Lawrence Radiation Laboratory, Berkeley, succeeded in making chloroplasts—which had been isolated from spinach leaves—perform photosynthesis at high rates. This makes possible the study of photosynthesis without interference from other chemical processes that occur in biochemistry of the living cell. The experiment was the first in which photosynthesis—the process in which green plants manufacture the earth's energy foods—has ever been conducted at high rates and in complete form outside the cells of green plants (see Figs. III–50 and 51). Future refinements of knowledge of photosynthetic mechanisms may ultimately make it possible to control the plant process in such a way as to raise the protein and fat content of conventional agricultural crops or to produce food crops in leaf plants not now cultivated.

Chloroplasts are membrane-enclosed subcellular particles which contain all the green pigment, chlorophyll, together with other pigments and enzymes required for photosynthesis in a highly organized system. This system absorbs solar energy and uses it to transfer hydrogen atoms from water to carbon dioxide. Thus, plants liberate oxygen and at the same time convert carbon dioxide to organic compounds such as food and fiber. The basic process of photosynthesis includes all the steps from the absorption of light to the formation of simple sugar phosphates by a cyclic sequence of reactions—the carbon cycle.

Until recently, the basic process could be performed by isolated chloroplasts at only a few percent of the rate found with intact cells. It is now possible to carry out such photosynthesis, at two-thirds the rate found in healthy intact leaves and to maintain this rate for about 15 minutes. This is long enough to permit study of the reactions of photosynthesis and their control by light and by added natural and synthetic chemicals.

Experiments with isolated chloroplasts and with radioisotopes have already given evidence for the location of two regulation points along the basic carbon cycle pathway. Enzymes at these points control the flow of carbon in the presence and absence of light and probably during growth and development of green leaves.

It appears that plants may regulate enzymic activity at one control point to adjust the amount of photosynthetic carbon used for carbohydrate synthesis (sugar, starch, etc.) as compared with the amount used for the synthesis of fats and proteins. Application of suitable chemicals alters control point activity. Thus, it may become possible to affect quantitatively the products of photosynthesis in green leaves.

275–845 O—68——20

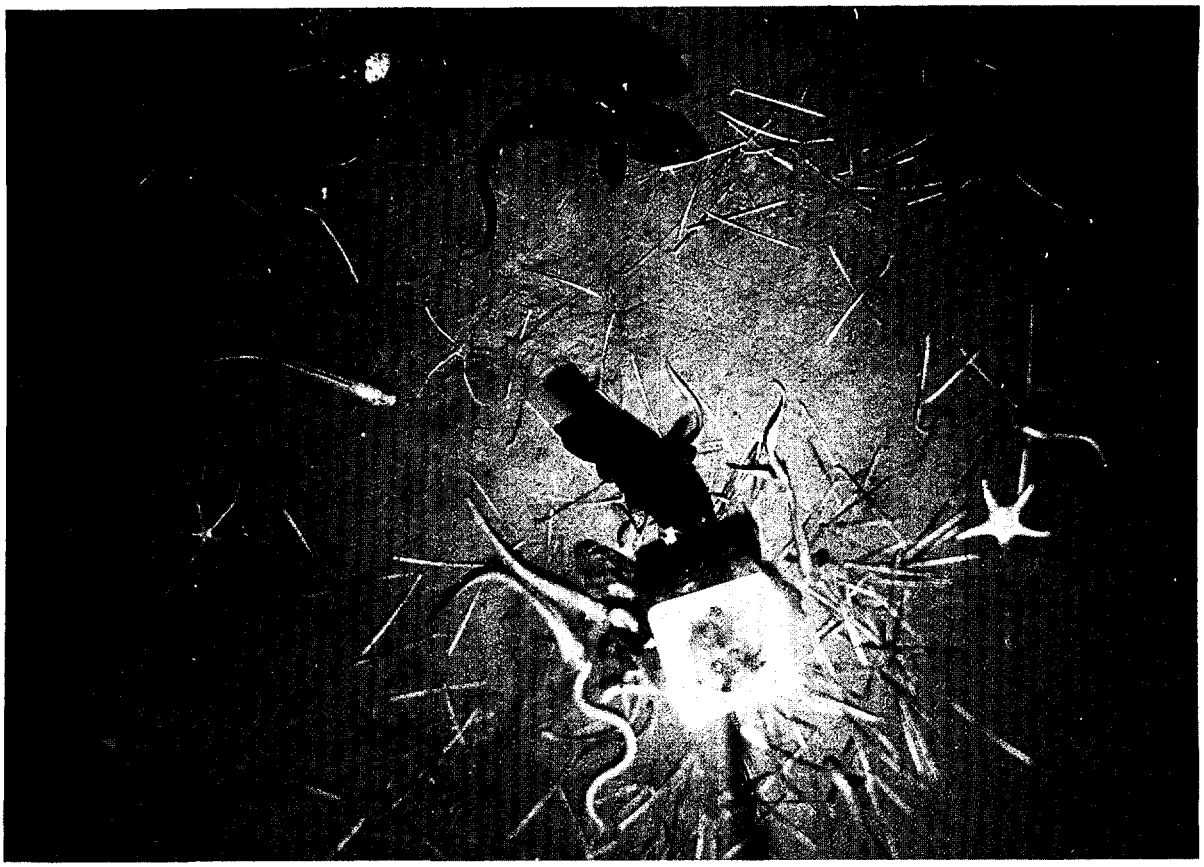

Fig. III–52. Deep-Sea Life. The AEC's environmental research program includes oceanographic studies associated with the fate and effect of radioactivity in the sea. The work provides much new "spin-off information of interest. For instance, through the use of a "Monster camera" developed by the Scripps Institutions of Oceanography (La Jolla, Calif.) of the University of California, pictures have revealed fish populations at least 10 times greater than were ever thought to exist in deep water. In this photo, taken at a depth of 1,098 fathoms (6,588 feet), a variety of fish are seen (Grenadier, Eel Pout, Hag fish, tube worms, starfish, and crabs). The bait can (at *bottom*) is 9.5 inches wide and 12.5 inches on the top diagonal. A companion photo to this shot, showed a 30-foot-long "sea creature" with eyes as big as dinner plates. It has been tentatively identified as a Greenland or Sleeper Shark, a type never before known in southern California waters.

ENVIRONMENTAL RADIATION STUDIES

The ultimate objective of environmental radiation studies is to be able to predict under any given set of circumstances the fate and effect of radionuclides in the environment. The number of environmental factor combinations and the huge number and kinds of organisms found within these diverse environments almost staggers the imagination. Fortunately, when radionuclides move through the environment, they leave "tracks," thus providing a means to trace the movement.

TERRESTRIAL ECOLOGY

By tagging components of a particular ecological system (ecosystem), it may be possible to unravel the movements of animal or insect pests, determine pesticide distribution, estimate the efficiency by which particular foods are used by wild or domesticated animals, locate sites of

Fig. III–53. Cycling of Radioactive DDT in Marsh. An Ohio State University field technician is shown collecting samples of plants and animals from a marsh treated with chlorine-36 labeled DDT. A punt boat was used to prevent disturbing the bottom of the marsh by wading. Over 6,000 samples of plants and animals were taken from the marsh to determine the distribution and translocation of the radioactively labeled DDT.

water or nutrient concentration, and many other ecological phenomena. The following AEC-sponsored studies indicate the usefulness of such isotope techniques.

Cycling of Radioactive DDT in a Marsh

Contamination of the environment by persistent chlorinated pesticides is essentially universal. Residues have been found in organisms taken from the Arctic to the Antarctic. The translocation and accumulation of DDT (dichlorodiphenyltrichloroethane) in a freshwater marsh has been studied at Ohio State University using the isotope chlorine-36 as a tracer (see Fig. III–53). A normal mosquito control application at the rate of 0.2 lb. of DDT per acre was laid down on a 4-acre marsh by helicopter in July 1964. More than 6,000 samples of water, soil, plants, and animals have since been radioassayed. Results of the assays indicate DDT is rapidly translocated throughout the marsh ecosystem and is rapidly accumulated by many organisms. For example, concentrations of DDT more than 3,000 times the amount applied were found in an aquatic plant 3 days after application. However, maximum accumulations in the predators, which feed on other animals and are in the higher levels of the food web, may not occur until a year or more later. In general, a steady state of accumulation and excretion occurred for most animals after about 2 months. Great variability in the levels observed in the same species strongly suggests that large numbers of samples are necessary to properly determine the accumulation of pesticides in natural systems. The use of isotopes to study pesticide translocation permits the analysis of

a large number of biological samples at comparatively low cost—approximately 1/5 of that for regular chemical procedures.

Ecology of Tick Vectors of Disease

It is recognized that small mammal populations serve as reservoirs for a number of diseases which plague mankind. It is equally well known that ticks are important vectors or transmitters of these diseases. However, little is known about the efficiency and conditions under which these diseases are transferred from wildlife to man. Much needs to be learned before reasonably accurate disease outbreak predictions can be made. Unfortunately, the feasibility of needed studies, particularly tick movement and population size, has been thwarted by lack of suitable techniques. During 1966, a study was undertaken by Old Dominion College, Norfolk, Va., to determine the feasibility of using radioisotopes as ecological tracers to investigate tick populations. The results of this study indicate that large numbers of tagged ticks can be raised with a very modest expenditure, that the ticks behave similarly to nontreated ones, that individual ticks are readily detectable, released ticks can be recaptured in large numbers on wild mammals, and that natural tick populations can be readily estimated. Carbon-14 seems best for this work. Other radioisotopes that have been tried include chromium-144, cesium-137, phosphorus-32, strontium-90, and tritium. Application of this promising radioisotope technique represents an important advance in the ability to investigate tick-borne diseases.

Estimation of Energy Requirements

At the AEC's Laboratory of Nuclear Medicine and Radiation Biology on the University of California at Los Angeles (UCLA) campus, investigations are being made on a method for evaluating the metabolic rate, and, consequently, the energy requirements of animals living in the Nevada desert. This will enable the UCLA ecologists to determine if production of animal food by desert plants is ample to support the population of small animals living there, or if these animals have a thin margin of safety between existence and starvation.

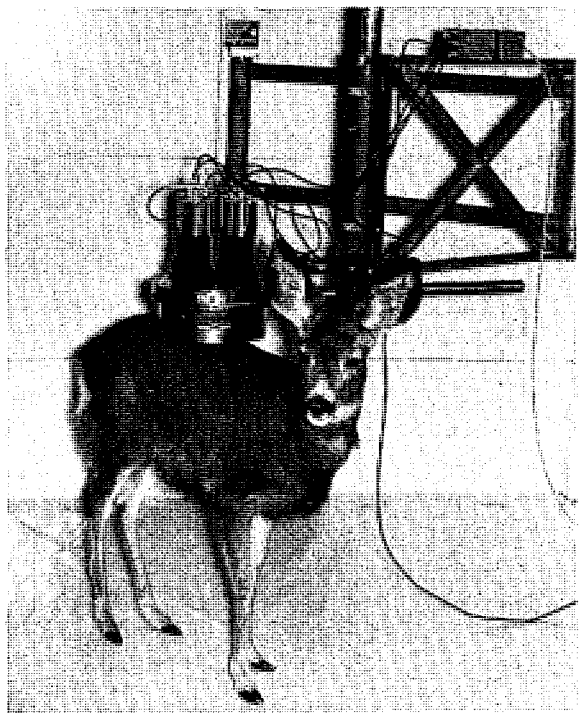

Fig. III–54. Concentration of Radionuclides Study. As a part of its studies on the translocation of airborne radioactivity through the plant-food chain cycle, the AEC sponsors continuing studies on the concentration of radionuclides in wild-life. Photo shows how minute quantities of fallout radioactivity are measured routinely in live deer using a whole-body counter at Colorado State University. Before being returned to their natural habitat, the radioactive body burdens of the deer are recorded and they are tagged for future identification.

The method uses the isotopes deuterium and oxygen-18. The body water of animals is enriched with these isotopes and they are then released to live their normal lives for a time. Later, the animals are recaptured and a tiny sample of blood is taken. The ratio of the two isotopes in the blood sample, when compared to the original concentrations, indicates the amount of carbon dioxide produced by metabolic processes. This can be converted to terms of energy. It is anticipated that the method will be useful

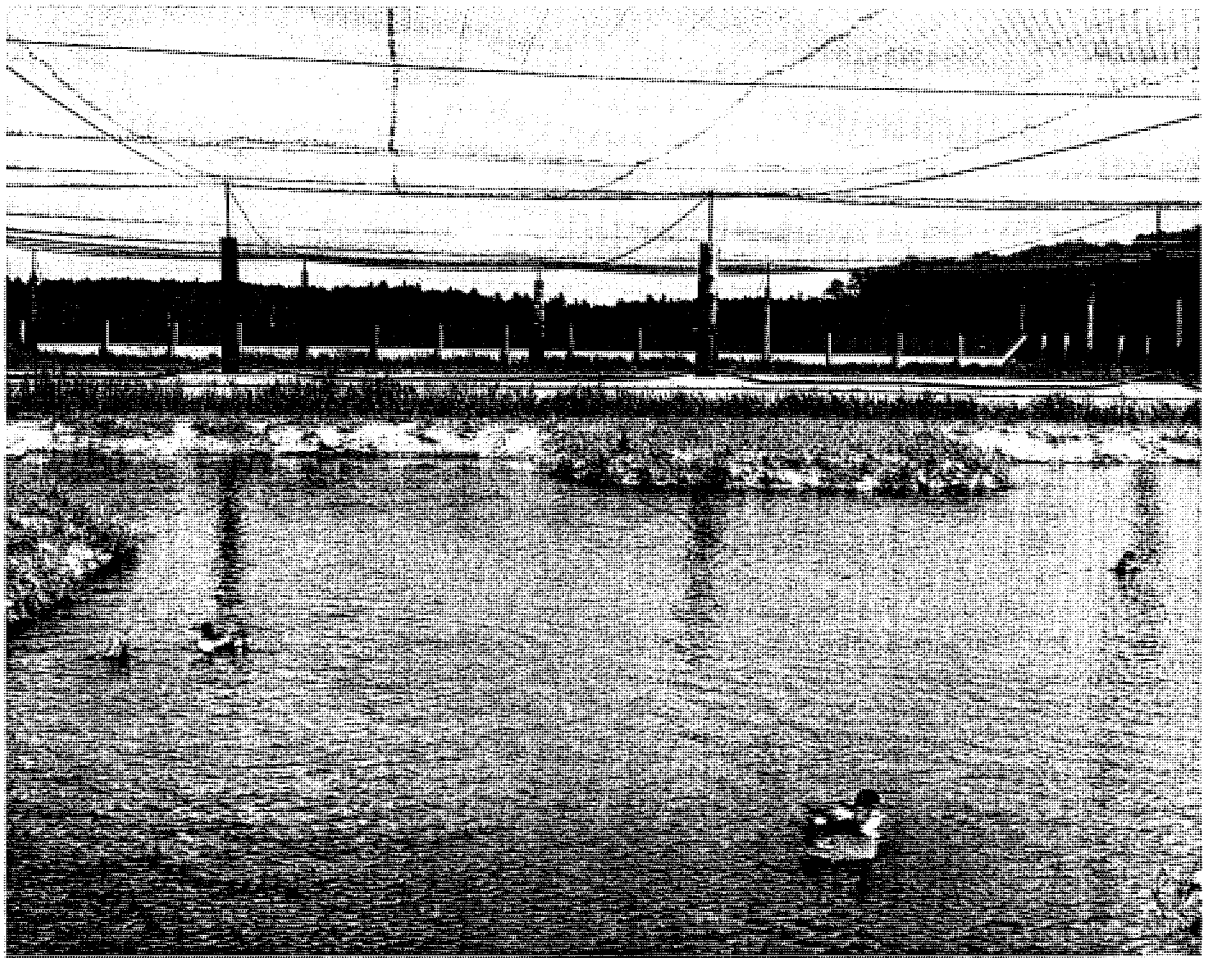

Fig. III–55. Behavior Study. Photo shows the large flight-pens used at the University of Minnesota to investigate effects of radiation on the aggressive behavior of breeding pairs of Shoveler ducks. Two pens, each measuring 90 ft. × 90 ft., provide breeding requirements for eight pairs. Data on hostile encounters are collected by observing from an elevated blind. Changes in territorial behavior resulting from irradiation can be measured accurately under these controlled conditions.

in evaluating slight amounts of radiation damage in animals and in estimating the population "carrying capacity" of this or other landscape regions.

Chromium-51 in Energy Flow Studies

Studies to determine the usefulness of radioactive chromium-51 in energy flow are being carried on at Michigan State University. A fast and convenient technique for obtaining pertinent digestive data is being developed using the ring-necked pheasants and white-tailed deer as experimental species.

It has been shown that chromium-51 is not metabolized in the body, and detection of the isotope in the feces of the animal enables determination of the rate of passage of labeled food. In addition, the ratio between the concentration of isotope in the food and its concentration in the feces permits evaluation of the proportion of the food which is absorbed during digestion. This information is essential to the study of animal energy metabolism. Neither the value of

chromium-51 for this type of work nor the energetics of the above species has been adequately investigated previously.

On a standard commercial diet, the average ring-necked pheasant tested passed the fecal residues of a meal beginning 1.5 hours and extending for 9 hours after eating. Different metabolizable energy values and passage rates occurred with different diets and when birds were molting.

In the white-tailed deer, approximately 60 percent of a standard sheep food diet was passed as feces. The first and last appearance of chromium-51 in the deer feces for this diet occurred at 10 and 36 hours, respectively. The variation in results which occurred among single individuals as well as that prevailing between animals of the same age and sex is being analyzed.

The chromium-51 technique has been found to have considerable research value. The suitability of the method for comparisons of the energy conversion capabilities of related species is next to be explored. Further studies also need to be made of the energy values of various feedstuffs and of procedures for relating the data of captive animals to those of animals living in the wild.

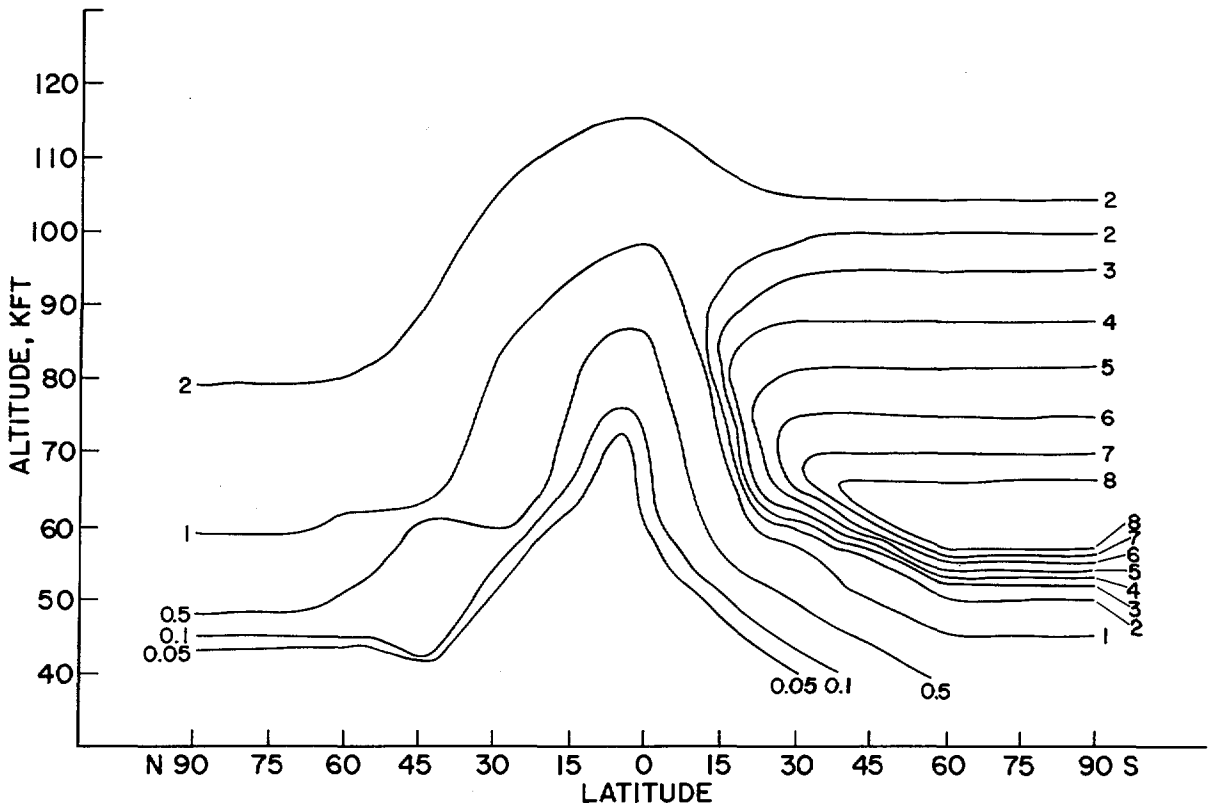

Fig. III–56. Plutonium-238 from SNAP–9A Burnup. Profiles of plutonium-238 activity in the stratosphere are based upon air sampling from aircraft and balloons and the above chart shows stratospheric distribution of plutonium-238, January through March 1966. Aircraft samples were collected along north-south pathways over the Western Hemisphere, and balloon samples were collected over Alaska, Texas, Panama, and Australia. Only very small amounts of plutonium-238 had reached the earth's surface by March 1966. The chart shows altitude in thousands of feet (KFT) and the concentration levels are based on plutonium-238 disintegrations per minute per thousand standard cubic feet (Pu^{238} dpm/KSCF). Summation of the radioactivity by the AEC's Health and Safety Laboratory, New York City, indicated a total of 15 kilocuries of plutonium-238 to be present in the atmosphere, accounting for essentially all of the 17 kilocuries, which had been placed in the SNAP–9A satellite generator. See page 290 for details.

ATMOSPHERIC RADIOACTIVITY AND FALLOUT

The AEC's research program in atmospheric radioactivity and fallout is concerned with the atmospheric transport and deposition of airborne radioactive debris, the nature and behavior of aerosols in the atmosphere, and sampling and analytic procedures applicable to the study of radioactivity in air, precipitation, soil, foods, and man for the purpose of predicting, as accurately as possible, the consequences of introducing radioactivity into the earth's atmosphere or biosphere. (See also "Atmospheric Sciences" section, page 297.)

ATMOSPHERIC DEPOSITION

In general, the amounts of radioactivity from nuclear weapons tests have continued to diminish in air, precipitation, soil, food, and man.

Debris, probably from the Red Chinese tests conducted at Lop Nor in the far northwestern

part of China (Lat. 40° N., Long. 90° E.), has remained largely within the Northern Hemisphere, whereas, debris from the French tests conducted at Mururoa Atoll in the South Pacific (Lat. 22° S., Long. 139° N.) has been similarly restricted to the Southern Hemisphere. The total amounts of strontium-90 and cesium-137 on the ground have begun to decrease as the loss through radioactive decay exceeds the new deposition of these radionuclides. The concentration of strontium-90 in adult human bone and that of carbon-14 in contemporary biological samples is still increasing slightly, because of the respective long biological retention time and atmospheric mixing time of these two radionuclides.

Current investigations continue to focus upon specific radionuclides which are of interest either because of their long half-lives and their biological significance (strontium-90, cesium-137, and iron-55) or because their unique manner of injection into the atmosphere (plutonium-238 from the SNAP-9A burnup) may add significantly to the knowledge of atmospheric processes.

Plutonium-238 from SNAP-9A Burnup

Approximately 17 kilocuries of plutonium-238 (Pu^{238}) were released into the upper stratosphere of the Southern Hemisphere in April 1964 when a SNAP-9A generator reentered the atmosphere following a rocket failure of a navigational satellite. The reentry was at about 11° S., over the Indian Ocean. SNAP-9A Pu^{238} has been collected by the AEC's High Altitude Balloon Sampling Program and the Defense Atomic Support Agency's aircraft sampling program (Project Stardust) at all altitudes in the stratosphere. As shown by the global distribution in Figure III–56 for the period January to March 1966, SNAP-9A debris has mixed poleward and downward, as predicted, with a minimum of material descending into the equatorial stratosphere.

Seasonal trends of stratospheric SNAP-9A Pu^{238} concentrations occur in the mid- and polar-regions of the stratosphere which suggest that above 80,000 feet, a downward flux of debris from upper altitudes occurs during the winter and spring followed by an apparent upward flux in the summer and fall. A cell of high concentration occurs in the 65,000- to 90,000-foot layer which apparently reflects an equator-ward mixing of debris from the polar regions at these altitudes. The pattern in the equatorial stratosphere was markedly different with little penetration of debris to the lower altitudes. Collections at Natal, Brazil (6° S.), up to 136,000 feet, which is close to the point of burnup, also revealed minimal plutonium-238 concentrations characteristic of the equatorial stratosphere. These findings are in good agreement with many aspects of existing stratospheric meridional circulation models.

Stratospheric inventory. The stratospheric inventory of plutonium-238 for the period January to March 1966 shown in Figure III–56 was derived from balloon and aircraft sampling measurements by the AEC's Health and Safety Laboratory (HASL), New York City. No SNAP-9A debris had been identified in the troposphere prior to this time, and only minute traces were found in surface air and deposition samples during this inventory period. Therefore, the integrity of the stratospheric reservoir of SNAP-9A plutonium-238 was essentially intact at this time, and no adjustment for deposition was required.

Upon integrating the contours in Figure III–57, 12 kilocuries (or 80%) of the SNAP-9A Pu^{238} was found in the southern Hemisphere stratosphere and three kilocuries (or 20%) in the Northern Hemisphere stratosphere. Therefore, during the 2-year interval after the burnup, the average rate of transfer from the Southern to the Northern Hemisphere was about 10 percent per year. Most of this transfer is believed to have occurred during the winter months of the Northern Hemisphere.

The total stratospheric inventory of 15 kilocuries accounts—within experimental uncertainties—for essentially all of the 17 kilocuries in the original source. While there has been strong speculative evidence earlier, this is the

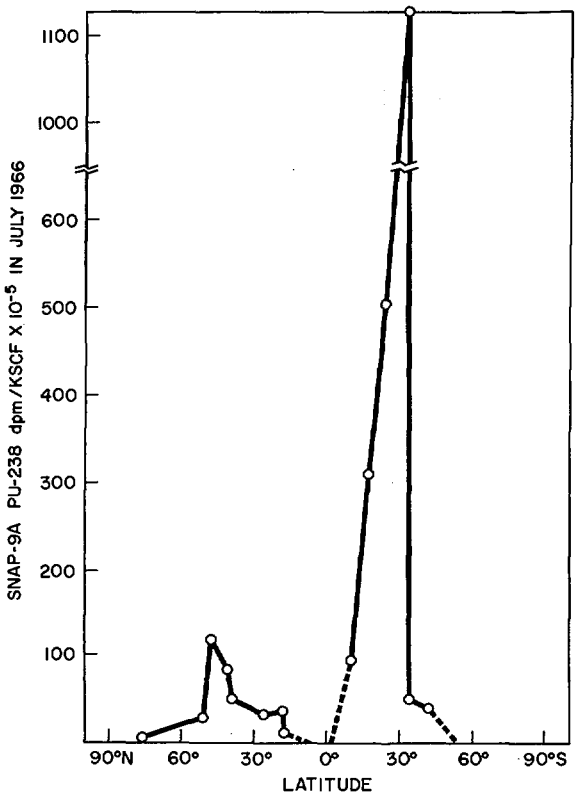

Fig. III–57. Stratospheric Inventory. Chart, produced by the AEC's Health and Safety Laboratory, shows the concentration of plutonium-238 in surface air as a function of latitude. Plutonium-238 was released at high altitude by the burnup of the navigational satellite SNAP–9A in April 1964. Two years elapsed before measurable amounts of plutonium-238 reached the earth's surface. Burnup slightly south of the equator accounts for the higher concentrations observed in Southern Hemisphere. These levels are well below those deemed safe for human exposure.

first direct accountability calculation which shows that the SNAP–9A generator completely vaporized into submicroscopic particles during reentry.

Particle size. The actual size of the particles from the vaporized SNAP–9A generator has been investigated by Tracerlab, Richland, Calif., using an autoradiographic technique by which particples containing plutonium-238 are identified, assayed, and the equivalent size of Pu^{238} dioxide spheres is calculated. Figure III–58 shows the calculated distribution of Pu^{238}

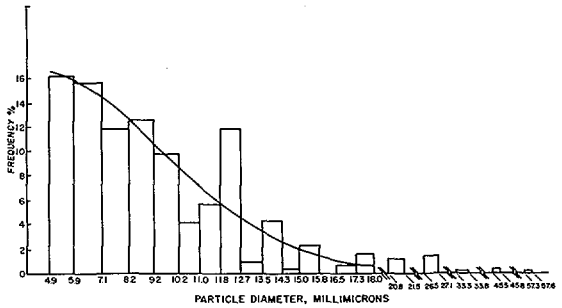

Fig. III–58. Particle Diameters in SNAP–9A Debris. The actual size of the submicroscopic particles of debris from the burnup of the SNAP–9A generator have been determined by Tracerlab-West, Richmond, Calif., using radioautography. Sensitive photographic emulsion was placed in close contact with filter material known to contain plutonium-238 bearing particles. The film was exposed for one year, and the number of alpha-tracks per particle was used to calculate an equivalent sphere of plutonium-238 oxide which would yield the same number of tracks during one year. The diameters range from 5 to 58 millimicrons (too small to be seen with the optical microscope) with an arithmetic mean of 9.7 millimicrons, indicating that burnup during reentry was quite complete.

spheres derived from a 1 year emulsion exposure of a filter sample known to contain SNAP–9A debris. The histogram represents the actual data, and the smoothed curve was obtained by graphical differentiation. A total of 1,008 particles was plotted; the diameters range from five to 58 millimicrons (10^{-3} microns) with the arithmetic mean at 9.7 millimicrons. These particle-size determinations confirmed the fact, derived earlier from the behavior of Pu^{238} concentrations with time, that the vaporized particles were submicroscopic and were not significantly influenced by gravity.

Surface air concentrations. While minute traces of SNAP–9A plutonium-238 was detected sporadically in surface air in March and April 1966, concentrations became more ubiguitous beginning in May 1966. By July, a monthly average latitudinal distribution of these concentrations was developed, by the HASL's Surface Air Sampling Program, which showed peak concentrations occurring in the mid-latitudes of each hemisphere similar to

the patterns produced by nuclear weapons tests fallout.

A significant difference from the strontium-90 (Sr^{90}) distribution is the 10 times higher concentrations of SNAP–9A plutonium-238 in the Southern Hemisphere as compared to the Northern Hemisphere. The season of the year bears upon the rate of transfer of stratospheric air to the troposphere, July is summer in the Northern Hemisphere, but winter in the Southern Hemisphere. This discrepancy in SNAP–9A plutonium-238 concentrations in the surface air of each hemisphere reflects the much larger burden of SNAP–9A debris in the Southern Hemisphere stratosphere.

The SNAP–9A plutonium-238 concentration in surface air in July 1966 reached a maximum average value of 0.011 dpm/10^3 SCF [22] at Portillo, Chile. This value should have increased by about three or four times in the spring months of that year (October, November, and December 1966). The maximum expected concentration in surface air is still only two ten-thousandths of the permissible concentration of the International Commission on Radiological Protection (ICRP) maximum for continuous exposure of industrial workers to soluble plutonium-238 aerosols and indicates an extremely low risk of hazard.

Deposition. Fallout of SNAP–9A plutonium-238 on the earth's surface was anticipated to be so small that special large-area collection systems had to be deployed. Only two sites were activated, one at New York City in the Northern Hemisphere and the other at Melbourne, Australia, in the Southern Hemisphere. The results for the first 11 months of 1966 from these two locations are shown in Table 2.

At New York, a pulse of SNAP–9A debris seems to have arrived in February 1966 but consistent and significant deposition did not begin until May. At Melbourne, sampling apparently was not begun soon enough because measurable levels of SNAP–9A plutonium-238 were detected in May 1966, the first sampling

TABLE 2.—PLUTONIUM-238 FALLOUT LEVELS

[10^{-4} millicuries per square kilometer]

Month	*New York*	*Melbourne*
January	0.20	----------
February	2.06	----------
March	0.59	----------
April	0.44	----------
May	4.41	0.43
June	0.98	3.0
July	2.25	[a] 8.23
August	1.96	3.9
September	1.62	4.76
October	1.18	26.9
November	--------	9.91
Total	15.69	57.13
Estimated hemispheric deposit.	Northern--0.19 (kilocuries)	
	Southern--1.02 (kilocuries)	

[a] Estimated.

period. Using the empirically derived relationship that for every millicurie deposited per square kilometer at New York City, 0.123 megacuries of deposition occurs in the Northern Hemisphere, the deposition of SNAP–9A plutonium-238 in the Northern Hemisphere through October 1966 was 0.19 kilocuries. Using an analogous ratio of 0.180 megacuries Southern Hemispheric deposition for every millicurie deposited per square kilometer at Melbourne, the deposition from May through November 1966 in the Southern Hemisphere was 1.02 kilocuries. Consequently, the global deposit of SNAP–9A plutonium-238 during 1966 was between 1.3 to 1.6 kilocuries, or about 8 to 10 percent of the total plutonium-238 released by the burnup.

Strontium-90 Deposition

A cooperative land and sea fallout sampling program has shown that strontium-90 deposition from the atmosphere is actually heavier over land than over the oceans, making previous theories untenable. The studies have also given new information that shows rainfall to be less over the sea than over adjacent land.

Action of sea-spray. To test the hypothesis that sea-spray may lead to higher fallout deposition over or near the ocean, the U.S. Department of Agriculture took soil samples on a transect running inland from the soil-beach

[22] dpm/10^3 SCF—disintegrations per minute per 1,000 standard cubic feet.

boundary at a small island site (Utsira, 59° N.) off the Norwegian coast. Another transect sampling was made in Iceland. In all instances, there was no indication of higher strontium-90 deposition in proximity to the ocean, nor were the strontium-90 levels on the islands higher than those observed at mainland sites experiencing comparable precipitation and situated at the same latitude. Thus, the supposition that seaspray, as such, leads to higher deposition of strontium-90 seems untenable.

Rainfall over the ocean. Four of the U.S. Coast Guard vessels serving as Atlantic Ocean Weather Observation stations were outfitted by HASL with new and improved equipment for strontium-90 sampling and rain measurement. Operation of these devices for 1 year has shown lower deposition of strontium-90 over the ocean compared to land sites at comparable latitudes, and furthermore, has indicated oceanic rainfall to be less than on adjacent land areas. Fallout in the oceans, by the mechanisms which cause deposition on land, has, therefore, probably been overestimated, and additional factors must be considered to account for the discrepancy between fallout rate as derived from the atmospheric inventory and the measured deposition. Such factors may include enhanced dry deposition due to terrain roughness and vegetation, as well as regional variations in the frequency and character of precipitation events.

High Altitude Sampling

Routine sampling by balloon has, since 1966, been conducted to a maximum altitude of 135,000 feet at all sampling sites. Sampling is carried out periodically at four locations: Fairbanks, Alaska, 65° N. (June); San Angelo, Tex., 31° N. (quarterly); Albrook Air Force Base, Canal Zone, 9° N. (December-April, and (September-October) and Mildura, Australia, 34° S. (quarterly). Sampling altitudes are 80,000, 90,000, 105,000, 120,000, and 135,000 feet. The Mildura station is operated by the Australian Department of Supply; the other sites are manned by the U.S. Air Force.

Five ALARR (Air Launch and Air Recovery Rocket)[23] sampling flights have been made. An option in sampling altitudes allows selection of one of three essentially equal altitude increments between 150,000 and 250,000 feet or an integral sample taken over this entire range. Sampling is done on the downward leg of the rocket trajectory, and about 10 standard cubic feet of air are sampled during each flight. This system has been designed and developed by the AEC and the Department of Defense and marks a significant increase in altitude range over that attainable by balloons.

The concentrations of weapon-produced radionuclides in the stratosphere have steadily decreased since 1962. Two innovations in the balloon sampling equipment have been introduced to permit the collection of larger samples, thereby increasing the precision of measurement of dwindling radionuclide concentrations. The first is the development of a much larger capacity sampler (50% higher) without a similar increase in payload weight for the balloon to lift. The second is the utilization of a hydrazine reactor instead of compressed nitrogen gas to generate greater power for the aspirator action of the sampler.

Seasonal trends in the strontium-90 concentrations at, and above 80,000 feet derived from the balloon program since 1963 have demonstrated a downward flux of stratospheric air at mid-latitudes in the winter and spring months followed by an upwelling in the summer and fall. Since strontium-90 concentrations decrease with increasing altitude upwards of 65,000 feet, such motions develop a minimum strontium-90 concentration in the spring followed by a maximum in the summer or fall. Oddly enough, this seasonal trend is just the reverse of that characteristic of fallout in surface air and deposited on the earth's surface. It, however, behaves the same as Pu^{238} which initially had higher concentrations at higher altitudes. The cyclic trend

[23] See p. 92, "Fundamental Nuclear Energy Research—1966."

was broken in the mid-latitudes of the Northern Hemisphere when a peak strontium-90 concentration occurred during the spring of 1966. It was also about this time that the half residence time of strontium-90 concentrations at these altitudes increased sharply indicating an incursion of additional strontium-90 or a drastic reduction in its removal processes.

Fresh debris, apparently from the Chinese nuclear weapon test of June 17, 1967, has been found in two balloon filter samples collected at an altitude of about 135,000 feet over San Angelo in July and August. Debris has also been observed in aircraft samples at altitudes up to 63,000 feet, but could not be found in balloon samples from 80,000 to 120,000 feet. These observations may be the first direct verification of an upper stratospheric circulation, rising over the north polar region in the summer and flowing towards the opposite pole, which was deduced from theoretical heat balance calculations by United Kingdom scientists in 1961. High-altitude sampling is being intensified to follow up the preliminary finding. The high altitude horizontal current is a necessary part of the seasonally oscillating vertical displacements observed in the Sr^{90} and Pu^{238} distributions.

HUMAN BODY UPTAKE

The major source of radiation dose to man from worldwide fallout results from the ingestion of strontium-90 (Sr^{90}) and cesium-137 (Cs^{137}) in foods. To estimate this dose, the concentrations of strontium-90 and cesium-137 in people and in their diets are being measured and attempts are being made to derive relations between fallout rates and dietary contamination levels, between dietary contamination levels and radionuclide concentrations in humans, and between radionuclide concentrations in humans and radiation doses.

Strontium-90 and Cesium-137 in Human Diet

The concentrations of both strontium-90 and cesium-137 have continued to drop in the human diet as the fallout rate has diminished. Because of the rapid turnover rate of cesium-137 in man (biological half-life of approximately 100 days[24]), the body-burden of this radionuclide has also decreased markedly in the past 2 years.

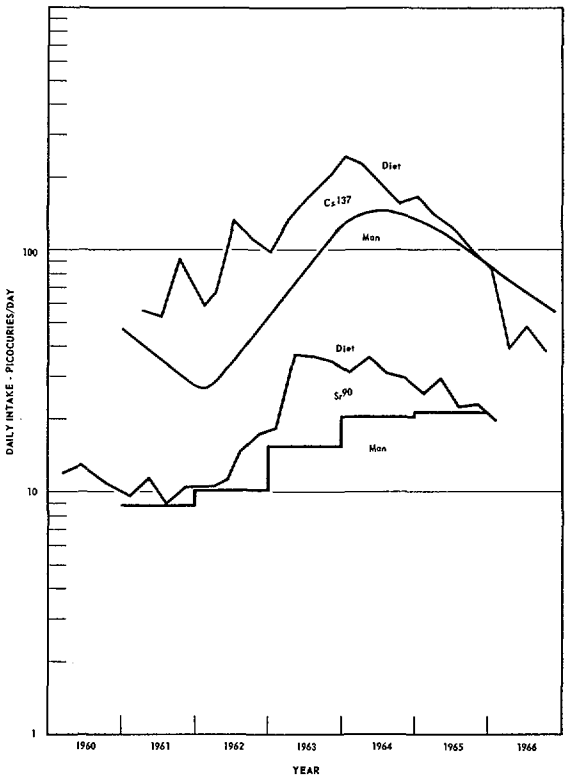

Fig. III–59. Strontium-90 and Cesium-137 in Human Diet. The amounts of strontium-90 (Sr^{90}) in an adult diet and in adult bone for the above chart were determined in New York City; the diet and whole-body measurements of cesium-137 (Cs^{137}) were made in Chicago. Increasing quantities of both radionuclides in food are evident as the fallout levels increased during 1961–1964, followed by decreasing diet levels as fallout lessened. The whole-body content of cesium-137 follows the diet closely because of its short biological retention time; however, the amount of strontium-90 in bone remains fairly constant during the last 2 or 3 years because of the long retention time of strontium-90 in bone. However, it is only a small fraction of the cumulative dose received from natural background. The surveys for data collection were made by the AEC's Health and Safety Laboratory and Argonne National Laboratory.

[24] The biological half-life is the time that is required for one half of the amount of a given radionuclide present in the body to be biologically eliminated, *i.e.*, excreted.

In contrast, the concentration of strontium-90 in human bone has remained essentially constant because of the long retention time of this calcium-like radionuclide in bone (biological half-life of approximately 18 years). Concentrations in bone have decreased only in the very young who reflect the contemporary diet levels of strontium-90, while older children and adults have shown nearly constant levels of bone strontium-90 during the past 2 or 3 years.

The trends of strontium-90 and cesium-137 in diet and man are illustrated in Figure III–59. The strontium-90 data in diet and human bone are for New York City and were obtained from a sampling program conducted by HASL. The cesium-137 data in diet and human adults are for Chicago and derive from programs in progress at Argonne National Laboratory.

Milk remains an important dietary source (about ⅓ of the daily intake) for both strontium-90 and cesium-137, with grain products assuming relatively greater importance with time (also about ⅓ of the daily intake). Meat supplies most of the remaining ⅓ of the cesium-137 intake, and fruits and vegetables combine to provide the remainder of the strontium-90 intake.

Bone Dose From Strontium-90

Calculations have been made at the AEC's Health and Safety Laboratory, New York City, of the radiation dose to bone from strontium-90 received by New York City residents. The results are shown in Table 3. These calculations use the empirically derived quantitative relations between fallout and diet strontium-90 concentrations, and diet and bone concentrations, that are described qualitatively in the preceding sections. Although the data upon which these calculations are based were limited to the New York City area, similarities in fallout and strontium-90 intake levels elsewhere make them applicable to a much larger geographic region.

It can be seen that the maximum radiation dose has been received by children 4 years of age in 1967. This maximum dose is 89 *millirads* (*mrads*). Adults greater than 32 years of age

TABLE 3.—BONE DOSES RECEIVED BY 1967

Age in 1967 (years)	*Dose Received (millirads)*
1	19
2	40
3	68
4	89
5	69
6	64
7	66
8	76
9	67
10	68
11	69
12	68
13	64
14	57
15	55
16	55
17	54
18	52
19	50
20	50

in 1967 have received only 16 *mrads*. If there are no further significant additions of strontium-90 to the atmosphere, then the maximum dose that will be attained by New York City residents living to age 70 will be those who were 4 years old in 1967. This maximum 70-year bone dose is estimated to be about 300 *mrads*. Since the radiation dose rate to bone from natural background is about 100 *mrads* per year, the dose accumulated over a 70-year lifespan is 7,000 *mrads*. The additional dose accumulated in a lifetime, therefore, amounts to at most four percent of that from natural sources. The variation of background dose rates to bones in large populated areas is commonly as great as 30 percent, hence, the risk associated with exposure to strontium-90 from fallout may be considerably less than that associated with a change in residence from one large city to another.

Iron-55 in Man and the Biosphere

Iron-55 has increased in relative importance from a minor fraction of fallout to the most abundant of all fallout isotopes since the 1961–62 nuclear tests. The study of the transfer of iron-55 and its concentration in the biosphere is of interest because iron is an essential element to

many organisms and is easily measured in almost all living organisms of the biosphere. The weak radiation associated with the iron-55 decay produces an extremely small radiation exposure as compared even with the normal potassium-40 body content. Human blood studies at Pacific Northwest Laboratory show that the levels of iron-55 in man ranged from five nanocuries [25] in South Africa to 2,300 nanocuries in some natives of Alaska (see Table 4). These studies show that the highest levels in humans are associated with a high consumption of ocean fish, especially salmon (the highest levels measured in any organism were in salmon). The average levels in women are significantly higher than men, probably because of a higher iron uptake caused by menstrual blood loss.

Table 4 represents results of a Pacific Northwest Laboratory survey of iron-55 in people throughout the world. These estimates were made by measuring iron-55 in blood samples obtained from blood banks or hospitals. Since blood banks do not accept blood from people deficient in iron (mostly women) the difference between the levels in men and women are not as great as when a random sampling of the general population is used. (There is no immediate explanation for the exceptions shown in the table for Winnipeg and Hamilton in Canada and Johannesburg, South Africa.)

[25] *Nano* is a prefix that divides a basic unit by 1 billion (10^9); thus, a *nanocurie* is one-billionth of a curie.

TABLE 4.—IRON-55 CONTENT IN HUMANS THROUGHOUT THE WORLD [a] [b]

[In nanocuries]

Sampling location	*Average iron-55 body burden*	
	Male	*Female*
Sydney, Australia	8.0	9.2
Caracas, Venezuela	7.4	----------
Johannesburg, South Africa	5.8	5.7
Toulouse, France	17.0	22.0
Tokai-Mura, Japan [c]	634.0	919.0
Oslo, Norway	58.0	64.0
Amsterdam, The Netherlands	9.1	14.3
Canada		
Calgary	18.0	24.0
Winnipeg	22.0	21.0
Hamilton	23.0	22.0
United States		
New York City, New York	22.0	26.0
Milwaukee, Wisconsin	13.0	20.0
Seattle, Washington	26.0	33.0
Bethel, Alaska (fish-eating natives) [c]	----------	[d] 1,100.0 (18)
Southeastern, Alaska—Yukon River mouth area (fish-eating natives) [c]	[d] 344.0 (6)	[d] 700.0 (7)
Tanana, Alaska (fish and caribou-eating natives) [c]	[d] 250.0 (6)	----------
Anaktuvuk, Alaska (caribou-eating natives) [c]	[d] 80.0 (6)	----------

[a] Blood specimens collected during first half of calendar year 1966.

[b] Body burdens were calculated by assuming a total blood volume of 5 liters and that 60% of the total iron is in the blood.

[c] Blood samples obtained from adult population and not blood banks.

[d] Numbers in parentheses indicate the number of samples analyzed.

Fig III–60. Terrain Effects on Diffusion and Transport. Possibly the greatest reason that man knows so little about flow patterns in the atmosphere is that air is invisible—consider what would be known of ocean waves and currents if water were also invisible. Cloud patterns, dust storms, fog, and smoke can make air movement visible. In studies by the AEC's Pacific Northwest Laboratory, Colorado State University, and the U.S. Navy smoke is used to determine terrain effects on atmospheric diffusion and transport over Point Arguello, Calif.; for how this "aerial" photo of Point Arguello, Calif., was made, see page 306, and Fig. III–68.

ATMOSPHERIC SCIENCES

The AEC sponsors a significant portion of the basic and applied research conducted in the field of meteorology in the United States, as well as some additional research abroad. The AEC's interest in this field originated in the 1940's from urgent needs for an ability to predict the behavior of radioactive gases and particles released to the atmosphere. These materials can be released both at very high elevations by nuclear explosives, and near the ground through venting of underground explosions, or through accidental releases from industrial plants using or producing radioactive products. Hence, a considerable range in kinds and scales of atmospheric process is pertinent to the AEC and the public interest.

Areas of Study

Radioactive materials placed in the atmosphere behave in most respects like nonradioactive pollutants of like size, density, and shape. And, like other pollutants, they react and interact with earth surfaces, and with sea salt, cloud droplets, dust particles, and rain or snow in the air. Because of this, AEC-sponsored meterological research frequently contributes directly to, and benefits from, research of other Federal and international agencies in the areas of air pollution, weather modification, and weather prediction. Therefore, it has been advantageous to cooperate with other organizations in the conduct of research on common meteorological problems.

Pollutant Transport Routes

Figure III–61 shows the routes a pollutant can follow, from both low and high elevation sources, until it finally returns to the earth through settling or impaction on surfaces (called dry deposition) or through the scrubbing action of rain and snow (called wet deposition, or precipitation scavenging). The travel from source to destination is appropriately called transport, and the spreading above, below, and to the side of the plume as it travels is called dispersion or diffusion. The complex air motions producing the diffusion are termed turbulence. Turbulent motions or eddies are also able to pick up material from the sea and ground. This entrainment accounts for the sub-

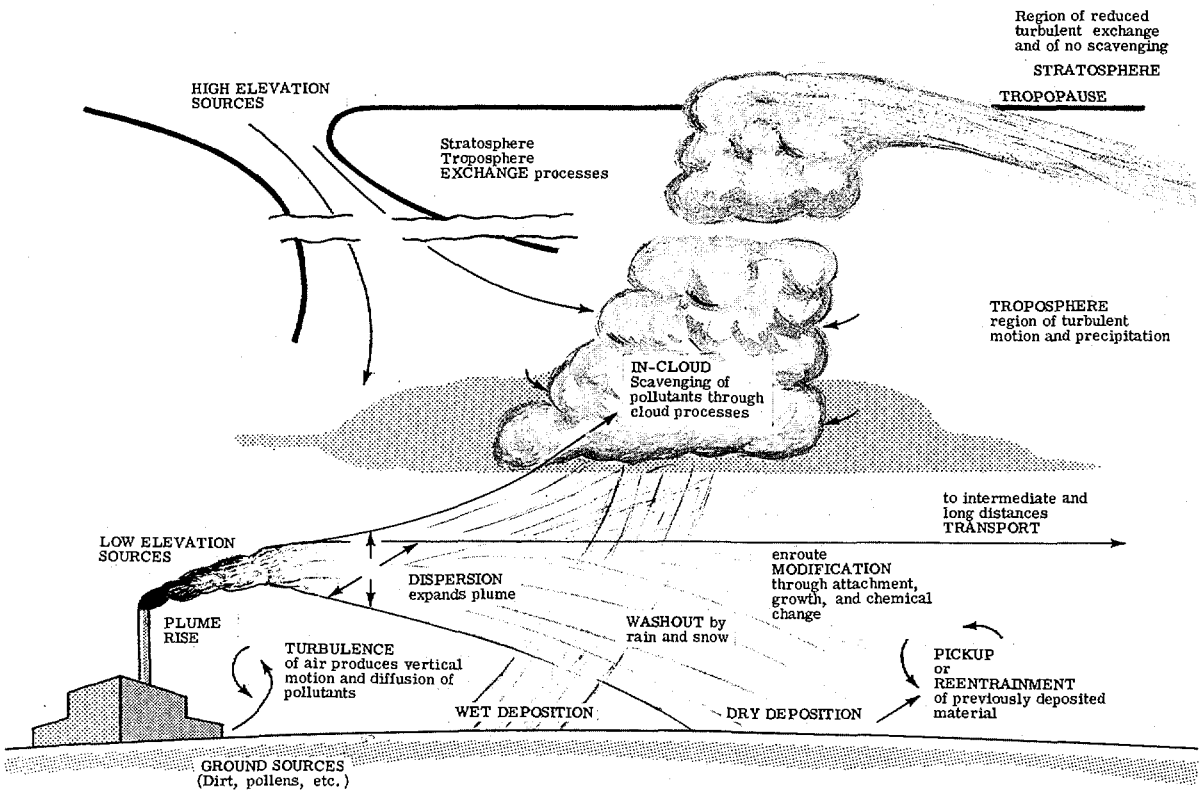

Fig. III–61. Pollutant Routes. Schematic drawing shows the meteorological influences on pollutant materials released to the atmosphere from ground sources (dirt, pollens, auto fumes, etc.); from low-elevation sources (stacks, fires, etc.); and high-elevation sources (nuclear weapons testing, extra terrestrial dust, etc.), and how these pollutants finally returned to earth.

stantial amounts of sea salt and dust in the air, and can lead to relocation of material deposited previously. Because the turbulence is highly dependent upon the change of wind and temperature with height, meteorologists are concerned with these items as well.

"Micrometeorology" is the study of the small-scale atmospheric processes—usually considered as up to about 10 miles in distance, and within the planetary boundary layer (lowest 3,000 ft.) of the atmosphere. Transport to greater distances—from about 10 to 125 miles—is classified as in the middle or "mesometeorological" regime, but the dividing line between micro and meso is somewhat arbitrary. In addition to these scales, there is the "macro" or "synoptic" scale of motions which involve the global transport of pollutants up to very high altitudes.[26] These motions transport pollutants in the higher atmosphere to those places where atmospheric motions can carry them to lower altitudes for removal. Most of the pollutants in the higher atmosphere are carried back to the earth as washout by rain and snow. Consequently, the AEC sponsors research closely allied to other agency research in cloud physics. This section deals with micro- and meso-scale research, and also includes some work on precipitation scavenging.

[26] See pp. 188–203, "Fundamental Nuclear Energy Research—1965."

BUOYANT PLUMES

When it is necessary to exhaust undesirable materials to the atmosphere, this is usually done from stacks or chimneys. Ideally, the resultant "plume" will diffuse or thin out enough to be acceptable by the time parts of it get near the ground. However, since persons at larger distances from a complex such as a city may receive contributions from numerous stacks, it is necessary to consider the diffusion of these plumes to rather long distances. The degree of dilution at the ground depends heavily upon the height of travel of the plume.

Plume Rise Variables

The plume from a well-designed stack will continue to rise for some distance downwind after it leaves that stack. This plume rise depends upon several factors:

(*1*) The plume exiting from the stack has an initial upward velocity which tends to continue, much as a stream of water from a water sprinkler. This upward momentum is greater for higher exhaust flow rates and for larger diameter stacks.

(*2*) The plume will also tend to rise if it is warmer (less dense) than the surrounding air, just as warm air in a room rises toward the ceiling. This buoyancy is usually caused by a temperature difference between the plume and the air, but it can also result from differences in the kinds of gases emitted. Hydrogen, for example, is lighter than air and has some tendency to increase plume rise.

(*3*) As the plume rises it entrains or collects additional air from around it. This air dilutes the plume and decreases the upward velocity and buoyancy effects by increasing the mass of the plume. The rate of entrainment depends upon the speed of rise, the diameter of the plume, and the atmospheric turbulence levels.

(*4*) As the plume rises it continually meets stronger and stronger wind speeds which reduce its ability to rise further.

(*5*) When the plume leaves the stack, the turbulent motions of the atmosphere mix clean air into the edges of the plume, increasing its size and carrying some of the gases outward, upward, and downward away from the plume core; this continues after the plume has ceased rising. The entrainment is accomplished by the turbulence generated by plume motion, and by natural forces.

Thus, not only the stack variables of diameter, height, temperature, and upward speed, but also the atmospheric variables of wind speed, temperature lapse rate, and turbulence influence the rise and spread of the plume. Theoretically, it should be possible for meteorologists to match these seven variables to observed plume rises and obtain prediction formulas. However, the problem has been under investigation for many years without solution. There are several reasons for this: (*a*) the final height of the plume is hard to measure—as it rises it also grows thinner, and photographs are hard to take and hard to interpret; (*b*) there are seven or more variables to be investigated, and meteorologists are only now able to combine some of them so as to reduce the number to be considered; (*c*) the turbulence variable is not something so simple that numbers or words can define it. In some ways the atmospheric motions are random and erratic, and in other ways they appear to be well organized. Not only does the turbulence change with height and distance from the stack, it also changes with time, with the weather, and with the underlying terrain and vegetation.

Numerous equations for predicting plume rise have been fitted to observed plume rise data from different stacks in the past. However, it appears that each group of data needs a different formula; and, unfortunately, most of the data have been taken over limited ranges of wind speed and stack variables. What is more, many of the formulas in current use are largely empirical, that is, they are derived from the data rather than from theory. However, considerable agreement between theory and experiment has been found.

Current Plume Studies

Plume Rise Models

Theoretical models of plume rise have been developed under AEC sponsorship by ESSA's [27] Atmospheric Turbulence and Diffusion Laboratory located at Oak Ridge, Tenn. The models take into account the initial plume buoyancy and momentum, as well as possible contributions to buoyancy from heating because of plume radioactivity. An important conclusion from these

[27] ESSA—Environmental Science Services Administration, which was formed in 1965 to consolidate the activities of the U.S. Weather Bureau with the U.S. Coast and Geodetic Survey, the National Environmental Satellite Center, the Institutes for Environmental Research, and the Environmental Data Service.

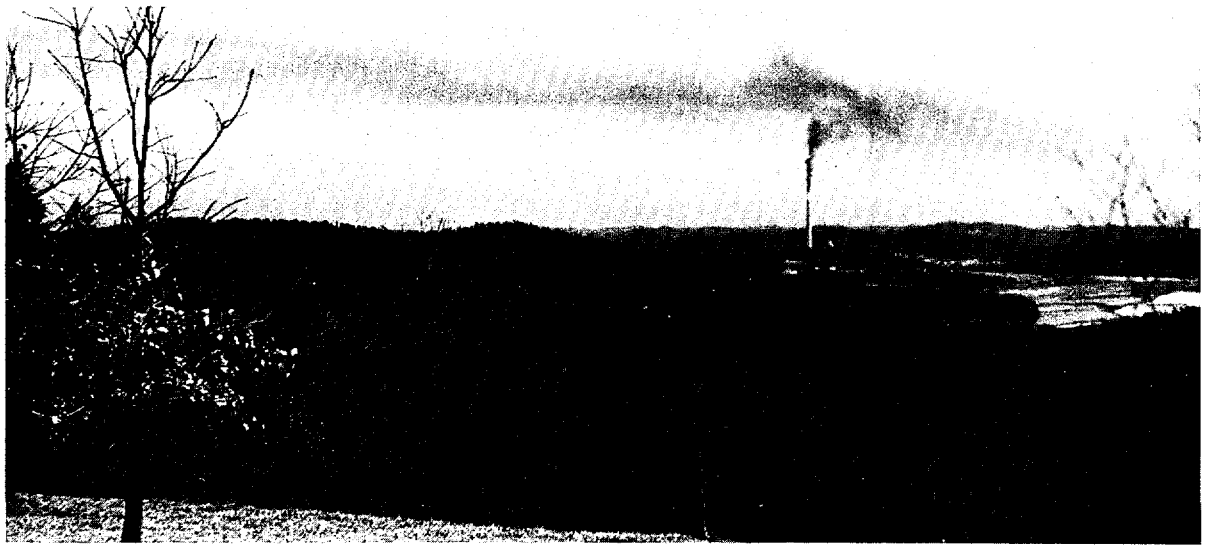

Figs. III–62 and 63. Plume Rise Variables. Photo *above* shows the smoke plume from TVA's Bull Run steam plant, Oak Ridge, illustrating the initial buoyant plume rise from the stack, and then the inhibiting effect on the plume rise by a temperature inversion aloft. Photo *below*, taken over Brookhaven National Laboratory shows an oil-fog smoke trail shortly after sunrise during a deep, temperature inversion extending well above the smoke trail. Some 3 miles of smoke trail are visible in the photo.

studies is that the rise depends mostly upon plume properties such as buoyancy and momentum, and only in the final stages upon atmospheric properties such as the change of temperature with elevation of the surrounding air. Observed plume rises are well described, over broad ranges of plume buoyancy and to great distances from the source, by the so-called "transitional rise" formulas.[28]

Hot "Puff" Studies

Similar studies at Brookhaven National Laboratory (BNL) are specifically concerned with the rise of very hot "puffs" of cloud, such as might result from accidents or spills involving radioactive material (see Fig. III–64).

The open burning of rocket propellant fuel serves as a source of bouyant clouds, the dimensions of which can be measured photographically and visually. Repeated experiments have produced consistent cloud behavior during temperature inversions while showing an expected variability during lapse conditions. Analyses of the time and space history of the cloud tops has established the usefulness of a method for distinguishing the initial cloud behavior from the subsequent expansion of the cloud caused by ambient turbulence. Since the heat release, cloud behavior, and meteorological factors are known from photographs and meteorological measurements made from nearby towers, it has been possible to study their interrelation and to make comparisons with theory.

Since the stability of the layer in which the cloud ascends is related to the work done in displacing a parcel of gas from one elevation to another, it can be expected that there will be a marked relationship between the height increase, Δh, and stability. This is indeed the case, and an equation of the same form as that proposed by a 1956 Brookhaven study describes the data very well.[29]

Stack Engineering

Plume rise studies have also been carried out at Argonne National Laboratory (ANL) over a limited, but controlled range of stack parameters. Consecutive photos, taken from the sides and bottoms of the plumes, have been superimposed to study the relationship between the instantaneous plume averaged over several periods of time. It is then possible to correlate the plume sizes to the wind characteristics over the same time intervals as the photographs (see Figs. III–65 and 66).

In another study at Argonne, many plume measurements made in the United States and Europe were analyzed for the purpose of arriv-

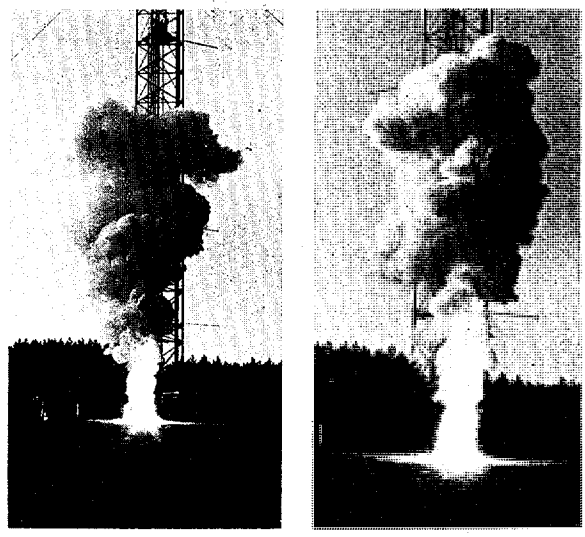

Fig. III–64. Hot "Puff" Studies. Small scale experiments conducted with burning rocket fuels provide data used in prediction of the diffusion and final height-of-rise of clouds from larger accidental releases. These are successive photos taken at Brookhaven National Laboratory. Wind and air temperature data are taken on nearby towers. The data have been described with equations similar to equations used in predicting plumes from stacks. Series of photos, taken from different angles, shows the rise of a hot "puff."

[28] These involve only plume buoyancy upward momentum, and wind speed, and take the simple form $h = C_1 F_m^{1/3} x^{1/3} \mu^{-2/3}$ for a momentum dominated plume, and $h = C_2 F^{1/3} x^{2/3} \mu$ for a buoyant plume. If the plume contains radioactive gases, the rise equation has the form $h = C_3 F^{1/3} \mu^{-4/3} x$. Here, x and μ represent distance from the stack and wind speed, while the F's are flux terms containing parameters such as air and plume temperature and stack diameter. The C's are theoretically determined constants.

[29] $\Delta h = 0.084 (Q/G)^{1/3}$

where $G = (g/T)\ (\partial\theta/\partial z)$ stability parameter (sec^{-2}).
θ = potential temperature (deg K).
g = gravity (cm/sec^2).
T = ambient temperature at source level (deg K).
$\partial\theta/\partial z$ = change of potential temperature with height (deg C/cm).

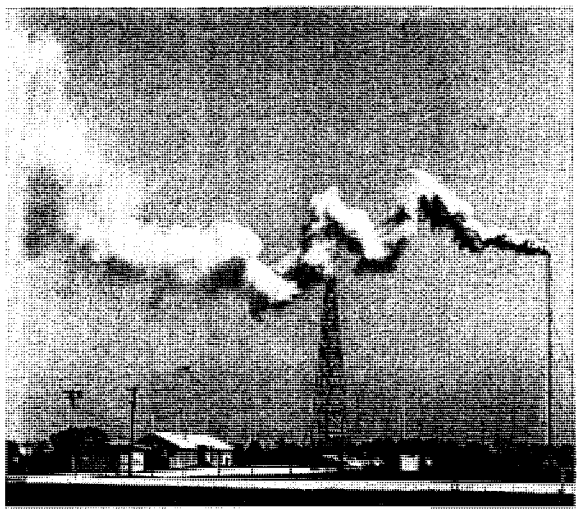

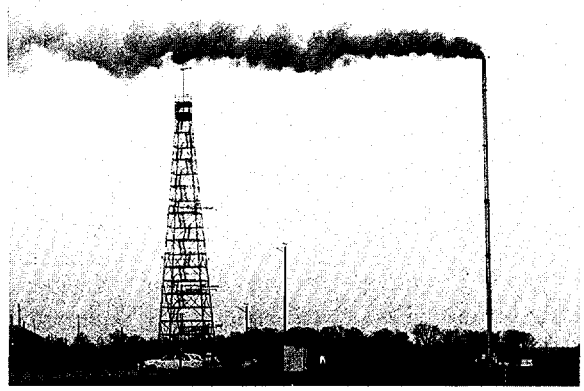

Figs. III–65 and 66. Effects of Atmospheric Conditions. Photo on the *left* shows a smoke plume ejected from an 111-foot stack at Argonne National Laboratory. The irregularity of this typical plume indicates unstable atmospheric conditions. The photo on the *right* was taken at sundown on the same day as that shown on the *left* and shows the typical plume behavior under moderately stable conditions. This stack has been designed so that its height can be varied by removing sections. The research up to now has involved only changes in flow rate and effluent temperature but not height changes.

ing at an improved technique for predicting plume rise from stack engineering and weather factors. This study included a large range of measurements on stacks varying from the small Argonne experimental stack to the giant ones of the Tennessee Valley Authority (TVA); the heat emission rate of the largest was 5,000 times that of the smallest. The study produced plume rise equations to be used in a handbook of the American Society of Mechanical Engineers (ASME).

Contaminant Suspensions

The University of Waterloo, Ontario, Canada, is carrying out studies under AEC contract on the behavior of relatively large particulate contaminants suspended in hot plumes. The work completed so far has provided additional information on the heights to which hot plumes may rise. The experimental work is carried out in three ways: (*a*) photographic, full-scale studies of industrial chimney plumes; (*b*) pilot-scale studies using the smoke-plume of a 20-foot-high model chimney over flat grassland, and; (*c*) wind-tunnel studies using a 3-inch diameter stack. The studies are complicated by the fact that although the particles are in a hot and therefore rising plume, they also exhibit their own downward drift, because of their weight.

Industrial Plant Stack Studies

To meet a growing need for reliable and comprehensive plume rise data from large industrial-type stack emissions, the Tennessee Valley Authority, under sponsorship of the U.S. Public Health Service, has conducted a special 3-year research study of plume rise at large electric generating stations. The Brookhaven National Laboratory staff provided important support to this study through interim reviews, analysis, and interpretation of the data with respect to principal plume rise formulas. The study was particularly timely because the experience, techniques, and special equipment developed in a preceding 5-year dispersion study were directly applicable. Also, available plant sizes, stack heights, and stack configurations accommodated full-scale assessment of plume rise over a wide range of conditions. The TVA fieldwork was

conducted on 50 days totaling about 311 hours of field sampling. Data include 1,580 plume photographs, 494 double- and single-theodolite pilot balloon runs, and 305 helicopter temperature profile runs. Total helicopter time was 188 hours. ESSA personnel from Oak Ridge provided valuable guidance in the programming and consolidation of these data.

Brookhaven is also analyzing measurements of sulfur dioxide at large distances from the stack in the case of "fumigation"—the term used to describe the sudden downward mixing of a plume once the reappearance of thermal convection following sunrise destroys the temperature inversion that has kept the pollutants aloft during the night. This is thought to be one way in which relatively large concentrations of a pollutant might be attained at the ground at large distances. The sulfur dioxide data collected and provided to BNL by the TVA from its coal-burning power plants are especially interesting because they concern plumes from very tall stacks. This kind of data has not been available before and will be invaluable in determining the value of tall stacks for dispersing pollution.

Diffusion or Dispersion

Concentration Prediction

In those cases where the meteorological parameters are known in advance (vertical temperature distribution, wind speed, direction, and wind variability), the concentration of contaminants out to a few miles can now be predicted with sufficient reliability for many operational requirements. For instance, average air concentrations from a radioactivity release at the Brookhaven National Laboratory during November 11–16, 1964, were predicted by BNL meteorologists to within a factor of two, *i.e.*, the concentrations were between ½ and twice the predicted values. Recent improvements in sensitive detection techniques have also permitted such comparisons with a full-year's data, using the minute amounts of iodine-131 routinely released from the stack of the Brookhaven Research Reactor. The prediction system is based on a single wind instrument located at the same height as the stack, and it has been found that the system predicts the observed concentrations at ground-level with reasonable accuracy. This accuracy might be improved somewhat if the short-term variability in the release of iodine were more closely defined, but the system is satisfactory to assure that concentrations are kept within the established safety margin. Most recent studies include the measurement of emitted argon-41.

Turbulent Energy Spectra

To describe turbulence in a quantitative manner, meteorologists—in common with other workers in fluid dynamics—distinguish between the average circulation velocity which prevails throughout a given volume of fluid for a period of time, and the instanteous departures of fluctuations from that mean (in both speed and direction) that occur at all intervening times and at all points within the volume. These instantaneous fluctuations are often termed "turbulent eddies," but by this it should not be inferred that the individual circulation elements themselves necessarily resemble small vortices. For example, they may simply be short-lived changes in linear speed. A record of fluid velocity obtained at any one point within the volume will be found to oscillate in an apparently random manner around a mean value; but statistical analysis reveals that these fluctuations actually occur in a fairly well organized fashion. This is shown in plots of the energy of the eddies versus their characteristic frequency, a type of graphical representation known as a "turbulence spectrum" and illustrated in Figure III–67.

Figure III–67 shows the averages of many such spectra measured at the Pacific Northwest Laboratory (PNL). The three average curves are for the horizontal eddies perpendicular to the average wind direction during sunny (unstable), nighttime (stable), and windy (neutral) conditions. While the turbulent energy is generally less at night for all frequencies, a higher percentage of the energy occurs in the

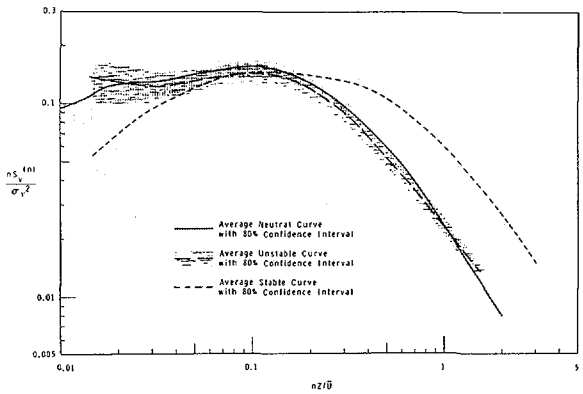

Fig. III–67. Turbulent Energy Spectra. Meteorologists describe the turbulence of the air by plotting a function of the turbulent eddy energies (formula shown on *left* scale of chart) against a function of the eddy sizes, nz/Ū (at *bottom* scale). The product of the turbulent wind fluctuation frequency, n, and the power spectral density of the turbulence, $S_v(n)$, divided by the total variance in the wind fluctuations, σv^2, gives a measure of the fraction of the total turbulent energy occurring in each eddy size. The wavelength of the eddy, estimated by Ū/n, where Ū is the mean wind speed, is divided in the figure by the height, z, to remove dependence of the spectral distribution on height. This Pacific Northwest Laboratory plot is of the energy in the crosswind component of the turbulent motions of the air during sunny (unstable), windy (neutral), and nighttime (stable) conditions. Some of the energy seems to shift from the low frequencies of the day to the higher frequencies of the night. (Curiously, this shift was not observed as markedly in the vertical and along-wind components.)

high frequencies at night than during the day. the low frequency eddies are large in size and are the ones that produce large snakelike patterns in a plume. The high frequency eddies are small in size and cause local expansion of the plume as it wanders under control of the larger eddies. Thus, the spectra can be directly related to the growth and meandering of a plume as it travels. Differences in the spectra between weather situations and between sites explain differences in diffusion between times and locations.

Useful information of another type is also contained in atmospheric turbulence spectra. Nature continuously adds energy to the turbulent circulations, but this takes place almost entirely at the low-frequency, large-scale end through the agency of "eddies" such as those associated with the formation of convective clouds. At the same time, an overall energy balance is maintained in the system by the continuous removal of turbulent energy at the very high-frequency end of the spectrum, where very small, rapid motions, ranging from millimeter sizes to near-molecular scale, continuously convert the kinetic energy of the moving air into heat through viscous friction. As a result, there exists an intermediate range of turbulent eddy sizes where little or no energy is either added or subtracted; instead, it is here merely handed down the scale, from larger to smaller eddies in a highly-organized cascade process.

Vertical Turbulent Exchanges

Work at Argonne National Laboratory has shown that the well-established, statistical properties of this organized turbulence regime (the so-called inertial subrange) can be used to evaluate vertical diffusion rates through the lowest 10 meters (32.8 feet) of the atmosphere. Since most of the energy input and at least half the energy losses of the entire atmospheric heat "engine" are transported by the turbulent exchange across this region, some method of measuring this transport of heat, moisture, and momentum over an appreciable portion of the earth's surface constitutes a major hurdle which must be crossed before significant improvement in weather forecasting can be obtained.

Up to now, it has not been feasible to treat storms as other than perpetual motion machines; forecasters, both human and electronic, have had to assume that cyclones and anticyclones neither gain nor lose energy as they move across the earth. In contrast to other techniques for evaluating these important vertical turbulent exchanges, the methods of analysis and instrumentation being developed at Argonne, are relatively simple; thus, they show promise of being adaptable to routine, world-wide meteorological measurement. For example, it has been shown that the downward flux of momentum associated with frictional losses sustained by the wind as it

rubs against the earth can be measured with the single cup anemometer, an instrument especially constructed at Argonne for this purpose. What is more, since the turbulent mechanisms which transport momentum in the atmosphere are identical with those which disperse pollutants, continuing studies with this instrument and its associated data-analysis procedure at Argonne will contribute further to knowledge of the atmosphere's ability to dilute waste materials introduced by industrialized civilization.

Turbulence Measurement

Unfortunately, the measurement of turbulence is a formidable problem. Considerable effort has been spent on the development of instruments able to measure eddies of all sizes and at frequencies up to hundreds of cycles per second. In this regard, one of the major simplifications achieved by the Argonne work described above lies in the fact that it has been shown that useful information on turbulence can be obtained using instrumentation with relatively limited (but fully understood) response characteristics. Measurements have also been made at ANL of the properties of turbulence artificially generated in laboratory wind tunnels and water channels in order to develop theories which might then be used in the outdoors. Much attention has been given to the relation between the turbulence measured at a point as the wind goes by (called an "Eulerian" measurement), and the turbulence carried within a "parcel" of the air as it moves around (called a "Lagrangian" measurement). (Whereas the turbulence at a stationary point is easier to measure, the turbulence in the moving parcel is what actually diffuses a plume.)

AEC laboratories and contractors use several methods in attempting to follow or trace the moving parcels. Particles and gases have been placed in the air and captured again downstream. Balloons have been tracked with optical, radar, and radio direction finding devices. Smokes have been generated and followed with optical and camera equipment.

The equipment and techniques developed under AEC contracts for tracing atmospheric motions are also profitably employed in research on similar problems for other agencies. The results of that work can be used in turn to predict the future course of radioactive materials. An example of this symbiotic relationship is the diffusion and transport work conducted by the Pacific Northwest Laboratory for the U.S. Air Force over the rugged Point Arguello terrain of the southern portion of Vandenberg Air Force Base in California.

Modeling Air Motion

The design of the Vandenberg Air Force Base experiments is essentially the same as that developed and used previously and currently for diffusion studies at the AEC's Hanford Works in southeastern Washington. The field samples are taken with Air Force-AEC developed samplers and engines, and are assayed on automatic counting equipment developed under AEC sponsorship.

The effects of large terrain features can be visualized from the photographs (Figs. III–60, and III–68) of a modeling study conducted in a wind tunnel at Colorado State University, Fort Collins. This modeling study, recently sponsored by the U.S. Navy was used to reveal flow characteristics which the design of full-scale tests must consider, and can be used to extend the results of full outdoor field tests to larger distances and other situations. The PNL meteorologists consider the results of the outdoor field tests and of the modeling studies when planning similar experiments for the AEC.

Aircraft Sampling

Although considerable progress has been made in the study of dispersion over short distances, longer-distance dispersion investigations are also required. The number of problems where the mixing and transport properties of the atmosphere are of concern on such a broad scale are increasing rapidly. This is be-

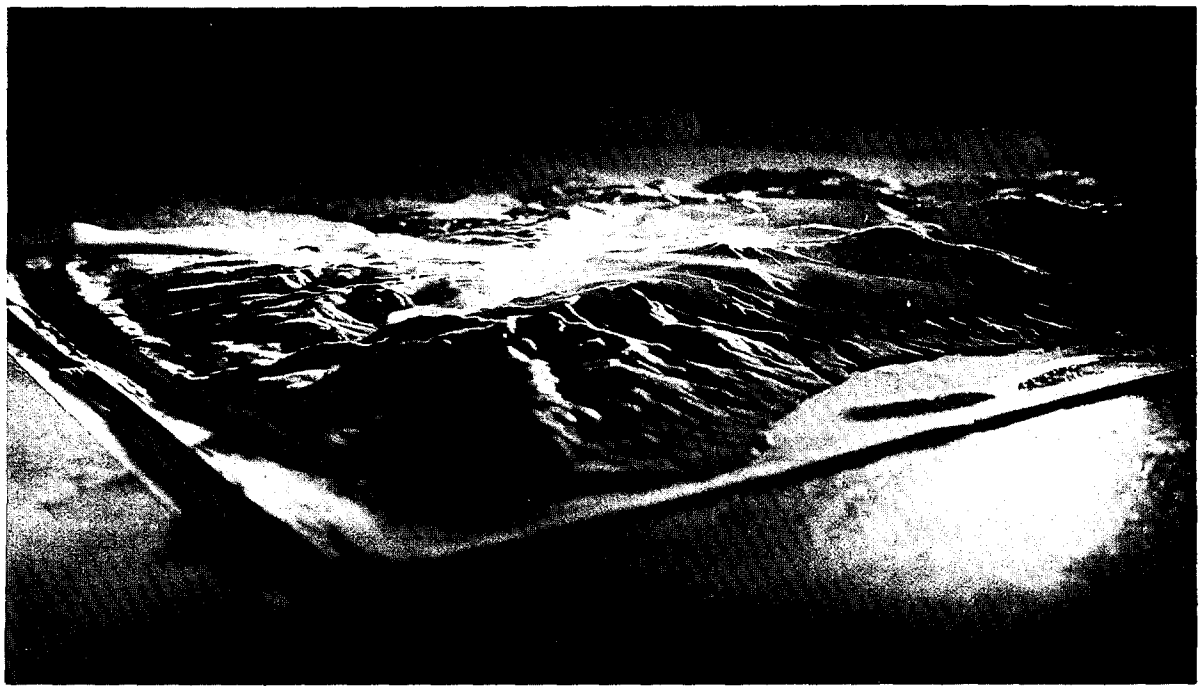

Fig. III–68. Modeling Terrain Effects. The "aerial" photo, Figure III–60, is of smoke patterns on a 1/12,000-scale model of the southern (Point Arguello), portion of the Vandenberg Air Force Base, Calif. It was taken in a meteorological wind tunnel at Colorado State University, Fort Collins, as a part of a U.S. Navy study. The view of the model is toward east northeast as if from a few miles out over the Pacific Ocean. The beach on the right lies on the Santa Barbara Channel, and Pismo Beach is to the left. The artificial smoke issues from cotton soaked with titanium tetrachloride at the left (NW) side of the model. The air masses in this region are quite stable—a result of warmer air at higher levels—during much of the year. This condition is simulated in the tunnel by refrigerating the tunnel floor and heating the air. Model studies such as these help meteorologists explain measurements in full-scale field tests. When the two flow patterns correspond, the model can be used to predict concentrations over the less accessible or more distant regions. Field equipment, procedures, and tracer techniques developed under AEC sponsorship are in use in field studies at this site.

cause of increases in the total amounts and in the toxicities of pollutants, and increases in the population densities around these pollutant sources. It is not sufficient to determine meteorological variables at a single point to predict contaminant dispersal in the atmosphere; the parameters important in describing the dispersion and transport can change radically with both time and distance because of changes in the meteorology and variations in the surface below.

Field experimental investigation of long range dispersion and transport is difficult. Sampler sensitivity must be high to detect low tracer concentrations. A high mobility must be available to rapidly sample tracers or contaminants. Pacific Northwest Laboratory uses two aircraft with AEC-developed "real-time samplers" [30] to extend sampling to heights, distances, and locations impossible for surface vehicles (see Fig. III–69). The aircraft and samplers are in use over both the Hanford site and the Vandenberg Air Force Base.

Through use of the aircraft and samplers, measurements of atmospheric tracers have shown an expected limitation on the upward plume growth when there is warmer air above. The effects of terrain variations on the plume growth also have been observed. In fact, the

[30] These real-time samplers are based on a Pacific Northwest Laboratory design reported on p. 97 of the "Fundamental Nuclear Energy Research—1966," as the "Rapid Response Recorder."

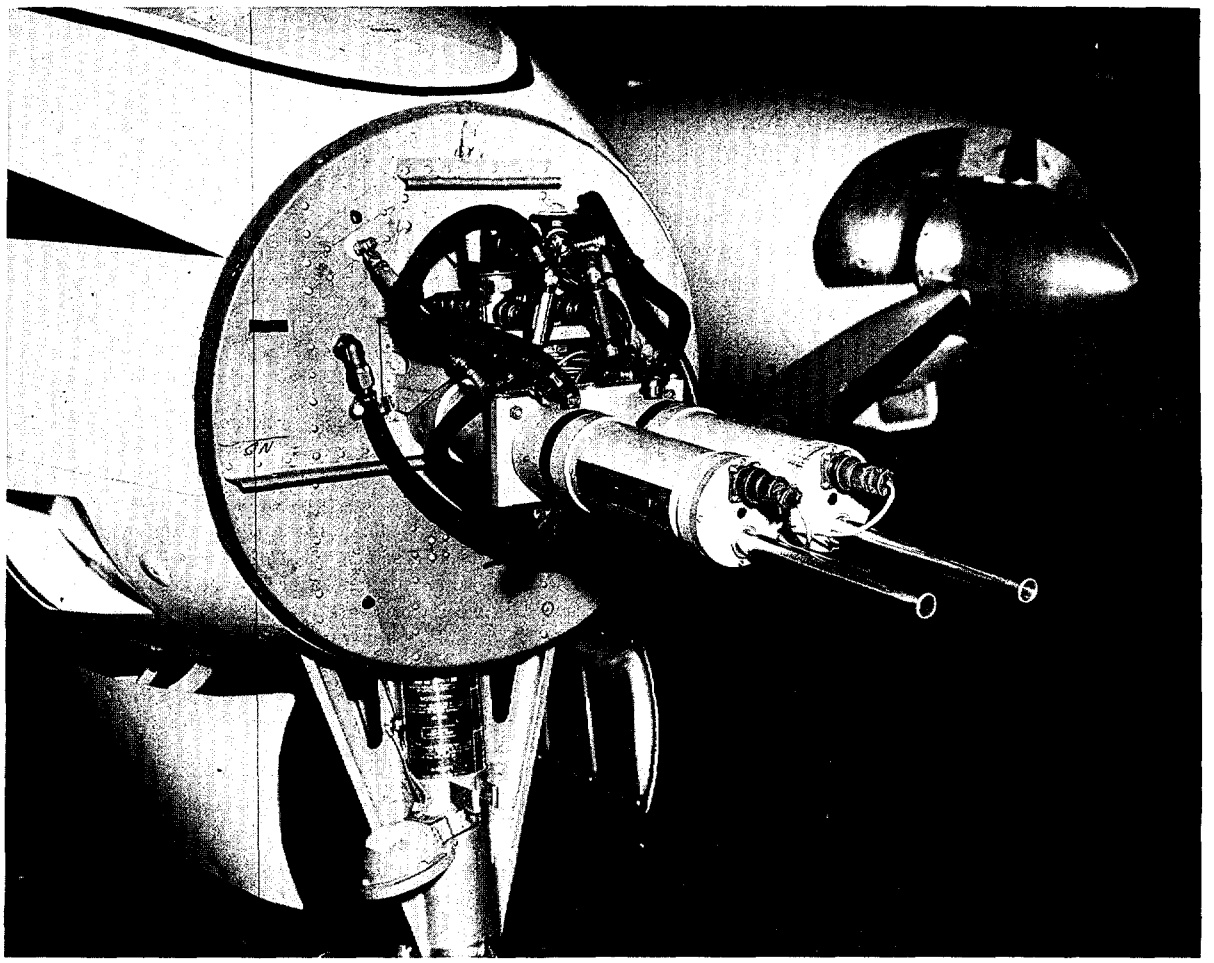

Fig. III–69. Airborne Tracer Sampler. Measurement of tracers from airborne platforms is necessary to extend the height and range of studies on the ability of the atmosphere to diffuse and transport pollutants. One tracer, used for many years, is a nontoxic zinc sulfide which phosphoresces after exposure to ultraviolet light. A sampler capable of measuring the phosphorescence of materials continuously during sampling was invented and developed at the Pacific Northwest Laboratory (PNL) and is now commercially available. The two samplers shown here are mounted in the nose section of PNL's flying atmospheric science laboratory. Systems of this type are used to follow tracers over mountainous terrain and adjacent seas. A similar ground-based sampler also provides comparisons of instantaneous measurements and average values (called peak-to-mean ratios), data not previously available in quantity.

mixing by mountains masks the mixing caused by ordinary surface roughness and that due to convective activity, and the usual seasonal and day-to-night differences in concentrations are considerably reduced at the Vandenberg site. Deviations in the paths of plumes over large distances as a result of large terrain obstructions have also been observed by PNL in its studies.

Transport Studies

The ability to predict the growth rates of plumes and the resultant concentrations of pollutants within narrow limits of error is of little use if the location of the plume cannot also be predicted. To predict the plume's centerline position, the meterologist: (*a*) gathers all available wind direction and speed data, (*b*) plots these

on maps, (*c*) draws flow lines to conform to the observed winds, and then (*d*) moves the plume along the flow lines with the measured wind speeds. Over flat land this usually works rather well for limited distances, but in mountainous or sparsely populated areas there are too few wind observations. Further difficulty arises because the wind speed and direction change with height. As a result, that part of a plume which diffuses or climbs upward is swept off in new directions with higher speeds—forcing the meteorologist to predict travel paths at several higher levels, and with still fewer wind measurements. It is also true that large air masses can climb or descend slowly with plumes contained within them, and that over large distances rather weak, unmeasured vertical motions can produce important changes in the travel heights of plumes.

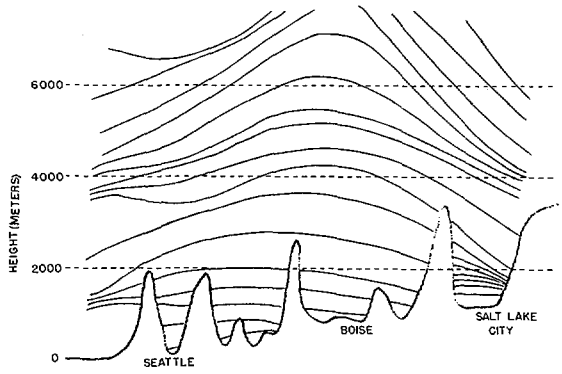

Fig. III–70. Long Range Transport Studies. This Pacific Northwest Laboratory drawing shows a slice of the atmosphere in the direction of the wind on a selected day. The surfaces of constant energy (isentropic surfaces) along which the parcels of air can be expected to travel are the thin, wave-like lines. Near the earth some of them intersect the mountainous land surface, which presents an obstacle to further motion of the air. The spacing of these lines indicates the stability of the air. The air above Salt Lake City in this case is quite stable, and pollutants in the vicinity cannot travel very far before intersecting the surrounding moutains.

"Isentropic" Trajectories

The best possible method for determining long-range trajectories uses the fact that the air tends to travel along surfaces of constant energy, called "isentropic surfaces." Material released at a position in air which has a certain energy will approximately travel so as to be in air of the same energy at points downwind. The heights and shapes of these constant energy surfaces are calculated from radiosonde reports (radio weather balloon observations taken twice daily throughout the world for use principally in weather forecasting). These calculations must be very accurate in order to compare with observed tracer movements, and are also quite tedious. Therefore, computer programs have been developed with AEC support by Pacific Northwest Laboratory, Pennsylvania State University, and the Illinois State Water Survey, and are used in their research studies of atmospheric tracers.

Figure III–70 is a vertical cross section of the atmosphere purposely selected to show how the isentropic surfaces can be used to predict gradual changes in the elevation of pollutants. This section lies with the wind direction (NW to SE) from Seattle, Wash., through Boise, Idaho, to Salt Lake City, Utah. Since pollutants placed on a surface will tend to remain there, on this particular day it may be predicted, for example, that:

(*1*) Pollutants released near the ground at Seattle will not get past the mountains immediately to the southeast;

(*2*) Pollutants released at 2,000 meters (6,500 feet) over Seattle may go through the mountain passes and get as far as the Boise area, but cannot penetrate the barrier protecting Salt Lake City; and

(*3*) Pollutants released at low levels in the Salt Lake Basin cannot escape and will continue to accumulate until a new storm comes in to exchange the air of the basin.

Progress in the ability to predict trajectories comes very slowly, primarily because of insufficient wind data, but also because predicted trajectories are seldom verified (concentrations become too low to measure or may not be obtainable for other reasons). The meteorologist pre-

dicts the long-range track of some material, but seldom learns whether he was right or wrong, and therefore cannot see how to improve his techniques. Recently meteorologists at the Lawrence Radiation Laboratory, Livermore, in studies aimed at developing atmospheric transport and dispersion models for the Plowshare Program, have been tracking exhaust from stationary experimental nuclear rocket engine test firings at the Nuclear Rocket Development Station, in Nevada, using aircraft equipped with sensitive detectors to follow the plumes for long distances.

Search for Better Tracers

Experiments to verify forecasts based upon semi-theoretical transport models call for further advances in tracer technology. Tracer sources of opportunity such as the nuclear rocket engine test (see above) are necessarily conducted too infrequently, and under too-highly restricted conditions, to permit sampling a suitable range of meteorological and topographic conditions. Several laboratories are therefore searching for techniques that will allow the measurement of minute amounts of a tracer material among the relatively large amounts of natural or "background" materials present in the air and in the material used for filters.

The University of Michigan and Pacific Northwest Laboratory are experimenting, independently, with some of the "rare earth" elements which have naturally low backgrounds. These elements are measured in quantities as small as one-billionth of a gram using the "neutron activation" technique. For this technique, the neutrons present in a reactor are used to make a sample radioactive (after it has been collected from the air), and then special counters determine how much of the resultant radioactivity is from the tracer material.

Some promise of a naturally occurring tracer is given by Pacific Northwest Laboratory's investigation of radionuclides normally produced in the air by cosmic rays. These radionuclides are formed continuously from oxygen, nitrogen, and argon, and have half-lives which vary from seconds to millions of years. The long-lived nuclides are useful in defining stratospheric-tropospheric exchange processes. The relative amounts of long-lived and short-lived nuclides in rain water are already providing insight into the scavenging processes at work in rain clouds. The research may consequently also have a payoff in weather modification.

PRECIPITATION SCAVENGING

The scavenging of the numerous pollutants placed in the air by both man and nature is essential to man's survival. The inability of dry deposition to cope with air pollution is evident in our cities and valleys during dry and stagnant conditions. That the entire earth's atmosphere is not intolerably defiled is due to rainout and washout by falling rain and snow.

Scavenging Processes

Conventionally, rainout is defined as those processes occurring within clouds, and washout as those processes occurring below clouds. However, this is not necessarily the best way to break up the research problem, since many of the processes within and below the clouds are the same, with only the size of the waterdrops and ice crystals doing the scavenging being different.

The process of collecting a particle by a bit of water or ice may be a simple matter of impaction or inertial collection, *i.e.*, the particle cannot make the turn to get out of the way of the falling droplet or snowflake. The collection process may also get some contribution from molecular diffusion and electrostatic forces, or from diffusiophoresis, which is the motion of the particle under the flow of water molecules rushing toward the growing water droplet in a supersaturated environment.

Determining the collision process, then, requires a nonlinear equation involving several forces, and the rather uncertain velocity field of the air flowing past the falling droplet or flake.

Mathematical computer solutions of this equation have been made only for uncharged particles of rather small size being overtaken by spherical raindrops. Because the equations are so difficult to adequately formulate for rain, and currently impossible for snowflakes, and because it is not certain that the particles will stick when they do strike the drop or snowflake, the scentists have had to rely mostly upon experimentation.

Scavenging Experiments

Much of the experimental work on precipitation scavenging has followed the method of: (*a*) measuring the collection of each size of drop on each size of particle, (*b*) independently measuring the sizes of drops that fall in a rain, and (*c*) then multiplying the results to obtain the total predicted washout. This is, of course, a very tedious though rewarding effort. Figure III–71 shows the results of such work with zinc sulfide particles at the Pacific Northwest Laboratories (PNL). These particles fluoresce a brilliant green under ultra violet light, and thus may be easily distinguished from the other dirt carried by the rain.

On the left of Fig. III–71 is an actual rain sample taken with a special paper. This paper is water sensitive and appropriate processing produces high contrast between the wetted and nonwetted portions of the paper. In rain samplers developed by PNL, this paper provides a permanent record of the raindrop's content and size. The spot sizes have been calibrated to yield the sizes of the raindrops producing them.

A raindrop which has fallen through a cloud of zinc sulfide particles typically presents a microscopic view such as in the upper right of Figure III–71. Background particles are observed on the paper outside the drop. Within the drop the particles are grouped mostly near the center of the image, a characteristic of scavenging by an artificial raindrop.

The image of a natural raindrop that has fallen through a plume of zinc sulfide and zinc-cadmium sulfide particles results in the zinc sulfide particles being distributed throughout the image rather than in groups. Yet, cadmium-zinc sulfide particles in the same natural raindrop will be all at one edge of the image. The differences noted may be due to electrical effects on the paper surface, or perhaps to differences in "wettability." (Wettability of a large solid is usually defined in terms of the angle between that solid and a touching water drop, but, in the case of a small particle, such definitions are tenuous.) Aerojet General Corp., Downey, Calif., has found that the speed at which a droplet envelops a particle depends upon the electrical charges present, and these results indicate that the drop will not wet the particle when there is no electrical field present.

The lower right of Fig. III–71 is a graph of collection efficiency *versus* particle diameter for several raindrop sizes. Theory predicts, when considering inertia only, that the effiicencies should lie in the shaded area. That they do not is only partially the result of experimental error; air flow patterns around the falling drops are different from the idealized patterns used in the theory. Still other effects appear to be involved.

Washout Below Clouds

When trying to measure washout of particles or gases in the field or in the laboratory, a major problem is to determine the concentration of the tracer in the path of the relatively small raindrop. The concentration will vary in all four dimensions, and yet the raindrop will sweep out a column of only pencil-lead size. It becomes necessary to average the collections of many raindrops, as well as to "fight" sampling errors.

A different approach to this problem is to release a measured quantity of tracer into the air, and mathematically evaluate the amount of tracer in the path of the rain or snow collected in buckets below. The falling precipitation integrates the plume vertically and precipitation samples collected along a line laid out crosswind integrates the plume cross-axis. By sampling precipitation during the entire plume passage, the plume is integrated down the axis. The indi-

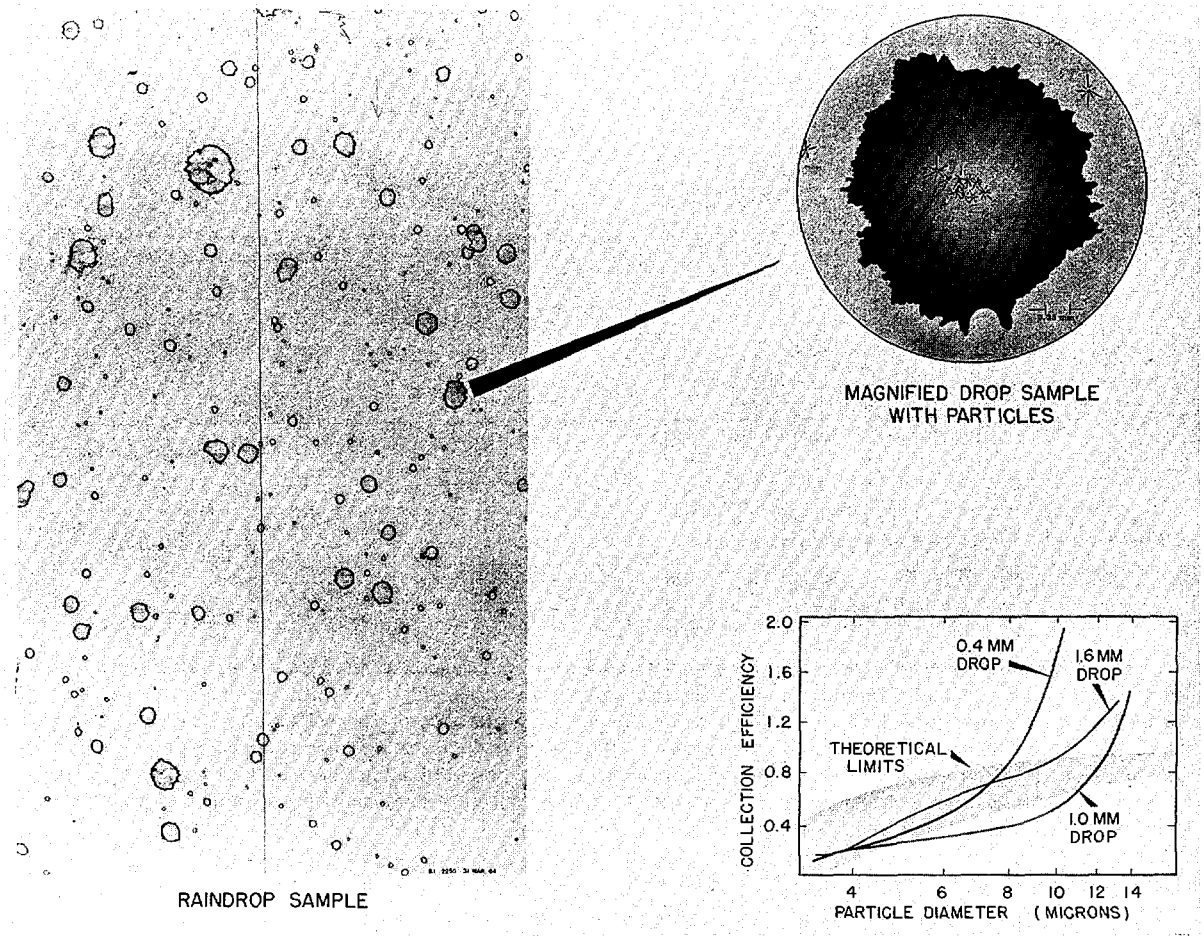

Fig. III–71. Raindrop Scavenging Studies. The water-sensitive paper shown at *left* is used to provide a permanent record of the particles washed from the air by raindrops of different sizes. A special particle tracer can be released into the air during rain and later be counted and sized by the individual raindrops collected on this paper. The fraction of the particles in the path of a drop which get collected is called the collection efficiency for that drop size. Studies using fluorescent zinc sulfide particles at Pacific Northwest Laboratory have shown some deviations from theoretical predictions. The results in the graph (*lower right*) show that the smaller raindrop has a higher collection efficiency—something that was not predicted by theory.

vidual samples are simply poured together to perform the integration. Then, from a measured wind speed, it can be calculated how long the plume was over the samples below, and finally the fraction of the plume washed out in a given time.

Pacific Northwest Laboratory has established an experimental site on an irrigation lake bed in the Cascade Mountains of Washington. A 40-foot tower (see Fig. III–72) is used for release of small quantities of bromine and iodine vapors and nonradioactive particulates. The ground-level collection buckets are located on concentric arcs, and are lined for each test with new plastic bags so that the samples are not contaminated. The bags are gathered after the plume has passed, the rain or snow in them is poured together, and the total sample is returned to the laboratory for neutron activation and radiochemical analysis.

The precipitation rate is determined from the amount of water collected over the known time

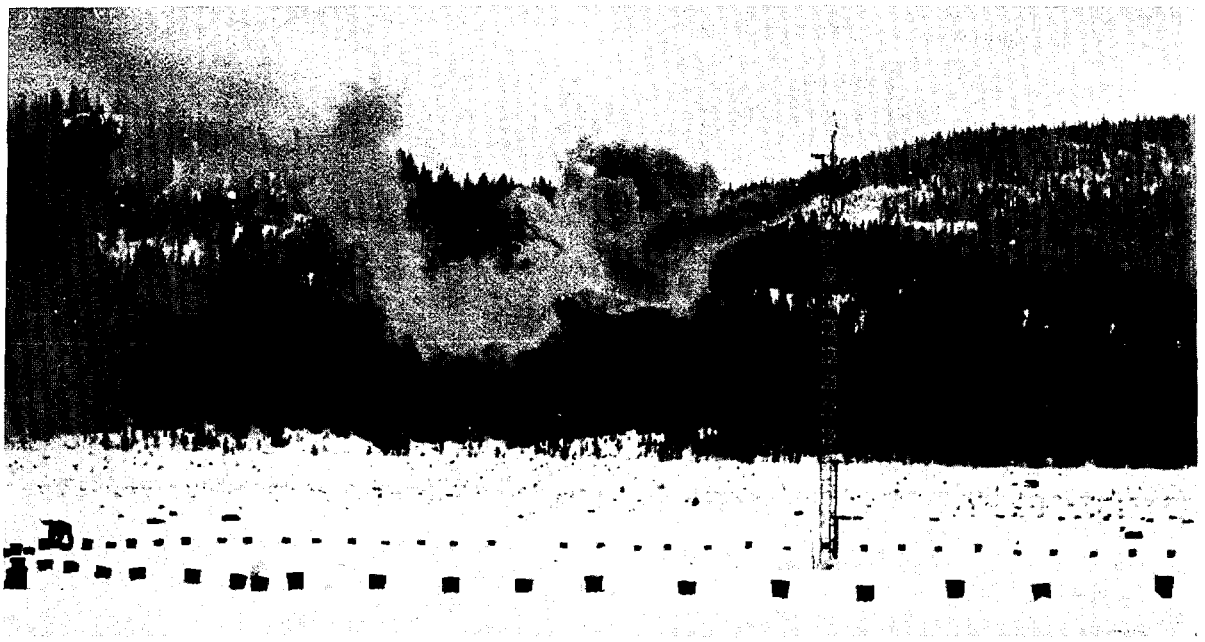

Fig. III–72. Washout Experiments. Various kinds of gases and particles are released from this 40-foot tower in the Cascade Mountains of Washington during rain and snowstorms. The precipitation picks up some of the released materials and falls into the buckets below. Laboratory analysis of the water later, reveals the rate at which the precipitation scrubbed the air of pollutants. This rate is found to depend upon the type and size of the snowflake or raindrop, upon the solubility and diffusion of the gas, and upon the size and electrical charge of the particles. An instrument to measure the electrical charge of individual snowflakes and raindrops is under development at Pacific Northwest Laboratory.

of release. The rate of rainfall can also be calculated from measurements of the drop size distributions made with water-sensitive paper (see Fig. III–73). The precipitation rate, the size of raindrop, crystal type of snowflake, and electrical charges have been found to determine variations in washout rates.

The collection efficiency becomes quite small as the particle size decreases—theoretically, it goes to zero in the absence of electrical forces, and raindrops could not then scavenge submicron (less than 1/25,000-inch) particles. PNL scientists have recently measured the scavenging rate of snow and rain on such small particles (and gases as well) using the neutron activation analysis techniques described above. The washout is attributed to molecular diffusion of small particles to the drop or flake, and to attraction of electrical charges on the rain and snow. Special equipment is being developed to measure such electrical charges on individual raindrops and snowflakes, whose sizes run from $\frac{1}{100}$ to $\frac{12}{100}$ of an inch in diameter.

DEPOSITION AND REENTRAINMENT

In the absence of precipitation, and when the pollutant source is near the ground, substantial amounts of airborne material may contact and remain on the earth's surface and vegetation. The delivery of the pollutant to the immediate vicinity of the surface is a turbulent exchange process, and obeys most of the same laws that the exchanges of heat, momentum, and water vapor follow. But travel through the last few inches or fractions of an inch to the earth and vegetation is determined by an uncertain mix of settling, electrical attraction, impaction on tiny hairs and stems in the case of particles, and of molecular diffusion and chemical reaction rates with the surfaces in the case of gases.

Dry Deposition

Theories of dry deposition are still rather unsatisfactory. In field experiments, meteorologists measure a quantity called "deposition velocity," which is merely the rate at which the pollutant is deposited on an area of surface, divided by the concentration of the pollutant in the air above. Although widely used for want of a better scientific approach, the use of deposition velocity does have some weaknesses. For one thing, the concentration of the pollutant in

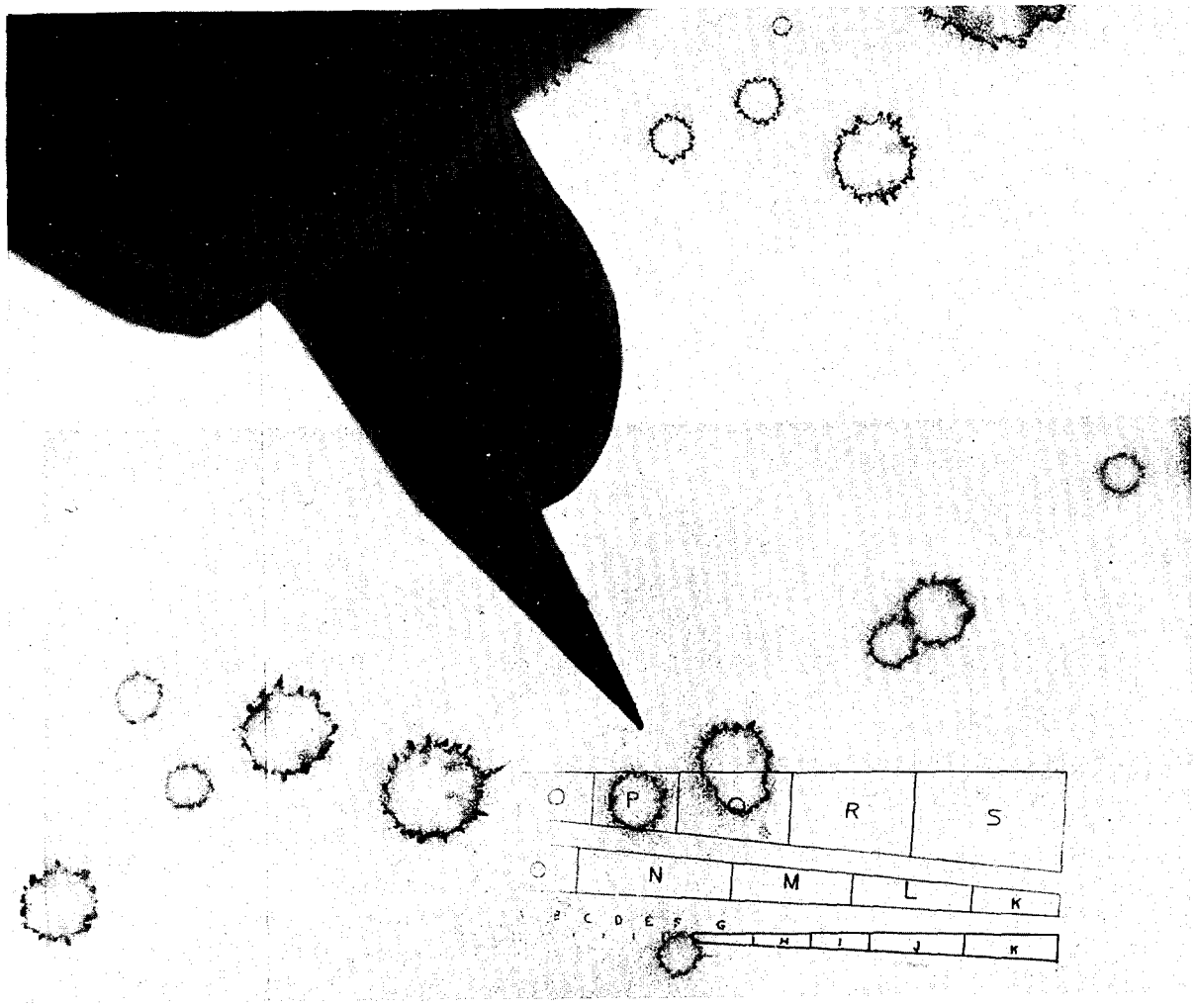

Fig. III–73. Size Distribution of Raindrops. The sizes of raindrops have been measured since before 1900 by means of the spots left on water-sensitive paper. Although modern methods include automated optical-electronic equipment, and cameras, water sensitive paper is still favored by scientists for some purposes. Here, an overlay is being used to separate rain spots into different size classes. The Pacific Northwest Laboratory uses letters rather than numbers on the overlay so as to prevent a subconscious preference for certain numbers (such as 5, 7, 10) from biasing the data. The wedge-shaped design of the overlay also reduces errors due to personal judgment. These spots are several times as large as the raindrops that made them. (This relationship was determined through laboratory tests using falling drops.) This paper is currently used only in light rains when it does not become quickly saturated. The spots can be later checked for particles "washed" from the atmosphere by the raindrops. Size distributions of raindrops obtained by this and other means are used to predict washout and radar wave reflectivity.

275–845 O—68——22

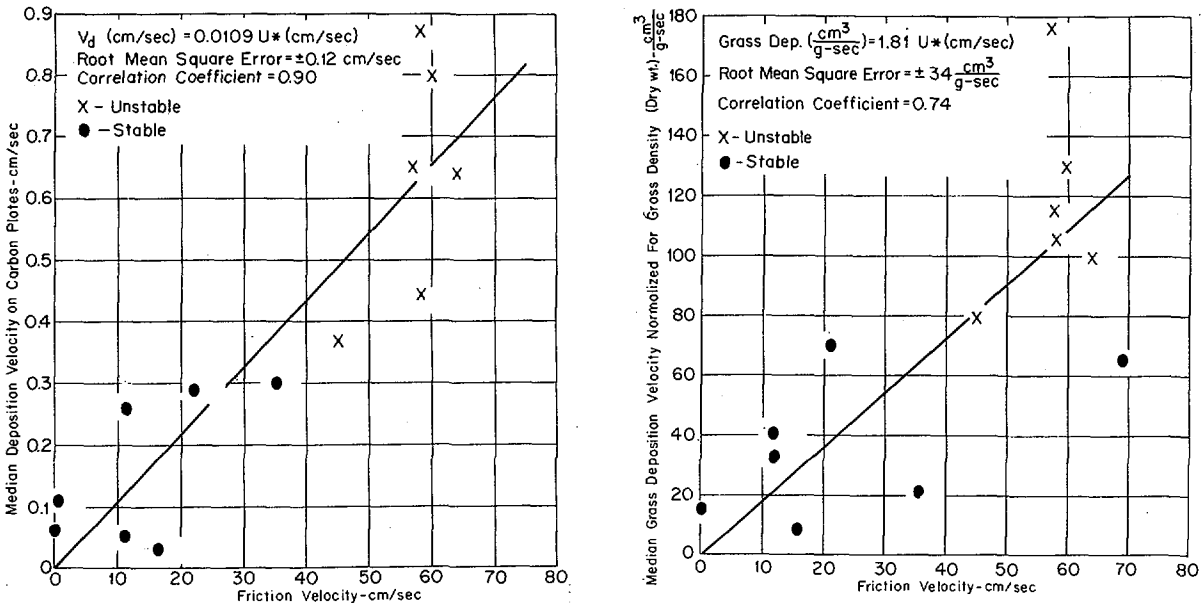

Figs. III–74 and 75. Iodine Tests at NRTS. Chart on *left* shows a scatter diagram of deposition velocity *vs* friction velocity, and the line of best fit, from data collected during experiments at the National Reactor Testing Station (NRTS) on the deposition of radioactive iodine (I^{131}) on carbon plates when released under stable and unstable atmospheric conditions. Chart on *right* shows the deposition velocity of I^{131} onto grass; it, too, appears to be linearly related to the friction velocity.

the air depends upon the height at which it is measured, and it also depends upon the distance away from the source. Secondly, the physical characteristics of most pollutants change with time and distance away from their source, becoming attached to dirt in the air, gaining or losing electrical charge, and reacting with water vapor in the air. Since the larger particles settle out nearer the source, there is obviously a change in the rate at which the remaining cloud deposits. And, strange things happen with such reactive gases as iodine, where the physical characteristics of the gas apparently change with time.

Deposition Measurement Tests

Field tests measuring the deposition velocity of radioactive iodine over pasture grass, and subsequent uptake by milk cows, have been conducted at the AEC's National Reactor Testing Station (NRTS) in Idaho, and at the Hanford operations site. Similar tests using small copper spheres, uranine dye, and pollen particles are being conducted at the Brookhaven National Laboratory site on eastern Long Island.[31]

Iodine tests at NRTS. In the field studies at the NRTS it has been found that the deposition velocity onto plates of activated charcoal is linearly related and highly correlated to the friction velocity. The friction velocity is a measure of the quantity of high frequency turbulence near the ground, and is linearly related to the average wind speed (see Fig. III–74). The deposition velocity onto grass divided by the grass density, expressed in dry weight per unit horizontal area, also appears to be linearly related to the friction velocity (see Fig. III–75).

Theoretical analyses of turbulence and air concentration profiles of iodine-131 to determine differences in the flux of momentum and of mass are also being carried out at NRTS. Interpretation of these results are complicated because neither carbon plates nor grass provide

[31] See pp. 196–208, "Fundamental Nuclear Energy Research—1965."

a perfect sink for iodine deposition. Carbon plates are about 20–30% efficient, while grass provides a variable sink which is dependent upon height, density plant metabolism, and probably other factors. Another significant finding of the NRTS field experiments is that from 30 to 50 percent of radioiodine released to the atmosphere in a gaseous form is irreversibly attached to the natural aerosol within a few seconds.

Brookhaven tests. In the Brookhaven experiments, the mean air concentration and deposition to both natural and artificial surfaces are measured simultaneously. Deposition is also calculated by computing the loss of airborne tracer material over specified distances. Measured values are usually no less than half nor more than twice the calculated values. Similar agreement is found with deposition computed using a statistical dispersion equation. Experimental results obtained indicate that deposition to a short grass-covered surface may average up to 50 percent higher than to a relatively smooth surface, such as the sticky paper and greased glass slides used as deposition collectors (see Fig. III–76).

Dispersion and deposition experiments conducted in a wooded region by BNL show that

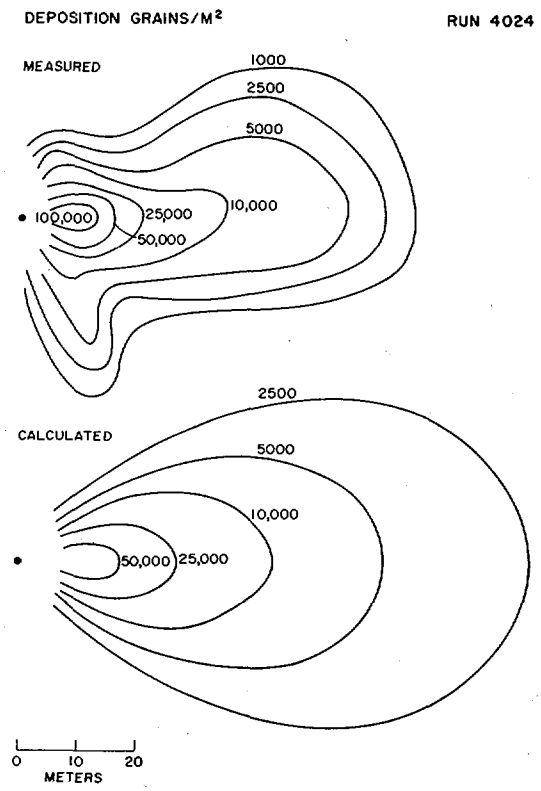

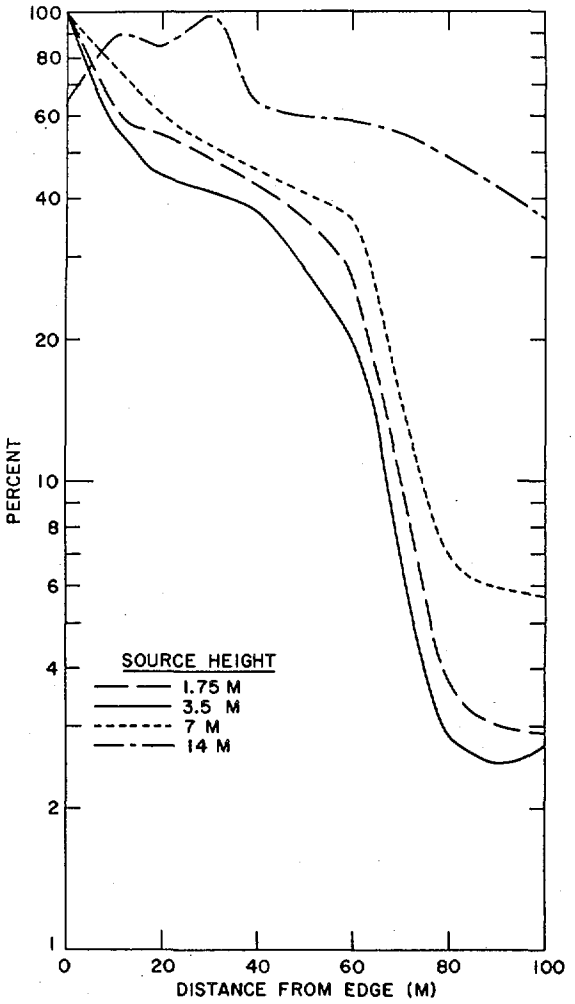

Figs. III–76 and 77. Field Deposition Experiments. At *left* are computed and measured deposition patterns from a dispersion experiment at Brookhaven National Laboratory over a grass-covered surface, using tracer particles 20-microns in diameter released from a height of 1.4 meters (4½ feet). Chart at *right*, shows the percent of 20-micron diameter particles remaining airborne while passing through or above a pine forest with 11-meter (36 feet) tall trees. The particles were emitted from four heights, as shown in the figure from a point 30 meters (98 feet) upwind of the forest edge.

particulate clouds carried into a forest are depleted at a faster rate than clouds passing over open terrain, since particles are lost by impaction on twigs and foliage as well as to the ground (see Fig. III–77). Deposition velocities calculated from field experiments are commonly several times the gravitational settling velocity of the tracer particle indicating the important role of turbulence impingement, impaction, and other nongravitational forces in the deposition process.

Pipe and duct tests. Deposition rates are also being measured within pipes and ducts by Pacific Northwest Laboratory at the Hanford site. Early theory assumes that particles move toward the wall of the tube according to the laws of turbulent diffusion, and that the tube wall holds the particles contacting it. Consequently, it is expected that the highest concentration of particles will be in the gas along the center of the tube, and that the particles will move toward the wall, according to the gradient of this concentration. With the wall acting as a perfect "sink," *i.e.*, keeping all the particles that strike it, the lowest concentration of particles in the air should be next to the wall.

For many conditions, greater amounts of particles have been observed moving down the tube very near the tube wall. This maximum near the wall was unexpected. If such a thing were to materialize, even momentarily, it should soon be destroyed by particles diffusing towards the tube center. Yet, results are quite reproducible. It is obvious that the diffusion of material from the central region of the tube to the wall cannot always be expressed by the simple diffusion of current theories. Meteorologists are not able to control all variables in the outdoors, so the hope is that laboratory tests of this type will provide clues to what occurs in the field.

The Pacific Northwest Laboratory data for particles 1/10,000-inch in size moving in tubes also suggest that all of those particles striking a plain surface do not remain, and that deposition on a tacky surface is significantly greater than for an untreated tube surface. These data show unexpectedly that for particles as small as 1/10,000-inch some rebounding or reentrainment may occur in an untreated tube. An "accommodation coefficient" appears to be required to account for these observations.

Particle Pickup and Reentrainment

Gases and particles previously in the oceans or on the earth may also become airborne through ill-defined evaporation processes, or through the dynamics of wind forces. Once airborne, they are subject to diffusion upwards by the turbulent atmosphere, and to horizontal transport by the average wind. Research on micrometeorological processes does not always require the use of tracers introduced specifically for those studies. Often, productive research can be accomplished with tracers unintentionally placed in the air. For instance, many radionuclides eventually become airborne as a result of normal reactor operations.

At AEC's Hanford plant, near Richland, Wash., water from the Columbia River is used as a reactor coolant, and then is retained in cooling ponds for a time before its return to the river. Air sampling studies by PNL have shown that not only do some of the gases in the water become airborne, but also some of the solid materials. Although these are in quantities too small to present health hazards, sophisticated counting equipment can measure their relative amounts. These include radionuclides without gaseous parents (manganese-56, sodium-24, zinc-65, copper-64, chromium-51, lanthanum-140, scandium-46, and cobalt-60), and radionuclides with gaseous parents (barium-140, cesium-137, and cesium-138), as well as gaseous radionuclides (iodine-133, iodine-134, iodine-135, and chlorine-38). Their physical and chemical forms have been studied in air samples taken at distances of 50 to 1,000 meters (160 to 3,200 feet) from the ponds.

The relative concentrations of the solid radionuclides in the air compared to their concentrations in water varied by as much as 1,500 times. Typical enrichment factors in air, using manganese as a base of comparison, are:

Manganese	1 time
Sodium	2.7 times
Arsenic	10 times
Zinc	40 times
Copper	100 times
Chromium	100 times
Lanthanum	400 times
Scandium	900 times
Cobalt	1,500 times

Future studies on the comparative evaporation of iodine, bromine, and chlorine from the same cooling basin may provide insight into why the concentrations in air of these three halogens are not in the same proportion as found in the sea—a question of current interest in precipitation scavenging research.

DATA COMPILATIONS

The bahavior of pollutants in the atmosphere is theoretically determined by numerous micrometeological parameters, *e.g.*, small scale variations in wind, temperature and energy. The AEC has had a continuing program of measurement on a number of these parameters since the 1940's and a large mass of data has been collected, processed to some degree, and stored for possible future use.

Site Data Accumulations

Each of the AEC's Laboratories has an accumulation of meteorological data peculiar to its own site, but in some ways similar to that at other sites. In a typical 20 minutes of record taken at Argonne National Laboratory, 6,000 measurements of wind direction, speed, and temperature can be extracted and processed by an electronic computer. The computer supplies graphic representations of the high frequency air motions in the form of "power spectra" of the wind and temperature. These power spectra are related to the friction of the air over the earth, and to the evaporation of water bodies, as well as to the rate of spread of pollutant plumes and puffs.

An example of the wealth of information available in these archives is provided by a dew point study conducted at Argonne. Figure III–78 shows the diurnal (daily) changes in the wind, temperature, dew point, and radiation (sunshine) for a few days' period. It is obvious that these variables are interdependent. Some of these changes are related to the loss of moisture from vegetation.

Similarly enormous volumes of data are collected on magnetic tape at the Brookhaven National Laboratory, partially processed by a computer, studied and then stored for possible future use. Studies are continuously underway to find better ways of grouping, classifying, and presenting such data.

Typical Use of Stored Data

An example of the use that can be made of long records of data is the prediction of the probability of extended periods of extremes or of unfavorable weather conditions. In the case of reactor hazard evaluation, satisfactory engineering solutions are available for the prediction of the hourly mean concentration from a continuous point source, based on field tests of diffusion for relatively short periods. However, it is not practical to conduct field tests for long time periods, so that meteorologists resort to a simple technique for estimating dosages for long-time periods, using the data taken in field tests over short periods. This technique involves calculating the concentration for the shorter periods of interest, and expanding the evaluation in time by summation of successive periods. The variability of wind direction, wind speed, and dispersion conditions is thus completely taken into account and an average dispersion climatology may be developed.

However, this technique cannot be readily used in estimating the worst possible conditions that might accompany a release of material, either accidental or routine, due to the limitation of available data. For periods up to 7 hours, it may be assumed that extremely adverse dispersion conditions could exist from any direction, but for longer periods that assumption is

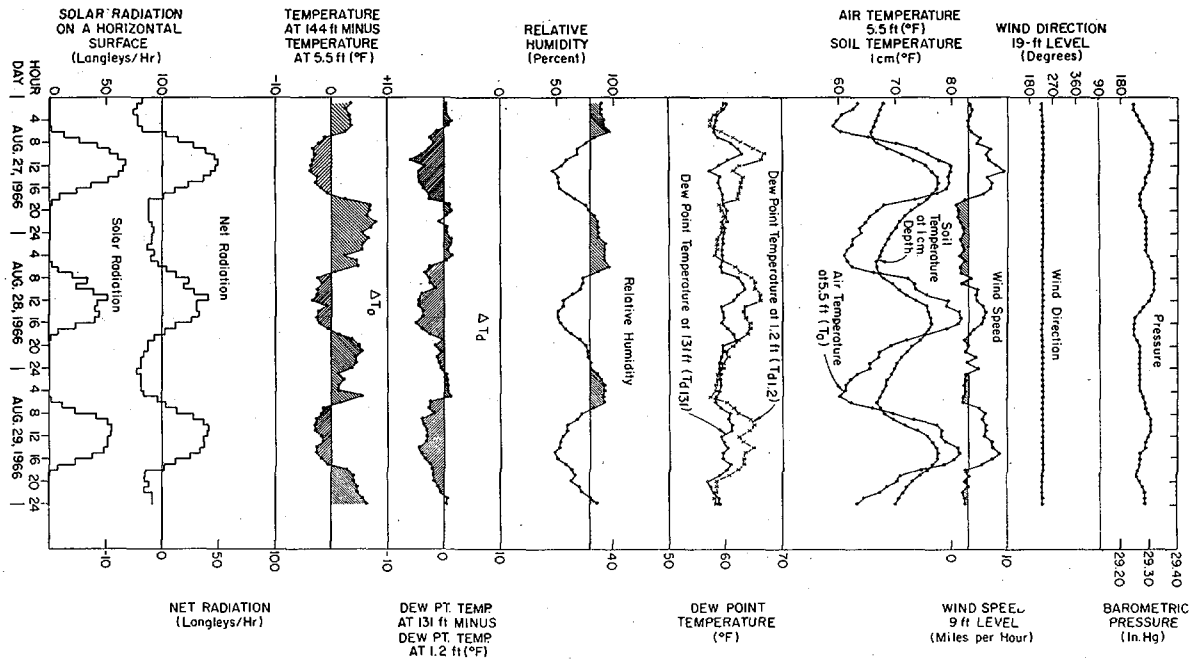

Fig. III–78. Portrayal of Micrometeorological Data. Large quantities of measurements of meteorological variables are computer processed and stored at the AEC's national laboratory sites. The interrelationships of these variables is demonstrated in these Argonne National Laboratory graphs of the dew point, temperature, wind, and solar radiation (sunshine) and other variables over a several-day period in 1966.

unrealistic, and the least favorable conditions are usually determined by the lack of variability in the wind direction.

The most common expression of direction variability is "persistence," in which the number of consecutive hours where the wind remains in some preselected annular direction sector is tabulated. This method can fail to indicate the extent of a given hazard, since the deviation of the wind from a given sector for an hour effectively ends a period of persistence even though the wind can resume the same direction immediately thereafter. To handle this failing, BNL meteorologists have applied the evaluation technique called constantly (steadiness) as a tool to indicate clearly the fluctuations of wind direction as a function of time with their associated probability of recurrence.

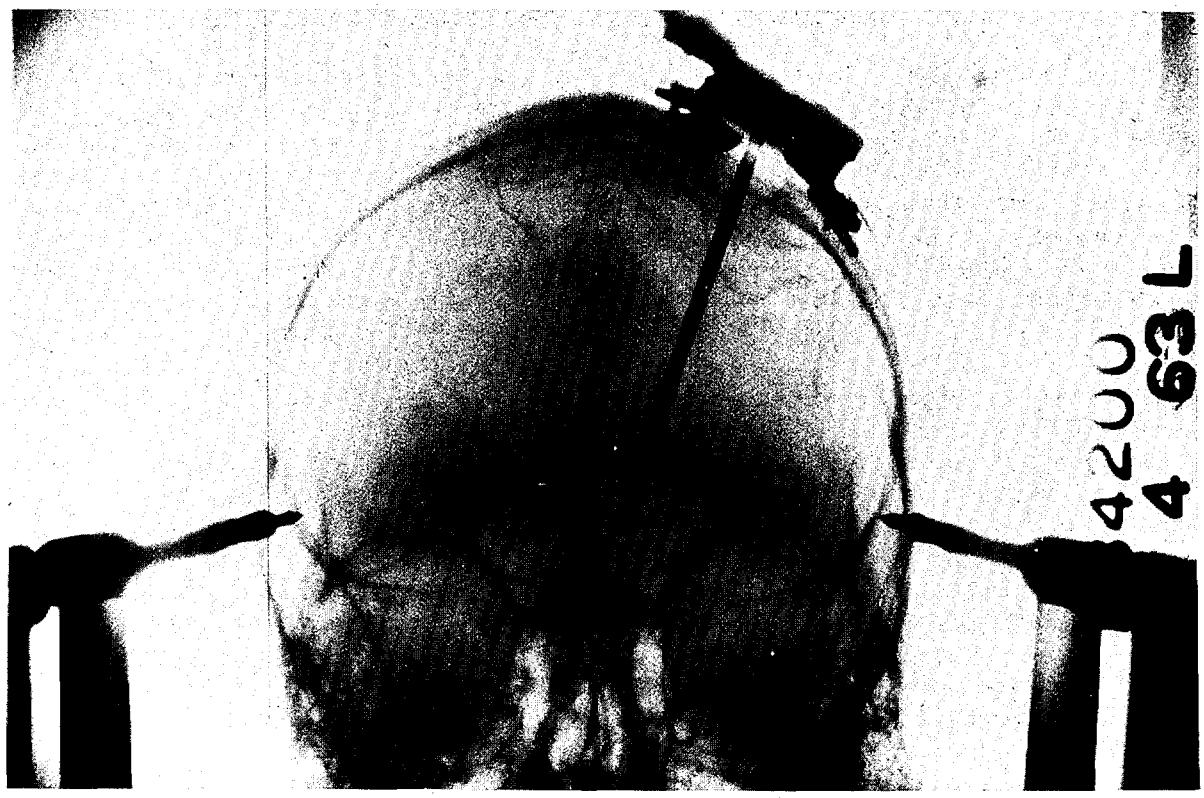

Fig. III–79. Brain Tumor Probe. The X-ray photograph shows a rigid silicon, beta-sensitive semiconductor detector probe placed in a patient with a malignant glioma (tumor) of the brain. The probe, developed by Solid State Radiations, Inc., Los Angeles, is undergoing evaluation at the University of California at Los Angeles and can accurately indicate the boundaries of a tumor as it passes through it. Little or no damage is done to the brain cells by the probe. See page 329 for details.

SEMICONDUCTOR DETECTOR APPLICATIONS

Semiconductor detector programs have been conducted by the AEC for several years because of their potential value for applications in biology and medicine. The smallest sizes possible are valuable for use as probes and implantable detectors for both clinical and experimental use and the considerably increased energy resolution can be applied to the analysis of radioactive materials. Except in situations wherein the environment of the early delicate detectors could be carefully controlled, *e.g.*, counting prepared radioactive samples, biomedical applications have been slow to develop, while applications in the physical sciences have been widespread since the first primitive detectors appeared. Exploitation and evaluation of semiconductor detectors from the biomedical programs by the physical scientists has, however, allowed the art to so advance that many valuable biomedical applications are now being developed.

SEMICONDUCTOR DETECTORS

A semiconductor is a material such as silicon or germanium through which the flow of electric current is extremely small compared to conductors like copper. However, this current is not absent as it is in insulators. Nuclear radiation such as an alpha particle absorbed by semi-

conductor materials causes the release of positive and negative electric charges within it. If an electric field is present, the charges released by the particle momentarily increase the flow of electric current, thus, providing a radiation detection mechanism. This situation is a solid state counterpart of the more familiar gaseous counter, wherein radiation causes the dissociation of gas molecules into positive and negative charges. The semiconductor radiation detector has the advantages of greater radiation absorption efficiency and mechanical simplicity.

Early attempts to develop "solid ionization chambers" were unsuccessful because the conductivity of the impure semiconductors then available resulted in background leakage currents that completely masked the signal pulses generated by radiation interactions in the detector materials. Other objectionable characteristics attributable to chemical impurities and crystalline imperfections caused these attempts to be abandoned. In recent years, single crystals of silicon and germanium have been produced of purity and crystalline perfection many times better than other available materials. However, at room temperature the conductivity of even these materials still produced excessive leakage currents.

Positive-Negative Charge Junctions

A technique that reduces the intrinsic conductivity problem has been successful in semiconductor detector fabrication. This method depends upon the controlled addition of small amounts of impurities into a sample of silicon or germanium so that the specimen is divided into two regions that differ in their electrical natures. This type of structure comprises what is termed a reverse-biased diode. If, in a silicon sample, impurity atoms such as boron are present (which are electron deficient relative to silicon), then an excess positive charge exists and an increased conductivity because of these charges is observed. Such material, exhibiting conductivity due to an excess of positive charges, is termed "P" (positive)-type material. However, if an excess of impurity atoms such as phosphorus is present (which have one more valence electron per atom than silicon), then a "N" (negative)-type silicon is obtained, wherein conductivity results from excess electrons. The reverse-biased diode type semiconductor detector is simply a specimen of silicon or germanium—typically disc shaped—wherein one section is "N"-type material in junction contact with a "P"-type section. This configuration is called a P–N junction. Diffused junction detectors are fabricated by exposing a specimen of, say, P-type silicon to an impurity dopant, *e.g.*, phosphorus, which will diffuse into the base material a short distance and establish a thin N-type layer. Excess of N-type material is removed so that the remaining layer is very thin. The junction is formed at this interface between the P-type base and the N-type layer.

P–N Pairs Created by Radiation

Electrical contacts are applied to each section and a potential difference is applied across the P–N structure so that the excess electrons in the N-type material and the excess positive charges in the P-type material are drawn away from the junction between the two types of material. A so-called depleted region is thus established in which an electric field exists when voltage is applied, similar in function to the sensitive volume of an ionization chamber (see Fig. III–80). Radiation entering the depleted region creates positive-negative charge pairs by ionization and the collection of these charge carriers produces the electrical signal as in an ionization chamber. However, the depth of the depleted region is limited in such detectors to about 1 millimeter because of residual leakage current. The principal origin of this leakage current is the detector surface and the control of such current "noise" has been one of the major research and development problems. However, even if surface leakage currents could be controlled, the relatively small amounts of impurities remaining in the available silicon would permit volume leakage currents sufficiently high to allow only thin

detectors to be made. The thin detectors are useful for alpha and moderate energy beta ray detection, and spectroscopy of some environmental and biological samples. However, they were not satisfactory for use as efficient gamma-ray detectors needed to analyze mixtures of environmental radioactive contamination and low-level radioactivity studies in both environmental and biological systems.

Historical Aspects

Program Initiated in 1958

A semiconductor radiation detector program for eventual biomedical use began at Oak Ridge National Laboratory (ORNL) shortly after the successful application of germanium junctions to a nuclear physics experiment at ORNL in 1958. An additional program was also estab-

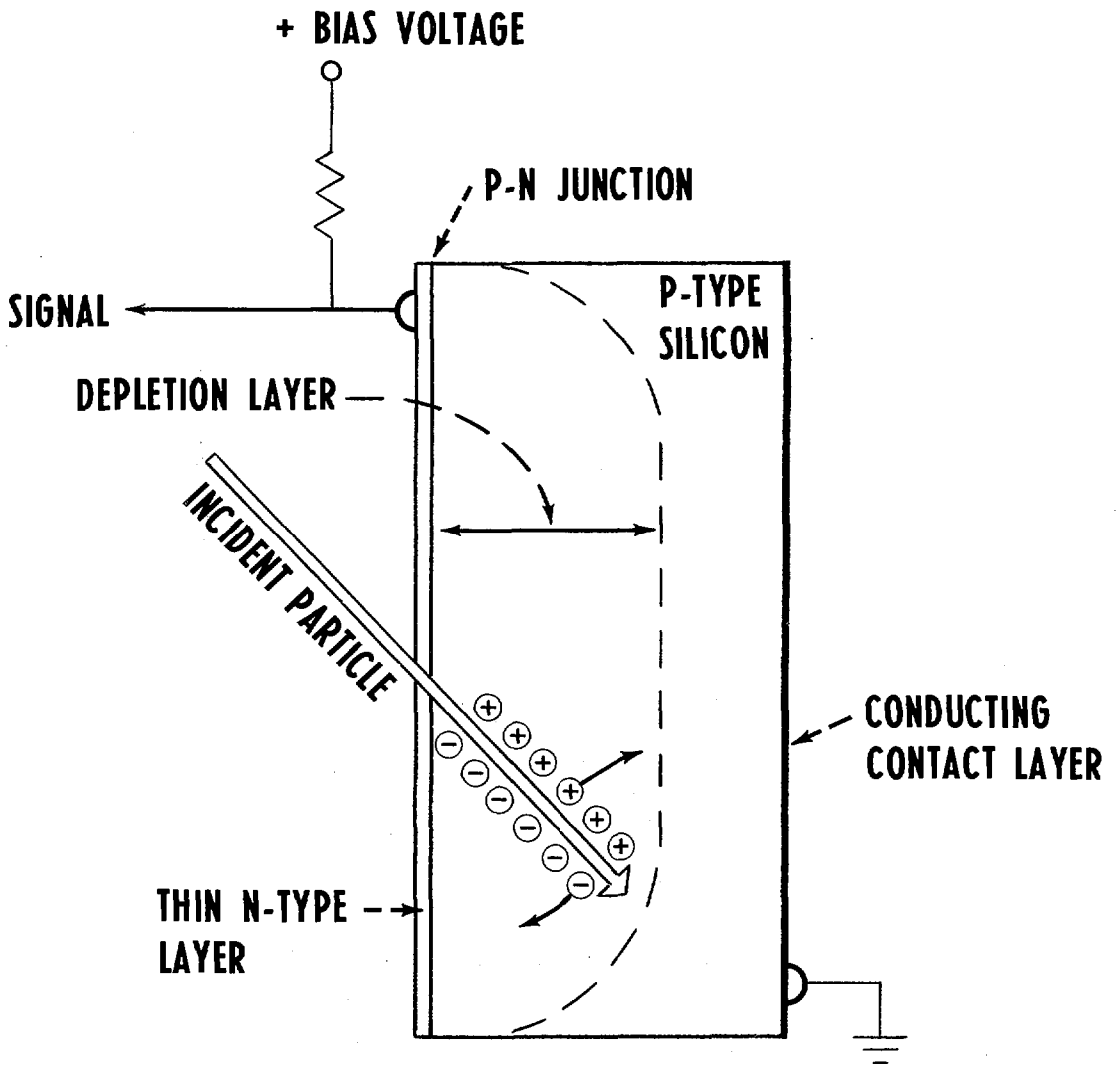

Fig. III–80. Functional Diagram of a Semiconductor Detector. During operation of a semiconductor detector, an electric field sufficient for the collection of charges released by incident radiation exists only in the depletion layer. The depletion layer depth depends on the value of externally applied bias voltage. Radiation reaching the depleted region from a source external to the detector creates positive-negative charge pairs by ionization; the collection of these charges produces an electronic signal indicating the detection of radiation.

275–845 O—68——23

lished at Brookhaven National Laboratory, which for a number of years was carried on jointly with the Bell Telephone Laboratories (BTL) at Murray Hill, N.J. These programs concentrated on study of the basic detector phenomena and the development of improved detectors and advanced circuitry. Biomedical applications of the technological advances at the AEC's national laboratories have often been carried on in off-site cooperative programs between commercial laboratories and appropriate biomedical investigators.

In 1962, it was shown that the few positively charged impurities remaining in high purity P-type silicon could be compensated for by drifting lithium through the lattice under an applied electric field which made it possible to obtain sensitive volumes of one centimeter or more in depth. The lithium atom acts as a singly charged electron donor which drifts with high mobility through the silicon crystal lattice. The lithium ions remain in the vicinity of acceptor (positively charged) sites as they are encountered and very effectively neutralize their electrical activity. At Brookhaven, the relevant parameters involved in this process were analyzed and apparatus was developed to drift the lithium at the most efficient rate. Germanium, the only other semiconductor material that has been developed to a very high degree of purity, is a heavier element and so more suitable for gamma-ray detection. However, at room temperature it has a very large leakage current and must be operated at liquid air temperature to function as a detector. This requirement precludes its use at present for many purposes, such as *in vivo* detectors. As for silicon, lithium compensation of the residual imperfections is necessary in germanium.

Since the drift rate becomes slower as the thickness of the compensated region increases, It is not practical to drift lithium more than a centimeter or so. Large volume detectors however, have been made at Argonne and Brookhaven National Laboratories by drifting lithium from the surface of a cylinder toward the center, leaving an axial core of uncompensated material. An alternative method of producing a fully compensated thick detector was initiated in 1966 at Argonne, where lithium was drifted from one side toward the center; then, after reversing the contacts, lithium was drifted from the opposite side until the two compensated regions met. At Brookhaven, the same effect was accomplished by performing the drift under an applied alternating electric field so that the drift proceeded from the two faces toward the center on alternate phases of the applied a.c. voltage.

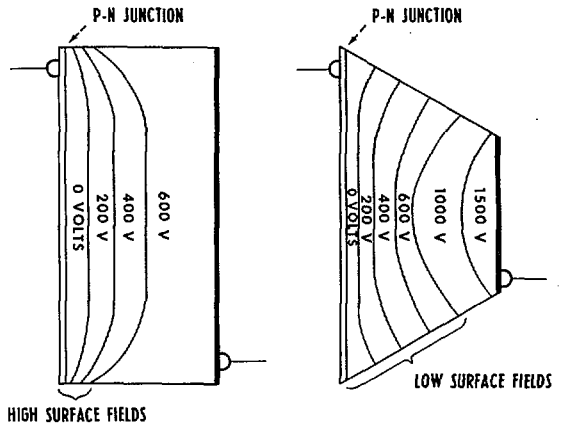

Fig. III–81. Contoured Amplifying Detector. The drawings show the effect of contouring on surface electric fields to reduce spurious electrical noise pulses in diffused junction detectors. The one on the *left* illustrates qualitatively the distribution of voltage levels in a detector such as shown in Fig. III–80. Close spacing of voltage levels at the surface indicates a concentration of high surface electric fields at the P–N junction. These high fields limit the voltage that can be applied without causing electrical breakdown. Drawing on *right*, illustrates the change in voltage distributions at the contoured surface, which results in substantially lower surface fields in the vicinity of the junction. Consequently, much higher external voltages can be applied without causing excessive surface breakage currents or electrical breakdown. The contouring approach was developed for the AEC by General Electric's Missile and Space Division, King of Prussia, Pa.

Amplifying Detectors

In 1963, an AEC-supported program was initiated at the General Electric Missile and Space Division, King of Prussia, Pa., to investi-

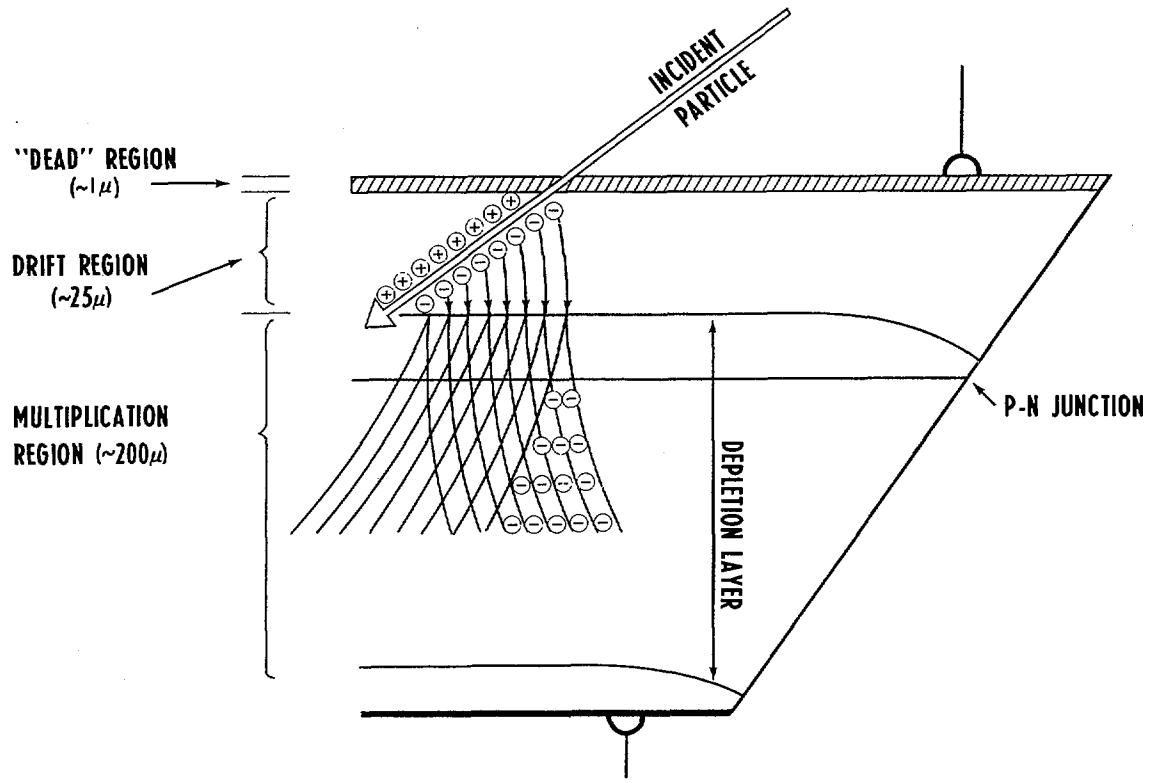

Fig. III–82. Contoured Avalanche Principle. Drawing illustrates the multiplication process in a contoured avalanche detector. Electrons originating in the "drift" region are moved to the depletion layer by a small but effective electric field arising from a gradient of positively charged dopant atoms. The large electric field existing in the depletion layer accelerates the electrons sufficiently to form an avalanche output pulse containing up to 1,000 times the original input charge.

gate a method of reducing surface noise currents in diffused junction detectors. For a variety of reasons, the exposed edge of a junction detector usually has physical and chemical characteristics that differ from the interior bulk material. These differing surface states generally distort the shape of the depletion region such that high electrical fields at the surface are concentrated near the P–N junction. This situation limits the amount of voltage that can be applied to create a depletion region and also causes the detector surface to be the principal source of spurious electrical noise pulses. The approach investigated by General Electric involved mechanically shaping the detector edge so that the maximum surface field would be moved away from the P–N junction (see Fig. III–81).

A series of discoveries resulted which led to the development of a unique thin silicon detector which exhibits controlled internal amplification. That is, charges released in the detector by, for example, a 20-kev. (kilo electron volts) electron are multiplied within the detector up to a thousandfold, so that the output signal would be equivalent to that of a 20-Mev. (million electron volts) particle deposited in a conventional nonamplifying detector.

The mechanism of the contoured avalanche amplifying detector is shown in Figure III–82. At the surface, a dead region, approximately one micron in thickness, exists which remains nearly constant for each detector regardless of the depth of the junction, indicating that the dead layer results from a surface recombination effect.

The "drift" region, approximately 25 microns thick, contains the gallium that was diffused into the base material to form the P-type section. The diminishing density of positively charged gallium atoms provides a low value electric field which is sufficient to move electrons released by radiation in the drift region toward the multiplication region.

In the junction space charge or multiplication region, a very high electric field exists because of the application of approximately 1,500 volts from an external power supply. The acceleration of electrons appearing in this high electric-field region is sufficient to cause them to release a few additional electrons at first and then an avalanche of electrons; thus a build-up occurs as they proceed toward the back contact of the detector. The magnitude of the resulting output pulse, however, depends on the path length of the electrons in the multiplication region. Thus, the charge deposited near the drift region is muliplied to a greater extent than that deposited farther back in the multiplying region. Because of this, random noise pulses—from thermally excited single electrons originating throughout the detector—are very seldom large enough to be mistaken for signal pulses caused by radiation interactions in or near the drift region.

This phenomenon allows detection of small numbers of very low-energy radiation interactions in the presence of significant noise levels. It is through use of this effect that it has been possible to detect very low-energy radiation such as 0.6-kev. oxygen fluorescence X-ray interactions using external amplifiers with noise levels equivalent to 10-kev. The detection efficiency for low-energy beta radiations of biologically significant materials such as those from tritium and carbon-14 has been investigated. Tritium detection efficiency which is found to be low because of the remaining one-micron thick surface dead layer, is of limited use at the present time. For higher energy beta emitters such as carbon-14, however, the efficiency is at least 50 percent, which is of considerable value.

CURRENT APPLICATIONS

Advances made in performance and stability of semiconductor detectors and associated circuitry and the appearance of larger-volume detectors in recent years have permitted the development of devices designed primarily for applications in biology and medicine. A program at the Lawrence Radiation Laboratory, Berkeley, was established in 1966 for general studies of semiconductor biomedical applications. Other more specific developments have been undertaken in several laboratories. A representative selection of such programs is described in this section.

High Speed Digital Counter

The amplification of the contoured detector under development at the General Electric Co. has made possible the development of a miniature detector-tunnel diode unit that can furnish sufficiently large signals for direct use by oscilloscopes and scalers.

A tunnel diode is a tiny solid state amplifying device which has a minimum sensitivity equivalent to about the amount of charge released in silicon by a 500-kev. particle. It has been demonstrated that amplification by the contoured detector makes it possible to activate the tunnel diode for particles with energies as low as 300 ev. The output pulses of the tunnel diode are identical regardless of the pulse size delivered to it by the contoured detector. The result is a simplified digital detection system analogous to a *Geiger* counter, but, in addition, it is capable of extreme speed. For example, signals from low-energy X-ray interactions can be detected and amplified in a unit less than 1 cubic inch in volume with counting rate ability shown to be in excess of 10 million per second. An extremely useful aspect of the detector-tunnel diode combination is that the internal thermally excited noise pulses in the silicon detector are not amplified sufficiently to trigger the tunnel diode amplifier. Consequently, this unit is an essentially noise-free detector of even

very low-energy interactions. Applications of this instrument are shown in Figs. III–83 and 84.

Gamma-Ray Area Monitor

The General Electric Co. has also collaborated with the Atomic Energy of Canada, Ltd. (AECL) in the evaluation of contoured amplifying detectors for health protection applications.

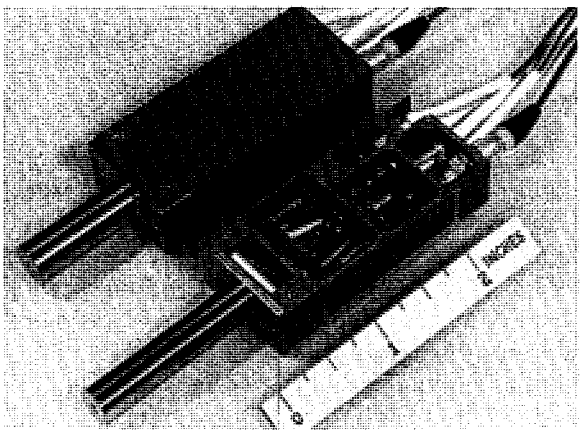

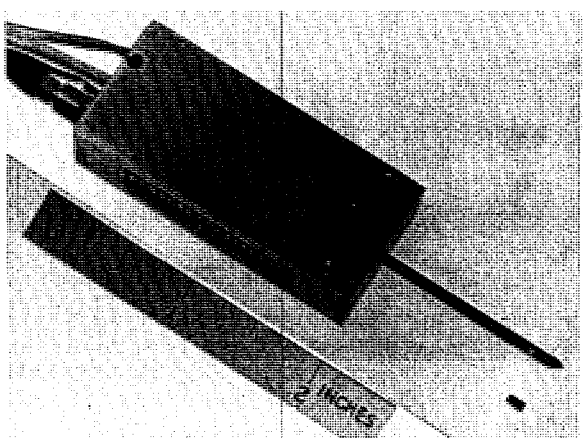

Fig. III–83 and 84. Noise-Free Detectors. By combining the high degree of amplification as obtained by contoured P–N junctions with tiny solid-state amplifying devices (tunnel diodes), the General Electric Co. has developed noise-free semiconductor detectors. Photo *above* shows a probe designed for *in vivo* studies utilizing low-energy radiation emitting isotopes which is being evaluated at the Pacific Northwest Laboratory and the University of Washington. The photo *below* is a probe designed by General Electric in collaboration with PNL for locating plutonium-239 embedded in wounds. An avalanche detector (small dark square in photo) is shown near the end of the probe to show its size and shape.

The AECL has developed a device utilizing the contoured detectors which monitors gamma-ray dose rates from two *millirad* to 2,000 *rad* per hour, with both logarithmic and linear display. The response of the monitor, as a function of photon energy, is designed to match the tissue absorbed dose from 30 kev. to 1.5 Mev.

In Vivo Plutonium-239 Mapping

An assessment of the total amount of plutonium-239 contamination in a wound can be made adequately by several methods. If the level of contamination is high enough to require removal, however, there is no satisfactory way of mapping the distribution of contamination within a wound nor of locating tiny particles that must be removed surgically. The application of semiconductor detectors to this important problem is being investigated at several laboratories.

At the Pacific Northwest Laboratory (PNL) semiconductor detectors are being used as spectrometers to estimate externally both the amount and depth of plutonium in wounds. The three low-energy X-rays, 13, 17, and 20 kev., associated with the decay of plutonium-239 are well resolved with these detectors and their relative attenuations, as a function of depth in tissue, permit depth estimates. The attenuation of the 13-kev. X-ray in tissue is about three times greater than that of the 20-kev. X-ray; therefore, the relative counting rates of these two photons define the depth of a point source or the average depth of a source spread in the wound. Figure III–85 illustrates the attenuation of the plutonium X-rays produced by various thicknesses of tissue equivalent absorbers. From the relative peak heights of the 13 and 20 kev. plutonium X-rays, the depth of deposition of plutonium in the wound can be estimated. In Figure III–86 the ratios of the 13 and 20 kev. peaks are plotted as a function of tissue absorber thickness and show a linear relationship between these ratios and tissue depth.

Because the internally amplifying detectors developed at the General Electric Co. are especially sensitive to low-energy X-rays and also retain their virtually noise-free operation at elevated temperature, their use inside living systems for plutonium-239 detection is being explored at PNL and at Argonne National Laboratory (ANL). The intrinsic efficiency of these detectors is about five percent for the 17-kev. average X-ray from plutonium-239 which is useful in treating plutonium-contaminated wounds. If this efficiency can be improved, these detectors would also be useful for kinetic transport studies in experimental animals wherein extremely small amounts of plutonium are used.

A wound probe has been developed by General Electric in collaboration with PNL for use in precise location of plutonium embedded in tissue (see Fig. III–84). The internal amplification feature of these detectors when used in conjunction with a tiny tunnel diode amplifier makes additional amplifiers unnecessary. Consequently, it is also feasible to use them in arrays. Such an array is under fabrication for use at the Pacific Northwest Laboratory in mapping plutonium-239 distributions in wounds prior to surgery.

Blood Flow Studies

Gastrointestinal tract. Detectors have been developed at the Lawrence Radiation Laboratory (LRL), Berkeley, for use in gastrointestinal tract studies at the University of Minnesota (Minneapolis) for the purpose of measuring blood flow. They have been made small enough to swallow so that it is possible to measure radioactivity that has been injected into a vein and is then carried to every part of the gastrointestinal tract by the blood. The detectors have been used to study the effect of a disturbed blood supply on the origin and pathological consequence of dis-

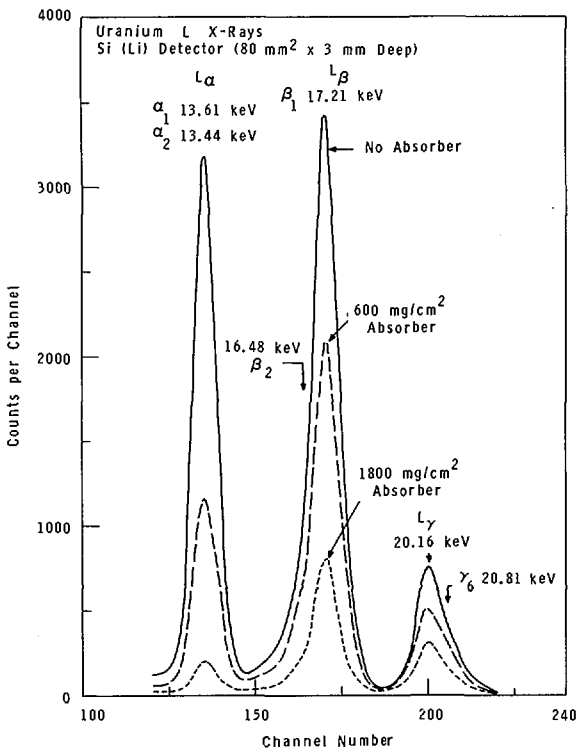

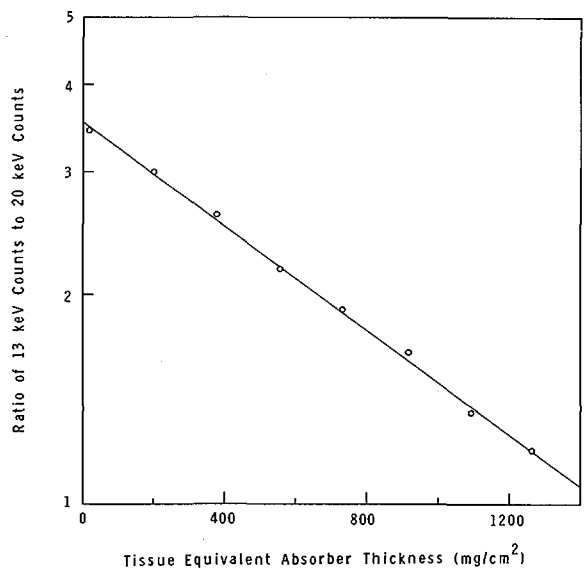

Figs. III–85 and 86. In Vivo Plutonium-239 Mapping. Semiconductor detectors are in use at the Pacific Northwest Laboratory for externally estimating both the amount and the depth of plutonium-239 (Pu^{239}) in wounds. On *left* is a Si(Li) diode spectra showing the attenuation produced by tissue equivalent absorbers in the X-rays emitted in the decay of Pu^{239}. On the *right* is the ratio of the observed intensities of the 13 and 20 Kev. X-rays, emitted in the decay of Pu^{239}, to the thickness of a tissue equivalent absorber.

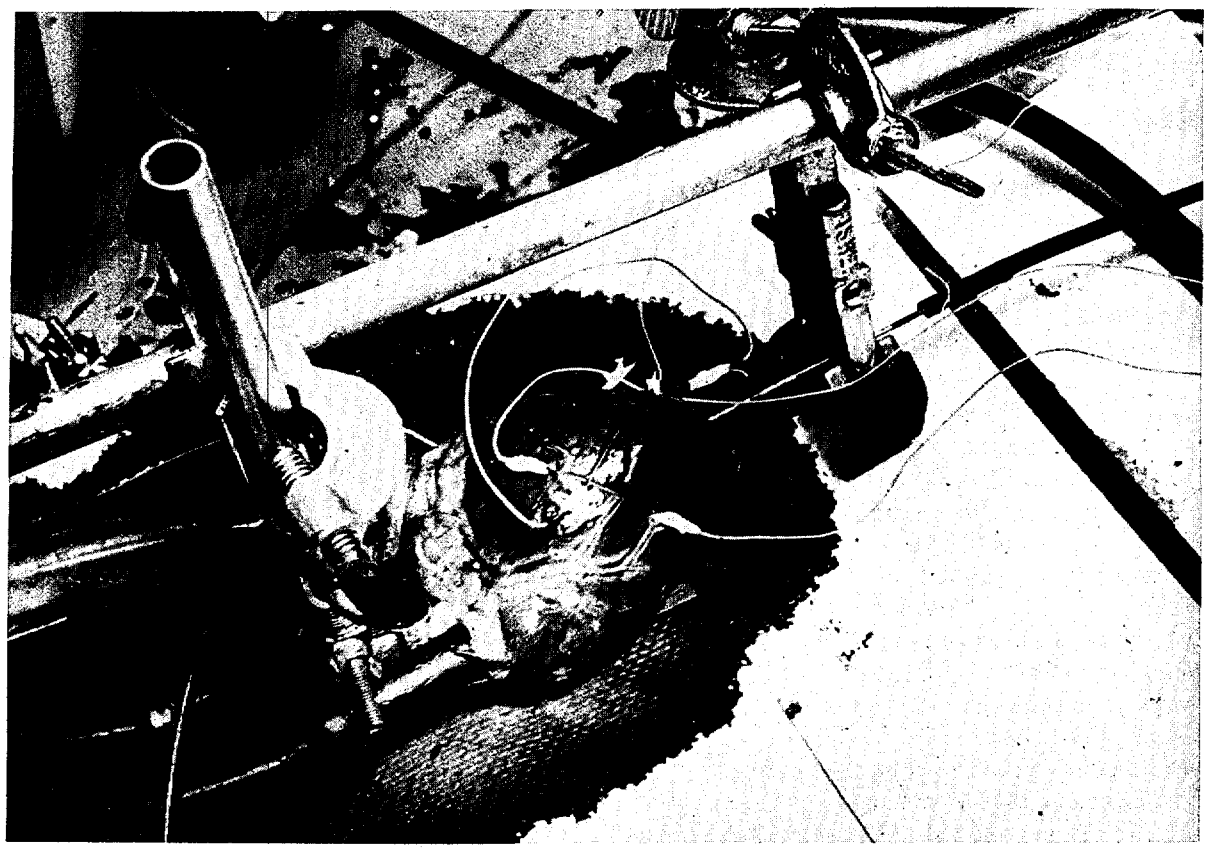

Fig. III–87. Heart-Region Detectors. Semiconductor detectors have been developed at Lawrence Radiation Laboratory, Berkeley, and the University of Minnesota for use in coronary blood flow studies. In photo, detectors are shown on surface of a functioning exteriorized dog heart. They are being used in studying the effect of changes in coronary blood flow and heart metabolism on the working capacity of the heart.

ease of the bowel. The use of semiconductor detectors allows measurements of the amount of blood that comes to any region of the bowel and its distribution in the various tissue layers by measuring changes in the pulse height spectrum. The use of remote detection of signals from a swallowed detector may also pinpoint bleeding sites within the bowel.

Heart regions. Detectors have also been developed at LRL, Berkeley, and the University of Minnesota for direct measurement of regional coronary blood flow at several regions of the heart simultaneously (see Fig. III–87). They are used in studying the effect of changes in coronary blood flow and heart metabolism on the working capacity of the heart. Over a wide range, it has been found that heart metabolism (as influenced by coronary blood flow) is a critical primary determinant of heart performance. It seems likely that the mechanism for this effect is related to the fact that coronary blood is not homogeneously distributed to the heart, but rather that some areas of the heart are less perfused with blood and do not contract fully, if at all. When coronary blood flow is increased, perfusion of these poorly contracting regions is improved and they are recruited into a stronger contraction. The distribution of coronary flow under altered conditions of flow and load have been studied with a double-label isotope technique (using potassium-42 and rubidium-86) in

the isolated heart and the data tend to support the hypothesis.

A probe has been constructed by the General Electric Co. incorporating amplifying detectors (see Fig. III–83) for use in blood flow studies, iron metabolism and, in general, laboratory and clinical situations where a low-energy emitting isotope such as iron-55 (5.9 kev.) would be useful. Initially, these probes are for evaluation at the Pacific Northwest Laboratory and at the University of Washington at Seattle.

Brain tissue. It is generally thought that blood flow within different parts of the cerebral tissue is regulated by the metabolism of the tissue itself. Measurements of blood flow in specific areas of the brain should, therefore, give information about the metabolism of the part studied. Some knowledge of regional blood flow has been obtained in the past from studies of cerebral structures that are accessible to detectors used at the surface. A method that was used in Norway involves monitoring the brain tissue clearance of xenon-133 or krypton-85 with external counters. Following injection into the carotid artery, either xenon-133 gamma activity from a portion of the brain or krypton-85 beta activity from superficial layers of the cortex can be recorded. Since a number of important neurological diseases are caused by subsurface disturbances, more refined methods for quantitative measurements in the depths of the brain are necessary. Observations of less accessible locations require semi-permanently implanted detectors which are sensitive primarily to beta particles so that the clearance curve obtained relates only to the circulation in the immediate vicinity of the detector. An investigative study is being carried on by AEC-supported groups in Oslo, Norway, and Lund, Sweden—in cooperation with Solid State Radiations, Inc., Los Angeles—to provide blood flow information at the same sites now being investigated by semi-permanently implanted voltage recording electrodes, in connection with the treatment of *Parkinson's* disease.

Semiconductor detectors in the form of cylinders one millimeter (0.0394-inch) in diameter and three millimeters in length have been prepared with platinum iridium leads soldered directly to the silicon contacts. Detector and leads are protected from contact with body fluids by deposition in high vacuum of a long-chain polymer of paraxylylene, which has proved resistant to the penetration of water (see Fig. III–88). An implantation of one of the small detectors was made in the thalamus of a cat during November 1966 in a Swedish experiment. Four months later the leads to the detector were extracted and connected to a recording system. When krypton-85, the radioisotope used, was injected, the normal clearance curve rate was observed, *i.e.*, the clearance rate was identical to that obtained by an external *Geiger-Mueller* counter, confirming the complete recovery of the condition of the thalamus.

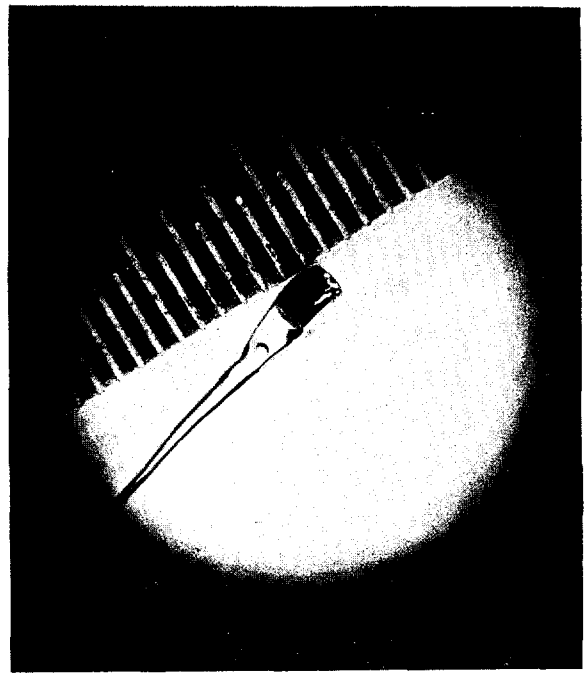

Fig. III–88. Brain Tissue Probe. Photomicrograph shows a miniature silicon detector developed by Solid State Radiations, Inc., Los Angeles, for brain implantation to allow blood flow studies. The scale shown is in millimeters (1 mm.=0.0394-inch). The platinum leads are soldered directly to the silicon contacts and the detector is covered with a long-chain polymer (paraxylylene) to protect it against body fluids. Data obtained with this tiny probe are as good, if not better, as those obtained by larger, more cumbersome methods.

If a clearance rate curve is obtained immediately upon implantation of the detector, abnormal circulatory patterns are observed. Thus, by following the procedure of implantation of the miniaturized semiconductor detectors, allowing for the recovery of the surrounding tissue and then using beta emitters, it is possible to obtain data on the circulatory system deep in brain matter and to locate defects in the circulation pattern.

Tumor Studies

Brain tumor localization. Probes incorporating beta sensitive semiconductor detectors have been developed at the Solid State Radiation, Inc., and evaluated at the University of California at Los Angeles (UCLA) Medical School for use in brain tumor surgery. Their use is based on the observation that phosphorus-32 concentrates relatively more in active brain tumors than in adjacent normal tissue. Because of this, a beta sensitive semiconductor detector probe inserted into the tumor site can indicate the boundaries of the tumor as the probe passes through it. Accurate tumor location is especially helpful where it is necessary to remove a sample of tumor material for microscopic study.

A small hole is drilled into the cranium under local anesthetic and a semiconductor detector of one to three millimeters in diameter which has been incorporated into the end of a hypodermic needle is used to probe the suspected volume of brain tissue for the presence of the radioactive isotope. Little or no damage is done to the brain cells with the use of such a probe. For normal cells, a count rate of five counts per minute is observed; upon entering the tumor tissue the count rate jumps to 100 to 300 counts per minute. By noting the length of the needle inserted, and the angle of insertion, the precise location of the tumor is determined.

Figure III–79, page 319, shows an X-ray photograph taken during biopsy on a patient with a malignant tumor (glioma) of the brain. The biopsy specimen was taken at a depth of five centimeters after final tumor boundary was determined by the silicon junction detector probe.

Neutron-capture therapy. Neutron-capture therapy is a technique for the possible destruction of brain tumor cells *in vivo* (within the body) by the introduction of a suitable neutron-capture isotope into the tumors and subsequent irradiation with a beam of thermal neutrons.

Two of the problems encountered are the limited concentration of boron-10 obtainable in the tumor during the irradiation and the lack of exact dose measurements during irradiation. Recent studies indicate the possibility of using solid state probes and detectors *in vivo* for the latter purposes in neutron-capture therapy.

Solid State Radiations, Inc., has designed an *in vivo* alpha-counting system to count alpha particles or estimate the alpha-particle dose from the boron-10 (n, α) lithium-7 reaction when tumors loaded with boron-10 are subjected to neutron bombardment in a nuclear reactor. The problem is the extremely large background count due to gamma-rays and direct interaction of neutrons with the detector. To circumvent these difficulties, a system has been developed which consists of: (*a*) a very thin low-resistivity silicon detector (whose sensitive volume is a disc millimeters in diameter and approximately 30 microns thick) enclosed in a 10-centimeter-long stainless steel tube that is sealed and coated with aluminum to eliminate sensitivity to light; and (*b*) a very fast current sensitive amplifier system to prevent the pile-up of the direct interaction events from being confused with alpha-particle pulses. The system response time is well below ten billionths of a second so that the discriminator is responsive only to single events and not to multiple pile-up events.

Experiments were conducted at Massachusetts General Hospital, Boston, to study the response of these semiconductor probes to alpha particles produced in neutron irradiated solutions with varying boron concentrations. The net response versus concentration of boron was observed to be sufficiently linear to allow accurate dose determinations to be made.

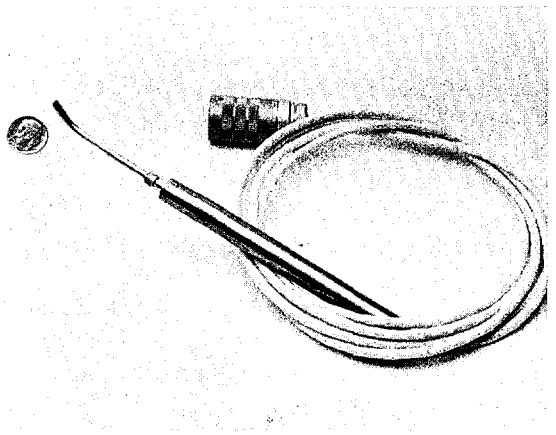

Fig. III–89. Eye Tumor Probe. A silicon beta detector (12-square-millimeter effective area) is within the tip of the curved probe end. The probe handle contains an electronic pre-amplifier. The probe was developed by Solid State Radiations, Inc., Los Angeles, in cooperation with Duke University, Durham, N.C., and the Veterans Administration Hospital, Houston, Tex.

Eye probes. Injected phosphorus-32, in the form of phosphate, remains selectively localized for several days in eye tumors. By probing the surfaces of the eye with a *Geiger-Mueller* probe, information about the location and extent of a tumor can be determined which is useful in outlining a suitable surgical procedure. Numerous objections to the *Geiger-Mueller* type instrumentation which have been expressed by clinicians have led to the development of semiconductor probes.

A program to investigate the use of semiconductor detectors in eye probes was initiated at Solid State Radiations, Inc., in cooperation with Duke University, Durham, N.C., and subsequently with the Veterans Administration Hospital in Houston, Tex.

A series of probes using lithium-drifted detectors packaged in the configuration shown in Figure III–89 has been designed. These detectors have rugged entrance windows, operate at low voltages, and when encapsulated with a paraxylylene coating, are proving to be impervious to body fluids. In addition, with the recent introduction of integrated electronic circuitry, much of the electronics required to operate the probe is mounted within the probe handle, thus, minimizing noise signals from external sources. Work is underway for the fabrication of improved versions of the detectors, detector holders, and electronics in order to: (*a*) lower the noise level, (*b*) improve beta detection and (*c*) obtain useful configurations of the probe system. The evaluation of these devices is being undertaken with the aid of the Veterans Administration Hospital in Houston, and the Eye Clinic of the University of California at Los Angeles.

In Vivo Radium Exposures

The study of the workers from the radium and luminous paint industries and takers of radium nostrums 30 to 50 years ago [32] is the principal source of knowledge on the long-term effects of radioactivity on human beings. Detailed understanding of the distribution of radium and mesothorium in the human body is necessary before complete correlations of radioactive body burden with health factors can be made. As part of the radium case study at the Radioactivity Center of the Massachusetts Institute of Technology, semiconductor detectors are being developed and used to determine the distribution of the alpha-ray emitters in samples of human tissue (principally bone, since radium deposits preferentially in calcified tissue).

The bone sample, a fraction of a square-inch in area, is bonded to a plastic holder by means of epoxy resin. The detector is then positioned above the surface of the sample in such a way as to expose the sensitive surface of the detector to the alpha-rays issuing from the bone surface. The detector produces a signal proportional to the energy of the alpha-ray striking it. Analysis of the final energy spectrum, after counting for a day, yields the values of the radium-226 concentration in the sample and, separately, also the values of the concentration of the short-lived decay products and of the long-lived

[32] See pp. 152–153, "Fundamental Nuclear Energy Research—1965."

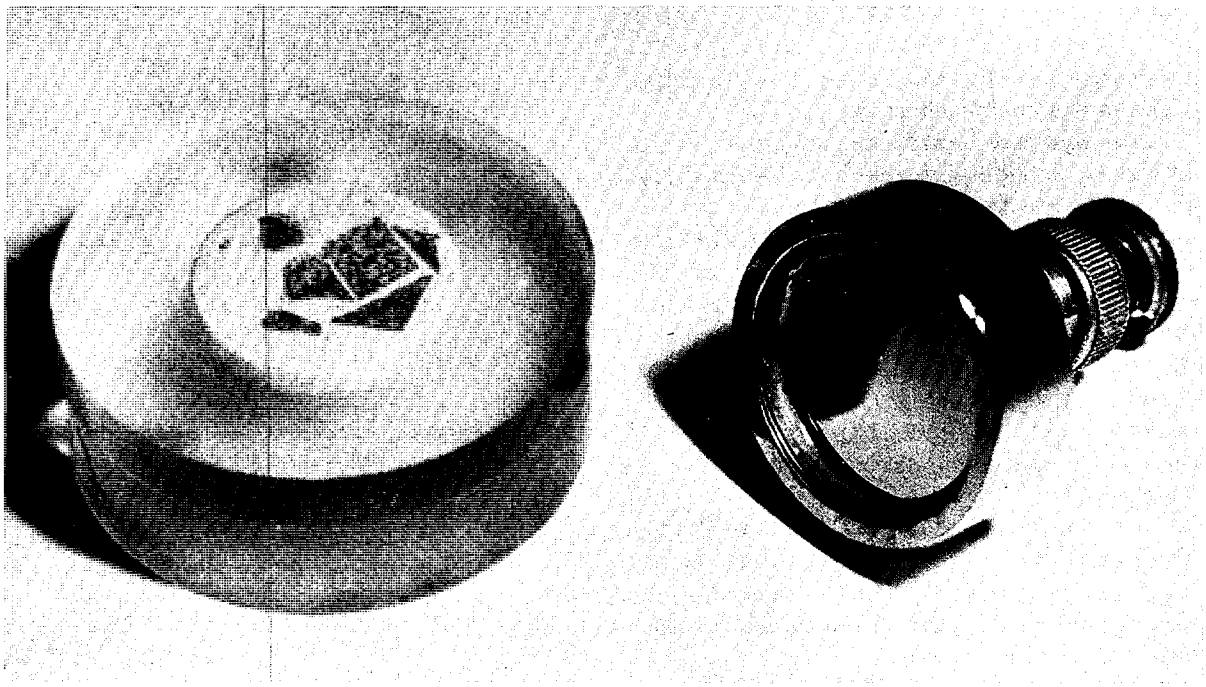

Fig. III–90. In Vivo Radium Exposures. As a part of radium case studies at the Massachusetts Institute of Technology, semiconductor detectors are being developed and used to determine the distribution of the alpha-ray emitters in samples of human tissue (principally bone, since radium deposits preferentially in calcified tissue). On *left* is a bone sample (portions of the parietal bone of the skull) embedded in epoxy resin in a plastic holder. At the *right* is a typical solid-state charged-particle detector used in this work. The diameter of the sensitive area of the detector is approximately 1 inch. During the measurement, both the detector and the sample are placed in a vacuum chamber to eliminate the slowing effect of air on the alpha particles.

decay products. In this respect, the method is superior to autoradiography (in which film is used as the detector of alpha-rays) since in autoradiography the amounts of the various radioactive species cannot be determined separately. Alpha-rays are able to penetrate only a very small thickness of bone, and for this reason the calculated concentrations refer only to the topmost layer of the bone sample. After completion of each measurement, the topmost layer of bone is cut away to expose a new surface. In this way, the distribution of the radium and its daughters can be followed through a complete specimen (see Fig. III–90).

Nine cases of the 500 studied so far at MIT have had soft-tissue cancers originating in the sinus cavities or in the mastoid air cells. This condition, which is very rare in the general population, is believed to be connected with special features of the physiology of the sinus and mastoid cavities. In these spaces, a thin layer of tissue overlays the radium-bearing bone and is, therefore, subject to bombardment of the alpha-rays from the bone. Bone samples from the sinus and mastoid regions are being studied with the solid state detector method to obtain an accurate measure of the dose rate to the soft tissue.

Neutron Activation Analysis

When bombarded with neutrons, many stable elements become temporarily radioactive, emitting gamma-rays of characteristic energy. Under favorable conditions, only a few hundred of the gamma-rays need be detected for a qualitative and quantitative indication of the pres-

ence of a particular element. Neutron activation analysis, therefore, forms a sensitive method of analysis, especially when used in conjunction with semiconductor detectors.

Tissue analysis. Trace elements are known to be widely distributed throughout the biosphere and many are known to have precise physiological functions in man. Many of these trace elements exist in the parts-per-billion range and the only sufficiently sensitive method for their precise measurement has been by neutron activation, followed by radiochemical separation. These very complicated and time-consuming radiochemical procedures have greatly limited the number of studies that have been performed on trace element deposition and behavior in both normal and diseased tissues. At the Pacific Northwest Laboratory, recently developed large-volume, coaxial-drifted germanium detectors have made possible the direct measurement of at least 14 trace elements in neutron-activated tissue samples. Figure III–91 shows the gamma-ray spectrum of a two-gram sample of neutron-activated lung tissue with a 20-cubic centimeter germanium (lithium drifted) detector as recorded three months after irradiation. In this spectrum, the photopeaks from 11 radionuclides are identified from which it is possible to measure 10 elements with reasonably good precision. These include selenium, iron, chromium, mercury, zinc, antimony, cesium, scandium, rubidium, and cobalt. In addition, phosphorus can be precisely determined from its *bremsstrahlung* [33] contribution to the spectrum. Sodium and bromine are easily measured from the characteristic gamma radiation of their radioactive daughters. Where larger samples or longer radiation times are employed, it is also possible to measure silver. This method for the direct measurement of trace elements in human tissues will allow the practical investigation of the natural abundance and the biological behavior of trace elements in the body. Its direct applicability to all manner of biological and environmental materials also appears certain.

[33] X-rays resulting from changing velocities of the phosphorus-32 beta particles.

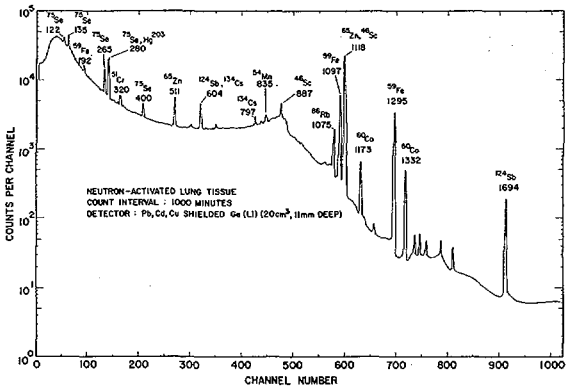

Fig. III–91. Neutron Activation Analysis. Trace elements are known to be well distributed throughout the biosphere and many are known to have precise physiological functions in man. Many of these trace elements exist in the parts-per-billion range and at the Pacific Northwest Laboratory, recently developed large-volume, coaxial-drifted germanium detectors make it possible to directly measure at least 14 trace elements in neutron-activated tissue samples. The chart shows the gamma-ray spectrum of a two-gram sample of neutron-activated lung tissue as recorded—three months after irradiation—with a 20-cubic centimeter germanium (lithium drifted) detector. In this spectrum, the photopeaks from 11 radionuclides are identified from which it is possible to measure 10 elements with reasonably good precision. These include selenium, iron, chromium, mercury, zinc, antimony, cesium, scandium, rubidium, and cobalt.

Atmospheric elements. Elements present in the atmosphere in trace amounts may in favorable cases be filtered out and identified with neutron activation analysis using no wet chemistry at any point in the procedure. Samples taken on the roof of a tall building on the MIT campus show clear evidence of bromine, zinc, and other elements. The method may also be useful in tracing the small-scale motions of air in and around a city if trace elements are injected into the atmosphere.

Oceanography

Investigations at the University of California's Scripps Institution of Oceanography, La Jolla, have used solid state semiconductors to assay, by alpha spectrometric techniques, the

amounts of members of the uranium and thorium naturally radioactive series in samples from the marine environment. Inasmuch as such elements are extensively involved in present day nuclear technologies, a knowledge of their behaviors in the oceanic system is needed to show the consequences of the release of controlled or uncontrolled amounts of them into the marine environment. Their distribution between the water, organisms of the sea, and marine sediments as a function of time has been studied. For example, it has been determined that uranium remains in solution for very long time periods (up to a million years) before precipitation to the sediments. On the other hand, thorium becomes very actively involved in chemical reactions upon introduction to sea water and probably stays in the oceanic system only for periods of about a hundred years before being accumulated in the sediments.

Measurements of the rates of accumulation of oceanic sediments have been made using the isotopes of thorium and uranium. In recent accumulations (those deposited over the past few hundred thousand years), rates of accumulation have been measured to be on the order of a few millimeters per thousand years. Of further interest have been the measurements of the rates of chemical precipitation on the sea floor. The ferromanganese minerals (oxides of iron and manganese) appear to accumulate at rates of about a layer one atom thick per day or less based on the concentrations of thorium and uranium isotopes within their matrices. This is perhaps one of the slowest chemical reactions for which rates have been accurately recorded.

APPENDIX

MAJOR RESEARCH AND DEVELOPMENT FACILITIES OF THE U.S. ATOMIC ENERGY COMMISSION

Ames Laboratory (Iowa State University of Science and Technology, contractor), Ames, Iowa

Director	DR. FRANK H. SPEDDING
Deputy Director	DR. MORTON SMUTZ
Assistant Director	DR. ALBERT F. VOIGT

Argonne Cancer Research Hospital (University of Chicago, contractor), Chicago, Ill.

Director	DR. ALEXANDER GOTTSCHALK
Associate Director	DR. SAMUEL B. WEISS
Assistant Director for Administration	CYRIL W. KUPFERBERG

Argonne National Laboratory (University of Chicago and Argonne Universities Association, contractors), Argonne (Lemont), Ill.

Director	DR. ROBERT B. DUFFIELD
Associate Director	DR. WINSTON M. MANNING
Associate Director	DR. STEPHEN LAWROSKI
Associate Director for High Energy Physics	DR. ROBERT G. SACHS
Assistant Director	DR. RICHARD M. ADAMS
Assistant Director for Personnel	JOHN T. BOBBITT
Business Manager	JOHN H. MCKINLEY
Manager, Technical Service	VICTOR H. MUNNECKE

University of Chicago

President	DR. GEORGE W. BEADLE
Vice President, Special Projects	W. B. HARRELL

Argonne Universities Association

Chairman, Board of Trustees.	DR. FRED H. HARRINGTON
President	DR. PHILIP N. POWERS

The participating institutions in the Argonne Universities Association are:

Carnegie-Mellon University
Case Institute of Technology
Illinois Institute of Technology
Indiana University
Iowa State University
Kansas State University
Loyola University
Marquette University
Michigan State University
Northwestern University
Ohio State University
Purdue University
St. Louis University
State University of Iowa
University of Arizona
University of Chicago
University of Cincinnati
University of Illinois
University of Kansas
University of Michigan
University of Minnesota
University of Missouri
University of Notre Dame
University of Wisconsin
Washington University (St. Louis)
Wayne State University

Associated Midwest Universities (Participants in "University-AEC Laboratory Cooperative Program" at Argonne National Laboratory)

President	DR. FREDERICK D. ROSSINI
Vice President	DR. ARMON F. YANDERS
Executive Director and Secretary	DR. JOHN H. ROBERSON
Treasurer	A. T. SCHMEHLING

The participating institutions are:

Carnegie-Mellon University
Case Western Reserve University
Illinois Institute of Technology
Indiana University
Iowa State University
Kansas State University
Loyola University (Chicago, Ill.)
Marquette University
Michigan Technological University
Michigan State University
Northwestern University
Ohio State University
Ohio University
Oklahoma State University
Pennsylvania State University

Purdue University
St. Louis University
Southern Illinois University
University of Arizona
University of Chicago
University of Cincinnati
University of Illinois
University of Iowa
University of Kansas
University of Michigan
University of Minnesota
University of Missouri
University of Nebraska
University of Notre Dame
University of Texas
University of Wisconsin
Washington University (St. Louis)
Wayne State University

Associated Colleges of Midwest (Participants in "University-AEC Laboratory Cooperative Program" at Argonne National Laboratory)

President	DR. BLAIR STEWART
Vice President	DR. HENRY M. HALSTED, III
Program Associate	DONALD R. LIGGETT

The participating institutions are:

Beloit College
Carleton College
Coe College
Cornell College (Iowa)
Grinnell College
Knox College
Lawrence College
Monmouth College
Ripon College
St. Olaf College

Associated Colleges of the Chicago Area (Participants in "University-AEC Laboratory Cooperative Program" at Argonne National Laboratory)

President	VICTOR ARNOLD
Vice President	CLIFFORD HOLMES
Secretary	REV. VIRGIL TRELO
Treasurer	CLIFFORD HOLMES

The participating institutions are:

Aurora College
Barat College
College of Saint Francis
Concordia College
Elmhurst College
George Williams College
Judson College
Lake Forest College
Lewis College
Mundelein College
North Central College
North Park College
Olivet Nazarene College
Rosary College
Saint Dominic College
Saint Procopius College
Saint Xavier College
Trinity Christian College
Wheaton College

Central States Universities Incorporated (Participants in "University-AEC Laboratory Cooperative Program" at Argonne National Laboratory)

President	H. F. HENRY
Vice President	GLENN BROWN
Treasurer	T. GRIFFITH
Secretary	G. E. BRADLEY

The participating institutions are:

Ball State Teachers College
Bowling Green State University
De Paul University
Depauw University
John Carroll University
Kent State University
Miami University
Northern Illinois University
Northern Michigan University
Ohio University
Southern Illinois University
State College of Iowa
University of Detroit
University of Toledo
Western Michigan University

Bettis Atomic Power Laboratory (Westinghouse Electric Corp., contractor), Pittsburgh, Pa.

General Manager	PHILIP N. ROSS
Manager, PWR Project	J. T. STIEFEL
Manager, Surface Ship Project.	ELLIS T. COX
Manager, Submarine Project.	N. A. BELDECOS

Brookhaven National Laboratory (Associated Universities, Inc., contractor), Upton, N.Y.

Director	DR. MAURICE GOLDHABER
Deputy Director	DR. GEORGE VINEYARD
Associate Director	DR. VICTOR P. BOND
Associate Director	DR. RODNEY L. COOL

Assistant Director	SAMUEL M. TUCKER
Assistant Director	DR. G. NORRIS GLASOE
Assistant Director	DR. R. C. ANDERSON
Assistant Director	DR. WILLIAM J. CATACOSINOS

Associated Universities, Inc.

Chairman, Board of Trustees.	DR. E. F. JOHNSON
President, AUI	DR. T. KEITH GLENNAN

The sponsoring institutions in Associated Universities, Inc., are:

Columbia University
Cornell University
Harvard University
The Johns Hopkins University
Massachusetts Institute of Technology
Princeton University
University of Pennsylvania
University of Rochester
Yale University

Cambridge Electron Accelerator (Massachusetts Institute of Technology and Harvard University, contractors), Cambridge, Mass.

Director	DR. CARL STRAUCH
Assistant Director	ROBERT E. CUMMINGS
Assistant Director	DR. THOMAS L. COLLINS
Assistant Director	DR. GUSTAV A. VOSS
Business Manager	WILLIAM B. BALCH

Health and Safety Laboratory (AEC operated), New York, N.Y.

Director	DR. JOHN H. HARLEY
Director, Environmental Studies Division.	EDWARD P. HARDY
Director, Health Protection Engineering Division.	ALFRED J. BRESLIN
Director, Instrumentation Division.	ROBERT T. GRAVESON
Director, Radiation Physics Division.	JAMES E. MCLAUGHLIN
Director, Radiochemistry Division.	GEORGE A. WELFORD

Knolls Atomic Power Laboratory (General Electric Co., contractors), Schenectady, N.Y.

General Manager	K. A. KESSELRING
Manager, S5G Project	H. E. STONE
Manager, D1G Project	W. H. BRUGGEMAN
Manager, SAR Project	E. C. RUMBAUGH

Laboratory of Nuclear Medicine and Radiation Biology (University of California at Los Angeles, contractor), Los Angeles, Calif.

Acting Director	PROF. OWEN R. LUNT
Project Manager	CLINTON LONGWILL

Laboratory of Radiobiology, San Francisco Medical Center (University of California, contractor), San Francisco, Calif.

Director	DR. HARVEY M. PATT

E. O. Lawrence Radiation Laboratory (University of California, contractor), facilities at Berkeley and Livermore, Calif.

Director	DR. EDWIN M. MCMILLAN
Director, Livermore Laboratory.	DR. MICHAEL M. MAY
Business Manager	RICHARD P. CONNELL
Deputy Business Manager	WILLIAM B. HARFORD

Associate Directors, Berkeley

Donner Laboratory of Medical Physics, Director.	DR. JOHN H. LAWRENCE
Inorganic Materials Research Division.	DR. LEO BREWER
Laboratory of Chemical Biodynamics, Director.	DR. MELVIN CALVIN
Nuclear Chemistry Division.	DR. ISADORE PERLMAN
Physics Division	DR. DAVID L. JUDD
Program and Planning	DR. ROBERT L. THORNTON
Administration	DR. HAROLD A. FIDLER
Support	DR. ELMER L. KELLY

Associate Directors, Livermore

Advanced Studies	DR. ARTHUR T. BIEHL
Biomedical Research	DR. JOHN W. GOFMAN
Chemistry and Space Reactors.	DR. ROGER E. BATZEL
Military Application	A. CARL HAUSSMANN
Nuclear Design	DR. JACK ROSENGREN
Nuclear Testing	DR. HARRY L. REYNOLDS
Physics	DR. EDWARD TELLER
Plowshare	DR. GLENN C. WERTH
Sherwood	DR. CHESTER M. VAN ATTA
Support	DUANE C. SEWELL

275-845 O - 68 - 24

Los Alamos Scientific Laboratory (University of California, contractor), Los Alamos, N. Mex.

Director	DR. NORRIS E. BRADBURY
Technical Associate Director.	DR. RAEMER E. SCHREIBER
Assistant Director	DR. JANE H. HALL
Assistant Director, Production.	DR. MAX F. ROY
Assistant Director, Classification and Security.	PHILLIP F. BELCHER
Assistant Director, Financial Planning.	LESLIE G. HAWKINS
Assistant Director, Administration.	HENRY R. HOYT

Mound Laboratory (Monsanto Research Corp., contractor), Miamisburg, Ohio

Project Director (President, Monsanto Research Corp.).	H. K. NASON
Plant Manager (Vice President, Monsanto Research Corp.).	DAVID L. SCOTT

National Reactor Testing Station (NRTS) (Six contractors—Argonne National Laboratory, General Electric, General Atomic, Idaho Nuclear, Phillips, and Westinghouse) Idaho Falls, Idaho

Argonne National Laboratory (ANL Idaho Division), Idaho Falls

Director	M. NOVICK
Associate Director	F. W. THALGOTT
EBR–II Reactor Project Manager.	R. E. RICE
Operations Manager	G. K. WHITHAM
Analysis and Test Manager.	R. R. SMITH
Engineering Manager	B. C. CERUTTI
Experimental Support Manager.	D. W. CISSEL
Fuel Cycle Facility Project Manager.	C. E. STEVENSON
Fuel Cycle Operations Manager.	M. J. FELDMAN
Fuel Cycle Analytical Laboratory Manager.	E. B. EBERSOLE
TREAT Project Manager	J. F. BOLAND
Fast Reactor Physics Experiments Manager.	W. J. DAVEY
ZPPR Project Manager	R. P. HEARN
ZPPR Technical Manager	H. LAWROSKI
ZPR–III Operations Manager.	R. L. MCVEAN

General Electric Co. (Idaho Test Station, Nuclear Materials and Propulsion Operation, Nuclear Energy Division), Idaho Falls

Manager	DR. J. W. MORFITT
Manager, Idaho Engineering.	DR. R. E. WOOD
Manager, Relations and Services.	L. A. MUNTHER
Manager, Materials Projects.	F. O. URBAN
Manager, Low Power Test Operations.	DR. J. DUNZE

General Electric Co. (Knolls Atomic Power Laboratory, S5G Field Office), Idaho Falls

Manager	E. R. SHOCK
Manager, Administrative Services	R. L. JORDAN

Idaho Nuclear Corp. (Jointly owned subsidiary of Aerojet General Corp. and Allied Chemical Corp.), Idaho Falls

President & Manager	DR. C. H. TRENT
Vice President & Deputy Manager.	F. H. ANDERSON
Manager, Administrative Division.	R. TRIPP
Manager, Engineering Division.	L. J. WEBER
Manager, Nuclear and Chemical Technology Division.	D. R. DEBOISBLANC
Acting Manager, Operations Division.	F. H. ANDERSON

Phillips Petroleum Co. (Atomic Energy Division), Idaho Falls

Manager	J. P. LYON
Assistant Manager, Technical Division.	S. G. FORBES
Assistant Manager, Administration.	L. L. LEEDY
Manager, Water Reactor Safety Program.	F. SCHROEDER
Manager, Nuclear Safety Research.	J. C. HAIRE
Manager, Plant Applications and Engineering Test Branch.	N. K. SOWARDS
Manager, Technical Services Branch.	M. E. THOMAS
Manager, Engineering and Test Branch.	T. R. WILSON

Westinghouse Electric Corp., Idaho Falls

Manager, Naval Reactors Facility.	R. C. MAIRSON
Manager, S1W Operations	H. D. RUPPEL
Manager, Expended Core Facility.	T. A. MANGELSDORF
Manager, A1W Operations	W. M. GAWJEWSKI
Manager, Administrative Services.	W. H. WALKER
Manager, Technical Services.	D. E. ANDERSON
Manager, Quality Engineering Control.	H. A. CLAWSON
Manager, Plant Services	W. H. MCKIM
Controller	J. L. TAYLOR

Associated Western Universities. Participants in "University-AEC Laboratory Cooperative Program" at the National Reactor Testing Station, as well as at the Los Alamos Scientific Laboratory, Sandia Laboratory, Lovelace Foundation (Albuquerque), Lawrence Radiation Laboratory (Berkeley and Livermore), Pacific Northwest Laboratory, Dow Chemical Co. (Rocky Flats).

Chairman, Board of Directors.	DR. W. E. MORGAN
Vice Chairman	DR. J. R. SMILEY
Secretary-Treasurer	DR. J. C. FLETCHER
Executive Director	DR. G. V. BEARD
Chairman, Nuclear Committee.	DR. QUENTIN FORD

The participating institutions are:

Brigham Young University
Colorado State University
Idaho State University
Montana State University
New Mexico Institute of Mining and Technology
New Mexico State University
San Jose State College
Texas Agriculture and Mechanical Arts University
University of Colorado
University of Denver
University of Idaho
University of Montana
University of New Mexico
University of Utah
University of Wyoming
Utah State University

ORAU Research Facilities (formerly Oak Ridge Institute of Nuclear Studies—ORINS) (Oak Ridge Associated Universities, contractor), Oak Ridge, Tenn.

President of Association	DR. PAUL M. GROSS
Chairman of Council	DR. H. W. DAVIS
Vice Chairman of Council	DR. G. B. HUFF
Executive Director of Association.	DR. WILLIAM G. POLLARD

The sponsoring institutions of the Association are:

Auburn University
Catholic University of America
Clemson University
College of William and Mary
Duke University
Emory University
Fisk University
Florida State University
Georgia Institute of Technology
Louisiana State University
Medical College of Virginia
Meharry Medical College
Mississippi State College
North Carolina State University
North Texas State University
Rice University
Southern Methodist University
Texas A. and M. University
Texas Christian University
Texas Women's University
Tulane University
Tuskegee Institute
University of Alabama
University of Arkansas
University of Florida
University of Georgia
University of Kentucky
University of Louisville
University of Maryland
University of Miami
University of Mississippi
University of North Carolina
University of Oklahoma
University of Puerto Rico
University of South Carolina
University of Tennessee
University of Texas
University of Virginia
Vanderbilt University
Virginia Polytechnic Institute
West Virginia University

Oak Ridge National Laboratory (Union Carbide Corp., Nuclear Division, contractor), Oak Ridge, Tenn.

Director	DR. A. M. WEINBERG
Deputy Director	H. G. MACPHERSON
Assistant Deputy Director	F. R. BRUCE
Assistant Director	G. E. BOYD
Assistant Director	W. H. JORDAN
Assistant Director	F. L. CULLER
Assistant Director	M. E. RAMSEY
Assistant Director	A. H. SNELL
Assistant Director	GALE YOUNG
Assistant Director	J. L. LIVERMAN

Pacific Northwest Laboratory (Battelle Memorial Institute, contractor), Richland, Wash.

Director	DR. S. L. FAWCETT
Associate Director	DR. F. W. ALBAUGH
Associate Director	DR. R. S. PAUL
Manager, Applied Physics and Electronics Dept.	D. C. WORLTON
Manager, Biology Dept	DR. H. A. KORNBERG
Manager, Chemistry Dept	DR. D. R. DEHALAS
Manager, Engineering Development Dept.	DR. J. M. BATCH
Manager, Engineering Services Dept.	W. D. RICHMOND
Manager, Environmental Health Dept.	A. R. KEENE
Manager, Environmental and Radiological Sciences Dept.	J. J. FUQUAY
Manager, Fast Flux Test Facility Project.	E. R. ASTLEY
Manager, Materials Dept	DR. E. A. EVANS
Manager, Mathematics Dept.	DR. C. A. BENNETT
Manager, Metallurgy Dept.	DR. J. J. CADWELL
Manager, Reactor Physics Dept.	F. G. DAWSON, JR.
Manager, Heavy Water Reactor Program Office.	HAROLD HARTY
Manager, Finance	WALLACE SALE
Manager, Planning, Programming, and Engineering.	R. F. DICKERSON
Manager, Technical and Public Services.	C. R. TIPTON, JR.

Princeton-Pennsylvania Accelerator (Princeton University and University of Pennsylvania, contractors), James Forrestal Research Center, Princeton, N.J.

Director	DR. MILTON G. WHITE
Assistant Director	DR. AARON LEMONICK
Assistant Director	DR. ALFRED K. MANN

Princeton Plasma Physics Laboratory (Princeton University, contractor), James Forrestal Research Center, Princeton N.J.

Director	DR. MELVIN B. GOTTLIEB
Associate Director	DR. EDWARD A. FRIEMAN
Assistant Director	DR. E. C. TANNER
Head, Experimental Division.	DR. TOM STIX
Head, Engineering and Development Division.	DR. ROBERT MILLS
Head, Theoretical Division	DR. J. M. DAWSON
Head, Administrative Division.	ROBERT VON VERDO

Puerto Rico Nuclear Center (University of Puerto Rico, contractor), San Juan and Mayaguez, P.R.

Director	DR. HENRY J. GOMBERG
Deputy Director	DR. AMADOR COBAS

Radiation Laboratory (University of Notre Dame, contractor), Notre Dame, Ind.

Director	DR. MILTON BURTON
Associate Director	DR. JOHN L. MAGEE
Assistant Director for Administration.	J. J. RISSER

Sandia Laboratory (Sandia Corp., contractor), facilities at Sandia Base, Albuquerque, N. Mex.; Livermore, Calif; and Tonopah, Nev.

President	J. A. HORNBECK
Vice President	W. J. HOWARD
Vice President	R. W. HENDERSON
Vice President	R. B. POWELL
Vice President	C. W. CAMPBELL
Vice President	R. C. FLETCHER
Vice President	C. T. ROSS, JR.
Vice President	R. A. BICE
Vice President	B. S. BIGGS
Vice President	G. A. FOWLER

Savannah River Laboratory (E. I. du Pont de Nemours & Co., contractor), Aiken, S.C.

Director	W. P. OVERBECK
Assistant Director	A. A. JOHNSON
Section Director—Physics Section.	G. DESSAUER
Section Director—Nuclear Engineering and Materials Section.	J. W. MORRIS

Section Director—Separations Chemistry and Engineering Section.	C. H. ICE

Stanford Linear Accelerator Center (Stanford University, contractor), Palo Alto, Calif.

Director	DR. W. K. H. PANOFSKY
Deputy Director	DR. M. SANDS
Research Division, Associate Director.	DR. J. BALLAM
Technical Division, Associate Director.	DR. R. B. NEAL
Business Service Division, Associate Director.	F. V. L. PINDAR
Administrative Service Division, Associate Director.	R. H. MOULTON, JR.

University of Rochester Atomic Energy Project (University of Rochester, contractor), Rochester, N.Y.

Director	DR. ASER ROTHSTEIN
Associate Director	DR. WILLIAM F. NEUMAN
Associate Director for Education.	DR. J. N. STANNARD
Business Manager	PAUL D. NICHOLSON

U.T.-AEC Agricultural Research Laboratory (University of Tennessee, contractor), Oak Ridge, Tenn.

Project Leader	DR. JOHN A. EWING
Laboratory Director	DR. N. S. HALL

INDEX

A

C

D

E

F

K

L

M

N

O

P

Q

R

S

U

V

W

X

Y

Z

U.S. GOVERNMENT PRINTING OFFICE: 1968 O—275-845